STIFF

NASA CONTRACTOR REPORT 166494

Laboratory Infrared Studies of Molecules of Atmospheric And Astrophysical Interest

K. Narahari Rao

CONTRACT NSG-2175
October 1982

NASA

NASA CONTRACTOR REPORT 166494

Laboratory Infrared Studies of Molecules of Atmospheric And Astrophysical Interest

K. Narahari Rao
Principal Investigator
Ohio State University
Department of Physics
174 West 18th Avenue
Columbus, Ohio 43210

Prepared for
Ames Research Center
Under Grant NSG-2175

National Aeronautics and
Space Administration

Ames Research Center
Moffett Field, California 94035

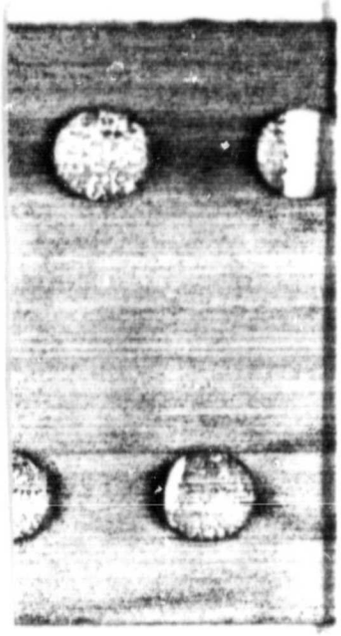

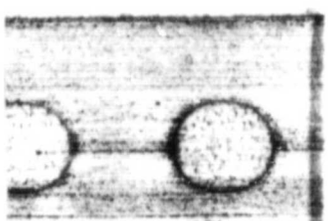

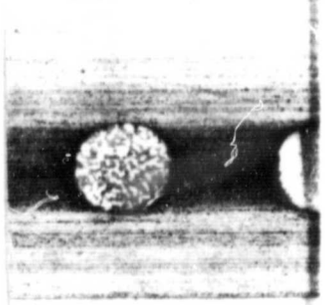

OSU

The Ohio State University
Department of Physics
174 West 18th Avenue
Columbus, Ohio 43210

Re: Laboratory Infrared Studies of Molecules of Atmospheric and Astrophysical Interest

Contract Number: NSG 2175

Duration: October 1, 1976--October 1, 1982

This NASA grant administered by Moffett Field (Supervisor, Dr. R. Boese) has provided funding for a period of three years. During the no-cost extension period, all research done has been published and the report is a compilation of nineteen reprints on the molecular species:

NO_2 ν_2 & $2\nu_2$; H_2O (6050-9730 cm^{-1}; O_3 ν_2; C_2H_2 ν_5 and 6680-6460 cm^{-1}; CH_3D ν_3 & ν_6; CH_3I ν_6; NH_3 ν_2, $2\nu_2$, ν_4; ND_3 ν_2; $^{13}C^{16}O_2$ ν_3; PH_3 ν_1 & ν_3; OCS ν_1; GeH_4 ν_4.

Much of the work was done by using the Doppler-limited resolution provided by diode lasers. The diode laser was used as a source to a grating spectrometer which has been used earlier for high resolution studies. This technique provided many advantages. Wherever possible, the studies have been directed to intensity determinations of infrared bands.

K. Narahari Rao

K. Narahari Rao
Principal Investigat

JOURNAL OF MOLECULAR SPECTROSCOPY 88, 251–258 (1981)

Diode Laser Measurements of Intensities, N_2-Broadening, and Self-Broadening Coefficients of Lines of the ν_2 Band of $^{14}N^{16}O_2$

V. MALATHY DEVI,[1] PALASH P. DAS,[2] A. BANO, AND K. NARAHARI RAO

Department of Physics, The Ohio State University, Columbus, Ohio 43210

AND

J.-M. FLAUD, C. CAMY-PEYRET, AND J.-P. CHEVILLARD

Laboratoire de Physique Moleculaire et d'Optique Atmospherique, Bât. 221, Campus d'Orsay, 91405 Orsay Cedex, France

A diode laser spectrometer (resolution 0.0013 cm^{-1}) was used to record, in the 12-μm region, high-quality spectra of the ν_2 band of NO_2. Using these spectra, it was possible to obtain the N_2-broadening coefficients and an average self-broadening coefficient from measurements made for several lines of this band. In addition, 30 single spin-component line intensities were measured. From them, through a least-squares fit, the purely vibrational transition moment of the ν_2 band, as well as two correcting rotational terms involved in the expansion of the transition moment operator, were obtained. These results led to the determination of the dipole moment derivative $\partial\mu_z/\partial q_2 = -0.0604_1 \pm 0.0037$ D. It was also demonstrated that there is good consistency between the correcting terms deduced from the observed intensities and their theoretical estimates. Finally, a complete spectrum of the ν_2 band of NO_2 was computed, providing a total band intensity $S_v(\nu_2) = 0.542 \times 10^{-18}$ cm^{-1}/molecule cm^{-2} at 296 K.

I. INTRODUCTION

Many high-resolution studies concerning the line positions of nitrogen dioxide in the infrared have been reported but much less work has been performed on NO_2 line intensities and widths (*1–4*). These line parameters are of importance for precise determinations of the concentration of nitrogen dioxide in the atmosphere and in combustion products. As a natural continuation of our study of the line positions of the ν_2 band of NO_2 (*5*), we present here results on intensities, N_2-broadening, and self-broadening coefficients of lines belonging to the ν_2 band of this molecule.

II. EXPERIMENTAL DETAILS

The diode laser spectrometer used in this investigation has been described earlier (*6*, *7*). A commercial sample of NO_2 was used. Although it was stated to

[1] Present address: NOAA–NESS, FB4, S/RE21, Washington, D. C. 20233.
[2] Present address: Tachisto Inc., 13 Highland Circle, Needham, Mass. 02194.

0022-2852/81/080251-08$02.00/0

be 99% pure, our experience indicated that it contained a significant amount of NO as an impurity. CO_2 is also believed to be another minor impurity in this gas. In order to purify the sample, NO_2 at about 100 Torr was introduced into a glass bulb connected to a mechanical pump and a diffusion pump. Using a mixture of methanol and dry ice the sample was then frozen to −78°C. This frozen solid usually had a bluish tinge indicating the presence of NO. In order to remove this NO, the frozen solid at −78°C was pumped for an hour, then warmed to room temperature, refrozen, and pumped again. This procedure removed the blue tinge completely, leaving behind a pure white solid. This procedure also eliminated CO_2. For line strength measurements, two Pyrex cells of lengths 101.6 and 201.6 cm were used. Since NO_2 reacts with H_2O to form HNO_3, which can cause interference, the cells and the gas-handling systems were pumped to pressures less than 10^{-5} Torr. KRS-5 windows were used for the cells. Ordinarily, the amount of dimer of NO_2, namely, N_2O_4, depends on the total gas pressure and temperature. If P_{NO_2} and $P_{N_2O_4}$ denote the pressures of NO_2 and N_2O_4 (in atmospheres), then, the equilibrium constant $k_p(T)$ for the reaction (8)

$$N_2O_4 \rightleftarrows 2NO_2$$

is given by

$$\frac{(P_{NO_2})^2}{P_{N_2O_4}} = k = 1.08 \times 10^{13} \times T^{-1.304} \exp\left(-\frac{14520}{1.987\,T}\right) = \frac{(P_{NO_2})^2}{P - P_{NO_2}}, \quad (1)$$

where $P = P_{NO_2} + P_{N_2O_4}$. For 296 K and a total pressure of 1 Torr, the above equation was solved numerically. It was found that only 1% of the gas was in the form of N_2O_4. Therefore, for all line strength measurements, pressures were kept below 1 Torr. The scans were taken within 1 hr after filling the cells and several repetitive scans were made on each line for various pressure × pathlength values. Pressures were measured with MKS Baratron gauges with an estimated uncertainty of less than 1% and the cell temperatures were monitored during each scan by precision thermistor probes. The dispersion was calculated from the wavenumbers of NO_2 lines recorded simultaneously with the fringes obtained with a 1-in.-long germanium etalon. The analog records were digitized with a Bendix Datagrid digitizer for processing. For self-broadening measurements we used three Pyrex cells 6.3, 11.3, and 21.7 cm in length and the pressure of NO_2 ranged from 12 to 30 Torr. For nitrogen-broadening experiments, a Pyrex cell, 201.6 cm long with total pressures up to 30 Torr and NO_2 pressures less than 1 Torr, was used.

III. MEASUREMENTS OF LINE INTENSITIES

We have selected 30 well-isolated lines, the equivalent widths of which have been measured several times at different pressures and path lengths. The intensity k_σ^p (in $cm^{-2}\,atm^{-1}$) of each line has been extracted from the equivalent width assuming a value of 0.112 $cm^{-1}\,atm^{-1}$ for the self-broadening coefficient and taking into account wing corrections. The results are given in Table I together with their statistical errors (one standard deviation).

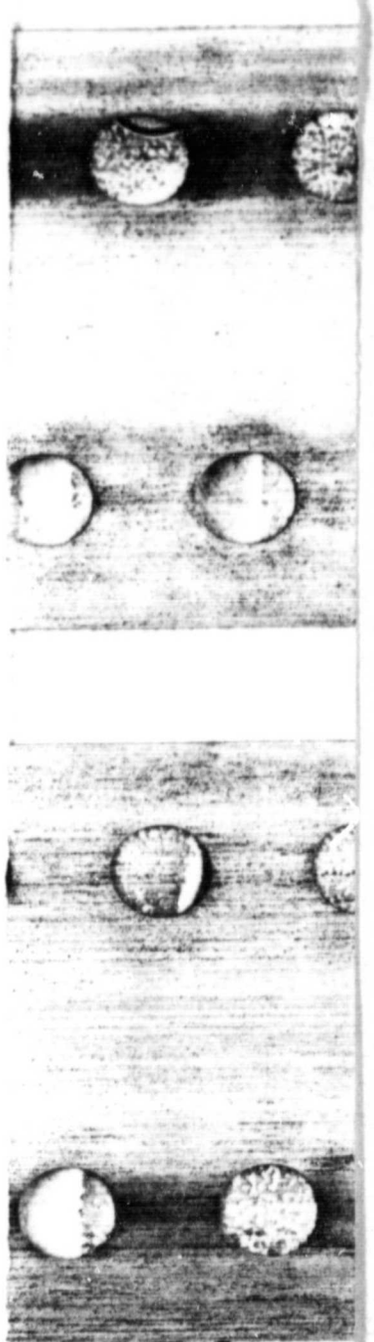

TABLE I

Measured and Calculated Line Intensities of the ν_3 Band of $^{14}N^{16}O_2$

SIGMA (cm^{-1})	N' K_a' K_c'	N K_a K_c	i·N	k_0^p (obs) ($10^{-3} cm^{-2} atm^{-1}$)	k_0^p (calc) ($10^{-3} cm^{-2} atm^{-1}$)	$\left\|\frac{k_0^p(obs) - k_0^p(calc)}{k_0^p(obs)}\right\|$
825.335	35 5 31	35 4 32	-1/2	2.067 ± 0.11	1.984	4%
825.345	36 5 31	36 4 32	+1/2	1.812 ± 0.14	1.812	0%
825.357	34 5 29	34 4 30	-1/2	2.174 ± 0.11	2.219	2%
825.381	35 5 31	35 4 32	+1/2	2.060 ± 0.12	2.041	1%
825.386	33 5 29	33 4 30	-1/2	2.349 ± 0.15	2.472	5%
825.476	29 5 25	29 4 26	-1/2	3.643 ± 0.18	3.595	1%
825.488	31 5 27	31 4 28	+1/2	3.252 ± 0.14	3.124	4%
825.495	28 5 23	28 4 24	-1/2	4.206 ± 0.18	3.917	7%
835.806	12 5 7	11 4 8	-1/2	6.819 ± 0.39	7.116	4%
836.648	13 5 9	12 4 8	-1/2	7.099 ± 0.44	7.116	0%
836.761	13 5 9	12 4 8	+1/2	7.548 ± 0.63	7.711	2%
837.488	14 5 9	13 4 10	-1/2	7.422 ± 0.44	7.116	4%
837.594	14 5 9	13 4 10	+1/2	7.283 ± 0.32	7.637	3%
839.166	16 5 11	15 4 12	-1/2	7.015 ± 0.19	6.967	2%
839.259	16 5 11	15 4 12	+1/2	7.063 ± 0.24	7.413	5%
843.705	25 6 20	25 5 21	+1/2	3.505 ± 0.20	3.446	2%
843.719	24 6 18	24 5 19	+1/2	3.547 ± 0.14	3.645	3%
843.732	23 6 18	23 5 19	+1/2	3.705 ± 0.16	3.843	4%
843.745	22 6 16	22 5 17	+1/2	3.833 ± 0.23	4.017	5%
843.758	21 6 16	21 5 17	+1/2	4.471 ± 0.19	4.190	6%
843.770	20 6 14	20 5 15	+1/2	4.229 ± 0.18	4.314	2%
843.783	19 6 14	19 5 15	+1/2	4.265 ± 0.19	4.438	4%
843.794	18 6 12	18 5 13	+1/2	4.367 ± 0.20	4.512	3%
843.806	17 6 12	17 5 13	+1/2	4.358 ± 0.17	4.537	4%
843.817	16 6 10	16 5 11	+1/2	4.348 ± 0.19	4.537	4%
861.929	28 7 21	28 6 22	+1/2	1.766 ± 0.074	1.778	1%
861.965	25 7 19	25 6 20	+1/2	2.115 ± 0.10	2.189	4%
862.032	19 7 13	19 6 14	+1/2	3.247 ± 0.15	2.777	15%
862.065	16 7 9	16 6 10	+1/2	2.937 ± 0.10	2.802	5%
862.100	13 7 7	13 6 8	+1/2	2.579 ± 0.12	2.529	2%

IV. MEASUREMENTS OF LINEWIDTHS

The instrumental function of the diode laser spectrometer has been shown to be Gaussian with a half-width at half-maximum (HWHM) $\gamma_I = 0.65 \times 10^{-3}$ cm^{-1} (*9*). We have measured the half-width γ^{obs} of the observed line absorption profile at $I_o(I_{min}/I_o)^{1/2}$, where I_o is the measured continuum or baseline determined from the region of no absorption and I_{min} is the measured absorption at the center of the line. This would give the true half-width at half-maximum of the absorption coefficient assuming no contribution from the apparatus function. As a first approximation, where γ_I is small compared to the half-width γ_V of the Voigt profile, the Lorentzian half-width γ_L can be obtained from γ^{obs} assuming $\gamma^{obs} \simeq \gamma_V$ through the relation (*10*)

$$\gamma_L = \gamma_V\left(7.7254 - 6.7254\left(1 + 0.3195\left(\frac{\gamma_D^{eff}}{\gamma_V}\right)^2\right)^{1/2}\right), \quad (2)$$

where $\gamma_D^{eff} = (\gamma_I^2 + \gamma_D^2)^{1/2}$. Then, using a program which explicitly performs

TABLE II

N_2-Broadening Coefficients for Seven Lines of the ν_2 Band of NO_2

SIGMA	N'	K'_a	K'_c	N	K_a	K_c	J'-N	$\gamma^0_{NO_2-N_2}$ (cm^{-1} atm^{-1}) measured (this work)
835.806	12	5	7	11	4	8	$-\frac{1}{2}$	0.079 ± 0.009
836.648	13	5	9	12	4	8	$-\frac{1}{2}$	0.078 ± 0.004
836.761	13	5	9	12	4	8	$+\frac{1}{2}$	0.076 ± 0.005
837.488	14	5	9	13	4	10	$-\frac{1}{2}$	0.078 ± 0.007
837.594	14	5	9	13	4	10	$+\frac{1}{2}$	0.076 ± 0.006
839.166	16	5	11	15	4	12	$-\frac{1}{2}$	0.075 ± 0.007
839.259	16	5	11	15	4	12	$+\frac{1}{2}$	0.075 ± 0.005

the convolution of the absorption profile with the Gaussian instrumental function (characterized by γ_I), we refined the value of γ_L in order to obtain the best agreement between the calculated half-width at $I_o(I_{min}/I_o)^{1/2}$ and γ^{obs}. The N_2-broadening coefficients $\gamma^0_{NO_2-N_2}$ measured in this work are gathered in Table II. It appears that the calculated values[3] are, on the average, 12% lower than the measured values but a slight decrease in the widths with N is predicted in the calculations. It has not been possible to detect any noticeable difference between the widths of the two spin components for a given transition. Since our set of measured values is limited to a few lines, no general statement about the variation with the quantum numbers of the N_2-broadening coefficients can be made based on these data.

We have attempted to determine the self-broadening coefficients for the same lines using the method described above; but this determination is much more difficult because of the dimerization of NO_2 into N_2O_4. Under these conditions, the quantity actually deduced from the experiment is $\gamma_L = \gamma^0_{NO_2-NO_2}P_{NO_2} + \gamma^0_{NO_2-N_2O_4}P_{N_2O_4}$. Because the only measured pressure is the total pressure P, we used the equilibrium constant $k_p(T)$ (*8*) of the reaction $2NO_2 \leftrightarrows N_2O_4$ in order to obtain the values of (P_{NO_2}) and $(P_{N_2O_4})$ and thus any error on $k_p(T)$ would produce errors on these two pressures. Moreover, in our experiment, the maximum pressure of NO_2 (P_{NO_2}) was 30 Torr, corresponding to a maximum pressure of N_2O_4 ($P_{N_2O_4}$) of 10 Torr; consequently, if one assumes that $\gamma^0_{NO_2-NO_2}/\gamma^0_{NO_2-N_2O_4} \geq 3$, the contribution of $(\gamma^0_{NO_2-N_2O_4}P_{N_2O_4})$ to γ_L would be less than 10%; that is the order of magnitude of the experimental error on γ_L. For all these reasons it has only been possible to determine an average value $\gamma^0_{NO_2-NO_2} = 0.112 \pm 0.013$ cm^{-1} from the seven lines we have studied. Some experiments which have been performed at a temperature of 45°C, where the influence of N_2O_4 is negligible, confirm the value of $\gamma^0_{NO_2-NO_2}$ that we have found.

V. CALCULATION OF LINE INTENSITIES

The intensity of a line in (cm^{-1}/molecule) cm^{-2} can be written as

$$k^N_\sigma = \frac{8\pi^3}{3hc4\pi\epsilon_o}\left(1 - \exp\left(-\frac{hc\sigma}{kT}\right)\right)\frac{g_A}{Z(T)}\exp\left(-\frac{E_A}{kT}\right)R^B_A \qquad (3)$$

[3] G. D. T. Tejwani and E. S. Young, Iowa State University, Ames (unpublished report (1975)).

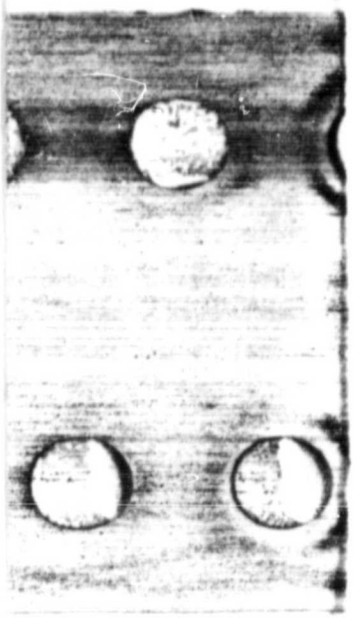

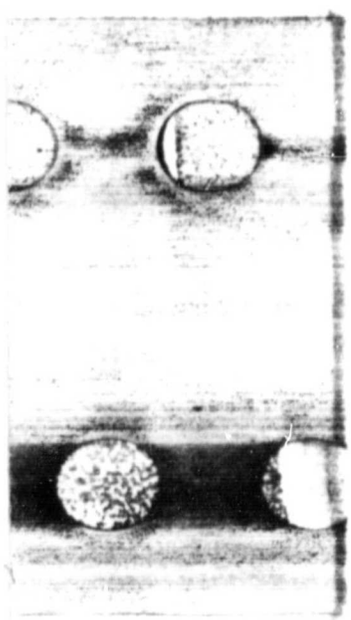

with

$$R_A^B = \sum_a \sum_b 3|\langle a|\mu_Z'|b\rangle|^2,$$

where

—A and B are respectively the lower and upper levels of the transition,
—$\sigma = (E_B - E_A)/hc$ is the wavenumber of the transition,
—$Z(T)$ is the partition function at the temperature T,
—g_A is the degeneracy due to the nuclear spin of the level A,
— $|a\rangle$ and $|b\rangle$ represent single states corresponding to the M_J degeneracy of the levels A and B.

To calculate the vibration–rotation energies (5) we have used a transformed Hamiltonian and determined its eigenstates $|v_1v_2v_3NK_aK_c\rangle$. For this reason, although the transformed dipole moment μ_Z' is more complicated than the non-transformed dipole moment μ_Z, we calculated the matrix elements of μ_Z' instead of those of μ_Z.

For NO_2, the single states $|a\rangle$ and $|b\rangle$ are the $|v_1v_2v_3NK_aK_cSJM_J\rangle$ states which can be expanded as

$$|v_1v_2v_3NK_aK_cSJM_J\rangle = \sum_{M_S+M_N=M_J} \langle NM_NSM_S|JM_J\rangle\,|v_1v_2v_3NK_aK_cM_N\rangle\,|SM_S\rangle. \quad (4)$$

From

$$R_B^A = 3\sum_{M_J} |\langle v_1v_2v_3NK_aK_cSJM_J|\mu_Z'|v_1'v_2'v_3'N'K_a'K_c'SJ'M_J\rangle|^2 \quad (5)$$

after some calculations, one obtains

$$R_A^B = (2J+1)(2J'+1)\begin{Bmatrix} J' & 1 & J \\ N & S & N' \end{Bmatrix}^2 |\langle v_1v_2v_3NK_aK_c|\mu_Z'|v_1'v_2'v_3'N'K_a'K_c'\rangle|^2, \quad (6)$$

where $\{\ \}$ represents the usual $6j$ coefficient.

Under these conditions, the transition strength R_A^B is the product of the spin-free transition strength $|\langle v_1v_2v_3NK_aK_c|\mu_Z'|v_1'v_2'v_3'N'K_a'K_c'\rangle|^2$ times the relative intensity $g(N, J, N', J')$ of the spin–rotation components (allowed or forbidden). Using the relation

$$\sum_\alpha (2\alpha+1)\begin{Bmatrix} a & b & \alpha \\ c & d & f \end{Bmatrix}\begin{Bmatrix} a & b & \alpha \\ c & d & g \end{Bmatrix} = \frac{1}{2f+1}\delta_{fg}, \quad (7)$$

it is easy to deduce that $\sum_{J,J'} g(N, J, N', J') = 2S + 1$; consequently, for a spin 1/2, one has $\sum_{J,J'} g(N, J, N', J') = 2$. The different values of the coefficients $g(N, J, N', J')$ for the different possible transitions are gathered in Table III.

To evaluate the matrix element of μ_Z', we will follow the general theory developed in Ref. (*11*) and we recall here only the relevant notations and formulas.

The wavefunctions $|v_1v_2v_3NK_aK_c\rangle$ have been obtained as a byproduct of the diagonalization of Watson's Hamiltonian for the (000) and the (010) vibrational states (*5*). One has

$$|v_1v_2v_3NK_aK_c\rangle = |v\rangle \sum_K C_K^\Gamma |NK\gamma\rangle$$

TABLE III

Relative Intensity $g(N, J, N', J')$ of the Spin-Rotation Components

N'	Spin component	J'	J	$G(N, J, N', J')$
$N' = N - 1$	$F_1' - F_1$	$J' = N' + \frac{1}{2}$	$J = N + \frac{1}{2}$	$\frac{2(N+1)}{2N+1}$
	$F_2' - F_2$	$J' = N' - \frac{1}{2}$	$J = N - \frac{1}{2}$	$\frac{2(N-1)}{2N-1}$
	$F_1' - F_2$	$J' = N' + \frac{1}{2}$	$J = N - \frac{1}{2}$	$\frac{2}{(2N-1)(2N+1)}$
$N' = N$	$F_1' - F_1$	$J' = N' + \frac{1}{2}$	$J = N + \frac{1}{2}$	$\frac{2N(2N+3)}{(2N+1)^2}$
	$F_2' - F_2$	$J' = N' - \frac{1}{2}$	$J = N - \frac{1}{2}$	$\frac{2(N+1)(2N-1)}{(2N+1)^2}$
	$F_2' - F_1$	$J' = N' - \frac{1}{2}$	$J = N + \frac{1}{2}$	
	$F_1' - F_2$	$J' = N' + \frac{1}{2}$	$J = N - \frac{1}{2}$	$\frac{2}{(2N+1)^2}$
$N' = N + 1$	$F_1' - F_1$	$J' = N' + \frac{1}{2}$	$J = N + \frac{1}{2}$	$\frac{2(N+2)}{2N+3}$
	$F_2' - F_2$	$J' = N' - \frac{1}{2}$	$J = N - \frac{1}{2}$	$\frac{2N}{2N+1}$
	$F_2' - F_1$	$J' = N' - \frac{1}{2}$	$J = N + \frac{1}{2}$	$\frac{2}{(2N+1)(2N+3)}$

with

$$v = 0 \text{ for } (000), \qquad v = 1 \text{ for } (010), \tag{8}$$

where the rotational functions $|NK\gamma\rangle$ are the usual Wang functions. The general form of the transformed dipole moment operator is

$$\mu_Z' = \sum_{v,v'} |v\rangle^{vv'}\mu_Z'\langle v'| \tag{9}$$

and its relevant part to be used for the ν_2 band is the transformed transition moment operator ${}^{01}\mu_Z'$ with

$${}^{01}\mu_Z' = {}^{01}\mu_1'\varphi_x + {}^{01}\mu_4'\{i\varphi_y, J_z\} + {}^{01}\mu_5'\{\varphi_z, iJ_y\} + \cdots, \tag{10}$$

where the transition moment constants ${}^{01}\mu_j'$ are to be determined from measured intensities. In Eq. (10), we have kept only terms which proved to be significant in the least-squares fit but the general form of ${}^{vv'}\mu_Z'$ as well as the matrix elements of the rotational operators involved in its expansion can be found in Ref. (*11*).

TABLE IV

Constants Involved in the Expansion of the Transformed Transition Moment Operator of the ν_2 Band of NO_2

Operator	Constant	Value in D
φ_x	$^{01}\mu_1'$	$(-0.427_2 \pm 0.026) \times 10^{-1}$
$\{i\varphi_y, J_z\}$	$^{01}\mu_4'$	$(0.40_3 \pm 0.25) \times 10^{-3}$
$\{i\varphi_z, iJ_y\}$	$^{01}\mu_5'$	$(0.108_3 \pm 0.028) \times 10^{-3}$

The errors quoted are 95% statistical confidence intervals.

Using the 30 measured intensities as input parameters in a least-squares fit, we were able to deduce the values of the $^{01}\mu_j'$'s quoted in Table IV. These constants were then used to compute the whole spectrum of the ν_2 band of NO_2 leading to a total band intensity (i.e., the sum of individual line strengths) of $S_r(\nu_2) = 0.542 \times 10^{-18}$ cm^{-1}/molecule cm^{-2} at 296 K.

In fact, since the intensity of a line is proportional to the square of the matrix element of the dipole moment, from the least-squares fit of the measured intensities it is only possible to determine the relative signs of the coefficients $^{01}\mu_j'$. The choice actually made is discussed in the next section.

VI. THEORETICAL DISCUSSION

The theory of the contact transformation used to obtain the transformed dipole moment has been developed by Legay (*12*). For molecules with a permanent dipole moment, one has, to the second order of approximation,

$$^{01}\mu_1' = \frac{1}{(2)^{1/2}}\,{}^{2}\mu_x,$$

$$^{01}\mu_4' = 2\cos\gamma\left(\frac{A}{\omega_2}\right)^{3/2}{}^{0}\mu_x,$$

$$^{01}\mu_5' = \frac{C\zeta_{23}^{\nu}(2\omega_2\omega_3)^{1/2}}{\omega_3^2 - \omega_2^2}\,{}^{3}\mu_z + 2\zeta_{13}^{\nu}\left(\frac{C}{\omega_2}\right)^{3/2}{}^{0}\mu_x. \tag{11}$$

Using the equilibrium geometry and force constants of Ref. (*13*) (leading to $\cos\gamma = 0.767$ and $\sin\gamma = 0.642$) one obtains

$$^{01}\mu_1' = \frac{1}{(2)^{1/2}}\,{}^{2}\mu_x, \tag{12}$$

$$^{01}\mu_4' = 0.1648 \times 10^{-2}\,{}^{0}\mu_x, \tag{13}$$

$$^{01}\mu_5' = -0.2656 \times 10^{-3}\,{}^{3}\mu_z + 0.1151 \times 10^{-4}\,{}^{0}\mu_x. \tag{14}$$

Assuming that the sign of $^{0}\mu_x$ corresponds, as shown by ab initio calculations (*14*),

to the polarity $N^+-O_2^-$ and that its value is not very different from the ground-state dipole moment $\mu_z(000)$ given in Ref. (*15*), we can take the value ${}^0\mu_z = 0.316$ D.

Then, Eq. (13) implies that ${}^{01}\mu_4$ must be positive. As we already said since the relative signs of the constant ${}^{01}\mu_j'$ are determined from the least-squares fit, the signs of these constants with respect to the sign of ${}^0\mu_z$ are then fixed.

Moreover, from Eq. (13) we obtain for ${}^{01}\mu_4'$ the calculated value $0.57_4 \times 10^{-3}$ D, which compares well with the value $(0.403 \pm 0.25) \times 10^{-3}$ D we have obtained. Using Eq. (12), one gets

$$^2\mu_z = (-0.604_1 \pm 0.037) \times 10^{-1} \text{ D}.$$

Finally, Eq. (14) allows us to deduce from ${}^{01}\mu_5'$ the value

$$^3\mu_z = -0.39_4 \pm 0.11 \text{ D}.$$

This value is to be compared to the value of ${}^3\mu_z$ deduced from the intensity of the ν_3 band. From the two values 1430 ± 300 cm^{-2} atm^{-1} at 40°C (*2*) and 2059 cm^{-2} atm^{-1} at 25°C (*1*), assuming that the ν_3 band can be treated in the rigid rotor approximation, one obtains

$$^3\mu_z = -0.411 \pm 0.043 \text{ D}$$

and

$$^3\mu_z = -0.483 \text{ D}.$$

It is of interest to note that the measurements of Goldman *et al.* (2) provide a better estimate of the ν_3 band intensity because they lead to a value of ${}^3\mu_z$ comparable to the present work.

ACKNOWLEDGMENTS

One of us (K.N.R.) expresses his gratitude to the National Aeronautics and Space Administration for support of this research.

RECEIVED: November 11, 1980

REFERENCES

1. A. GUELTMAN, *J. Quant. Spectrosc. Radiat. Transfer* **2**, 1–15 (1962).
2. A. GOLDMAN, F. S. BONOMO, W. J. WILLIAMS, AND D. G. MURCRAY, *J. Quant. Spectrosc. Radiat. Transfer* **15**, 107–112 (1975).
3. J. H. SHAFFER AND C. YOUNG, *Appl. Opt.* **15**, 2551–2553 (1976).
4. R. A. TOTH AND R. H. HUNT, *J. Mol. Spectrosc.* **79**, 182–202 (1980).
5. J.-M. FLAUD, C. CAMY-PEYRET, V. MALATHY DEVI, PALASH P. DAS, AND K. NARAHARI RAO, *J. Mol. Spectrosc.* **84**, 234–242 (1980).
6. S. P. REDDY, W. IVANCIC, V. MALATHY DEVI, A. BALACCI, K. NARAHARI RAO, A. W. MANTZ, AND R. S. ENG, *Appl. Opt.* **18**, 1350–1354 (1979).
7. P. P. DAS, V. MALATHY DEVI, AND K. NARAHARI RAO, *J. Mol. Spectrosc.* **84**, 305–318 (1980).
8. K. SCHOFIELD, *J. Phys. Chem. Ref. Data* **2**, 25–84 (1973).
9. P. P. DAS, Ph.D. dissertation, Ohio State University, 1980.
10. J. J. OLIVERO AND R. L. LONGBOTHUM, *J. Quant. Spectrosc. Radiat. Transfer* **17**, 233–236 (1977).
11. J.-M. FLAUD AND C. CAMY-PEYRET, *J. Mol. Spectrosc.* **55**, 278–310 (1975).
12. F. LEGAY, *Cah. Phys.* **12**, 416–436 (1958).
13. G. K. SPEIRS AND V. SPIRKO, *J. Mol. Spectrosc.* **56**, 104–123 (1975).
14. G. D. GILLIPSIE, A. V. KHAN, A. C. WAHL, R. P. HOSTENY, AND M. KRAUSS, *J. Chem. Phys.* **63**, 3425–3444 (1975).
15. J. A. HODGESON, E. R. SILBERT, AND R. F. CURL, *J. Phys. Chem.* **67**, 2833–2835 (1963).

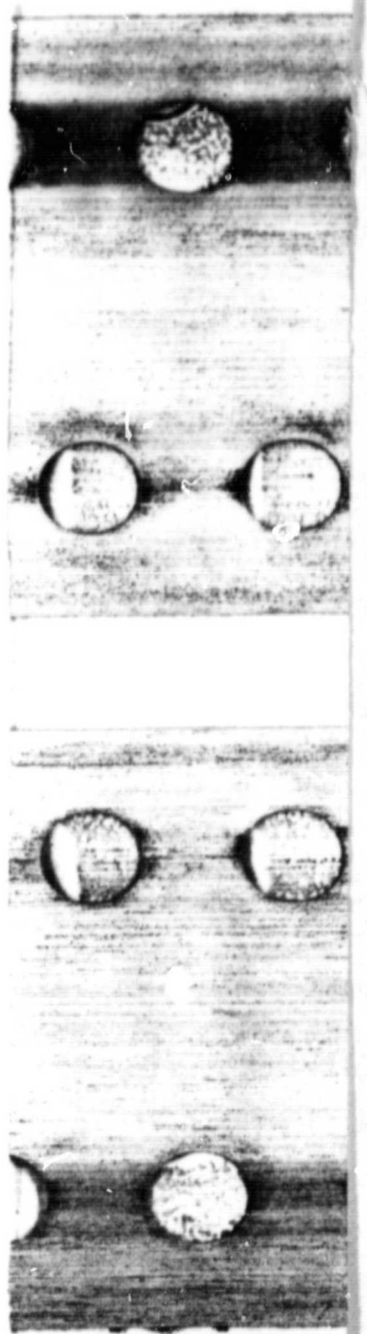

JOURNAL OF MOLECULAR SPECTROSCOPY 84, 234–242 (1980)

Diode Laser Spectra of the ν_2 Band of $^{14}N^{16}O_2$: The (010) State of NO_2

J.-M. FLAUD AND C. CAMY-PEYRET

Laboratoire de Physique Moleculaire et d'Optique Atmospherique,[1] CNRS, Bat. 221, Campus d'Orsay, 91405 Orsay Cedex, France

AND

V. MALATHY DEVI,* PALASH P. DAS,† AND K. NARAHARI RAO[2]

Department of Physics, The Ohio State University, Columbus, Ohio 43210

Diode laser spectra of the ν_2 band of NO_2 are recorded and analyzed. Due to the very high resolution (0.002 cm^{-1}), the Q branches are compietely resolved. Although the whole ν_2 band is not completely covered, the quality of the spectra led to an improved set of rotational and spin–rotation constants. The band center is found to be $\nu_2 = 749.6541 \pm 0.0012$ cm^{-1}.

INTRODUCTION

The importance of nitrogen dioxide in the photochemistry of the atmosphere has stimulated many high-resolution studies of the infrared spectra of this molecule. Moreover, a good knowledge of the lowest vibrorotational levels of the electronic ground state is very helpful to assign visible fluorescence or absorption spectra involving higher vibronic states.

This paper reports the analysis of diode laser spectra of the ν_2 band of $^{14}N^{16}O_2$. Previous studies of this band using spectra recorded on grating spectrometers (resolution $\simeq 0.040$ cm^{-1}) have been performed by Hurlock *et al.* (*1*) and by Cabana *et al.* (*2*). The resolution of the diode laser spectra ($\simeq 0.002$ cm^{-1}) allows a much better analysis, particularly in the Q branches, which are now completely resolved. However, it has not been possible with the diode used in this study to cover continuously the whole extent of the ν_2 band. Nevertheless, the positions of about 380 lines were precisely determined and from them, improved band center, rotational, and spin–rotation constants for the (010) vibrational state were obtained.

EXPERIMENTAL DETAILS

The experimental setup used in this study has been described elsewhere (*3*). Two diode lasers operating between 687–720 and 820–865 cm^{-1} were used. Only

[1] Financial support from the University Pierre and Marie Curie (Paris) is acknowledged.

[2] The support extended this research by the National Aeronautics and Space Administration is gratefully acknowledged.

Present address: *NOAA-NESS, FB4, S/RE21, Washington, D. C. 20233 and †Tachisto Inc., 13 Highland Circle, Needham, Mass. 02194.

0022-2852/80/110234-05$02.00/0

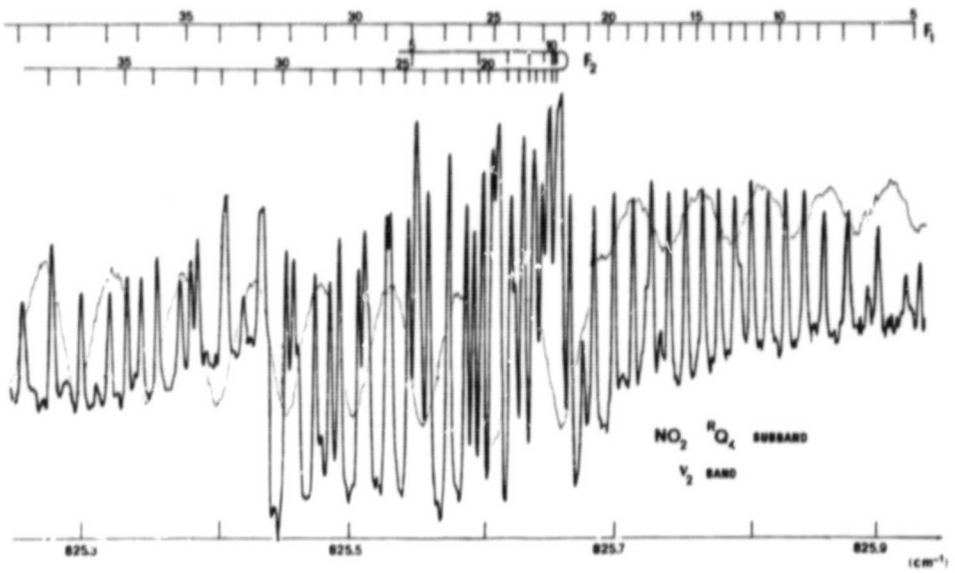

FIG. 1. Example of a resolved Q branch of $^{14}N^{16}O_2$.

those modes were scanned where suitable calibration lines were available. In the 14-μm region ν_2 and $\nu_1 - \nu_2$ band lines (*4*) of $^{12}C^{16}O_2$, ν_2 band lines of $H^{12}C^{14}N$ (*3*) and in the 12-μm region ν_1 band lines of OCS (*5*) were used for determining the absolute positions of the lines. A commercial sample of NO_2, at pressures ranging from 0.5 to 1 Torr, was contained in a multipass cell with a total path length of 12 m. Some impurity lines, especially CO_2 and HNO_3, were observed. A 33-cm-long air-spaced etalon with 0.015-cm^{-1} fringe spacing was used in the 14-μm region while a 2.54-cm (1-in)-long germanium etalon with 0.049-cm^{-1} fringe separation was employed in the 12-μm region for producing wavenumber scales on the spectra. The relative accuracy of our measurements was estimated to be about ± 0.0005 cm^{-1} and the absolute accuracy is believed to be about ± 0.002 cm^{-1}.

To show the quality of the spectra, we present a reproduction of the $^RQ_4$ branch around 825.500 cm^{-1} (Fig. 1). On the high wavenumber edge of this region, the lines corresponding to the F_1 component appear clearly whereas around 825.650 cm^{-1} they are superimposed on the lines corresponding to the F_2 component. On the low wavenumber edge of the region, the F_1 and F_2 series are again relatively well separated. At high K_a, near the origins of the Q branches the spin splitting is expected to be very large. This can be clearly seen in the spectrum of $^RQ_5$ displayed in Fig. 2. For example, for $N = 20$, the splitting between the F_1 and F_2 components is as much as ~ 0.1 cm^{-1}. The observation of such splittings helped us to determine the spin–rotation interaction constants more precisely than before.

DATA ANALYSIS AND RESULTS

NO_2 is an asymmetric top molecule belonging to the C_{2v} group with the complication that the spin–rotation interaction must be considered. Under these

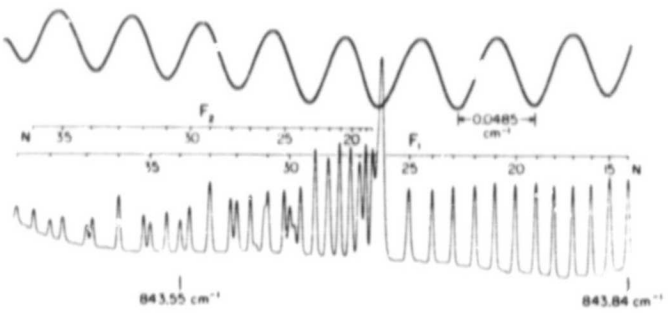

FIG. 2. $^RQ_5$ subband of ν_2 of $^{14}N^{16}O_2$.

conditions, the energy of a level can be expressed as the sum of a rotational energy E_r and of a contribution due to the spin–rotation interaction. Treating this interaction up to second order of perturbation (*2*, *6*, *7*) one obtains:

—For $J = N + 1/2$

$$F_1 = \frac{E_r}{hc} + \frac{1}{2(N+1)}\left[(\epsilon_{aa} - \bar{\epsilon})K_a^2 + \bar{\epsilon}N(N+1) + \gamma\frac{(\epsilon_{bb} - \epsilon_{cc})}{4}\delta_{1,K_a}N(N+1) + \eta_{aaaa}K_a^4 - \frac{(\epsilon_{aa} - \bar{\epsilon})^2}{4\bar{B}}K_a^2\left(1 - \frac{K_a^2}{(N+1)^2}\right)\right],$$

—For $J = N - 1/2$

$$F_2 = \frac{E_r}{hc} - \frac{1}{2N}\left[(\epsilon_{aa} - \bar{\epsilon})K_a^2 + \bar{\epsilon}N(N+1) + \gamma\frac{(\epsilon_{bb} - \epsilon_{cc})}{4}\delta_{1,K_a}N(N+1) + \eta_{aaaa}K_a^4 - \frac{(\epsilon_{aa} - \bar{\epsilon})^2}{4\bar{B}}K_a^2\left(1 - \frac{K_a^2}{N^2}\right)\right],$$

In these equations $\bar{\epsilon} = (1/2)(\epsilon_{bb} + \epsilon_{cc})$, $\bar{B} = (1/2)(B + C)$, and

$\gamma = -1$ for N odd,

$\gamma = +1$ for N even.

The rotational energy E_r is calculated by diagonalizing a Watson-type Hamiltonian (*8*)

$$H_{vv} = \frac{E_v}{hc} + [A^v - (1/2)(B^v + C^v)]P_z^2 + (1/2)(B^v + C^v)P^2 + (1/2)(B^v - C^v)P_{xy}^2 - \Delta_K^v P_z^4 - \Delta_{NK}^v P_z^2P^2 - \Delta_N^v(P^2)^2 - \delta_K^v\{P_z^2, P_{xy}^2\} - 2\delta_N^v P_{xy}^2P^2 + H_K^v P_z^6 + H_{KN}^v P_z^4P^2 + H_{NK}^v P_z^2(P^2)^2 + H_N^v(P^2)^3 + h_K^v\{P_z^4, P_{xy}^2\} + h_{NK}^v\{P_z^2, P_{xy}^2\}P^2 + 2h_N^v P_{xy}^2(P^2)^2 + L_K^v P_z^8,$$

where $P_{xy}^2 = P_x^2 - P_y^2$, $\{A,B\} = AB + BA$, and $(P_x \mp iP_y)|NK\rangle = (N(N+1) - K(K \pm 1))^{1/2}|NK \pm 1\rangle$.

TABLE I

Rotational Constants (in cm^{-1}) of $^{14}N^{16}O_2$

	(000)[a]	(010)
E_v		$749.654_1 \pm 0.0012$[b]
A^v	8.0023657	$8.373661_1 \pm 0.00010$
B^v	0.43370797	$0.4336271_5 \pm 0.0000067$
C^v	0.41044536	$0.4095770_5 \pm 0.0000050$
Δ_K^v	0.26881×10^{-2}	$(0.34139_5 \pm 0.00042) \times 10^{-2}$
Δ_{NK}^v	-0.19499×10^{-4}	$(-0.2160_5 \pm 0.0010) \times 10^{-4}$
Δ_N^v	0.20068×10^{-6}	$(0.3071_6 \pm 0.0028) \times 10^{-6}$
δ_K^v	0.413×10^{-5}	$(0.46_3 \pm 0.40) \times 10^{-5}$
δ_N^v	0.3179×10^{-7}	$(0.308_2 \pm 0.022) \times 10^{-7}$
H_K^v	0.2946×10^{-5}	$(0.3948_2 \pm 0.0053) \times 10^{-5}$
H_{KN}^v	-0.197×10^{-7}	$(-0.322_0 \pm 0.022) \times 10^{-7}$
H_{NK}^v	-0.370×10^{-9}	
H_N^v	0.52×10^{-12}	0.53×10^{-12}[c]
h_K^v	-0.78×10^{-7}	
h_N^v	0.22×10^{-12}	
L_K^v	-0.355×10^{-8}	

[a] Ground state constants taken from Lafferty and Sams (9).

[b] Uncertainties cited are one standard deviation.

[c] Fixed to the ground state value.

As a starting point in the analysis of the diode laser spectra, we computed a theoretical spectrum of the ν_2 band of NO_2 using the rotational and spin–rotation constants of the (010) and (000) states given in Refs. (*2*, *9*, *10*). With this calculation, we assigned the most intense lines lying in the available spectral intervals. The upper-state energies deduced from these transitions and from the ground-state energy levels calculated with the constants of Ref. (*9*) (see Tables I and II) were introduced in a nonlinear least-squares fit to obtain refined molecular constants for the (010) vibrational state. We repeated this procedure up to the point where all the NO_2 lines were assigned and the set of constants determined from the final fit is given in Table I for the rotational constants and in Table II for the spin–rotation

TABLE II

Spin–Rotation Constants (in cm^{-1}) of $^{14}N^{16}O_2$

	(000)	(010)	
$\epsilon_{aa} - \frac{1}{2}(\epsilon_{bb} + \epsilon_{cc})$	0.181644^a	0.19930_8	$\pm 0.00070^c$
$\frac{1}{2}(\epsilon_{bb} + \epsilon_{cc})$	-0.0014608^a	-0.0015193_4	± 0.000011
$\epsilon_{bb} - \epsilon_{cc}$	0.0034319^a	0.00384_0	± 0.00022
η_{aaaa}	$-0.1^{\cdot}8 \times 10^{-3}$ [b]	$(-0.2001_4$	$\pm 0.017) \times 10^{-3}$

[a] Taken from microwave work of Lees et al. [10].

[b] Taken from Cabana et al. [2].

[c] Uncertainties cited are one standard deviation.

constants. An improved band center was obtained: $\nu_2 = 749.6541 \pm 0.0012\ cm^{-1}$. With this final set of constants, we calculated the whole spectrum of the ν_2 band and Table III presents the experimental and calculated wavenumbers together with the assignments of the lines.

DISCUSSION

A few comments are to be made about the assignment problem. First, only stretches of the whole band were recorded with the diode laser spectrometer. Except for the $^RQ_4$ subband which is completely covered (see Fig. 1), only parts of the $^PQ_5$, $^PQ_4$, $^PQ_3$ subbands as well as parts of the $^RQ_5$ and $^RQ_6$ subbands were available together with less crowded intervals. Second, some interferences with impurities (particularly HNO_3 and CO_2) complicated the assignment. However, because a good self-consistency in the calibration of wavenumbers was achieved, a very satisfactory fit was finally obtained (the unweighted standard deviation of $0.0018\ cm^{-1}$ is to be compared with the estimated precision of the position of the lines, i.e., $0.002\ cm^{-1}$). From the set of energy levels of (010) deduced in this work, it was not possible to determine the value of the octic constant L_K. Indeed the highest K'_a value reached in our study is 7. However, our calculations reproduce very satisfactorily the positions of the $^RQ_7$ ($K'_a = 8$) and $^RQ_8$ ($K'_a = 9$) subbands observed at lower resolution in Ref. (*1*). Indeed, in the $^RQ_7$ subband, the calculated intensities peak for $J = 17, 18, 19$ at $880.367\ cm^{-1}$ in the F_1 component and at 880.199 in the F_2 component and these calculated positions compare well with the maxima observed in Ref. (*1*) at 880.339 and 880.186 cm^{-1}. The same agreement was obtained for the $^RQ_8$ subband: calculated maxima ($J = 18, 19, 20$) at 898.680 and 898.496 cm^{-1} are to be compared with the observed ones at 898.604 and 898.455 cm^{-1}.

It is important to emphasize that both the rotational and spin–rotation constants of the (010) vibrational state are highly dependent on the parameters assumed

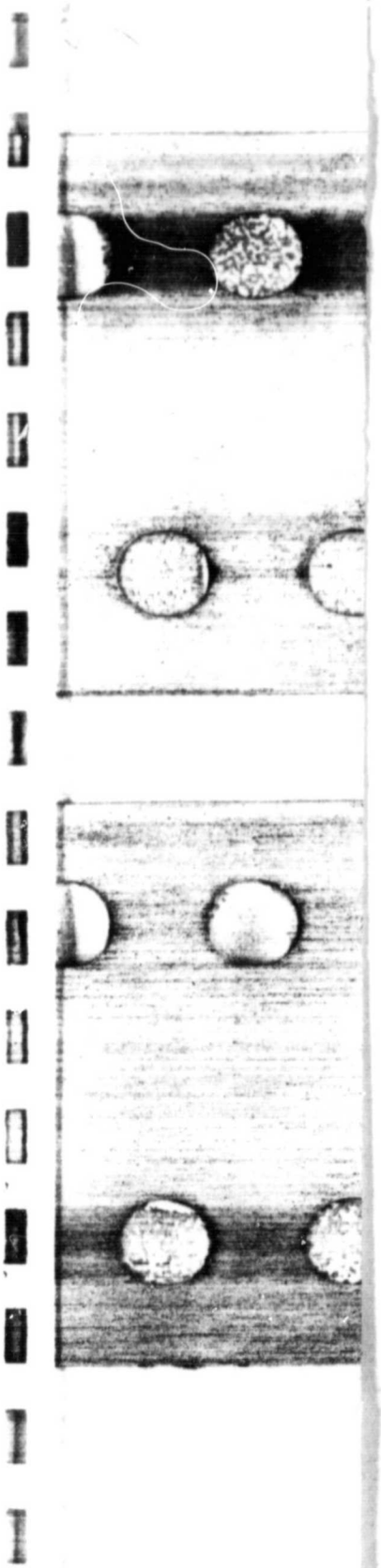

TABLE III

List of the Observed ν_2 Lines (in vac.-cm^{-1}) of $^{14}N^{16}O_2$

σ_{obs}	σ_{calc}	N'	K'_a	K'_c	N	K_a	K_c	J-N	σ_{obs}	σ_{calc}	N'	K'_a	K'_c	N	K_a	K_c	J-N
687.3857	.387	37	4	34	35	5	33	+1/2	700.3829	.384	7	3	5	7	4	4	-1/2
.3936	.395	38	4	34	38	5	33	-1/2	.4056	.406	6	3	3	6	4	2	-1/2
.4188	.421	37	4	34	37	5	33	-1/2	.4341	.435	5	3	3	5	4	2	-1/2
.4260	.428	36	4	32	36	5	31	+1/2	.4781	.477	4	3	1	4	4	0	-1/2
.4533	.455	35	4	32	35	5	31	+1/2	.6399	.640	15	4	12	14	5	9	+1/2
.4601	.463	36	4	32	36	5	31	-1/2	.6651	.665	14	2	12	15	3	13	+1/2
.4883	.491	35	4	32	35	5	31	-1/2	.7089	.709	14	2	12	15	3	13	-1/2
.4905	.493	34	4	30	34	5	29	+1/2	.7386	.739	15	4	12	14	5	9	-1/2
.5189	.521	33	4	30	33	5	29	+1/2									
.5237	.526	14	3	11	15	4	12	+1/2	706.4127	.414	22	4	18	21	5	17	+1/2
.5260	.529	34	4	30	34	5	29	-1/2	.4292	.432	36	5	31	35	6	30	+1/2
.5547	.556	32	4	28	32	5	27	+1/2	.4740	.477	36	5	31	35	6	30	-1/2
.5557	.559	33	4	30	33	5	29	-1/2	.4783	.479	22	4	18	21	5	17	-1/2
.5827	.583	14	3	11	15	4	12	-1/2	.5773[b]	.575	7	2	6	8	3	5	+1/2
	.585	31	4	28	31	5	27	+1/2		.577	48	0	48	49	1	49	-1/2
.5936	.595	32	4	28	32	5	27	-1/2	.6156	.615	48	0	48	49	1	49	+1/2
.6178	.618	30	4	26	30	5	25	+1/2	.6516	.653	7	2	6	8	3	5	-1/2
.6246	.625	31	4	28	31	5	27	-1/2	.9796	.980	8	3	5	7	4	4	+1/2
.6466	.646	29	4	26	29	5	25	+1/2	707.1472	.148	8	3	5	7	4	4	-1/2
.6521	.654	13	5	9	12	6	6	+1/2									
.6574	.659	30	4	26	30	5	25	-1/2	712.7576[b]	.759	25	2	24	25	3	23	+1/2
.6757	.677	28	4	24	28	5	23	+1/2	.7760[b]	.782	40	0	40	41	1	41	+1/2
.6870	.689	29	4	26	29	5	25	-1/2	.7907	.790	25	2	24	25	3	23	-1/2
.7041	.705	27	4	24	27	5	23	+1/2	.8364	.838	15	3	13	14	4	10	+1/2
.7194	.720	28	4	24	28	5	23	-1/2	.8798	.884	23	2	22	23	3	21	+1/2
.7323	.733	26	4	22	26	5	21	+1/2	.9177	.916	15	3	13	14	4	10	-1/2
.7484	.750	27	4	24	27	5	23	-1/2	.9195[b]	.917	23	2	22	23	3	21	-1/2
.7590	.760	25	4	22	25	5	21	+1/2	.9428[b]	.945	30	4	26	29	5	25	+1/2
									.9876	.989	21	2	20	21	3	19	+1/2
699.8218	.819	31	3	29	31	4	28	+1/2	.9908	.992	30	4	26	29	5	25	-1/2
.8530	.853	31	3	29	31	4	28	-1/2	713.0226	.025	21	2	20	21	3	19	-1/2
.8784	.876	29	3	27	29	4	26	+1/2	.0762[b]	.077	19	2	18	19	3	17	+1/2
.8959	.894	34	3	31	34	4	30	+1/2	.1172[b]	.116	19	2	18	19	3	17	-1/2
	.891	36	3	33	36	4	32	+1/2	.1477	.148	17	2	16	17	3	15	+1/2
.9005	.902	38	3	35	38	4	34	+1/2		.141	18	1	17	19	2	18	+1/2
.9071	.908	32	3	29	32	4	28	+1/2		.146	18	1	17	19	2	18	-1/2
.9120	.912	29	3	27	29	4	26	-1/2	.1934	.192	17	2	16	17	3	15	-1/2
.9170	.917	14	4	10	13	5	9	-1/2	.2070	.205	15	2	14	15	3	13	+1/2
.9237	.923	34	3	31	34	4	30	-1/2	.2548	.255	15	2	14	15	3	13	-1/2
	.920	36	3	33	36	4	32	-1/2		.250	13	2	12	13	3	11	+1/2
.9311	.930	27	3	25	27	4	24	+1/2	.2840	.284	11	2	10	11	3	9	+1/2
	.930	30	3	27	30	4	26	+1/2	.2929[b]	.291	3	2	2	3	3	1	+1/2
	.930	38	3	35	38	4	34	-1/2	.3061[b]	.307	13	2	12	13	3	11	-1/2
	.929	40	3	37	40	4	36	+1/2		.307	9	2	8	9	3	7	+1/2
.9391	.940	32	3	29	32	4	28	-1/2	.3120	.311	4	2	2	4	3	1	+1/2
.9579	.955	40	3	37	40	4	36	-1/2	.3207	.320	12	2	10	12	3	9	+1/2
.9310	.958	28	3	25	28	4	24	+1/2		.319	7	2	6	7	3	5	+1/2
.9646	.964	30	3	27	30	4	26	-1/2		.318	5	2	4	5	3	3	+1/2
.9677	.967	27	3	25	27	4	24	-1/2	.3245	.324	10	2	8	10	3	7	+1/2
.9777	.975	42	3	39	42	4	38	+1/2		.325	6	2	4	6	3	3	+1/2
.9802	.979	25	3	23	25	4	22	+1/2	.3274	.327	14	2	12	14	3	11	+1/2
	.979	28	5	23	27	6	22	+1/2		.326	8	2	6	8	3	5	+1/2
.9922	.990	26	3	23	26	4	22	+1/2	.3423	.342	16	2	14	16	3	13	+1/2
.9943	.994	28	3	25	28	4	24	-1/2	.3498	.350	11	2	10	11	3	9	-1/2
700.0192	.019	25	3	23	25	4	22	-1/2	.3716	.371	18	2	16	18	3	15	+1/2
.0261	.025	23	3	21	23	4	20	+1/2	.3784	.380	14	2	12	14	3	11	-1/2
	.025	24	3	21	24	4	20	+1/2	.3822	.384	12	2	10	12	3	9	-1/2
.0284	.029	26	3	23	26	4	22	-1/2	.3868	.388	16	2	14	16	3	13	-1/2
.0356	.037	25	1	25	26	2	24	+1/2		.388	9	2	8	9	3	7	-1/2
	.033	42	1	41	43	2	42	-1/2	.3958	.397	10	2	8	10	3	7	-1/2
	.037	28	5	23	27	6	22	-1/2	.4110	.413	18	2	16	18	3	15	-1/2
.0600[b]	.061	22	3	19	22	4	18	+1/2	.4170	.417	8	2	6	8	3	5	-1/2
.0687	.068	21	3	19	21	4	18	+1/2	.4230	.419	20	2	18	20	3	17	+1/2
	.067	24	3	21	24	4	20	-1/2		.423	7	2	6	7	3	5	-1/2
	.069	23	3	21	23	4	20	-1/2	.4454	.445	6	2	4	6	3	3	-1/2
.0780	.079	25	1	25	26	2	24	-1/2	.4550	.457	20	2	18	20	3	17	-1/2
.0966	.096	20	3	17	20	4	16	+1/2	.4632	.463	5	2	4	5	3	3	-1/2
.1074	.106	22	3	19	22	4	18	-1/2	.4946	.492	22	2	20	22	3	19	+1/2
	.107	19	3	17	19	4	16	+1/2		.493	4	2	2	4	3	1	-1/2
.1163	.116	21	3	19	21	4	18	-1/2		.492	45	1	45	45	2	44	-1/2

Note. The different diode laser spectra are separated. The superscript b after an observed wavenumber means that the line is blended with an interfering line (CO_2, HNO_3). When several lines are assigned to the same observed line, they are listed in the order of decreasing intensity.

TABLE III—*Continued*

σ_{obs}	σ_{calc}	N' K'_a K'_c	N K_a K_c	J-N	σ_{obs}	σ_{calc}	N' K'_a K'_c	N K_a K_c	J-N
713.5219	.526	22 2 20	22 3 19	-1/2	825.5966	.595	26 5 21	26 4 22	+1/2
.5411	.541	3 2 2	3 3 1	-1/2	.6024	.601	21 5 17	21 4 18	-1/2
.5946	.592	24 2 22	24 3 21	+1/2		.599	6 5 1	6 4 2	-1/2
.6209	.624	24 2 22	24 3 21	-1/2		.602	40 3 37	39 2 38	-1/2
					.6101	.612	20 5 15	20 4 16	-1/2
717.0916	.081	34 0 34	35 1 35	-1/2		.608	21 4 18	20 3 17	+1/2
.1009	.107	34 0 34	35 1 35	+1/2	.6150	.614	25 5 21	25 4 22	+1/2
.1928	.192	12 1 11	13 2 12	+1/2	.6247	.622	19 5 15	19 4 16	-1/2
.2136	.213	12 1 11	13 2 12	-1/2		.624	7 5 3	7 4 4	-1/2
						.621	40 3 37	39 2 38	+1/2
717.8002	.799	21 3 19	20 4 16	+1/2	.6332	.631	18 5 13	18 4 14	-1/2
.8448	.849	36 4 32	35 5 31	-1/2		.632	24 5 19	24 4 20	+1/2
.8541	.854	21 3 19	20 4 16	-1/2	.6422	.639	17 5 13	17 4 14	-1/2
	.861	39 1 39	40 0 40	-1/2		.639	8 5 3	8 4 4	-1/2
.9008	.901	37 1 37	32 2 36	+1/2	.6486	.645	16 5 11	16 4 12	-1/2
.9497	.952	37 1 37	37 2 36	-1/2	.6528	.651	15 5 11	15 4 12	-1/2
						.649	23 5 19	23 4 20	+1/2
719.4295	.428	38 4 34	37 5 33	+1/2		.649	9 5 5	9 4 6	-1/2
.4450	.444	23 3 21	22 4 18	+1/2	.6589	.655	14 5 9	14 4 10	-1/2
.4656	.465	38 4 34	37 5 33	-1/2		.655	10 5 5	10 4 6	-1/2
.4946	.494	23 3 21	22 4 18	-1/2	.6611	.658	13 5 9	13 4 10	-1/2
.8151	.817	33 1 33	33 2 32	+1/2		.658	11 5 7	11 4 8	-1/2
.8492	.844	30 0 30	31 1 31	-1/2		.659	12 5 7	12 4 8	-1/2
	.851	37 1 37	38 0 38	+1/2	.6693	.665	22 5 17	22 4 18	+1/2
.8614[b]	.866	30 0 30	31 1 31	+1/2	.6849	.681	21 5 17	21 4 18	+1/2
.8646	.865	33 1 33	32 2 32	-1/2	.6970	.696	20 5 15	20 4 16	+1/2
					.7112	.711	19 5 15	19 4 16	+1/2
824.7863	.789	20 4 16	19 3 17	+1/2	.7248	.725	18 5 13	18 4 14	+1/2
825.0677	.071	21 6 16	22 5 17	-1/2	.7377	.738	17 5 13	17 4 14	+1/2
.0921	.088	42 5 37	42 4 38	-1/2	.7507	.751	16 5 11	16 4 12	+1/2
.1091	.109	43 5 39	43 4 40	+1/2	.7628	.764	15 5 11	15 4 12	+1/2
.1276	.126	42 5 37	42 4 38	+1/2	.7753	.776	14 5 9	14 4 10	+1/2
.1509[b]	.146	41 5 37	41 4 38	-1/2	.7883	.789	13 5 9	13 4 10	+1/2
.1694	.166	40 5 35	40 4 36	-1/2	.8001	.801	12 5 7	12 4 8	+1/2
.1792	.181	21 6 16	22 5 17	+1/2	.8126	.814	11 5 7	11 4 8	+1/2
.1864	.185	41 5 37	41 4 38	+1/2	.8263	.827	10 5 5	10 4 6	+1/2
.2079	.206	40 5 35	40 4 36	+1/2	.8418	.842	9 5 5	9 4 6	+1/2
.2170	.214	39 5 35	39 4 36	-1/2	.8577	.858	8 5 3	8 4 4	+1/2
.2370	.236	38 5 33	38 4 34	-1/2	.8774	.877	7 5 3	7 4 4	+1/2
.2575	.256	39 5 35	39 4 36	+1/2	.9007	.901	6 5 1	6 4 2	+1/2
.2788	.277	37 5 33	37 4 34	-1/2	.9225	.922	20 6 14	21 5 17	-1/2
	.279	38 5 33	38 4 34	+1/2	.9317	.933	5 5 1	5 4 2	+1/2
.3002	.300	36 5 31	36 4 32	-1/2	826.0396	.038	20 6 14	21 5 17	+1/2
.3213	.321	37 5 33	37 4 34	+1/2	829.3173[b]	.316	16 6 10	17 5 13	-1/2
.3348	.334	35 5 31	35 4 32	-1/2	.4665[b]	.465	16 6 10	17 5 13	+1/2
.3452	.345	36 5 31	36 4 32	+1/2					
.3566	.357	34 5 29	34 4 30	-1/2	830.1059	.105	5 5 1	4 4 0	+1/2
.3808	.381	35 5 31	35 4 32	+1/2	.1624	.162	15 6 10	16 5 11	-1/2
.3861	.387	33 5 29	33 4 30	-1/2	.3234	.322	15 6 10	16 5 11	+1/2
.4056	.405	34 5 29	34 4 30	+1/2	.4741	.472	27 4 24	26 3 23	-1/2
.4073	.408	32 5 27	32 4 28	-1/2	.5158	.515	27 4 24	26 3 23	+1/2
.4342	.434	31 5 27	31 4 28	-1/2					
.4363	.436	33 5 29	33 4 30	+1/2	830.9327	.934	6 5 1	5 4 2	+1/2
.4543	.454	30 5 25	30 4 26	-1/2	831.0068	.006	14 6 8	15 5 11	-1/2
.4599	.460	32 5 27	32 4 28	+1/2	.1790	.179	14 6 8	15 5 11	+1/2
.4763	.476	29 5 25	29 4 26	-1/2	.3292	.329	28 4 24	27 3 25	-1/2
.4876	.487	31 5 27	31 4 28	+1/2	.3704	.370	28 4 24	27 3 25	+1/2
.4948	.495	28 5 23	28 4 24	-1/2	.5718	.572	7 5 3	6 4 2	-1/2
.5099	.509	30 5 25	30 4 26	+1/2	.7648	.764	7 5 3	6 4 2	+1/2
.5143	.514	27 5 23	27 4 24	-1/2	.8506	.849	13 6 8	14 5 9	-1/2
.5313	.531	26 5 21	26 4 22	-1/2	.9050	.905	46 3 43	45 2 44	-1/2
.5336	.533	29 5 25	29 4 26	+1/2	.9196[b]	.921	46 3 43	45 2 44	+1/2
.5475	.547	25 5 21	25 4 22	-1/2	832.0357[b]	.037	13 6 8	14 5 9	+1/2
.5538	.552	21 4 18	20 3 17	-1/2	.0927	.092	29 4 26	28 3 25	-1/2
	.554	28 5 23	28 4 24	+1/2	.1330	.132	29 4 26	28 3 25	+1/2
	.557	5 5 1	5 4 2	-1/2	.4233	.423	8 5 3	7 4 4	-1/2
.5625	.562	24 5 19	24 4 20	-1/2					
.5775	.576	23 5 19	23 4 20	-1/2	832.8943	.895	12 6 6	13 5 9	+1/2
	.576	27 5 23	27 4 24	+1/2	.9698	.967	30 4 26	29 3 27	-1/2
.5919	.589	22 5 17	22 4 18	-1/2	833.0070	.005	30 4 26	29 3 27	+1/2

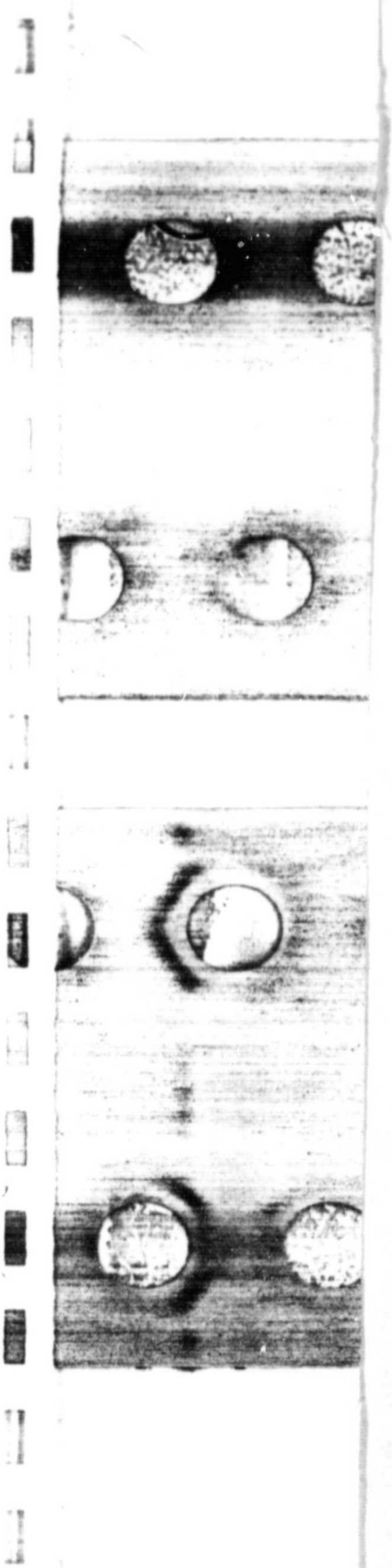

TABLE III—*Continued*

σ_{obs}	σ_{calc}	N' K'_a K'_c	N K_a K_c	J-N
833.0674[b]	.074	33 7 27	34 6 28	-1/2
.1547	.156	33 7 27	34 6 28	+1/2
.2725	.272	9 5 5	8 4 4	-1/2
.4272	.428	9 5 5	8 4 4	+1/2
.5280	.527	11 6 6	12 5 7	-1/2
835.9300[b]	.928	12 5 7	11 4 8	+1/2
836.2339[b]	.232	34 4 30	33 3 31	-1/2
.2615[b]	.266	34 4 30	33 3 31	+1/2
836.6488	.648	13 5 9	12 4 8	-1/2
.7621	.761	13 5 9	12 4 8	+1/2
837.4403	.439	28 7 21	29 6 24	+1/2
.4869	.488	14 5 9	13 4 10	-1/2
.5942	.594	14 5 9	13 4 10	+1/2
837.8640	.860	36 4 32	35 3 33	-1/2
.8989	.892	36 4 32	35 3 33	+1/2
838.1936	.193	27 7 21	28 6 22	-1/2
839.1520	.150	26 7 19	27 6 22	+1/2
.1659	.165	16 5 11	15 4 12	-1/2
.2604	.259	16 5 11	15 4 12	+1/2
839.9584[b]	.961	39 4 36	38 3 35	-1/2
.9831[b]	.990	39 4 36	38 3 35	+1/2
840.0015[b]	.002	17 5 13	16 4 12	-1/2
.0972[b]	.091	17 5 13	16 4 12	-1/2
843.5509	.550	34 6 28	34 5 29	+1/2
.5565	.557	30 6 24	30 5 25	-1/2
.5705	.572	29 6 24	29 5 25	-1/2
	.570	33 6 28	33 5 29	+1/2
.5860	.586	28 6 22	28 5 23	-1/2
.5892	.590	32 6 26	32 5 27	+1/2
	.588	6 6 0	6 5 1	-1/2
.6027[b]	.599	27 6 22	27 5 23	-1/2
.6065[b]	.611	26 6 20	26 5 21	-1/2
	.608	31 6 26	31 5 27	+1/2
.6231	.622	25 6 20	25 5 21	-1/2
.6261	.626	30 6 24	30 5 25	+1/2
	.626	7 6 2	7 5 3	-1/2
.6327	.633	24 6 18	24 5 19	-1/2
.6426	.643	23 6 18	23 5 19	-1/2
	.643	29 6 24	29 5 25	+1/2
.6513	.652	22 6 16	22 5 17	-1/2
	.650	8 6 2	8 5 3	-1/2
.6586	.660	21 6 16	21 5 17	-1/2
	.660	28 6 22	28 5 23	+1/2
.6676	.667	20 6 14	20 5 15	-1/2
	.666	9 6 4	9 5 5	-1/2
.6744	.674	19 6 4	19 5 15	-1/2
	.676	27 6 22	27 5 23	+1/2
.6782	.679	18 6 12	18 5 13	-1/2
	.677	10 6 4	10 5 5	-1/2
.6858	.684	17 6 12	17 5 13	-1/2
	.684	11 6 6	11 5 7	-1/2
.6891	.687	16 6 10	16 5 11	-1/2
	.688	12 6 6	12 5 7	-1/2
	.690	15 6 10	15 5 11	-1/2
	.690	13 6 8	13 5 9	-1/2
	.691	14 6 8	14 5 9	-1/2
	.691	26 6 20	26 5 21	+1/2
.7050	.706	25 6 20	25 5 21	+1/2
.7186	.720	24 6 18	24 5 19	+1/2
.7322	.734	23 6 18	23 5 19	+1/2
.7453	.747	22 6 16	22 5 17	+1/2
.7579	.760	21 6 16	21 5 17	+1/2
.7704	.773	20 6 14	20 5 15	+1/2
843.7827	.785	19 6 14	19 5 15	+1/2
.7943	.797	18 6 12	18 5 13	+1/2
.8062	.808	17 6 12	17 5 13	+1/2
.8173[b]	.820	16 6 10	16 5 11	+1/2
.8277[b]	.832	15 6 10	15 5 11	+1/2
.8399	.843	14 5 8	14 5 9	+1/2
.8514	.855	13 6 8	13 5 9	+1/2
.8638	.868	12 6 6	12 5 7	+1/2
.8808	.881	11 6 6	11 5 7	+1/2
.8955	.896	10 6 4	10 5 5	+1/2
.9103	.912	9 6 4	9 5 5	+1/2
.9300	.931	8 6 2	8 5 3	+1/2
.9534	.955	7 6 2	7 5 3	+1/2
.9832	.986	6 6 0	6 5 1	+1/2
844.1706	.171	22 5 17	21 4 18	-1/2
847.4858	.487	26 5 21	25 4 22	-1/2
.5256	.524	16 7 9	17 6 12	-1/2
.5460	.546	26 5 21	25 4 22	+1/2
.7106	.706	16 7 9	17 6 12	+1/2
856.3734	.374	15 6 10	14 5 9	-1/2
.4981	.496	15 6 10	14 5 9	+1/2
	.496	37 5 33	36 4 32	-1/2
.5397	.537	37 5 33	36 4 32	+1/2
861.9155	.918	29 7 23	29 6 24	+1/2
.9286	.931	28 7 21	28 6 22	+1/2
.9416	.943	27 7 21	27 6 22	+1/2
.9534	.955	26 7 19	26 6 20	+1/2
.9650	.967	25 7 19	25 6 20	+1/2
.9770	.979	24 7 17	24 6 18	+1/2
.9877	.990	23 7 17	23 6 18	+1/2
862.0001	.001	22 7 15	22 6 16	+1/2
.0107	.012	21 7 15	21 6 16	+1/2
.0215	.023	20 7 13	20 6 14	+1/2
.0318	.033	19 7 13	19 6 14	+1/2
.0425	.044	18 7 11	18 6 12	+1/2
.0539	.054	17 7 11	17 6 12	+1/2
.0650	.065	16 7 9	16 6 10	+1/2
.0752	.076	15 7 9	15 6 10	+1/2
.0868	.087	14 7 7	14 6 8	+1/2
.1002	.099	13 7 7	13 6 8	+1/2
.1111	.112	12 7 5	12 6 6	+1/2
.1264	.127	11 7 5	11 6 6	+1/2
.1450	.143	10 7 3	10 6 4	+1/2
.1604	.162	9 7 3	9 6 4	+1/2
.1767	.183	44 5 39	43 4 40	+1/2
.1822	.185	8 7 1	7 6 2	+1/2
.2121	.214	7 7 1	7 6 2	+1/2

for the (000) state. This is because the observed energy levels of (010) used as input in the fit were obtained by adding the observed line positions to the calculated energy levels of the ground state.

RECEIVED: December 10, 1979

REFERENCES

1. S. C. HURLOCK, K. NARAHARI RAO, L. A. WELLER, AND P. K. L. YIN, *J. Mol. Spectrosc.* **48,** 372–394 (1973).
2. A. CABANA, M. LAURIN, W. J. LAFFERTY, AND R. L. SAMS, *Canad. J. Phys.* **53,** 1902–1926 (1975).
3. S. PADDI REDDY, W. IVANCIC, V. MALATHY DEVI, A. BALDACCI, K. NARAHARI RAO, A. W. MANTZ, AND R. S. ENG, *Appl. Optics* **18,** 1350–1354 (1979).
4. R. PASO, J. KAUPPINEN, AND R. ANTILLA, *J. Mol. Spectrosc.* **79,** 236–253 (1980).
5. A. G. MAKI, WM. B. OLSON, AND R. L. SAMS, *J. Mol. Spectrosc.* **81,** 122–138 (1980).
6. C. C. LIN, *Phys. Rev.* **116,** 903–906 (1959).
7. W. T. RAYNES, *J. Chem. Phys.* **41,** 3020–3032 (1964).
8. J. K. G. WATSON, *J. Chem. Phys.* **46,** 1935–1949 (1967).
9. W. J. LAFFERTY AND R. L. SAMS, *J. Mol. Spectrosc.* **66,** 478–492 (1977).
10. R. M. LEES, R. F. CURL, AND J. G. BAKER, *J. Chem. Phys.* **45,** 2037–2040 (1966).

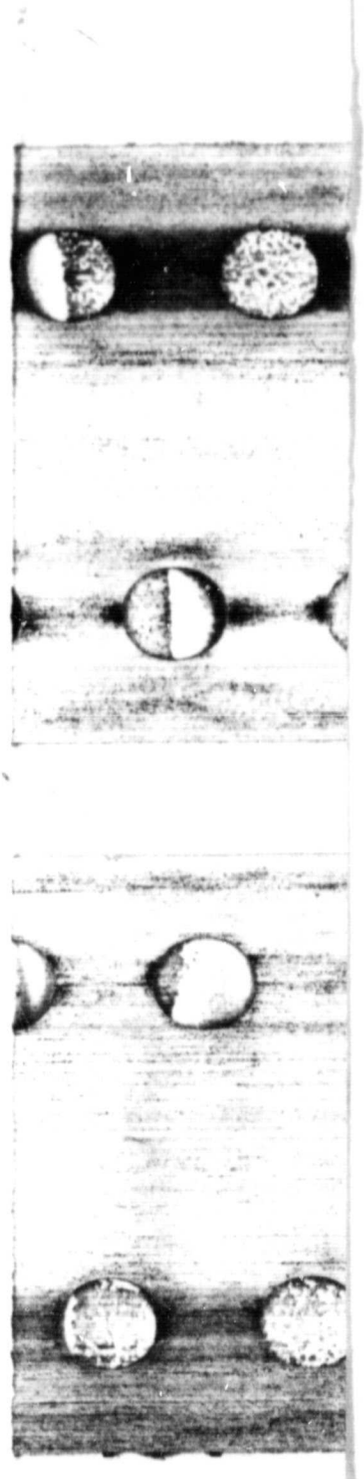

JOURNAL OF MOLECULAR SPECTROSCOPY 75, 339–362 (1979)

Spectrum of Water Vapor between 8050 and 9370 cm^{-1}

J.-M. FLAUD AND C. CAMY-PEYRET

Laboratoire de Physique Moléculaire et d'Optique Atmosphérique, C.N.R.S., Bât. 221, Campus d'Orsay, 91405 Orsay Cedex, France

K. NARAHARI RAO, DA-WUN CHEN, AND YAN-SHEK HOH

Department of Physics, The Ohio State University, Columbus, Ohio 43210

AND

J.-P. MAILLARD

Observatoire de Meudon, 1 Place J. Janssen, 92190 Meudon, France

Measurements of the line positions of $H_2{}^{16}O$ in the 8050 to 9370 cm^{-1} region have been performed at a spectral resolution of 0.07 cm^{-1}. A grating spectrum of room-temperature water vapor and a Fourier transform spectrum of heated water vapor (T = 60°C) were used in the interpretation. A careful analysis of the bands $\nu_1 + 3\nu_2$, $3\nu_2 + \nu_3$, $2\nu_1 + \nu_2$, $\nu_1 + \nu_2 + \nu_3$, and $\nu_2 + 2\nu_3$ has led to a set of rotational levels belonging to the vibrational states (130), (031), (210), (111), and (012). Many vibrorotational resonances were detected.

INTRODUCTION

The vibration–rotation spectrum of the water molecule begins to be understood in great detail in the 6.3-μm (*1–3*), 2.7-μm (*4–6*), 1.9-μm (*1*,*6*,*7*), and 1.4-μm (*8*,*9*) regions. Toward the photographic infrared and the visible, the situation is not so favorable because the bands are weak and also because of the possibility that multiple resonances will make both the assignment and the calculation of spectra much more difficult. However, it is important to improve our knowledge of these spectral regions from both practical considerations (atmospheric studies) and theoretical reasons (determination of the potential function). A systematic effort to analyze the H_2O spectra in these regions was performed earlier by Benedict (*10*). In the present paper, we report an experimental investigation of the spectrum of water vapor from 8050 to 9370 cm^{-1}; we have been able to assign about 1200 vibration–rotation lines belonging to the $\nu_1 + 3\nu_2$, $3\nu_2 + \nu_3$, $2\nu_1 + \nu_2$, $\nu_1 + \nu_2 + \nu_3$, and $\nu_2 + 2\nu_3$ bands. From the observed line positions, an extensive set of experimental rotational levels has been obtained for the vibrational states (130), (031), (210), (111), and (012).

0022-2852/79/060339-24$02.00/0

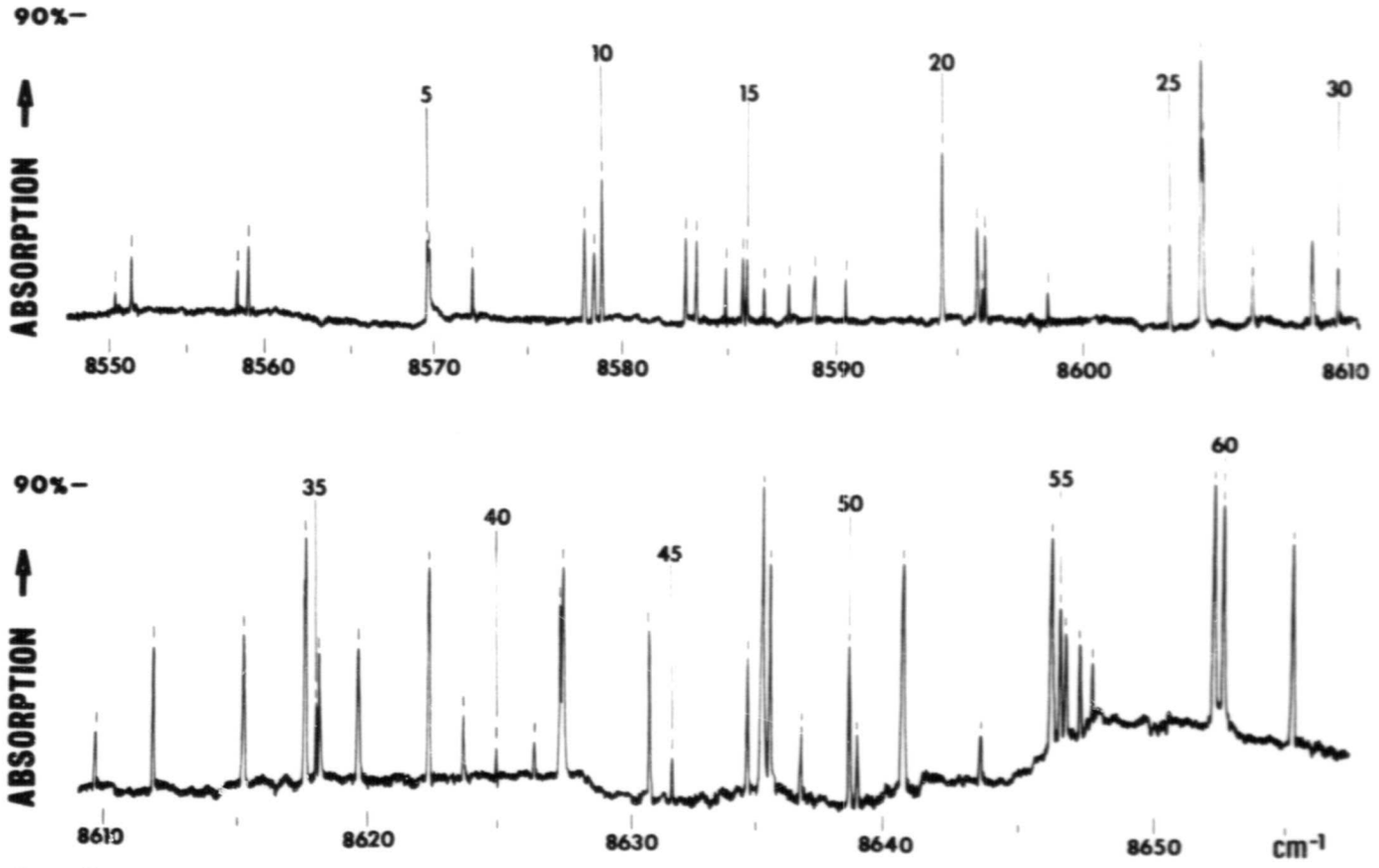

FIG. 1. Room-temperature water vapor spectrum (grating spectrometer, resolution 0.07 cm^{-1}) between 8550 and 9024 cm^{-1} (L = 100 m, P = 7 Torr).

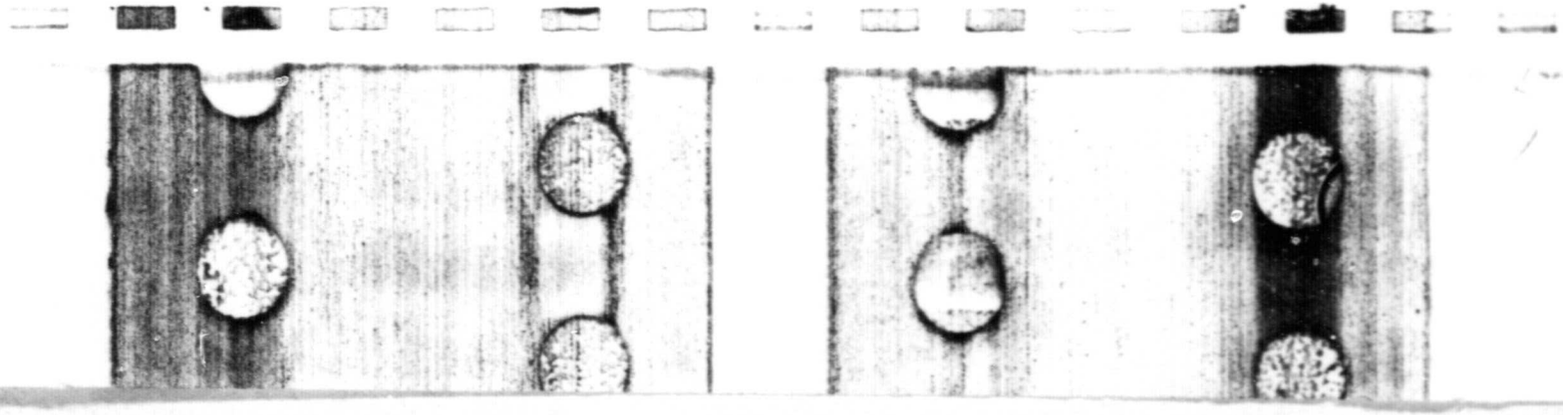

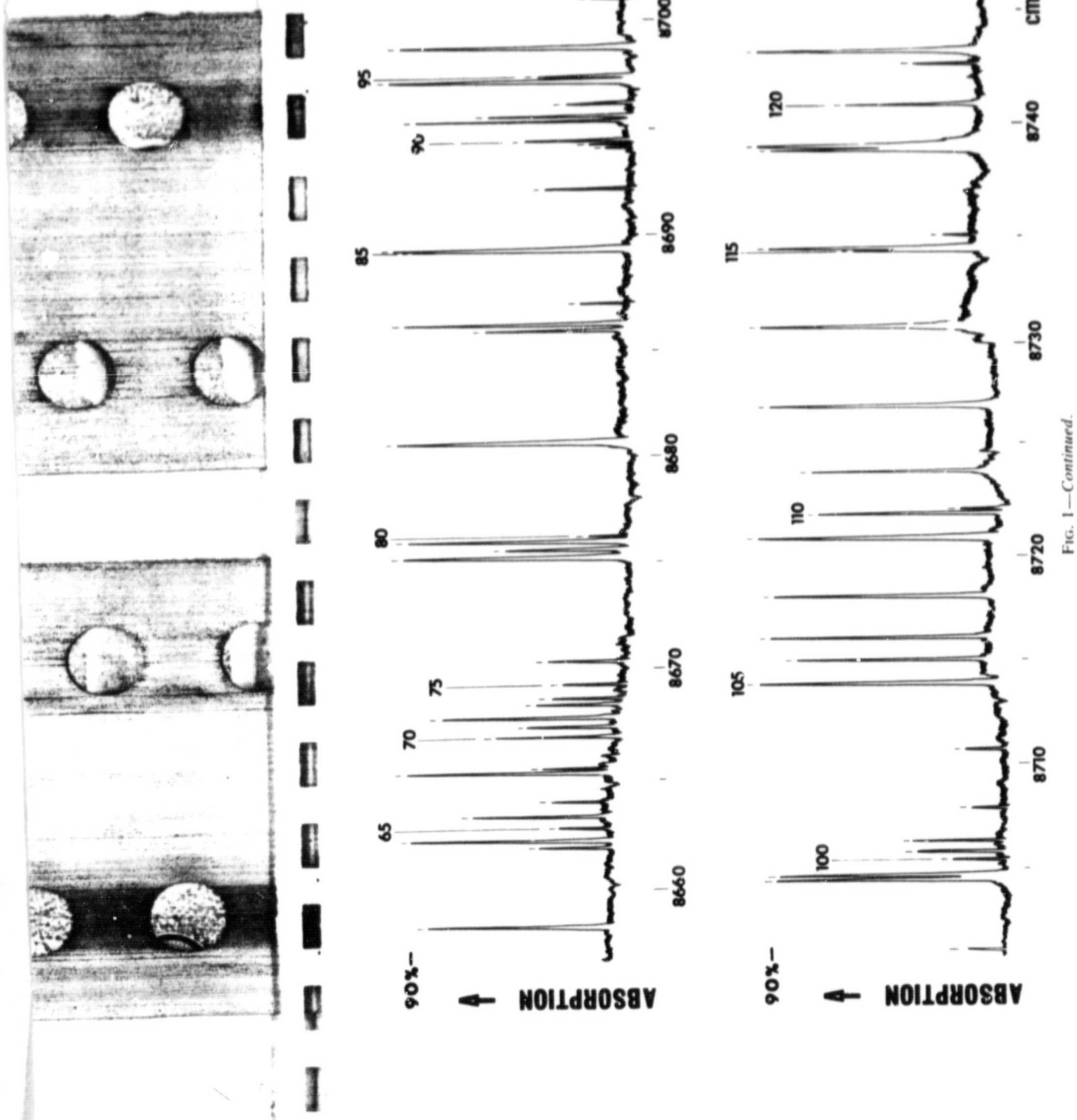

FIG. 1—*Continued.*

FIG. 1—*Continued.*

FIG. 1—*Continued.*

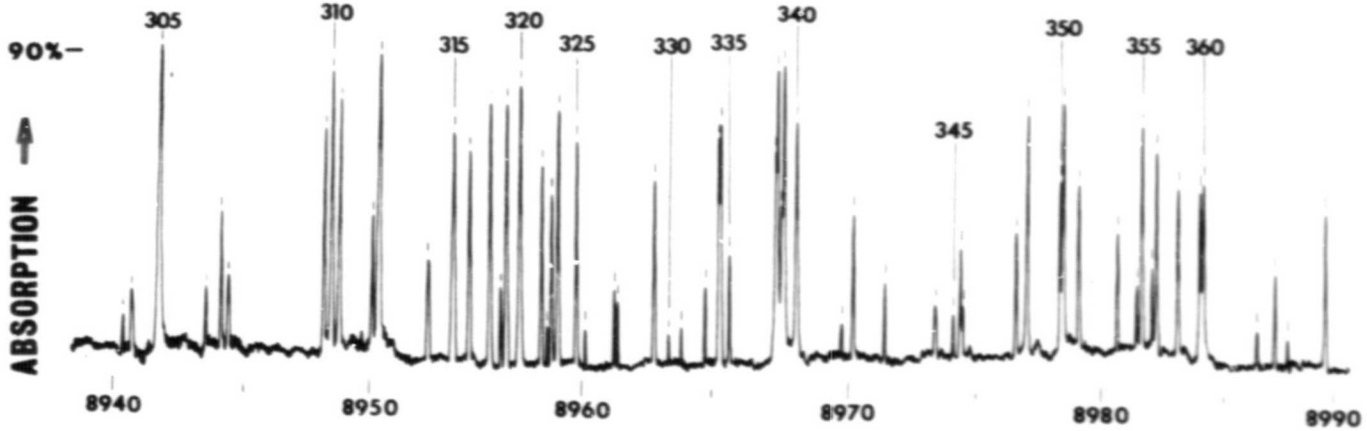

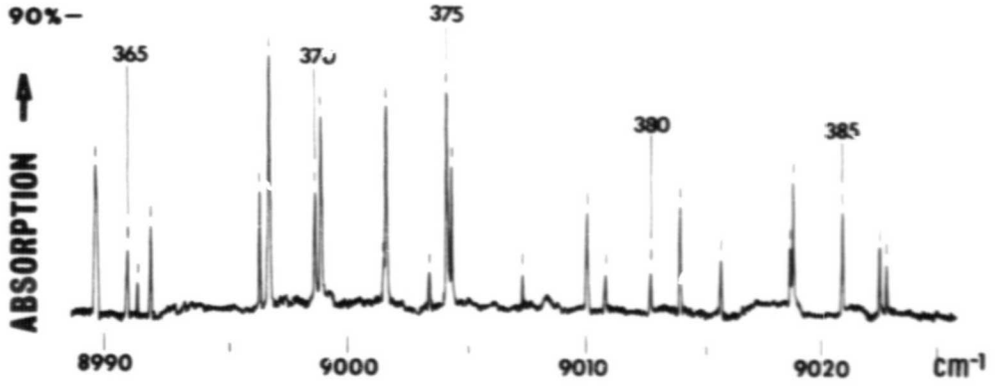

FIG. 1—*Continued.*

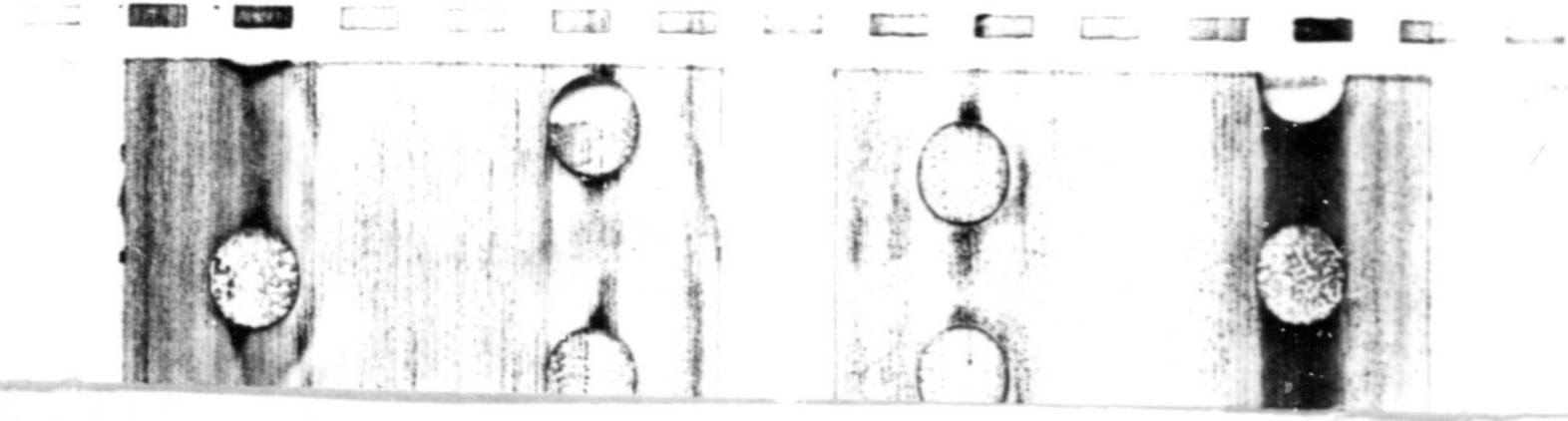

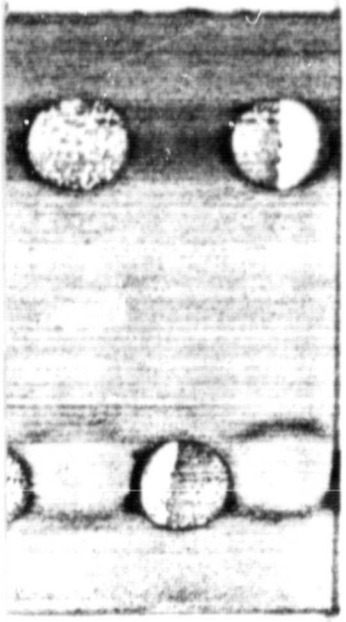

EXPERIMENTAL DETAILS

For this study, we analyzed two different spectra. For the strongest lines, we used the line positions given by a room-temperature spectrum recorded from 8550 to 9024 cm^{-1}. The positions of the weaker lines were deduced from a Fourier transform spectrum of heated water vapor extending from 8050 to 9370 cm^{-1}. The characteristics of the two spectra are given below:

Room-Temperature Spectrum

A 10-m focal length Czerny–Turner vacuum spectrometer at the Ohio State University was used to record the spectrum. This spectrometer employed a 40 $\times$ 20-cm^2 (16 $\times$ 8-$in.^2$) echelle with 79 grooves per millimeter on its surface and blazed at an angle of about 63°. The source of continuous infrared radiation was a carbon rod furnace working at an input power of 3.4 kW (10 V at 340 A). A description of this spectrometer was given previously (*11*). The infrared radiation was detected with two detectors—InSb for the CO calibrating lines and a liquid-nitrogen-cooled photomultiplier for the water vapor spectrum. The signal was amplified by a Princeton Applied Research Model HR-8 phase-sensitive amplifier and then recorded on a strip chart recorder. The resolution was about 0.07 cm^{-1} and the precision of the positions of the lines is approximately $\pm$0.005 cm^{-1}. Figure 1 shows a reproduction of this spectrum. The water vapor partial pressure used was 7 mm Hg, and the length of the absorption path was 100 m.

Fourier Transform Spectrum

The water vapor was introduced into a heated multiple-path cell ($T \simeq 60$°C, $P \simeq 90$ Torr, total length $L = 40$ m) and the spectrum was recorded by one of us (J.-P.M.) with a resolution $\delta\sigma = 0.070$ cm^{-1}. Under these conditions, the experimental linewidth at half height was approximately 0.11 cm^{-1}, and the precision of the positions of the lines was $\pm$0.005 cm^{-1}. Figure 2 shows a reproduction of the observed spectrum.

For unblended and unsaturated lines common to both spectra we have noticed that the line positions agree to within the stated experimental uncertainties, that is $\pm$0.005 cm^{-1}.

DATA ANALYSIS AND RESULTS

The identification of the lines of $H_2{}^{16}O$ was facilitated by the previous work of Benedict (*10*) and with the help of the available rotational energy levels for the (000) and (111) vibrational states of $H_2{}^{16}O$ (*12*, *13*).

In the 1.1-μm region, the *A*-type band $\nu_1 + \nu_2 + \nu_3$ is much stronger (see the strong *Q* branch at 8807 cm^{-1}) than the bands $\nu_1 + 3\nu_2$, $3\nu_2 + \nu_3$, $2\nu_1 + \nu_2$, and $\nu_2 + 2\nu_3$. Consequently, the number of levels determined for the (111) state is larger than the number determined for the (130), (031), (210), and (012) states. Also, since the $\nu_1 + \nu_2 + \nu_3$ band center (8807.000 cm^{-1}) is close to the $2\nu_1 + \nu_2$ band center (8761.579 cm^{-1}), the lines of this weak band are often blended with lines of the strong band, which complicated the interpretation.

FIG. 2. Heated water vapor spectrum (Fourier transform spectrometer, resolution 0.07 cm^{-1}) between 8050 and 9370 cm^{-1} (L = 40 m, P = 90 Torr, T = 60°C).

FIG. 2—*Continued.*

FIG. 2—*Continued.*

FIG. 2—*Continued.*

FIG. 2—*Continued.*

FIG. 2—*Continued.*

FIG. 2—*Continued.*

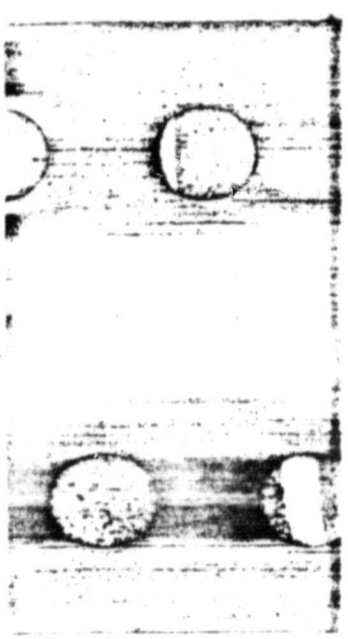

TABLE I

List of the Lines of Water Vapor between 8050 and 9370 cm^{-1} [a]

v'	v	SIGMA	J'	KA'	KC'	J	KA	KC	P1	P2	G	I
15	0	8060.1451	9	0	9	10	110		7		100	0
15	0	8062.2909	9	1	9	10	010		4		100	0
16	0	8082.9210	6	2	4	7	4	3	3		1	0
15	0	8084.5096	8	0	8	9	1	9	5		100	0
16	0	8085.8634	8	1	8	9	0	9	11		100	0
15	0	8107.6925	7	0	7	8	1	8	19		100	0
16	0	8108.3160	8	1	7	9	2	8	4		10	0
15	0	8109.8407	7	1	7	8	0	8	6		100	0
15	0	8111.4436	4	2	3	5	3	2	10		100	0
16	0	8112.1967	11	11	1	12	12	0	4		10	0
15	0	8112.6795	5	2	3	6	3	4	7		100	0
15	0	8118.1377	5	1	5	6	2	5	10		10	0
15	0	8121.8689	6	3	3	7	4	4	9		100	0
15	0	8124.0256	8	2	7	9	1	8	5		100	0
15	0	8127.8580	6	1	5	7	2	6	4		0	0
15	0	8129.1353	4	2	2	5	3	3	5		10	0
15	0	8129.4951	5	0	5	7	1	7	13		100	0
15	0	8133.1522	5	1	4	7	0	7	32		100	0
16	0	8137.1984	5	1	4	6	2	5	12		100	0
15	0	8137.8947	10	01	0	11	01	1	6		100	0
16	0	8140.5870	3	1	3	4	1	4	5		1	0
15	0	8143.4910	3	2	2	4	3	1	5		10	0
15	0	8144.3095	7	1	7	7	2	6	5		100	0
15	0	8146.1592	4	3	2	5	4	1	4		100	0
15	0	8147.0199	4	3	1	5	4	2	3		100	0
15	0	8147.5860	4	1	3	5	2	4	7		10	0
16	0	8148.0786	4	1	4	5	2	3	5		10	0
15	0	8148.6333	5	0	5	6	1	6	42		10	0
15	0	8149.5336	3	2	1	4	3	2	42		1	0
15	0	8151.9096	2	1	2	3	2	1	14		100	0
16	0	8155.2790	4	1	3	5	3	2	4		1	0
15	0	8156.1007	5	1	5	5	0	5	1		100	0
15	0	8160.4005	3	1	2	4	2	3	25		100	0
		8161.1416							5		1	
16	0	8161.6793	9	0	9	10	010		6		100	0
16	0	8162.9312	9	1	9	10	110		16		100	0
15	0	8166.5175	6	1	6	7	2	5	6		10	0
15	0	8166.7729	6	2	5	7	1	6	12		100	0
15	0	8168.0421	4	0	4	5	1	5	17		100	0
15	0	8171.5258	2	2	1	3	3	0	27		100	0
15	0	8172.5373	2	2	0	3	3	1	19		100	0
15	0	8172.6222	3	3	0	4	4	1	19		10	0
15	0	8175.0360	2	1	1	3	2	2	10		10	0
15	0	8179.0216	4	1	4	5	0	5	45		100	0
15	0	8184.7649	3	0	3	4	1	4	43		100	0
16	0	8185.5422	8	0	8	9	0	9	30		100	0
16	0	8187.0720	8	1	8	9	1	9	10		10	0
15	0	8187.1289	1	1	1	2	2	0	9		100	0
15	0	8187.3722	4	1	3	5	2	4	17		10	0
15	0	8187.3722	4	4	0	5	5	1	13		0	0
15	0	8192.1624	5	2	4	6	1	5	6		100	0
15	0	8194.4427	1	1	0	2	2	1	25		100	0
15	0	8194.8145	9	1	8	10	1	9	5		1	0
15	0	8197.4419	5	0	5	5	1	4	13		10	0
15	0	8200.9067	2	0	2	3	1	3	17		100	0
16	0	8201.0501	9	2	8	10	2	9	7		100	0
15	0	8202.5530	3	1	3	4	0	4	19		100	0
16	0	8202.7505	8	2	6	9	2	7	8		100	0
15	0	8204.0090	4	1	4	4	2	3	13		100	0
16	0	8205.1095	8	1	7	9	1	8	17		100	0
16	0	8209.3604	7	0	7	8	0	8	19		100	0
		8210.0465							4		100	
16	0	8210.5492	7	1	7	8	1	8	39		100	0
15	0	8212.1622	5	2	0	6	3	1	5		100	0
16	0	8216.7291	8	3	5	9	3	6	11		100	0
15	0	8217.8833	1	0	1	2	1	2	40		100	0
15	0	8218.3148	3	1	3	3	2	2	7		10	0
15	0	8219.1798	4	2	3	4	1	4	7		100	0
16	0	8219.3844	4	2	3	5	1	5	9		0	0
15	0	8220.8081	4	2	3	5	1	4	13		100	0
16	0	8221.0917	8	0	8	9	2	7	6		1	0
15	0	8221.3467	7	1	6	8	2	7	6		10	0
16	0	8222.0319	7	1	6	8	1	7	15		100	0
16	0	8227.2969	2	1	2	3	0	3	37		100	0
15	0	8228.1556	2	1	2	3	0	3	14		100	0
16	0	8230.2770	2	1	1	3	1	2	1		1	0
16	0	8231.0007	6	0	6	7	0	7	64		100	0
16	0	8231.5096	6	2	4	7	2	5	10		10	0
16	0	8231.6626	6	2	4	7	2	5	14		100	0
16	0	8233.1563	6	1	6	7	1	7	7		100	0
16	0	8234.5330	6	1	6	7	1	6	44		100	0
16	0	8234.6564	6	1	5	7	1	6	44		100	0
15	0	8236.2368	3	0	3	3	1	2	32		100	0
15	0	8236.8404	3	0	3	4	1	4	8		100	0
15	0	8237.7323	4	2	3	4	3	2	7		10	0
15	0	8237.9891	7	2	6	8	2	7	30		100	0
15	0	8238.6632	6	3	4	7	2	5	28		100	0
		8238.9692							5		100	
15	0	8243.3507	5	1	4	6	2	5	25		100	0
16	0	8243.9308	7	0	7	8	2	6	4		10	0
16	0	8244.1766	7	3	4	8	3	5	4		10	0
15	0	8246.0951	2	2	1	3	3	0	5		1	0
15	0	8246.7045	3	2	1	4	3	2	6		1	0
15	0	8248.0105	2	0	2	3	1	3	16		100	0
16	0	8248.1019	5	1	4	6	1	5	37		10	0
15	0	8248.1019	4	1	3	4	2	2	37		1	0
15	0	8248.3071	3	1	2	4	3	1	32		100	0
16	0	8249.4038	8	3	6	9	3	7	4		1	0
16	0	8250.4420	7	1	7	7	1	6	3		0	0
15	0	8251.2964	5	0	5	6	1	6	31		100	0
15	0	8251.8189	3	2	2	4	1	3	6		10	0
15	0	8252.8472	5	2	3	5	3	2	11		100	0
15	0	8253.2148	1	1	1	2	1	2	8		10	0
15	0	8255.0084	1	1	0	2	1	1	37		100	0
16	0	8255.2305	5	1	5	6	1	6	74		100	0
15	0	8255.5586	7	2	5	7	3	4	5		100	0
16	0	8255.8285	5	2	3	6	2	4	17		100	0
16	0	8257.1756	6	2	5	7	2	6	19		100	0

[a] The columns mean:

v', v Labels of the upper and lower vibrational states of the transition with the correspondence:

0 = (000), 1 = (010), 20 = (060),
15 = (130), 16 = (031), 17 = (210),
18 = (111), 19 = (012), 24 = (121).

Sigma Observed wavenumber of the transition (in cm^{-1})

$J'K_a'K_c'JK_aK_c$ Rotational quantum numbers of the upper and lower levels

P_1, P_2 Percentages of absorption at the center of the line for the heated and room-temperature spectra

G Statistical weight of the line

I Isotopic species with the notation 0 = $H_2{}^{16}O$, 1 = $H_2{}^{17}O$, 2 = $H_2{}^{18}O$

TABLE I—*Continued*

V'	V	SIGMA	J'KA'KC'	J	KA	KC	P1	P2	G	I
16	0	8257.1460	6 2 4	6	4	3	4		100	0
15	0	8264.1124	6 3 3	6	4	2	4		10	0
16	0	8274.4485	6 1 5	6	4	3	77		100	0
14	0	8278.2340	5 1 5	5	4	1	4		1	0
15	0	8282.1940	4 1 4	4	4	0	2		0	0
14	0	8289.0060	4 3 1	4	4	1	2		0	0
14	0	8289.3243	4 3 2	4	4	0	2		0	0
16	0	8270.1154	6 0 6	6	5	2	87		100	0
15	0	8271.5849	5 3 3	5	5	0	5		100	0
16	0	8274.4200	6 3 3	6	5	2	26		100	0
16	0	8275.5598	6 1 6	6	5	2	42		100	0
16	0	8277.2546	5 2 4	5	5	1	56		100	0
		8281.4498					9		100	
16	0	8281.5061	5 0 5	5	5	1	5		0	0
16	0	8281.9604	6 2 5	6	5	1	68		100	0
15	0	8283.4940	5 2 3	5	5	0	3		10	0
16	0	8284.6467	3 1 2	4	3	2	47		100	0
16	0	8288.1173	3 1 3	4	3	1	49		100	0
16	0	8291.8884	3 2 2	4	3	2	8		100	0
15	0	8295.2275	4 0 4	4	2	3	9		100	0
16	0	8298.1722	3 1 3	4	2	2	88		100	0
16	0	8298.1951	5 1 5	5	3	2	53		10	0
14	0	8303.0455	5 1 4	5	3	1	9		1	0
15	0	8305.5629	5 1 5	5	3	1	57		100	0
16	0	8305.6629	5 1 5	6	3	1	57		1	0
15	0	8306.0431	2 0 2	3	1	3	8		10	0
16	0	8306.6844	2 0 2	3	1	2	96		100	0
15	0	8307.1058	3 2 2	4	1	4	19		10	0
16	0	8307.4731	3 2 2	4	1	3	98		100	0
15	0	8310.0322	4 3 2	5	2	3	10		10	0
14	0	8310.2178	3 2 1	4	2	2	36		100	0
15	0	8312.1377	3 1 3	4	2	2	21		10	0
14	0	8313.4250	3 1 2	4	2	2	4		0	0
15	0	8314.1953	5 2 3	6	4	2	7		1	0
16	0	8315.0718	5 3 3	6	4	3	47		100	0
14	0	8320.1418	3 2 2	4	2	3	98		100	0
16	0	8320.4900	3 1 2	4	2	3	79		100	0
15	0	8323.2605	3 1 3	4	2	2	17		10	0
15	0	8324.0036	3 1 2	4	2	3	38		100	0
15	0	8325.5726	5 3 2	6	2	5	7		10	0
16	0	8327.1907	5 0 5	6	2	5	53		100	0
14	0	8328.0071	4 1 4	5	2	3	9		1	0
15	0	8330.1027	3 0 3	4	2	2	24		100	0
14	0	8332.1873	4 1 3	5	2	4	42		100	0
16	0	8335.2362	4 1 3	5	2	3	52		100	0
16	0	8336.4675	2 2 1	3	2	1	68		100	0
16	0	8339.2737	4 3 2	5	3	3	24		100	0
15	0	8340.2577	2 1 2	3	2	1	36		100	0
15	0	8341.1036	7 2 6	7	2	5	6		10	0
16	0	8341.6877	4 1 4	5	2	4	78		100	0
15	0	8341.8130	4 1 3	5	2	4	9		10	0
16	0	8342.9104	6 4 2	7	4	3	24		100	0
16	0	8343.4610	2 2 1	3	2	2	32		100	0
15	0	8344.8599	3 1 1	4	2	2	4		100	0
16	0	8345.8825	6 4 3	7	4	4	9		100	0
16	0	8349.7551	3 1 3	3	1	2	21		10	0
16	0	8350.0540	3 0 3	3	1	3	76		100	0
15	0	8352.3907	4 0 4	3	2	2	10		100	0
16	0	8354.5115	3 1 3	3	2	2	19		100	0
15	0	8357.5961	4 2 2	4	1	3	14		10	0
16	0	8357.9981	4 1 3	3	2	2	14		1	0
15	0	8358.1408	3 2 1	3	1	2	46		1	0
		8361.4860					3		100	
15	0	8362.2005	5 2 3	5	1	4	30		100	0
15	0	8362.5975	5 2 3	5	1	5	7		100	0
16	0	8362.8069	3 3 1	4	3	2	22		100	0
16	0	8364.0108	3 3 1	4	3	2	52		100	0
		8364.9500					4		1	
15	0	8364.9778	5 1 4	5	0	5	20		100	0
		8365.3277					1		1	
16	0	8366.3533	7 1 7	8	3	6	7		100	0
16	0	8367.2785	7 1 7	8	3	5	30		100	0
15	0	8367.6039	4 1 4	5	0	5	36		100	0
16	0	8369.2174	8 3 5	9	5	4	8		1	0
16	0	8370.3185	5 4 1	6	4	2	12		100	0
15	0	8371.2303	5 4 2	6	4	3	31		100	0
15	0	8372.0486	5 3 3	6	4	3	28		100	0
15	0	8374.1606	6 2 4	6	3	3	10		1	0
15	0	8377.4527	6 2 4	6	3	3	19		100	0
16	0	8378.8137	6 1 5	6	3	4	91		100	0
16	0	8380.5259	7 2 5	8	3	6	10		10	0
15	0	8380.7408	5 2 4	6	3	4	10		100	0
16	0	8383.6615	5 2 4	6	3	3	29		100	0
15	0	8385.0518	7 2 6	8	3	5	6		100	0
16	0	8385.3538	7 2 6	8	3	5	10		100	0
15	0	8389.3450	6 0 6	6	4	3	6		1	0
15	0	8389.7460	5 1 5	6	4	2	6		1	0
16	0	8390.2273	1 1 0	1	1	1	48		100	0
17	0	8393.7032	8 3 6	9	4	5	7		10	0
15	0	8394.0514	5 1 5	6	4	3	21		100	0
15	0	8395.4267	4 2 3	5	4	1	20		100	0
		8395.6760					3		0	
16	0	8396.2571	4 4 0	5	4	1	33		100	0
16	0	8396.4708	4 4 1	5	4	2	12		100	0
16	0	8397.4846	1 0 1	0	0	0	39		100	0
		8398.0981					9		100	
16	0	8398.8786	4 2 3	4	2	2	19		100	0
		8400.2295					1		100	
16	0	8401.3447	2 1 2	2	1	2	59		100	0
16	0	8403.1271	4 2 2	5	0	5	10		100	0
		8403.4784					5		100	
15	0	8404.5909	7 0 7	6	1	6	14		100	0
15	0	8407.1648	7 1 6	6	0	6	5		0	0
15	0	8408.4438	5 2 4	5	1	5	8		100	0
16	0	8408.4801	5 2 3	5	1	4	74		100	0
16	0	8410.5527	6 5 2	7	5	3	6		100	0
16	0	8410.8184	6 5 1	7	5	2	18		100	0
16	0	8412.6770	6 3 3	7	1	6	5		0	0

TABLE I—*Continued*

V'	V	SIGMA	J'KA'KC'	J	KA	KC	P1	P2	G	I
16	0	8413.8029	2 2 1	2	2	0	66		100	0
16	0	8414.2441	2 2 0	3	1	3	6		1	0
16	0	8414.5786	2 2 1	3	1	2	42		100	0
15	0	8416.1197	2 2 0	2	2	1	100		100	0
15	0	8417.5292	7 1 6	7	0	7	14		10	0
16	0	8417.6636	3 1 2	3	1	3	16		100	0
		8418.4830					7		100	
16	0	8419.7065	3 2 1	3	2	2	48		10	0
16	0	8419.8538	2 0 2	1	1	1	93		100	0
16	0	8420.6248	2 2 0	1	1	1	21		100	0
15	0	8421.2151	5 1 5	5	2	4	8		100	0
14	0	8422.1788	5 1 5	6	5	2	7		1	0
14	0	8423.1957	6 2 5	7	4	4	9		100	0
15	0	8423.7345	6 2 5	6	4	3	11		100	0
16	0	8425.3221	2 1 2	1	1	1	43		100	0
17	0	8425.6380	5 0 5	6	3	4	5		1	0
16	0	8428.1111	4 2 2	4	2	3	48		100	0
		8430.8703					1		100	
15	0	8432.0819	5 3 2	5	2	3	23		1	0
15	0	8432.1147	3 2 2	3	2	1	23		1	0
		8432.8710					6		0	
16	0	8433.7022	7 3 5	7	3	4	10		100	0
16	0	8435.4675	5 3 3	6	3	4	25		10	0
16	0	8435.4679	5 3 3	6	3	4	25		1	0
		8436.0150					8		0	
15	0	8436.5910	14 0 14	15	0	15	6		1	0
14	0	8436.5910	14 1 14	15	1	15	6		1	0
16	0	8438.4632	2 1 2	1	1	0	81		100	0
16	0	8439.2697	4 1 3	4	1	4	28		100	0
16	0	8440.2801	3 0 3	2	0	2	63		100	0
		8441.1043					4		100	
15	0	8441.3503	4 3 1	4	2	2	4		100	0
16	0	8442.3792	5 2 4	5	2	4	12		100	0
16	0	8443.6146	3 1 3	3	1	2	95		100	0
15	0	8446.9098	6 2 5	6	2	4	29		100	0
15	0	8446.9921	6 3 4	6	3	3	10		100	0
15	0	8447.8043	7 1 6	7	1	6	5		100	0
15	0	8448.5798	7 3 5	7	3	4	29		100	0
15	0	8448.9325	7 2 5	6	3	4	7		10	0
		8449.9685					100		100	
15	0	8450.8255	7 1 6	6	2	5	3		1	0
16	0	8451.5128	7 6 2	8	6	3	12		10	0
16	0	8451.5126	7 6 1	8	6	2	12		1	0
15	0	8452.4548	4 3 1	5	3	2	9		100	0
0	0	8452.6313	3 3 1	3	3	1	1		1	0
15	0	8454.3420	3 3 1	3	3	0	11		10	0
16	0	8455.2353	6 0 6	7	2	5	58		100	0
14	0	8455.4317	6 0 6	7	2	5	14		10	0
15	0	8456.1711	4 3 2	4	2	3	31		100	0
16	0	8458.8203	4 0 4	3	0	3	100		100	0
16	0	8459.3048	4 3 2	4	3	1	38		100	0
15	0	8460.1491	5 2 4	5	2	4	10		100	0
16	0	8461.1085	3 3 1	3	3	0	100		100	0
16	0	8461.1895	4 1 4	3	1	3	8		0	0
16	0	8461.4278	3 3 0	3	3	1	88		10	0
16	0	8461.5281	4 3 2	4	3	1	75		100	0
16	0	8463.1277	5 3 3	5	3	2	21		100	0
16	0	8463.7726	6 5 1	6	5	2	1		100	0
16	0	8464.3595	5 1 4	5	1	5	6		10	0
16	0	8464.9682	3 1 2	3	1	2	61		100	0
16	0	8466.2700	13 1 13	14	1	14	20		10	0
18	0	8466.2700	13 0 13	14	0	14	20		1	0
16	0	8467.9063	6 3 3	6	3	4	29		100	0
15	0	8468.1577	6 3 3	6	2	5	24		100	0
16	0	8468.7503	6 4 2	6	3	3	17		100	0
17	0	8469.2398	6 4 3	7	5	2	15		100	0
20	0	8469.4000	6 6 0	7	4	3	8		1	0
15	0	8471.5144	6 2 5	5	1	4	17		10	0
		8472.4033					8		100	
18	0	8474.0452	5 1 5	6	3	4	23		10	0
16	0	8475.9412	5 0 5	7	0	7	81		100	0
16	0	8476.2926	6 6 1	7	6	2	10		10	0
16	0	8476.2926	6 6 1	5	1	5	10		1	0
16	0	8477.6471	5 1 5	7	1	6	93		100	0
16	0	8484.1891	3 2 2	3	0	3	14		100	0
16	0	8486.0506	3 2 2	2	2	1	79		100	0
16	0	8489.8270	3 2 1	2	2	0	5		100	0
16	0	8489.9134	12 11 1	13	11	2	15		1	0
16	0	8490.7368	12 11 2	13	12	2	94		100	0
18	0	8491.3551	12 11 1	13	12	2	9		1	0
18	0	8491.4461	6 1 5	6	1	6	17		10	0
18	0	8491.4461	5 2 3	6	4	2	17		10	0
16	0	8491.8960	6 0 6	5	0	5	96		100	0
16	0	8492.5530	4 2 3	4	3	2	10		1	0
16	0	8493.0173	8 1 8	8	1	8	7		100	0
16	0	8493.5252	8 1 7	8	1	7	7		100	0
18	0	8494.7874	12 11 2	13	11	3	14		100	0
18	0	8495.0676	12 0 12	13	0	13	38		100	0
18	0	8496.3090	4 2 3	5	2	4	7		100	0
15	0	8496.6150	6 1 5	7	1	6	38		100	0
15	0	8498.8944	8 2 7	8	2	6	5		100	0
16	0	8501.3052	11 4 8	12	4	9	14		100	0
		8502.0196					18		100	
16	0	8504.8206	8 2 6	8	2	6	15		100	0
18	0	8505.6635	10 4 6	11	4	7	14		100	0
16	0	8506.7231	10 0 7	11	0	11	47		100	0
16	0	8507.4621	7 1 7	6	1	6	90		10	0
18	0	8507.4621	10 3 7	11	3	8	90		1	0
16	0	8508.3066	4 1 3	3	1	3	91		100	0
18	0	8508.8705	14 2 13	15	2	13	18		100	0
18	0	8511.1763	9 3 6	9	4	5	28		100	0
16	0	8512.1503	7 4 4	7	4	3	20		100	0
16	0	8515.5096	5 1 4	4	1	3	50		100	0
16	0	8515.8442	6 4 3	6	4	2	17		100	0
15	0	8516.3156	4 2 2	3	2	1	90		100	0
16	0	8517.4225	6 4 2	6	4	3	53		100	0
16	0	8517.6123	6 4 3	7	4	4	87		10	0
18	0	8517.6123	11 2 10	12	2	11	87		0	0

TABLE I—*Continued*

V'	V	SIGMA	J'	KA'	KC'	J	KA	KC	P1	P2	G	I
16	0	8517.9877	5	4	1	5	4	2	35		100	0
16	0	8518.4879	5	4	2	5	4	1	100		10	0
16	0	8518.4879	4	4	1	4	4	0	107		0	0
15	0	8518.9806	5	0	5	6	2	4	25		100	0
18	0	8519.9576	11	110		12	111		10		100	0
16	0	8520.4627	7	0	7	7	1	6	28		100	0
16	0	8520.7353	8	1	8	7	3	5	28		100	0
18	0	8521.1626	4	1	4	5	3	3	11		0	0
15	0	8521.7042	10	5	5	11	0	6	8		10	0
14	0	8521.7042	3	3	1	4	1	4	8		1	0
18	0	8523.5765	11	111		12	112		80		10	0
14	0	8523.5765	11	011		12	012		80		1	
		8523.9302							4		100	
15	0	8524.3764	3	3	1	2	2	0	18		10	0
17	0	8524.9820	10	4	7	11	3	8	15		100	0
		8525.3764							7		100	
15	0	8525.8393	3	3	0	2	2	1	40		10	0
18	0	8525.9150	7	2	2	8	1	8	8		10	0
15	0	8526.1631	7	4	3	7	3	4	10		1	
18	0	8526.1988	10	3	8	11	2	9	22		100	0
14	0	8526.1988	10	6	7	11	2	8	7		100	0
		8529.1813							7		100	
16	0	8529.8104	5	2	4	4	2	3	87		100	0
14	0	8530.4329	10	5	6	11	5	7	9		100	0
14	0	8532.0343	3	2	1	4	1	0	10		100	0
16	0	8533.1459	9	0	9	8	1	8	27		100	0
16	0	8533.3177	9	1	9	8	1	8	50		100	0
18	0	8534.1232	10	2	8	11	2	9	18		100	0
18	0	8534.1232	10	2	8	11	2	9	30		100	0
18	0	8536.5412	9	3	6	10	3	7	16		100	0
15	0	8536.8253	5	2	3	4	1	4	7		100	0
16	0	8537.3495	7	2	6	7	0	7	8		10	0
16	0	8539.2268	6	1	5	5	1	4	80		10	0
14	0	8539.2268	6	4	3	10	4	6	80		10	0
18	0	8539.9638	5	1	4	6	3	3	13		1	0
		8540.9638							13		100	0
17	0	8542.2026	4	3	2	5	4	1	13		100	0
16	0	8542.8200	5	2	3	4	2	2	55		100	0
14	0	8542.9420	10	2	9	11	2	10	29		100	0
17	0	8543.5384	4	3	1	5	4	2	8		100	0
14	0	8544.0312	10	1	9	11	1	10	63		100	0
14	0	8544.2709	4	3	2	3	2	1	14		100	0
14	0	8544.8406	10	010		9	0	9	41		100	0
		8545.0385							8		100	
16	0	8545.4870	10	2	8	11	011		46		100	0
		8545.7511							5		10	
15	0	8546.9309	4	4	1	4	3	2	14		100	0
		8547.8073							8		100	
		8548.2069							8		100	
16	0	8550.5796	6	2	5	5	2	4	38		100	0
14	0	8550.6925	10	110		11	111		63		100	0
15	0	8550.8461	4	3	1	3	2	2	3		1	0
14	0	8551.6491	10	010		11	011		88		100	0
17	0	8551.9914	8	3	6	9	2	7	7		10	0

V'	V	SIGMA	J'	KA'	KC'	J	KA	KC	P1	P2	G	I
17	0	8552.3381	4	2	3	5	3	2	31		100	0
16	0	8555.0040	9	2	7	10	2	8	37		100	0
16	0	8555.1427	7	5	2	10	5	5	4		100	0
16	0	8555.5078	7	4	4	10	4	7	86		1	
10	0	8555.5078	11	111		10	110		88		1	
17	0	8555.8280	9	5	5	10	4	7	13		100	0
15	0	8557.0619	10	3	8	11	1	11	25		100	0
24	1	8557.1372	7	1	7	8	1	8	8		1	0
16	0	8558.0239	4	3	2	3	3	1	33	13	100	0
16	0	8558.5315	4	3	1	3	3	0	43	26	100	0
18	0	8558.9824	9	3	7	10	3	8	64	16	100	0
		8559.1224							8		100	
18	0	8559.6581	9	3	7	10	3	8	27		100	0
16	0	8561.8310	9	3	6	10	1	10	22		100	0
16	0	8562.0192	7	1	6	7	1	7	27		100	0
24	1	8562.6080	6	2	4	6	2	5	1		1	0
18	0	8563.1329	3	1	3	4	0	4	38	14	100	0
18	0	8563.6099	3	3	0	4	3	1	81	26	100	0
16	0	8564.1124	9	2	8	9	2	7	64		100	0
17	0	8565.3284	9	0	9	10	1	10	10		10	0
18	0	8565.3684	9	6	3	10	6	4	10		10	0
16	0	8565.9320	6	3	4	7	0	7	4		100	0
16	0	8565.9540	12	012		11	011		13		10	0
18	0	8566.1926	9	6	4	10	6	5	12		100	0
18	0	8567.3581	6	2	4	7	2	5	81	26	100	0
18	0	8568.6174	3	3	1	4	4	1	5		1	0
17	0	8569.8044	7	3	5	8	3	6	14	7	10	0
16	0	8570.6868	7	2	6	7	2	5	72	24	10	0
18	0	8570.8204	9	2	8	10	2	9	93	31	100	0
18	0	8570.8835	6	1	5	7	1	6	9	23	9	0
16	0	8571.0340	7	3	5	8	3	6	6		100	0
18	0	8571.9770	8	3	6	9	3	7	6		10	0
18	0	8572.6539	8	4	4	9	4	5	72	21	100	0
17	0	8572.1418	8	3	5	9	3	6	9		10	0
17	0	8573.3924	4	3	2	5	3	3	9		1	0
15	0	8574.5560	6	3	4	5	2	3	21	9	10	0
		8575.5781							10		10	
18	0	8576.8238	4	0	4	5	2	3	63	24	100	0
18	0	8577.2770	8	2	6	9	2	7	88	30	100	0
18	0	8577.6828	9	2	7	10	2	8	78	29	100	0
18	0	8578.0574	9	1	9	10	1	10	100	34	100	0
15	0	8578.1530	5	3	2	6	2	5	14		9	0
16	0	8579.6093	7	5	3	7	5	2	10		10	0
16	0	8580.6823	7	5	2	7	5	3	33		100	0
16	0	8581.5424	5	5	1	5	5	0	27		100	0
16	0	8582.0004	5	5	1	5	5	0	92	34	1	0
16	0	8582.0004	5	5	0	5	5	1	92	34	0	0
16	0	8582.0004	6	5	1	6	5	2	92	34	0	0
16	0	8583.2836	8	4	5	9	4	6	99	36	10	0
16	0	8582.2906	5	3	2	4	3	1	99	16	0	0

TABLE I—*Continued*

V'	V	SIGMA	J'	KA'	KC'	J	KA	KC	P1	P2	G	I
16	0	8583.9737	8	1	7	7	1	6	52	16	100	0
18	0	8584.1676	8	1	8	7	1	6	61	18	100	0
17	0	8584.6877	8	3	5	9	2	8	5		10	0
17	0	8584.8597	7	3	5	8	2	7	14		13	0
16	0	8585.1703	10	010		10	2	9	10		100	0
17	0	8585.9098	3	2	2	4	3	1	19		100	0
14	0	8586.9497	8	5	4	9	5	5	52	10	100	0
16	0	8588.2881	7	5	3	8	5	4	41	10	100	0
15	0	8589.5799	8	4	5	9	3	6	23		100	0
15	0	8590.0416	8	5	3	9	5	4	38	10	100	0
16	0	8590.1671	8	2	7	8	2	6	21	7	100	0
17	0	8590.8980	8	1	8	9	2	7	9		100	0
18	0	8592.3650	9	1	9	9	1	8	100	37	100	0
18	0	8593.8338	8	1	7	9	1	8	86	27	100	0
17	0	8594.0193	7	3	4	8	3	5	24	8	100	0
18	0	8594.1800	7	3	5	8	3	6	67	20	100	0
16	0	8595.6449	8	0	8	9	0	9	19		100	0
18	0	8595.8417	3	1	2	4	3	1	16		10	0
		8596.3778							4		100	
16	0	8596.8980	7	2	5	8	2	6	20		10	0
16	0	8597.2901	9	3	7	9	1	8	8		100	0
		8598.3987							5		100	
19	3	8598.6760	9	5	4	10	6	5	4		100	0
18	0	8599.9998	9	2	7	9	2	8	10		0	
17	0	8601.2457	5	1	4	6	2	5	14		100	0
18	0	8601.9879	7	2	6	8	2	7	80	25	100	0
18	0	8603.3041	8	0	8	9	0	9	100	79	100	0
18	0	8603.4000	8	1	8	9	0	9	8	53	10	0
24	1	8604.0200	5	1	5	6	1	6	11		1	0
		8604.5341							8		100	
16	0	8604.5781	6	3	4	5	3	3	28	10	100	0
16	0	8604.9497	7	4	3	8	4	4	10		100	0
15	0	8605.5295	7	4	4	8	4	5	59	22	100	0
24	1	8606.7970	7	4	3	8	4	4	9		1	0
18	0	8607.6796	6	2	4	7	3	5	9		10	0
16	0	8608.0670	6	3	3	7	3	4	53	28	100	0
16	0	8608.4260	6	3	3	7	3	4	36	10	100	0
16	0	8609.8272	7	3	4	8	3	5	100	61	100	0
18	0	8611.3834	7	4	4	8	4	5	93	42	100	0
18	0	8611.8281	7	0	7	8	2	6	10		100	0
18	0	8613.5283	7	0	7	8	1	8	27		100	0
18	0	8614.2385	5	1	5	6	3	4	14		10	0
17	0	8614.4172	5	2	4	6	3	3	49	21	100	0
14	0	8614.8411	8	7	2	9	7	3	100	56	100	0
18	0	8615.8411	8	7	1	9	7	2	10		10	0
18	0	8615.8411	8	7	2	9	7	3	10		1	0
17	0	8616.8040	6	1	5	7	2	6	10		100	0
18	0	8617.3823	7	5	2	8	5	3	33	11	1	0
18	0	8617.5850	7	5	3	8	5	4	8	63	1	0
18	0	8617.6414	7	2	5	8	2	6	100	81	10	0
18	0	8618.0596	7	2	6	8	2	7	71	23	10	0
18	0	8618.0596	7	2	1	8	2	0	71	23	1	0
20	0	8618.2303	6	1	6	7	2	5	100	48	100	0
		8619.2981							10		100	

V'	V	SIGMA	J'	KA'	KC'	J	KA	KC	P1	P2	G	I
15	0	8619.8257	6	5	2	7	5	3	95	66	100	0
		8620.0440							4		100	
17	0	8621.1285	7	0	7	7	1	6	9		100	0
16	0	8622.2576	6	2	5	7	2	6	31	10	100	0
19	0	8622.7980	6	3	3	7	3	4	100		100	0
19	0	8623.0134	7	6	1	8	7	2	14		10	0
19	0	8623.0134	7	6	2	8	7	1	14		1	0
24	1	8624.1988	7	0	7	8	1	8	22		10	0
18	0	8624.1988	3	0	3	4	0	4	22		10	0
		8624.4925							22		100	
18	0	8625.5127	7	6	2	8	6	3	38		10	0
18	0	8625.5127	7	6	1	8	6	3	38		10	0
16	0	8627.0696	7	3	5	8	3	6	82		100	0
		8627.4304							8		100	
18	0	8628.3416	7	0	7	8	0	8	78		100	0
18	0	8628.3416	7	1	7	8	1	8	87		100	0
17	0	8630.6844	7	5	2	8	5	3	7		10	0
17	0	8631.8473	6	3	4	7	2	5	97	60	100	0
		8632.2885							6		100	
16	0	8632.8256	7	3	4	8	3	5	44	24	1	0
18	0	8633.3989	4	2	3	5	2	4	8		1	0
		8634.0498							5		100	
18	0	8634.1176	5	3	3	6	3	4	9		100	2
		8634.1400							4		0	
18	0	8634.8383	6	3	4	7	3	5	96	86	100	0
18	0	8636.7684	6	1	6	7	1	7	100	92	100	0
18	0	8636.9700	6	4	2	7	4	3	100	88	100	0
18	0	8637.8747	6	2	5	7	2	6	90	17	100	0
18	0	8638.3874	6	0	6	7	0	7	8		100	0
18	0	8639.1388	5	2	3	6	2	4	86		100	0
18	0	8639.5869	6	4	3	7	4	4	86	37	100	0
17	0	8639.7156	6	4	2	7	4	3	19	11	10	0
18	0	8639.8811	6	4	1	7	4	4	48	23	100	0
16	0	8639.9985	5	4	1	6	4	2	14	11	100	0
		8640.3972							4		100	
18	0	8640.7114	8	1	8	9	1	9	200		100	0
18	0	8641.3368	8	1	7	9	1	8	100	72	100	0
18	0	8641.5983	7	2	6	8	2	7	18		10	0
24	1	8641.9309	7	2	5	8	2	6	18		1	0
		8642.3009							10		100	
18	0	8644.0283	4	4	1	5	3	2	31	15	100	0
24	1	8644.2838	4	4	0	5	3	3	1		100	0
24	1	8644.2838	3	3	1	4	3	2	1		100	0
24	1	8644.2218	4	3	2	4	3	1	21		100	0
18	0	8644.3969	9	1	8	9	2	7	13		1	0
18	0	8644.4230	9	1	9	9	2	8	13		100	0
18	0	8644.6650	5	2	3	6	3	4	87	32	100	0
18	0	8644.7720	6	2	4	7	2	5	94	38	100	0
18	0	8644.8469	6	5	2	7	5	3	73	21	10	0
18	0	8644.8469	6	5	1	7	5	2	73	21	1	0
16	0	8644.9469	7	6	2	7	6	1	71	23	10	0
16	0	8647.4396	6	6	1	6	6	0	71	23	1	0

TABLE I—*Continued*

V'	V	SIGMA	J'	KA'	KC'	J	KA	KC	P1	P2	G	I
18	0	8647.8708	4	2	2	5	2	3	6		100	2
24	1	8648.7474	3	1	3	4	1	4	20		100	0
16	0	8648.9980	8	3	6	7	3	5	14		100	0
18	0	8649.0419	5	1	5	6	1	6	10		100	2
17	0	8649.2473	6	0	6	6	1	5	5		1	0
19	0	8649.2473	7	5	3	8	6	2	5		0	0
19	0	8649.9046	7	5	2	8	6	3	10		100	0
17	0	8649.6576	4	0	4	5	1	5	7		100	0
19	0	8650.1534	7	2	6	8	3	5	10		10	0
17	0	8650.6456	2	1	1	3	2	2	15		100	0
		8650.9374							9		100	
19	0	8651.3486	6	1	6	7	2	5	14		100	0
18	0	8652.0451	6	0	6	7	0	7	100	99	100	0
18	0	8652.1956	6	1	6	7	1	7	100	91	100	0
18	0	8653.1627	4	1	3	5	1	4	10		100	2
17	0	8654.3164	4	1	4	5	0	5	11		100	0
18	0	8654.8239	5	3	2	6	3	3	100	76	100	0
19	0	8654.9601	6	6	1	7	6	2	38	17	0	0
18	0	8654.9601	6	6	0	7	6	1	38	17	0	0
24	1	8655.2561	2	1	1	3	1	2	14		100	0
18	0	8656.5007	8	2	6	8	4	5	12		100	0
18	0	8657.1494	7	2	5	7	4	4	15		10	0
17	0	8657.1494	6	2	5	6	3	4	15		10	0
16	0	8657.2897	8	3	5	7	3	4	30	11	100	0
18	0	8658.0776	5	1	4	6	1	5	100	90	100	0
18	0	8660.2139	3	1	3	3	3	0	14		100	0
		8660.3754							5		100	
17	0	8660.9714	5	1	5	5	2	4	15		1	0
16	0	8660.9714	7	4	4	7	2	5	15		1	0
17	0	8661.6993	4	2	3	5	1	4	50	29	100	0
18	0	8662.0152	5	3	3	5	3	4	100	91	100	0
18	0	8662.5946	7	0	7	7	2	6	45	16	10	0
19	0	8663.1525	2	0	2	3	2	1	88	59	100	0
16	0	8663.5076	6	4	3	5	4	2	22	10	10	0
17	0	8663.5076	1	1	1	2	2	0	22	10	0	0
16	0	8663.9057	6	4	2	5	4	1	44	21	100	0
18	0	8665.1329	5	2	4	6	2	5	100	99	100	0
18	0	8665.3269	8	1	7	8	3	5	8	16	100	0
19	0	8665.5421	6	3	3	6	4	2	5		1	0
18	0	8666.7625	5	4	1	6	4	2	84	53	100	0
19	0	8667.2144	5	0	5	6	3	4	70	35	100	0
18	0	8667.6609	5	4	2	6	4	3	100	86	100	0
19	0	8668.2522	7	1	7	7	1	5	71	37	100	0
17	0	8668.5216	5	3	3	6	2	4	46	23	100	0
		8668.7689							5		100	
17	0	8669.1921	3	0	3	4	1	4	34	20	100	0
17	0	8669.6148	5	2	4	5	3	3	6		1	0
19	0	8669.6148	4	0	4	5	0	5	6		1	2
17	0	8670.2563	1	1	0	2	2	1	50	26	100	0
24	1	8670.6905	2	1	2	3	1	3	12		10	0
16	0	8670.6905	4	3	1	3	1	2	12		10	0
18	0	8671.7047	5	0	5	6	0	6	5		10	2
19	0	8673.8559	7	4	3	8	5	4	7		100	0
19	0	8675.0079	4	2	2	5	2	3	100	100	100	0
18	0	8675.0480	5	0	5	6	0	6	8		10	0
19	0	8675.3975	5	5	1	6	5	2	100	53	10	0
18	0	8675.3975	5	5	0	6	5	1	100	53	0	0
18	0	8675.7797	6	1	5	6	1	6	100	99	100	0
17	0	8676.1490	5	0	5	5	1	4	8	9	100	0
17	0	8678.4108	3	1	3	4	0	4	6		10	0
17	0	8678.6305	4	2	3	4	3	2	12		100	0
17	0	8679.2915	4	1	4	4	2	3	21		100	0
19	0	8680.2593	4	1	3	5	1	4	100	98	100	0
19	0	8681.2614	7	1	6	7	3	5	23		100	0
24	1	8682.9122	1	1	0	2	1	1	5		10	0
18	0	8685.4213	6	0	6	6	2	5	90	55	100	0
18	0	8685.7167	4	3	1	5	3	2	100	98	100	0
15	0	8686.5743	6	4	3	5	3	2	9		1	0
16	0	8686.6638	7	4	4	6	4	3	38	12	100	0
24	1	8687.0194	1	0	1	2	0	2	4		100	0
		8687.1648							8		100	
17	0	8687.2497	2	0	2	3	1	3	23	10	100	0
16	0	8687.3833	7	4	3	6	4	2	11		10	0
18	0	8688.6043	3	3	1	4	3	2	5		10	2
18	0	8689.1910	4	3	2	5	3	3	8	90	100	0
18	0	8689.2177	4	2	3	5	2	4	100	99	100	0
18	0	8690.8701	10	[illegible]	8	10	3	7	6		100	0
18	0	8691.3091	8	2	7	8	2	6	22		100	0
18	0	8691.9912	6	1	5	6	3	4	70	37	100	0
24	1	8692.6678	1	1	1	2	1	2	9		100	0
		8692.8594							9		100	
18	0	8693.9054	3	1	3	4	1	4	8		100	2
18	0	8694.0690	1	0	1	2	2	0	31	18	100	0
17	0	8694.2608	3	2	2	4	1	3	68	32	100	0
18	0	8695.1902	4	4	0	5	4	1	100	82	100	0
18	0	8695.3867	4	4	1	5	4	2	76	54	100	0
17	0	8695.8518	5	2	3	5	3	2	8		1	0
18	0	8695.9748	6	1	6	6	1	5	45	23	100	0
19	0	8696.4842	6	4	3	7	5	2	14		1	0
18	0	8696.9975	4	0	4	5	0	5	100	100	100	0
18	0	8697.1970	4	1	3	4	3	2	8	39	100	0
24	1	8697.9098	3	1	3	3	1	2	5		10	0
19	0	8697.9098	6	4	2	7	5	3	5		10	0
18	0	8698.5257	4	1	4	5	1	5	100	99	100	0
19	0	8700.1275	5	5	1	6	6	0	14		1	0
19	0	8700.1275	5	5	0	6	6	1	14		100	0
		8700.6325							3		1	
17	0	8700.8018	4	0	4	4	1	3	24	16	100	0
19	0	8703.0176	6	2	5	7	3	4	12		100	0
17	0	8703.5188	2	1	2	3	0	3	11		1	0
18	0	8704.1744	3	1	2	4	1	3	100	96	100	0
18	0	8704.3898	3	2	1	4	2	2	100	95	100	0
17	0	8705.1591	1	0	1	2	1	2	33	27	100	0
17	0	8705.3781	2	1	2	2	2	1	8	11	1	0
18	0	8705.5327	5	0	5	5	2	4	65	38	100	0
17	0	8706.0975	4	3	2	5	2	3	69	34	100	0
18	0	8706.4383	2	2	0	3	2	1	6		100	2
17	0	8707.6510	5	1	4	5	2	3	27	12	100	0

TABLE I—*Continued*

V'	V	SIGMA	J'	KA'	KC'	J	KA	KC	P1	P2	G	I
		8708.6333							8		100	
		8709.1897							12		100	
16	0	8709.9441	8	7	1	8	7	2	22		10	0
16	0	8709.9441	8	7	2	8	7	1	22		1	0
24	1	8710.1515	0	0	0	1	0	1	8		10	0
16	0	8710.4766	7	7	1	7	7	0	55	12	10	0
16	0	8710.4766	7	7	0	7	7	1	55	12	1	0
18	0	8711.1327	2	2	1	3	2	2	4		10	2
18	0	8711.5296	2	0	2	3	0	3	14		100	2
16	0	8712.3018	8	4	4	7	4	3	9		1	0
19	0	8713.6555	3	2	2	4	2	3	100	100	100	0
18	0	8714.7567	3	3	0	4	3	1	100	93	100	0
18	0	8715.8799	3	3	1	4	3	2	100	96	100	0
17	0	8717.2447	4	1	3	4	2	2	9		100	0
19	0	8717.9115	3	0	3	4	0	4	100	99	100	0
17	0	8720.1071	7	5	2	8	4	5	14		1	0
18	0	8720.8239	3	1	3	4	1	4	100	100	100	0
18	0	8720.9239	7	2	6	7	2	5	8	100	1	0
19	0	8721.9730	4	0	4	4	2	3	97	78	100	0
18	0	8722.1674	9	3	7	9	3	6	41	25	10	0
19	0	8723.3196	5	4	2	6	5	1	5		10	0
19	0	8723.2132	5	4	1	6	5	2	13		100	0
18	0	8723.5738	5	1	5	5	1	4	90	75	100	0
17	0	8724.4423	0	0	0	1	1	1	11		100	0
		8725.4361							6		100	
17	0	8726.4714	2	2	1	3	1	2	100	96	100	0
18	0	8727.6969	1	1	0	2	1	1	4		1	2
		8727.9383							3		100	
16	0	8728.1267	6	5	2	5	5	1	8		100	0
16	0	8728.5721	6	5	1	5	5	0	26	11	100	0
24	1	8729.2114	1	1	1	1	1	0	14	10	100	0
19	0	8730.1293	2	1	1	3	1	2	100	100	100	0
		8731.5100							5		1	
		8732.6415							5		100	
19	0	8732.9797	1	0	1	2	0	2	6		100	2
18	0	8733.6692	3	0	3	3	2	2	9	50	10	0
19	0	8733.9064	2	2	0	3	2	1	100	100	10	0
17	0	8734.3543	2	0	2	2	1	1	23	12	100	0
24	1	8736.8376	2	2	1	2	2	0	9		100	0
17	0	8737.4387	4	3	1	5	2	4	17		100	0
18	0	8737.9190	1	1	1	2	1	2	5		0	2
18	0	8738.3312	2	2	1	3	2	2	100	93	100	0
18	0	8738.5468	2	0	2	3	0	3	100	100	100	0
24	1	8739.2230	2	2	0	2	2	1	23		100	0
19	0	8740.4098	2	0	2	2	2	1	83	54	100	0
24	1	8741.3191	4	3	1	4	3	2	9		1	0
17	0	8741.9956	3	3	1	4	2	2	12		10	0
17	0	8742.2452	1	0	1	1	1	0	37	71	100	0
24	1	8742.4130	3	3	1	3	3	0	9		100	0
18	0	8742.9781	2	1	2	3	1	3	100	100	100	0
19	0	8744.9148	5	3	3	6	4	2	12		1	0
18	0	8744.9148	3	1	3	3	1	2	12		0	2
18	0	8746.4565	8	2	7	7	4	4	6		1	0
19	0	8747.2317	10	0	10	11	1	11	6		10	0
19	0	8747.3495	10	1	10	11	0	11	17		100	0
24	1	8747.7507	4	4	0	4	4	1	9		10	0
24	1	8747.7507	4	4	1	4	4	0	9		0	0
18	0	8748.1755	6	2	5	6	2	4	67	34	100	0
19	0	8748.8765	4	4	1	5	5	0	20	10	100	0
18	0	8749.6548	4	1	4	4	1	3	90	63	100	0
16	0	8749.7977	7	5	2	6	5	1	5		1	0
15	0	8750.0697	5	[illegible]	4	6	3	3	7		10	0
15	0	8750.2357	8	3	6	8	3	5	28	10	100	0
24	1	8750.6371	2	1	1	2	1	2	7		1	0
17	0	8750.7132	4	2	2	5	1	5	7		1	0
19	0	8751.0862	3	0	3	4	3	2	4		10	0
19	0	8751.5048	5	3	2	6	4	3	30	10	100	0
17	0	8751.7166	3	2	1	4	1	4	55	30	100	0
16	0	8751.9172	7	5	3	6	5	2	29	8	100	0
24	1	8752.3508	5	5	1	5	5	0	6		10	0
24	1	8752.3508	5	5	0	5	5	1	6		1	0
		8752.9511							3		100	
		8753.1231							5		100	
		8753.8941							6		1	
18	0	8754.9316	1	1	0	2	1	1	100	94	100	0
18	0	8755.9653	0	0	0	1	0	1	[illegible]		100	2
24	1	8757.2675	1	0	1	0	0	0	4		1	0
17	0	8757.4013	5	2	3	6	1	6	14		10	0
17	0	8757.5596	3	3	0	4	2	3	32	17	100	0
		8759.4309							14	5	100	
18	0	8760.1386	1	0	1	2	0	2	100	97	100	0
17	0	8760.4229	2	2	0	3	1	3	8	22	100	0
		8762.7618							23		100	
19	0	8763.1262	9	1	8	10	2	9	12		100	0
19	0	8763.4394	9	2	8	10	1	9	4		1	0
18	0	8765.0393	1	1	1	2	1	2	100	100	100	0
		8768.1349							4		100	
15	0	8769.1185	5	5	0	4	4	1	20		100	0
		8769.6668							3		10	
19	0	8770.1287	7	2	5	8	3	6	12		100	0
18	0	8771.5278	5	2	4	5	2	3	100	89	100	0
18	0	8772.2915	3	1	3	3	1	2	100	95	100	0
19	0	8772.7716	4	3	2	5	4	1	28	16	100	0
19	0	8773.1106	9	0	9	10	1	10	24	10	100	0
19	0	8773.2179	9	1	9	10	0	10	7		100	0
18	0	8773.5903	7	3	5	7	3	4	90	53	100	0
18	0	8774.4156	3	2	2	3	2	1	17		100	2
19	0	8774.5258	4	3	1	5	4	2	12		1	0
18	0	8774.8231	1	1	1	1	1	0	11		100	2
24	1	8775.2076	2	1	2	1	1	1	10		100	0
18	0	8776.6010	9	4	6	9	4	5	35	10	100	0
		8778.2395							4		10	
24	1	8778.6572	2	0	2	1	0	1	21		100	0
18	0	8781.0914	2	2	1	2	2	0	9		100	2
17	0	8781.3610	1	1	0	1	0	1	47	22	100	0
19	0	8782.4985	6	2	4	7	3	5	8		10	0
18	0	8783.2057	0	0	0	1	0	1	100	100	100	0
18	0	8783.7543	2	2	0	2	2	1	17	10	100	2

TABLE I—*Continued*

V'	V	SIGMA	J'KA'KC'	J	KA	KC	P1	P2	G	I
18	0	8784.7457	4 3 1	4	3	2	5		100	2
18	0	8785.5741	3 3 1	3	3	0	15		100	2
18	0	8785.6803	3 3 0	3	3	1	4		1	2
18	0	8785.9935	3 3 1	3	3	1	8		100	2
17	0	8786.6671	2 2 1	2	2	0	22	11	100	0
24	1	8787.1741	2 2 1	2	2	0	12		100	0
19	0	8789.2228	6 2 5	6	1	5	14		100	0
19	0	8790.3961	6 2 5	6	1	5	26	14	100	0
18	0	8790.6491	4 2 3	4	2	2	96	83	100	0
18	0	8790.8278	2 1 2	2	1	1	100	90	100	0
18	0	8791.1867	6 3 4	6	3	3	85	49	100	0
17	0	8791.9129	6 3 4	6	3	3	5		100	0
18	0	8792.4043	2 0 2	1	1	1	43	14	1	0
17	0	8792.4043	2 0 2	1	1	1	43	14	1	0
		8792.8634					5		100	0
24	1	8793.2780	3 1 3	2	1	2	17		100	0
19	0	8793.6490	6 3 4	6	3	3	4		100	0
		8793.9514					4		100	0
18	0	8794.3196	4 1 3	3	3	0	19		1	0
18	0	8794.4640	6 5 1	6	4	3	5		100	2
18	0	8795.0787	4 3 1	5	1	4	19		100	0
19	0	8795.7094	5 2 3	5	0	5	33	12	100	0
19	0	8796.1457	4 2 2	5	0	5	14	10	100	0
17	0	8796.4250	3 1 2	5	0	5	65	32	100	0
18	0	8796.7497	11 6 6	11	6	5	6		100	0
		8797.0868					9		100	0
24	1	8797.2672	3 0 3	2	0	2	9		100	0
17	0	8797.8030	7 5 2	6	4	3	13		1	0
19	0	8797.9872	8 2 6	9	1	9	17		10	0
18	0	8798.1360	5 2 3	5	1	4	4		100	0
19	0	8798.3578	5 3 3	4	4	0	42	16	100	0
19	0	8799.0735	5 3 3	4	4	1	10		100	0
19	0	8799.3760	5 3 3	4	4	1	36	15	100	0
17	0	8799.6537	5 3 3	4	4	1	19	13	10	0
18	0	8801.0784	9 5 5	9	5	4	28	7	100	0
18	0	8801.9655	3 2 2	3	2	1	100	100	100	0
18	0	8802.1954	3 2 2	3	2	1	100	100	10	0
18	0	8802.6654	5 3 3	5	3	2	100	100	1	0
18	0	8802.8518	7 4 4	7	4	3	100	55	100	0
17	0	8803.1785	5 2 3	5	1	4	47	39	100	0
18	0	8803.7959	3 1 2	3	1	2	8	4	10	0
17	0	8803.9091	6 3 4	5	4	1	14		10	0
17	0	8804.4803	6 3 4	5	4	1	12		100	0
17	0	8804.6963	6 3 4	5	4	1	36	20	10	0
16	0	8805.9526	5 0 5	4	2	2	8		10	0
19	0	8806.6720	7 1 6	6	3	3	27		100	0
19	0	8807.1802	5 0 5	5	1	5	73	33	100	0
17	0	8807.5191	2 2 0	2	1	1	28	22	100	0
18	0	8807.9848	5 2 4	5	0	5	28	14	100	0
18	0	8808.4667	5 2 4	5	0	5	28	14	100	0
18	0	8809.0776	6 5 1	6	4	3	65	22	10	0
18	0	8809.2712	4 3 2	4	3	1	100	94	10	0
18	0	8809.5346	7 4 3	7	4	4	85	53	10	0
18	0	8809.5346	7 4 3	7	4	4	85	53	0	0

V'	V	SIGMA	J'KA'KC'	J	KA	KC	P1	P2	G	I
18	0	8805.7891	9 3 6	9	3	7	17		100	0
18	0	8810.1774	8 4 4	8	4	5	51	41	100	0
18	0	8811.0616	2 2 0	2	2	1	100	100	100	0
18	0	8811.4853	6 4 3	6	4	3	100	83	100	0
18	0	8811.6056	4 3 2	4	3	1	100	86	100	0
18	0	8811.9752	6 3 4	6	3	3	100	79	100	0
18	0	8812.0752	1 1 1	1	1	0	100	100	1	0
18	0	8812.0752	1 1 0	1	1	1	100	100	10	0
18	0	8813.3872	3 3 0	3	3	1	100	98	100	0
18	0	8813.3872	3 3 1	3	3	1	100	98	1	0
18	0	8813.8720	7 5 3	7	5	2	100	94	100	0
18	0	8814.0287	5 4 1	5	4	2	100	93	100	0
18	0	8814.4289	5 4 1	5	4	2	100	90	100	0
17	0	8815.5389	7 5 3	6	5	2	1	1	100	0
16	0	8815.7758	6 5 1	6	5	2	8		1	0
18	0	8815.8433	6 5 2	6	5	1	8	5	1	0
18	0	8816.4849	6 3 4	6	3	3	50	15	100	0
17	0	8816.4849	6 3 4	6	3	3	84	77	100	0
		8816.4849					50	46	10	0
		8816.8443					14	5	100	0
18	0	8817.1640	4 4 1	4	4	0	8		10	0
18	0	8817.4120	4 4 0	4	4	1	100	100	100	0
18	0	8818.0010	7 6 2	7	6	1	90	90	0	0
18	0	8818.1786	7 6 1	7	6	2	28		0	0
19	0	8818.4083	7 6 2	7	6	1	28		10	0
17	0	8820.3383	2 2 1	2	2	1	100	92	100	0
18	0	8820.6881	2 2 1	2	1	2	8	8	10	0
18	0	8821.0341	7 6 2	7	6	2	61	50	1	0
18	0	8821.1591	4 2 2	4	2	3	100	98	100	0
16	0	8821.6765	6 5 1	6	5	2	28	22	10	0
18	0	8821.9198	5 5 0	5	5	1	100	90	10	0
18	0	8822.1241	5 5 1	5	5	0	8		1	0
19	0	8822.3376	3 2 2	3	2	1	8	10	100	0
19	0	8822.7355	7 6 2	7	6	1	86	25	100	0
18	0	8823.3207	10 4 6	10	4	7	14		1	0
18	0	8823.9993	3 2 1	3	2	2	100	98	100	0
24	1	8825.1757	5 3 3	4	3	2	22		100	0
19	0	8825.8218	5 5 1	5	5	0	8	3	100	0
19	0	8826.1540	6 6 1	6	6	0	95	74	10	0
18	0	8826.1540	6 6 1	6	6	1	95	74	1	0
24	1	8827.1649	5 5 1	4	5	0	7		100	0
16	0	8827.3273	8 5 4	8	5	3	8		100	0
17	0	8827.4987	3 2 2	3	1	3	5		0	0
18	0	8827.6087	7 3 5	7	3	4	36	14	100	0
18	0	8827.8849	4 1 3	4	1	4	9		10	2
18	0	8827.8849	4 1 3	4	1	4	9		10	2
17	0	8828.5759	5 3 3	5	2	3	80	23	100	0
16	0	8828.8108	7 3 5	6	1	5	14	9	1	0
17	0	8828.8108	5 1 4	5	0	5	14	9	10	0
		8828.9878					5	7	100	

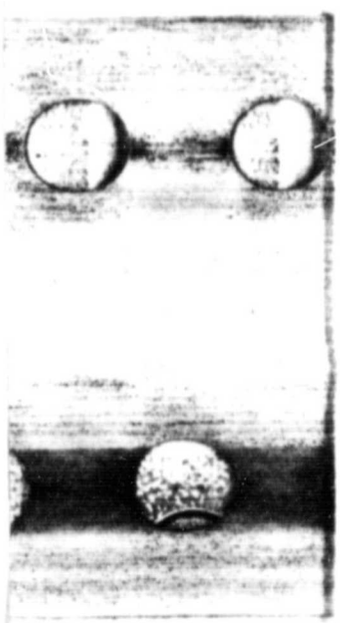

TABLE I—*Continued*

V'	V	SIGMA	J'KA'KC'	J	KA	KC	P1	P2	G	I
19	0	8829.9808	3 2 1	4	3	2	37	23	100	0
18	0	8830.2374	1 0 1	0	0	0	100	98	100	0
17	0	8830.4176	3 1 3	2	0	2	9	27	10	0
		8831.5041					7		1	
18	0	8831.6655	2 1 1	1	1	0	11	5	10	2
18	0	8832.1611	6 5 2	5	3	2	21	10	100	0
18	0	8833.0359	5 2 3	5	2	4	98	84	100	0
18	0	8833.3137	9 7 3	9	7	2	12		10	0
18	0	8833.3137	9 7 2	9	7	3	12		1	0
17	0	8834.0208	4 0 4	3	1	3	30	18	100	0
24	1	8835.2583	4 1 3	3	2	2	16		100	0
19	0	8835.7351	8 7 2	8	7	2	45	11	10	0
18	0	8835.7351	8 7 2	8	7	1	45	11	1	0
18	0	8836.4326	7 1 6	6	3	3	9		1	0
		8837.6135					7		100	
18	0	8837.3985	3 1 2	3	1	3	92	81	100	0
18	0	8837.4802	7 7 1	7	7	0	8	37	10	0
18	0	8837.4802	7 7 0	7	7	1	8	37	1	0
17	0	8837.8649	4 3 1	4	2	2	37	12	100	0
		8838.4646					5		100	
18	0	8838.7515	3 1 3	2	1	2	18	10	100	2
24	1	8839.2134	6 1 6	5	1	5	7		100	0
24	1	8840.2850	6 0 6	5	0	5	21	6	100	0
18	0	8840.4092	8 3 5	8	1	8	49	18	100	0
19	0	8841.1550	6 2 5	6	1	6	36	13	100	0
16	0	8841.4519	5 6 2	5	2	3	14		100	0
19	0	8842.0628	5 1 4	5	0	5	42	21	100	0
18	0	8842.3206	6 3 4	6	2	5	8		100	2
17	0	8842.8501	4 1 4	3	0	3	68	56	100	0
		8843.5565					5		100	
		8844.5845					6		100	
19	0	8844.7340	7 5 3	7	6	2	9		100	0
19	0	8844.9271	7 5 2	7	6	1	23	5	100	0
17	0	8845.2676	7 5 3	7	5	3	63	32	100	0
19	0	8846.0444	6 0 6	7	2	6	8	15	10	0
19	0	8846.0920	6 5 2	6	6	1	56	13	100	0
19	0	8846.0920	6 5 1	6	6	0	56	13	0	0
		8846.5134					4		100	
24	1	8846.7285	5 2 4	4	2	3	8		100	0
19	0	8847.0178	6 6 1	6	5	2	60	27	100	0
19	0	8847.2577	6 6 0	6	5	1	73	36	100	0
20	0	8847.7355	6 1 6	6	2	5	37	24	100	0
18	0	8848.0710	2 1 2	1	1	1	100	98	100	0
15	0	8849.3204	6 5 2	6	2	5	70	33	10	0
18	0	8849.3204	3 3 1	3	3	0	70	33	1	0
18	0	8849.3204	9 8 2	9	8	1	70	33	1	0
18	0	8849.5264	9 8 1	9	8	2	70	33	10	0
17	0	8850.7268	5 0 5	4	3	1	65	45	100	0
18	0	8851.0239	8 8 1	8	8	0	23	6	10	0
18	0	8851.0239	8 8 0	8	8	1	23	6	1	0
18	0	8851.5128	2 0 2	1	0	1	100	100	100	0
19	0	8852.0468	2 2 0	3	3	1	19	11	10	0
17	0	8853.2391	4 1 3	4	2	3	75	43	100	0
17	0	8853.7068	5 1 4	4	2	3	14	7	10	0

V'	V	SIGMA	J'KA'KC'	J	KA	KC	P1	P2	G	I
18	0	8854.8754	4 1 3	4	1	4	95	90	100	0
17	0	8855.1055	5 1 5	4	0	4	42	32	1	0
17	0	8855.1055	5 3 3	5	2	4	42	32	1	0
		8855.5414					4		1	
18	0	8856.6108	3 1 2	2	1	1	17	7	100	2
19	0	8857.0291	4 1 3	5	2	4	14	9	100	0
17	0	8857.4641	2 2 1	1	1	0	100	99	100	0
		8857.9100					14	11	10	
18	0	8858.4820	9 3 6	9	3	7	4		100	0
		8858.7064					5		100	
24	1	8858.8730	5 3 3	4	3	2	13		100	0
		8859.8210					4		100	
18	0	8861.1219	2 1 1	1	1	0	100	100	100	0
19	0	8861.3630	6 3 4	6	2	5	8	50	100	0
19	0	8862.6738	7 3 4	7	2	6	8		100	0
15	0	8863.3442	7 5 3	7	2	6	12		100	0
18	0	8863.7677	5 3 3	5	1	5	9		1	0
24	1	8864.7610	6 0 6	7	0	7	7		1	0
17	0	8865.0359	7 1 6	7	0	7	34	21	1	0
18	0	8866.1659	3 1 3	2	1	2	100	100	100	0
17	0	8867.2901	6 1 6	5	0	5	61	48	100	0
		8868.0339					4		100	
19	0	8868.7377	5 2 4	5	1	5	14		10	0
19	0	8868.9381	5 0 5	6	1	6	79	48	100	0
18	0	8869.6731	3 0 3	2	0	2	100	100	100	0
19	0	8870.3930	6 1 5	6	0	6	34	20	100	0
18	0	8870.5823	5 1 5	4	1	4	14		100	0
24	1	8871.4765	5 2 4	5	1	5	5		1	0
18	0	8871.4765	5 4 2	6	2	5	13		1	0
18	0	8871.7072	5 0 5	4	0	4	7		100	2
		8872.0395					10		100	
19	0	8872.1391	3 1 2	4	2	3	63	32	100	0
		8873.6505					5		100	
18	0	8874.3315	5 1 4	5	1	5	67	53	100	0
17	0	8874.5754	3 2 2	2	0	2	96	74	10	0
18	0	8874.5754	3 2 1	2	0	2	96	74	10	0
18	0	8875.2862	7 2 6	7	2	6	43	21	100	0
16	0	8877.2551	3 2 2	3	0	3	94	78	100	0
		8877.6251					5		10	
17	0	8878.1881	7 0 7	6	1	6	58	37	100	0
17	0	8878.4453	7 1 7	6	0	6	5		100	0
15	0	8878.8198	3 1 2	3	1	2	8		100	2
16	0	8879.1180	3 2 2	2	2	1	100	100	100	0
24	1	8880.0249	7 2 6	6	2	5	9		100	0
		8880.5269					38		100	
		8881.3004					22		100	
18	0	8881.7191	4 3 1	3	3	0	7		100	2
18	0	8882.2058	4 2 2	3	2	1	8		100	2
18	0	8882.8721	4 1 4	3	1	3	100	100	100	0
18	0	8883.3757	4 2 3	4	0	4	48	45	100	0
18	0	8884.0055	3 2 1	2	2	0	100	98	100	0
18	0	8884.4973	3 1 2	2	1	1	100	95	100	0
18	0	8885.5730	4 0 4	3	0	3	100	100	100	0
17	0	8887.7775	4 2 3	3	1	2	100	83	100	0

TABLE I—*Continued*

V'	V	SIGMA	J'	KA'	KC'	J	KA	KC	P1	P2	G	I
24	1	8888.2788	6	4	2	5	4	1	6		100	0
19	0	8888.8594	4	0	4	3	2	2	23	15	100	0
19	0	8889.5197	4	0	4	5	1	5	49	30	100	0
17	0	8889.8822	8	0	8	7	1	7	24	14	100	0
17	0	8890.2586	8	1	8	7	0	7	63	32	100	0
16	0	8890.6460	7	4	4	6	2	5	9		0	0
17	0	8892.2688	10	4	7	10	3	8	8		1	0
17	0	8892.6956	5	2	4	5	0	5	100	77	100	0
19	0	8893.1127	6	1	6	5	0	5	67	67	100	0
18	0	8893.5121	8	2	6	8	2	7	8	27	10	0
18	0	8893.9214	6	1	5	6	1	6	87	70	100	0
		8894.1432							4		100	
19	0	8894.5433	6	2	5	6	3	4	5		0	0
		8894.9504							10		100	
17	0	8895.3638	3	2	1	2	1	2	10		100	0
		8897.6781							10		1	
18	0	8898.1917	5	1	5	4	1	4	100	100	10	0
19	0	8898.7493	4	2	3	5	1	4	19	14	100	0
19	0	8899.1256	4	2	3	3	2	2	100	97	10	0
19	0	8899.4917	4	2	3	4	0	4	100	97	100	0
17	0	8900.1080	9	1	9	8	1	8	40	20	100	0
17	0	8900.7405	9	1	9	8	0	8	17		10	0
19	0	8900.4420	5	1	5	5	2	4	8		0	0
19	0	8901.0243	1	1	1	2	2	0	16	10	100	0
19	0	8904.3551	6	2	5	6	0	6	18	14	100	0
19	0	8905.2711	7	3	4	7	1	6	8		100	0
16	0	8905.7430	8	1	7	7	0	7	8		1	0
16	0	8905.7430	8	1	7	7	1	7	8		0	0
16	0	8906.3495	4	1	3	3	1	2	100	100	100	0
17	0	8906.8615	6	2	5	5	1	4	8	48	100	0
18	0	8907.3023	4	1	2	3	2	1	100	90	10	0
18	0	8907.9023	1	1	0	2	2	1	8		0	0
19	0	8908.7403	4	0	3	4	1	3	45	40	100	0
19	0	8909.1093	4	1	3	3	0	3	100	97	100	0
19	0	8909.3614	4	2	2	3	2	1	100	100	100	0
14	0	8909.4227	5	3	4	6	1	5	27	25	100	0
		8910.5028							5		100	
17	0	8910.8733	10	110		9	0	9	32	12	1	0
19	0	8911.4320	5	3	3	4	1	4	58	52	10	0
18	0	8911.9320	7	1	6	7	1	7	68	52	0	0
14	0	8911.9342	7	3	5	7	1	6	36	35	100	0
19	0	8912.2534	6	1	6	5	1	5	100	94	100	0
16	0	8912.9408	6	0	6	5	0	5	100	100	100	0
19	0	8914.1192	0	1	1	1	1	0	9		10	0
19	0	8914.8010	7	2	5	6	1	6	31	11	10	0
19	0	8915.6913	4	2	3	4	1	3	7		100	0
		8915.9478							5		100	
		8916.2147							14		100	
		8916.4356							7		100	
18	0	8917.0272	7	2	6	7	0	7	64	56	10	0
19	0	8917.0272	5	1	5	4	0	4	64	56	10	0
		8917.3741							8	9	10	
14	0	8917.6788	5	2	4	4	2	3	100	98	100	0
19	0	8918.4172	4	1	4	4	2	3	12		10	0
17	0	8918.4872	11	011		10	1	10	12		1	0
		8918.6196							8		100	
		8920.4450							5		100	
		8920.8070							22	11	100	
		8921.0818							5		10	
17	0	8921.1632	3	3	0	3	0	3	5		100	0
18	0	8922.1656	2	2	0	1	0	1	77	53	100	0
		8922.5740							7		100	
17	0	8924.1741	8	2	7	7	1	6	36	19	10	0
		8924.3566							7		100	
18	0	8925.0337	3	3	1	3	1	2	8	25	100	0
18	0	8925.2217	7	1	7	6	1	6	100	97	100	0
18	0	8925.4974	5	1	4	4	1	3	100	97	10	0
18	0	8925.4974	7	0	7	6	0	6	100	97	10	0
16	0	8926.0006	9	3	7	9	1	8	17	12	100	0
19	0	8926.4714	2	0	2	3	1	3	35	21	100	0
18	0	8927.2816	8	1	7	8	1	8	59	23	100	0
		8927.5062							4		100	
		8927.7390							8		100	
18	0	8928.4751	5	3	3	4	3	2	100	74	100	0
17	0	8929.1704	9	1	8	8	2	7	17		1	0
18	0	8930.1499	8	2	7	8	0	8	32		100	0
19	0	8930.4711	3	2	2	4	1	3	15		100	0
		8930.8263							5		100	
18	0	8931.1558	10	2	8	10	2	9	11		100	0
19	0	8931.3352	4	2	2	4	1	3	8		100	0
17	0	8931.5846	4	3	1	4	0	4	12		1	0
16	0	8932.2207	9	1	9	8	1	8	27	21	10	0
18	0	8932.5277	5	3	2	4	3	1	100	87	100	0
19	0	8933.4674	5	2	3	4	2	2	100	95	100	0
19	0	8933.6722	5	0	5	4	3	2	96	56	100	0
19	0	8933.8638	7	2	5	7	3	4	7		1	0
		8934.1280							7		100	
18	0	8934.7396	6	2	5	5	2	4	100	92	100	0
19	0	8935.8881	5	2	3	5	3	2	5		100	0
18	0	8936.2642	5	4	2	4	4	1	100	88	100	0
18	0	8936.4108	5	4	1	4	4	0	82	71	10	0
18	0	8936.8330	5	1	5	4	1	4	100	88	100	0
18	0	8937.1338	8	0	8	7	0	7	100	98	100	0
16	0	8940.2640	5	5	0	4	3	1	14	6	10	0
17	0	8940.4505	4	3	2	3	2	1	26	12	100	0
19	0	8940.5461	4	0	4	4	1	3	5		100	0
18	0	8941.5157	6	1	5	5	1	4	100	99	100	0
19	0	8943.3827	2	1	2	2	2	1	18	12	100	0
19	0	8943.7946	2	1	2	2	1	1	18	12	100	0
18	0	8944.2873	9	2	8	9	0	9	34	11	100	0
17	0	8945.6195	10	2	9	9	1	8	15		1	0
18	0	8946.5436	11	3	9	11	1	10	8		100	0
		8946.9815							5		100	
17	0	8947.3261	4	3	1	3	2	2	5		1	0
18	0	8948.1481	9	0	9	8	0	8	91	74	100	0
18	0	8948.4418	9	1	9	8	1	8	100	85	100	0
18	0	8948.7634	6	3	4	5	3	3	100	84	100	0
		8949.7514							5		100	

TABLE I—*Continued*

V'	V	SIGMA	J'	KA'	KC'	J	KA	KC	P1	P2	G	I
18	0	8950.0850	3	2	1	2	0	2	47	38	100	0
18	0	8950.3160	7	2	6	6	2	5	100	96	100	0
18	0	8951.6859	7	6	6	7	2	5	20		100	0
		8952.1081							6		100	
16	0	8952.4300	10	2	8	9	0	9	82	44	100	0
18	0	8953.6782	6	2	4	5	2	3	100	96	10	0
14	0	8954.1285	6	5	2	5	2	3	100	88	100	0
19	0	8955.0918	7	1	6	6	1	5	97	83	100	0
18	0	8955.4135	5	3	3	4	2	2	23	23	100	0
18	0	8955.7196	5	3	2	5	2	3	97	90	100	0
18	0	8956.2926	6	3	3	5	3	2	100	94	100	0
18	0	8957.2016	6	4	3	5	4	2	93	66	100	0
19	0	8957.4585	4	1	3	4	2	2	8	12	100	0
18	0	8957.6015	10	4	110	9	4	9	51	40	100	0
18	0	8957.8687	6	4	2	5	4	1	100	95	100	0
18	0	8958.0323	10	010		9	0	9	97	77	100	0
19	0	8958.0975	2	1	1	2	2	0	14	10	100	0
19	0	8960.2700	3	0	3	3	1	2	46	26	100	0
19	0	8960.3487	3	1	2	3	2	1	46	24	100	0
16	0	8961.9449	6	5	1	5	3	2	94	62	100	0
		8962.1509							5		100	
19	0	8962.4769	2	2	1	3	1	2	19	10	10	0
19	0	8962.8272	5	4	1	6	3	4	4		1	0
19	0	8963.0031	0	0	0	1	1	1	24	11	100	0
15	0	8964.0065	10	1	8	9	0	9	62	26	100	0
19	0	8964.5294	6	5	2	5	5	1	8	8	0	0
18	0	8964.5296	6	5	1	5	5	0	100	73	1	0
19	0	8964.8150	8	2	7	7	2	6	8	75	10	0
17	0	8964.9959	7	3	5	6	2	4	46	33	100	0
18	0	8965.9325	11	210	11	10	1	9	7		10	0
		8965.9831							6		100	
16	0	8966.2506	6	5	2	5	3	3	13		10	0
19	0	8966.8674	11	011	10	10	0	10	8	63	1	0
18	0	8966.8676	11	111	10	10	1	10	100	63	1	0
18	0	8966.9650	7	3	5	6	3	4	100	96	100	0
19	0	8967.1406	1	1	1	2	0	2	8	49	1	0
18	0	8967.3705	8	1	7	7	1	6	100	96	100	0
17	0	8967.7431	6	3	4	5	2	3	100	82	100	0
18	0	8969.4098	4	3	2	4	3	1	22	8	100	0
18	0	8970.1740	7	5	3	6	5	2	46	40	100	0
17	0	8971.5187	8	3	6	7	2	5	60	24	10	0
		8973.4307							5		100	
19	0	8973.5831	2	0	2	2	1	1	31	18	10	0
18	0	8974.1351	12	112	11	11	1	11	56	14	100	0
18	0	8974.6260	12	012	11	11	0	11	56	33	100	0
17	0	8974.7219	5	3	2	4	2	3	8	13	100	0
		8976.1729							9		100	
16	0	8976.9088	7	5	2	6	3	3	79	38	100	0
18	0	8977.3624	7	4	4	6	4	3	100	81	10	0
18	0	8977.6717	5	4	2	5	3	2	14		10	0
19	0	8978.7432	9	1	9	8	1	7	8	56	100	0
15	0	8979.4531	9	2	8	8	2	7	100	82	100	0
19	0	8979.5263	7	4	3	6	4	2	86	52	100	0
		8980.4537							16		100	
		8980.9293							7		100	
19	0	8981.1218	1	0	1	1	1	0	58	36	100	0
18	0	8981.9404	13	113	12	112		51	20	10	0	
18	0	8981.9404	13	013	12	012		51	20	1	0	
18	0	8982.1302	7	2	5	6	2	4	81	74	10	0
		8982.6011	4	1	1	3	3	0	32	28	100	0
18	0	8982.7578	7	3	4	6	3	3	83	67	100	0
		8983.1740							4		100	
18	0	8983.7047	8	3	6	7	3	5	94	58	100	0
18	0	8984.6452	7	5	3	6	5	2	97	65	1	0
18	0	8984.6452	7	5	2	6	5	1	97	65	1	0
16	0	8986.7548	4	2	2	3	0	3	80	70	100	0
19	0	8987.0001	6	1	6	5	2	3	29	11	100	0
18	0	8987.6940	10	2	9	9	1	8	81	30	100	0
18	0	8988.2282	14	014	13	013		44			10	0
18	0	8988.2282	14	114	13	113		44			1	0
18	0	8989.7959	10	1	9	9	1	8	94	61	100	0
16	0	8991.0780	8	5	3	7	3	4	57	22	100	0
		8991.4088							5		100	
16	0	8991.5440	7	5	3	6	3	4	31	5	100	0
18	0	8992.0657	7	6	2	6	6	1	72	25	10	0
18	0	8992.0657	7	6	1	6	6	0	72	25	1	0
		8993.4145							5		100	
18	0	8993.5459	15	115	14	114		18			10	0
18	0	8993.5459	15	015	14	014		18			1	0
		8994.7906							5		100	
		8995.4047							4		1	
		8995.7122							5		100	
18	0	8996.4363	8	4	5	7	4	4	64	38	100	0
18	0	8996.8064	8	2	6	7	2	5	100	84	100	0
		8997.5090							15		100	
18	0	8997.9827	16	016	15	015		8			10	0
18	0	8997.9827	16	116	15	115		8			1	0
18	0	8998.7171	11	210	10	2	9	65	38	100	0	
18	0	8998.9692	9	3	7	8	3	6	95	66	100	0
		8999.2684							5		100	
18	0	9001.5656	11	110	10	1	9	8	12	10	0	
18	0	9001.6588	8	4	4	7	4	3	100	69	10	0
18	0	9003.4361	3	3	0	2	1	1	18	10	100	0
18	0	9004.1748	8	3	5	7	3	4	100	80	100	0
18	0	9004.4043	8	5	3	7	5	2	57	43	100	0
		9004.9576							4		100	
18	0	9005.1416	4	4	0	4	2	3	7		10	0
19	0	9006.3407	9	2	8	8	3	5	11		1	0
18	0	9007.4059	12	111	11	11	0	11	68	12	100	0
18	0	9008.3140	5	4	1	5	2	4	5		1	0
18	0	9008.5642	12	211	11	210		26			100	0
19	0	9009.2787	8	6	3	7	7	0	11		10	0
		9009.5620							4		100	
18	0	9010.0650	9	2	7	8	2	6	85	39	100	0
18	0	9010.8133	8	6	2	7	6	1	85	15	100	0
18	0	9010.9459	8	6	3	7	6	2	21		1	0
		9011.4359							16		100	
18	0	9012.7908	10	3	8	9	3	7	65	18	100	0

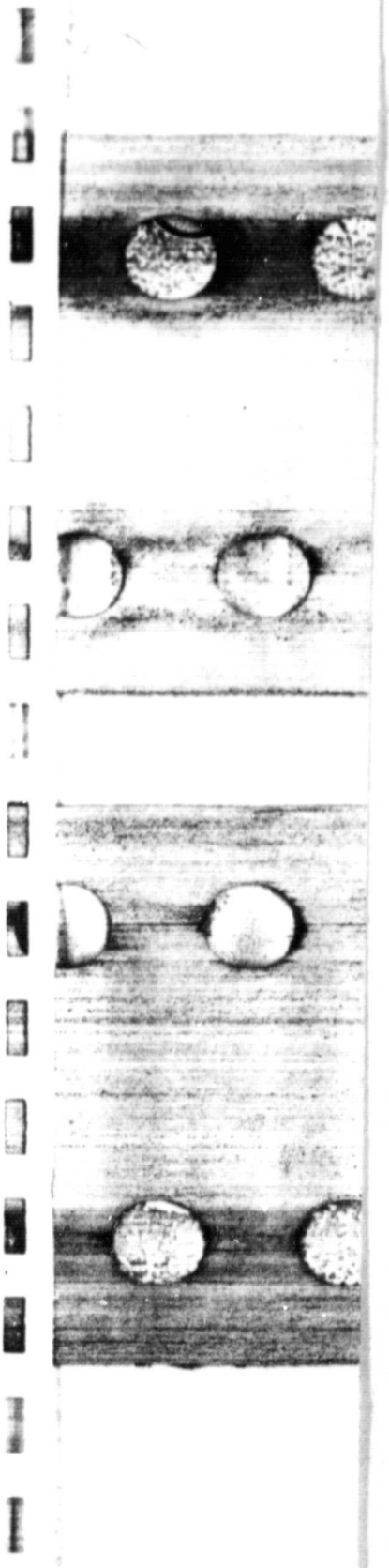

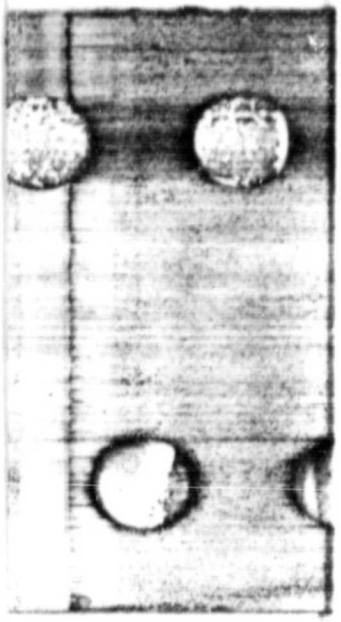

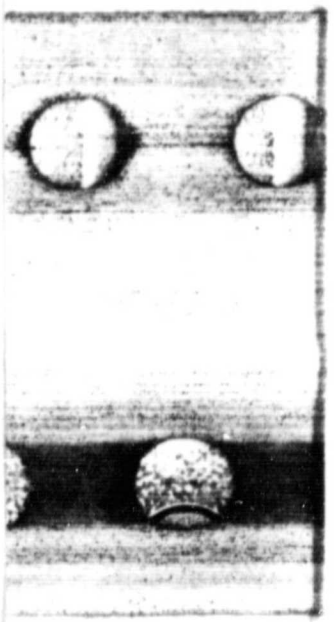

TABLE I—*Continued*

V'	V	SIGMA	J'KA'KC'J	KA	KC	P1	P2	G	I
18	0	9014.1298	9 4 6	8 4 5	100	46	100	0
18	0	9015.0075	13 4 10	12 4 9	97		100	0
18	0	9015.2870	13 4 9	12 4 8	11		10	0
17	0	9015.9994	10 5 6	9 5 5	66	17	100	0
19	0	9016.0421	7 5 3	6 5 2	6		1	0
18	0	9016.7429	13 12 2	12 11 1	15		100	0
18	0	9017.8325	6 3 3	5 1 5	9		1	0
18	0	9018.9025	3 1 3	2 1 2	22	17	100	0
19	0	9019.2496	1 1 0	1 0 1	83	43	100	0
		9020.6980			11		100	
18	0	9021.1638	4 3 1	3 1 2	80	44	100	0
18	0	9022.8680	10 2 8	9 2 7	81	36	100	0
18	0	9023.3070	9 5 5	8 5 4	79	27	100	0
18	0	9023.9154	9 4 5	8 4 4	82		0	
18	0	9023.9154	9 5 4	8 5 3	82		1	
18	0	9024.3268	9 5 4	8 5 3	56		100	0
18	0	9024.7579	14 11 3	13 11 2	10		100	0
18	0	9025.0675	7 1 7	7 0 7	38		100	0
18	0	9025.2490	11 3 9	10 3 8	73		100	0
19	0	9025.9438	8 2 7	7 3 4	11		10	0
		9026.4709			8		100	
18	0	9027.1043	5 4 3	4 0 4	50		100	0
18	0	9027.9504	5 4 2	4 0 4	18		10	0
18	0	9029.5659	9 5 4	8 5 3	44		100	0
18	0	9029.6215	11 2 9	10 2 8	8		1	0
18	0	9030.3024	10 4 7	9 4 6	42		100	0
19	0	9031.0112	2 0 2	1 1 1	31		10	0
19	0	9031.0112	8 7 2	7 7 1	31		10	0
		9034.3411			6		100	
19	0	9035.7435	3 1 2	3 0 3	72		100	0
18	0	9036.4444	12 3 10	11 3 9	17		10	0
19	0	9037.1985	1 1 1	0 0 0	25		100	0
18	0	9037.7650	10 3 7	9 3 6	64		10	0
19	0	9038.2211	8 3 6	7 3 5	13		100	0
19	0	9039.1013	3 2 1	3 1 2	75		100	0
19	0	9039.8039	5 3 2	4 1 3	41		100	0
18	0	9040.4125	12 2 10	11 2 9	39		100	0
18	0	9040.4707	5 3 2	4 1 3	48		100	0
18	0	9041.2432	10 5 6	9 5 5	10		10	0
18	0	9042.0782	2 2 0	2 1 1	27		100	0
18	0	9042.6744	3 2 2	2 1 1	54		10	0
19	0	9044.4398	10 4 6	9 4 5	58		100	0
18	0	9044.9255	11 4 8	10 4 7	32		100	0
18	0	9045.0514	6 3 3	5 3 2	27		100	0
19	0	9045.2356	5 3 3	5 1 4	64		100	0
		9046.5556			9		100	
18	0	9046.5556	13 3 11	12 3 10	17		100	0
		9046.8597			9		100	
18	0	9047.0444	10 6 4	9 6 3	23		100	0
		9047.9118			10		100	
		9049.0980			8		100	
		9052.1707			15		100	
18	0	9050.4434	4 3 2	3 1 3	17		100	0

V'	V	SIGMA	J'KA'KC'J	KA	KC	P1	P2	G	I
19	0	9051.1834	4 1 3	4 0 4	26			100	0
18	0	9053.2108	9 1 9	8 1 8	18			10	0
18	0	9053.2108	9 2 8	8 2 7	18			10	0
19	0	9054.1337	3 2 1	3 1 2	44			100	0
19	0	9054.4827	3 2 2	3 1 3	44			100	0
18	0	9054.8002	14 2 12	13 2 11	7			10	0
17	0	9055.2917	10 4 7	9 3 6	58			100	0
		9056.0575			4			1	
19	0	9056.3388	2 2 1	2 1 2	29			100	0
		9056.8869			8			1	
		9057.1753			10			10	
18	0	9058.0176	11 5 7	10 5 6	29			100	0
		9060.4168			14			10	
19	0	9061.7193	5 3 2	5 2 3	52			100	0
19	0	9062.2535	9 5 4	8 5 3	7			10	0
		9062.6657			11			100	
		9062.8858			5			100	
19	0	9063.0982	3 2 2	3 1 3	29			100	0
		9063.9051			18			100	
18	0	9065.0498	6 3 3	5 1 4	85			100	0
18	0	9065.7045	11 6 6	10 6 5	8			0	0
		9066.3647			11			100	
		9068.3085			13			100	
19	0	9068.3980	4 3 1	4 2 2	29			100	0
19	0	9068.9773	4 3 1	4 2 2	29			100	0
19	0	9069.5281	5 1 4	5 0 5	43			100	0
		9070.0906			10			1	
18	0	9071.2007	8 5 3	8 1 8	17			100	0
18	0	9072.0274	7 5 2	7 1 6	27			100	0
18	0	9072.3710	4 3 1	4 1 4	97			100	0
18	0	9073.8698	4 0 4	3 1 3	15			100	0
18	0	9073.9602	10 7 4	9 7 3	3			1	0
18	0	9073.9602	10 7 3	9 7 2	3			1	0
18	0	9074.3983	12 3 9	11 3 8	13			100	0
18	0	9074.8427	6 2 4	5 2 3	22			100	0
18	0	9075.2815	6 3 3	5 3 2	52			10	0
18	0	9075.7218	6 3 4	5 3 3	52			10	0
15	0	9076.8832	3 2 2	3 0 3	20			100	0
19	0	9080.9068	3 3 1	3 2 2	20			100	0
19	0	9082.0993	4 1 4	3 0 3	45			100	0
18	0	9082.5892	12 4 8	11 4 7	8			100	0
19	0	9082.7545	4 3 2	4 2 3	45			100	0
18	0	9083.2015	5 3 3	4 2 2	21			100	0
18	0	9086.1526	5 3 3	5 1 4	30			100	0
19	0	9086.5060	5 3 3	5 1 4	18			10	0
19	0	9086.6586	7 4 3	7 1 6	11			100	0
19	0	9086.7296	6 1 5	6 0 6	15			100	0
17	0	9088.0046	6 3 4	5 0 5	8			100	0
		9090.2526			9			10	
19	0	9091.0561	5 0 5	4 1 4	57			100	0
18	0	9091.6237	10 8 2	9 8 1	6			1	0
18	0	9091.6237	10 8 3	9 8 2	6			1	0
18	0	9092.3335	6 3 4	6 2 5	33			100	0
18	0	9093.3676	4 4 0	3 2 1	8			0	0

TABLE I—*Continued*

V'	V	SIGMA	J'KA'KC'J	KA	KC	P1	P2	G	I
19	0	9093.4728	2 2 1	1 1 0	69			100	0
19	0	9094.4807	11 7 5	10 7 4	3			10	0
19	0	9094.6116	5 1 4	4 2 3	12			100	0
19	0	9095.0372	5 1 5	4 0 4	17			100	0
16	0	9095.5511	7 5 2	6 1 5	15			100	0
19	0	9096.0107	6 4 2	5 3 3	12			100	0
19	0	9098.1138	6 2 5	5 1 4	41			100	0
18	0	9099.2038	4 4 1	3 3 1	9			1	0
19	0	9100.1010	2 1 2	1 1 1	37			10	0
19	0	9100.1480	7 3 5	7 2 6	8			1	0
		9101.2558			3			100	
18	0	9101.3090	7 3 4	6 1 5	24			100	0
19	0	9102.0958	5 4 1	5 3 2	28			100	0
19	0	9105.8934	6 0 6	5 1 5	6			100	0
19	0	9106.0279	7 1 6	7 0 7	28			100	0
19	0	9107.1455	4 4 0	4 3 1	12			100	0
19	0	9107.3299	6 4 3	5 3 4	28			100	0
19	0	9107.5686	5 4 2	5 3 3	10			10	0
19	0	9108.1615	6 1 6	5 0 5	23			100	0
19	0	9108.2961	7 4 4	7 3 5	6			100	0
19	0	9108.4360	4 4 1	4 3 2	23			100	0
19	0	9108.7645	5 4 1	4 3 2	17			100	0
		9109.5515			5			100	
19	0	9109.7777	8 3 6	8 2 7	15			100	0
19	0	9110.7919	7 2 5	7 1 6	35			100	0
19	0	9110.8692	8 4 5	8 3 6	9			1	0
19	0	9113.9535	7 2 6	7 1 7	11			10	0
19	0	9118.5398	7 0 7	7 1 6	9			100	0
19	0	9119.9052	7 0 7	6 0 6	4			1	0
18	0	9121.7005	6 4 2	5 2 3	48			100	0
18	0	9124.0119	5 4 2	4 2 3	41			100	0
19	0	9124.1230	8 2 7	8 1 8	7			0	0
19	0	9124.5440	4 2 3	3 1 2	44			100	0
18	0	9126.0491	6 3 4	5 1 5	16			100	0
16	0	9129.2208	8 5 3	7 4 4	9			100	0
19	0	9129.8885	7 5 2	7 4 3	10			100	0
19	0	9132.2972	8 1 8	7 0 7	6			1	0
19	0	9132.9710	3 2 1	2 1 2	44			100	0
19	0	9133.4062	6 5 1	6 4 2	7			100	0
19	0	9134.4359	6 5 2	6 4 3	12			10	0
19	0	9134.5284	6 5 2	6 4 3	16			10	0
19	0	9134.7501	5 5 0	5 4 1	13			100	0
19	0	9135.1019	5 5 1	5 4 2	5			0	0
19	0	9136.1408	5 2 4	4 1 3	12			100	0
19	0	9136.5826	9 1 8	9 0 9	7			100	0
19	0	9138.1985	7 2 5	6 0 6	10			100	0
19	0	9139.7557	7 1 6	7 0 7	6			100	0
19	0	9142.3167	8 3 5	8 2 6	33			100	0
19	0	9145.9101	6 2 5	5 1 4	26			100	0
18	0	9150.4829	8 4 4	7 2 5	39			100	0
19	0	9151.0601	3 3 1	2 2 0	40			10	0
18	0	9151.0631	6 4 3	5 2 4	40			1	0
19	0	9152.5360	3 3 0	2 2 1	72			100	0
		9153.4169			6			10	

V'	V	SIGMA	J'KA'KC'J	KA	KC	P1	P2	G	I
19	0	9154.0954	8 2 7	7 1 6	7			100	0
18	0	9156.6964	7 3 5	6 1 6	31			100	0
19	0	9157.8504	7 3 5	6 1 6	60			100	0
19	0	9172.8896	4 2 3	3 1 3	6			1	0
18	0	9172.7529	9 4 5	8 2 6	10			1	0
19	0	9178.3507	4 3 1	3 2 2	20			100	0
18	0	9181.1781	7 4 4	6 2 5	29			100	0
18	0	9181.4807	5 5 1	4 3 2	7			100	0
		9184.1744			5			100	
19	0	9185.9175	5 3 3	4 2 2	15			100	0
18	0	9192.9583	8 2 6	7 0 7	11			100	0
		9193.6964			5			100	
18	0	9197.7942	6 5 1	5 3 2	10			100	0
19	0	9198.7448	6 3 4	5 2 3	25			100	0
19	0	9205.5366	4 4 1	3 3 0	64			100	0
19	0	9205.7561	4 4 0	3 3 1	29			100	0
19	0	9206.0944	7 3 5	6 2 5	5			1	0
19	0	9207.8700	5 3 2	4 2 3	34			100	0
18	0	9211.7401	7 5 2	6 3 3	9			10	0
19	0	9219.8520	5 2 3	4 1 4	14			100	0
18	0	9221.8964	8 5 3	7 3 4	10			1	0
18	0	9222.2478	8 5 3	6 3 4	13			100	0
19	0	9227.6997	5 4 1	4 3 2	20			100	0
19	0	9229.2919	5 4 1	4 3 2	46			100	0
18	0	9237.8018	10 5 5	9 3 6	7			100	0
19	0	9241.5674	6 3 3	5 2 4	4			1	0
18	0	9241.5674	10 3 7	9 1 8	4			0	0
		9242.1965			4			1	
		9242.1972			4			1	
18	0	9246.8544	8 5 4	7 3 5	5			1	0
19	0	9247.4971	6 4 3	5 3 2	34			100	0
18	0	9251.2366	6 4 2	5 3 3	10			100	0
19	0	9253.5810	6 4 2	5 3 3	13			100	0
		9253.8425			5			100	
19	0	9257.0865	5 5 0	4 4 1	61			10	0
19	0	9257.0865	5 5 1	4 4 0	61			0	0
18	0	9260.9210	9 3 7	8 1 8	6			100	0
19	0	9263.4294	7 4 4	6 3 3	6			100	0
18	0	9272.2696	7 5 3	6 3 4	10			10	0
19	0	9274.6446	8 4 5	7 3 4	17			100	0
19	0	9280.0295	7 4 3	6 3 4	19			100	0
19	0	9280.8090	6 5 2	5 4 1	26			100	0
19	0	9282.0820	6 5 2	5 4 1	11			100	0
19	0	9283.9903	7 3 4	6 2 5	6			10	0
19	0	9303.1354	7 5 3	6 4 2	10			100	0
19	0	9304.4030	7 5 2	6 4 3	21			100	0
19	0	9305.4474	6 6 1	5 5 0	34			1	0
19	0	9305.4474	6 6 0	5 5 1	34			1	0
19	0	9323.1785	8 5 4	7 4 3	9			100	0
19	0	9325.1167	7 6 1	6 5 2	18			100	0
18	0	9342.6449	7 7 0	6 5 2	10			1	0
18	0	9343.6845	7 7 1	6 5 2	10			10	0
19	0	9350.3930	7 7 0	6 6 1	15			10	0
19	0	9350.3939	7 7 1	6 6 0	15			1	0
18	0	9366.6107	8 7 1	7 5 2	10			100	0

TABLE II

Energies (cm^{-1}) of the Rotational Levels for the Vibrational States (130), (031), (210), (111), (012), of $H_2{}^{16}O$[a]

			130		031		210		111		012	
0	0	0	8273.9773	4.4	8373.0603	4.4	8761.5792	4.4	8807.0010	3.9	9000.1402	4.4
1	0	1	8277.3796	3.1	8397.4830	3.1	8784.0558	3.1	8830.2312	2.0	9023.4019	3.1
1	1	1	8323.2928	3.4	8421.1844	3.1	8788.8337	2.3	8844.5359	1.2	9037.1983	3.0
1	1	0	8329.3609	3.1	8427.2637	3.1	8805.1568	3.1	8850.1080	3.1	9042.8439	2.7
2	0	2	8383.1850	2.9	8443.6836	2.9	8823.5288	3.0	8875.3083	1.8	9066.7813	3.4
2	1	2	8384.0504	2.2	8452.4572	2.5	8840.2777	6.1	8885.2066	1.7	9076.2809	3.1
2	1	1	8392.2364	3.1	8480.4370	2.5	8850.1708	3.1	8903.4987	1.6	9095.1801	2.5
2	2	1	8458.9658	3.1	8548.2845	3.1	8932.8358	3.1	8984.5342	1.8	9135.8415	2.4
2	2	0	8457.7039	2.5	8551.0218	3.0	8982.8982	3.1	8985.9637	1.8	9137.2954	3.4
3	0	3	8829.0012	2.9	8910.3702	3.1	9439.0325	3.1	8930.9827	2.2	9133.5830	2.9
3	1	3	8826.0255	2.9	8923.1118	2.5	9900.4782	4.5	8965.8598	1.9	9139.0860	3.0
3	1	2	8860.7838	2.5	8960.1832	2.5	8933.2035	4.4	8979.8738	2.5	9172.5037	2.5
3	2	2	8927.3272	3.1	8970.9527	2.2	8998.5588	2.9	9018.0205	1.9	9205.9008	2.2
3	2	1	8932.1365	3.1	8975.7357	2.2	9003.3368	2.9	9023.8171	1.9	9210.6670	2.5
3	3	1	8980.0428	3.4	8746.4252	2.8	9057.7603	6.7	9098.3981	1.9	9267.2101	2.9
3	3	0	8980.7358	3.4	8746.4899	2.8	9057.8223	2.4	9098.4084	2.5	9267.4380	2.9
4	0	4	8828.8711	2.5	8990.4853	2.4	3976.2935	2.5	9022.3352	1.9	9218.1858	2.5
4	1	4	8508.3887	2.5	8803.4868	4.1	8979.8505	2.5	9025.1514	2.4	9218.8589	2.9
4	1	3	8583.8702	4.8	8868.1068	2.4	8933.1188	3.1	8979.5108	1.6	9223.2371	2.5
4	2	3	8731.6623	2.5	8716.4727	2.5	8991.3614	2.8	9105.4278	2.1	9288.2882	3.0
4	2	2	8x.3.0088	2.5	8718.4727	2.5	8991.3614	2.8	9121.1535	2.7	9288.2882	3.0
4	3	2	8758.5328	2.8	8843.2414	2.4	9152.8041	2.4	9193.5218	2.7	9383.1149	2.9
4	3	1	8757.1324	3.0	8884.0888	2.4	9153.9803	2.4	9194.5308	1.6	9384.0525	3.2
4	4	1	8829.6461	3.0	8928.5844	2.4	9268.3198	4.4	9305.4078	1.6	9490.0935	2.5
4	4	0	8829.6 12	4.4	8928.5972	3.8			9305.5177	1.6	9490.0951	3.1
5	0	5	8508.8040	3.1	8837.4038	3.1	8973.1081	3.0	9121.7439	2.3	9318.1913	3.1
5	1	5	8802.7902	3.1	8702.4849	3.1	8977.1602	2.7	9121.9877	2.7	9318.2867	3.1
5	1	4	8838.1884	2.5	8741.0025	3.4	8158.1503	2.7	9230.0872	2.5	9384.9735	2.5
5	2	4	87.5.0885	2.5	8830.1738	2.2	9173.5732	6.7	9218.0416	1.6	9411.6330	2.7
5	2	3	8761.0008	2.5	8858.9305	2.2	9028.0525	3.1	9219.8539	1.9	9481.0148	2.5
5	3	3	8878.5382	2.5	8958.3305	2.5	9028.0525	3.1	9260.2838	1.9	9481.0148	2.5
5	3	2	8878.5771	3.5	8967.0971	4.1	9275.0853	3.1	9316.3083	1.9	9508.2306	2.5
5	4	2			9127.2563	2.5			9428.3703	1.6	9511.5430	3.6
5	4	1	9257.2230	3.1	9128.0890	2.5			9428.5665	1.5	9511.8005	2.5
5	5	1			9328.1049	4.7			9563.9955	1.4	9765.1889	2.9
6	0	6	8715.9734	4.1	8817.2438	3.1	9192.1531	13.7	9238.3301	1.7	9432.8197	3.0
6	1	6	8719.4058	2.9	8819.0620	3.1	9192.6302	3.8	9238.8775	1.6	9433.5066	2.2
6	1	5	8817.4772	3.1	8918.0839	3.4			9280.9730	1.6	9535.4284	3.1
6	2	5	8870.9849	2.9	8950.7863	3.1	9320.1287	2.9	9350.9674	1.5	9585.3715	2.2
6	2	4	8981.0708	13.7	9014.2706	2.5			9392.9025	1.6	9588.1927	2.2
6	3	4	9021.0687	2.7	9100.0810	2.2	9418.2541	2.1	9482.7704	1.5	9683.2880	2.5
6	3	3			9110.8796	2.5	9423.0824	13.7	9485.1056	1.7	9687.7762	13.7
6	4	3	9195.1863	13.7	9273.0251	2.9	9529.0768	4.4	9587.3072	2.1	9788.3094	3.0
6	4	2			9273.0251	2.9			9588.2110	1.7	9787.9568	2.9
6	5	2	9402.2322	2.4	9470.2024	2.9			9706.6003	1.5	9891.1512	2.9
6	5	1			9470.0538	2.1			9706.6041	1.5	9891.1921	3.1
6	6	1			9692.4809	2.7			9871.1654	2.1	10047.5235	2.7
6	6	0			9692.4918	5.5			9871.1654	2.1	10047.5206	13.7
7	0	7	8851.0539	3.1	8953.4288	2.9	9325.4601	3.1	9372.2070	2.5	9568.8053	3.1
7	1	7	8851.0113	3.1	8954.7127	3.8	9325.1122	7.7	9372.6791	1.9	9568.8930	4.1
7	1	6	9001.7539	4.2	9104.2240	3.1	9451.2791	13.7	9497.9818	1.9	9702.2702	3.1
7	2	6			9123.5037	3.1	9451.9871	7.7	9503.2881	1.9	9700.5289	3.5
7	2	5	9097.9145	3.8	9190.0717	7.7			9584.8901	2.1	9776.2821	3.0
7	3	5			9270.0900	4.1	9567.7702	3.8	9615.9858	1.7	9805.7808	3.8
7	3	4			9270.3600	4.1			9615.9858	1.7	9805.7808	3.8
7	4	4			9463.3877	3.0			9738.0008	1.6	9926.9702	3.1
7	4	3	9368.5000	13.7	9465.1638	7.7			9737.1063	2.1	9929.0155	2.9
7	5	3	9572.0515	2.5	9662.0192	4.1			9873.2298	1.5	10060.9193	3.1
7	5	2			9662.0192	4.1			9873.2815	1.5	10061.1218	3.1
7	6	2			9863.1290	4.7	9842.8384	9.7	10037.1241	1.8	10231.9132	3.1
7	6	1			9863.1503	13.7			10037.1248	4.8	10231.9133	3.8
7	7	1			10105.2904	7.7			10232.2935	2.4	10305.4570	13.7
7	7	0			10105.2904	13.7			10232.2935	2.4	10305.4517	7.7
8	0	8	9006.7208	4.4	9108.7078	3.0	9478.3614	4.5	9523.4770	1.7	9718.1985	3.7
8	1	8	9006.2325	4.4	9107.2178	3.1	9478.6921	3.1	9523.6795	1.7	9718.5372	4.1
8	1	7	9188.7016	7.7	9288.1887	3.1			9573.4853	1.7		
8	2	7	9203.1071	3.1	9290.7728	3.1	9628.3863	7.7	9674.2183	3.0	9868.3053	2.9
8	2	6			9405.0698	3.1			9772.2065	1.9		
8	3	6			9405.0537	3.1	9753.9269	4.5	9800.4003	1.9	9995.3733	3.1
8	3	5			9490.0454	2.5			9868.5303	2.1		
8	4	5							9924.1815	2.1	10116.9933	3.1
8	4	4			9644.2291	13.7			9932.9911	1.5	10254.4153	3.1
8	5	4			9837.4377	2.5			10083.8749	1.9		
8	5	3							10084.2817	1.9		
8	6	3			10057.6604	3.1			10227.1594	2.2	10404.0925	7.7
8	6	2			10300.3398	13.7			10227.0275	1.9		
8	7	2			10300.5398	8.7			10426.4300	2.0		
8	7	1							10426.7 100	2.0		
8	8	1							10660.0601	2.1		
8	8	0							10650.0801	2.1		
9	0	9	9178.6967	4.4	9277.2107	3.1	9864.6817	7.7	9892.2202	1.7	9887.9602	4.4
9	1	9	9178.8249	4.4	9277.4787	3.1	9864.8167	7.7	9892.6008	1.7	9887.7519	4.4
9	1	8			9487.0402	3.1	9814.7708	13.7	9981.6329	2.0	10058.7981	3.1
9	2	8			9494.8834	3.1			9981.8540	2.0	10058.4787	9.7
9	2	7							9992.0765	2.2		
9	3	7			9678.3777	2.8			10005.0809	1.7		
9	3	6							10074.6895	2.2		
9	4	6							10138.8380	2.2		
9	4	5							10138.8758	6.7		
9	5	5							10278.3741	1.8		
9	5	4							10279.8548	3.0	10473.8535	3.8
9	6	4							10441.1731	1.8		
9	6	3							10660.8301	1.8		
9	7	3							10663.9116	1.6		
9	7	2							10663.9166	2.6		
9	8	2							10159.1300	2.0		
9	8	1							10159.1026	2.5		

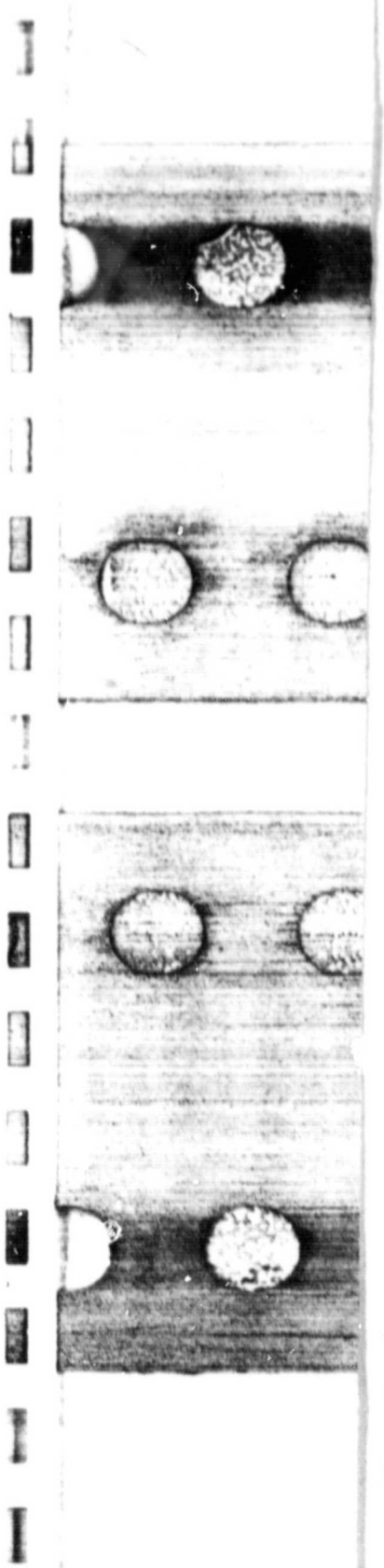

TABLE II—*Continued*

			130		031		210		111		012	
10	0	10			9465.0067	3.1			9878.8033	2.0	10074.3509	7.7
10	1	10					9830.8424	13.7	9877.8116	2.2	10074.4590	4.4
10	1	9							10068.8783	1.7		
10	2	9					10024.6995	13.7	10068.0852	3.2		
10	2	8			9872.5978	3.1			10224.7803	1.7		
10	3	8	9884.1735	3.1			10217.8216	3.1	10229.0228	2.0		
10	3	7							10320.6766	1.9		
10	4	7					10338.2134	3.0	10371.1895	2.2		
10	4	6							10404.6785	1.5		
10	5	6							10516.2311	3.0		
10	5	5							10520.7198	2.2		
10	6	5										
10	6	4							10678.4300	1.4		
10	7	4							10884.5511	6.2		
10	7	3							10884.5611	1.8		
10	8	3							11101.4461	2.1		
10	8	2							11101.4461	2.1		
11	0	11					10033.0368	13.7	10081.4128	5.7		
11	1	11			9673.0490	6.7			10081.4199	2.3		
11	1	10							10294.5809	2.3		
11	2	10							10292.3490	1.7		
11	2	9							10467.6181	2.6		
11	3	9							10471.3833	1.9		
11	3	8										
11	4	8							10626.2573	1.7		
11	4	7										
11	5	7							10776.7348	2.0		
11	5	6										
11	6	6							10940.8063	1.6		
11	6	5										
11	7	5							11148.8318	1.5		
11	7	4										
11	8	4							11366.7813	2.4		
11	8	3							11366.7858	3.3		
12	0	12			9892.8635	7.7			10301.7397	1.8		
12	1	12							10301.4562	2.1		
12	1	11							10532.2571	1.8		
12	2	11							10533.7093	2.3		
12	2	10							10731.0768	1.8		
12	3	10							10731.5106	2.1		
12	3	9							10887.6173	2.3		
12	4	9										
12	4	8							10981.4963	1.8		
12	5	8										
12	5	7							11078.8781	2.0		
12	6	7										
12	6	6							11224.9451	1.6		
12	7	6										
12	7	5										
12	8	5										
12	8	4							11654.8053	5.8		
13	0	13							10539.7870	3.1		
13	1	13							10539.7897	1.7		
13	1	12							10791.4120	5.4		
13	2	12							10789.7624	1.8		
13	2	11							11004.1858	2.1		
13	3	11							11009.0592	1.8		
13	3	10										
13	4	10							11194.8327	2.0		
13	4	9										
13	5	9										
13	5	8										
13	6	8							11532.6720	1.7		

[a] To the right of each energy level (in cm^{-1}) the statistical uncertainty (68% confidence interval in 10^{-3} cm^{-1}) is given. Additional level appearing through perturbation: (060) [616] 9400.6409 2.4.

Particular attention was paid to lines originating from resonant levels which, as already mentioned, are quite numerous.[1] In general, perturbed lines were located by considering strong lines which cannot be attributed to normal lines of the strongest band, $\nu_1 + \nu_2 + \nu_3$. Among these perturbations are two interesting examples:

—The perturbation between the levels (210)[221] and (111)[211] leads to doublets of lines of nearly equal intensity, instead of the usual single lines belonging to the strongest *A*-type band $\nu_1 + \nu_2 + \nu_3$ (*10*).

—An extreme example of resonance is the quadruple resonance between the levels (060)[616], (130)[652], (210)[634], and (111)[624]. In this case, the labeling of the levels will be definitive only when a theoretical calculation provides the mixing coefficients. It may be emphasized that the $6\nu_2$ band appears only through lines originating in the perturbed level (060)[616]; this behavior is similar to that of the

[1] These resonances can be classified for the hexad of the vibrational states {(050), (130), (031), (210), (111), (012)} under study as follows: Coriolis-type interactions between $(v_1\ v_2\ v_3)$ and $(v_1 - 1\ v_2\ v_3 + 1)$; $(v_1 v_2 v_3)$ and $(v_1 v_2 - 2 v_3 + 1)$; Fermi-type interaction between $(v_1 v_2 v_3)$ and $(v_1 - 1 v_2 + 2 v_3)$; and Darling–Dennison-type interaction between $(v_1\ v_2\ v_3)$ and $(v_1 - 2\ v_2\ v_3 + 2)$.

$4\nu_2$ band, in the 1.4-μm region, which appears only through lines originating in the perturbed level (040)[945], (*14*).

Because of the large value of the $P \times L$ product for the heated spectrum, we have been able to detect lines belonging to the "hot" band $\nu_1 + 2\nu_2 + \nu_3 - \nu_2$ (relative intensity compared to $\nu_1 + \nu_2 + \nu_3 \simeq 0.2\%$) and lines belonging to the $\nu_1 + \nu_2 + \nu_3$ band of $H_2{}^{18}O$ (relative isotopic abundance $\simeq 0.2\%$). The assignment of this band of $H_2{}^{18}O$ has been facilitated by knowledge of the ground state of $H_2{}^{18}O$ (*15*, *16*). The complete list of the transitions with their assignments and the percent absorption at the center of the lines is given in Table I. From these lines and from the ground-state energy levels, we deduced the vibration–rotation energy levels of the upper states, which are given in Table II.

Since the rotational levels of the (111) vibrational state were obtained previously from the study of a flame spectrum (*13*), we combined the data originating from the latter work and the present study to obtain what we consider to be the most reliable set of rotational energy levels for this state. In the present work, we did not observe lines involving high rotational quantum numbers, and, therefore, we limited the levels listed in Table II to $J \leq 13$. Reference (*13*) gives the information for $J > 13$ of the (111) state.

ACKNOWLEDGMENTS

The authors wish to thank Professor W. S. Benedict for valuable comments about this paper. One of us (K.N.R.) expresses his gratitude to the Atmospheric Research Section of the National Science Foundation and the National Aeronautics and Space Administration for the support provided for this investigation.

RECEIVED: May 19, 1978

REFERENCES

1. W. S. BENEDICT AND R. F. CALFEE, ESSA Prof. Paper 2, 1967.
2. C. CAMY-PEYRET AND J.-M. FLAUD, *Mol. Phys.* **32**, 523–537, (1976).
3. J.-M. FLAUD, C. CAMY-PEYRET, J.-Y. MANDIN, AND G. GUELACHVILI, *Mol. Phys.* **34**, 413–426, (1977).
4. D. M. GATES, R. F. CALFEE, D. W. HANSEN AND W. S. BENEDICT, *Nat. Bur. Stand. (U. S.) Monogr.* **71**, 1964.
5. J.-M. FLAUD AND C. CAMY-PEYRET, *J. Mol. Spectrosc.* **55**, 278–310, (1975).
6. L. A. PUGH, Ph.D. dissertation, The Ohio State University, 1972.
7. C. CAMY-PEYRET, J.-M. FLAUD, AND R. A. TOTH, *J. Mol. Spectrosc.* **67**, 117–131, (1977).
8. R. A. TOTH AND J. S. MARGOLIS, *J. Mol. Spectrosc.* **55**, 229–251, (1975).
9. C. CAMY-PEYRET AND J.-M. FLAUD, Thèse, CNRS, AO 11443, Université Pierre et Marie Curie, Paris, 1975.
10. W. S. BENEDICT, *Phys. Rev.* **74**, 1246–1247, (1948); J. W. SWENSSON, W. S. BENEDICT, L. DELBOUILLE, AND G. ROLAND, *Mem. Soc. Roy. Sci. Liège, Vol. Hors Ser.*, No. 5, **8**, 1970.
11. B. D. ALPERT, Ph.D. dissertation, The Ohio State University, 1970.
12. J.-M. FLAUD, C. CAMY-PEYRET, AND J.-P. MAILLARD, *Mol. Phys.* **32**, 499–521, (1976).
13. C. CAMY-PEYRET, J.-M. FLAUD, J.-P. MAILLARD, AND G. GUELACHVILI, *Mol. Phys.* **33**, 1641–1650, (1977).
14. W. S. BENEDICT, M. A. POLLACK, AND W. J. TOMLINSON, *IEEE J. Quantum Electron.* **5**, 108–124, (1969).
15. R. A. TOTH, J.-M. FLAUD, AND C. CAMY-PEYRET, *J. Mol. Spectrosc.* **67**, 185–205, (1977).
16. J.-M. FLAUD, C. CAMY-PEYRET, AND R. A. TOTH, *J. Mol. Spectrosc.* **68**, 280–287, (1977).

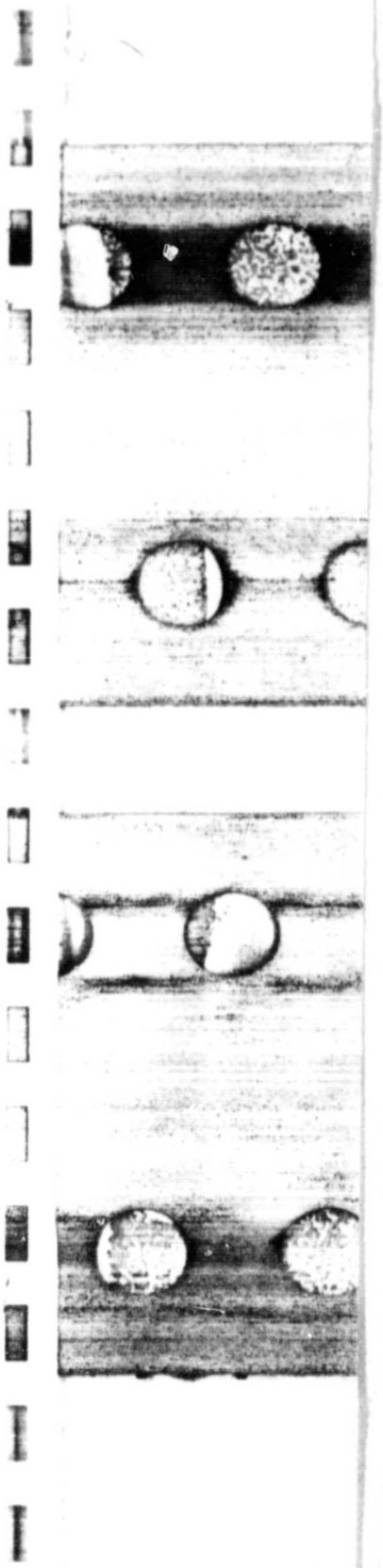

JOURNAL OF MOLECULAR SPECTROSCOPY 77, 156–159 (1979)

Interpretation of Diode Laser Spectra of Ozone at 14 μm: (010) and (020) States of Ozone

Introduction. In the present investigation, ozone spectra at different wavenumber intervals have been recorded in the 14-μm region with a resolution of about 0.002 cm^{-1} using a tunable diode laser. As may be noticed from Fig. 1, which gives a reproduction of a small portion of the spectrum, the structure is well resolved. Almost all the observed lines have now been assigned to the ν_2 fundamental and to the associated "hot" band $2\nu_2-\nu_2$ of ozone.

ν_2 band lines of ozone. In interpreting the diode laser spectra, use has been made of the molecular constants reported recently by Monnanteuil *et al.* (*1*) for the (010) state of ozone. A synthetic spectrum of the ν_2 band of ozone has been calculated according to the method suggested in Ref. (*2*). Seventy-eight transitions belonging to the ν_2 band have thus been assigned, and their wavenumbers together with these assignments are given in Table I. This study has given a value for the ν_2 band center as $\nu_0 = 700.9316 \pm 0.0030$ cm^{-1}, which is in good agreement with the value of 700.933 ± 0.005 cm^{-1} suggested in Ref. (*1*).

$2\nu_2-\nu_2$ band lines. Using the rotational constants of Ref. (*1*) and an estimated band center, we have calculated a synthetic spectrum of the $2\nu_2-\nu_2$ band. As the uncertainty in the estimated band center is almost as large as the spectral range of the diode laser spectra (the extension of which is typically 1 cm^{-1}), it was not readily possible to match the calculated spectrum with the weak unassigned lines of the diode laser spectra. By trial and error, we finally succeeded in assigning 34 lines in the regions studied to the $2\nu_2-\nu_2$ band, and these data are also presented in Table I. Combining these data with the 10 microwave transitions observed in the (020) state (*1*, *3*), a least-squares fit was performed, and the rotational constants thus obtained are given in Table II. For this calculation the sextic centrifugal coefficients have been extrapolated from the values relative to the (000) and (010) states. This procedure seems to be better than fixing the values of the sextic coefficients for the (020) state to those of the ground state. The agreement between the observed microwave transitions as well as that between the observed and calculated energy levels for the (020) state is close, as can be seen from Table III.

Discussion. As a result of the above analysis, it has become possible to locate for the first time

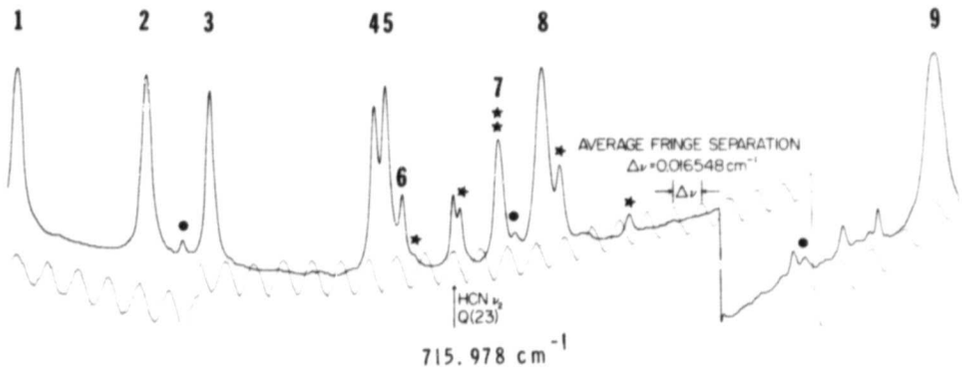

FIG. 1. A sample spectrum of ozone at 14 μm obtained with a tunable diode laser spectrometer. Lines with asterisks are due to the $2\nu_2-\nu_2$ band and the numerals 1 to 9 are used to locate conveniently the corresponding lines in Table I. Filled circles indicate unassigned lines.

0022-2852/79/080156-04$02.00/0

TABLE I

Wavenumbers (cm^{-1} -vac) and Assignments for Some of the Ozone Lines at 14 μm

OBS.	CALC.	J'	K'_a	K'_c	J''	K''_a	K''_c			OBS.	CALC.	J'	K'_a	K'_c	J''	K''_a	K''_c			
683.0760	.076	26	6	20	25	7	19	ν_2		704.9286	.931	1	1	1	0	0	0	ν_2		
.1386	.144	16	0	16	17	1	17		$2\nu_2-\nu_2$	.9318	.934	5	2	4	6	1	5	ν_2		
.1916	.197	41	8	34	40	9	31	ν_2		.9747	.977	16	1	15	15	2	14		$2\nu_2-\nu_2$	
	.189	23	5	19	22	6	16		$2\nu_2-\nu_2$	.9814	.982	8	0	8	7	1	7	ν_2		
.2405	.240	23	1	23	23	2	22	ν_2		705.0143	.015	8	1	7	8	0	8	ν_2		
.2772	.279	30	1	29	30	2	28		$2\nu_2-\nu_2$	.0412	.047	41	4	38	40	5	35	ν_2		
.3087	.308	19	5	15	18	6	12	ν_2		.0645										
.3261	.325	5	1	5	6	2	4		$2\nu_2-\nu_2$	.0880										
.3419										.1015	.095	41	7	35	42	6	36 ?	ν_2		
.3544										.2021	.207	34	6	28	35	5	21	ν_2		
.3628										.2055										
.3685	.370	21	2	20	21	3	19	ν_2		.2197										
.4563	.458	6	1	5	7	2	6		$2\nu_2-\nu_2$	.2483	.250	20	4	16	21	3	19	ν_2		
.4772	.479	26	0	26	26	1	25	ν_2		.3242	.326	5	1	5	4	0	4		$2\nu_2-\nu_2$	
.4998	.501	23	2	22	24	1	23	ν_2		.3499										
.5070	.508	12	4	8	11	5	7	ν_2		.3579	.358	6	2	4	7	1	7	ν_2		
.5377	.541	34	7	27	33	8	26	ν_2		.4934	.493	14	1	13	13	2	12	ν_2		
.5442	.545	21	2	20	22	1	21		$2\nu_2-\nu_2$	.5021	.501	10	3	7	11	2	10		$2\nu_2-\nu_2$	
.5581	.558	10	1	9	11	2	10	ν_2			.510	45	5	41	45	6	40	ν_2		
.5875	.588	16	4	12	15	5	11		$2\nu_2-\nu_2$	.5598	.560	10	1	9	10	0	10	ν_2		
.6237	.624	18	2	16	18	3	15		$2\nu_2-\nu_2$	.5847	.585	17	4	14	18	3	15		$2\nu_2-\nu_2$	
.6430										.6091										
.6725										.6196										
.6786	.678	5	3	3	4	4	0	ν_2		.6233										
.8370	.836	27	6	22	26	7	19	ν_2		.7030	.702	19	4	16	20	3	17	ν_2		
	.840	34	2	32	34	3	31		$2\nu_2-\nu_2$	.8356	.833	16	1	15	16	0	16		$2\nu_2-\nu_2$	
.9078	.906	19	2	18	19	3	17	ν_2												
.9224	.920	7	1	7	8	2	6	ν_2		715.1221	.120	9	4	6	10	3	7	ν_2		
										.1832										
696.1343	.131	20	3	17	19	4	16	ν_2		.2353	.233	31	7	25	32	6	26	ν_2		
.1615	.160	5	1	5	6	0	6		$2\nu_2-\nu_2$	.2412	.239	28	1	27	28	0	28		$2\nu_2-\nu_2$	
.2456	.245	25	3	23	24	4	20		$2\nu_2-\nu_2$	.2471										
.2539	.253	25	1	25	24	2	22	ν_2		.2666	.264	21	3	19	21	2	20		$2\nu_2-\nu_2$	
.2856	.283	13	1	13	12	2	10		$2\nu_2-\nu_2$	.2920	.298	50	4	46	50	3	47	ν_2		
.3247	.321	8	1	7	7	2	6		$2\nu_2-\nu_2$	.3107										
.3655	.366	27	4	24	28	3	25	ν_2		.4459										
.4113	.412	28	4	24	27	5	23	ν_2		.4626	.464	42	3	39	42	2	40	ν_2		
.4273	.427	21	3	19	20	4	16	ν_2		.4747										
.4567										.5092	.508	25	2	24	25	1	25		$2\nu_2-\nu_2$	
.5918	.592	7	1	7	6	2	4	ν_2		.5437	.542	16	3	13	16	2	14	ν_2		
.6066	.610	36	5	31	35	6	30	ν_2		.5637										
.6619	.661	8	0	8	8	1	7	ν_2		.5924	.591	16	5	11	17	4	14	ν_2		
.6898	.689	7	1	7	8	0	8	ν_2			.591	23	3	21	23	2	22		$2\nu_2-\nu_2$	
.6976	.700	19	2	18	18	3	15		$2\nu_2-\nu_2$	.6407										
.7088	.715	44	6	38	43	7	37	ν_2		.6877	.686	11	2	10	10	1	9		$2\nu_2-\nu_2$	
701.4894	.490	38	3	35	39	2	38	ν_2		.7018	.703	38	4	34	38	3	35	ν_2		
.5094	.499	50	6	44	49	7	43 ?	ν_2		.7107	.709	20	0	20	19	1	19	ν_2		S.No.*
.5566	.554	16	2	14	17	1	17	ν_2		.7309	.729	21	2	20	21	1	21	ν_2		1
.6038	.606	18	2	16	19	1	19	ν_2		.8008	.799	7	2	6	6	1	5	ν_2		2
.6210	.624	18	3	15	19	2	18	ν_2		.8201										
.6548	.657	2	1	1	2	0	2		$2\nu_2-\nu_2$	.8358	.836	26	1	25	26	0	26	ν_2		3
.6939	.701	42	5	37	41	6	36	ν_2		.9314	.932	34	2	32	34	1	33	ν_2		4
	.699	43	5	39	42	6	36	ν_2		.9384	.937	6	2	4	5	1	5	ν_2		5
.7203	.720	24	4	20	25	3	23	ν_2		.9479	.947	23	6	18	24	5	19	ν_2		6
.7703	.771	29	2	28	28	3	25	ν_2		.9540	.955	21	6	16	22	5	17		$2\nu_2-\nu_2$	
.7963	.797	25	2	24	24	3	21	ν_2		.9821	.982	26	1	25	25	2	24		$2\nu_2-\nu_2$	
.8038	.804	14	2	12	15	1	15	ν_2												
.8212	.823	4	1	3	4	0	4		$2\nu_2-\nu_2$	716.0060	.005	8	4	4	9	3	7	ν_2		7
.8252	.827	29	3	27	28	4	24	ν_2			.004	23	1	23	22	0	22		$2\nu_2-\nu_2$	
.8488	.850	18	2	16	17	3	15	ν_2			.006	25	3	23	25	2	24		$2\nu_2-\nu_2$	
.8629	.866	34	4	30	33	5	29	ν_2		.0163										
	.877	37	6	32	38	5	33	ν_2		.0319	.029	14	3	11	14	2	12	ν_2		8
.9499	.951	27	2	26	26	3	23	ν_2		.0426	.041	24	0	24	23	1	23		$2\nu_2-\nu_2$	
.9608	.963	20	2	18	21	1	21	ν_2		.0841	.084	32	4	28	32	3	29		$2\nu_2-\nu_2$	
.9673	.968	26	3	23	25	4	22	ν_2		.1773	.190	52	4	48	52	3	49	ν_2		
										.2054	.210	30	7	23	31	6	26	ν_2		
702.0035	.004	15	3	13	16	2	14	ν_2		.2200										
.0983	.099	6	1	5	7	0	6		$2\nu_2-\nu_2$	.2550	.256	19	1	19	18	0	18	ν_2		9
.2549										.3314	.332	32	2	30	31	3	29		$2\nu_2-\nu_2$	
										.3689	.371	37	8	30	38	7	31	ν_2		
											.376	46	4	42	45	5	41	ν_2		
										.4085	.408	12	3	9	12	2	10	ν_2		

*These serial numbers correspond to the ones in Fig. 1.

the vibrational energy $E_{(020)}$ for the (020) state of ozone. The value obtained is $E_{(020)} = 1399.2744 \pm 0.0035\ cm^{-1}$.

From the two vibrational energy values $E_{(010)}$ and $E_{(020)}$ obtained here, the value of x_{22} is obtained using the relation $2x_{22} = E_{(020)} - 2E_{(010)}$ as $x_{22} = -1.294 \pm 0.006\ cm^{-1}$, which compares reasonably well with the value $x_{22} = -1.0\ cm^{-1}$ obtained in Ref. (*4*).

TABLE II

Rotational Constants for the (020) Vibrational State of O_3

E_v	1399.2743_6 ± 0.0035	δ_J^v	$(0.68458_9$ ± 0.00097) x 10^{-7}
A^v	3.66240909_2 ± 0.0000057	H_K^v	0.52703 x 10^{-7}
B^v	0.44274491_9 ± 0.00000076	H_{KJ}^v	-0.2098 x 10^{-8}
C^v	0.39007248_5 ± 0.00000026	H_{JK}^v	-0.6004 x 10^{-11}
Δ_K^v	$(0.25660_6$ ± 0.00069) x 10^{-3}	H_J^v	0.3669 x 10^{-12}
Δ_{JK}	$(-0.1792_0$ ± 0.0034) x 10^{-5}	h_K^v	0.2902 x 10^{-8}
Δ_J^v	$(0.4574_2$ ± 0.0012) x 10^{-6}	h_{JK}^v	-0.6004 x 10^{-11}
δ_K^v	$(0.4583_9$ ± 0.0013) x 10^{-5}	h_J^v	0.2035 x 10^{-12}

The quoted errors are one standard deviation.

The sextic coefficients have been extrapolated from the values relative to the (000) and (010) states of Ref. [1].

TABLE III

Agreement between Observation and Calculation for the (020) State of Ozone

Microwave Transitions

J'	K_a'	K_c'	J	K_a	K_c	OBS (in MHz)	OBS-CALC (in MHz)
18	3	15	19	2	18	46 326.84	0.00
1	1	1	2	0	2	46 600.95	-0.01
16	2	14	17	1	17	46 977.39	0.00
15	3	13	16	2	14	48 532.34	0.00
14	2	12	15	1	15	49 041.20	-0.03
18	2	16	19	1	19	54 725.88	0.01
12	2	10	13	1	13	60 443.46	0.04
6	0	6	5	1	5	63 115.29	0.01
7	2	6	8	1	7	64 381.84	0.00
12	1	11	11	2	10	66 210.13	0.00

Infrared levels

J	K_a	K_c	OBS (in cm^{-1})	OBS-CALC (in cm^{-1})
2	1	1	1405.0951	-0.0024
4	1	3	1411.1079	-0.0018
5	1	5	1414.6135	0.0007
6	1	5	1420.5506	-0.0009
8	1	7	1433.4184	0.0036
11	2	10	1467.1482	0.0018
13	1	13	1475.7092	0.0029
16	0	16	1510.7506	-0.0050
16	1	15	1518.7821	0.0003
16	4	12	1564.5287	-0.0005
17	4	14	1578.7103	-0.0008
18	2	16	1556.7493	-0.0002
19	2	18	1569.8232	-0.0023
21	2	20	1603.6494	-0.0007
21	3	19	1621.2083	0.0026
24	0	24	1642.3163	0.0019
25	2	24	1680.9773	0.0015
26	1	25	1699.6124	0.0001
28	1	27	1745.2668	0.0019
30	1	29	1793.9980	-0.0019
32	2	30	1861.3107	-0.0006
32	4	28	1892.8885	-0.0001

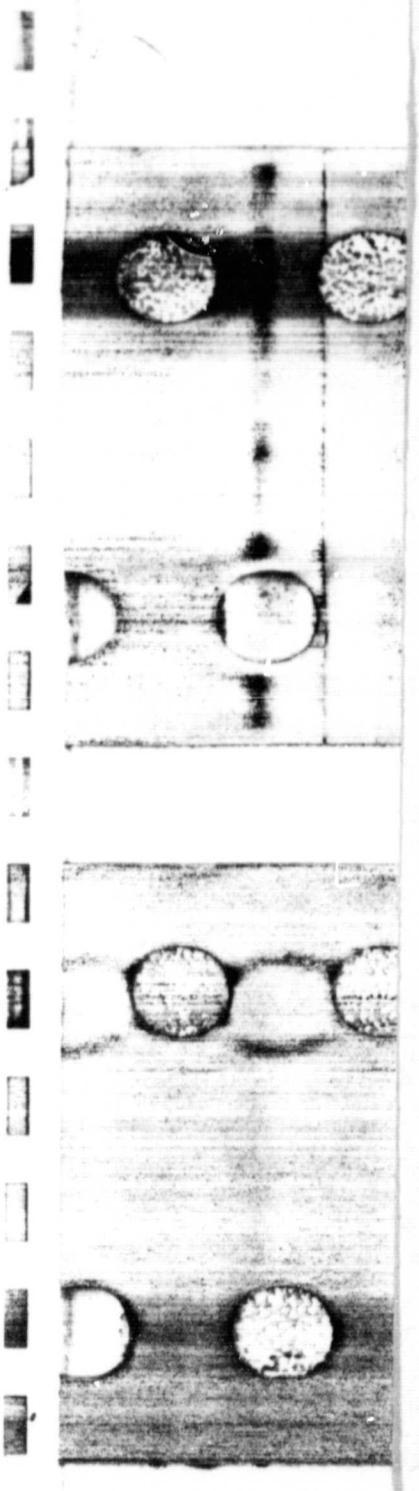

ACKNOWLEDGMENT

One of us (K.N.R.) expresses his gratitude for the support extended to this research by the National Aeronautics and Space Administration.

REFERENCES

1. N. Monnanteuil, J. C. Depannemaecker, J. Bellet, A. Barbe, C. Secroun, P. Jouve, S. Giorgianni, Y.-S. Hoh, and K. Narahari Rao, *J. Mol. Spectrosc.* **71,** 399–414 (1978).
2. C. Camy-Peyret and J.-M. Flaud, *Mol. Phys.* **32,** 523–537 (1976).
3. T. Tanaka and Y. Morino, *J. Mol. Spectrosc.* **33,** 538–551 (1970).
4. A. Barbe, C. Secroun, and P. Jouve, *J. Mol. Spectrosc.* **49,** 171–182 (1974).

V. Malathy Devi
S. P. Reddy
K. Narahari Rao

The Ohio State University
Department of Physics
Columbus, Ohio 43210

J.-M. Flaud
C. Camy-Peyret

Laboratoire de Physique Moléculaire et d'Optique Atmosphérique
C.N.R.S., Bâtiment 221,
Campus d'Orsay
91405 Orsay, France

Received October 15, 1978

JOURNAL OF MOLECULAR SPECTROSCOPY 71, 399–413 (1978)

Microwave and Infrared Study of the ν_2 State of $^{16}O_3$ and Identification of the $(\nu_3 + \nu_2) - \nu_2$ Band Lines at 10 μm

N. MONNANTEUIL, J. C. DEPANNEMAECKER, AND J. BELLET

Laboratoire de Spectroscopie Hertzienne—L.A. 249, Universite de Lille I, B. P. 36, 59650 Villeneuve d'Ascq, France

A. BARBE, C. SECROUN, AND P. JOUVE

Laboratoire de Physique Moleculaire—E. R. A., Faculte des Sciences de Reims, B. P. 347, 51100 Reims, France

AND

S. GIORGIANNI,[1] YAN-SHEK HOH, AND K. NARAHARI RAO

Department of Physics, The Ohio State University, Columbus, Ohio 43210

A study of the ν_2 state of ozone is presented both in the microwave and infrared regions. Forty observed microwave lines led to the determination of molecular parameters which allowed the calculation of the ν_2 state energy levels. One-hundred and twenty transitions of the $(\nu_3 + \nu_2) - \nu_2$ band, observed as a residual spectrum of the ν_3 band, are identified leading to the determination of the band center of the ν_2 fundamental. The interpretation of an observed spectrum of the ν_2 band which is consistent with these molecular parameters is presented.

INTRODUCTION

Ozone, a bent triatomic molecule has its three fundamental vibrations located at 701 cm^{-1} (ν_2), 1042 cm^{-1} (ν_3), and 1103 cm^{-1} (ν_1). Microwave study of the ground state (*1*) and of the two excited states ν_3 and ν_1 which are strongly coupled by a Coriolis interaction have previously allowed an analysis of the ν_3 state both in the microwave and infrared regions (*2*, *3*). In the same way, the microwave study of the ν_2 state (Section I) leads to the possibility of computing the ν_2 state energy levels. These calculated levels along with the values for the energy levels of the $(\nu_3 + \nu_2)$ state obtained from the study of the $(\nu_3 + \nu_2)$ band (*4*) have allowed the assignment of 120 transitions of the $(\nu_3 + \nu_2) - \nu_2$ band (Section II). In Section III, we present an interpretation of the ν_2 band which is consistent with the information summarized in Sections I and II.

[1] Present Address: Istituto di Chimica Organica dell 'Universita', Calle Larga S. Marta 2137, Venezia, Italy.

0022-2852/78/7113-0399$02.00/0

TABLE I

Microwave Lines in the ν_3 State (values in MHz)

	Lower State			Upper State			Calculated frequency	σ	Observed frequency	Obs.-Calc.
	J	K_{-1}	K_1	J	K_{-1}	K_1				
*	3	1	3	4	0	4	9 077.27	0.01	9 077.22	-0.05
	32	3	29	33	2	32	20 050.16	0.05	20 050.14	-0.02
	22	3	19	23	2	22	23 551.10	0.02	23 551.12	0.02
	24	3	21	23	4	20	27 947.62	0.02	27 947.60	-0.02
	17	3	15	18	2	16	28 915.19	0.02	28 915.23	0.04
	34	5	29	35	4	32	32 932.60	0.03	32 932.55	-0.05
	19	2	18	18	3	15	34 916.39	0.02	34 916.38	-0.01
	17	1	17	16	2	14	36 141.37	0.02	36 141.37	0.00
*	25	4	22	26	3	23	39 094.94	0.03	39 094.99	0.05
*	16	2	14	15	3	13	39 149.89	0.02	39 149.83	-0.06
*	15	1	15	14	2	12	39 459.17	0.02	39 459.16	-0.01
*	24	3	21	25	2	24	41 922.18	0.02	41 922.10	-0.08
*	19	1	19	18	2	16	42 427.71	0.03	42 427.79	0.08
	28	4	24	29	3	27	43 051.91	0.02	43 051.91	0.00
	25	3	23	24	4	20	43 190.86	0.02	43 190.82	-0.04
*	2	0	2	1	1	1	44 686.12	0.01	44 686.09	-0.03
	33	5	29	34	4	30	46 169.38	0.04	46 169.36	-0.02
	39	5	35	38	6	32	46 861.45	0.03	46 861.46	0.01
	28	3	25	29	2	28	51 274.31	0.03	51 274.34	0.03
	26	3	23	27	2	26	51 462.79	0.03	51 462.88	0.09
	13	1	13	12	2	10	51 913.40	0.02	51 913.37	-0.03
	41	6	36	42	5	37	54 981.47	0.05	54 981.45	-0.02
	21	1	21	20	2	18	58 385.94	0.04	58 385.92	-0.02
	8	1	7	7	2	6	58 950.79	0.02	58 950.80	0.01
	42	6	36	43	5	39	59 189.98	0.05	59 190.01	0.03
	38	5	33	37	6	32	64 861.30	0.03	64 861.26	-0.04
	5	1	5	6	0	6	65 267.06	0.02	65 266.99	-0.07
	31	4	28	30	5	25	67 701.47	0.03	67 701.46	-0.01
	11	2	10	12	1	11	71 449.28	0.02	71 449.18	-0.10
	17	2	16	16	3	13	72 473.72	0.02	72 473.66	-0.06
	11	1	11	10	2	8	72 657.43	0.02	72 657.44	0.01
	30	4	26	29	5	25	78 487.62	0.03	78 487.63	0.01
	30	4	26	31	3	29	80 191.49	0.03	80 191.46	-0.03
	2	0	2	2	1	1	97 930.66	0.02	97 930.68	0.02
	37	5	33	36	6	30	100 209.86	0.04	100 209.87	0.01
	9	1	9	8	2	6	100 582.93	0.02	100 582.92	-0.01
	19	3	17	20	2	18	100 899.89	0.03	100 899.88	-0.01
	14	2	12	13	3	11	103 150.32	0.03	103 150.39	0.07
	4	0	4	4	1	3	103 554.00	0.03	103 554.07	0.07
	29	4	26	28	5	23	119 316.35	0.03	119 316.39	0.04

* Lines measured by TANAKA and MORINO (5).

I. MICROWAVE STUDY OF THE ν_3 STATE

The pure rotational spectrum of ozone in the ν_2 state was first studied by Tanaka and Morino (*5*). They measured and assigned 17 lines with $J \leq 26$ and $K_{-1} \leq 4$. In determining the rotational constants they assumed τ_{zzzz}, τ_{zzzz}, and τ_{zzzz} to have the same values as given by Pierce (*6*) for the ground state; τ_{zzzz} was chosen to obtain the best fit of the observed with the calculated frequencies of all the 17 lines. The rotational constants thus obtained are:

$A = 108137.57 \pm 3$ MHz, $B = 13311.20 \pm 0.6$ MHz, $C = 11765.17 \pm 0.6$ MHz, with $\tau_{zzzz} = -27.245$ MHz.

In the present investigation, new measurements were made in the range 18 to 120 GHz, using a classical Stark modulation spectrometer. A modulation frequency of

TABLE II

Rotational Constants of the Ground, ν_3 and $2\nu_3$ States (Values in MHz $\times 10^x$)

CONSTANTS	x	GROUND STATE (†) Constants	σ	ν_2 STATE Constants	σ	$2\nu_2$ STATE Constants	σ
A	0	106 536.236	0.004	106 137.97	0.03	109 796.25	0.09
B	0	13 369.2548	0.0007	13 311.443	0.004	13 273.153	0.008
C	0	11 834.3613	0.0006	11 765.034	0.003	11 694.077	0.009
Δ_J	2	1.3618	0.0002	1.367	0.001	1.36	0.02
Δ_{JK}	2	-5.534	0.004	-5.45	0.03	-5.6	0.6
Δ_K	2	634.54	0.03	698.2	0.2	770	4
δ_J	2	0.20924	0.00002	0.20744	0.00009	0.205	0.001
δ_K	2	9.692	0.003	11.647	0.009	13.73	0.01
H_J	6	0.011	0.002	0.011*	-	0.011*	-
H_{JK}	6	-0.18	0.07	-0.18*	-	-0.18*	-
H_{KJ}	6	-55.1	0.5	-59	2	-55.1	-
H_K	6	1 178	7	1 379	44	1 178*	-
h_J	6	0.0053	0.0002	0.0057	0.0003	0.0053*	-
h_{JK}	6	-0.18	0.06	-0.18*	-	-0.18*	-
h_K	6	67	4	77	4	67*	-
g_K	6	0.021	0.003				

† Ref. (1)

* Fixed to the ground state value.

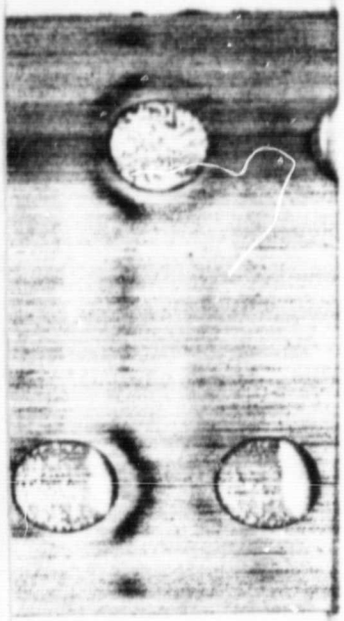

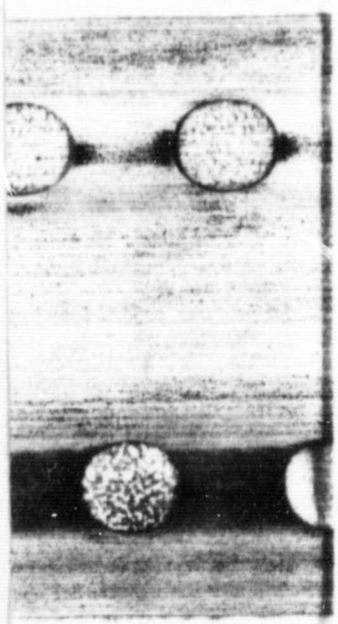

50 KHz was employed. The cell, cooled with dry ice, is a 3 m long cell in a RG 52 U guide and the source is a klystron locked by a Schommand, FDS unit.

Thirty-three lines, twenty-three of them being new and corresponding to $J \leq 43$ and $K_{-1} \leq 6$ were measured. Using a Watson-type Hamiltonian developed up to P^6 terms in angular momentum, forty transitions (Table I) were fitted by a least squares process. The molecular constants thus obtained are given in Table II. The uncertainties

TABLE III

Microwave Lines in the $2\nu_3$ State (Values in MHz)

Lower State J	K_{-1}	K_1	Upper State J	K_{-1}	K_1	Calculated Frequency	σ	Observed Frequency	Obs.-Calc.
19	2	18	18	3	15	46 326.84	0.04	46 326.84	0.00
* 2	0	2	1	1	1	46 600.96	0.03	46 600.95	-0.01
*17	1	17	16	2	14	46 977.39	0.03	46 977.39	0.00
16	2	14	15	3	13	48 532.34	0.04	48 532.34	0.00
15	1	15	14	2	12	49 041.24	0.02	49 041.20	-0.04
*19	1	19	18	2	16	54 725.88	0.04	54 725.88	0.00
13	1	13	12	2	10	60 443.43	0.03	60 443.46	0.03
5	1	5	6	0	6	63 115.28	0.03	63 115.29	0.01
8	1	7	7	2	6	64 381.84	0.04	64 381.84	0.00
11	2	10	12	1	11	66 210.14	0.04	66 210.13	-0.01

*Lines measured by Tanaka and Horino (5).

TABLE IV

Evolution of the τ_{aaaa}'s with Respect to the Quantum Number v_2 (Values in MHz)

	Ground State	v_2 State	$2v_2$ State
τ_{xxxx}	- 0.071211	- 0.07128	- 0.0708
τ_{yyyy}	- 0.037733	- 0.03809	- 0.0381
τ_{zzzz}	-25.215	-27.77	-30.6

σ for the parameters and for the calculated frequencies are also reported in Table II and Table I, respectively.

Molecular parameters are presented for the $2\nu_2$ state in Table II. These were obtained by a least squares process in which some of the constants, as indicated in Table II, were constrained to ground state values. The input data of the analysis consisted of ten lines in the $2\nu_2$ state (Table III), some of which were measured previously by Tanaka and Morino (*5*), and the remaining ones by the present experiments.

The molecular parameters of the ν_2 and $2\nu_2$ states can be compared to those of the ground state (recalled in Table II), which were obtained by fitting 107 microwave lines with $J \leq 56$ and $K_{-1} \leq 8$ (*1*). In particular, it may be pointed out that Δ_J, Δ_{JK}, and δ_J have almost the same values in these three states. On the other hand, the corresponding values of Δ_K and δ_K differ significantly. This is to be expected because the bending vibration ν_2 induces an important alteration in the value of τ_{zzzz}. In Table IV the values of τ_{aaaa} for the ground, ν_2 and $2\nu_2$ states are compared. Interestingly, the τ_{zzzz} varies almost linearly with respect to the vibrational quantum number (see also Ref. 7).

II. INFRARED STUDY OF THE $(\nu_3 + \nu_2) - \nu_2$ BAND

Ozone has taken on a new practical significance because of atmospheric considerations. In particular, the ν_3 band appears in the atmospheric window in the 10 μm region. Therefore, this band has been chosen for laboratory study. It was recorded using a SISAM spectrometer with a resolution of 0.012 cm^{-1} (*3*). About 1200 lines have been obtained with a calibration precision of 1.10^{-3} cm^{-1}. Most of these lines have been assigned to the (001) ← (000) band (*2*, *3*). As the average population in the (010) state is about 3.1% of the average population in the ground state at 296 K (experimental temperature), most of the residual spectrum can be attributed to the (011) ← (010) band.

Calculations

The spectra of the $(\nu_1 + \nu_2)$ and $(\nu_3 + \nu_2)$ bands have also been recorded with resolution of 0.017 cm^{-1} by means of the Reims-SISAM (*8*). The (011) and (110) states in Coriolis resonance have been fitted using a Watson-type Hamiltonian and the results will be published separately (*4*). From this work we have a knowledge of energy levels for the (011) state. The (010) energy levels can be derived from the rotational constants obtained by the microwave study (Section I) and the ν_2 band center, 700.93 cm^{-1}, given

by Tanaka and Morino (*9*). Thus, we can compare the observed spectrum of the "hot" band $(\nu_3 + \nu_2) - \nu_2$ with a calculated one. Most of the lines of the residual spectrum in the ν_3 region have been assigned by adopting a slightly different value for the ν_2 band center: 700.933 cm^{-1}. The uncertainty in this value is taken as the sum of the uncertainties in the $(\nu_3 + \nu_2)$ and $(\nu_3 + \nu_2) - \nu_2$ band centers (respectively, 1726.5277 ± 0.0027 cm^{-1} and 1025.594 ± 0.0018 cm^{-1}), that is 0.005 cm^{-1}.

Atlas of the $(\nu_3 + \nu_2) - \nu_2$ *Band*

Table V gives the listing of this band with calculated wavenumbers and assignments. The absolute intensities have been derived taking into account the Boltzmann factor at 296 K. Only the lines of absolute intensity larger than 0.3 cm·molecule^{-1},[2] in the range 985 to 1052 cm^{-1}, are reported. In fact, only 120 lines have been observed because several lines are blended by the ν_3 lines.

III. INFRARED STUDY OF THE ν_2 BAND

Experimental Procedure

High resolution infrared studies of the ν_2 band of ozone have been sparse because in the region where it occurs the technology progressed somewhat more slowly than elsewhere. Also, in the same region, the strong ν_2 fundamental of carbon dioxide is observed and so it is necessary to use a vacuum spectrograph to record its spectrum. In 1955, Nexsen (*10*) recorded the spectrum using a one-meter focal length Pfund-type vacuum grating spectrograph equipped with a thermocouple as a detector. Although the resolution was not very high, as mentioned in the above section, Tanaka and Morino (*9*) were able to reinterpret his data and thereby obtain a value for the band center. The present measurements also used a vacuum grating spectrograph. However, it was possible to employ a liquid helium cooled Ge:Cu detector and therefore improved results were obtained. Actually, the resolution achieved was about 0.1 cm^{-1}. The spectral positions were determined relative to the absorption standards of carbon monoxide (*11*). The ozone sample was prepared by flowing dry and pure oxygen through a silent electric discharge. The gas was condensed in a liquid nitrogen trap and the ozone concentration was increased by pumping off excess oxygen. An estimate of the concentration of ozone was made using chemical methods. Figure 1 illustrates the observed spectrum which corresponds to the data of Table VI. The ν_2 band which is a B-type band shows an irregular structure with no distinct Q branch present. The lines indicated by an asterisk[3] in Fig. 1 are due to the CO_2 present in the ozone sample because of reaction with the cell which is made out of stainless steel. Earlier measurements (*12*) of some of these CO_2 lines served as internal standards in the measurement of the ozone spectrum.

[2] Conversion factors to obtain other intensity units are available in Chapter 4 of Molecular Spectroscopy: Modern Research (K. Narahari Rao, Ed.), Academic Press (1976).

[3] These asterisks are placed below the lead marks used for indicating the serial numbers of the lines in Fig. 1. They are somewhat difficult to locate in the reduced spectrum. The extent of the CO_2 interference can be inferred from the Q-branch region of the ν_2 band at 667 cm^{-1}.

TABLE V

Wavenumbers and Assignments of the $(\nu_3 + \nu_2) - \nu_2$ Band of Ozone

Calc. wavenumber (cm^{-1})	Upper state J' K_{-1}' K_{+1}'	Lower state J'' K_{-1}'' K_{+1}''	Lower state energy $E''(cm^{-1})$	Obs. Int. 10^{-21} cm mol^{-1}	O − C (10^{-3} cm^{-1})
987.191	36 1 36	37 1 37	1 266.658	0.309	
988.606	35 1 35	36 1 35	1 262.606	0.306	
988.663	35 0 35	36 0 36	1 237.052	0.368	
989.361	34 1 33	35 1 35	1 256.733	0.302	
989.601	34 2 33	35 2 34	1 233.863	0.361	
989.877	34 1 34	35 1 35	1 258.576	0.289	
990.577	33 1 32	34 1 33	1 236.223	0.327	
990.731	33 2 31	34 2 32	1 231.637	0.349	
990.853	33 1 33	34 1 34	1 256.398	0.382	
991.106	32 0 32	33 0 33	1 180.619	1.433	
991.185	32 4 29	33 4 30	1 222.439	1.338	
991.760	32 1 30	33 1 31	1 199.227	1.378	
992.021	32 2 31	33 2 32	1 177.672	2.626	
992.100	31 1 30	32 1 31	1 222.999	0.321	
992.317	31 0 31	32 0 32	1 153.617	0.680	
992.580	31 4 27	32 4 28	1 195.695	0.370	
992.916	31 1 30	32 1 31	1 176.803	0.607	
993.096	31 2 29	32 2 30	1 166.659	0.636	
993.314	31 1 31	32 1 32	1 169.369	0.672	
993.288	30 1 30	31 1 31	1 196.096	0.351	
993.521	31 0 31	32 0 32	1 127.303	0.530	
993.760	30 4 27	31 4 28	1 167.857	0.611	
993.891	30 2 29	31 2 30	1 206.761	0.325	
994.296	30 5 26	31 5 27	1 166.978	0.663	
994.396	30 2 29	31 2 30	1 136.260	0.517	
994.665	29 5 25	30 5 25	1 170.115	0.389	
994.710	29 3 26	30 3 27	1 101.887	0.582	
994.897	29 4 25	30 4 26	1 162.303	0.450	
995.062	28 4 25	29 4 26	1 179.608	0.356	
995.220	29 3 26	30 3 27	1 122.878	0.657	
995.410	29 1 29	30 1 30	1 110.719	0.530	
995.535	29 2 27	30 2 28	1 196.600	0.309	
995.595	29 1 28	30 1 29	1 097.321	0.570	
995.596	28 5 24	29 5 25	1 166.921	0.625	
995.890	29 0 29	30 0 30	1 077.105	0.636	
996.087	28 4 25	29 4 26	1 138.633	0.693	
996.182	27 4 23	28 4 24	1 155.316	0.384	
996.406	28 3 26	29 3 27	1 096.306	0.555	
996.657	26 7 20	27 7 21	1 172.961	0.333	
996.719	28 2 27	29 2 28	1 076.182	0.617	
996.735	27 5 22	28 5 23	1 120.613	0.661	
997.056	28 1 28	29 1 29	1 053.277	0.691	
997.180	27 5 23	28 4 24	1 092.568	0.535	
997.316	26 6 21	27 6 22	1 131.182	0.616	
997.491	27 3 24	28 3 25	1 072.469	0.596	
997.551	27 0 27	28 0 28	1 009.787	0.353	
997.780	25 7 18	26 7 19	1 150.384	0.356	
997.866	26 5 22	27 5 23	1 097.118	0.698	
997.890	27 1 26	28 1 27	1 068.260	0.676	
998.211	27 0 27	28 0 28	1 030.026	0.768	
998.316	26 3 23	27 3 24	1 068.776	0.379	
998.435	25 6 19	26 6 20	1 109.263	0.666	
998.676	26 3 24	27 3 25	1 068.122	0.653	
998.853	26 7 20	27 7 21	1 128.603	0.379	
998.898	26 1 25	27 1 26	1 076.687	0.725	
998.998	26 2 25	27 2 26	1 027.301	0.723	
999.239	25 5 21	26 5 22	1 155.098	0.389	
999.353	26 1 26	27 1 27	1 067.803	0.806	
999.427	25 4 21	26 4 22	1 148.370	0.622	
999.567	25 5 20	26 5 21	1 087.676	0.673	
999.731	25 3 22	26 3 23	1 035.588	0.693	
999.912	25 2 23	26 2 24	1 013.166	0.760	
999.995	25 7 18	26 7 19	1 137.679	0.600	
1 000.096	26 0 26	27 0 27	1 051.683	0.771	
1 000.133	25 1 24	26 1 25	1 002.601	0.786	
1 000.336	22 8 15	23 8 16	1 135.009	0.323	
1 000.683	25 0 25	26 0 26	986.061	0.862	
1 000.842	24 6 19	25 6 20	1 096.342	0.665	
1 000.868	25 4 22	26 4 23	1 066.139	0.501	
1 000.901	24 3 22	25 3 23	1 001.969	0.750	
1 001.088	23 7 16	24 7 17	1 087.592	0.620	
1 001.196	23 3 21	24 3 22	1 031.731	0.698	
1 001.236	24 2 23	25 2 24	983.629	0.829	
1 001.418	23 8 15	24 8 16	1 115.765	0.336	
1 001.602	24 1 24	25 1 25	965.667	0.917	
1 001.638	23 6 19	24 6 20	1 003.389	0.738	
1 001.739	23 2 22	24 2 23	964.662	0.727	
1 001.938	23 3 20	24 3 21	982.230	0.790	
1 002.105	23 2 21	24 2 22	949.600	0.866	
1 002.170	21 7 14	22 7 15	1 068.363	0.638	
1 002.286	22 5 18	23 5 19	1 011.613	0.698	
1 002.336	23 1 22	24 1 23	959.670	0.894	
1 002.691	20 8 13	21 8 14	1 097.358	0.366	
1 002.706	23 0 23	24 0 24	963.212	0.972	
1 002.731	22 4 19	23 4 20	983.663	0.765	
1 002.819	21 6 15	22 6 16	1 027.184	0.550	
1 003.086	22 3 20	23 3 21	960.898	0.862	
1 003.241	20 7 14	21 7 15	1 069.931	0.652	
1 003.364	21 5 16	22 5 17	992.361	0.668	
1 003.416	22 2 21	23 2 22	943.169	0.929	
1 003.554	19 8 11	20 8 12	1 079.787	0.353	
1 003.801	22 1 22	23 1 23	926.272	1.02	
1 003.805	21 6 17	22 6 18	963.910	0.781	
1 003.886	21 4 17	22 4 18	1 008.784	0.571	
1 004.110	21 3 18	22 3 19	962.383	0.879	
1 004.260	21 2 19	22 2 20	929.063	0.963	
1 004.302	19 7 12	20 7 13	1 032.356	0.666	
1 004.435	20 5 15	21 5 16	973.907	0.696	
1 004.672	21 1 20	22 1 21	920.106	0.996	
1 004.686	18 8 11	19 8 12	1 063.052	0.357	
1 004.873	21 0 21	22 0 22	907.477	1.07	
1 004.878	20 6 15	21 6 16	945.611	0.816	
1 004.963	20 4 17	21 4 18	991.185	0.587	
1 005.230	20 3 18	21 3 19	923.181	0.922	
1 005.333	18 7 12	19 7 13	1 015.619	0.671	
1 005.496	19 5 14	20 5 15	956.336	0.718	
1 005.517	19 3 16	20 3 17	905.964	1.02	
1 005.664	17 8 9	18 8 10	1 067.155	0.356	
1 005.936	19 4 15	20 4 16	927.820	0.862	
1 005.951	20 1 20	21 1 21	890.226	1.11	
1 005.998	19 6 13	20 6 14	916.660	0.799	
1 006.264	19 2 18	20 2 19	906.023	0.957	
1 006.383	19 3 17	20 3 18	892.176	1.03	
1 006.392	17 7 10	18 7 11	999.718	0.676	
1 006.562	18 5 14	19 5 15	939.560	0.736	
1 006.576	18 3 16	19 3 17	883.743	1.08	
1 006.679	16 8 9	17 8 10	1 052.096	0.352	
1 006.986	18 4 15	19 4 16	911.029	0.865	
1 006.989	19 0 19	20 0 20	872.854	1.15	
1 007.032	18 6 13	19 6 14	898.642	0.606	
1 007.333	18 5 14	19 5 15	888.808	0.983	-2
1 007.421	16 7 10	17 7 11	986.655	0.672	
1 007.580	17 5 12	18 5 13	923.647	0.765	
1 007.682	18 1 17	19 1 18	871.954	1.08	-4
1 007.699	15 8 7	16 8 8	1 017.869	0.362	
1 008.020	17 6 11	18 6 12	895.109	0.881	-2
1 008.050	18 1 18	19 1 19	857.336	1.18	1
1 008.082	17 4 13	18 4 14	903.667	0.607	
1 008.138	17 3 14	18 3 15	873.126	1.00	-4
1 008.439	15 7 8	16 7 9	970.629	0.666	
1 008.673	17 2 15	18 2 16	850.751	1.08	
1 008.697	16 5 11	17 5 12	908.172	0.750	0
1 008.836	17 1 16	18 1 17	850.833	1.16	-2
1 008.908	16 8 9	17 8 9	1 006.681	0.327	
1 009.069	16 6 11	17 6 12	880.012	0.891	
1 009.051	17 0 17	18 0 18	861.363	1.21	
1 009.081	15 6 9	16 6 10	939.238	0.602	
1 009.196	16 3 14	17 3 15	857.787	1.02	
1 009.467	16 4 13	17 4 14	857.139	0.869	-1
1 009.623	15 5 10	16 5 11	896.336	0.768	
1 009.703	16 2 15	17 2 16	841.262	1.12	
1 009.705	13 8 5	14 8 6	991.930	0.305	
1 010.064	15 3 12	16 3 13	865.769	0.892	
1 010.087	14 6 9	15 6 10	915.844	0.589	
1 010.100	16 1 16	17 1 17	827.610	1.22	
1 010.189	15 3 12	16 3 13	863.659	1.02	-1
1 010.539	15 2 13	16 2 14	864.687	0.628	
1 010.629	14 5 10	15 5 11	880.960	0.758	0
1 010.656	15 1 14	16 1 15	830.815	1.17	2
1 011.060	13 0 13	14 0 14	812.967	1.34	2
1 011.070	14 1 13	15 1 14	857.259	0.885	
1 011.082	13 6 7	14 6 8	903.292	0.568	
1 011.413	14 3 12	15 3 13	850.122	1.02	
1 011.428	12 7 6	13 7 7	932.772	0.398	
1 011.623	13 4 9	14 4 10	868.581	0.719	2
1 011.710	14 2 13	15 2 14	813.803	1.13	-1
1 012.064	13 4 9	14 4 10	859.796	0.869	0
1 012.066	12 6 7	13 6 8	891.375	0.539	-2
1 012.100	13 2 11	14 2 12	801.056	1.23	
1 012.195	13 3 10	14 3 11	817.606	1.00	2
1 012.402	11 7 4	12 7 5	921.896	0.360	-4
1 012.550	13 2 11	14 2 12	802.376	1.11	
1 012.607	12 5 8	13 5 9	858.663	0.691	-3
1 012.662	13 1 12	14 1 13	796.328	1.17	-1
1 013.018	13 0 13	14 0 14	787.680	1.22	
1 013.039	11 6 5	12 6 6	880.695	0.500	
1 013.068	12 6 7	13 6 8	838.384	0.863	
1 013.366	12 4 9	13 4 10	911.083	0.533	
1 013.390	12 3 10	13 3 11	805.815	0.981	
1 013.579	11 5 6	12 5 7	865.779	0.652	
1 013.675	12 2 11	13 2 12	789.657	1.10	2
1 014.002	10 7 3	11 7 4	870.683	0.651	
1 014.020	11 4 7	12 4 8	817.179	0.806	1
1 014.050	12 1 12	13 1 13	777.690	1.19	3
1 014.356	11 3 8	12 3 9	796.963	0.965	-2
1 014.532	11 2 9	12 2 10	779.122	1.06	
1 014.540	10 5 6	11 5 7	835.735	0.603	
1 014.593	11 1 10	12 1 11	771.199	1.12	
1 014.929	11 0 11	12 0 12	765.563	1.17	-2
1 014.951	9 6 3	10 6 4	861.668	0.391	-3
1 014.983	10 6 5	11 6 5	807.130	0.757	1
1 015.123	10 5 6	11 5 6	784.868	0.900	3
1 015.490	9 5 4	10 5 5	826.528	0.567	-3
1 015.596	10 2 9	11 2 10	768.816	1.02	
1 015.891	8 6 3	9 6 4	853.080	0.318	
1 015.891	9 4 5	10 4 6	797.921	0.697	1
1 015.952	11 1 10	11 1 11	757.517	1.11	
1 016.271	9 3 6	10 3 7	775.661	0.861	
1 016.629	8 5 4	9 5 5	818.159	0.668	
1 016.669	9 1 8	10 1 9	759.961	0.957	
1 016.707	9 1 8	10 1 9	751.659	1.02	
1 016.799	9 0 9	10 0 10	746.627	1.07	
1 016.870	8 6 3	9 6 4	789.569	0.636	
1 017.213	8 3 6	9 3 7	767.778	0.771	-1
1 017.357	7 7 1	8 7 2	810.627	0.381	
1 017.675	8 2 7	9 2 8	751.791	0.891	-4
1 017.798	7 6 2	8 6 3	782.016	0.538	
1 017.805	8 1 8	9 1 9	760.550	0.979	
1 018.162	7 5 3	8 5 4	759.363	0.687	
1 018.357	7 3 5	8 3 6	763.905	0.809	
1 018.386	7 1 6	8 1 7	735.136	0.883	
1 018.630	7 0 7	8 0 8	730.910	0.920	
1 018.716	6 6 1	7 6 2	775.320	0.637	
1 018.964	11 11 0	11 11 1	1 138.678	0.329	
1 019.057	6 3 4	7 3 5	753.063	0.590	-4
1 019.111	6 2 5	7 2 6	737.092	0.717	-3
1 019.510	6 1 5	7 1 6	726.799	0.807	-2
1 019.619	5 4 1	6 4 2	769.462	0.318	
1 019.811	12 10 3	12 10 2	1 082.787	0.327	
1 019.957	11 10 1	11 10 2	1 072.756	0.375	
1 019.967	5 3 3	6 3 3	767.184	0.478	-4
1 020.091	10 10 1	10 10 0	1 063.551	0.431	-3
1 020.196	5 2 3	6 2 4	731.286	0.612	
1 020.231	5 1 4	6 1 5	722.215	0.697	
1 020.627	5 0 5	6 0 6	718.451	0.733	-4
1 020.685	11 9 3	11 9 2	1 033.865	0.310	
1 020.758	12 9 4	12 9 3	1 022.987	0.356	
1 020.855	4 3 2	5 3 3	762.162	0.368	
1 020.871	11 9 2	11 9 3	1 012.966	0.406	
1 021.009	10 9 2	10 9 1	1 003.762	0.467	
1 021.105	4 2 3	5 2 4	726.227	0.496	
1 021.128	9 9 0	9 9 1	995.376	0.539	
1 021.367	4 1 4	5 1 5	716.276	0.596	
1 021.430	13 8 5	13 8 6	980.216	0.318	

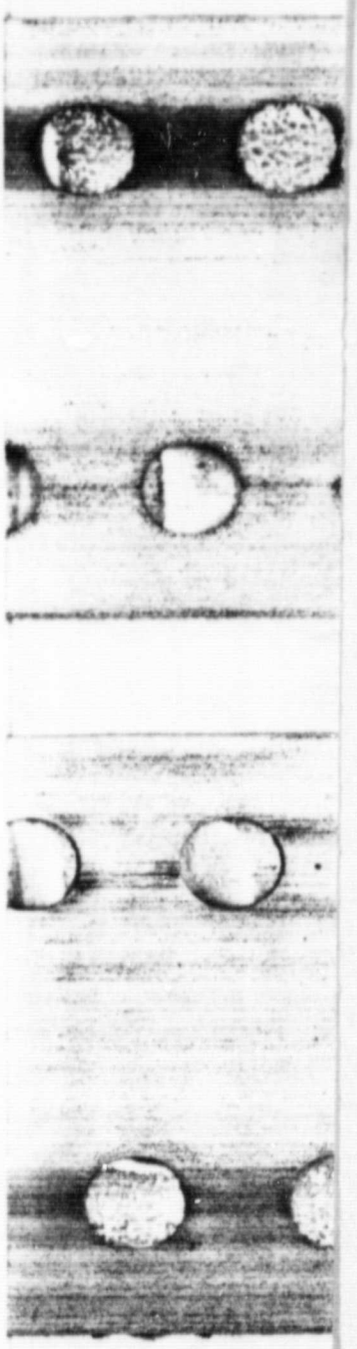

TABLE V—*Continued*

Calc. Wavenumber (cm^{-1})	Upper state $J\ K_{-1}\ K_{+1}$	Lower state $J\ K_{-1}\ K_{+1}$	Lower state energy (cm^{-1})	Abs. Int. (10^{-21} cm mol^{-1})	O − C (10^{-3} cm^{-1})
1 030.126	6 1 6	5 1 5	716.336	0.736	
1 030.177	6 1 5	5 1 4	716.337	0.620	−6
1 030.352	7 1 7	6 1 6	769.662	0.667	3
1 030.436	8 1 8	7 1 7	803.933	0.391	
1 030.499	7 1 6	6 1 5	767.186	0.609	+3
1 030.650	8 1 7	7 1 6	803.934	0.527	
1 030.977	7 1 7	6 1 6	731.586	0.735	
1 031.089	7 0 7	6 0 6	718.631	0.849	
1 031.099	8 1 8	7 1 7	775.320	0.553	
1 031.291	7 1 7	6 1 6	722.232	0.822	
1 031.391	6 1 6	5 1 5	810.677	0.682	
1 031.647	8 1 8	7 1 7	753.063	0.706	
1 031.736	8 1 8	7 1 7	726.799	0.913	
1 031.776	10 0 10	9 0 9	803.080	0.603	
1 031.847	11 1 11	10 1 10	902.668	0.323	
1 031.876	8 2 7	7 2 6	737.092	0.832	
1 032.038	9 4 5	8 4 4	782.016	0.843	+5
1 032.116	10 5 6	9 5 5	818.159	0.760	+6
1 032.181	9 5 5	8 5 4	818.159	0.796	
1 032.287	11 6 6	10 6 5	861.668	0.667	+3
1 032.367	12 7 6	11 7 5	911.857	0.373	
1 032.502	9 2 7	8 2 6	763.905	0.919	3
1 032.546	9 3 7	8 3 6	780.910	0.802	
1 032.562	10 4 7	9 4 6	789.564	0.721	
1 032.830	11 5 6	10 5 5	826.538	0.635	
1 032.860	9 1 8	8 1 7	730.126	1.00	
1 032.913	10 3 8	9 3 7	767.778	0.870	
1 032.919	10 1 10	9 1 9	960.550	1.07	
1 032.973	14 6 7	13 6 8	980.736	0.317	
1 032.989	12 6 7	11 6 6	870.653	0.519	
1 033.038	13 7 7	12 7 6	921.896	0.410	
1 033.121	10 2 9	9 2 8	751.791	0.992	
1 033.278	11 4 7	10 4 6	797.921	0.786	
1 033.533	12 5 8	11 5 7	835.735	0.678	
1 033.638	13 8 6	14 8 7	991.930	0.361	
1 033.640	11 3 9	10 3 8	775.661	0.936	2
1 033.679	13 6 8	12 6 7	880.695	0.561	
1 033.734	14 7 8	13 7 7	932.772	0.446	
1 033.863	11 0 11	10 0 10	766.677	1.15	
1 033.983	12 1 9	11 1 8	807.130	0.859	−1
1 034.013	11 2 9	10 2 8	771.961	1.09	
1 034.223	12 1 12	11 1 11	757.537	1.18	
1 034.225	13 5 8	12 5 7	845.779	0.720	
1 034.291	14 8 7	15 8 8	1 006.481	0.358	
1 034.332	11 1 10	10 1 9	751.459	1.13	
1 037.802	17 3 14	16 3 13	861.659	1.08	
1 037.985	22 8 15	21 8 14	1 097.358	0.358	
1 038.001	18 6 13	17 6 12	880.012	0.938	
1 038.157	21 7 14	20 7 13	1 032.356	0.682	
1 038.161	19 5 14	18 5 13	923.667	0.782	
1 038.216	20 6 15	19 6 14	976.660	0.636	
1 038.354	18 3 16	17 3 15	851.787	1.07	
1 038.369	18 2 17	17 2 16	861.362	1.11	
1 038.408	17 2 15	16 2 14	828.816	1.19	
1 038.652	17 1 16	16 1 15	820.815	1.21	
1 038.500	19 0 19	18 0 18	861.363	1.23	
1 038.584	23 8 15	22 8 14	1 135.765	0.365	
1 038.665	19 4 15	18 4 14	890.109	0.934	
1 038.749	22 7 16	21 7 15	1 069.931	0.468	
1 038.781	20 5 16	19 5 15	939.560	0.786	
1 038.830	21 6 15	20 6 14	991.103	0.611	
1 038.861	20 4 17	19 4 16	897.536	1.10	
1 039.132	24 8 17	23 8 16	1 135.009	0.331	
1 039.163	19 3 16	18 3 15	873.126	1.05	
1 039.261	20 6 17	19 6 16	911.029	0.903	
1 039.331	23 7 16	22 7 15	1 068.363	0.651	
1 039.393	21 5 16	20 5 15	956.316	0.765	
1 039.416	22 6 17	21 6 16	1 008.766	0.591	
1 039.496	21 0 21	20 0 20	872.854	1.16	
1 039.537	20 3 18	19 3 17	871.959	1.12	
1 039.603	20 2 18	19 2 17	880.898	1.07	
1 039.686	19 1 18	18 1 17	850.633	1.20	
1 039.691	25 8 17	24 8 16	1 155.090	0.315	
1 039.805	19 2 17	18 2 16	858.751	1.15	
1 039.867	22 1 22	21 1 21	890.226	1.11	
1 039.896	21 4 17	20 4 16	927.820	0.876	
1 039.903	24 7 18	23 7 17	1 087.592	0.631	
1 039.991	23 5 18	22 5 17	973.907	0.719	
1 040.003	23 6 18	22 6 17	1 027.186	0.568	
1 040.039	23 0 23	22 0 22	907.677	1.06	
1 040.046	25 7 18	24 7 17	1 107.679	0.610	
1 040.070	21 3 18	20 3 17	906.023	0.996	
1 040.182	22 4 19	21 4 18	961.611	0.864	
1 040.279	24 6 19	23 6 18	1 064.462	0.562	
1 040.386	23 5 18	22 5 17	992.361	0.690	
1 040.663	22 2 21	21 2 20	905.960	1.06	
1 040.796	24 1 24	23 1 23	926.272	1.01	
1 040.803	22 3 20	21 3 19	923.181	0.955	
1 040.852	21 1 20	20 1 19	883.763	1.13	
1 041.018	26 7 20	25 7 19	1 128.603	0.387	
1 041.115	23 6 19	22 6 18	963.915	0.808	
1 041.165	25 6 19	24 6 18	1 066.539	0.516	
1 041.157	21 2 19	20 2 18	891.176	1.09	
1 041.266	26 7 20	25 7 19	1 151.613	0.457	
1 041.332	25 0 25	24 0 24	965.212	0.956	
1 041.560	27 7 20	26 7 19	1 150.364	0.363	
1 041.661	24 4 21	23 4 20	982.163	0.768	1
1 041.690	24 2 23	23 2 22	963.165	0.966	2
1 041.702	24 6 21	23 6 20	1 087.474	0.686	
1 041.761	25 5 20	24 5 19	1 031.731	0.672	
1 041.893	25 3 22	24 3 21	967.383	0.915	
1 041.893	23 1 22	22 1 21	920.106	1.03	0
1 041.951	24 3 22	23 3 21	960.898	0.867	0
1 042.092	28 7 22	27 7 21	1 172.963	0.338	
1 042.175	27 0 27	26 0 26	986.061	0.860	+2
1 042.250	27 1 27	26 1 26	1 109.264	0.653	3
1 042.301	26 5 22	25 5 21	1 052.683	0.585	0
1 042.307	25 6 21	24 6 20	1 003.389	0.727	6
1 042.439	23 2 21	22 2 20	929.065	0.996	1
1 042.519	28 7 22	27 7 21	1 087.803	0.781	0
1 042.613	29 7 22	28 7 21	1 196.490	0.313	1
1 042.676	26 2 25	25 2 24	983.629	0.836	1
1 042.787	28 6 23	27 6 22	1 131.862	0.477	1
1 042.805	26 4 23	25 4 22	1 039.284	0.683	1
1 042.861	27 5 22	26 5 21	1 096.487	0.567	3
1 042.864	25 1 24	24 1 23	959.670	0.917	1
1 042.971	29 0 29	28 0 28	1 030.024	0.723	2
1 043.068	26 3 24	25 3 23	1 001.965	0.768	0
1 043.095	25 3 23	24 3 22	981.230	0.821	3
1 043.316	30 1 30	29 1 29	1 053.277	0.666	2
1 043.316	29 6 23	28 6 22	1 135.336	0.391	2
1 043.399	28 5 24	27 5 23	1 097.118	0.509	1
1 043.418	27 6 22	26 6 21	1 051.270	0.638	1
1 043.595	28 2 27	27 2 26	1 027.306	0.734	3
1 043.658	25 2 23	24 2 22	969.400	0.809	1
1 043.719	31 0 31	30 0 30	1 077.105	0.610	2
1 043.749	27 1 26	26 1 25	1 027.401	0.799	1
1 043.838	30 6 25	29 6 24	1 179.408	0.360	1
1 043.906	28 6 25	27 6 26	1 068.776	0.593	5
1 043.968	29 5 25	28 5 23	1 120.613	0.470	4
1 044.051	32 1 32	31 1 31	1 101.883	0.556	+1
1 044.087	28 3 26	27 3 25	1 044.322	0.666	7
1 044.364	31 6 25	30 6 24	1 206.761	0.329	
1 044.373	27 5 24	26 5 23	1 085.588	0.730	2
1 044.430	33 0 33	32 0 32	1 117.303	0.505	−6
1 044.456	30 2 29	29 2 28	1 076.180	0.615	7
1 044.461	30 5 26	29 5 25	1 146.921	0.433	−1
1 044.557	29 1 28	28 1 27	1 068.260	0.681	
1 044.632	29 4 25	28 4 26	1 092.568	0.568	3
1 044.737	34 1 34	33 1 33	1 153.617	0.456	−6
1 044.803	27 2 25	26 2 26	1 013.366	0.775	+2
1 044.866	32 6 27	31 6 26	1 230.712	0.300	3
1 044.966	30 4 27	29 4 26	1 116.833	0.703	0
1 045.003	31 5 26	30 5 25	1 170.115	0.396	
1 045.062	30 5 28	29 5 27	1 099.006	0.584	0
1 045.075	35 0 35	34 0 34	1 180.619	0.610	−7
1 045.252	32 2 31	31 2 30	1 126.260	0.511	6
1 045.297	31 1 30	30 1 29	1 097.221	0.570	
1 045.372	28 3 26	27 3 25	1 038.476	0.367	
1 045.486	32 5 28	31 5 27	1 196.096	0.360	
1 045.628	29 3 26	28 3 25	1 072.669	0.617	
1 045.682	37 0 37	36 0 36	1 237.052	0.327	
1 045.775	31 0 31	30 0 30	1 167.303	0.681	3
1 045.863	29 2 27	28 2 26	1 060.366	0.660	3
1 045.976	32 4 29	31 4 28	1 167.857	0.458	
1 045.980	33 1 32	32 1 31	1 169.369	0.667	
1 045.989	32 3 30	31 3 29	1 166.978	0.668	
1 045.992	34 2 33	33 2 32	1 177.672	0.416	
1 046.030	33 5 28	32 5 27	1 222.999	0.326	
1 046.036	35 1 34	34 1 33	1 206.398	0.376	
1 046.077	34 1 33	33 1 32	1 183.863	0.333	
1 046.076	31 2 29	30 2 28	1 110.719	0.550	
1 046.061	31 5 28	30 5 27	1 122.078	0.518	
1 046.067	34 3 32	33 3 31	1 199.227	0.381	
1 046.117	33 4 29	32 4 28	1 195.496	0.379	
1 046.161	34 4 31	33 4 32	1 222.639	0.360	7
1 046.646	36 5 34	35 5 33	1 256.733	0.303	
1 046.709	33 2 31	32 2 30	1 164.459	0.469	
1 046.996	33 3 30	32 3 29	1 176.803	0.425	
1 047.064	35 4 31	34 4 30	1 251.178	0.307	
1 048.486	35 2 33	34 2 32	1 221.637	0.358	
1 049.083	35 3 32	34 3 31	1 236.223	0.361	

TABLE VI

Wavenumbers and Assignments of the ν_3 Band of Ozone

Line No.	Observed Wavenumber (cm^{-1})	Lower State J′	K′$_a$	K′$_c$	Upper State J′	K′$_a$	K′$_c$	I_c
678	613.156	16	16	2	15	13	3	0.63
693	614.063	15	14	2	14	13	1	0.63
695	614.187	20	13	7	19	12	8	0.63
706	614.953	16	16	0	15	13	3	0.68
707	615.153	19	15	5	18	12	7	0.68
708	615.301	26	12	15	25	11	15	0.63
722	616.222	23	12	12	22	11	11	0.67
730	616.688	17	15	3	16	12	4	0.53
736	617.189	22	12	10	21	11	11	0.51
766	617.833	16	13	3	15	12	4	0.58
769	618.138	21	12	10	20	11	9	0.53
773	618.395	26	11	15	25	10	16	0.68
757	618.757	15	15	1	14	12	2	0.84
765	619.289	25	11	15	26	10	16	0.52
769	619.631	16	15	1	15	12	3	0.63
770	619.716	30	10	20	29	9	21	0.61
773	619.935	16	12	4	15	11	5	0.63
777	620.282	26	11	15	25	10	16	0.57
778	620.476	13	13	1	12	12	0	0.67
780	620.633	29	10	20	28	9	19	0.68
787	620.800	18	12	6	17	11	7	0.67
787	621.168	23	11	13	22	10	12	0.67
793	621.583	28	10	18	27	9	19	0.51
796	621.723	17	12	6	16	11	5	0.71
799	622.082	22	11	11	21	10	12	0.67
805	622.510	27	10	18	26	9	17	0.58
807	622.689	16	12	4	15	11	5	0.76
811	622.980	21	11	11	20	10	10	0.72
817	623.488	36	10	26	35	9	27	0.62
823	623.936	20	11	9	19	10	10	0.77
828	624.361	35	10	26	34	9	25	0.67
836	624.826	19	11	9	18	10	8	0.83
839	625.087	30	9	21	29	8	22	0.52
845	625.536	26	10	16	25	9	17	0.73
865	625.536	17	11	7	17	10	8	0.88
867	625.867	29	9	21	28	8	20	0.58
871	626.182	12	12	0	11	11	1	0.96
1056	665.720	13	8	6	12	7	5	1.06
1056	665.961	19	10	10	19	9	11	0.75
1057	665.993	16	10	6	16	9	7	0.69
1058	666.091	25	8	20	26	5	19	1.32
1059	666.167	15	10	6	15	9	7	0.85
1062	666.350	16	10	6	16	9	7	0.59
1064	666.762	18	7	11	17	6	12	1.58
1065	666.893	26	6	18	25	5	19	1.43
1067	667.156	30	5	25	29	4	26	0.88
1070	667.336	17	7	11	16	6	10	1.07
1072	667.511	25	6	18	22	5	17	1.56
1080	668.081	18	7	9	17	6	10	1.06
1082	668.196	22	6	16	21	5	17	1.65
1083	668.199	28	5	23	27	4	24	1.08
1086	668.295	9	8	2	8	7	1	2.31
1087	668.410	15	7	9	16	6	8	2.15
1088	668.625	21	6	16	20	5	15	1.76
1089	668.696	33	5	29	33	4	29	0.48
1090	668.792	32	5	27	32	4	28	0.53
1093	630.117	8	8	0	7	7	1	2.58
1096	650.299	29	9	21	29	8	22	0.69
1097	650.496	28	9	19	27	8	20	0.79
1099	650.757	25	9	17	25	8	18	0.89
1100	650.863	20	9	11	20	8	12	1.06
1101	650.956	21	9	13	21	8	14	1.06
1102	651.057	19	9	11	19	8	12	1.01
1103	651.165	18	9	9	18	8	10	1.06
1106	651.231	17	9	9	17	8	10	1.06
1105	651.338	16	9	7	15	8	8	0.96
1108	651.396	12	9	3	12	8	5	0.90
		13	9	5	13	8	6	0.81
		12	9	3	12	8	4	0.71
		11	9	3	11	8	4	0.58
		10	9	1	10	8	2	0.42
		19	8	14	18	7	13	1.48
1109	666.238	35	6	30	35	5	31	0.83
		40	6	34	40	5	35	0.65
		38	6	32	38	5	33	0.59
1161	666.176	33	6	28	33	5	29	1.02
		36	6	30	36	5	31	0.89
1164	666.485	32	6	26	32	5	27	1.13
1165	666.523	31	6	26	31	5	27	1.26
1167	666.622	30	6	24	30	5	25	1.35
		35	6	30	35	5	31	0.83
		20	3	17	19	2	18	1.48
1168	666.655	39	1	39	38	0	38	1.63
		29	6	24	29	5	25	1.48
1169	666.731	28	6	22	28	5	23	1.70
1171	666.839	27	6	22	27	5	23	1.70
1172	666.887	8	5	3	7	4	4	2.76
		26	6	20	26	5	21	1.71
1173	666.925	37	5	33	36	4	33	1.46
1176	666.950	25	6	20	25	5	21	1.92
1178	667.070	24	6	18	24	5	19	2.03
1178	667.097	23	6	18	23	5	19	2.13
1179	667.164	22	6	16	22	5	17	2.22
1180	667.210	21	6	16	21	5	17	2.30
1181	667.264	20	6	14	20	5	15	2.36
1213	667.312	19	6	14	19	5	15	2.41
1184	667.381	18	6	12	18	5	13	2.44
1186	667.453	17	6	12	17	5	13	2.46
		16	6	10	13	3	11	2.58
1187	667.522	16	6	10	16	5	11	2.63
1188	667.581	15	6	10	15	5	11	2.70
1189	667.617	14	6	8	14	5	9	2.73
1190	667.669	38	0	38	37	1	37	1.83
		13	6	8	13	5	9	2.22
		37	2	36	36	1	35	1.32
1191	667.712	14	7	8	13	6	7	2.76
		7	5	3	6	4	2	2.76
		25	3	23	24	2	22	1.62
1192	667.769	11	6	6	11	5	7	1.93
		10	6	4	10	5	5	1.73
1193	667.831	9	6	4	9	5	5	1.49
		38	1	37	37	2	36	1.19
		8	6	2	8	5	3	1.21
1301	668.368	13	9	10	12	8	9	0.63
1308	668.562	37	1	37	36	0	36	2.06
1309	668.583	6	5	1	5	4	1	2.77
1317	668.964	18	3	15	17	2	16	1.95
1327	669.460	18	2	16	17	1	17	0.69
		5	5	1	4	4	0	2.79
1329	669.566	36	0	36	35	1	35	1.30
1335	669.879	36	1	35	35	2	34	1.46
1348	670.695	19	3	17	18	2	16	2.16
1350	670.828	33	2	32	32	1	31	1.91
1352	670.975	10	4	6	9	3	7	2.69
1354	671.096	16	3	13	15	2	14	2.20
1360	671.428	36	0	36	35	1	35	1.62
1363	671.562	37	2	36	37	1	37	0.44
1363	671.619	41	3	39	41	2	40	0.41
		37	3	35	37	4	34	0.80
1369	671.905	35	3	33	35	4	32	1.01
		17	3	15	16	2	14	2.30
1370	671.970	34	3	32	33	4	32	1.75
1373	672.134	33	3	29	33	4	30	1.25
1375	672.259	33	3	30	32	0	32	3.11
		32	3	30	32	4	28	1.20
1378	672.707	31	3	29	31	4	28	1.51
1382	672.821	27	3	25	27	4	24	2.07
1383	672.898	8	6	4	7	5	3	2.66
1386	672.737	25	3	23	25	4	22	2.30
1388	673.037	16	3	14	15	2	13	0.96
		32	3	29	32	4	28	1.39
1387	672.966	22	3	19	21	4	18	2.71
1388	673.009	21	3	19	20	4	16	2.89
1389	673.069	20	3	17	20	4	16	2.89
		36	1	35	36	0	36	0.51
1390	673.099	19	3	15	19	4	16	2.96
		16	3	13	16	4	12	2.38
1391	673.162	18	3	15	18	4	14	3.00
1392	673.189	17	3	13	1	4	14	5.02
1393	673.232	16	3	13	16	4	12	3.01
		15	3	13	14	2	12	2.63
1395	673.312	15	3	11	15	4	12	2.98
		32	0	32	31	1	31	1.61
1396	673.380	16	3	9	16	4	12	2.91
		35	2	34	35	1	35	0.58
		13	3	9	13	4	10	2.81
1397	673.447	36	1	35	36	0	36	0.92
		12	3	7	12	4	8	2.68
1398	673.505	11	3	9	11	4	8	2.53
		10	3	7	10	4	6	2.31
1399	673.551	9	3	7	9	4	6	2.06
		8	3	5	8	4	4	1.78
1400	673.591	7	3	5	7	4	4	1.44
		29	2	28	28	1	27	1.48
		6	3	4	6	4	2	1.06
1403	673.767	38	1	37	38	0	38	0.73
1409	674.090	31	1	31	30	0	30	3.71
1410	674.118	32	1	31	31	1	31	1.05
		36	2	34	35	3	33	0.75
1413	674.268	40	1	39	40	0	40	0.57
		39	1	38	39	1	39	0.61
1421	674.716	13	3	11	12	2	10	2.51
1426	675.016	12	3	9	11	2	10	2.68
1429	675.126	36	1	33	36	0	36	0.67
1430	675.179	30	0	30	29	1	29	4.02
		33	1	33	32	3	30	0.76
		37	4	34	37	5	33	0.88
1431	675.298	5	4	2	4	3	1	2.55
1432	675.362	15	3	13	14	2	12	2.51
1433	675.603	40	2	38	40	0	40	0.51
1446	675.876	29	1	29	28	0	28	4.33
1446	675.985	35	4	32	35	5	31	1.16
		35	2	34	34	1	33	2.91
1449	676.099	16	2	12	15	3	13	1.22
1450	676.136	16	3	13	15	4	12	1.22
		6	4	0	5	5	1	2.56
1452	676.251	11	3	9	10	2	8	2.53
1453	676.313	35	1	35	35	0	35	1.00
1454	676.367	30	2	29	29	3	27	2.33
1459	676.665	33	4	30	33	5	31	1.42
1465	676.869	10	3	7	9	2	8	2.49
1465	676.938	31	2	30	31	1	31	0.97
1466	677.063	36	2	35	36	1	36	0.51
		28	0	28	27	1	27	4.63
1467	677.088	23	2	22	22	1	21	3.06
1469	677.186	32	1	31	32	0	32	0.87
		31	2	30	31	1	31	0.76
1475	677.672	19	4	16	19	5	15	2.09
		33	3	31	33	2	32	1.29
1479	677.898	9	3	7	8	2	6	2.68
1482	678.067	27	4	24	27	5	23	1.66
1486	678.117	21	2	20	20	1	19	3.11
1487	678.326	25	4	22	25	5	21	2.78
1492	678.663	29	2	28	29	1	29	1.23
		8	3	5	7	4	4	2.62
1495	678.763	28	1	27	27	2	26	2.37
		21	4	18	21	5	17	3.35

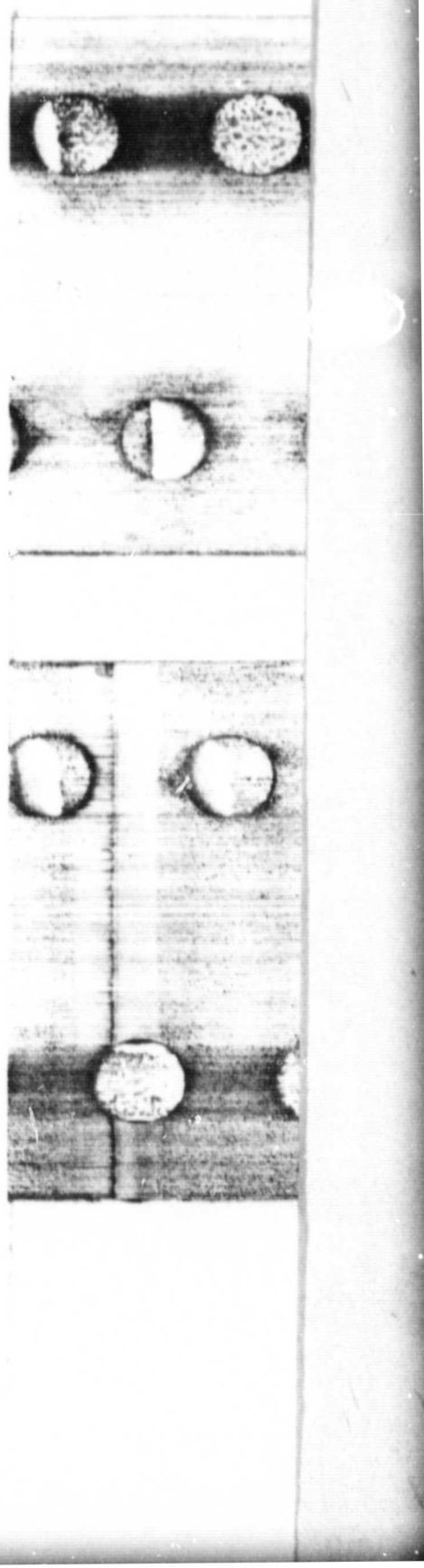

TABLE VI—*Continued*

Line No.	Observed Wavenumber (cm^{-1}vac.)	Lower State J''	K_a''	K_c''	Upper State J'	K_a'	K_c'	I_r
1500	678.966	31	3	29	31	2	30	1.63
		12	2	10	11	1	11	1.69
1501	679.052	17	4	14	17	3	15	3.61
1502	679.137	19	2	18	18	1	17	3.13
		19	4	16	18	3	15	3.60
1504	679.225	16	4	12	16	3	13	3.62
		18	4	14	18	3	15	3.60
		13	4	10	13	3	11	3.62
1505	679.310	20	3	17	21	4	18	0.69
		14	4	10	14	3	11	3.52
		20	4	16	20	3	17	3.67
		30	1	29	30	0	30	1.33
1506	679.307	12	4	8	12	3	9	3.59
		11	4	8	11	3	9	3.61
1507	679.351	10	4	6	10	3	7	2.90
		25	1	25	26	0	26	5.53
1508	679.390	13	4	8	14	3	9	0.50
		9	4	6	9	3	7	1.65
		22	4	18	22	3	19	3.23
		6	4	4	6	3	3	2.36
1509	679.455	7	4	4	7	3	5	2.02
		5	4	2	5	3	3	1.63
		5	4	2	5	3	3	1.19
		4	4	0	4	3	1	0.66
1510	679.555	7	3	5	8	2	6	2.36
1516	679.892	26	4	22	26	3	23	2.71
1517	680.007	32	2	30	31	3	29	0.97
		36	2	34	36	1	35	0.97
		21	3	19	22	4	18	0.69
1518	680.053	29	3	27	29	2	28	2.02
1519	680.159	16	4	8	15	3	13	0.35
		17	2	16	16	1	15	3.09
1521	680.256	27	2	26	27	1	27	1.53
1522	680.296	28	4	24	28	3	25	2.61
1536	680.397	4	3	3	4	2	2	2.38
1539	681.037	23	1	23	22	0	22	6.01
		26	1	25	25	2	24	2.75
1540	681.078	27	3	25	27	2	26	1.63
1543	681.236	15	2	14	14	1	13	2.99
1546	681.286	5	3	3	4	2	2	2.19
		32	4	28	32	3	29	1.81
1545	681.391	28	1	27	28	0	28	1.63
1548	681.565	23	2	22	24	1	24	0.68
		10	2	8	9	1	9	1.69
1551	681.738	16	4	10	17	3	15	0.63
1552	681.796	25	2	24	25	1	25	1.86
1719	691.752	14	4	10	15	3	13	1.07
1720	691.791	6	2	4	7	1	7	0.88
1723	692.023	6	2	4	6	1	5	2.92
		20	2	18	20	1	19	6.33
1727	692.252	22	3	19	23	4	20	0.86
		12	2	10	11	1	11	1.69
1729	692.486	18	2	16	18	1	17	6.73
		10	2	8	10	1	9	4.93
		7	1	7	6	0	6	3.61
1730	692.596	12	0	12	11	1	11	5.19
1731	692.686	12	2	10	12	1	11	5.80
		15	4	12	16	3	13	1.12
		16	1	15	16	0	16	4.87
		16	2	14	16	1	15	6.77
		14	4	10	14	3	11	6.66
1732	692.730	14	2	12	14	1	13	6.44
1736	692.857	8	3	5	9	2	8	0.86
1738	693.090	23	5	19	24	4	20	0.83
1742	693.336	16	4	12	17	3	15	1.16
1744	693.552	16	1	15	15	2	14	1.31
1746	693.621	10	3	27	29	4	26	0.69
1751	693.926	9	3	7	10	2	8	0.98
		5	1	5	4	0	4	2.75
1752	694.007	16	3	13	16	2	14	3.57
1758	694.372	17	4	14	18	3	15	1.16
		10	3	7	11	2	10	1.07
1762	694.665	10	0	10	9	1	9	4.37
1766	694.897	18	4	14	19	3	17	1.15
1773	695.364	6	2	4	5	1	5	0.69
		26	5	21	27	4	24	0.72
1774	695.402	3	1	3	2	0	2	1.86
1780	695.723	33	3	31	34	4	30	0.41
		11	3	9	12	2	10	1.19
1782	695.861	12	3	9	13	2	12	1.23
1784	695.982	10	1	9	10	0	10	6.25
		14	1	13	13	2	12	2.26
1785	696.128	19	4	16	20	3	17	1.15
1787	696.356	28	3	25	27	4	24	0.80
1788	696.413	27	5	23	28	4	24	0.68
		20	4	16	21	3	19	1.12
1792	696.591	6	2	4	7	1	7	0.77
1793	696.668	8	1	7	8	0	8	5.98
		8	0	8	7	1	7	5.44
1796	696.977	1	1	1	0	0	0	0.95
		31	3	29	30	4	26	0.36
1798	697.103	5	1	5	4	1	4	0.77
		20	2	18	19	3	17	1.48
19 8	70x.990	17	2	16	18	1	17	2.85
		6	1	5	6	2	4	3.06
1961	710.275	4	1	3	4	2	2	1.97
1962	710.444	8	0	8	9	1	9	4.66
1963	710.578	26	1	25	26	2	24	4.19
		13	1	13	14	0	14	6.18
1964	710.650	15	3	13	14	4	10	1.13
		3	1	3	3	2	2	1.35
1967	710.884	5	1	5	5	2	4	2.25
1968	710.920	22	4	18	21	3	17	0.93
1969	710.998	20	0	20	20	1	19	3.82
1970	711.169	7	2	6	6	3	3	0.58
		29	5	25	28	6	22	0.53
		7	1	7	7	2	6	2.96
1974	711.498	25	3	23	26	2	24	1.36
		14	3	11	13	4	10	1.07
		9	1	9	9	2	8	3.42
1975	711.621	10	0	10	11	1	11	5.45
		28	1	27	28	2	26	3.33
		33	4	30	34	3	31	0.51
1977	711.813	32	2	30	32	3	29	3.69
		30	2	28	30	3	27	3.23
1978	712.030	11	1	11	11	3	9	3.69
		34	2	32	34	3	31	3.55
		28	2	26	28	3	25	3.75
1980	712.236	19	2	18	20	1	19	3.01
		1	1	1	2	2	0	1.41
1981	712.377	15	1	15	16	0	16	6.69
1982	712.478	13	3	11	12	4	8	1.00
		26	2	24	26	3	23	4.18
		36	2	34	36	3	33	1.65
1983	712.556	22	2	20	22	1	21	2.98
		13	1	13	13	2	12	3.77
1985	712.772	12	0	12	13	1	13	6.15
1986	712.879	30	1	29	30	2	28	2.58
1987	712.997	2	1	1	3	2	2	1.57
		27	3	25	28	3	26	4.52
1990	713.233	15	1	15	15	2	14	3.68
		38	2	36	38	3	35	1.23
1991	713.333	12	3	9	11	4	8	0.92
1996	713.652	22	2	20	22	3	19	4.36
2000	713.909	16	0	16	15	1	15	6.68
2001	713.968	17	1	17	17	2	16	3.47
2002	714.026	3	1	3	4	2	2	1.66
		27	3	25	28	2	26	1.28
		26	5	21	25	6	20	0.64
2003	714.069	17	1	17	18	0	18	6.97
2004	714.165	26	0	26	26	1	25	2.63
2005	714.222	40	2	38	40	3	37	0.88
		11	3	9	10	4	6	0.82
2006	714.328	20	2	18	20	3	17	4.86
		44	3	41	44	4	40	0.51
		35	4	32	36	3	33	0.63
		33	1	33	32	2	30	1.95
2007	714.466	4	1	3	3	2	2	1.93
		21	2	20	22	1	21	3.11
2008	714.561	41	3	39	42	4	38	0.69
2009	714.677	18	4	14	17	5	13	0.95
2011	714.807	19	1	19	19	2	18	3.16
2012	714.965	18	2	16	18	3	15	4.87
2014	715.064	16	0	16	17	1	17	7.00
2020	715.348	16	2	14	16	3	13	4.79
2021	715.705	38	3	35	38	4	34	1.16
		19	1	19	20	0	20	6.99
		21	1	21	21	2	20	2.80
2022	715.804	6	1	5	7	2	6	2.29
		26	0	26	26	1	25	1.97
2023	715.961	34	1	33	34	2	32	1.44
		5	1	5	6	2	4	1.87
2024	716.014	16	2	14	15	3	13	4.59
2026	716.254	18	0	18	19	1	19	7.09
2027	716.407	12	2	10	12	3	9	4.26
2028	716.513	16	4	12	15	5	11	0.90
		36	3	33	36	4	32	1.60
2029	716.655	29	3	27	30	2	28	1.19
		23	2	22	24	1	23	3.11
		10	2	8	10	3	7	3.79
2030	716.871	8	2	6	9	1	9	3.17
2031	717.001	11	2	10	11	3	9	3.98
		6	2	4	6	3	3	2.38
		9	2	8	9	3	7	3.68
		13	2	12	13	3	11	4.31
		7	2	6	7	3	5	2.79
		5	2	4	5	3	3	1.92
		15	2	14	15	3	13	4.66
		4	2	2	4	3	1	1.60
		8	2	7	8	3	6	2.63
2032	717.132	17	2	16	17	3	15	4.66
2033	717.281	21	1	21	22	0	22	6.77
		19	2	18	19	3	17	4.26
2034	717.427	15	4	12	14	5	9	0.86
		34	3	31	34	4	30	1.69
2035	717.478	20	0	20	21	1	21	6.96
		28	0	28	28	1	27	1.58
2036	717.546	21	2	20	21	3	19	3.97
2037	717.597	36	1	35	36	2	34	1.08
2038	717.761	25	1	25	25	2	24	2.06
2039	717.855	23	2	22	23	3	21	3.58
2040	717.904	7	1	7	8	2	6	1.96
2042	718.161	10	1	9	11	2	10	2.90
2044	718.271	25	2	24	25	3	23	3.16
2046	718.398	22	2	20	22	3	19	2.00
2051	718.733	22	0	22	23	1	23	6.67
		25	2	24	26	1	25	3.03
		21	3	19	20	4	16	0.76
		13	1	13	14	0	14	6.37
		27	2	26	27	3	25	2.68
2052	718.871	27	1	27	27	2	26	1.69
2054	719.109	28	2	26	27	3	25	0.65
		30	0	30	30	1	29	1.25
		31	3	29	32	2	30	0.58
2055	719.183	13	4	10	12	5	7	0.73
		12	1	11	13	2	12	2.13
2056	719.295	30	3	27	30	4	26	2.33
2057	719.353	29	3	27	29	4	25	2.35
2059	719.570	2	2	0	3	3	1	2.25
2062	719.953	26	0	26	25	1	25	6.16
2065	720.171	14	1	13	15	2	14	3.31
		28	2	26	28	3	25	2.86
		9	1	9	10	2	8	1.86
		25	1	25	26	0	26	5.86
2069	720.420	3	2	2	4	3	1	2.32
2073	720.708	32	0	32	33	1	33	0.98
		27	2	26	28	1	27	2.86
2075	720.916	26	3	23	26	4	22	3.02
2076	720.983	16	1	15	17	2	16	3.43
2080	721.232	31	1	31	31	2	30	1.09
		7	2	6	7	3	5	2.43
		26	0	26	27	1	27	5.54
2084	721.522	26	3	23	26	4	20	3.36
2085	721.597	27	1	27	28	0	28	5.21
		35	2	34	35	3	33	1.12
2086	721.765	18	1	17	19	2	18	3.48
2089	722.061	5	2	4	6	3	3	2.53
		22	3	19	22	4	18	3.65
2090	722.226	36	0	36	36	1	35	0.76

TABLE VI—*Continued*

Line No.	Observed Wavenumber (cm^{-1}vac.)	Lower State J'' K_a'' K_c''	Upper State J' K_a' K_c'	I_r
2091	722.416	17 5 13	16 4 10	0.70
		33 1 33	33 2 31	0.86
2092	722.526	20 3 17	20 4 16	1.89
		38 0 38	39 1 39	1.69
		20 1 19	21 2 20	3.68
2093	722.579	29 3 27	29 4 26	2.35
		37 2 36	37 3 35	0.86
		27 1 25	27 4 24	2.76
		31 3 29	31 4 28	1.96
		29 2 28	30 1 29	1.62
2094	722.628	25 3 23	25 4 22	3.12
		11 1 11	12 2 10	1.66
		33 3 31	33 4 30	1.61
2095	722.725	23 3 21	23 4 20	3.66
		62 1 61	62 2 60	0.61
2096	722.825	18 3 15	18 4 14	4.03
		35 3 33	35 4 32	1.38
		6 2 4	7 5 3	2.63
2097	722.963	21 3 19	21 4 18	3.75
		29 1 29	30 0 30	4.55
		19 3 17	19 4 16	3.95
2098	723.089	16 5 13	16 4 12	4.05
		37 3 35	37 4 34	1.00
2099	723.236	17 3 15	17 4 14	4.05
		22 1 21	23 2 22	3.62
		15 3 13	15 4 12	4.01
2100	723.367	16 3 13	16 4 12	3.96
		13 3 11	13 4 10	3.83
		12 1 11	12 4 8	3.16
2101	723.480	11 3 9	11 4 8	3.49
		10 3 7	10 4 6	3.25
2102	723.556	9 3 7	9 4 6	2.97
		8 3 5	8 4 4	2.84
2103	723.616	7 3 5	7 4 4	2.78
		6 3 3	6 4 2	1.83
2104	723.675	5 3 3	5 4 2	1.33
		35 1 35	35 2 34	0.66
		36 0 36	36 1 35	0.58
		4 3 1	4 4 0	0.34
		3 2 2	3 3 1	2.71
2105	723.784	30 0 30	31 1 31	4.22
2107	723.950	26 1 25	27 2 26	3.78
2108	724.054	35 3 33	36 2 34	0.85
2111	724.295	31 1 31	32 2 30	3.68
		31 2 30	32 1 31	2.33
2112	724.394	8 2 6	9 3 7	2.79
2197	733.201	26 2 24	27 3 25	1.71
		40 3 35	40 4 36	0.54
2200	733.425	41 5 37	41 6 36	0.67
		68 0 68	67 1 67	0.66
2201	733.494	11 5 9	12 4 8	3.16
2202	733.585	28 2 26	29 3 27	1.52
2203	733.775	38 3 35	38 4 34	0.70
2204	733.920	30 2 28	31 3 29	1.36
2206	733.975	67 1 67	68 0 68	0.55
2209	734.214	36 5 31	36 6 30	0.89
		32 2 30	33 3 31	1.17
2210	734.262	12 3 9	13 4 10	3.11
2211	734.358	19 3 17	20 4 16	3.98
		34 2 32	35 3 33	1.00
		35 5 31	35 6 30	0.99
		68 0 68	69 1 69	0.67
		5 5 1	6 4 2	1.30
2214	734.859	33 5 29	33 6 28	1.22
		36 2 34	37 3 35	0.85
2215	734.969	32 3 29	32 4 28	1.35
2217	735.072	13 5 11	14 4 10	3.07
2219	735.177	31 5 27	31 6 26	1.48
2220	735.287	38 2 36	39 3 37	0.71
		30 5 25	30 6 24	1.61
2221	735.406	5 4 2	6 3 3	3.28
		29 5 25	29 6 24	1.75
2222	735.555	28 5 23	28 6 22	1.89
2223	735.706	27 5 23	27 6 22	2.03
2225	735.812	16 3 13	15 4 12	3.00
		[illegible] 5 21	26 6 20	2.16
2226	735.969	[illegible] 5 21	25 6 20	2.30
2227	[illegible]	[illegible] 5 19	26 6 18	2.42
2228	736.137	23 5 19	23 6 18	2.54
2229	736.218	6 4 2	7 5 3	3.29
		22 5 17	22 6 16	2.65
2230	736.314	21 5 17	21 6 16	2.74
2231	736.405	20 5 15	20 6 14	2.82
2232	736.497	19 5 15	19 6 14	2.71
2233	736.566	18 5 13	18 6 12	2.91
2235	736.650	15 3 13	16 4 12	2.92
		17 5 13	17 6 12	2.92
2236	736.720	16 5 11	16 6 10	2.90
2237	736.770	15 5 11	15 6 10	2.85
2238	736.851	14 5 9	14 6 8	2.77
		13 5 9	13 6 8	2.65
2239	736.987	12 5 7	12 6 6	2.50
2363	750.068	23 7 17	23 8 16	1.66
		26 4 20	25 5 21	1.82
2364	750.172	15 5 11	16 6 10	2.91
		21 7 15	21 8 14	1.78
		31 3 29	32 4 28	0.78
2365	750.276	20 7 13	20 8 12	1.82
2366	750.409	18 7 11	18 8 10	1.85
2367	750.516	16 7 9	16 8 8	1.80
2368	750.598	15 7 9	15 8 8	2.00
2369	750.678	14 7 7	14 8 6	1.65
		7 6 2	8 7 1	3.32
2370	750.738	13 7 7	13 8 6	1.53
		12 7 5	12 8 4	1.38
		11 7 5	11 8 4	1.20
2371	750.864	10 7 3	10 8 2	0.97
		25 4 22	26 5 21	1.68
		9 7 3	9 8 2	0.71
2372	750.932	16 5 11	17 6 12	2.80
2376	751.418	26 4 22	27 5 23	1.54
2375	751.495	8 6 2	9 7 3	3.26
2377	751.713	17 5 13	18 6 12	2.68
2382	752.310	9 6 4	10 7 3	3.20
2383	752.484	18 5 13	19 6 14	2.56
2385	752.761	28 4 26	29 5 25	1.28
2390	753.100	6 6 4	11 5 7	3.16
391	753.251	19 5 15	20 6 14	2.43
2395	753.775	29 4 26	30 5 25	1.15
2396	753.903	11 6 6	12 7 5	3.07
2397	754.009	30 4 26	31 5 27	1.06
		20 5 15	21 6 16	2.30
2402	754.709	12 6 6	13 7 7	3.00
2403	754.772	21 5 17	22 6 16	2.16
2408	755.111	32 4 28	33 5 29	0.83
2407	755.219	31 4 28	32 5 27	0.92
2410	755.499	13 6 8	14 7 7	2.91
		22 5 17	23 6 18	2.03
2411	755.634	35 0 35	35 9 27	0.51
2413	755.790	36 1 35	36 8 29	0.57
2413	755.956	33 0 33	33 9 25	0.63
2414	756.093	32 0 32	32 9 23	0.70
2415	756.177	34 4 30	35 5 31	0.84
		31 0 31	31 9 23	0.76
2416	756.254	23 5 19	24 6 18	1.89
		14 6 8	15 7 9	2.82
2417	756.413	29 0 29	29 9 21	0.90
2116	726.713	26 1 25	27 2 26	3.09
2118	725.063	32 0 32	33 1 33	3.56
2123	725.322	13 1 13	14 2 12	1.38
		9 2 8	10 3 7	2.82
2123	725.559	28 1 27	29 2 28	2.83
		35 1 35	36 0 36	3.25
2126	725.888	10 2 8	11 3 9	2.87
2127	725.[illegible]0	34 2 32	34 3 31	2.02
2128	726.131	36 4 32	36 5 31	1.06
2129	726.293	36 0 36	35 1 35	2.95
2130	726.407	30 1 29	31 2 30	2.53
2136	726.865	36 2 34	36 3 33	1.66
		34 4 30	34 5 29	1.31
2137	727.036	3 3 1	4 4 0	2.89
		11 2 10	12 3 9	2.83
2140	727.281	12 2 10	13 3 11	2.87
2141	727.350	14 2 12	15 3 13	2.72
		32 5 31	33 2 32	2.20
2142	727.507	32 4 28	32 5 27	1.60
		19 6 14	18 7 11	0.34
		35 2 34	36 1 35	1.70
		36 0 36	37 1 37	2.[illegible]
		37 4 34	37 5 33	0.93
2146	727.776	35 4 32	35 5 31	1.17
2147	727.868	4 3 1	5 2 3	2.92
2148	728.049	30 5 26	30 5 25	1.91
2149	728.086	33 4 30	33 5 29	1.66
		37 1 37	38 0 38	2.16
2168	728.363	15 4 12	16 5 12	1.08
2169	728.518	31 4 28	31 5 27	1.75
		34 1 33	35 2 34	1.87
2150	728.618	18 6 12	17 7 11	0.52
		28 6 24	28 5 23	1.26
2151	728.551	39 5 35	40 2 38	0.61
		14 2 12	13 3 13	2.80
		29 4 26	29 5 25	2.07
2152	728.676	5 3 3	6 4 2	2.97
2153	728.775	38 0 38	39 1 39	1.91
		13 2 12	14 3 11	2.76
		36 4 32	36 5 31	2.56
		27 4 24	27 5 23	1.60
		23 2 22	24 3 21	1.28
2154	728.969	37 2 36	38 1 37	1.39
2155	729.097	25 4 22	25 5 21	2.72
		24 4 20	24 5 19	2.87
2156	729.319	23 4 20	23 5 19	3.01
		17 6 12	16 7 9	0.42
		11 5 7	11 5 6	2.31
		7 4 4	8 5 3	3.30
		10 5 5	10 6 4	2.07
2160	737.089	9 5 5	9 6 4	0.78
		8 6 2	8 5 3	1.65
		7 6 2	7 5 3	1.05
2161	737.298	16 3 13	17 4 14	2.83
2166	737.618	9 5 5	8 6 4	3.30
2250	738.207	17 5 13	18 4 14	2.72
2253	738.618	9 4 6	10 5 5	3.30
2254	738.732	18 3 15	19 4 16	2.61
2258	739.159	23 2 22	24 3 21	1.28
2261	739.433	10 4 6	11 5 7	3.28
2265	739.773	19 3 17	20 4 16	2.66
2267	740.095	20 3 17	21 4 18	2.36
2268	740.227	11 4 8	12 5 7	3.25
2273	741.021	13 4 10	12 5 7	3.21
2278	741.366	22 3 19	23 4 20	2.06
		21 3 19	22 4 18	2.18
2279	741.616	36 6 30	36 7 29	0.73
2281	741.780	35 6 30	35 7 29	0.82
2282	741.732	36 4 32	36 5 31	0.91
2283	741.815	13 4 10	14 5 9	3.15
2284	741.875	33 6 28	33 7 27	1.01
2285	741.912	25 2 24	26 3 23	0.96
2286	742.026	32 2 30	32 3 29	1.11
2287	742.178	31 6 26	31 7 25	1.22
		5 5 1	6 6 0	3.65
2288	742.331	30 6 24	30 7 23	1.33
2289	742.460	29 6 24	29 7 23	1.46
		26 3 23	25 6 22	1.78
2290	742.535	28 6 22	28 7 21	1.56
2291	742.588	14 6 10	15 5 11	3.07
2292	742.638	27 6 22	27 7 21	1.67
2296	742.769	26 6 20	26 7 19	1.78
2295	742.855	25 6 20	25 7 19	1.89
2296	742.913	23 3 21	24 4 20	1.88
		24 6 18	24 7 17	1.99
2297	742.982	6 5 2	7 6 2	3.41
		23 6 18	23 7 17	2.09
2298	743.133	22 6 16	22 7 15	2.17
2299	743.251	21 6 16	21 7 15	2.26
2300	743.353	20 6 14	20 7 13	2.30
		15 4 12	16 5 11	2.98
		19 6 14	19 7 13	2.36
2318	756.355	28 8 20	28 9 19	0.97
2319	756.669	27 8 20	27 9 19	1.06
		33 4 30	36 5 29	0.72
2320	756.766	26 8 18	26 9 17	1.11
2321	756.836	25 8 18	25 9 17	1.17
2322	757.002	24 8 16	24 9 15	1.23
		25 5 19	25 6 20	1.75
2323	757.058	23 8 16	23 9 15	1.28
		15 0 10	16 1 9	2.72
2326	757.119	22 8 14	22 9 13	1.33
2325	757.202	21 8 14	21 9 13	1.36
2326	757.328	19 8 12	19 9 11	1.40
2327	757.516	18 8 10	18 9 9	1.33
2328	757.626	15 7 9	15 8 7	1.27
		7 7 1	8 8 0	3.13
		16 8 8	16 9 7	1.18
2329	757.720	13 8 6	13 9 5	1.07
		25 5 21	25 6 20	1.62
		12 8 4	12 9 3	0.93
2330	757.815	11 8 4	11 9 3	0.76
		16 6 10	17 7 11	2.61
		10 8 2	10 9 1	0.59
2333	758.161	35 4 32	36 5 31	0.56
2336	758.437	26 5 21	27 6 22	1.69
		8 7 1	9 8 2	3.05
2337	758.660	17 7 11	18 8 11	2.50
2662	759.166	27 5 23	28 6 22	1.36
2663	759.225	9 7 3	10 8 2	2.97
2664	759.367	18 6 12	19 7 13	2.38
2667	759.670	28 5 24	29 6 24	1.26
2668	760.038	10 7 3	11 8 4	2.90
2669	760.138	19 6 14	20 7 13	2.26
2653	760.576	29 5 25	30 6 24	1.12
2656	760.854	11 7 5	12 8 4	2.87
		20 6 14	21 7 15	2.13
2661	761.250	30 5 25	31 6 26	1.01
2666	761.663	12 7 5	13 8 6	2.76
		21 6 16	22 7 15	2.00
2667	761.990	31 5 27	32 6 26	0.90
2670	762.608	22 6 16	23 7 17	1.87
		13 7 7	14 8 6	2.65
2672	762.626	32 5 27	33 6 28	0.81
2677	763.166	23 6 18	24 7 17	1.76
		32 9 23	32 10 22	0.53
2678	763.215	14 7 7	15 8 8	2.56
2679	763.366	33 5 29	34 6 28	0.72
2157	729.503	21 5 17	21 6 16	2.82
		6 3 3	7 4 4	3.03
		20 4 16	20 5 15	3.35
2158	729.677	19 4 16	19 5 15	3.62
		18 2 16	17 3 15	2.67
2159	729.752	18 4 14	18 5 13	2.67
2160	729.836	17 4 14	17 5 13	3.69
2161	729.931	16 4 12	16 5 11	3.68
		60 0 60	61 1 61	1.69
		15 4 12	15 5 11	3.66
2162	730.013	14 4 10	14 5 9	3.37
2163	730.076	13 4 10	13 5 9	3.25
2164	730.113	12 4 8	12 5 7	3.10
2165	730.150	11 4 8	11 5 7	2.91
2166	730.201	16 6 10	1- 7 9	0.66
		10 4 6	10 5 5	2.67
		9 4 6	9 5 5	2.39
		8 4 4	8 5 3	2.05
2167	730.282	8 4 4	8 5 3	2.05
		7 4 4	7 5 3	1.98
2168	730.365	7 4 4	7 5 3	1.66
		6 4 2	6 5 1	1.21
2169	730.500	39 2 38	40 1 39	1.12
		5 4 2	5 5 1	0.66
		38 1 37	39 2 38	1.36
		61 1 61	62 0 62	1.31
2170	730.556	15 2 14	16 3 13	2.56
2171	730.666	14 2 12	15 3 13	2.50
2176	731.101	8 3 5	9 4 6	3.12
		13 6 10	14 7 7	0.62
		62 0 62	63 1 63	1.35
2179	731.669	20 2 18	21 3 19	2.31
		17 1 17	18 2 16	0.80
2181	731.690	61 2 60	62 1 61	0.68
		63 1 63	64 0 64	1.00
		22 3 19	21 4 18	0.60
2183	731.895	9 3 7	10 4 6	3.14
2187	732.185	22 2 20	23 3 21	2.11
2191	732.679	17 2 16	18 3 15	2.29
2193	732.710	10 3 7	11 4 8	3.13
		26 2 22	25 3 23	1.91
		62 1 61	63 2 62	0.77
2196	732.862	65 1 65	66 0 66	0.79
2195	732.983	63 2 62	66 1 63	0.87
2351	763.426	26 3 23	27 4 24	1.50
		18 6 12	18 7 11	2.36
2302	763.517	17 6 12	17 7 11	2.36
		16 6 10	16 7 9	2.33
2303	763.665	15 6 10	15 7 9	2.27
2306	763.721	14 6 8	14 7 7	2.19
		13 6 8	13 7 7	2.07
2305	763.805	12 6 6	12 7 5	1.92
		7 5 3	8 6 2	3.18
		11 6 6	11 7 5	1.72
2306	763.919	10 6 4	10 7 3	1.49
		9 6 4	9 7 3	1.31
2308	764.131	16 4 12	17 5 13	2.88
2309	764.235	28 3 25	29 4 26	1.25
2313	764.610	25 3 23	26 4 22	1.58
		8 5 3	9 6 4	3.35
2315	764.883	11 5 7	12 6 6	3.02
		17 4 14	18 5 13	2.77
2319	765.326	32 3 29	33 4 30	0.83
2320	765.429	9 5 5	10 6 4	3.32
2322	765.660	18 4 14	19 5 15	2.65
2329	766.218	10 5 5	11 6 6	3.27
2330	766.323	27 3 25	28 4 26	1.29
2331	766.420	19 4 16	20 5 15	2.52
2338	767.028	11 5 7	12 6 6	3.22
2339	767.162	20 4 16	21 5 17	2.39
2343	767.817	12 5 7	13 6 8	3.16
2346	767.919	21 4 18	22 5 17	2.25
2348	768.189	29 3 27	30 4 26	1.02
2351	768.612	13 5 9	14 6 8	3.09
		22 4 18	23 5 19	2.10
		35 2 29	35 3 28	0.66
2352	768.765	36 2 27	36 3 26	0.73
2353	768.903	33 2 27	33 3 26	0.81
2354	769.053	32 2 25	32 3 24	0.89
2355	769.157	31 2 25	31 3 24	0.98
2357	769.320	30 2 23	30 3 22	1.07
2358	769.398	16 5 9	15 6 10	3.00
		23 4 20	24 5 19	1.96
		29 2 23	29 3 22	1.16
2359	769.562	28 2 21	28 3 20	1.25
2360	769.635	27 2 21	27 3 20	1.34
2361	769.726	26 2 19	26 3 18	1.43
2362	769.872	25 2 19	25 3 18	1.51
		6 6 0	7 7 1	3.38
		24 7 17	24 8 16	1.59
2681	783.491	29 9 21	30 10 20	0.63
2682	783.600	28 9 19	28 10 18	0.73
2683	783.701	27 9 19	27 10 18	0.78
2686	783.807	26 9 17	26 10 16	0.83
2685	783.909	24 6 18	25 7 19	1.61
		25 9 17	25 10 16	0.88
2686	783.979	15 7 9	16 8 8	2.66
		24 9 15	24 10 14	0.92
2687	784.084	23 9 15	23 10 14	0.96
2688	784.153	22 9 13	22 10 12	0.99
2689	784.266	21 9 13	21 10 12	1.01
2690	784.328	20 9 11	20 10 10	1.07
2691	784.448	18 9 9	18 10 8	1.01
2692	784.615	16 9 7	16 10 6	0.96
		25 6 20	26 7 19	1.69
		15 9 7	15 10 6	0.88
2693	784.758	17 9 9	17 10 8	1.00
2699	785.337	26 6 20	27 7 21	1.37
2500	785.425	8 6 0	9 9 1	2.75
2501	785.537	17 7 11	18 8 10	2.36
2507	786.089	27 5 23	28 6 22	0.63
		27 6 22	28 7 21	1.25
2508	786.262	9 8 2	10 9 1	2.66
2509	786.313	18 7 11	19 8 12	2.13
2517	786.517	28 5 24	29 6 23	1.24
2511	787.060	10 8 2	11 9 3	2.58
		19 7 13	20 8 12	2.02
2521	787.533	29 6 24	30 7 23	1.03
2523	787.836	11 8 4	12 9 3	2.50
		20 7 13	21 8 14	1.90
2526	788.232	30 6 24	31 7 25	0.93
2530	788.625	21 7 15	22 8 14	1.78
		12 8 4	13 9 5	2.62
2532	788.979	31 6 26	32 7 25	0.83
2535	789.326	22 7 15	23 8 16	1.66
2536	789.395	13 8 6	14 9 5	2.33
2538	789.637	32 6 26	33 7 27	0.76
2542	790.117	24 7 17	24 8 16	1.55
2543	790.209	14 8 6	15 9 7	2.26
2545	790.358	33 6 28	34 7 27	0.66
		31 10 22	31 11 21	0.43
2546	790.491	30 10 20	30 11 19	0.46
2547	790.569	29 10 20	29 11 19	0.50
2548	790.716	28 10 18	28 11 17	0.54
2549	790.806	27 10 18	27 11 17	0.57

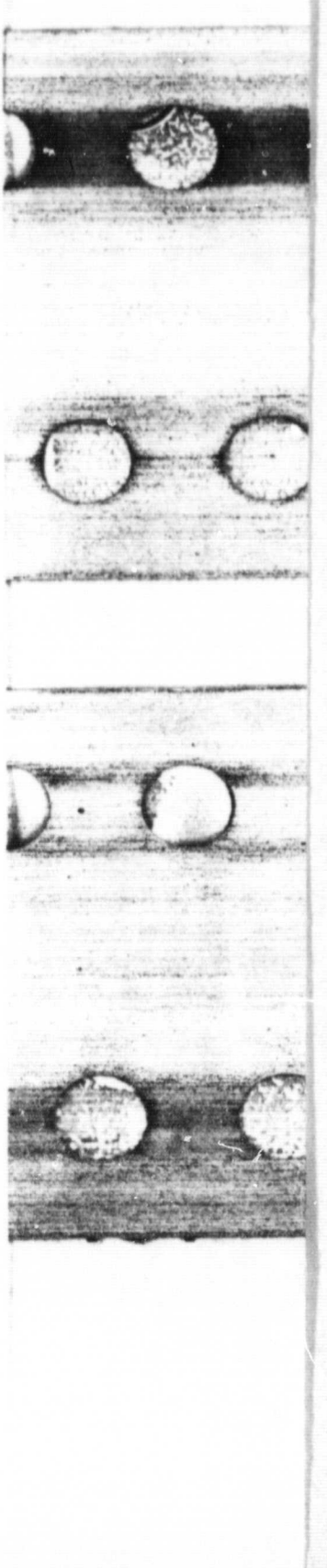

TABLE VI—*Continued*

Line No.	Observed Wavenumber (cm^{-1} vac.)	Lower State J'' K_a'' K_c''	Upper State J' K_a' K_c'	I_r
2550	770.857	26 7 19	25 8 18	1.63
2551	771.001	15 8 8	16 9 7	2.36
2552	771.070	26 10 16	26 11 15	0.67
2553	771.253	22 10 12	22 11 11	0.71
2555	771.582	25 7 19	26 8 18	1.32
2557	771.757	16 8 8	17 9 9	2.05
2562	772.360	26 7 19	27 8 20	1.21
2566	772.551	17 8 10	18 9 9	1.95
2568	772.857	23 7 21	28 8 20	1.10
2569	773.303	9 9 1	10 10 0	2.30
		18 8 10	19 9 11	1.86
2573	773.766	28 7 21	29 8 22	1.00
2577	774.083	19 8 12	20 9 11	1.76
		10 9 1	11 10 2	2.22
2579	774.521	29 7 23	30 8 22	0.91
2581	774.866	20 8 12	21 9 13	1.84
		11 9 3	12 10 2	2.34
2583	775.236	30 7 23	31 8 24	0.82
2586	775.606	21 8 14	22 9 13	1.53
2587	775.675	12 9 3	13 10 4	2.06
2589	775.920	31 7 25	32 8 24	0.74
2592	776.338	22 8 14	23 9 15	1.43
2593	776.461	13 9 5	14 10 4	1.98
2596	776.651	32 7 25	33 8 26	0.66
2598	777.117	23 8 16	24 9 15	1.33
2599	777.360	14 9 5	15 10 6	1.89
2600	777.367	33 7 27	34 8 26	0.58
2606	777.581	24 8 16	25 9 17	1.23
2607	778.051	15 9 7	16 10 6	1.81
		26 11 15	26 12 14	0.63
		36 7 29	35 8 28	0.52
2610	778.597	25 8 18	26 9 17	1.13
2612	778.825	16 9 7	17 10 8	1.72
2618	779.386	26 8 18	27 9 19	1.03
2620	779.592	17 9 9	18 10 8	1.63
2623	780.077	27 8 20	28 9 19	0.96
2625	780.363	18 9 9	19 10 10	1.54
2628	780.790	28 8 20	29 9 21	0.86
2631	781.157	19 9 11	20 10 10	1.43
		10 10 0	11 11 1	1.85
2636	781.511	29 8 22	30 9 21	0.77
2637	781.897	20 9 11	21 10 12	1.36
2638	782.078	11 10 2	12 11 1	1.77
2644	782.672	21 9 13	22 10 12	1.27
2645	782.777	12 10 2	13 11 3	1.70
2647	782.975	31 8 24	32 9 23	0.63
2650	783.606	22 9 13	23 10 14	1.19
2651	783.563	13 10 4	14 11 3	1.62
2652	783.680	32 8 24	33 9 25	0.56
2656	784.165	23 9 15	24 10 14	1.10
2657	784.354	14 10 4	15 11 5	1.55
2662	784.908	24 9 15	25 10 16	1.01
2663	785.110	15 10 6	16 11 5	1.68
2667	785.673	25 9 17	26 10 16	0.93
2669	785.902	16 10 6	17 11 7	1.60
2674	786.398	26 9 17	27 10 18	0.85
2676	786.696	17 10 8	18 11 7	1.53
2680	787.151	27 9 19	28 10 18	0.78
2681	787.434	28 10 8	19 11 9	1.25
2683	787.855	28 9 19	29 10 20	0.81
2686	788.232	19 10 10	20 11 9	1.18
2694	788.991	30 10 10	21 11 11	1.10
2695	789.121	11 11 1	12 12 0	1.47
2696	789.377	30 9 21	31 10 22	0.57
2697	789.750	21 10 12	22 11 11	1.03
2698	789.86_	17 11 1	13 12 2	1.35
2700	790.038	31 9 23	32 10 22	0.51
2704	790.577	22 10 12	23 11 13	0.95
2705	790.674	13 11 3	14 12 2	1.29
2706	790.731	32 9 23	33 10 24	0.66
2711	791.254	23 10 14	24 11 13	0.88
2717	791.667	33 9 25	34 10 24	0.61
2717	791.995	24 10 14	25 11 15	0.81
2720	792.280	15 11 5	16 12 4	1.17
2723	792.761	25 10 16	26 11 15	0.75
2725	793.035	16 11 5	17 12 6	1.11
2728	793.500	26 10 16	27 11 17	0.68
2731	793.822	17 11 7	18 12 6	1.06
2735	794.261	27 10 18	28 11 17	0.62
2738	794.590	18 11 7	19 12 8	0.98
2740	794.954	28 10 18	29 11 19	0.54
2743	795.362	19 11 9	20 12 8	0.92
2744	795.699	29 10 20	30 11 19	0.51
2746	796.106	20 11 9	21 12 10	0.86
2754	796.678	21 11 11	22 12 10	0.80
2762	797.630	22 11 11	23 12 12	0.74
2764	797.861	13 12 2	14 13 1	1.00
2768	798.389	23 11 13	24 12 12	0.69
2770	798.653	14 12 2	15 13 3	0.96
2773	799.133	24 11 13	25 12 14	0.63
2779	799.697	25 11 15	26 12 14	0.58
2781	800.195	16 12 4	17 13 5	0.85
2783	800.423	26 11 15	27 12 16	0.53
2786	800.962	17 12 6	18 13 5	0.80
2788	801.367	27 11 17	28 12 16	0.68
2789	801.763	18 12 6	19 13 7	0.75
2791	802.083	28 11 17	29 12 18	0.66
2797	802.503	19 12 8	20 13 7	0.70
2801	803.238	20 12 8	21 13 9	0.65
2807	804.023	21 12 10	22 13 9	0.61
2810	804.853	22 12 10	23 13 11	0.56
2815	805.000	13 13 1	14 14 0	0.76
2819	805.528	23 12 12	24 13 11	0.52
2820	805.800	14 13 1	15 14 2	0.70
2825	806.582	15 13 3	16 14 2	0.66

The following assignments have been omitted in the above list.

Line No.	Observed Wavenumber (cm^{-1} vac.)	Lower State J'' K_a'' K_c''	Upper State J' K_a' K_c'	I_r	
1606	686.852	20 6 14	21 5 17	0.68	
1613	686.475	6 3 3	6 2 4	1.20	
		8 3 5	etc. as in the above list		
1766	694.731	26 5 21	26 4 22	0.76	
1770	695.112	12 1 11	12 0 12	5.08	
1861	701.818	24 5 21	etc. as in the above list		plot
		17 3 15	18 2 16	1.50	
2023	715.961	36 1 33	etc. as in the above list		plot
		26 5 19	25 6 18	2.69	
2209	736.214	45 2 44	46 1 45	0.51	
		36 5 31	etc. as in the above list		
2693	784.768	13 9 5	13 10 4	0.69	
		16 7 9	17 8 10	1.35	

Interpretation of the ν_2 Structure of Ozone

Table VI gives the measured positions and assignments of some of the structure observed for the ν_2 band.[4] The basis of these assignments was the computed spectrum for the ν_2 band. For these computations the energy levels for the ground state were obtained by using 107 microwave lines with $J \leq 56$ and $K_{-1} \leq 8$. The ν_2 state levels were also calculated by making use of the microwave data discussed in Section I and of the band center already described in Section II. The relative intensities of the lines are also important parameters and they were calculated[5] according to the formula

$$I_r = S[\exp(-W/kT) - \exp(-W'/kT)],$$

where S is the calculated line strength of the transitions, W and W' are the energies of the ground state and z_2 state levels, respectively, and T is the temperature, set to 300 K. Table VI includes I_r values also. About 950 lines in the observed spectrum have been identified in this manner with J values up to 46 and K_{-1} values up to 14 with $I_r \geq 0.4$ which corresponds to 1/18 of the intensity of the strongest line. The spectrum itself showed several other weaker features which were all documented by Hoh (*13*). In fact, the serial numbers given in the first column of Table VI were taken from Hoh's compilation.

[4] In Table VI the ozone assignments were omitted whenever there was interference due to impurity lines of CO_2. Also, the assignments are given in terms of JK_aK_c instead of $JK_{-1}K_{+1}$ used in the rest of the paper. Both these equivalent notations appear in the literature (see, for instance, K. Narahari Rao in Physical Chemistry (D. A. Ramsay, Ed.), Series 2 Vol. 3, p. 348, Butterworths (1976)).

[5] Details of these calculations are available in Ref. (2).

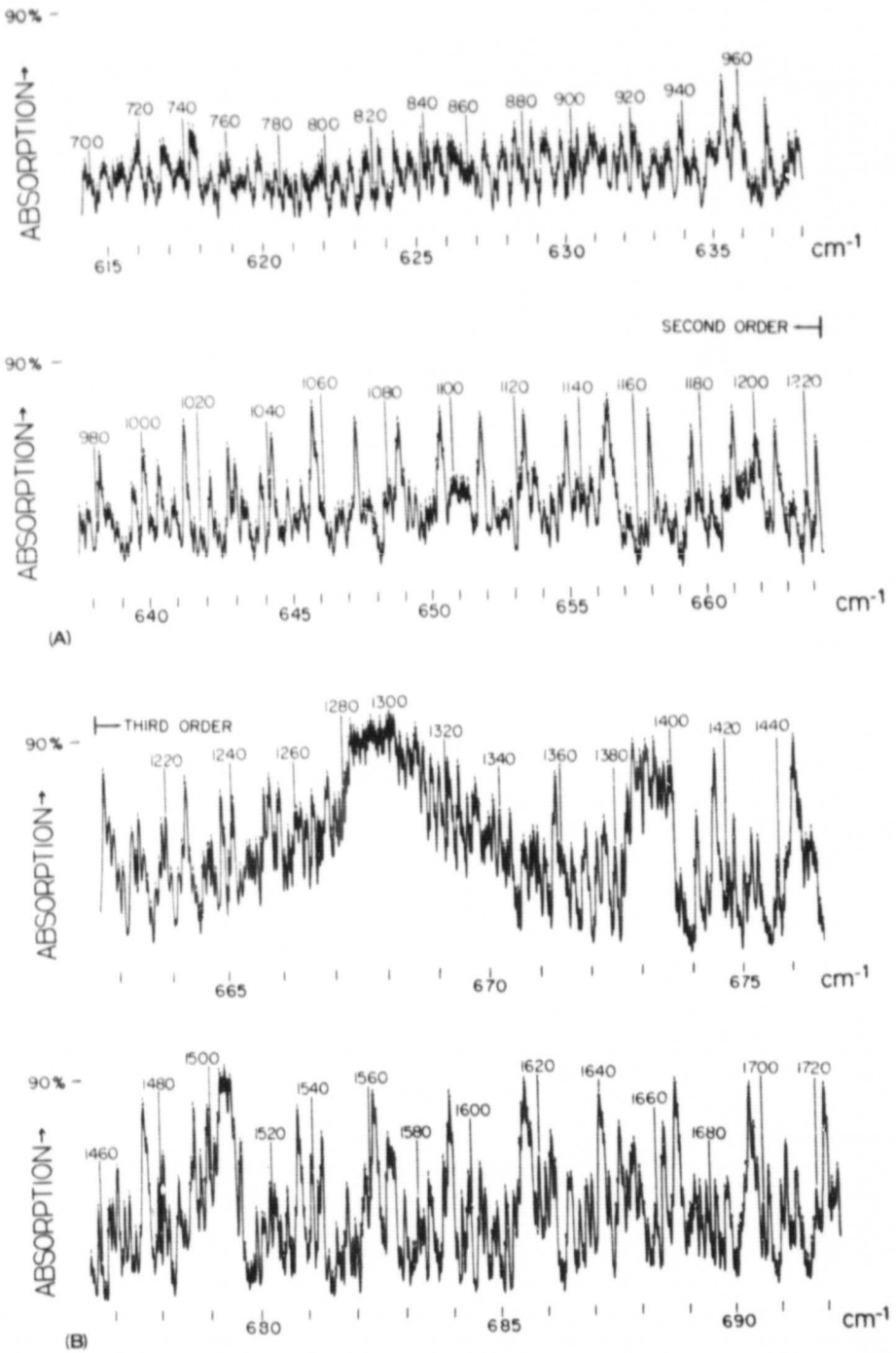

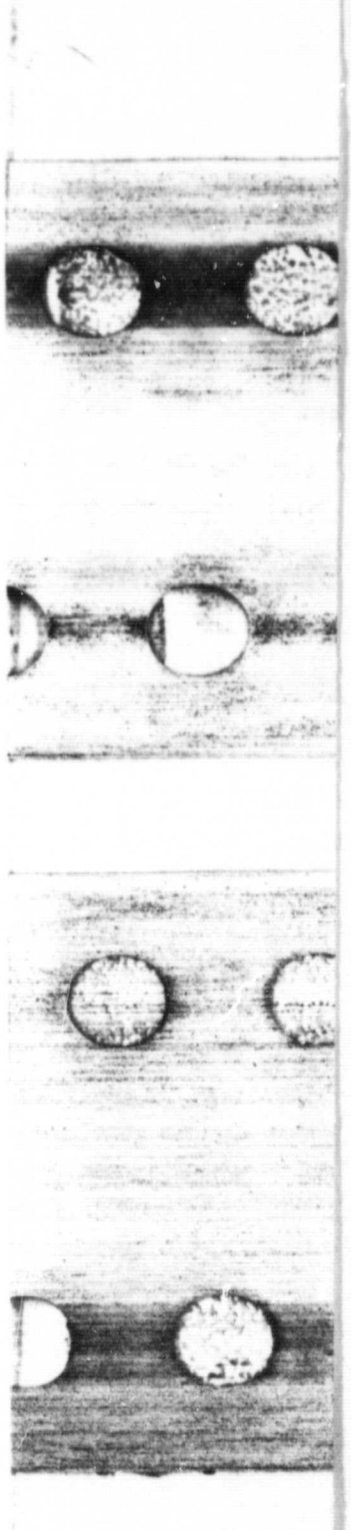

FIG. 1. ν_3 band region of $^{16}O_3$ from 615 to 806 cm^{-1}. Path length: 4 meters. Pressure: 25 mm of Hg. Ozone concentration: 50 to 35% Temperature of cell: 300 K.

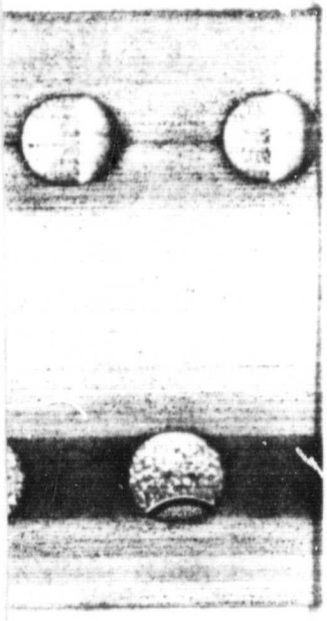

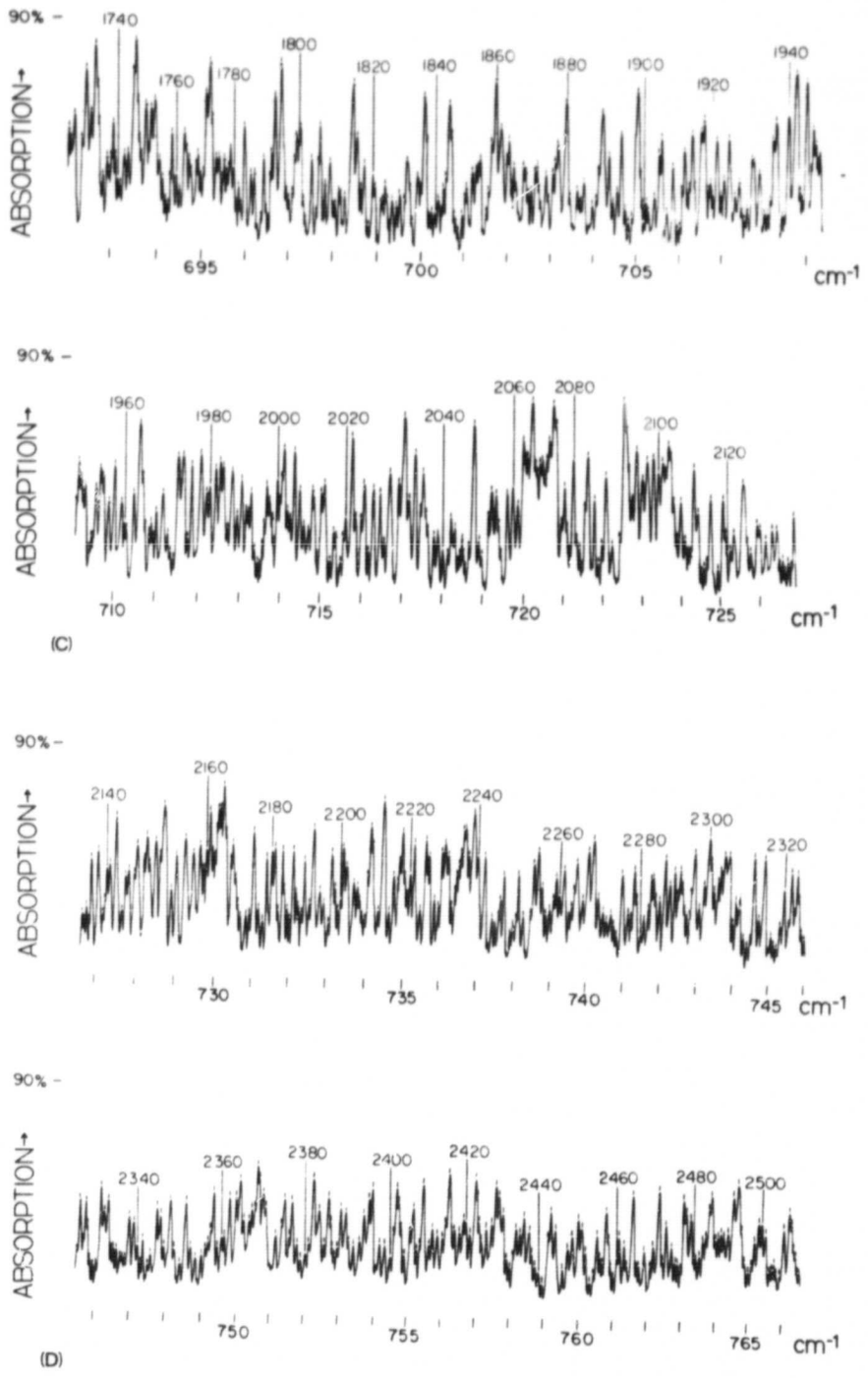

FIG. 1—*Continued*

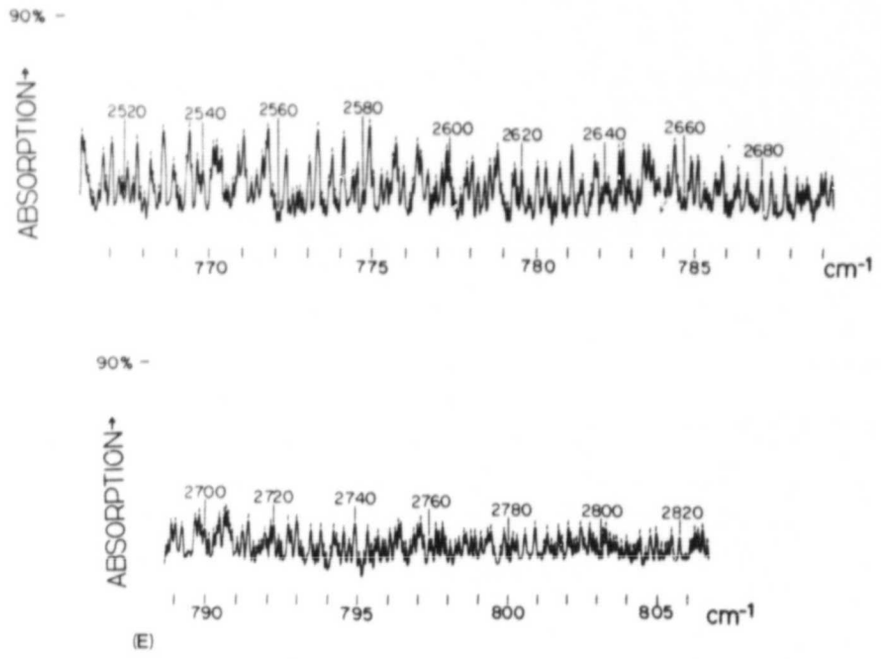

FIG. 1—*Continued*

Since the tunable diode laser spectroscopy in this region is progressing rapidly (*14*), before long it should be possible to record the ν_2 band of ozone with a resolution of 0.002 cm^{-1} and improve on the present analysis.

ACKNOWLEDGMENTS

The support extended to the Ohio State University research programs by the National Environmental Satellite Service, National Oceanic and Atmospheric Administration (NESS-NOAA), the Atmospheric Research Section of the National Science Foundation, and the National Aeronautics and Space Administration is gratefully acknowledged.

We also wish to express our thanks to Dr. C. Camy-Peyret and Dr. J. M. Flaud for participating in the calculations of the $(\nu_2 + \nu_3) - \nu_2$ band.

RECEIVED: September 1, 1977

REFERENCES

1. J. C. DEPANNEMAECKER, B. DUTERAGE, AND J. BELLET, *J. Quant. Spectrosc. Radiat. Transfer* **17** 519–530 (1977).
2. N. MONNANTEUIL, Thesis, Universite de Lille I (1976).
3. A. BARBE, C. SECROUN, P. JOUVE, N. MONNANTEUIL, J. C. DEPANNEMAECKER, B. DUTERAGE, J. BELLET, AND P. PINSON, *J. Mol. Spectrosc.* **64**, 343–364 (1977).
4. A. BARBE, C. SECROUN, P. JOUVE, C. CAMY-PEYRET, AND J. M. FLAUD (to be published).
5. T. TANAKA AND Y. MORINO, *J. Mol. Spectrosc.* **33**, 538–551 (1970).

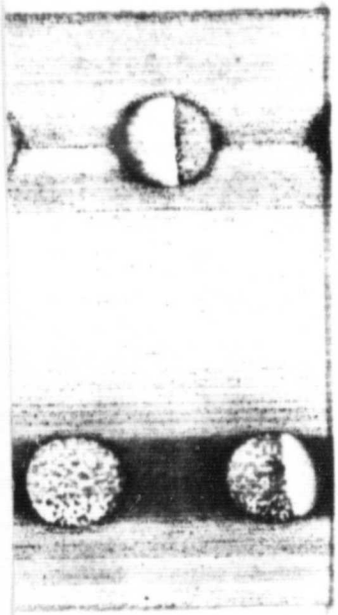

6. L. Pierce, *J. Chem. Phys.* **24**, 139–142 (1956).
7. J. C. Depannemaecker and J. Bellet, *J. Mol. Spectrosc.* **66**, 106–120 (1977).
8. A. Barbe, Thesis, Faculte des Sciences de Reims (1974).
9. T. Tanaka and Y. Morino, *J. Mol. Sepectrosc.* **33**, 552–553 (1970).
10. W. E. Nexsen, Jr., Ph.D. dissertation, The Ohio State University (1955).
11. K. Narahari Rao, C. J. Humphreys, and D. H. Rank, "Wavelength Standards in the Infrared," Academic Press, New York (1966).
12. H. R. Gordon and T. K. McCubbin, Jr., *J. Mol. Spectrosc.* **18**, 73–82 (1965).
13. Yan-Shek Hoh, Ph.D. dissertation, The Ohio State University (1976).
14. J. S. Knoll, G. L. Tettemer, W. G. Planet, K. Narahari Rao, Da-Wun Chen, and L. A. Pugh, *Appl. Opt.* **15**, 2973–2974 (1976).

JOURNAL OF MOLECULAR SPECTROSCOPY 84, 313–317 (1980)

NOTE

Diode Laser Spectra of Acetylene: ν_5 Region at 15 μm[1]

In 1979, during the early studies of diode laser spectra in this laboratory (*1*) it became evident that useful spectroscopic information can be derived for the acetylene molecule and its isotopic species even though only limited regions can be scanned by this technique. In the present study, the Q branches of the ν_5 of $^{12}C_2H_2$ and $2\nu_5^0-\nu_5^1$ "hot" bands of $^{12}C_2H_2$, $^{12}C^{13}CH_2$, and $^{13}C_2H_2$, all occurring in a natural sample of acetylene, were recorded and measured by using a diode laser spectrometer. For wavenumber calibration, lines from the ν_2 bands of HCN (*2*) and CO_2 (*3*) were used. The data obtained are estimated to be internally consistent to within ± 0.0005 cm^{-1} (*4*). Figure 1 gives an illustration of the spectra obtained along with a small portion of the grating spectrum (*5*).

In obtaining molecular constants from the observational data, for the ν_5^1 and $2\nu_5^0$ states of $^{12}C_2H_2$ we combined our data with those of Ref. (*5*). This resulted in improved values for the band centers and some of the rotational constants. Tables I–III present experimental data and the molecular constants determined.

While treating the data for $\Pi-\Sigma$ bands, we found it convenient to use the following expressions:

For the P and R transitions of ν_5 ($\Pi \leftarrow \Sigma$)

$$\nu(m) = (\nu_0 - B_r' - D_r' - H_r') + (B_r' + B_r'' + 2D_r' + 3H_r')m + (B_r' - B_r'' + D_r' + D_r'')m^2$$
$$+ (-2D_r' - 2D_r'' - 5H_r' + H_r'')m^3 + (-D_r' + D_r'' - 3H_r'')m^4$$
$$+ 3(H_r' + H_r'')m^5 + (H_r' - H_r'')m^6 \cdots,$$

For above Eq. and what follows below in Eq. 2

$$m = -J \text{ for a } P \text{ line}$$
$$= J + 1 \text{ for a } R \text{ line},$$

and

$$B_r = B_i - (1/2)(q_i - 2q_i^J + 3q_i^{JJ}),$$
$$B_f = B_i + (1/2)(q_i - 2q_i^J + 3q_i^{JJ}),$$
$$D_r = D_i - (1/2)(q_i^J - 3q_i^{JJ}),$$
$$D_f = D_i + (1/2)(q_i^J - 3q_i^{JJ}),$$
$$H_r = H_i - (1/2)q_i^{JJ},$$
$$H_f = H_i + (1/2)q_i^{JJ}. \quad (1)$$

The meaning of the q constants has been given by Maki and Lide (*6*).

For the Q transitions of the ν_5 band

$$Q(J) = [\nu_0 + (q_i - q_i^J + q_i^{JJ}) - B_f' - D_f' - H_f'] + (B_f' - B_f'' + 2D_f' + 3H_f')\{J(J+1)\}$$
$$+ (-D_f' + D_f'' - 3H_f')\{J^2(J+1)^2\} + (H_f' - H_f'')\{J^3(J+1)^3\}. \quad (2)$$

From these equations we note that the band origin ν_0 has been identified with a P or R branch transition. As a result, a $Q(J)$ transition for a $\Pi \leftarrow \Sigma$ band is essentially shifted by $(q_i - q_i^J + q_i^{JJ})$.

[1] Support extended this research by the National Aeronautics and Space Administration is gratefully acknowledged.

0022-2852/80/110313-05$02.00/0

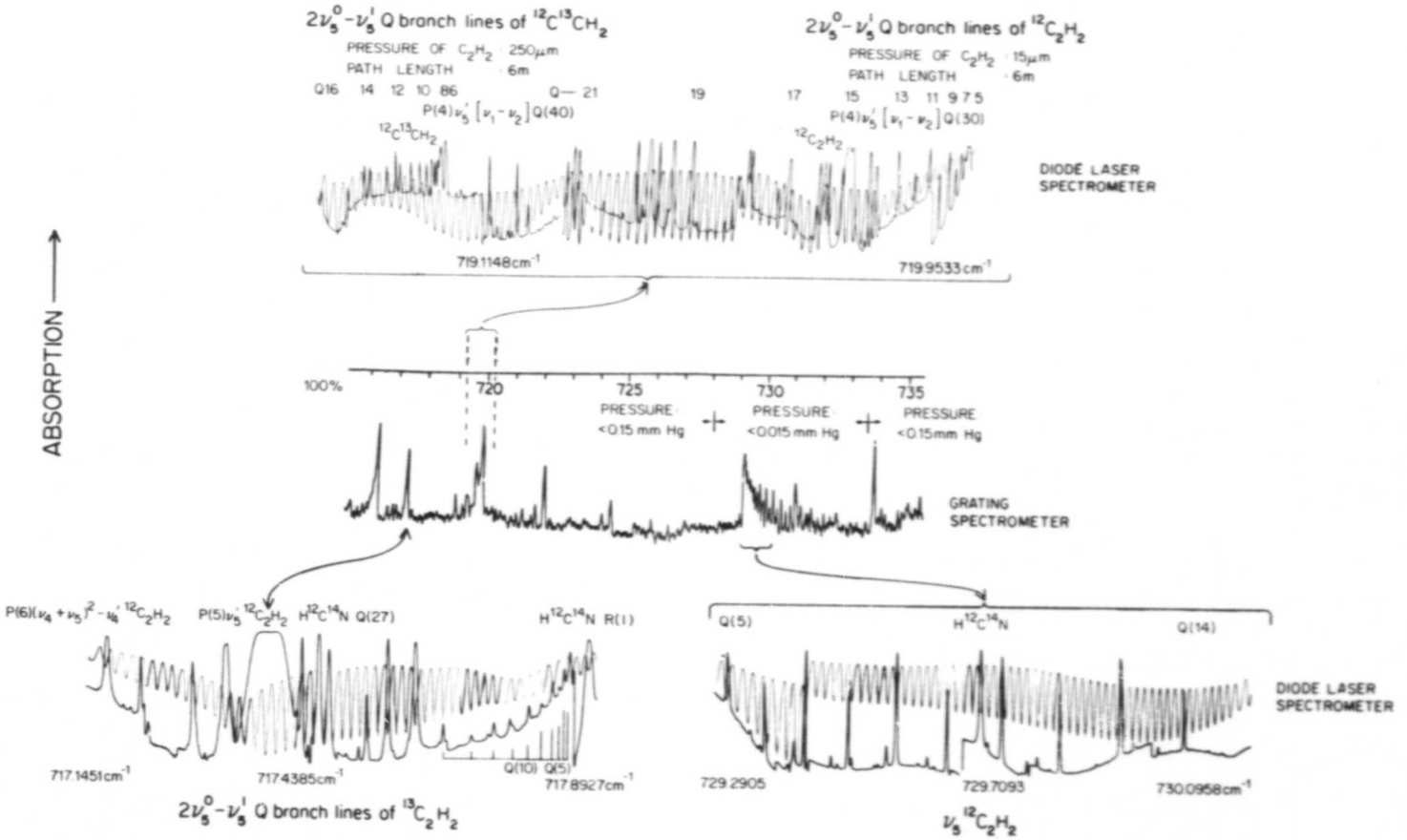

FIG. 1. Acetylene spectrum at 15 μm.

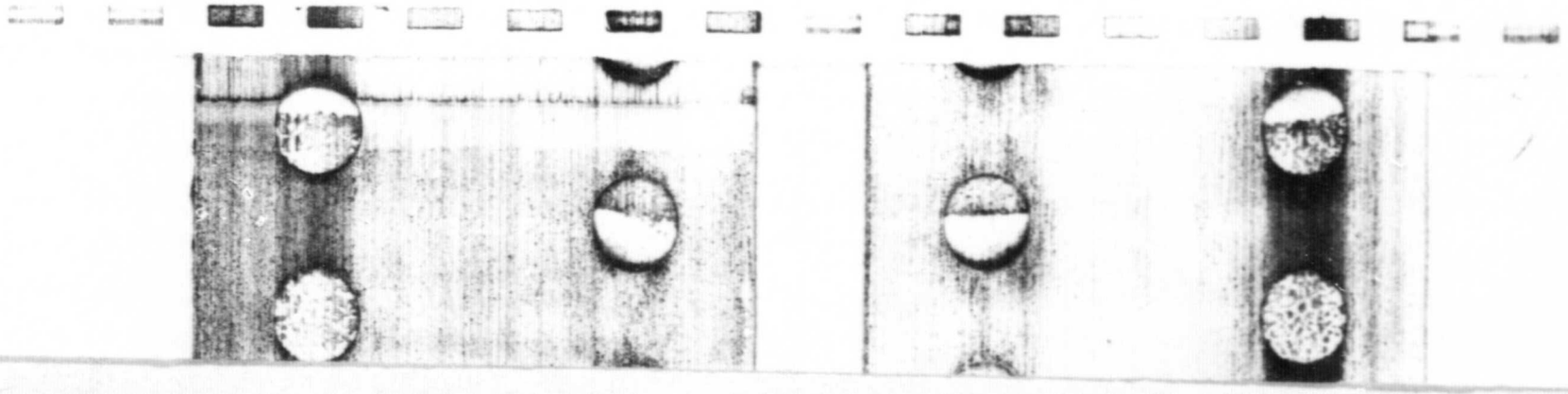

TABLE I

Wavenumbers (vac. cm^{-1}) and Molecular Constants (in cm^{-1}) for the Q Branch of the ν_5^1 Band of $^{12}C_2H_2$

Q(J)	$\nu_{calculated}$	(O-C)x10^4
Q(2)	729.1832	7
Q(3)	729.2101	- 6
Q(4)	729.2459	2
Q(5)	729.2907	- 2
Q(6)	729.3444	0
Q(7)	729.4070	0
Q(8)	729.4787	- 5
Q(9)	729.5592	1
Q(10)	729.6487	- 2
Q(11)	729.7472	2
Q(12)	729.8546	6
Q(13)	729.9710	3
Q(14)	730.0963	- 5

$\nu_o - B_f' - D_f' + q$ = 729.15639 ± 0.00019

$B_f' - B_e'' + 2D_f'$ = 0.0044759 ± 0.0000018

TABLE II

Wavenumbers (vac. cm^{-1}) and Molecular Constants (in cm^{-1}) for the Q Branch of the $2\nu_5^0 - \nu_5^1$ Band of $^{12}C_2H_2$, $^{12}C^{13}CH_2$, and $^{13}C_2H_2$. The ν's in columns 2, 4 and 6 are calculated values

	$^{12}C_2H_2$		$^{12}C^{13}CH_2$		$^{13}C_2H_2$	
Q(J)	ν	(O-C)x10^4	ν	(O-C)x10^4	ν	(O-C)x10^4
Q(5)	719.9533	2			717.8709	1
Q(6)	719.9491	1	719.0239	- 2	717.8652	- 2
Q(7)	719.9428	1	719.0190	2	717.8570	- 3
Q(8)	719.9341	- 2	719.0123*		717.8457	2
Q(9)	719.9224	- 2	719.0034	0	717.8304	4
Q(10)	719.9069	- 3	718.9918	0	717.8105	1
Q(11)	719.8869	0	718.9768	0	717.7851	- 1
Q(12)	719.8618	- 4	718.9577	- 1	717.7533	- 3
Q(13)	719.8308	6	718.9338	- 1	717.7144	- 2
Q(14)	719.7932	6	718.9041	2	717.6675	3
Q(15)	719.7481	- 3	718.8678	0	717.6119	2
Q(16)	719.6948	0	718.8237	0	717.5468	- 2
Q(17)	719.6327	- 4				
Q(18)	719.5609	2				
Q(19)	719.4789	4				
Q(20)	719.3862	- 2				
Q(21)	719.2822	- 5				
Q(22)	719.1667	3				

	$^{12}C_2H_2$	$^{12}C^{13}CH_2$	$^{13}C_2H_2$
$\nu_o + B_f'' + D_f''$	719.95970 ± 0.00037	719.03330 ± 0.00038	717.87953 ± 0.00055
$B_e' - B_f'' - 2D_f''$	(- 1.072 ± 0.064)x10^{-4}	(- 1.345 ± 0.097)x10^{-4}	(- 1.54 ± 0.15)x10^{-4}
$D_e' - D_f''$	(3.535 ± 0.029)x10^{-6}	(2.119 ± 0.070)x10^{-6}	(4.55 ± 0.12)x10^{-6}
$H_e' - H_f''$	(1.283 ± 0.036)x10^{-9}	(-0.81 ± 0.15)x10^{-9}	(2.29 ± 0.25)x10^{-9}

TABLE III

Molecular Constants of $^{12}C_2H_2$ (in cm^{-1})

$\nu_0(0000^0{}_1{}^1 \leftarrow 0000^0{}_0{}^0) = 730.33281 \pm 0.00019$ $\quad$ $\nu_0(0000^0{}_2{}^0 \leftarrow 0000^0{}_1{}^1) = 718.78334 \pm 0.00037$

$0000^0{}_0{}^0$	$0000^0{}_1{}^1$	$0000^0{}_2{}^0$
$B_0 = 1.176608 \pm 0.000014$*	$B = 1.178768 \pm 0.000023$	$B = 1.181008 \pm 0.000014$
$D_0 = (1.610 \pm 0.007) \times 10^{-6}$*	$D = (1.633 \pm 0.013) \times 10^{-6}$*	$D = (5.190 \pm 0.031) \times 10^{-6}$**
	$q_v = 0.004711 \pm 0.000023$*	$H = (1.283 \pm 0.036) \times 10^{-9}$**
	$q_v^J = (4.5 \pm 1.3) \times 10^{-8}$*	

*Values taken from Ref. (5).

**Represent only effective constants

In the case of the $2\nu_5^0-\nu_5^1$ band ($\Sigma \leftarrow \Pi$), P and R transitions have been represented by

$$\nu(m) = (\nu_0 + B_v'' + D_v'' + H_v'') + (B_v' + B_v'' + 2D_v'' + 3H_v'')m + (B_v' - B_v'' - D_v' - D_v'')m^2 + (-2D_v' - 2D_v'' + H_v' - 5H_v'')m^3 + (-D_v' + D_v'' + 3H_v')m^4 + 3(H_v' + H_v'')m^5 + (H_v' - H_v'')m^6 \cdots \quad (3)$$

In this case, the Q branch transitions would be given by

$$Q(J) = [\nu_0 - (q_v'' - q_v''^J + q_v''^{JJ}) + B_f'' + D_f'' + H_f''] + (B_v' - B_f'' - 2D_f'' - 3H_f'')J(J+1) + \{-(D_v' - D_f'') + 3H_f''\}J^2(J+1)^2 + (H_v' - H_f'')J_3(J+1)^3. \quad (4)$$

The reliability of the molecular constants given in Tables I–III and the validity of the equations (1)–(4) were checked by calculating the wavenumbers of some $P(J)$ and $R(J)$ lines which were also recorded in this work. The observed wavenumbers for $P(4)$ and $P(5)$ of the ν_5 band of $^{12}C_2H_2$ are 719.7408 and 717.3875 cm^{-1}, which agree well with our calculated values of 719.7416 and 717.3873 cm^{-1}, respectively. Similarly, for the $2\nu_5^0-\nu_5^1$ band, the observed wavenumbers of $P(1)$ and $R(3)$ lines are 717.6070 and 729.4612 cm^{-1} and the corresponding calculated wavenumbers are 717.6069 and 729.4611 cm^{-1}.

In conclusion, it may be mentioned that the astrophysical interest in these bands of C_2H_2 was pointed out by Ridgway (7), who identified them in the infrared spectrum of Jupiter. Measurements of intensities of these 15-μm lines of acetylene have been deferred until we have access to another diode laser operating at these wavelengths because the present one ceased to function after the recording of the above spectra.

REFERENCES

1. S. P. Reddy, V. Malathy Devi, A. Baldacci, W. Ivancic, and K. Narahari Rao, *J. Mol. Spectrosc.* **74,** 217–223 (1979).
2. S. P. Reddy, W. Ivancic, V. Malathy Devi, A. Baldacci, K. Narahari Rao, A. W. Mantz, and R. S. Eng, *Appl. Optics* **18,** 1350–1354 (1979).
3. R. Paso, J. Kauppinen, and R. Antilla, *J. Mol. Spectrosc.* **79,** 236–253 (1980).
4. V. Malathy Devi, Palash P. Das, and K. Narahari Rao, *Appl. Optics* **18,** 2918–2919 (1979).
5. K. F. Palmer, M. Mickelson, and K. Narahari Rao, *J. Mol. Spectrosc.* **44,** 131–144 (1972).

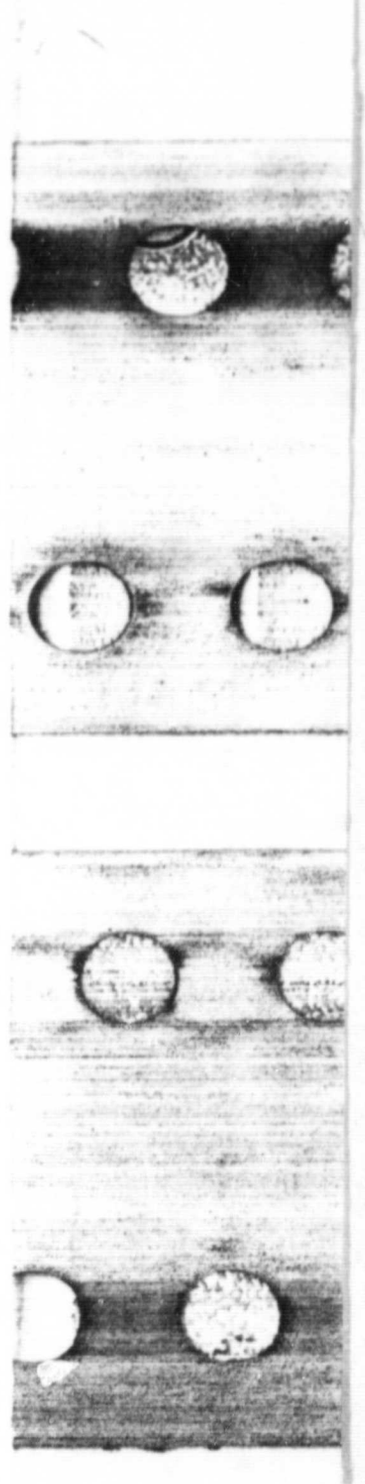

6. A. G. MAKI AND D. R. LIDE, JR., *J. Chem. Phys.* **47,** 3206–3210 (1967).
7. S. T. RIDGWAY, *Astrophys. J.* **187,** L41–L43 (1974)

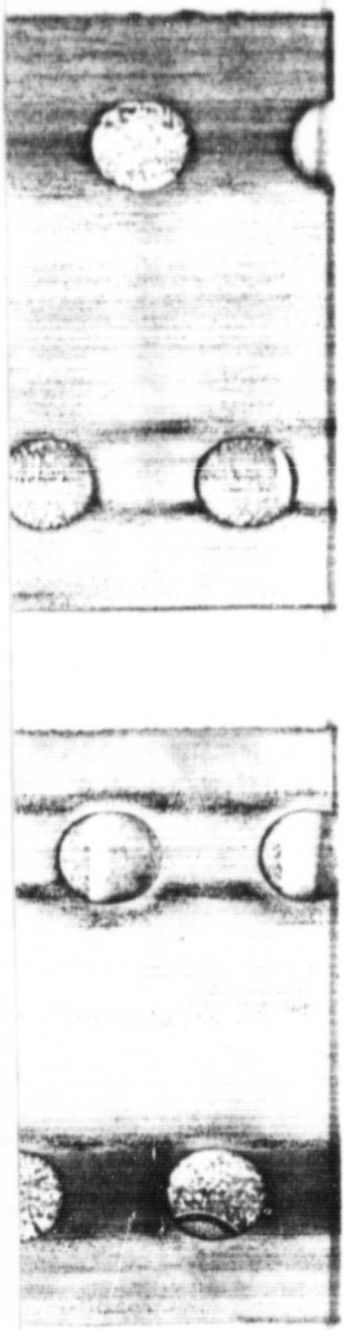

PALASH P. DAS*
V. MALATHY DEVI
K. NARAHARI RAO

Department of Physics,
The Ohio State University,
Columbus, Ohio 43210

Received March 1, 1980

* Present address: Tachisto Inc., 13 Highland Circle, Needham, Mass. 02194

JOURNAL OF MOLECULAR SPECTROSCOPY 74, 217–223 (1979)

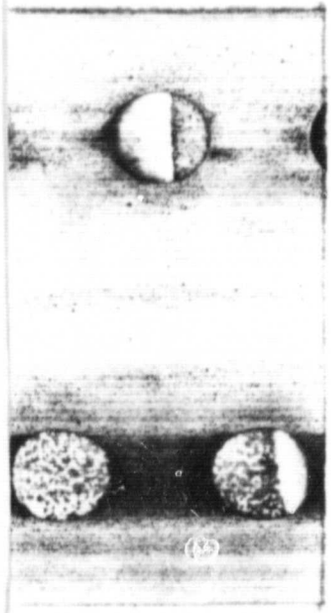

Acetylene Spectra with a Tunable Diode Laser: $(\nu_4 + \nu_5)^{0+} - \nu_4^{1f}$ Q Branches of $^{12}C_2H_2$ and $^{12}C^{13}CH_2$

S. PADDI REDDY,* V. MALATHY DEVI, A. BALDACCI, W. IVANCIC, AND K. NARAHARI RAO

Department of Physics, The Ohio State University, 174 West 18th Avenue, Columbus, Ohio 43210

The rotational structure of the Q branches of the $(\nu_4 + \nu_5)^{0+} - \nu_4^{1f}$ bands of $^{12}C_2H_2$ and $^{12}C^{13}CH_2$ at 13.7 μm has been observed in a natural sample of acetylene by using a tunable diode laser as a source in a high-resolution infrared grating spectrometer equipped with a precision grating drive. Altogether 23 lines from $J = 6$ to 28 for $^{12}C_2H_2$ and 15 lines from $J = 6$ to 20 for $^{12}C^{13}CH_2$ have been identified. The observed full width at half maximum of the resolved lines of these Q branches is very close to the calculated Doppler width. Molecular constants $\nu_0 + B''$, $B' - B'' - 2D''$, $D' - D''$, and $H' - H''$ have been derived from the measured line positions of the rotational structure.

I. INTRODUCTION

The objective of this paper is to report the observation and interpretation of tunable diode laser data for the rotational structure of the Q branches of the $(\nu_4 + \nu_5)^{0+}(\Sigma^+) - \nu_4^{1f}(\Pi)$ band of $^{12}C_2H_2$ and $^{12}C^{13}CH_2$ at 13.7 μm. In recent years diode lasers have been in use for the studies of molecular spectra at Doppler-limited spectral resolution. The present paper not only confirms these findings but also provides an example to demonstrate the sensitivity of the technique by observing the "hot" band of the carbon-13 variety of acetylene occurring in the natural sample. The previous grating data obtained with a conventional source did not have even an indication of this $^{12}C^{13}CH_2$ Q branch.

A large amount of experimental data on the high-resolution infrared absorption spectra of acetylene ($^{12}C_2H_2$) and its isotopic species using conventional thermal radiation sources such as a carbon rod furnace have been obtained over the past several years (see, e.g., Ref. (*1*)). In particular, in the spectral region near 13.7 μm the infrared active $\nu_5^1(\Pi)$ band of $^{12}C_2H_2$ and its five "hot" bands, $2\nu_5^{0,2} - \nu_5^1$ and $(\nu_4 + \nu_5)^{0+,0-,2} - \nu_4^1$, have been studied in considerable detail by Palmer *et al.* (*2*) at a spectral resolution of ~0.04 cm^{-1}. In the present study the high intensity and the narrow width of the modes of the PbSnTe tunable diode laser have made it possible to resolve and analyze the structure of the two

* On sabbatical leave (1977–1978) from Memorial University of Newfoundland, St. John's, Newfoundland A1B 3X7, Canada.

0022-2852/79/020217-07$02.00/0

Q branches of the acetylenes $^{12}C_2H_2$ and $^{12}C^{13}CH_2$ occurring in the spectral region 715.0–716.5 cm^{-1}, both in a commercial sample of acetylene.

II. EXPERIMENTAL DETAILS

The experimental technique employed in the present investigation has been described in detail elsewhere by Reddy *et al.* (3). The tunable diode laser assembly used was supplied by Laser Analytics, Inc. A closed-cycle cryogenic helium compressor unit cooled the crystal diode, a cryogenic temperature stabilizer maintained the required temperature in the range 10–100 K in the diode, and a laser control module unit enabled precise current tuning in the laser thereby producing different laser modes or sweeping a given laser mode continuously through its lasing region.

A 2-m focal length Czerny–Turner vacuum spectrometer equipped with a 31-grooves/mm echelle grating having a ruled area of 25 × 12.5 cm^2 was used for the laser mode separation. With the help of a precision drive, the grating position could be set to match one of the laser modes and the speed of rotation of the grating conveniently adjusted so that it would efficiently synchronize with the sweep rate of a particular laser mode. A wedge-shaped KBr window was used as a beam-splitter after the exit slit of the spectrometer. The transmitted beam from the beam-splitter reached a liquid-nitrogen-cooled HgCdTe detector after passing through the absorption cells. The reflected beam from the front surface of the beam-splitter reached a second liquid-nitrogen-cooled HgCdTe detector after passing through an air-spaced etalon 30.09 cm long in order to produce a Fabry–Perot fringe pattern. The air-spaced etalon consisted of two CdTe plates mounted on the parallel ends of a quartz tube spacer. The absorption spectrum and the Fabry–Perot fringes were simultaneously recorded on a chart paper with a two-pen recorder. The fringe spacing of the etalon in the spectral region under study was 0.016548 ± 0.000030 cm^{-1}. The line positions of the acetylene spectra relative to the absorption lines of the reference spectra were measured as a function of fractional fringe position. Spectra of acetylene in the region 715.0–716.5 cm^{-1} were recorded with an absorption cell 6 m long using gas pressures in the range 50–170 μm of Hg. In the spectral region investigated, four lines $Q(21)$–$Q(24)$ of ν_2^1 band of $H^{12}C^{14}N$ with a sample path length of 20 cm and a pressure of about 1 mm of Hg and two lines $(\nu_1 - \nu_2^1)P(7)$ and ν_2^1 $R(60)$ of $^{12}C^{16}O_2$ with a sample path length of 1.4 m and a pressure of about 2 mm of Hg were also recorded. The wavenumbers of the acetylene lines were measured relative to the four Q lines of $H^{12}C^{14}N$, the positions of which were calculated from the rotational constants given by Maki (*4*, *5*) and the vibrational band origin given by Yin and Rao (*6*). The calculated wavenumbers of $Q(21)$, $Q(22)$, $Q(23)$, and $Q(24)$ of the ν_2^1 band of $H^{12}C^{14}N$ are 715.3307, 715.6474, 715.9779, and 716.3224 cm^{-1}, respectively. The separations $\Delta\nu = Q(J + 1) - Q(J)$ thus calculated agree within a few ten-thousandths of 1 cm^{-1} with those obtained experimentally in Ref. (*6*) and by Wang and Overend (*7*). It is to be noted that the band origin of the ν_2 band of $H^{12}C^{14}N$ determined by Yin and Rao is 0.002 cm^{-1} less than that determined by Wang and

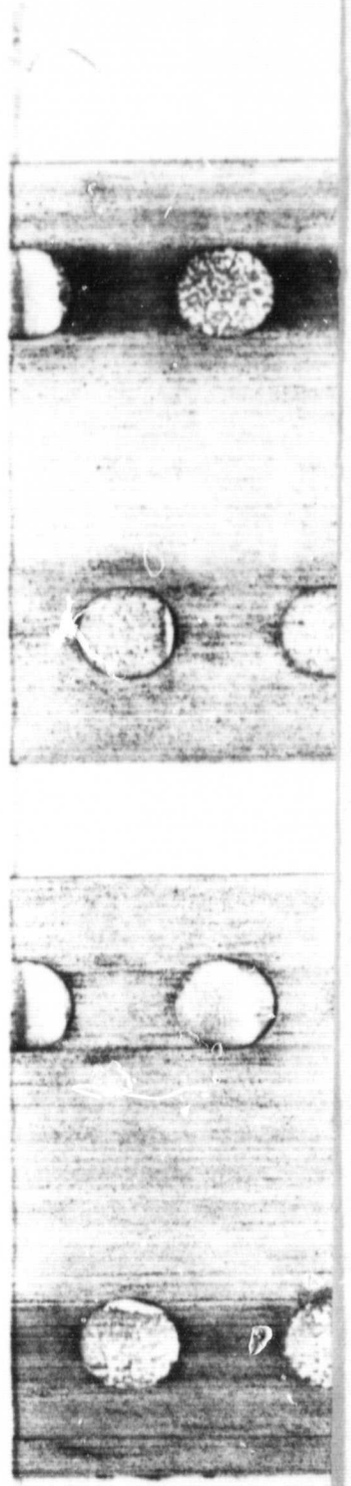

TABLE I

Wavenumbers (in cm^{-1} vac.) of the Q branches in the $(\nu_4 + \nu_5)^{0+} - \nu_4^{1f}$ bands of $^{12}C_2H_2$ and $^{12}C^{13}CH_2$

	$^{12}C_2H_2$			$^{12}C^{13}CH_2$		
J	Observed Q(J)	Observed $\Delta\nu$	$(\Delta\nu_{obs.} - \Delta\nu_{calc.}) \times 10^4$	Observed Q(J)	Observed $\Delta\nu$	$(\Delta\nu_{obs.} - \Delta\nu_{calc.}) \times 10^4$
6	716.3752	-0.0035	-0.6	715.4805	-0.0033	-3.3
7	.3717	-0.0048	0.0	.4772	-0.0039	1.5
8	.3669	-0.0066	-1.1	.4733	-0.0052	2.1
9	.3603	-0.0084	1.6	.4681	-0.0070	0.7
10	.3519	-0.0109	1.5	.4611	-0.0089	1.7
11	.3410	-0.0141	-1.2	.4522	-0.0111	3.2
12	.3269	-0.0172	2.1	.4411	-0.0144	-2.1
13	.3097	-0.0215	-1.4	.4267	-0.0177	-3.1
14	.2882	-0.0262	-3.5	.4090	-0.0215	-4.5
15	.2620	-0.0307	2.2	.3875	-0.0251	1.1
16	.2313	-0.0363	3.1	.3624	-0.0293	6.1
17	.1950	-0.0426	3.2	.3331	-0.0362	-10.2
18	.1524	-0.0500	-1.0	.2969	-0.0402	8.4
19	.1024	-0.0578	-2.5	.2567	-0.0477	-1.6
20	.0446	-0.0655	-5.7	.2090		
21	715.9781	-0.0752	-2.5			
22	.9029	-0.0844	3.1			
23	.8185	-0.0952	0.2			
24	.7233	-0.1069	-4.3			
25	.6164	-0.1172	12.4			
26	.4992	-0.1311	0.6			
27	.3681	-0.1452	-5.7			
28	.2229					

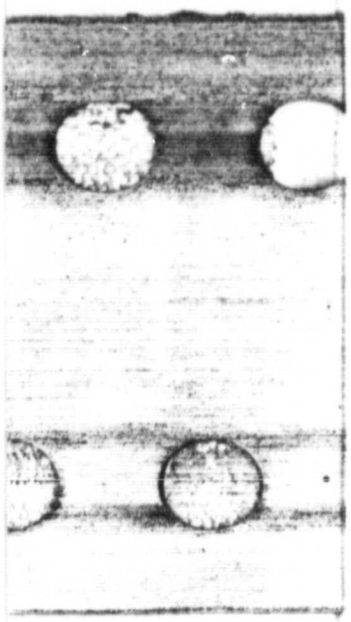

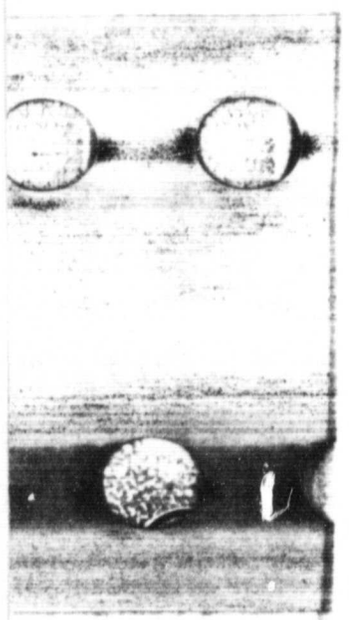

Overend and these two studies agree with one another within their respective uncertainties. Considering all aspects, the absolute wavenumbers of the acetylene lines given in Table I are believed to have an uncertainty of about ± 0.003 cm^{-1} at the most. The wavenumbers of $(\nu_1 - \nu_2^1)$ $P(7)$ and ν_2^1 $R(60)$ of $^{12}C^{16}O_2$ calculated in a similar way are 715.3195 and 716.4285 cm^{-1}, respectively, whereas the values determined by Gordon and McCubbin (*8*) are 715.321 and 716.426 cm^{-1}, respectively. In the spectral region 715.0–716.5 cm^{-1}, in addition to the two Q branch lines presented in this paper, five absorption lines of acetylene were also observed. One of these lines was unambiguously assigned as the $P(2)$ line of $2\nu_5^0-\nu_5^1$ band of $^{12}C_2H_2$. The estimated wavenumber of this line in the present work is 715.2645 cm^{-1} as compared to the value of 715.262 cm^{-1} reported in the previous work (*2*).

III. RESULTS

Observed Spectra

A major portion of the spectrum observed for the Q branch of the $(\nu_4 + \nu_5)^{0+}(\Sigma_u^+)-\nu_4^{1f}(\Pi g)$ band of $^{12}C_2H_2$ is reproduced in Fig. 1. The vibrational assignment of this band was made with the help of the previous work (*2*). As $^{12}C_2H_2$ has a center of symmetry (point group $D_{\infty h}$) and the nuclear spins of

FIG. 1. A major portion of the observed Q branch of the $(\nu_4 + \nu_5)^{0+}(\Sigma_u^-) - \nu_4^1(\Pi_g)$ band of $^{12}C_2H_2$. Also shown are the $Q(24)$ line of the ν_2^1 band of $H^{12}C^{14}N$ and the $R(60)$ line of ν_2^1 band of $^{12}C^{16}O_2$. (Sample path length: 6 m; pressure of gas: 70 μm of Hg).

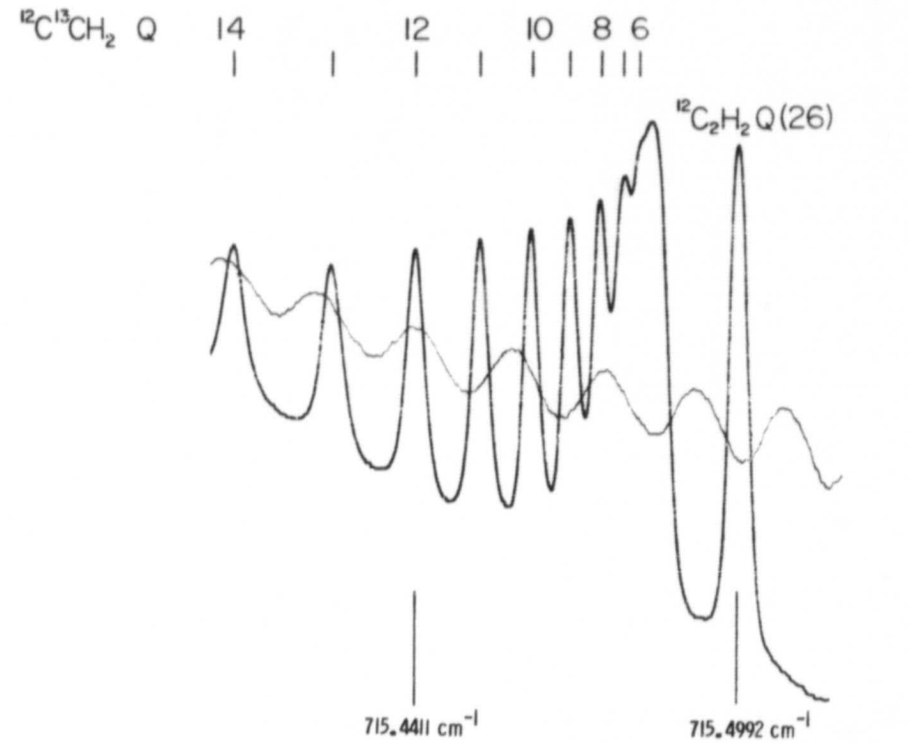

FIG. 2. A portion of the observed Q branch of the $(\nu_4 + \nu_5)^{0+}(\Sigma^+) - \nu_4^{1f}(\Pi)$ band of $^{12}C^{13}CH_2$. Also shown is the $Q(26)$ line of the corresponding band of $^{12}C_2H_2$. (Sample path length: 6 m; pressure of gas: 160 μm of Hg).

^{12}C and H atoms are 0 and ½, respectively, the rotational levels with even and odd J of the $0001^{1f}0$ state have statistical weights 3 and 1, respectively (9). In fact, the observed spectrum shows such an alternation of intensity in the rotational structure of the Q branch (Fig. 1). In assigning the J numbers to the rotational structure the calculated line positions and the intensity alternation within

TABLE II

Molecular constants* (in cm^{-1} vac.) for the $(\nu_4 + \nu_5)^{0+} - \nu_4^{1f}$ bands of $^{12}C_2H_2$ and $^{12}C^{13}CH_2$

Molecule	$\nu_0 + B''$	$B'-B''-2D''$	$(D'-D'')\times10^6$	$(H'-H'')\times10^{10}$	Std. dev. of fit
$^{12}C_2H_2$	716.3809 ±0.0030	-0.000068 ±0.000006	-1.828 ±0.019	1.91 ±0.02	1.9×10^{-5}
$^{12}C^{13}CH_2$	715.4852 ±0.0051	-0.000076 ±0.000009	-1.39 ±0.02		3.2×10^{-5}

*The values of $\nu_0 + B''$ are obtained from a least-squares fit of the observed data to Eq. (1) and those of the remaining parameters are obtained from a similar fit of $\Delta\nu$ to Eq. (2). The errors quoted are standard deviations

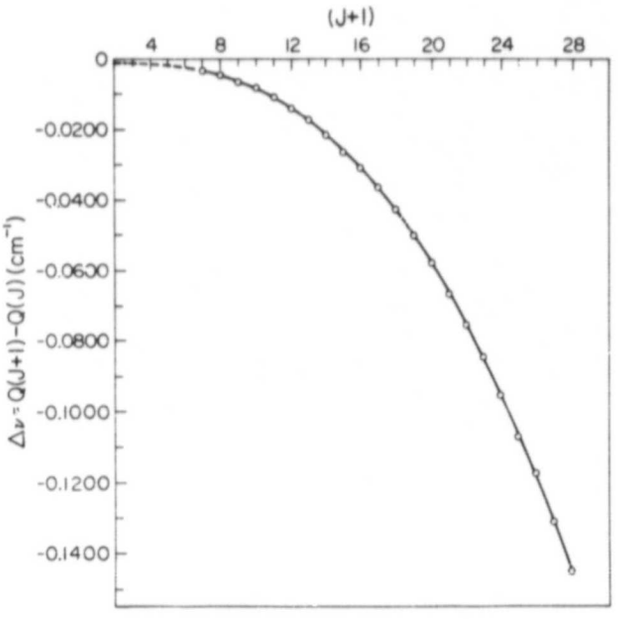

FIG. 3. A plot of $\Delta\nu[=Q(J+1)-Q(J)]$ versus $(J+1)$ for the $(\nu_4+\nu_5)^{0+}(\Sigma^+)-\nu_4^1{}^f(\Pi_g)$ band of $^{12}C_2H_2$.

the Q branch were taken into account. Altogether 23 lines from $J = 6$ to 28 were identified for the Q branch of this band of $^{12}C_2H_2$. For the resolved lines of this branch the full width at half maximum absorption is found to be 0.0025 cm^{-1} whereas the calculated Doppler width of these lines of $^{12}C_2H_2$ at room temperature is 0.0017 cm^{-1}.

A portion of the spectrum of the Q branch of the $(\nu_4+\nu_5)^{0+}(\Sigma^+)-\nu_4^1{}^f(\Pi)$ band of $^{12}C^{13}CH_2$ is reproduced in Fig. 2. Although lines from $J = 6$ to 20 are identified, only the ones up to $J = 14$ are shown in this figure. As $^{12}C^{13}CH_2$ does not have a center of symmetry (point group $C_{\infty v}$) no alternation of intensity is expected in any given branch of a band of this molecule, and this is what in fact has been observed experimentally (Fig. 2) and was responsible for its identification. The J assignments of the rotational structure of the Q branch of $^{12}C^{13}CH_2$ were confirmed by the rotational constants of this molecule obtained in the previous studies (*10, 11*).

The wavenumbers (in cm^{-1}vac.) and the J assignments for the lines measured in this work are listed in Table I.

Evaluation of Molecular Constants

The wavenumber data were fitted by least-squares techniques to not only the relation representing the $Q(J)$ lines but also the $\Delta\nu$ formula which can be readily represented, respectively, by the following equations:

$$Q(J) = \nu_0 + B'[J(J+1) - l'^2] - D'[J(J+1) - l'^2]^2 + H'[J(J+1) - l'^2]^3 - B''[J(J+1) - l''^2] + D''[J(J+1) - l''^2]^2 - H''[J(J+1) - l''^2]^3. \quad (1)$$

Here $\nu_0 = G_0(v',l') - G_0(v'',l'')$ is the vibrational band origin, $l' = 0$ for the upper Σ state, $l'' = 1$ for the lower Π state, and the constants of the lower state refer to the f-sublevels.

$$\Delta\nu = 2[B' - B'' + 2(D'l'^2 - D''l''^2) + 3(H'l'^4 - H''l''^4)](J+1) - 2[2(D' - D'') + 6(H'l'^2 - H''l''^2) - (H' - H'')](J+1)^3 + 6(H' - H'')(J+1)^5. \quad (2)$$

The molecular constants so derived are presented in Table II. That the relative accuracy of the data is high is clearly indicated by the fact that the observed $\Delta\nu$ values could be reproduced to within a few ten-thousandths of a cm^{-1} by the molecular constants (see also Fig. 3). Although the J values observed in the present work are not very high, there is definitely a need to include the H terms in Eqs. (1) and (2).

ACKNOWLEDGMENTS

The support received from the National Aeronautics and Space Administration is gratefully acknowledged.

RECEIVED: June 15, 1978

REFERENCES

1. S. C. HURLOCK, S. GHERSETTI, AND K. NARAHARI RAO, *Mem. Roy. Soc. Liege, Collect.* 87–97 (1971), and references therein.
2. K. F. PALMER, M. E. MICKELSON, AND K. NARAHARI RAO, *J. Mol. Spectrosc.* **44**, 131–144 (1972).
3. S. P. REDDY, W. IVANCIC, V. MALATHY DEVI, A. BALDACCI, K. NARAHARI RAO, A. W. MANTZ, AND R. S. ENG, to be published.
4. A. G. MAKI, *J. Mol. Spectrosc.* **58**, 308–315 (1975).
5. A. G. MAKI, *J. Phys. Chem. Ref. Data* **3**, 221–244 (1974).
6. P. K. L. YIN AND K. NARAHARI RAO, *J. Mol. Spectrosc.* **42**, 385–392 (1972).
7. V. K. WANG AND J. OVEREND, *Spectrochim. Acta A* **29**, 687–705 (1973).
8. H. R. GORDON AND T. K. MCCUBBIN, JR., *J. Mol. Spectrosc.* **18**, 73–82 (1965).
9. G. HERZBERG, "Molecular Spectra and Molecular Structure, Infrared and Raman Spectra of Polyatomic Molecules", Van Nostrand, Princeton, N. J., 1945.
10. S. GHERSETTI, A. BALDACCI, S. GIORGIANNI, R. H. BARNES, AND K. NARAHARI RAO, *Gazz. Chim. Italiana.* **105**, 875–900 (1975).
11. W. J. LAFFERTY AND R. J. THIBAULT, *J. Mol. Spectrosc.* **14**, 79–96 (1964).

JOURNAL OF MOLECULAR SPECTROSCOPY 68, 183–194 (1977)

Interpretation of the Acetylene Spectrum at 1.5 μm

A. BALDACCI AND S. GHERSETTI

Department of Organic Chemistry, University of Venice, Calle Larga S. Marta 2137, Venezia, Italy

AND

K. NARAHARI RAO

Department of Physics, The Ohio State University, Columbus, Ohio, 43210

Bands of acetylene in the region 6680–6460 cm^{-1} recorded with a high resolution infrared spectrograph are assigned to transitions and molecular constants of the levels involved have been evaluated.

INTRODUCTION

This article presents an analysis of the band systems observed in the absorption spectrum of acetylene at 1.5 μm (between 6680 and 6460 cm^{-1}). Numerous overlapping bands of both $^{12}C_2H_2$ and $^{12}C^{13}CH_2$ occur here and the interpretation of the spectrum has been done by adopting procedures described in previous publications. These procedures involve the use of graphical plots, examination of the patterns of intensity alternation, and evaluation of approximate vibrational term values.

Figure 1 shows a reproduction of the acetylene absorption spectrum observed in the present study. The conditions of the experiment along with the identifications of the different bands are given in the caption to this figure. The effective spectral resolution of the data achieved was about 0.03 cm^{-1}. About 80% of the nearly 1000 lines recorded have been given assignments. The next section summarizes the results along with a discussion of some of the more important aspects of the spectrum.

RESULTS AND DISCUSSION

Main Features (Combination Bands and Some "Hot" Bands)

The $\nu_1 + \nu_3$ and $\nu_1 + \nu_2 + (\nu_4 + \nu_5)^0$ bands of $^{12}C_2H_2$ originating from the ground state of this molecule represent the stronger absorptions. They are the bands labeled *A* and *Q* in Fig. 1. The two bands centered at about 6529.8 and at 6534.7 cm^{-1} are, respectively, the "hot" bands $\nu_1 + \nu_3 + \nu_4^1 - \nu_4^1$ and $\nu_1 + \nu_3 + \nu_5^1 - \nu_5^1$ of this molecular species.

For all these four bands, the present study gives improved values for the molecular constants of the levels involved in these transitions as compared to previous work in this region (*1*). The improvements reflect the better technology available at this time.

ISSN 0022-2852

FIG. 1. Reproduction of the rotational structure for the acetylene bands at 1.5 μm. Spectrograph used: 10-m-focal-length Czerny–Turner vacuum spectrograph at The Ohio State University equipped with a 79-grooves/mm 40 × 20-cm² (16 × 8-in.²) echelle. Detector: PbS cooled to dry ice temperature. Path length and pressure: An absorption path of 24 m with pressure of acetylene ranging between 0.2 and 10 Torr was used. The identification of the bands[1] marked A, B, C, D, etc., is given below (L, M, N refer to $^{12}C^{13}CH_2$ and the rest to $^{12}C_2H_2$):

A. $\nu_1 + \nu_3$
B. $\nu_1 + \nu_3 + \nu_4^1 - \nu_4^1$
C. $\nu_1 + \nu_3 + \nu_5^1 - \nu_5^1$
D. $\nu_1 + \nu_3 + 2\nu_4^0 - 2\nu_4^0$
E. $\nu_1 + \nu_3 + 2\nu_4^2 - 2\nu_4^2$
F. $\nu_1 + \nu_3 + (\nu_4 + \nu_5)_+^0 - (\nu_4 + \nu_5)_+^0$
G. $\nu_1 + \nu_3 + (\nu_4 + \nu_5)^2 - (\nu_4 + \nu_5)^2$
H. $\nu_1 + \nu_3 + 2\nu_5^0 - 2\nu_5^0$
I. $\nu_1 + \nu_3 + 2\nu_5^2 - 2\nu_5^2$
L. $\nu_1 + \nu_3$
M. $2\nu_3$
N. $\nu_1 + \nu_3 + \nu_4^1 - \nu_4^1$
O. $2\nu_1 + \nu_4^1 - \nu_5^1$
P. $\nu_1 + \nu_3 + (2\nu_4 + \nu_5)_{II}^1 - \nu_4^1$
Q. $\nu_1 + \nu_3 + (\nu_4 + \nu_5)_+^0$
R. $\nu_1 + \nu_3 + (2\nu_4 + \nu_5)_I^1 - \nu_4^1$
S. $\nu_1 + \nu_3 + (\nu_4 + 2\nu_5)_{II}^1 - \nu_5^1$
T. $2\nu_3 + \nu_5^1 - \nu_4^1$

[1] The levels $(\nu_4 + \nu_5)_+^0$, $(\nu_4 + \nu_5)_-^0$, $(\nu_4 + \nu_5)^2$ have, respectively, the symmetries Σ_u^+, Σ_u^-, Δ_u. The subscript I refers to the upper and II to the lower level of the doublet.

FIG. 1—*continued*

TABLE I

Vibrational Term Values (cm^{-1}) of $^{12}C_2H_2$ Obtained from the Bands at 1.5 μm

LEVEL	SPECIES	$G_0(v)$ (cm^{-1})
$10^10^20^0$	Σ_u^+	6556.461±2
$110(11)^0$	Σ_u^+	6623.140±2
10^111^0	Π_u	7142.657±6
$110(21)^1$ II	Π_u	7207.113±9
0020^01^1	Π_u	7219.370±8
$110(21)^1$ I	Π_u	7229.448±10
$10^20^11^1$	Π_g	7265.060±6
2001^10^0	Π_g	7297.547±8
$110(..)^1$ II	Π_g	7330.531±12
$10^12^20^0$	Σ_u^+	7732.78 ±6
$10^12^20^2$	Δ_u	7737.03 ±6
$101(11)^0$	Σ_g^+	7835.014±12
$101(11)^2$	Δ_g	7852.417±9
$10^20^12^0$	Σ_u^+	7961.837±8
$10^20^12^2$	Δ_u	7976.274±9

Other "Hot" Bands from the 0001^10^0 and 0000^01^1 Levels

The medium intensity band at 6567.2 cm^{-1} belongs to a transition arising from a *u* state as shown by the type of the intensity alternation in the *R* branch (no splitting was observed in the *P* branch): on this basis and in agreement with a vibrational calculation it was assigned to the $2001^10^0 \leftarrow 0000^01^1$ transition.

The medium-weak band at 6606.5 cm^{-1} presents the *l*-type doublets resolved in both *P* and *R* branches with the intensity alternation for a *g* vibrational lower state and the $B''_{c/d}$ constants are close to those measured for the 0001^10^0 state [see Refs. (*2*, *3*)]. Among the possible transitions compatible by symmetry and expected to occur in this wavenumber range, the most probable one is the transition $0020^01^1 \leftarrow 0001^10^0$: in fact from Keller's results for $2\nu_3 + \nu_5^1$ (*4*) and from ν_4^1 (*2*, *3*) a band origin at 6605.8 cm^{-1} is calculated.

Three additional weak bands were assigned as "hot" bands accompanying the main transition $110(11)_+^0 \leftarrow 0000^00^0$ which absorbs at 6623.1 cm^{-1}. The band at 6594.2 cm^{-1} belongs to a transition arising from the 0001^10^0 state and was identified as $\nu_1 + \nu_2 + (2\nu_4 + \nu_5)_{II}^1 - \nu_4^1$. By using the results at 5 μm (*2*), a second band ($\nu_1 + \nu_2 + (2\nu_4 + \nu_5)_I^1 - \nu_4^1$) should be located at about 20 cm^{-1} higher, that is at about 6614.2 cm^{-1}. The only absorption observed in this range is a weak badly overlapped band at 6616.6 cm^{-1} which was tentatively assigned to this transition. In passing, it may be noted that the *c* and *d* rotational sublevels[2] of the upper state $[(11021)_I^1]$ appear here much closer to each other than in the II states in general.

[2] It may be noted that the recommendation of J. M. Brown, J. T. Hougen, K.-P. Huber, J. W. C. Johns, I. Kopp, H. Lefebvre-Brion, A. S. Merer, D. A. Ramsay, J. Rostas, and R. N. Zare [*J. Mol. Spectrosc.* **55**, 500 (1975)] designates the *c* and *d* labels as *e* and *f*.

The band at 6600.2 cm^{-1} was attributed to the $(11012)_{II}^{1} \leftarrow 0000^{0}1^{1}$ transition. A value of about 6601 cm^{-1} was estimated for the band origin on the basis of vibrational calculations. The rotational constants, as well as the type of the alternation of intensity are in agreement with such an assignment for the lower state. No band of a transition from the same lower state to the $(11012)_{I}^{1}$ level could be identified.

"Hot" Bands Arising from the $0002^{0,3}0^{0}$, $0000^{0}2^{0,2}$ and $000(11)^{0,2}$ States

The band at 6502.4 cm^{-1} was assigned to the $\Sigma_u^+ \leftarrow \Sigma_g^+$ $1012^{0}0^{0} \leftarrow 0002^{0}0^{0}$ transition ($\nu_1 + \nu_3 + 2\nu_4^0 - 2\nu_4^0$) on the basis of the appropriate term values known from the literature ($1012^{0}0^{0}$ given by Keller (*4*), and $0002^{0}0^{0}$ quoted by Plíva (*5*)). It may be recalled that although the type of alternation of intensity agrees with a *g* vibrational

TABLE II

Spectroscopic Constants (cm^{-1}) of $^{13}C_2H_2$ Obtained from the Bands at 1.5 μm

LEVELS		Species of States	$\nu_0 = B'(l'+1)^2 + B''(l''+1)^2$	$(B'-B'')\times10^3$	$(D'-D'')\times10^6$
UPPER	LOWER				
$1010^{0}0^{0}$	$0000^{0}0^{0}$	$\Sigma_u^+ - \Sigma_g^+$	6556.461±0.002	-12.865±0.008	-0.029±0.006
$(1010^{0}1^{1})_c$	$(0000^{0}1^{1})_c$	$\Pi_g - \Pi_u$	6534.742±0.004	-12.90 ±0.02	-0.01 ±0.02
$(1010^{0}1^{1})_d$	$(0000^{0}1^{1})_d$			-12.68 ±0.02	0.03 ±0.02
$(1011^{1}0^{0})_c$	$(0001^{1}0^{0})_c$	$\Pi_u - \Pi_g$	6529.800±0.004	-12.60 ±0.02	0.02 ±0.02
$(1011^{1}0^{0})_d$	$(0001^{1}0^{0})_d$			-12.39 ±0.02	0.02 ±0.02
$1010^{0}2^{2}$	$0000^{0}2^{2}$	$\Delta_u - \Delta_g$	6513.265±0.005	-12.65 ±0.09	0.5 ±0.4
$1010^{0}2^{0}$	$0000^{0}2^{0}$	$\Sigma_u^+ - \Sigma_g^+$	6512.716±0.004	-12.69 ±0.09	-1.1 ±0.4
$(10111)^{0}$	$(00011)^{0}$	$\Sigma_g^+ - \Sigma_u^+$	6506.927±0.007	-12.65 ±0.11	-0.6 ±0.4
$(10111)^{2}$	$(00011)^{2}$	$\Delta_g - \Delta_u$	6504.949±0.005	-12.46 ±0.09	-0.5 ±0.3
$(1012^{2}0^{0})_c$	$(0002^{2}0^{0})_c$	$\Delta_u - \Delta_g$	6503.563±0.008	-14.87 ±0.08(†)	-3.3 ±0.2
$(1012^{2}0^{0})_d$	$(0002^{2}0^{0})_d$			-12.06 ±0.08(†)	0.6 ±0.3
$1012^{0}0^{0}$	$0002^{0}0^{0}$	$\Sigma_u^+ - \Sigma_g^+$	6502.389±0.006	-9.7 ±0.2	2.1 ±0.9
$(11011)^{0}$	$0000^{0}0^{0}$	$\Sigma_u^+ - \Sigma_g^+$	6623.140±0.002	-8.77 ±0.02	1.98 ±0.03
$(11021)^{1}_{c}$(I)	$(0001^{1}0^{0})_c$	$\Pi_u - \Pi_g$	6616.586±0.006	-7.03 ±0.10	-2.7 ±0.4
$(11021)^{1}_{d}$(†)	$(0001^{1}0^{0})_d$			-8.60 ±0.05	0.8 ±0.2
$(11012)^{1}_{c}$(II)	$(0000^{0}1^{1})_c$	$\Pi_g - \Pi_u$	6600.205±0.010	-11.36 ±0.10	0.6 ±0.3
$(11012)^{1}_{d}$(II)	$(0000^{0}1^{1})_d$			-5.77 ±0.10	0.6 ±0.3
$(11021)^{1}_{c}$(II)	$(0001^{1}0^{0})_c$	$\Pi_u - \Pi_g$	6594.251±0.007	-10.48 ±0.05	1.07 ±0.10
$(11021)^{1}_{d}$(II)	$(0001^{1}0^{0})_d$			-5.51 ±0.06	1.94 ±0.13
$(0020^{0}1^{1})_c$	$(0001^{1}0^{0})_c$	$\Pi_u - \Pi_g$	6606.510±0.006	-8.98 ±0.05	0.3 ±0.1
$(0020^{0}1^{1})_d$	$(0001^{1}0^{0})_d$			-11.65 ±0.08	0.5 ±0.2
$(2001^{1}0^{0})_c$	$(0000^{0}1^{1})_c$	$\Pi_g - \Pi_u$	6567.231±0.006	-14.56 ±0.04	-0.41 ±0.06
$(2001^{1}0^{0})_d$	$(0000^{0}1^{1})_d$			-13.96 ±0.04	-0.09 ±0.07

(†) Effective values

TABLE III

Wavenumbers (vac. cm^{-1}) of the Rotational Structure of $\Sigma_{u(g)}^{+} \leftarrow \Sigma_{g(u)}^{+}$ Bands of $^{12}C_2H_2$ (Estimated Accuracy of Data: $\pm 0.005\ cm^{-1}$)

	$1010^{0}0^{0} - 0000^{0}0^{0}$		$110(11)^{0} - 0000^{0}0^{0}$		$1012^{0}0^{0} - 0002^{0}0^{0}$		$101(11)^{0} - 000(11)^{0}$		$1010^{0}2^{0} - 0000^{0}2^{0}$		
J	R(J)OBS.	P(J)OBS.	R(J)OBS.	P(J)OBS.	R(J)OBS.	P(J)OBS.	R(J)OBS.	P(J)OBS.	R(J)OBS.	P(J)OBS.	J
0	6558.798		6625.489								0
1	6561.087	6554.119	6627.789	6620.800	6507.056	6500.044			6517.363	6510.342	1
2	6563.374	6551.714	6630.111	6618.425		6497.671	6513.846		6519.652	6507.981	2
3	6565.621	6549.337	6632.367	6616.025	6511.620	6495.243	6516.136†	6499.741†	6521.911	6505.556	3
4	6567.842	6546.878	6634.648	6613.624		6492.836	6518.336		6524.137		4
5	6570.050	6544.442	6636.874	6611.185	6516.136†	6490.375	6520.577†	6494.890	6526.352	6500.665	5
6	6572.205	6541.942	6639.107	6608.756	6518.336†	6487.925†			6528.501†	6498.160	6
7	6574.378	6539.455	6641.321	6606.284	6520.577	6485.424†	6524.899	6489.918†	6530.693	6495.664	7
8	6576.471	6536.905	6643.499	6603.822		6482.944	6527.017	6487.347	6532.799	6493.108†	8
9	6578.581	6534.367	6645.685	6601.305	6524.939	6480.414		6484.789	6534.933	6490.567†	9
10	6580.640	6531.768	6647.808	6598.813	6527.062	6477.893†	6531.221	6482.205	6536.994	6488.024†	10
11	6582.680	6529.173	6649.949			6475.311	6533.255	6479.602	6539.065†	6485.375†	11
12	6584.713	6526.538	6652.052	6593.726		6472.710	6535.305		6541.103†	6482.761	12
13	6586.679	6523.868	6654.142	6591.137		6470.112	6537.327	6474.296	6543.105†	6480.108	13
14	6588.659	6521.203	6656.218	6588.557		6467.423†	6539.282	6471.633	6545.110	6477.427	14
15	6590.593	6518.468	6658.227	6585.928		6464.778		6468.940†		6474.729	15
16	6592.488	6515.761	6660.255	6583.298		6462.073		6466.195			16
17	6594.394	6512.983	6662.237					6463.431†		6469.257	17
18	6596.238	6510.214	6664.179	6577.948				6460.671			18
19	6598.069	6507.397	6666.133	6575.243							19
20	6599.882	6504.550	6668.018	6572.508							20
21	6601.640	6501.713	6669.888	6569.754							21
22	6603.414	6498.815	6671.754								22
23	6605.142	6495.903	6673.546	6564.131							23
24	6606.821	6492.988	6675.329	6561.292							24
25	6608.512	6490.012	6677.094	6558.431							25
26	6610.161	6487.047	6678.799	6555.531							26
27	6611.784	6484.043	6680.468								27
28	6613.371	6480.999									28
29	6614.951	6477.950									29
30	6616.474	6474.887									30
31	6617.995	6471.767									31
32	6619.497	6468.666									32
33	6620.948	6465.494									33
34	6622.371	6462.295									34
35	6623.793										35
36	6625.178										36
37	6626.512										37
38	6627.835										38
39	6629.148										39
40	6630.410										40
41	6631.650										41
42	6632.866										42
43	6634.074										43

† Lines not used in calculations.

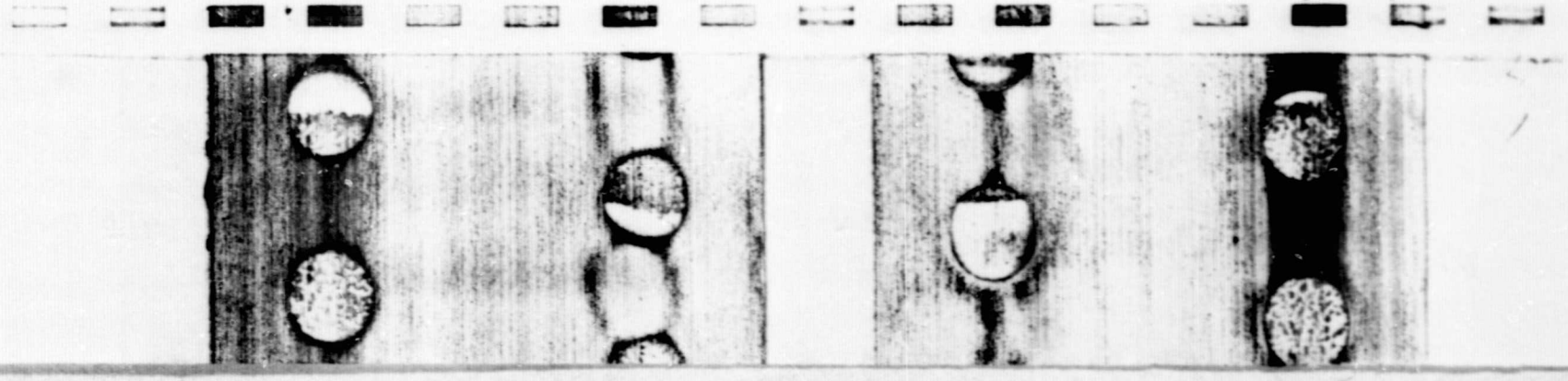

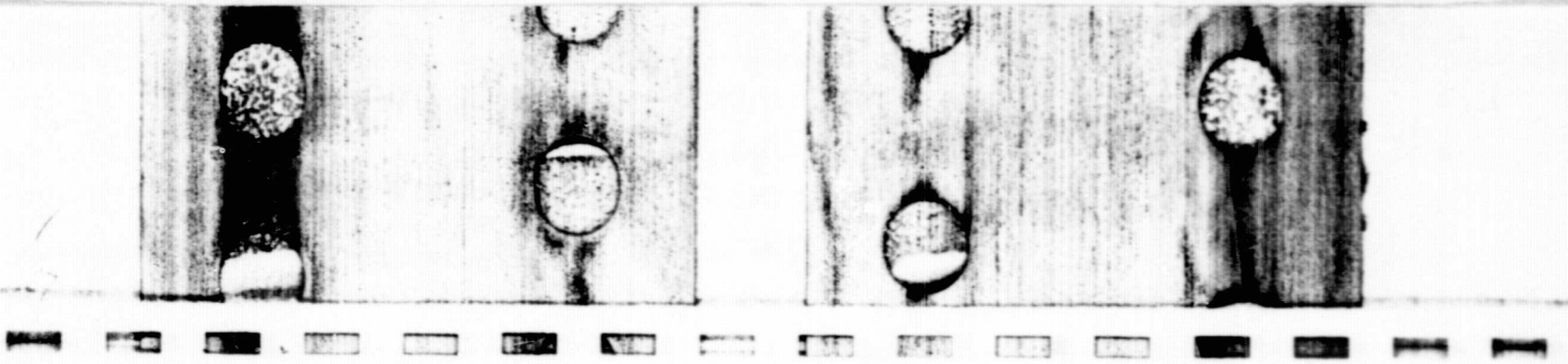

TABLE IV

Wavenumbers (vac. cm^{-1}) of the Rotational Structure of $\Pi_{u(g)} \leftarrow \Pi_{g(u)}$ Bands of $^{12}C_2H_2$ (Estimated Accuracy of Data: ± 0.005 cm^{-1})

	$1011^10^0 - 0001^10^0$				$1010^01^1 - 0000^01^1$				$0020^01^1 - 0001^10^0$				
	c - c		d - d		c - c		d - d		c - c		d - d		
J	R(J)OBS.	P(J)OBS.	R(J)OBS.	P(J)OBS.	R(J)OBS.	P(J)OBS.	R(J)OBS.	P(J)OBS.	R(J)OBS.	P(J)OBS.	R(J)OBS.	P(J)OBS.	J
1	6534.428		6534.428		6539.406†		6539.406						1
2	6536.705	6525.073	6536.718	6525.073	6541.645	6530.016	6541.645	6530.016†	6613.446	6601.776†	6613.446	6601.746	2
3	6538.955	6522.664	6538.994	6522.664	6543.903	6527.577	6543.935	6527.577	6615.733	6599.396	6615.733	6599.354	3
4	6541.173	6520.246†	6541.230	6520.209†	6546.116	6525.184	6546.163	6525.148†		6596.990		6596.900	4
5	6543.366	6517.788	6543.438	6517.736†	6548.311	6522.710	6548.376	6522.634	6520.258	6594.580	6620.200	6594.483	5
6	6545.552	6515.329	6545.633	6515.275	6550.491	6520.246	6550.564	6520.209†	6622.461	6592.125		6591.987†	6
7	6547.682	6512.816	6547.783	6512.754	6552.621	6517.736	6552.709	6517.657	6624.691	6589.693	6624.583†	6589.488	7
8	6549.825	6510.294	6549.938		6554.763	6515.210	6554.865	6515.145	6626.854		6626.696	6586.953	8
9	6551.895†	6507.746	6552.026	6507.667	6556.833	6512.641	6556.949	6512.571	6629.035		6628.828	6584.429	9
10	6553.995†	6505.160		6505.076	6558.922	6510.057	6559.054	6509.978	6631.175	6582.186	6630.929		10
11	6556.023	6502.573	6556.174	6502.494	6560.951	6507.443		6507.382	6633.296	6579.680	6632.988	6579.262	11
12	6558.051	6499.927	6558.230	6499.831	6562.966	6504.804	6563.127	6504.719	6635.418		6635.061†	6576.636	12
13	6560.052	6497.304	6560.242	6497.202	6564.964	6502.168	6565.136	6502.076	6637.483	6574.585	6637.055	6574.009	13
14	6561.997	6494.603	6562.206	6494.498	6566.910	6499.460	6567.096	6499.365	6639.578	6571.974	6639.057	6571.322	14
15	6563.960	6491.923	6564.187	6491.808	6568.865	6496.771	6569.069	6496.672	6641.614	6569.384	6641.052	6568.610	15
16	6565.862	6489.191	6566.104	6489.076	6570.756	6494.021	6570.973	6493.922	6643.629	6566.778	6642.986	6565.927	16
17	6567.756	6486.441	6568.018	6486.321	6572.635	6491.264	6572.876	6491.156			6644.926	6563.177	17
18	6569.638	6483.685	6569.911	6483.566	6574.506	6488.493	6574.758	6488.386	6647.620		6646.823	6560.435	18
19	6571.441	6480.866	6571.744	6480.745	6576.303	6485.661	6576.582	6485.547	6649.582				19
20	6573.270	6478.071	6573.596		6578.128	6482.851	6578.421	6482.739	6651.548				20
21	6575.059	6475.207	6575.397	6475.090	6579.915	6479.983	6580.205	6479.872	6653.439				21
22	6576.799	6472.330	6577.153	6472.203	6581.638	6477.092	6581.961	6476.972					22
23		6469.461	6578.932	6469.337†	6583.381	6474.204	6583.719	6474.084	6657.226				23
24	6580.246	6466.510		6466.379	6585.071	6471.252	6585.444	6471.136					24
25	6581.916	6463.565	6582.337	6463.431		6468.298	6587.100	6468.173					25
26	6583.601	6460.611	6584.044	6460.481	6586.386†	6465.312	6588.776	6465.187					26
27	6585.218†		6585.676		6590.003	6462.295	6590.407†	6462.162					27
28	6586.789†		6587.294		6591.585		6591.987						28
29	6588.386†		6588.906		6593.141		6593.599						29
30	6589.941		6590.478		6594.688†		6595.177†						30
31	6591.451		6591.987†				6596.671						31
32			6593.541		6597.663		6598.169						32
33			6595.035										33
34			6596.491										34
35			6597.951										35

† Lines not used in calculations.

TABLE IV—*continued*

	$110(21)^1 - 0001^1 0^0$				$110(21)^1 - 0001^1 0^0$				$110(12)^1 - 0000^0 1^1$				
	c - c		d - d		c - c		d - d		c - c		d - d		
J	R(J)OBS.	P(J)OBS.	R(J)OBS.	P(J)OBS.	R(J)OBS.	P(J)OBS.	R(J)OBS.	P(J)OBS.	R(J)OBS.	P(J)OBS.	R(J)OBS.	P(J)OBS.	J
1	6598.919†		6598.919		6621.261		6621.261						1
2	6601.197†	6589.532		6589.532†	6623.579	6611.838†	6623.579	6611.838†					2
3			6603.597		6625.857	6609.482	6625.857				6609.519†		3
4	6605.697		6605.884†		6628.131†	6607.077	6628.131†	6607.038†	6611.612†		6611.838†	6590.700	4
5	6607.908	6582.284	6608.179†	6582.337†	6630.410†	6604.699	6630.410†	6604.629†	6613.840	6588.206	6614.140	6588.265	5
6		6579.845	6610.465		6632.632†	6602.250	6632.632	6602.140		6585.734			6
7	6612.289	6577.358	6612.718	6577.486	6634.898			6599.690†	6618.201		6618.708†	6583.443	7
8	6614.474	6574.876	6614.992		6637.126		6637.055†	6597.198†	6620.363†	6580.723†		6580.975	8
9	6616.579	6572.336	6617.210	6572.587	6639.349	6594.944	6639.251	6594.688†	6622.461†		6623.188		9
10	6618.708†	6569.813		6570.129	6641.557		6641.412	6592.204†	6624.583†	6575.648	6625.426	6576.089	10
11		6567.227	6621.668	6567.655	6643.757†	6590.003†	6643.548	6589.693†	6626.633	6573.089	6627.625		11
12	6622.858	6564.675	6623.875	6565.186†	6645.965†	6587.523†			6628.693	6570.467	6629.847	6571.096†	12
13	6624.921	6562.043	6626.051	6562.659	6648.105	6585.018†	6647.761†	6584.543	6630.725		6632.012	6568.610†	13
14	6626.914	6559.435	6628.207	6560.147		6582.511	6649.861		6632.695	6565.186†	6634.209		14
15	6628.917	6556.753	6630.361	6557.594	6652.425		6651.913			6562.495†	6636.354†	6563.558	15
16	6630.882		6632.474	6555.069			6653.963		6636.617†	6559.827	6638.488†		16
17	6632.807	6551.380		6552.475	6656.713†		6655.983		6638.539		6640.634	6558.483	17
18	6634.742†	6548.669	6636.684		6658.830†		6657.969		6640.453		6642.741†		18
19	6636.617†	6545.918	6638.765	6547.316							6644.849†		19
20	6638.488†		6640.826	6544.712			6661.904						20
21	6640.335	6540.367		6542.047									21
22			6644.849†										22
23	6643.909												23

	$2001^1 0^0 - 0000^0 1^1$				$2001^1 0^0 - 0000^0 1^1$			
	c - c	d - d			c - c	d - d		
J	R(J)OBS.	R(J)OBS.	[b]P(J)OBS.	J	R(J)OBS.	R(J)OBS.	[b]P(J)OBS.	
1	6571.848	6571.848		14	6599.055	6599.319†	6531.672	
2	6574.133	6574.133	6562.495	15	6600.913	6601.197†	6528.891	
3	6576.393†	6576.393		16	6602.778	6603.090	6526.153†	
4			6557.638	17	6604.629†	6604.962	6523.312	
5	6580.723†	6580.809	6555.152	18	6606.400	6606.771	6520.511	
6	6582.886	6582.980	6552.647	19	6608.179†	6608.572	6517.638	
7	6585.018	6585.123	6550.116	20	6609.931	6610.352	6514.747	
8	6587.100†		6547.582	21	6611.612†	6612.084	6511.843	
9	6589.174	6589.326	6544.976	22	6613.319	6613.840†		
10	6591.180	6591.352	6542.389	23		6615.501	6505.956	
11	6593.202	6593.392	6539.730	24				
12	6595.177	6595.391	6537.086	25		6618.796		
13	6597.108	6597.347†						

[b] No splitting is observed in the P branch.

† Lines not used in calculations.

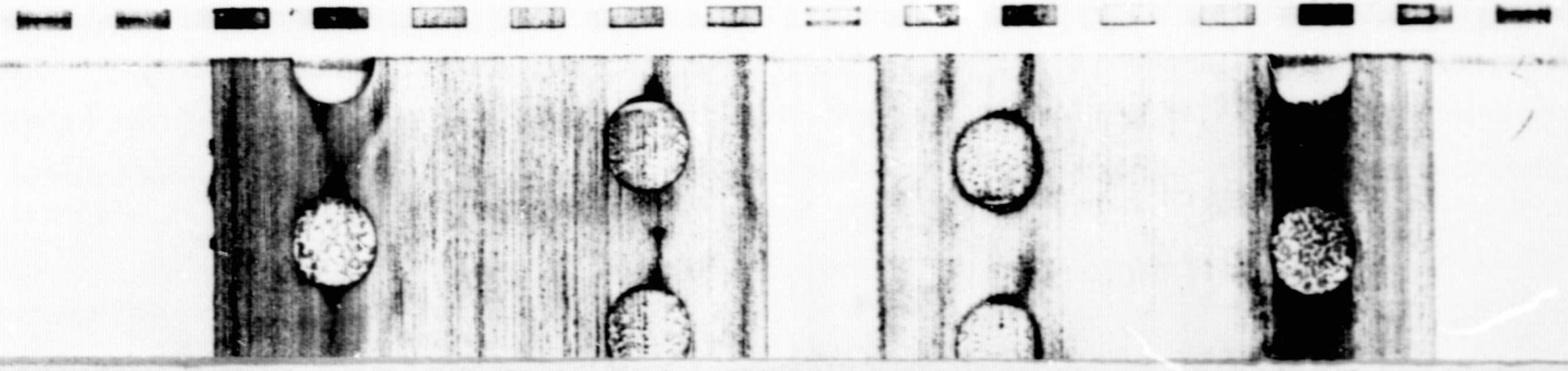

TABLE V

Wavenumbers (vac. cm^{-1}) of the Rotational Structure of $\Delta_{u(g)} \leftarrow \Delta_{g(u)}$ Bands of $^{13}C_3H_2$ (Estimated Accuracy of Data: ± 0.005 cm^{-1})

	$1012^{1}0^{0} - 0002^{1}0^{0}$				$101(11)^{2} - 000(11)^{2}$		$1010^{0}2^{2} - 0000^{0}2^{2}$		
	$c - c$		$d - d$						
J	R(J)OBS.	P(J)OBS.	R(J)OBS.	P(J)OBS.	R(J)OBS.	P(J)OBS.	R(J)OBS.	P(J)OBS.	J
2	6510.481		6510.481		6511.880				2
3	6512.717	6496.406	6512.717	6496.406	6514.123	6497.803	6522.459	6506.106	3
4	6514.919	6493.962	6514.968	6493.962	6516.380	6495.352	6524.694	6503.660	4
5	6517.108	6491.510	6517.177	6491.510	6518.555*	6492.919	6526.897	6501.211	5
6	6519.242	6489.032	6519.361	6489.032	6520.776	6490.410	6529.061*	6498.715	6
7		6486.486	6521.535	6486.539*	6522.913	6487.925*	6531.221*	6496.205	7
8	6523.431	6483.956	6523.651	6484.009*		6485.375	6533.345*	6493.671	8
9	6525.497	6481.353	6525.788	6481.449	6527.164		6535.476	6491.094	9
10	6527.512	6478.770*	6523.839*	6478.896	6529.258	6480.241	6537.534	6488.517*	10
11	6529.530	6476.112	6529.926	6476.278	6531.306	6477.650	6539.615	6485.885*	11
12	6531.520	6473.486	6531.946	6473.675	6533.345*	6475.022		6483.277	12
13	6533.474	6470.811	6533.967	6471.017	6535.366	6472.355*	6543.643	6480.579*	13
14	6535.430	6468.111	6535.952	6468.345	6537.372	6469.701*		6477.893*	14
15	6537.327	6465.402	6537.904			6466.972	6547.539		15
16	6539.220*	6462.632*	6539.858*	6462.901	6541.283	6464.251	6549.458*		16
17	6541.103*	6459.898	6541.768*	6460.164		6461.485	6551.380*		17
18	6542.932						6553.219		18
19	6544.761								19
20	6546.551								20

* Lines not used in calculations.

lower state, a check by the B'' and D'' constants could not be made since they are not available at this time. The corresponding $\Delta_u \leftarrow \Delta_g$ transition ($\nu_1 + \nu_3 + 2\nu_4^2 - 2\nu_4^2$) has been tentatively assigned to the nearby weak band at 6503.6 cm^{-1} because only higher order terms are responsible for different spectral positions for the two vibrational transitions and they are known to be rather small.

From a rotational analysis of this band a set of molecular parameters is obtained and they give rise to an unusually large splitting between the c and d components both in the upper and in the lower states. It may be noted that Innes (*6*) also obtains from uv data similar results for the 0002^20^0 state.

By comparing the above mentioned $\Sigma^+ \leftarrow \Sigma^+$ and $\Delta \leftarrow \Delta$ transitions, it may be noted that the Δ-Σ^+ separation in the upper states is 4.2 cm^{-1}, which is of the same order of magnitude as that quoted for the lower states (3.1 cm^{-1}) (*5*).

The two bands at 6512.7 and 6513.3 cm^{-1} are, respectively, assigned to the $1010^02^0 \leftarrow 0000^02^0$ and $1010^02^2 \leftarrow 0000^02^2$ transitions. Such an assignment can also be supported by an approximate vibrational calculation.[3] These two bands are distinguished from one another by consideration of the intensity alternations and the molecular constants of the lower levels.

It is of interest to note that in this case the separation between the Σ^+ and Δ levels is 14.4 cm^{-1} for the upper states $1010^02^{0,2}$. This may be compared to the value 13.9 cm^{-1} found for the $0000^02^{0,2}$ levels (*3, 5*). It may be recalled that in the previous section the Δ-Σ^+ separation was found to be 4.2 cm^{-1} which is an order of magnitude lower. That means $g_{55} > g_{44}$ which agrees with Ref. (*5*)

"Double hot" bands can also arise from the $(\nu_4 + \nu_5)_{+/-}^{0,2}$ levels. Again, by an

[3] ν_0 of $\nu_1 + \nu_3 = 6556.5$; ν_0 of $\nu_1 + \nu_3 + \nu_5^1 - \nu_5^1 = 6534.7$. The difference of 21.8 $cm^{-1} \simeq -(x_{15} + x_{35})$. Therefore, ν_0 of $(\nu_1 + \nu_3 + 2\nu_5^{0,2} - 2\nu_5^{0,2}) \simeq \nu_0$ of $(\nu_1 + \nu_3) + 2(x_{15} + x_{35}) \simeq 6512.9$.

TABLE VI

Wavenumbers (vac. cm^{-1}) and Spectroscopic Constants (cm^{-1}) of the Bands Pertaining to the $^{12}C^{13}CH_2$ Species in Natural Abundance (Estimated Accuracy of Data: ± 0.005 cm^{-1})

	$10^{1}0^{2}0^{2} - 00^{0}0^{0}0^{0}$		$00^{2}0^{2}0^{2} - 00^{0}0^{0}0^{0}$		$10^{1}1^{0}0^{2} - 00^{0}0^{1}0^{2}$				
					c - c		d - d		
J	R(J)OBS.	P(J)OBS.	R(J)OBS.	P(J)OBS.	R(J)OBS.	P(J)OBS.	R(J)OBS.	P(J)OBS.	J
0	6545.155		6495.151*						0
1	6547.380	6543.381	6497.392	6490.567*	6521.644		6521.699		1
2	6549.630	6538.246	6499.600	6488.261		6512.534*		6512.534*	2
3	6551.801	6535.916	6501.822	6485.885*	6526.055*		6526.153*		3
4		6533.529	6503.996		6528.261	6507.842	6528.327	6507.842	4
5	6556.141	6531.149	6506.175	6481.143*	6530.404*	6505.444	6530.514	6505.444	5
6	6558.279	6528.722	6508.303	6478.770	6532.535	6503.018	6532.625*	6503.018	6
7	6560.381	6526.295	6510.429	6476.321		6500.600	6534.764		7
8	6562.465	6523.830	6512.534*	6473.890		6498.160*		6498.101	8
9	6564.519	6521.348	6514.596	6471.509	6538.782	6495.664*		6495.607	9
10	6566.526	6518.810	6516.660	6468.940	6540.819	6493.159	6540.988	6493.108*	10
11	6568.546	6516.295	6518.670		6542.796*	6490.615	6543.023	6490.567*	11
12	6570.516	6513.710	6520.707	6461.856	6544.823	6488.093	6545.024	6488.024*	12
13	6572.464	6511.145			6546.785	6485.502	6547.016		13
14		6508.516	6524.642		6548.756	6482.944	6548.965		14
15	6576.303*	6505.901	6526.592*			6480.307	6550.873*	6480.241*	15
16	6578.180	6503.235	6528.501*			6477.697	6552.798		16
17	6580.041	6500.554	6530.504*				6554.702	6474.941	17
18	6581.849	6497.864*	6532.244				6556.532	6472.237	18
19	6583.670	6495.151*							19
20	6585.444	6492.391							20
21	6587.193	6489.601							21
22	6588.940	6486.811							22
23		6484.009*							23
24	6592.305	6481.143*							24
25	6593.978	6478.293							25
26	6595.596	6475.430							26
27	6597.198	6472.465							27
28		6469.526							28
29	6600.335	6466.584							29
30	6601.848								30
31									31
32	6604.818*								32

* Lines not used in calculations.

LEVELS		Species of States	$(B'+B'')$	$(B'-B'')\times10^{3}$	$(D'-D'')\times10^{6}$
UPPER	LOWER				
$10^{1}0^{2}0^{2}$	$00^{0}0^{0}0^{0}$	$\Sigma^{+} - \Sigma^{+}$	6542.873±0.002	-12.11±0.02	1.02±0.02
$00^{2}0^{2}0^{2}$	$00^{0}0^{0}0^{0}$	$\Sigma^{+} - \Sigma^{+}$	6492.86±0.005	-10.88±0.08	1.0 ±0.4
$(10^{1}1^{0}0^{2})_{c}$	$(00^{0}1^{0}0^{2})_{c}$	$\Delta - \Delta$	6517.152±0.008	-11.96±0.10	-1.5 ±0.4
$(10^{1}1^{0}0^{2})_{d}$	$(00^{0}1^{0}0^{2})_{d}$			-11.[illegible].11	0.4 ±0.3

approximate vibrational calculation[4] they can be predicted to be located at about 6508 cm^{-1}. Out of the three bands $\Delta_g \leftarrow \Delta_u$, $\Sigma_g^+ \leftarrow \Sigma_u^+$, $\Sigma_g^- \leftarrow \Sigma_u^-$ allowed by symmetry, two could be located both at a wavenumber value slightly lower than that expected. The first of these ($\nu_0 = 6506.9$ cm^{-1}) arises from the $000(11)_+^0$ level according to the alternation of intensity of the rotational lines and to the value of B'', and therefore it is assigned to the $(10111)_+^0 \leftarrow (00011)_+^0$ transition. The second one ($\nu_0 = 6504.9$ cm^{-1}), which arises from the $(00011)^2$ level has been assigned to the $(10111)^2 \leftarrow (00011)^2$ transition. The separation between the Σ^+ and Δ states is 17.7 cm^{-1} in the upper state as compared to the value of 19.4 cm^{-1} found for the lower state (*5*).

[4] ν_0 of $\nu_1 + \nu_3 = 6556.5$; ν_0 of $\nu_1 + \nu_3 + \nu_4^1 - \nu_4^1 = 6529.8$. The difference of 26.7 $cm^{-1} \simeq -(x_{14} + x_{34})$. $(x_{15} + x_{35}) = -21.8$ (see footnote 2). Therefore, ν_0 of $(\nu_1 + \nu_3 + (\nu_4 + \nu_5)_{+/-}^{0,2} - (\nu_4 + \nu_5)_{+/-}^{0,2}) \simeq \nu_0$ of $(\nu_1 + \nu_3) + (x_{14} + x_{34} + x_{15} + x_{35}) = 6508.0$.

VIBRATIONAL LEVELS OF ACETYLENE

Table I lists 15 vibrational levels of the $^{12}C_2H_2$ molecule referred to the ground vibrational state which were obtained by the present analysis. Although a few of these were previously measured, all were reported here because of the better resolution achieved in the present work and the internal consistency of the data. The molecular constants for these levels are presented in Table II and the observational data along with the assignments are given in Tables III–V. The data for the higher vibrational levels of acetylene like the ones obtained in the present study should be useful for the force field calculations of the type discussed by Strey and Mills (*8*).

BANDS PERTAINING TO $^{12}C^{13}CH_2$

Although the concentration of the isotopic species $^{12}C^{13}CH_2$ in the natural sample is only around 1%, there were observed, measured, and assigned a few sequences belonging to such an isotopic variety. Of course, no alternation of intensity was either expected or observed in the rotational structure. The $\nu_1 + \nu_3$ and $2\nu_3$ bands were already measured by using an enriched sample (*7*) although the basic observational data for the bands were not given in this publication. As far as we are aware the $\nu_1 + \nu_5 + \nu_4^1 - \nu_4^1$ band was measured here for the first time. The wavenumbers of the individual lines of all the three bands and the spectroscopic constants determined from these data are summarized in Table VI.

ASTROPHYSICAL INTEREST OF ACETYLENE

In recent years the acetylene spectrum in the infrared has assumed much astrophysical importance. In 1974, from observations made in the 10-μm window acetylene has been identified as a constituent of the atmosphere of Jupiter (*9*). About the same time, it has also been identified in the spectra of stellar photospheres; from observations made in the photographic infrared, bands of $^{12}C_2H_2$ have been identified in carbon stars by Hirai (*10*). In addition, the strong absorption features in the spectra of carbon stars at longer wavelengths as, for instance, at 3 μm may be, at least in part, due to acetylene (*11*). To maintain consistency in the notation as compared to current laboratory studies (*12*), the $^{12}C_2H_2$ bands at 9802, 9668, and 9603 cm^{-1} would, respectively, be due to the transitions 2011^10^0–0001^10^0, 1112^00–0000^00^0, and 0031^10^0–0001^10^0 instead of as indicated in Ref. (*10*).

ACKNOWLEDGMENTS

One of us (K.N.R.) expresses thanks to the Atmospheric Research Section of the National Science Foundation and the National Aeronautic and Space Administration for support of this research.

RECEIVED: January 10, 1977

REFERENCES

1. E. K. PLYLER, E. D. TIDWELL, AND T. A. WIGGINS, *J. Opt. Soc. Amer.* **53**, 589–593 (1963).
2. J. PLÍVA, *J. Mol. Spectrosc.* **44**, 145–164 (1972).
3. K. F. PALMER, M. E. MICHELSON, AND K. NARAHARI RAO, *J. Mol. Spectrosc.* **44**, 131–144 (1972).
4. F. L. KELLER, Ph.D. Dissertation, The University of Tennessee, Knoxville, 1956.
5. J. PLÍVA, *J. Mol. Spectrosc.* **44**, 165–182 (1972).

6. K. K. INNES, *J. Chem. Phys.* **22**, 863–876 (1954).
7. W. J. LAFFERTY AND R. J. THIBAULT, *J. Mol. Spectrosc.* **14**, 79–96 (1964).
8. G. STREY AND I. M. MILLS, *J. Mol. Spectrosc.* **59**, 103–115 (1976).
9. S. T. RIDGWAY, *Astrophys. J. Lett.* **187**, L41 (1974); M. COMBES, TH. ENCRENAZ, L. VAPILLON, Y. ZEAU, AND C. LESQUEREN, *Astron. Astrophys.* **34**, 33–35 (1974).
10. M. HIRAI, *Publ. Astron. Soc. Japan* **26**, 163–188 (1974); *Proc. Jap. Acad.* **50**, 743–746 (1974).
11. K. M. MERRILL AND W. A. STEIN, *Publ. Astron. Soc. Pacific* **88**, 285–293 (1976).
12. S. GHERSETTI, J. E. ADAMS, AND K. NARAHARI RAO, *J. Mol. Spectrosc.* **64**, 157–161 (1977).

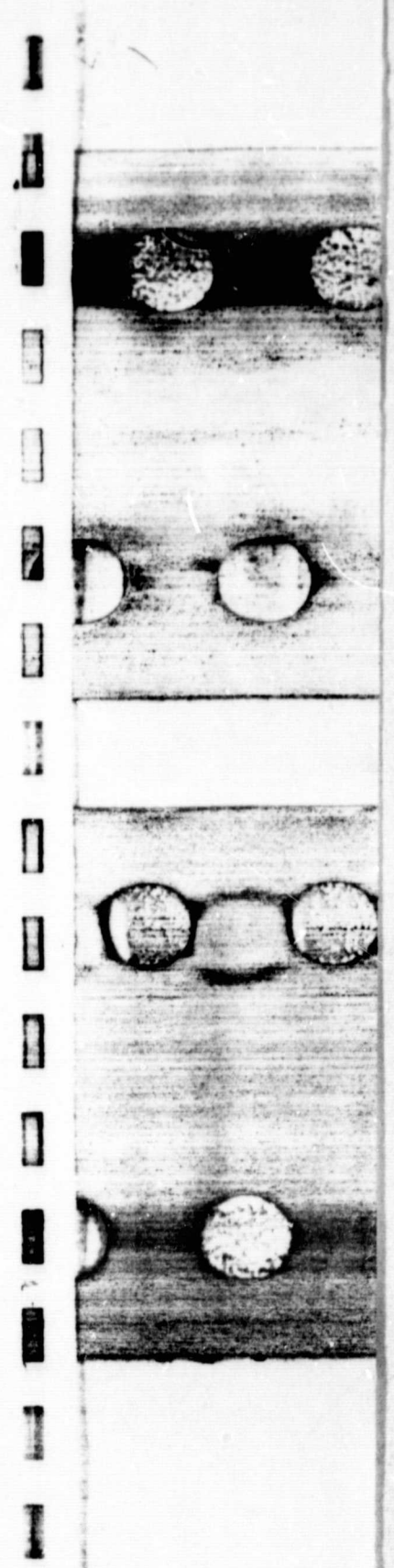

JOURNAL OF MOLECULAR SPECTROSCOPY 79, 31–46 (1980)

Analysis of the ν_3 Band of $^{12}CH_3D$ at 7.6 μm

GINETTE TARRAGO

Laboratorie d'Infrarouge, Associé au CNRS, Campus d'Orsay, Batiment 350, 91405 Orsay, Cedex, France

K. NARAHARI RAO AND L. W. PINKLEY

Department of Physics, The Ohio State University, Columbus, Ohio 43210

The previously reported (*J. Mol. Spectrosc.* **68**, 195–222 (1977)) study of the CH_3D spectrum occurring at 1033–1270 cm^{-1} which was mainly concerned with the ν_6 fundamental has now been extended to cover the region 1270–1420 cm^{-1}. In all, 342 transitions belonging to the ν_3 band are now assigned. Both the ν_3 and ν_6 bands are processed simultaneously taking into account of the Coriolis interaction between them, and the fitting of all the experimental data led to 21 significant spectroscopic constants for the states $v_6 = 1$ and $v_3 = 1$ of CH_3D.

INTRODUCTION AND EXPERIMENTAL RESULTS

In a previous paper (*1*), the absorption spectrum of $^{12}CH_3D$ was investigated in the range 1033–1270 cm^{-1}. The perpendicular-type $\nu_6(E)$ band, responsible for the absorption in this region, was analyzed up to $J' = 17$. A second-order Coriolis interaction with the parallel-type $\nu_3(A_1)$ band was expected to perturb transitions $PP(J, |K|)$, $PQ(J, |K|)$, and $PR(J, |K|)$ near $|K| = 13, 14$. Unfortunately, such transitions were generally too weak in our spectra of ν_6 to be observed or unambiguously assigned. On the other hand, the same perturbation was predicted to be observed in the ν_3 band for lower $|K|$ values, the subbands $|K| = 10, 11$ being expected to be the most perturbed.

In the present paper, the investigation of the spectrum of $^{12}CH_3D$ is extended to the range 1270–1420 cm^{-1}, where the absorption is mostly due to the ν_3 band. The investigated spectra are recorded with a resolution of about 0.04 cm^{-1} (*2*), which is better than previous recordings in the same region (*3*, *4*).

A reproduction of this spectrum is given in Fig. 1, which can be added to Fig. 1 of Ref. (*1*) to get the overall absorption of $^{12}CH_3D$ between 1033 and 1420 cm^{-1}.

The identified transitions of ν_3 run from 1155 to 1420 cm^{-1} with three very strong absorption peaks in the Q branch at 1303.898, 1305.709, and 1306.771 cm^{-1}. The high frequency side of the band is progressively overlapped by the very strong ν_2 band of H_2O, and also by transitions assigned to the ν_5 band of $^{12}CH_3D$. In addition, lines belonging to the ν_4 band of $^{12}CH_4$ are also identified throughout the spectrum showing the presence of this molecule as impurity in the gas sample.

0022-2852/80/010031-16$02.00/0

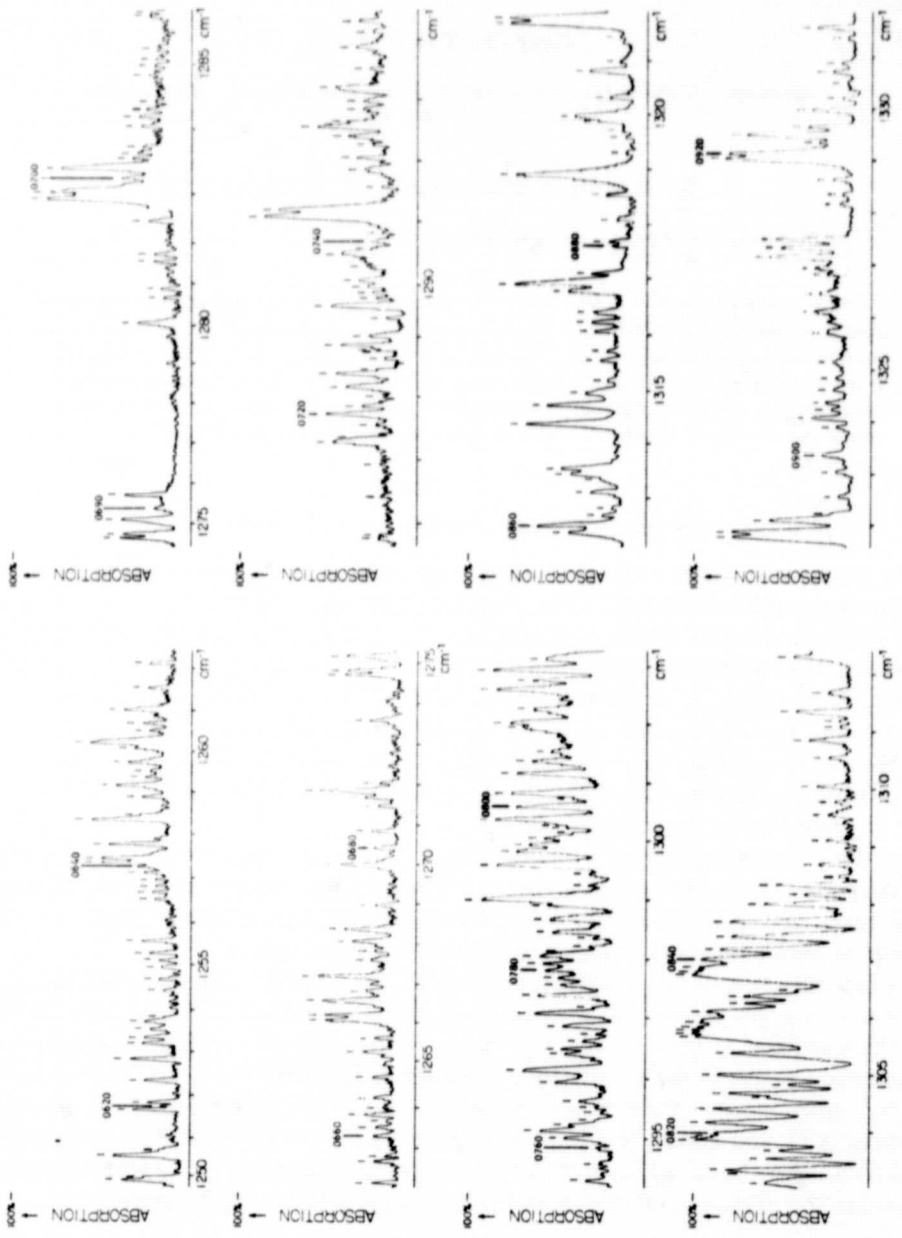

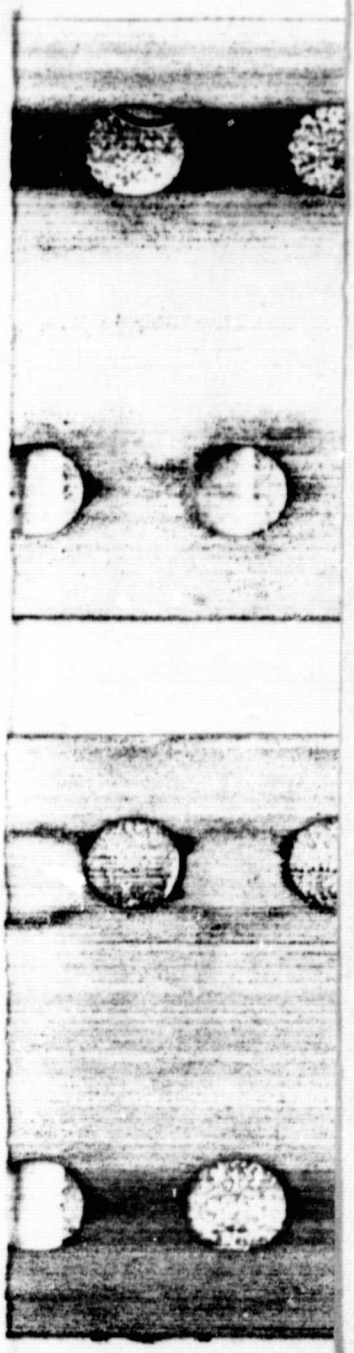

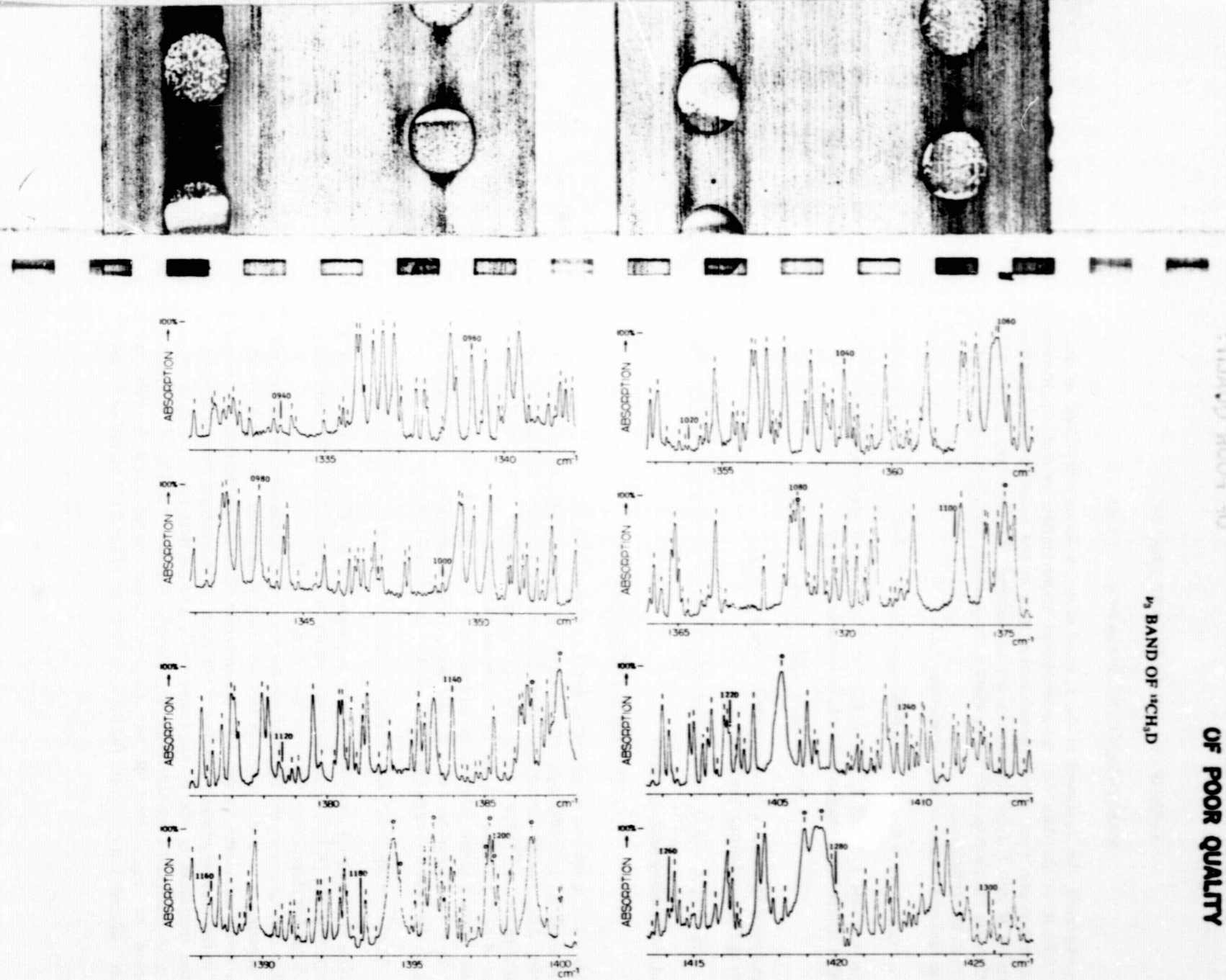

FIG. 1. The spectrum of $^{12}CH_3D$ from 1270–1420 cm^{-1}. The reproduced spectra were recorded with the gas sample contained within a 1-m-length absorption cell at a pressure of 30 Torr.

VIBROTATIONAL ENERGIES IN $v_3 = 1$ STATE

As expected, the treatment of the ν_3 band alone, without vibrational interaction, fails to fit the data within experimental uncertainties; in fact, anomalous deviations occur even if vibrational corrections to the fourth-order distortion constants H and K-type resonances are considered. As discussed in Ref. (*1*), the Coriolis interaction with the ν_6 band is responsible for at least a part of the observed discrepancies.

The first-order term of this interaction, i.e.,

$$(v_3 = 1, v_6 = 0, J, K, l_6 = 0|H|v_3 = 0, v_6 = 1, J, K \pm 1, l_6 = \pm 1) \qquad (1)$$

connects levels $J|K|$ of $v_3 = 1$ to the two Coriolis components of $v_6 = 1$, the coupled levels being roughly spaced, in terms of $|K|$, by

$$\Delta E_1^{\pm} = 151 \pm 3.5|K| \text{ (in cm}^{-1}\text{)}$$

for the positive and negative component, respectively.

For the second-order term, i.e.,

$$(v_3 = 1, v_6 = 0, J, K, l_6 = 0|H|v_3 = 0, v_6 = 1, J, K \pm 2, l_6 = \mp 1) \qquad (2)$$

the corresponding spacings are

$$\Delta E_2^{\pm} = 128 \pm 11.7|K| \text{ (in cm}^{-1}\text{)}.$$

Higher order terms can be neglected for the present purpose.

The spacings $\Delta E_1^{\pm}$ and ΔE_2^{+} remain large for any observed value of $|K|$, the spacing ΔE_2^{-} rapidly decreases when $|K|$ increases, thus making clear the possibility of a "second-order level crossing" between the two rotational series of $v_3 = 1$ and $v_6 = 1$, for $|K|$ between 10 and 11.

Now, if the Coriolis interaction between $v_3 = 1$ and the other near degenerate state $v_5 = 1$ is considered in a similar way, using a preliminary analysis of the ν_5 band, the related quantities $\Delta E_1^{\pm\prime}$ and $\Delta E_2^{\pm\prime}$ are found to be

$$\Delta E_1^{\pm\prime} = -169 \mp 5.5|K| \qquad \text{and} \qquad \Delta E_2^{\pm\prime} = -165 \pm 2.7|K| \text{ (in cm}^{-1}\text{)}$$

showing that no level crossing between rotational series of $v_3 = 1$ and $v_5 = 1$ is expected before $|K| \cong 30$ (for interactions up to second order). The same situation holds for interactions between $v_6 = 1$ and $v_5 = 1$.

So, a convenient model for available data is one in which the Coriolis interaction between $v_3 = 1$ and $v_6 = 1$ is treated exactly, all other vibrational interactions being calculated as usual by perturbation. The computational procedure used in the present analysis consists of the same three steps previously described for the treatment of the ν_6 band alone (*1*), except that now the data on ν_3 and ν_6 are analyzed simultaneously. The energies for $v_3 = 1$ and $v_6 = 1$ states are obtained as eigenvalues of an effective twice transformed Hamiltonian ${}^{(C)}_{(v_s,v_t)}H^{+}$, diagonal in v_s, except for the two elements (*1*) and (*2*) mentioned above

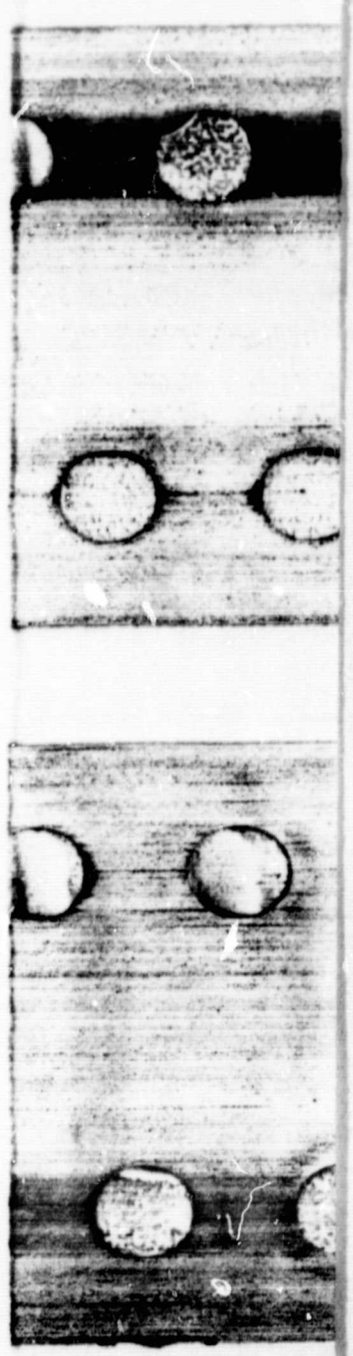

(5). These elements, expanded up to quadratic corrections in J and K, have the following general expressions:

$$(v_n, v_t, J, K, l_t|^{(C)}_{(v_n,v_t)}H^+/hc|v_n + 1, v_t - 1, J, K \pm 1, l_t \pm 1)$$
$$= ((v_n + 1)(v_t \mp l_t))^{1/2} \times \sqrt{J(J+1) - K(K \pm 1)}[C^{(1)}_{11} \pm C^{(2)}_{11}(2K \pm 1)$$
$$+ C^{(3a)}_{11}J(J+1) + C^{(3b)}_{11}(2K \pm 1)^2 + C^{(3c)}_{11}]$$
$$= (v_n + 1, v_t - 1, J, K \pm 1, l_t \pm 1|^{(C)}_{(v_n,v_t)}H^+/hc|v_n, v_t, J, K, l_t). \quad (3)$$

Coefficients $C^{(1)}_{11}$, $C^{(2)}_{11}$, and $C^{(3i)}_{11}$ ($i = a$, b, or c) originate with first, second, and third order terms of the Hamiltonian, respectively. $C^{(1)}_{11}$ has a well-known expression in terms of molecular parameters, i.e.,

$$C^{(1)}_{11} = \frac{B_e\zeta_{nt}}{2} \times \frac{\lambda_n^{1/2} + \lambda_t^{1/2}}{\lambda_n^{1/4}\lambda_t^{1/4}}$$

where ($\zeta_{nt} = \zeta^x_{nt_b} = -\zeta^y_{nt_a}$)

$$(v_n, v_t, J, K, l_t|^{(C)}_{(v_n,v_t)}H^+/hc|v_n + 1, v_t - 1, J, K \pm 2, l_t \mp 1)$$
$$= \mp((v_n + 1)(v_t \pm l_t))^{1/2} \times (J(J+1) - K(K \pm 1))^{1/2}(J(J+1) - (K \pm 2))^{1/2}$$
$$\times [C^{(2)}_{21} \mp C^{(3)}_{21}(2K \pm 2) + C^{(4a)}_{21}J(J+1) + C^{(4b)}_{21}(2K \pm 2)^2 + C^{(4c)}_{21}]$$
$$= (v_n + 1, v_t - 1, J, K \pm 2, l_t \mp 1|^{(C)}_{(v_n,v_t)}H^+/hc|v_n, v_t, J, K, l_t). \quad (4)$$

Coefficients $C^{(2)}_{21}$, $C^{(3)}_{21}$, and $C^{(4i)}_{21}$ ($i = a$, b, or c) originate from second, third, and fourth order terms of the Hamiltonian, respectively. Of course, any analysis does not allow us to separate the constant $C^{(3c)}_{11}$ from $C^{(1)}_{11}$ in Eq. (3), and $C^{(4c)}_{21}$ from $C^{(2)}_{21}$ in Eq. (4).

Expressions (3) and (4) assume for basis eigenvectors, the phase conventions defined in Ref. (6).

Besides the vibrational interaction terms given by Eqs. (3) and (4), the energy matrix $|^{(C)}_{(v_3,v_6)}H^+|$ includes of course the usual essential resonances within $v_3 = 1$ and $v_6 = 1$. The related terms, i.e., "2, 2," "1, −2," "3, 0," and "4, −2" are expressed elsewhere (1, 6).

RELATIVE INTENSITIES OF LINES

The method described in Ref. (1) is extended to take into account transitions going up to levels with $v_3 = 1$ besides $v_6 = 1$. The leading operator of M_Z responsible for all investigated transitions may be written as

$$(M_Z)_{3,6} = d_6[\cos(Z,x)q_{6a} + \cos(Z,y)q_{6b} + \rho_{3,6}\cos(Z,z)q_3] \quad (5)$$

where

$$d_6 = \frac{\partial M_x}{\partial q_{6a}} = \frac{\partial M_y}{\partial q_{6b}}; \qquad \rho_{3,6} = \frac{d_3}{d_6} \qquad \text{with} \qquad d_3 = \frac{\partial M_Z}{\partial q_3}.$$

The coefficient $\rho_{3,6}$, as well as the eigenvectors arising from the diagonalization of the matrix $|^{(C)}_{(v_3,v_6)}H^+|$, are involved in the calculation of the relative intensities. The values of these intensities are obtained in the same arbitrary scale as in Ref. (1).

TABLE I

Observed and Calculated Wavenumbers of ν_3 of $^{12}CH_3D$[a]

(I)	(II)	(III)				(IV)	(V)	(VI)	(VII)	(VIII)
ν_3 TRANSITIONS										
	$^{P}P(18, 3, A1)$	17	3	3	A2		1145.7929		0.170E+03	0.0
	$^{P}P(18, 6, A)$	17	6	6	A		1148.6981		0.258E+03	0.0
	$^{P}P(17, 0, A2)$	16	0	0	A1		1154.8298		0.346E+03	0.0
	$^{P}P(17, 1, E)$	16	1	1	E		1154.6270		0.343E+03	0.0
	$^{P}P(17, 2, E)$	16	2	2	E		1154.9979		0.333E+03	0.0
	$^{P}P(17, 3, A2)$	16	3	3	A1		1155.4510		0.316E+03	0.0
	$^{P}P(17, 3, A1)$	16	3	3	A2		1155.4641		0.316E+03	0.0
	$^{P}P(17, 4, E)$	16	4	4	E		1156.1918		0.294E+03	0.0
	$^{P}P(17, 6, A)$	16	6	6	A		1158.3437		0.476E+03	0.0
	$^{P}P(17, 9, A)$	16	9	9	A		1163.8956		0.270E+03	0.0
	$^{P}P(16, 0, A1)$	15	0	0	A2		1164.1822		0.623E+03	0.0
318	$^{P}P(16, 1, E)$	15	1	1	E	1164.2580	1164.2860	-27	0.616E+03	1.0
320	$^{P}P(16, 2, E)$	15	2	2	E	1164.5590	1164.5979	-38	0.597E+03	1.0
322	$^{P}P(16, 3, A1)$	15	3	3	A2	1165.1358	1165.1145	21	0.566E+03	0.0
322	$^{P}P(16, 3, A2)$	15	3	3	A1	1165.1358	1165.1256	10	0.566E+03	1.0
325	$^{P}P(16, 4, E)$	15	4	4	E	1165.8049	1165.8556	-50	0.525E+03	0.0
330	$^{P}P(16, 5, E)$	15	5	5	E	1166.8190	1166.8112	7	0.476E+03	1.0
334	$^{P}P(16, 6, A)$	15	6	6	A	1168.0755	1167.9961	79	0.841E+03	0.0
340	$^{P}P(16, 7, E)$	15	7	7	E	1169.4448	1169.4284	16	0.361E+03	1.0
344	$^{P}P(16, 8, E)$	15	8	8	E	1171.1640	1171.1465	17	0.300E+03	1.0
351	$^{P}P(16, 9, A)$	15	9	9	A	1173.2588	1173.2597	-19	0.471E+03	1.0
	$^{P}P(16, 12, A)$	15	12	12	A		1177.8617		0.206E+03	0.0
353	$^{P}P(15, 0, A2)$	14	0	0	A1	1173.7931	1173.8284	-35	0.107E+04	0.0
354	$^{P}P(15, 1, E)$	14	1	1	E	1173.9249	1173.9328	-7	0.106E+04	1.0
355	$^{P}P(15, 2, E)$	14	2	2	E	1174.1964	1174.2465	-50	0.103E+04	0.0
357	$^{P}P(15, 3, A2)$	14	3	3	A1	1174.7739	1174.7665	7	0.972E+03	1.0
357	$^{P}P(15, 3, A1)$	14	3	3	A2	1174.7739	1174.7753	-1	0.972E+03	1.0
362	$^{P}P(15, 4, E)$	14	4	4	E	1175.5188	1175.5086	10	0.878E+03	1.0
367	$^{P}P(15, 5, E)$	14	5	5	E	1176.4744	1176.4639	10	0.809E+03	1.0
371	$^{P}P(15, 6, A)$	14	6	6	A	1177.6501	1177.6492	6	0.142E+04	*1.0
375	$^{P}P(15, 7, E)$	14	7	7	E	1179.1112	1179.0575	53	0.605E+03	0.0
378	$^{P}P(15, 8, E)$	14	8	8	E	1180.7354	1180.7295	5	0.497E+03	1.0
384	$^{P}P(15, 9, A)$	14	9	9	A	1182.7048	1182.7223	-17	0.777E+03	1.0
388	$^{P}P(14, 0, A1)$	13	0	0	A2	1183.4514	1183.4456	5	0.178E+04	1.0
389	$^{P}P(14, 1, E)$	13	1	1	E	1183.5609	1183.5508	10	0.176E+04	1.0
390	$^{P}P(14, 2, E)$	13	2	2	E	1183.8797	1183.8666	13	0.170E+04	1.0
392	$^{P}P(16, 3, A1)$	13	3	3	A2	1184.4081	1184.3908	17	0.160E+04	1.0
392	$^{P}P(14, 3, A2)$	13	3	3	A1	1184.4081	1184.3975	10	0.160E+04	1.0
393	$^{P}P(14, 4, E)$	13	4	4	E	1185.1478	1185.1356	12	0.147E+04	1.0
394	$^{P}P(15, 10, E)$	14	10	10	E	1185.2783	1185.3481	-69	0.265E+03	0.0
399	$^{P}P(14, 5, E)$	13	5	5	E	1186.0982	1186.0933	4	0.132E+04	1.0
403	$^{P}P(14, 6, A)$	13	6	6	A	1187.2654	1187.2718	-6	0.229E+04	*1.0
	$^{P}P(15, 12, A)$	14	12	12	A		1189.4033		0.300E+03	0.0
408	$^{P}P(14, 7, E)$	13	7	7	E	1188.6720	1188.6772	-5	0.963E+03	1.0
413	$^{P}P(14, 8, E)$	13	8	8	E	1190.3491	1190.3206	22	0.780E+03	1.0
417	$^{P}P(14, 9, A)$	13	9	9	A	1192.2039	1192.2295	-25	0.120E+04	1.0
420	$^{P}P(13, 0, A2)$	12	0	0	A1	1192.9809	1193.0178	-37	0.282E+04	0.0
421	$^{P}P(13, 1, E)$	12	1	1	E	1193.1356	1193.1238	11	0.279E+04	1.0
422	$^{P}P(13, 2, E)$	12	2	2	E	1193.4270	1193.4423	-15	0.268E+04	1.0
423	$^{P}P(13, 3, A2)$	12	3	3	A1	1193.9889	1193.9718	17	0.252E+04	1.0
423	$^{P}P(13, 3, A1)$	12	3	3	A2	1193.9889	1193.9765	12	0.252E+04	1.0
425	$^{P}P(14, 10, E)$	13	10	10	E	1194.5055	1194.5436	-38	0.416E+03	0.0
426	$^{P}P(13, 4, E)$	12	4	4	E	1194.7925	1194.7208	11	0.230E+04	1.0
	$^{P}P(14, 11, E)$	13	11	11	E		1195.4468		0.268E+03	0.0
428	$^{P}P(13, 5, E)$	12	5	5	E	1195.7023	1195.6844	17	0.204E+04	1.0
430	$^{P}P(13, 6, A)$	12	6	6	A	1196.8711	1196.8678	3	0.350E+04	*1.0
436	$^{P}P(13, 7, E)$	12	7	7	E	1198.2676	1198.2745	-6	0.145E+04	1.0
438	$^{P}P(14, 12, A)$	13	12	12	A	1198.7052	1198.7185	-13	0.370E+03	1.0
441	$^{P}P(13, 8, E)$	12	8	8	E	1199.8936	1199.9090	-15	0.115E+04	1.0

[a] (I) Serial number. (II) Transition. (III) Values of J', $|K'|$, $|K' - l_6'|$, C' for upper levels of the transitions. (IV) Observed wavenumber in cm^{-1}. (V) Calculated wavenumber in cm^{-1}. (VI) (Expt − Calc) in 10^{-3} cm^{-1}. (VII) Calculated relative intensity. (VIII) Statistical weight.

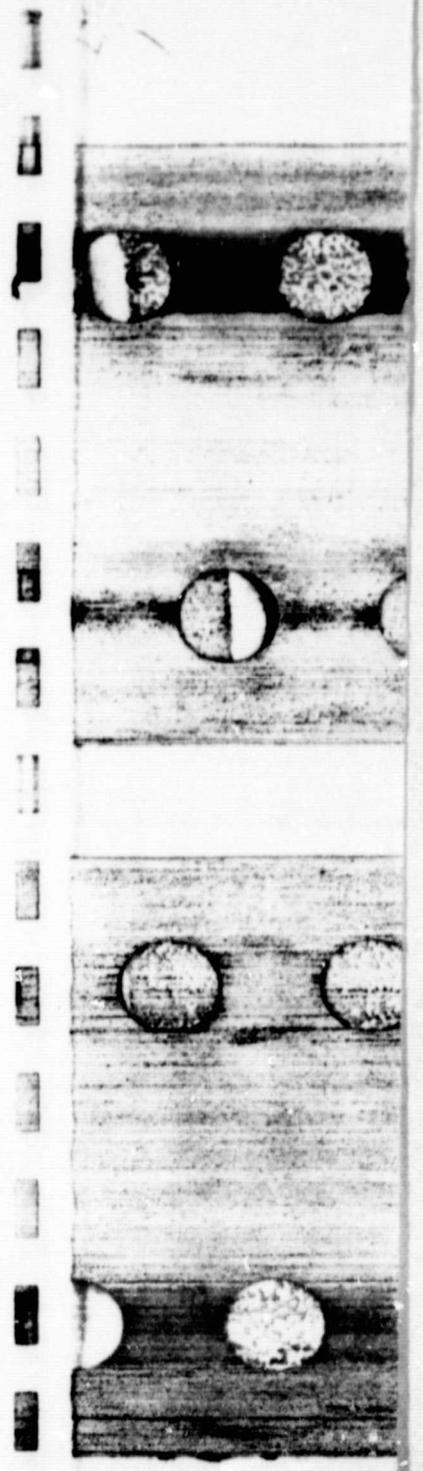

TABLE I—*Continued*

(I)	(II)	(III)				(IV)	(V)	(VI)	(VII)	(VIII)
445	QP(13, 9,A)	12	9	9	A	1201.7507	1201.7783	-27	0.171E+04	1.0
447	QP(12, 0,A1)	11	0	0	A2	1202.5402	1202.5291	11	0.429E+04	1.0
448	QP(12, 1,E)	11	1	1	E	1202.6779	1202.6362	41	0.423E+04	0.0
449	QP(12, 2,E)	11	2	2	E	1202.9688	1203.9580	10	0.406E+04	1.0
450	QP(12, 3,A1)	11	3	3	A2	1203.4982	1203.4935	4	0.379E+04	1.0
450	QP(12, 3,A2)	11	3	3	A1	1203.4982	1203.4967	1	0.379E+04	1.0
451	QP(13,10,E)	12	10	10	F	1203.8745	1203.9091	-28	0.583E+03	1.0
453	QP(12, 4,E)	11	4	4	F	1204.3074	1204.2981	58	0.343E+04	0.0
455	QP(12, 5,E)	11	5	5	F	1205.2216	1205.2218	0	0.301E+04	1.0
457	QP(13,11,E)	12	11	11	F	1206.0421	1206.0514	-9	0.364E+03	1.0
459	QP(12, 6,A)	11	6	6	A	1206.3928	1206.4158	-22	0.508E+04	0.0
461	QP(12, 7,E)	11	7	7	F	1207.8265	1207.8339	-7	0.205E+04	1.0
465	QP(13,12,A)	12	12	12	A	1208.7193	1208.7508	-31	0.326E+03	0.0
467	QP(12, 8,E)	11	8	8	F	1209.4808	1209.4795	1	0.156E+04	1.0
472	QP(12, 9,A)	11	9	9	A	1211.3415	1211.3555	-14	0.220E+04	1.0
474	QP(11, 0,A2)	10	0	0	A1	1211.9584	1211.9639	-5	0.629E+04	1.0
475	QP(11, 1,E)	10	1	1	E	1212.0776	1212.0723	5	0.614E+04	1.0
477	QP(11, 2,E)	10	2	2	E	1212.3965	1212.3979	-1	0.587E+04	1.0
480	QP(11, 3,A2)	10	3	3	A1	1212.9444	1212.9404	4	0.544E+04	1.0
480	QP(11, 3,A1)	10	3	3	A2	1212.9444	1212.9474	1	0.544E+04	1.0
482	QP(12,10,E)	11	10	10	F	1213.4594	1213.4594	0	0.683E+03	1.0
484	QP(11, 4,E)	10	4	4	E	1213.6911	1213.7045	-13	0.487E+04	1.0
485	QP(11, 5,E)	10	5	5	E	1214.6878	1214.6894	-1	0.420E+04	1.0
490	QP(11, 6,A)	10	6	6	A	1215.8939	1215.8992	-5	0.691E+04	*1.0
490	QP(12,11,E)	11	11	11	F	1215.8939	1215.9285	-34	0.311E+03	0.0
492	QP(11, 7,E)	10	7	7	E	1217.3227	1217.3381	-15	0.269E+04	1.0
498	QP(11, 8,E)	10	8	8	E	1218.9610	1219.0129	-51	0.193E+04	0.0
503	QP(11, 9,A)	10	9	9	A	1220.9409	1220.9376	2	0.249E+04	1.0
505	QP(10, 0,A1)	9	0	0	A2	1221.3077	1221.3071	0	0.865E+04	1.0
506	QP(10, 1,E)	9	1	1	E	1221.4196	1221.4169	2	0.850E+04	1.0
508	QP(10, 2,E)	9	2	2	E	1221.7480	1221.7466	2	0.809E+04	1.0
512	QP(10, 3,A1)	9	3	3	A2	1222.2995	1222.2968	-3	0.742E+04	1.0
512	QP(10, 3,A2)	9	3	3	A1	1222.2995	1222.2980	-4	0.742E+04	1.0
515	QP(10, 4,E)	9	4	4	E	1223.0681	1223.0711	-3	0.654E+04	1.0
516	QP(11,10,E)	10	10	10	E	1223.1984	1223.1768	21	0.562E+03	0.0
518	QP(10, 5,E)	9	5	5	E	1224.0597	1224.0707	-11	0.550E+04	1.0
523	QP(10, 6,A)	9	6	6	A	1225.2924	1225.3007	-8	0.874E+04	*1.0
531	QP(10, 7,E)	9	7	7	E	1226.7681	1226.7681	0	0.320E+04	1.0
535	QP(10, 8,E)	9	8	8	E	1228.4843	1228.4868	-2	0.205E+04	1.0
542	QP(10, 9,A)	9	9	9	A	1230.5376	1230.4937	43	0.199E+04	0.0
542	QP(9, 0,A2)	8	0	0	A1	1230.5376	1230.5435	-5	0.114E+05	1.0
543	QP(9, 1,E)	8	1	1	E	1230.6298	1230.6548	-25	0.112E+05	1.0
545	QP(9, 2,E)	8	2	2	E	1230.9809	1230.9891	-8	0.106E+05	1.0
548	QP(9, 3,A2)	8	3	3	A1	1231.5364	1231.5474	-10	0.959E+04	1.0
548	QP(9, 3,A1)	8	3	3	A2	1231.5364	1231.5480	-11	0.959E+04	1.0
550	QP(9, 4,E)	8	4	4	E	1232.3263	1232.3331	-6	0.827E+04	1.0
555	QP(9, 5,E)	8	5	5	E	1233.3071	1233.3492	-42	0.671E+04	0.0
558	QP(9, 6,A)	8	6	6	A	1234.5985	1234.6024	-3	0.100E+05	*1.0
563	QP(9, 7,E)	8	7	7	E	1236.1423	1236.1039	38	0.928E+04	0.0
570	QP(9, 8,E)	8	8	8	E	1237.9018	1237.8773	24	0.158E+04	1.0
577	QP(8, 0,A1)	7	0	0	A2	1239.6404	1239.6589	-18	0.144E+05	1.0
578	QP(8, 1,E)	7	1	1	E	1239.7643	1239.7717	-7	0.141E+05	1.0
580	QP(8, 2,E)	7	2	2	E	1240.1023	1240.1106	-8	0.131E+05	1.0
582	QP(8, 3,A1)	7	3	3	A2	1240.6633	1240.6771	-13	0.117E+05	1.0
582	QP(8, 3,A2)	7	3	3	A1	1240.6633	1240.6774	-14	0.117E+05	1.0
585	QP(8, 4,E)	7	4	4	E	1241.4707	1241.4748	-4	0.972E+04	1.0
588	QP(8, 5,E)	7	5	5	E	1242.5048	1242.5083	-3	0.744E+04	1.0
593	QP(8, 6,A)	7	6	6	A	1243.7885	1243.7865	1	0.995E+04	*1.0
598	QP(8, 7,E)	7	7	7	E	1245.3489	1245.3254	23	0.245E+04	1.0
609	QP(7, 0,A2)	6	0	0	A1	1248.4365	1248.4396	-3	0.172E+05	1.0

TABLE I—*Continued*

(I)	(II)	(III)	(IV)	(V)	(VI)	(VII)	(VIII)
610	2P(7, 1,E)	6 1 1 E	1248.7396	1248.7539	-14	0.167E+05	1.0
611	2P(7, 2,E)	6 2 2 E	1249.0912	1249.0973	-6	0.154E+05	1.0
614	2P(7, 3,A2)	6 3 3 A1	1249.6617	1249.6719	-10	0.132E+05	1.0
614	2P(7, 3,A1)	6 3 3 A2	1249.6617	1249.6719	-10	0.132E+05	1.0
617	2P(7, 4,E)	6 4 4 E	1250.4849	1250.4814	3	0.104E+05	1.0
619	2P(7, 5,E)	6 5 5 E	1251.5391	1251.5324	6	0.713E+04	1.0
623	2P(7, 6,A)	6 6 6 A	1252.8577	1252.8360	21	0.719E+04	*1.0
641	2P(6, 0,A1)	5 0 0 A2	1257.4662	1257.4729	-6	0.193E+05	1.0
642	2P(6, 1,E)	5 1 1 E	1257.5778	1257.5885	-10	0.186E+05	1.0
643	2P(6, 2,E)	5 2 2 E	1257.9910	1257.9961	-5	0.167E+05	1.0
644	2P(6, 3,A1)	5 3 3 A2	1258.5261	1258.5181	7	0.136E+05	1.0
644	2P(6, 3,A2)	5 3 3 A1	1258.5261	1258.5182	7	0.136E+05	1.0
647	2P(6, 4,E)	5 4 4 E	1259.3419	1259.3390	2	0.966E+04	1.0
652	2P(6, 5,E)	5 5 5 E	1260.3726	1260.4066	-33	0.501E+04	0.0
669	2P(5, 0,A2)	4 0 0 A1	1266.1437	1266.1472	-3	0.209E+05	1.0
670	2P(5, 1,E)	4 1 1 E	1266.2601	1266.2640	-3	0.194E+05	1.0
671	2P(5, 2,E)	4 2 2 E	1266.6180	1266.6154	2	0.166E+05	1.0
673	2P(5, 3,A2)	4 3 3 A1	1267.2121	1267.2039	8	0.123E+05	1.0
673	2P(5, 3,A1)	4 3 3 A2	1267.2121	1267.2040	8	0.123E+05	1.0
676	2P(5, 4,E)	4 4 4 E	1268.0493	1268.0349	14	0.659E+04	1.0
687	2P(4, 0,A1)	3 0 0 A2	1274.6616	1274.6524	9	0.198E+05	1.0
688	2P(4, 1,E)	3 1 1 E	1274.7719	1274.7702	1	0.184E+05	1.0
689	2P(4, 2,E)	3 2 2 E	1275.1281	1275.1246	3	0.145E+05	1.0
691	2P(4, 3,A1)	3 3 3 A2	1275.7297	1275.7186	11	0.816E+04	1.0
691	2P(4, 3,A2)	3 3 3 A1	1275.7297	1275.7186	11	0.816E+04	1.0
698	2P(3, 0,A2)	2 0 0 A1	1282.9901	1282.9788	12	0.174E+05	1.0
699	2P(3, 1,E)	2 1 1 E	1283.1074	1283.0983	9	0.153E+05	1.0
711	2P(3, 2,E)	2 2 2 E	1283.4689	1283.4550	13	0.940E+04	1.0
716	2P(17, 6,A)	17 6 6 A	1287.0584	1287.0198	38	0.150E+03	0.0
730	2P(16, 6,A)	16 6 6 A	1289.1281	1289.1021	22	0.300E+03	0.0
735	2P(15, 5,E)	15 5 5 E	1290.0299	1290.0282	1	0.218E+03	1.0
	2P(14, 3,A2)	14 3 3 A1		1290.4359		0.184E+03	0.0
742	2P(14, 4,E)	14 4 4 E	1291.1430	1291.1526	-10	0.278E+03	1.0
742	2P(15, 6,A)	15 6 6 A	1291.1430	1291.1707	-28	0.582E+03	*1.0
742	2P(2, 0,A1)	1 0 0 A2	1291.1430	1291.1226	19	0.131E+05	1.0
743	2P(2, 1,E)	1 1 1 E	1291.2522	1291.2415	10	0.973E+04	1.0
746	2P(14, 5,E)	14 5 5 E	1292.0914	1292.0753	16	0.409E+03	1.0
748	2P(13, 3,A1)	13 3 3 A2	1292.4438	1292.4328	10	0.298E+03	1.0
748	2P(13, 3,A2)	13 3 3 A1	1292.4438	1292.4395	4	0.298E+03	1.0
749	2P(15, 7,E)	15 7 7 E	1292.5970	1292.5527	44	0.362E+03	0.0
754	2P(13, 4,E)	13 4 4 E	1293.2126	1293.1595	59	0.506E+03	0.0
754	2P(14, 6,A)	14 6 6 A	1293.2126	1293.2145	-1	0.109E+04	*1.0
	2P(13, 5,E)	13 5 5 E		1294.0807		0.745E+03	0.0
757	2P(15, 8,E)	15 8 8 E	1294.2333	1294.2126	20	0.423E+03	1.0
757	2P(17,12,A)	17 12 12 A	1294.2333	1294.2292	4	0.262E+03	1.0
758	2P(12, 3,A2)	12 3 3 A1	1294.3861	1294.3690	17	0.526E+03	1.0
758	2P(12, 3,A1)	12 3 3 A2	1294.3861	1294.3738	12	0.526E+03	1.0
758	2P(16, 9,A)	16 9 9 A	1294.3861	1294.4098	-23	0.468E+03	0.0
759	2P(14, 7,E)	14 7 7 E	1294.5814	1294.5814	0	0.681E+03	1.0
761	2P(12, 4,E)	12 4 4 E	1295.1044	1295.0958	8	0.892E+03	1.0
762	2P(13, 6,A)	13 6 6 A	1295.2281	1295.2216	6	0.199E+04	*1.0
	2P(14,11,E)	13 11 11 E		1195.4468		0.268E+03	0.0
767	2P(11, 2,E)	11 2 2 E	1295.7084	1295.7092	0	0.413E+03	1.0
768	2P(12, 5,E)	12 5 5 E	1296.0429	1296.0307	12	0.131E+04	1.0
769	2P(11, 3,A1)	11 3 3 A2	1296.2981	1296.2901	8	0.899E+03	1.0
769	2P(11, 3,A2)	11 3 3 A1	1296.2981	1296.2333	4	0.899E+03	1.0
769	2P(14, 8,E)	14 8 8 E	1296.2981	1296.1985	39	0.799E+03	0.0
769	2P(15, 9,A)	15 9 9 A	1296.2981	1296.3198	-21	0.929E+03	0.0
770	2P(15,11,E)	15 11 11 E	1296.4855	1296.4795	11	0.404E+03	1.0
771	2P(13, 7,E)	13 7 7 E	1296.9876	1296.9829	5	0.124E+04	1.0

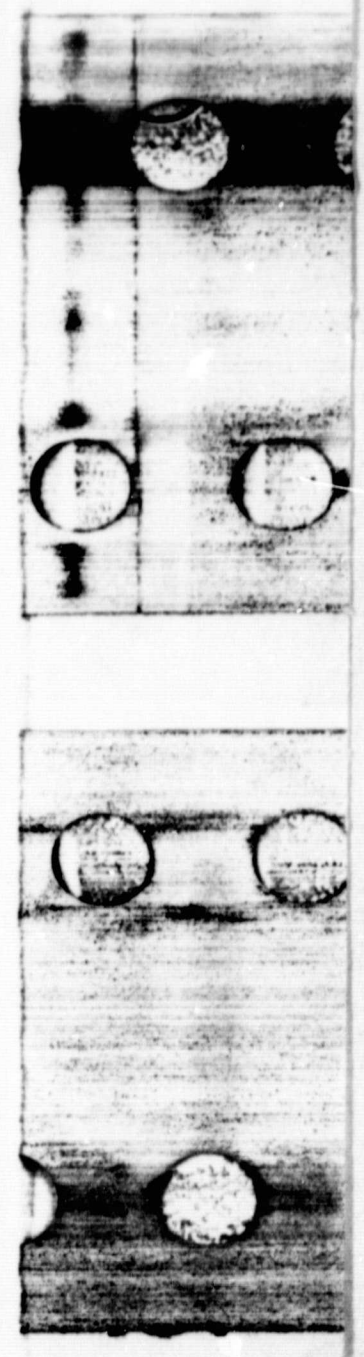

TABLE I—*Continued*

(I)	(II)	(III)			(IV)	(V)	(VI)	(VII)	(VIII)
774	00(11, 4,E)	11	4	4 E	1296.9681	1296.9650	3	0.153E+04	1.0
775	00(10, 1,F)	10	1	1 F	1297.1873	1297.1550	32	0.175E+03	0.0
775	00(12, 6,A)	12	6	6 A	1297.1873	1297.1790	8	0.351E+04	*1.0
777	00(10, 2,F)	10	2	2 F	1297.4844	1297.4726	11	0.685E+03	1.0
777	00(16,12,A)	16	12	12 A	1297.4844	1297.4760	8	0.546E+03	1.0
780	00(11, 5,F)	11	5	5 F	1297.9049	1297.9111	-6	0.224E+04	1.0
781	00(10, 3,A2)	10	3	3 A1	1298.0035	1298.0016	1	0.149E+04	1.0
781	00(10, 3,A1)	10	3	3 A2	1298.0035	1298.0034	0	0.149E+04	1.0
782	00(14, 9,A)	14	9	9 A	1298.1384	1298.1291	9	0.177E+04	1.0
783	00(13, 8,F)	13	8	8 F	1298.1843	1298.1744	9	0.146E+04	1.0
786	00(12, 7,F)	12	7	7 F	1298.5400	1298.5442	-4	0.219E+04	1.0
787	00(9, 1,F)	9	1	1 F	1298.7523	1298.8085	-56	0.282E+03	0.0
787	00(10, 4,F)	10	4	4 F	1298.7523	1298.7665	5	0.259E+04	1.0
789	00(9, 2,F)	9	2	2 F	1299.0926	1299.1308	-38	0.111E+04	0.0
789	00(15,10,F)	15	10	10 F	1299.0926	1299.1781	-85	0.429E+03	0.0
789	00(1, 0,A2)	0	0	0 A1	1299.0926	1299.0756	16	0.709E+04	1.0
789	00(11, 6,A)	11	6	6 A	1299.0926	1299.0725	20	0.601E+04	*1.0
792	00(9, 3,A1)	9	3	3 A2	1299.6747	1299.6686	6	0.241E+04	1.0
792	00(9, 3,A2)	9	3	3 A1	1299.6747	1299.6698	4	0.241E+04	1.0
792	00(10, 5,F)	10	5	5 F	1299.6747	1299.7069	-32	0.379E+04	0.0
793	00(14,11,E)	14	11	11 E	1299.8933	1299.8481	45	0.816E+03	0.0
794	00(13, 9,A)	13	9	9 A	1300.0061	1300.0248	-18	0.926E+04	1.0
795	00(12, 8,F)	12	8	8 F	1300.1177	1300.1307	-12	0.258E+04	1.0
798	00(8, 1,F)	8	1	1 F	1300.3989	1300.3939	-4	0.443E+03	1.0
799	00(9, 4,F)	9	4	4 F	1300.4355	1300.4356	9	0.409E+04	1.0
799	00(11, 7,F)	11	7	7 F	1300.4355	1300.4522	-16	0.375E+04	1.0
800	00(8, 2,F)	8	2	2 F	1300.6453	1300.6705	-25	0.174E+04	1.0
800	00(14,10,F)	14	10	10 F	1300.6453	1300.6849	-39	0.859E+03	0.0
800	00(15,12,A)	15	12	12 A	1300.6453	1300.6563	90	0.110E+04	0.0
801	00(16,13,F)	16	13	13 F	1300.7709	1300.7889	21	0.288E+03	1.0
803	00(10, 6,A)	10	6	6 A	1300.8746	1300.8867	-12	0.998E+04	*1.0
803	00(8, 3,A2)	8	3	3 A1	1301.2119	1301.2176	-5	0.378E+04	1.0
803	00(8, 3,A1)	8	3	3 A2	1301.2119	1301.2182	-6	0.378E+04	1.0
804	00(9, 5,E)	9	5	5 E	1301.3914	1301.4029	-11	0.601E+04	1.0
	00(7, 1,F)	7	1	1 F		1301.7451		0.681E+03	0.0
806	00(8, 4,F)	8	4	4 F	1301.9490	1301.9876	-38	0.642E+04	0.0
806	00(12, 9,A)	12	9	9 A	1301.9490	1301.9494	-3	0.582E+04	1.0
807	00(7, 2,F)	7	2	2 F	1302.0441	1302.0780	-33	0.267E+04	0.0
807	00(11, 8,F)	11	8	8 F	1302.0441	1302.0532	-9	0.443E+04	1.0
808	00(10, 7,E)	10	7	7 F	1302.2682	1302.2902	-21	0.623E+04	1.0
808	00(13,10,F)	13	10	10 F	1302.2682	1302.2794	-5	0.167E+04	1.0
809	00(7, 3,A1)	7	3	3 A2	1302.6104	1302.6345	-24	0.581E+04	1.0
809	00(7, 3,A2)	7	3	3 A1	1302.6104	1302.6348	-24	0.581E+04	1.0
809	00(9, 6,A)	9	6	6 A	1302.6104	1302.6054	4	0.161E+05	*1.0
811	00(6, 1,E)	6	1	1 F	1302.9755	1303.0025	-27	0.103E+04	1.0
811	00(8, 5,E)	8	5	5 E	1302.9755	1302.9855	-8	0.946E+04	1.0
812	00(13,11,E)	13	11	11 E	1303.1502	1303.1039	46	0.165E+04	0.0
813	00(6, 2,F)	6	2	2 F	1303.3233	1303.3407	-17	0.402E+04	1.0
814	00(7, 4,F)	7	4	4 E	1303.3894	1303.4182	-28	0.987E+04	1.0
815	00(14,12,A)	14	12	12 A	1303.5787	1303.5775	1	0.212E+04	1.0
816	00(15,13,E)	15	13	13 F	1303.7317	1303.7349	-13	0.567E+03	1.0
817	00(6, 3,A2)	6	3	3 A1	1303.8981	1303.9064	-8	0.876E+04	1.0
817	00(6, 3,A1)	6	3	3 A2	1303.8981	1303.9065	-8	0.876E+04	1.0
817	00(10, 8,E)	10	8	8 E	1303.8981	1303.9239	-25	0.737E+04	1.0
817	00(11, 9,A)	11	9	9 A	1303.8981	1303.8785	19	0.100E+05	1.0
817	00(16,14,F)	16	14	14 E	1303.8981	1303.8947	3	0.284E+03	1.0
819	00(9, 7,F)	9	7	7 E	1304.0919	1304.0405	-8	0.101E+05	1.0
819	00(12,10,E)	12	10	10 F	1304.0919	1304.0089	22	0.911E+04	0.0
820	00(5, 1,E)	5	1	1 E	1304.0760	1304.1037	-27	0.153E+04	1.0
820	00(17,15,A)	17	15	15 A	1304.0760	1304.0857	-9	0.769E+03	1.0

TABLE I—*Continued*

(I)	(II)	(III)	(IV)	(V)	(VI)	(VII)	(VIII)
821	20(8, 6,A)	8 6 6 A	1304.2096	1304.2120	-2	0.253E+05	*1.0
822	20(5, 2,E)	5 2 2 E	1304.4384	1304.4468	-8	0.598E+04	1.0
823	20(7, 5,E)	7 5 5 E	1304.4384	1304.4398	-4	0.145E+05	1.0
824	20(6, 4,E)	6 4 4 E	1304.7002	1304.7038	-9	0.149E+05	1.0
825	20(4, 1,E)	4 1 1 E	1305.0240	1305.0382	-14	0.226E+04	1.0
826	20(5, 3,A1)	5 3 3 A2	1305.0240	1305.0212	2	0.130E+05	1.0
826	20(5, 3,A2)	5 3 3 A1	1305.0240	1305.0212	2	0.130E+05	1.0
	20(4, 2,E)	4 2 2 E	1305.4025	1305.3857	16	0.888E+04	1.0
828	20(7, 6,A)	7 6 6 A	1305.7093	1305.6899	19	0.389E+05	*1.0
828	20(8, 7,E)	8 7 7 E	1305.7093	1305.6843	25	0.158E+05	1.0
828	20(9, 8,E)	9 8 8 E	1305.7093	1305.7217	-12	0.119E+05	1.0
829	20(6, 5,E)	6 5 5 E	1305.7566	1305.7390	17	0.219E+05	1.0
830	20(3, 1,E)	3 1 1 F	1305.8102	1305.7970	13	0.342E+04	1.0
830	20(10, 9,A)	10 9 9 A	1305.8102	1305.8020	8	0.167E+05	1.0
830	20(5, 4,E)	5 4 4 E	1305.8102	1305.8316	-21	0.221E+05	1.0
832	20(4, 3,A1)	4 3 3 A2	1305.9571	1305.9680	-10	0.193E+05	1.0
832	20(4, 3,A2)	4 3 3 A1	1305.9571	1305.9680	-10	0.193E+05	1.0
832	20(11,10,E)	11 10 10 E	1305.9571	1305.9246	32	0.548E+04	0.0
833	20(3, 2,E)	3 2 2 F	1306.1419	1306.1484	-6	0.134E+05	1.0
833	20(12,11,E)	12 11 11 E	1306.1419	1306.0889	52	0.338E+04	0.0
834	20(13,12,A)	13 12 12 A	1306.2735	1306.2956	-22	0.392E+04	1.0
835	20(2, 1,E)	2 1 1 E	1306.3951	1306.3729	22	0.547E+04	1.0
836	20(14,13,E)	14 13 13 E	1306.5175	1306.5429	-25	0.107E+04	1.0
837	20(1, 1,E)	1 1 1 E	1306.7719	1306.7600	11	0.106E+05	1.0
837	20(2, 2,E)	2 2 2 E	1306.7719	1306.7272	44	0.214E+05	0.0
837	20(3, 3,A1)	3 3 3 A2	1306.7719	1306.7374	33	0.292E+05	0.0
837	20(3, 3,A2)	3 3 3 A1	1306.7719	1306.7374	33	0.292E+05	1.0
837	20(4, 4,E)	4 4 4 F	1306.7719	1306.7902	-18	0.328E+05	1.0
837	20(15,14,E)	15 14 14 F	1306.7719	1306.8308	-59	0.554E+03	0.0
838	20(5, 5,E)	5 5 5 F	1306.8995	1306.8856	13	0.326E+05	1.0
839	20(6, 6,A)	6 6 6 A	1307.0292	1307.0292	16	0.586E+05	*1.0
	20(16,15,A)	16 15 15 A		1307.1586		0.542E+03	0.0
840	20(7, 7,E)	7 7 7 E	1307.2200	1307.2037	17	0.249E+05	1.0
841	20(8, 8,E)	8 8 8 F	1307.4439	1307.4298	20	0.187E+05	1.0
842	20(9, 9,A)	9 9 9 A	1307.7097	1307.6860	23	0.269E+05	1.0
843	20(10,10,E)	10 10 10 F	1308.0147	1307.9889	25	0.909E+04	1.0
845	20(11,11,E)	11 11 11 E	1308.3554	1308.3318	23	0.577E+04	1.0
847	20(12,12,A)	12 12 12 A	1308.7345	1308.7141	20	0.690E+04	1.0
848	20(13,13,E)	13 13 13 E	1309.1452	1309.1352	9	0.195E+04	1.0
849	20(14,14,E)	14 14 14 F	1309.6168	1309.5944	22	0.104E+04	1.0
851	20(15,15,A)	15 15 15 A	1310.1039	1310.0909	12	0.105E+04	1.0
866	2R(0, 0,A1)	1 0 0 A2	1314.4156	1314.4017	13	0.749E+04	1.0
893	2R(1, 0,A2)	2 0 0 A1	1321.7890	1321.7741	8	0.144E+05	1.0
894	2R(1, 1,E)	2 1 1 F	1321.8905	1321.8919	0	0.107E+05	1.0
918	2R(2, 0,A1)	3 0 0 A2	1328.9691	1328.9555	7	0.202E+05	1.0
919	2R(2, 1,E)	3 1 1 E	1329.0740	1329.0716	2	0.178E+05	1.0
921	2R(2, 2,E)	3 2 2 E	1329.4305	1329.4257	9	0.109E+05	1.0
946	2R(3, 0,A2)	4 0 0 A1	1335.9591	1335.9434	8	0.241E+05	1.0
947	2R(3, 1,F)	4 1 1 E	1336.0644	1336.0640	0	0.238E+05	1.0
949	2R(3, 2,E)	4 2 2 F	1336.4160	1336.4095	6	0.176E+05	1.0
951	2R(3, 3,A2)	4 3 3 A1	1336.8994	1336.8868	6	0.994E+04	1.0
911	2R(3, 3,A1)	4 3 3 A2	1336.8994	1336.8868	6	0.994E+04	1.0
975	2R(4, 0,A1)	5 0 0 A2	1342.7661	1342.7649	0	0.260E+05	1.0
976	2R(4, 1,E)	5 1 1 E	1342.8796	1342.8778	-4	0.248E+05	1.0
978	2R(4, 2,E)	5 2 2 E	1343.2119	1343.2171	-9	0.213E+05	1.0
979	2R(4, 3,A1)	5 3 3 A2	1343.7819	1343.7859	-9	0.157E+05	1.0
979	2R(4, 3,A2)	5 3 3 A1	1343.7819	1343.7894	-9	0.157E+05	1.0
983	2R(4, 4,E)	5 4 4 E	1344.5969	1344.5869	7	0.844E+04	1.0
1000	2R(5, 0,A2)	6 0 0 A1	1349.9969	1349.6047	-11	0.260E+05	1.0
1001	2R(5, 1,E)	6 1 1 E	1349.9020	1349.9177	-19	0.251E+05	1.0

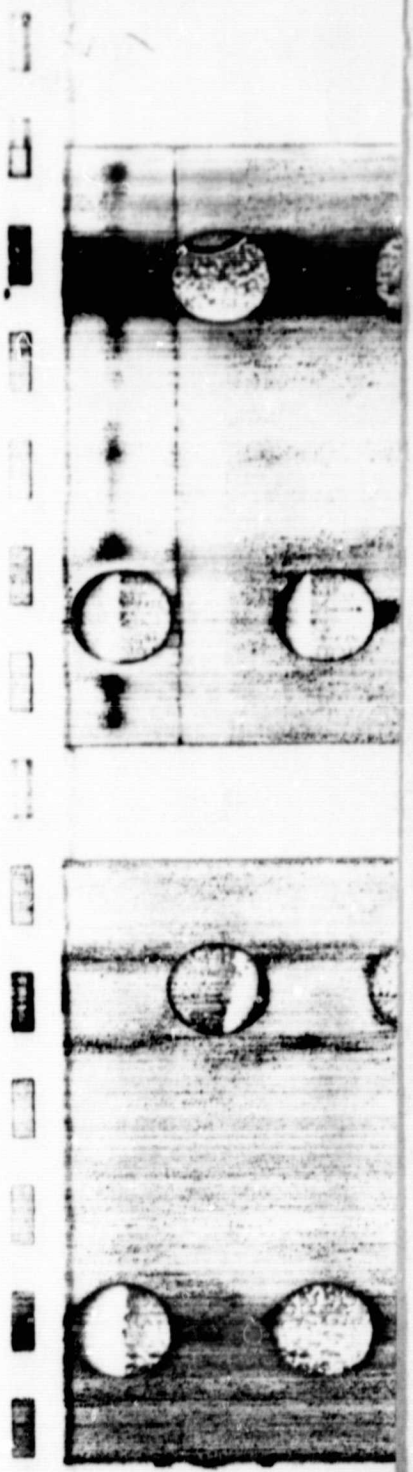

TABLE I—*Continued*

(I)	(II)	(III)	(IV)	(V)	(VI)	(VII)	(VIII)
1002	QR(5, 2,E)	6 2 2 E	1949.8421	1949.8513	-9	0.225E+05	1.0
1003	QR(5, 3,A2)	6 3 3 A1	1950.3876	1950.4095	-21	0.194E+05	1.0
1003	QR(5, 3,A1)	6 3 3 A2	1950.3876	1950.4097	-22	0.194E+05	1.0
1007	QR(5, 4,E)	6 4 4 E	1951.1921	1951.1964	-4	0.190E+05	1.0
1012	QR(5, 5,E)	6 5 5 F	1952.2212	1952.2180	3	0.674E+04	1.0
1026	QR(6, 0,A1)	7 0 0 A2	1955.8864	1955.8863	1	0.243E+05	1.0
1027	QR(6, 1,E)	7 1 1 E	1955.9870	1955.9937	-6	0.236E+05	1.0
1028	QR(6, 2,E)	7 2 2 E	1956.3208	1956.3214	0	0.217E+05	1.0
1032	QR(6, 3,A1)	7 3 3 A2	1956.8564	1956.8692	-12	0.187E+05	1.0
1032	QR(6, 3,A2)	7 3 3 A1	1956.8564	1956.8695	-13	0.187E+05	1.0
1034	QR(6, 4,E)	7 4 4 F	1957.6307	1957.6406	-9	0.147E+05	1.0
1039	QR(6, 5,E)	7 5 5 F	1958.6395	1958.6403	-6	0.101E+05	1.0
1045	QR(6, 6,A)	7 6 6 A	1959.8701	1959.8773	-7	0.102E+05	*1.0
1054	QR(7, 0,A2)	8 0 0 A1	1962.2049	1962.2093	-4	0.214E+05	1.0
1055	QR(7, 1,E)	8 1 1 F	1962.3025	1962.3163	-13	0.209E+05	1.0
1046	QR(7, 2,E)	8 2 2 E	1962.6080	1962.6379	-29	0.195E+05	0.0
1058	QR(7, 3,A2)	8 3 3 A1	1963.1878	1963.1750	12	0.173E+05	1.0
1058	QR(7, 3,A1)	8 3 3 A2	1963.1878	1963.1756	12	0.173E+05	0.0
1062	QR(7, 4,E)	8 4 4 F	1963.9271	1963.9310	-3	0.144E+05	1.0
1067	QR(7, 5,E)	8 5 5 E	1964.9040	1964.9090	-4	0.110E+05	1.0
1073	QR(7, 6,A)	8 6 6 A	1966.1061	1966.1154	-9	0.148E+05	*1.0
1075	QR(7, 7,E)	8 7 7 E	1967.5674	1967.5616	5	0.363E+04	1.0
1077	QR(8, 0,A1)	9 0 0 A2	1968.3960	1968.3915	5	0.179E+05	1.0
1078	QR(8, 1,E)	9 1 1 E	1968.5051	1968.4966	8	0.175E+05	1.0
1080	QR(8, 2,E)	9 2 2 F	1968.8034	1968.8122	-8	0.145E+05	1.0
1083	QR(8, 3,A1)	9 3 3 A2	1969.3358	1969.3388	-3	0.150E+05	1.0
1083	QR(8, 3,A2)	9 3 3 A1	1969.3358	1969.3400	-4	0.150E+05	1.0
1087	QR(8, 4,E)	9 4 4 F	1970.0711	1970.0801	-9	0.129E+05	1.0
1092	QR(8, 5,E)	9 5 5 F	1971.0278	1971.0372	-9	0.105E+05	1.0
1098	QR(8, 6,A)	9 6 6 A	1972.2223	1972.2151	7	0.156E+05	*1.0
1099	QR(8, 7,E)	9 7 7 E	1973.6214	1973.6209	10	0.511E+04	1.0
1102	QR(9, 0,A2)	10 0 0 A1	1974.4501	1974.4434	6	0.142E+05	1.0
1103	QR(9, 1,E)	10 1 1 E	1974.5460	1974.5467	0	0.139E+05	1.0
1105	QR(9, 2,E)	10 2 2 E	1974.8679	1974.8566	11	0.133E+05	1.0
1107	QR(8, 8,E)	9 8 8 E	1975.2606	1975.2683	-7	0.246E+04	1.0
1108	QR(9, 3,A2)	10 3 3 A1	1975.3711	1975.3732	-2	0.121E+05	1.0
1108	QR(9, 3,A1)	10 3 3 A2	1975.3711	1975.3752	-4	0.121E+05	1.0
1110	QR(9, 4,E)	10 4 4 F	1976.1021	1976.1010	1	0.107E+05	1.0
1114	QR(9, 5,E)	10 5 5 F	1977.0329	1977.0391	-6	0.900E+04	1.0
1118	QR(9, 6,A)	10 6 6 A	1978.1756	1978.1915	-15	0.143E+05	*1.0
1122	QR(9, 7,E)	10 7 7 E	1979.5650	1979.5626	2	0.522E+04	1.0
1126	QR(10, 0,A1)	11 0 0 A2	1980.3909	1980.3775	13	0.107E+05	1.0
1127	QR(10, 1,E)	11 1 1 F	1980.4863	1980.4700	7	0.106E+05	1.0
1129	QR(10, 2,E)	11 2 2 E	1980.7962	1980.7838	10	0.101E+05	1.0
1131	QR(9, 8,E)	10 8 8 E	1981.1403	1981.1588	-9	0.334E+04	1.0
1132	QR(10, 3,A1)	11 3 3 A2	1981.2967	1981.2911	5	0.935E+04	1.0
1132	QR(10, 3,A2)	11 3 3 A1	1981.2967	1981.2943	2	0.935E+04	1.0
1134	QR(10, 4,E)	11 4 4 F	1982.0293	1982.0070	16	0.836E+04	1.0
1136	QR(9, 9,A)	10 9 9 A	1982.9629	1982.9943	-31	0.317E+04	0.0
1136	QR(10, 5,E)	11 5 5 F	1982.9629	1982.9286	34	0.720E+04	1.0
1140	QR(10, 6,A)	11 6 6 A	1984.0487	1984.0601	-11	0.118E+05	*1.0
1146	QR(10, 7,E)	11 7 7 F	1985.3866	1985.4042	-17	0.440E+04	1.0
1149	QR(11, 0,A2)	12 0 0 A1	1986.2256	1986.2067	18	0.776E+04	1.0
1150	QR(11, 1,E)	12 1 1 E	1986.3259	1986.3066	19	0.765E+04	1.0
1152	QR(11, 2,E)	12 2 2 E	1986.5920	1986.6068	-14	0.734E+04	1.0
1154	QR(10, 8,E)	11 8 8 F	1986.9508	1986.9642	-13	0.329E+04	1.0
1155	QR(11, 3,A2)	12 3 3 A1	1987.1179	1987.1056	12	0.684E+04	1.0
1155	QR(11, 3,A1)	12 3 3 A2	1987.1179	1987.1103	7	0.684E+04	1.0
1158	QR(11, 4,E)	12 4 4 E	1987.8121	1987.8117	0	0.619E+04	1.0
1161	QR(11, 5,E)	12 5 5 F	1988.7247	1988.7201	4	0.541E+04	1.0

C2

TABLE I—*Continued*

(I)	(II)	(III)				(IV)	(V)	(VI)	(VII)	(VIII)
1161	OR(10, 9,A)	11	9	9	A	1388.7247	1388.7429	-18	0.413E+04	1.0
1166	OR(11, 6,A)	12	6	6	A	1389.8852	1389.8358	49	0.912E+04	0.0
1168	OR(10,10,E)	11	10	10	E	1390.7500	1390.7367	13	0.967E+03	1.0
1170	OR(11, 7,E)	12	7	7	E	1391.1547	1391.1624	-7	0.367E+04	1.0
1173	OR(12, 0,A1)	13	0	0	A2	1391.9574	1391.9441	13	0.536E+04	1.0
1174	OR(12, 1,E)	13	1	1	E	1392.0592	1392.0426	10	0.529E+04	1.0
1175	OR(12, 2,E)	13	2	2	E	1392.3553	1392.3387	16	0.510E+04	1.0
1176	OR(11, 8,E)	12	8	8	E	1392.6906	1392.7043	-13	0.279E+04	1.0
1177	OR(12, 3,A1)	13	3	3	A2	1392.8453	1392.8301	15	0.478E+04	1.0
1177	OR(12, 3,A2)	13	3	3	A1	1392.8453	1392.8368	8	0.478E+04	1.0
1181	OR(12, 4,E)	13	4	4	E	1393.5445	1393.5285	15	0.435E+04	1.0
1183	OR(11, 9,A)	12	9	9	A	1394.4789	1394.4684	10	0.390E+04	1.0
1183	OR(12, 5,E)	13	5	5	E	1394.4789	1394.4270	51	0.385E+04	0.0
1187	OR(12, 6,A)	13	6	6	A	1395.5291	1395.5339	-5	0.660E+04	*1.0
1189	OR(11,10,E)	12	10	10	E	1396.5253	1396.4751	50	0.117E+04	0.0
1195	OR(12, 7,E)	13	7	7	E	1396.8570	1396.8522	4	0.272E+04	1.0
1198	OR(13, 0,A2)	14	0	0	A1	1397.5992	1397.6091	-9	0.358E+04	1.0
1199	OR(13, 1,E)	14	1	1	E	1397.7299	1397.7004	22	0.351E+04	0.0
1201	OR(13, 2,E)	14	2	2	E	1397.9883	1397.9931	-4	0.338E+04	1.0
1202	OR(12, 9,E)	13	9	9	E	1398.3840	1398.3961	-12	0.213E+04	1.0
1203	OR(13, 3,A2)	14	3	3	A1	1398.4775	1398.4779	0	0.318E+04	1.0
1203	OR(13, 3,A1)	14	3	3	A2	1398.4775	1398.4868	-9	0.318E+04	1.0
1203	OR(11,11,E)	12	11	11	E	1398.4775	1398.4926	-15	0.561E+03	1.0
	OR(13, 4,E)	14	4	4	E		1399.1708		0.292E+04	0.0
1206	OR(13, 5,E)	14	5	5	E	1400.0892	1400.0627	20	0.261E+04	1.0
1207	OR(12, 9,A)	13	9	9	A	1400.1623	1400.1919	-29	0.314E+04	1.0
1210	OR(13, 6,A)	14	6	6	A	1401.1829	1401.1644	18	0.4[illegible]E+04	*1.0
1214	OR(12,10,E)	13	10	10	E	1402.3239	1402.3792	-55	0.100E+04	0.0
1215	OR(13, 7,E)	14	7	7	E	1402.5100	1402.4868	23	0.189E+04	1.0
1219	OR(14, 0,A1)	15	0	0	A2	1403.1619	1403.1975	-35	0.225E+04	1.0
1219	OR(12,11,E)	13	11	11	E	1403.1619	1403.1418	20	0.625E+03	1.0
1220	OR(14, 1,E)	15	1	1	E	1403.2580	1403.2938	-35	0.223E+04	1.0
1222	OR(14, 2,E)	15	2	2	E	1403.5545	1403.5834	-28	0.215E+04	1.0
1224	OR(14, 3,A1)	15	3	3	A2	1404.0544	1404.0626	-8	0.203E+04	1.0
1224	OR(14, 3,A2)	15	3	3	A1	1404.0544	1404.0737	-19	0.203E+04	1.0
1224	OR(13, 8,E)	14	8	8	E	1404.0544	1404.0524	2	0.151E+04	1.0
	OR(14, 4,E)	15	4	4	E		1404.7514		0.187E+04	0.0
1226	OR(14, 5,E)	15	5	5	E	1405.6479	1405.6396	8	0.168E+04	1.0
1227	OR(13, 9,A)	14	9	9	A	1405.8946	1405.9244	-29	0.228E+04	1.0
1229	OR(12,12,A)	13	12	12	A	1406.2498	1406.2589	-9	0.618E+03	1.0
1230	OR(14, 6,A)	15	6	6	A	1406.7701	1406.7420	28	0.294E+04	*1.0
1232	OR(13,11,E)	14	11	11	E	1407.5922	1407.5051	87	0.521E+03	0.0
1235	OR(14, 7,E)	15	7	7	E	1408.1144	1408.0766	37	0.124E+04	1.0
1236	OR(13,10,E)	14	10	10	E	1408.3797	1408.4147	-35	0.724E+03	1.0
1238	OR(15, 0,A2)	16	0	0	A1	1408.7720	1408.7417	30	0.137E+04	1.0
1238	OR(15, 1,E)	16	1	1	E	1408.7721	1408.8370	-65	0.136E+04	0.0
1239	OR(15, 2,E)	16	2	2	E	1409.0475	1409.1237	-76	0.131E+04	0.0
1241	OR(15, 3,A2)	16	3	3	A1	1409.5328	1409.5978	-65	0.124E+04	0.0
1241	OR(15, 3,A1)	16	3	3	A2	1409.5328	1409.6110	-78	0.124E+04	0.0
1242	OR(14, 9,E)	15	8	8	E	1409.7259	1409.6817	44	0.101E+04	0.0
1245	OR(15, 4,E)	16	4	4	E	1410.2175	1410.2839	-65	0.115E+04	0.0
1248	OR(15, 5,E)	16	5	5	E	1411.1606	1411.1697	-9	0.104E+04	1.0
1248	OR(13,12,A)	14	12	12	A	1411.1606	1411.1545	6	0.736E+03	1.0
1251	OR(14, 9,A)	15	9	9	A	1411.6885	1411.6665	21	0.139E+04	1.0
1251	OR(14,11,E)	15	11	11	E	1411.7527	1411.7329	19	0.985E+03	1.0
1254	OR(15, 6,A)	16	6	6	A	1412.3049	1412.2767	28	0.182E+04	*1.0
1259	OR(15, 7,E)	16	7	7	E	1413.6711	1413.6304	40	0.775E+03	1.0
1261	OR(16, 0,A1)	17	0	0	A2	1414.1771	1414.2513	-74	0.801E+03	0.0
1262	OR(16, 1,E)	17	1	1	E	1414.3022	1414.3495	-49	0.795E+03	1.0
1263	OR(14,10,E)	15	10	10	E	1414.4855	1414.5152	-29	0.475E+03	1.0

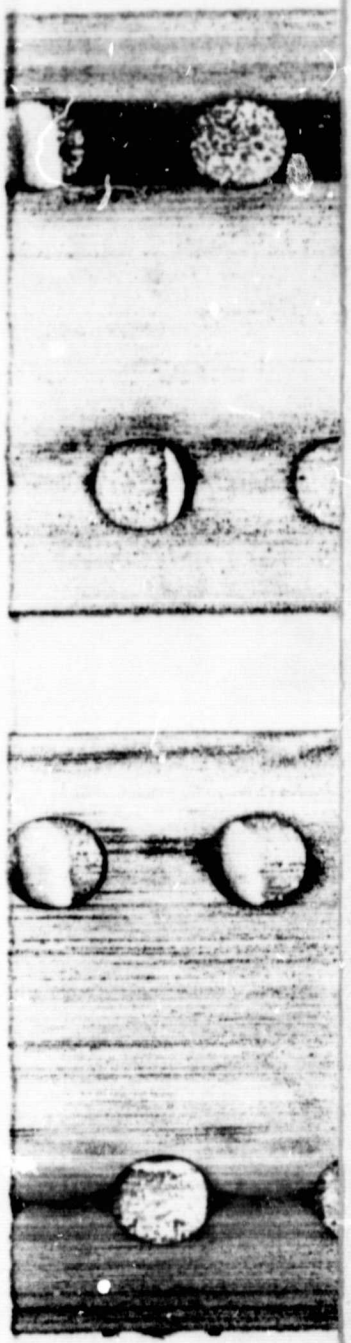

TABLE I—*Continued*

(I)	(II)	(III)	(IV)	(V)	(VI)	(VII)	(VIII)
	QR(16, 2,E)	17 2 2 E		1414.6791		0.768E+03	0.0
	QR(16, 3,A1)	17 3 3 A2		1415.0983		0.728E+03	0.0
	QR(16, 3,A2)	17 3 3 A1		1415.1129		0.728E+03	0.0
1266	QR(15, 8,E)	16 8 8 E	1415.3525	1415.2882	64	0.639E+03	0.0
1267	QR(14,12,A)	15 12 12 A	1415.7685	1415.7894	-20	0.630E+03	1.0
1267	QR(16, 4,E)	17 4 4 E	1415.7685	1415.7800	-11	0.675E+03	1.0
	QR(15,11,E)	16 11 11 E		1415.8919		0.261E+03	0.0
1272	QR(16, 5,E)	17 5 5 E	1416.6427	1416.6652	-22	0.612E+03	1.0
	QR(15, 9,A)	16 9 9 A		1417.4099		0.961E+03	0.0
1275	QR(16, 6,A)	17 6 6 A	1417.8119	1417.7782	33	0.108E+04	0.0
	QR(16, 7,E)	17 7 7 E		1419.1547		0.461E+03	0.0
1281	QR(15,12,A)	16 12 12 A	1420.2789	1420.2295	49	0.461E+03	0.0
1283	QR(15,10,E)	16 10 10 E	1420.6842	1420.6171	67	0.293E+03	0.0
	QR(16, 8,E)	17 8 8 E		1420.8723		0.378E+03	0.0
1293	QR(16, 9,A)	17 9 9 A	1423.1916	1423.1406	51	0.573E+03	0.0
1297	QR(16,12,A)	17 12 12 A	1424.5292	1424.5432	-13	0.305E+03	1.0
1305	QR(16,10,E)	17 10 10 E	1426.6585	1426.6719	-13	0.172E+03	1.0
ν_6 TRANSITIONS NEWLY ASSIGNED							
35	PP(16, 9,A)	15 8 9 A	1055.6194	1055.6275	-9	0.511E+03	1.0
63	PP(16,12,A)	15 11 12 A	1067.5848	1067.6641	-79	0.422E+03	0.0
67	PP(15,10,E)	14 9 10 E	1068.8419	1068.8537	-11	0.458E+03	1.0
77	PP(15,11,E)	14 10 11 E	1073.0915	1073.0654	-33	0.434E+03	1.0
86	PP(15,12,A)	14 11 12 A	1077.3242	1077.3384	-14	0.799E+03	1.0
93	PP(15,13,E)	14 12 13 E	1081.3394	1081.3713	-31	0.323E+03	1.0
94	PP(14,11,E)	13 10 11 E	1082.3541	1082.4020	-47	0.772E+03	1.0
103	PP(14,12,A)	13 11 12 A	1086.8476	1086.8741	-25	0.144E+04	1.0
113	PP(14,13,E)	13 12 13 E	1091.3393	1091.3372	2	0.617E+03	1.0
126	PP(14,14,E)	13 13 14 E	1097.5688	1097.6238	-55	0.532E+03	0.0
352	PQ(16, 8,E)	16 7 8 E	1173.3725	1173.4016	-29	0.294E+03	0.0
383	PQ(15,10,E)	15 9 10 E	1182.4813	1182.5157	-34	0.289E+03	1.0
418	PQ(14,12,A)	14 11 12 A	1192.4664	1192.5126	-46	0.373E+03	0.0

RESULTS AND DISCUSSION

All experimental data assigned to the ν_3 band of $^{12}CH_3D$ are listed in Table I, column IV. ν_6 transitions involving upper levels near the crossing, which could not be identified from the separated analysis of the ν_6 band are now reported at the end of Table I. Serial numbers of column I refer to the numbering of the lines in Fig. 1 of the present paper and in Fig. 1 of Ref. (*1*). Assignments and specifications of the upper state levels of the transitions are reported in columns II and III of the table.

In all, 342 transitions belonging to ν_3 are retained to be fitted besides 641 ν_6 transitions previously assigned in Ref. (*1*), or newly assigned in the present paper. Statistical weights equal to 1.0 are attributed to all data. For transitions going up to levels with $|K - l_6| = 0$ or 3 for $v_6 = 1$, and with $|K| = 3$ for $v_6 = 1$, A_1A_2 splittings are theoretically predicted, which correspond to observable effects; then, weights equal to 1.0 are assigned to each component $A_1 \rightarrow A_2$ and $A_2 \rightarrow A_1$. For transitions going up to levels with $|K - l_6| = 6, 9$ ($l_6 = 0$ for $v_3 = 1$), no splitting is expected and the overall weights are equally distributed for the two components transitions with asterisk in column VIII of Table I.

The fitting of the data leads to 21 significant constants. Six of these constants are related to $v_3 = 1$, 12 are related to $v_6 = 1$, and 3 are interaction constants between the two states; these last, i.e., $C_{21}^{(2)}$, $C_{21}^{(3)}$, and $C_{21}^{(4a)}$ result from the second-order Coriolis interaction defined by Eq. (4). All constants involved in the first-order

TABLE II

Spectroscopic Constants for Vibrational States $v_3 = 1$ and $v_6 = 1$ of $^{12}CH_3D$

CONSTANT	VALUE IN cm^{-1}	STANDARD DEVIATION IN cm^{-1}	99.5% CONFIDENCE INTERVAL IN cm^{-1}
$^*\nu_3$	1306.836	0.002	0.02
$^*B_v^3$	3.78294	0.00006	0.0004
$^*A_v^3$	5.27208	0.00007	0.0005
$^*D_J^3$	2.396 10^{-4}	0.008 10^{-4}	0.05 10^{-4}
$^*D_{JK}^3$	- 1.268 10^{-4}	0.006 10^{-4}	0.04 10^{-4}
$^*D_K^3$	- 8.33 10^{-6}	0.31 10^{-6}	2.0 10^{-6}
$^*\nu_6$	1161.096	0.002	0.011
$^*(A\zeta)_v^6$	3.1118	0.0002	0.0012
$^*B_v^6$	3.83481	0.00003	0.0002
$^*A_v^6$	5.26735	0.00006	0.0004
$^*D_J^6$	4.490 10^{-5}	0.014 10^{-5}	0.09 10^{-5}
$^*D_{JK}^6$	1.636 10^{-4}	0.004 10^{-4}	0.03 10^{-4}
$^*D_K^6$	- 8.95 10^{-5}	0.04 10^{-5}	0.25 10^{-5}
$^*\eta_J^6$	1.424 10^{-3}	0.011 10^{-3}	0.07 10^{-3}
$^*\eta_K^6$	- 4.94 10^{-4}	0.11 10^{-4}	0.72 10^{-4}
$^*q_{22}^6$	- 1.742 10^{-2}	0.002 10^{-2}	0.011 10^{-2}
$^*f_{22}^{6,J}$	4.03 10^{-6}	0.08 10^{-6}	0.49 10^{-6}
$^*q_{12}^6$	ϵ 1.84 10^{-2}	0.03 10^{-2}	0.17 10^{-2}
$C_{21}^{(2)}$	ϵ' 2.42 10^{-2}	0.02 10^{-2}	0.15 10^{-2}
$C_{21}^{(3)}$	ϵ' 6.18 10^{-4}	0.09 10^{-4}	0.60 10^{-4}
$C_{21}^{(4a)}$	$-\epsilon'$ 3.93 10^{-5}	0.08 10^{-5}	0.53 10^{-5}
Constants fixed to their ground state values (7)			
$H^J = H_0^J$	1.172 10^{-9}	$\epsilon = \pm 1$	
$H^{JJK} = H_0^{JJK}$	1.200 10^{-8}	$\epsilon' = \pm 1$	
$H^{JKK} = H_0^{JKK}$	- 1.042 10^{-8}		

Coriolis term, given by Eq. (2), are insignificant, verifying that no direct estimate of the Coriolis constant ζ_{36} can be obtained from available data.

The constants deduced from the fitting are reported in Table II, with their standard deviations and 99.5% confidence intervals. The fourth-order distortion constants H^J, H^{JJK}, and H^{JKK}, constrained in $v_3 = 1$ and $v_6 = 1$ to the ground state values determined elsewhere (*7*), are recalled at the bottom of the table. The 18 constants related to $v_3 = 1$ and $v_6 = 1$ are written using the usual notations, except the asterisks point out that they do not involve exactly the same contributions as in the individual analyses of the bands.

The constants of Table II reproduce the 983 fitted data points with an overall standard deviation equal to 0.016 cm^{-1}. Calculated wavenumbers and deviations (obs − calc) are listed in columns V and VII of Table I for ν_3 and the newly assigned ν_6 transitions. For all other ν_6 transitions, these quantities do not differ significantly from those given in Table I of Ref. (*1*) and are not repeated here. Table I includes also predicted wavenumbers for unobserved ν_3 transitions with calculated relative intensities $\geq 0.200 \times 10^3$ in our arbitrary scale. This value corresponds to a limit for observation in the most favorable parts of our spectra. The transitions, for which no A_1A_2 splitting is expected, are reported in Table I with overall notation $A \rightarrow A$. The relative intensities of transitions are calculated according to Eq. (5). Unfortunately, no experimental measurements of line intensities are now available for getting an accurate value of the coefficient $\rho_{3,6}$ involved in Eq. (3). A theoretical estimate of this coefficient can be deduced from band strengths of ν_3 and ν_4 of $^{12}CH_4$ (*8*). Assuming that the variation of dipole moment with vibration is not significantly affected by the substitution of H by D, two values are expected for $\rho_{3,6}$, i.e.,

$$\rho_{3,6} = 1.11 \quad \text{and} \quad \rho_{3,6} = 1.16$$

according as the derivatives $\partial M_\alpha/\partial Q_{3\alpha}$ and $\partial M_\alpha/\partial Q_{4\alpha}$ ($\alpha = x, y, z$) of dipole moment in methane have same or opposite signs. In fact, the value which seems to give the best qualitative agreement with observed intensities is $\rho_{3,6} = 1.19$ which is consistent with previous results on opposite signs of the two quantities $\partial M_\alpha/\partial Q_{3\alpha}$ and $\partial M_\alpha/\partial Q_{4\alpha}$ (*9*,*10*). Relative intensities of the ν_3 transitions, calculated for $\rho = 1.19$, are listed in column VII of Table I. Values for ν_6 transitions are not significantly different from those tabulated in Table I of Ref. (*1*).

Finally, it may be noted that:

—$^*f^6_{12}$, $^*f^6_{42}$, and $^*H^A$ are found to be not significant, pointing out that the corresponding constants f^6_{12}, f^6_{42}, and H^A, in the individual analysis of ν_6, contribute essentially in relation with the Coriolis interaction between $v_6 = 1$ and $v_3 = 1$.

—The distortion constants related to $v_3 = 1$, i.e., $^*D^3_J$, $^*D^3_{JK}$, and $^*D^3_K$, show large deviations from their ground state values. The magnitude and the sign of these deviations are consistent with the expected effect of the Coriolis interaction between $v_3 = 1$ and $v_5 = 1$ when the predicted value of ζ_{35}, i.e., 0.57 is used. Unfortunately, the data now available on the ν_5 band do not allow us to have more information on this interaction.

—The present analysis predicts for ν_3 transitions belonging to the subband $|K| = 3$, A_1A_2 splittings up to 0.015 cm^{-1} for $J' = 17$. Experimentally, such splittings are observed as broadenings of the lines, but are not resolved.

ACKNOWLEDGMENTS

We would like to convey our thanks to M. Dang-Nhu and G. Poussigue for helpful discussions. One of us (K.N.R.) is also grateful to the National Aeronautics and Space Administration for support of some of this research.

RECEIVED: August 12, 1978

REFERENCES

1. L. W. PINKLEY, K. NARAHARI RAO, G. TARRAGO, G. POUSSIGUE, AND M. DANG-NHU, *J. Mol. Spectrosc.* **68,** 195–222 (1977).
2. L. W. PINKLEY, Ph.D. dissertation, The Ohio State University, 1974.
3. F. A. ANDERSON, *Mat. Fys. Madd. Dan. Vid. Selsk.* **33,** no. 12, 1 (1963).
4. A. G. MORITZ, *Spectrochim. Acta* **22,** 385–388 (1966).
5. S. MAES, *J. Phys.* **27,** 37–42 (1966).
6. G. TARRAGO, *Cah. Phys.* **19,** 149–217 (1965).
7. G. TARRAGO, G. POUSSIGUE, M. DANG-NHU, A. VALENTIN, AND P. CARDINET, *J. Mol. Spectrosc.* **60,** 429–432 (1976).
8. S. SAEKI, M. MIZUNO, AND S. KONDO, *Spectrochim. Acta A* **32,** 403–413 (1976).
9. K. FOX, *Phys. Rev. Lett.* **27,** 233–236 (1971).
10. I. M. MILLS, *Mol. Phys.* **1,** 107–122 (1958).

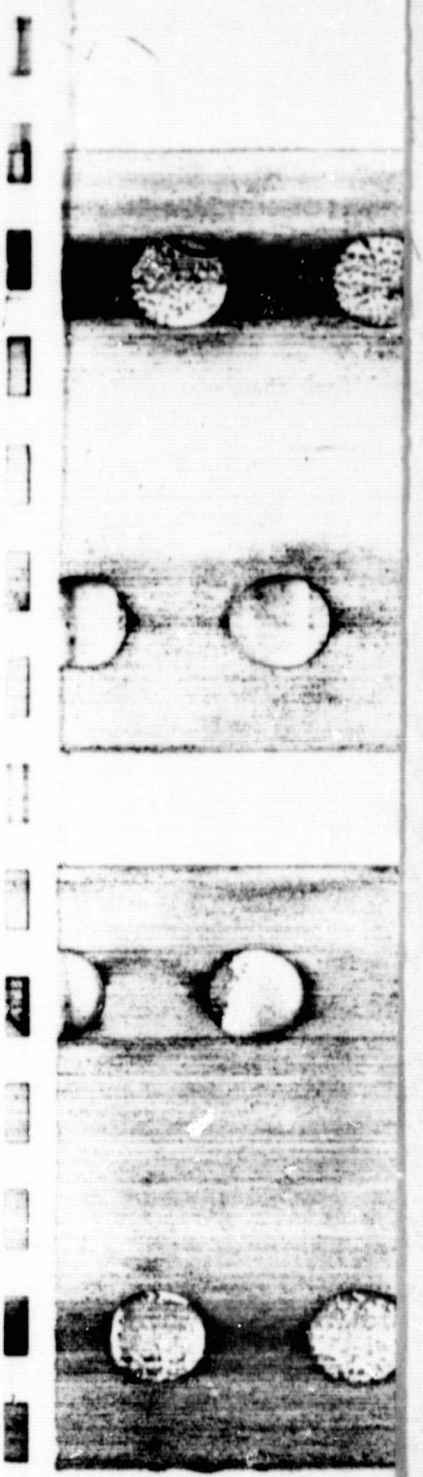

JOURNAL OF MOLECULAR SPECTROSCOPY 68, 195–222 (1977)

Analysis of the ν_6 Band of $^{12}CH_3D$ at 8.6 μm

LARY W. PINKLEY[1] AND K. NARAHARI RAO[2]

Department of Physics, The Ohio State University, Columbus, Ohio 43210

AND

G. TARRAGO, G. POUSSIGUE, AND M. DANG-NHU

Laboratoire de Spectroscopie Moléculaire I, Université Pierre et Marie Curie, Tour 13, 3ème étage, Place Jussieu, 75005 Paris, France

The $\nu_6(E)$ fundamental vibration–rotation band of monodeuteromethane ($^{12}CH_3D$) has been recorded in the spectral range 1033–1270 cm^{-1} with a resolution of approximately 0.04 cm^{-1}. Of the 669 transitions with $J' \leq 17$ identified, 633 have been retained for the determination of the rotational levels in the upper state $v_6 = 1$. The Coriolis interaction between the $v_6 = 1(E)$ and $v_3 = 1(A_1)$ vibrational states of $^{12}CH_3D$ results in large A_1A_2 splittings of levels with $v_6 = 1$ and $|K - l_6| = 0$ or 3; the mixing in K and l_6 also gives rise to some ten forbiuden transitions observed in the spectra. These effects have been very well explained within the formulation based on the contact transformation method. Values of 15 molecular structure constants of the $v_6 = 1$ state have been determined from a least-squares analysis of the 633 retained transitions. These constants can be used to estimate values of the upper-state energies up to fourth order, and through them the spectral positions of the 633 retained transitions are reproduced with an overall standard deviation of 0.013 cm^{-1}, which is within experimental uncertainties.

I. INTRODUCTION

The absorption spectrum of $^{12}CH_3D$ in the range 1033–1270 cm^{-1} is mainly due to transitions of the perpendicular-type $\nu_6(E)$ band, the lowest fundamental vibration–rotation band of $^{12}CH_3D$. This band, recently recorded (*1*) with a resolution of about 0.04 cm^{-1}, exhibits a very well resolved but rather complicated rotational structure. Indeed, because of large values of $A'-A_0$ and $B'-B_0$, very little extended J and K structure can be easily and reliably identified, except in the $^RQ_0$ subbranch. Moreover, the structure of the spectrum is further complicated by A_1A_2 splittings for $J' \geq 8$; the effects of notably large second-order corrections to the energies in the $v_6 = 1$ vibrational state are observed. The Coriolis interaction with the nearest band, the parallel-type $\nu_3(A_1)$ band centered near 1306.8 cm^{-1}, is clearly responsible for the observed features.

With the experimental data presently available, the analysis of the ν_6 band of $^{12}CH_3D$

[1] Present address: Lockheed Missiles & Space Co., Inc., P.O. Box 1103, Huntsville, Al. 35807.

[2] K.N.R. expresses gratefulness for the partial support extended to this research by the National Aeronautics and Space Administration and to the Atmospheric Research Section of the National Science Foundation.

ISSN 0022-2852

can be considered in two different ways: (a) In the first case, the Coriolis interactions are considered to be small and the analysis of the experimental data can utilize results from the usual contact transformation method (*2*). It is well known that such a formulation can satisfactorily explain giant A_1A_2 splittings as long as the numerical solution obtained from the analysis remains convergent; that is, as long as the values determined for the structure constants are consistent with their assumed order of magnitude in the expanded matrix energy. (b) In the second case, the Coriolis interactions are considered to be large and the ν_6 band can no longer be analyzed separately from other bands. Then, the treatment becomes more complex: The dimensions of the matrices to be diagonalized are greatly increased; but also, in the present case, the contributions due to the two kinds of vibration–rotation interaction terms, diagonal and nondiagonal in v_6, cannot be always separated unambiguously. This point will be discussed in the last part of this paper. Previously, Deroche *et al.* (*3*) reported results of the analysis of the ν_6 band of $^{12}CH_3D$ which explicitly included diagonal contributions up to the third order and nondiagonal contributions between the $v_6 = 1$ and $v_3 = 1$ vibrational states. Their study led to an effective value of the coupling constant ζ_{36}^{x} which is very small, i.e., $|\zeta_{36}^{x}| = 0.041$; this indicates that the magnitude of the Coriolis interaction between the $\nu_6 = 1$ and $\nu_3 = 1$ vibrational states is relatively weak. Unfortunately, their formulation failed to explain the A_1A_2 splittings observed in the P_3, Q_3, and R_3 subbranches for $J > 9$.

In the present work, we show that the available data of the ν_6 band of $^{12}CH_3D$ (including J values up to 17) can be interpreted within the formulation based on contact transformations. Many previously unidentified transitions of the ν_6 band are assigned to lines recorded in the range 1033–1270 cm^{-1}. Also, owing to the well-resolved spectra, it is now possible to determine values of molecular structure constants through fourth order.

II. EXPERIMENTAL DETAILS

The 3.5-m Littrow-type vacuum spectrograph, operating in the single pass configuration, used to record spectra of $^{12}CH_3D$ has been previously described by Mickelson (*4*). The data recorded from 1033 to 1270 cm^{-1} have been obtained in the sixth and seventh orders of the grating with an operating resolution of approximately 0.04 cm^{-1} over most of the range investigated.

All $^{12}CH_3D$ spectra have been recorded with the gas sample contained in a 1-m-long absorption cell at room temperature. The data have been recorded twice with a gas pressure of 18 Torr and twice with a gas pressure of 30 Torr. Most of the stronger absorption lines have been measured at least three times and some have been measured six times.

All data have been measured relative to the 1–0 band of CO and several water vapor lines using the single pen technique described by Rao *et al.* (*5*). These calibration standards are considered accurate to at least ± 0.002 cm^{-1} (*5*, *6*). All data have been calibrated relative to the accepted standards by the polynomial regression and stepwise multiple regression analysis computer programs described elsewhere (*1*). The calculated spectral positions of the stronger unblended lines vary no more than ± 0.0025 cm^{-1} from the corresponding mean values.

Figure 1 is a reproduction of the recorded spectrum; this region includes all identified

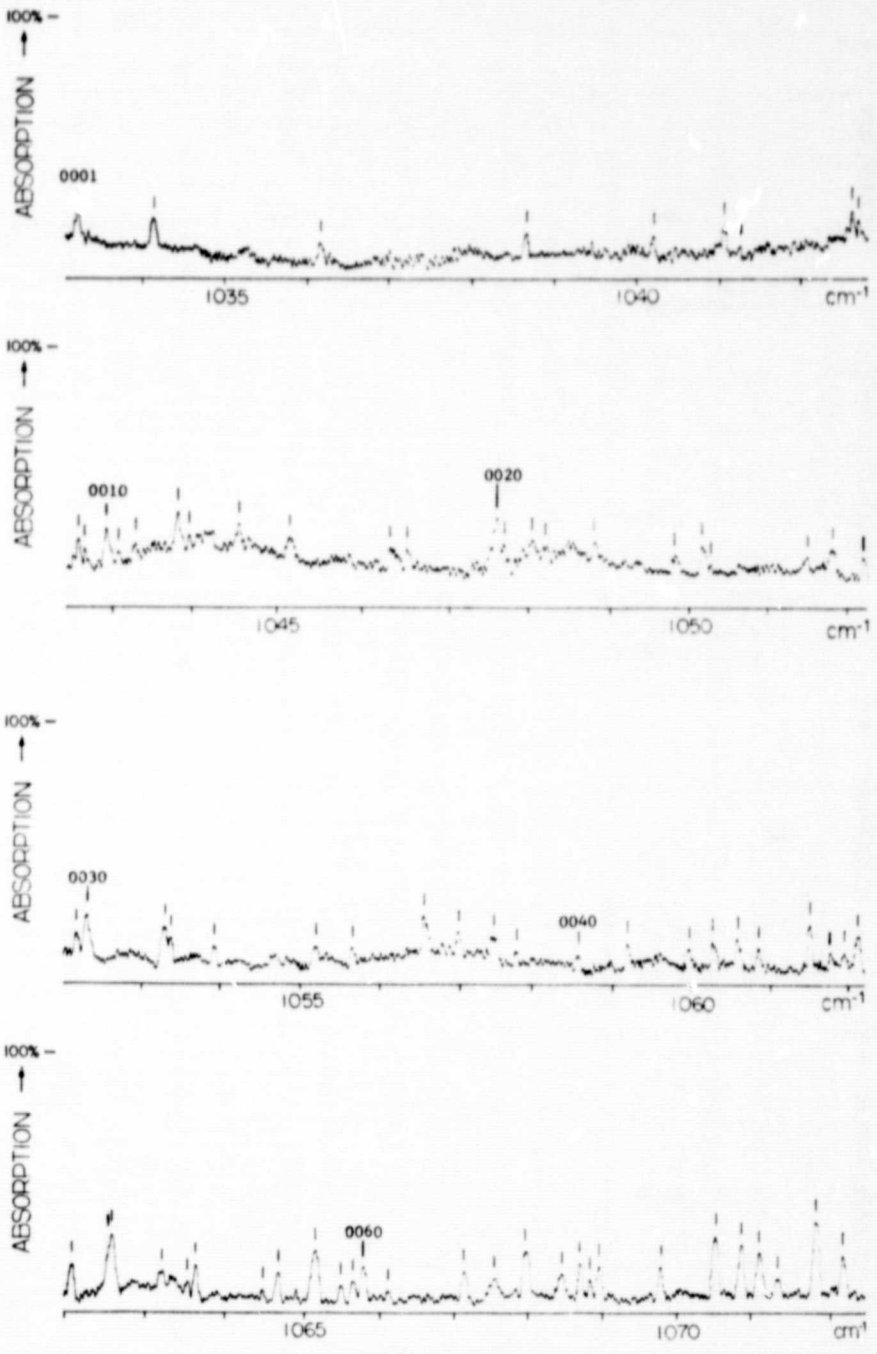

FIG. 1. The spectrum of $^{13}CH_3D$ from 1033 to 1270 cm^{-1}. The reproduced spectra were recorded with the gas sample contained within a 1-m-length absorption cell at a pressure of 30 Torr.

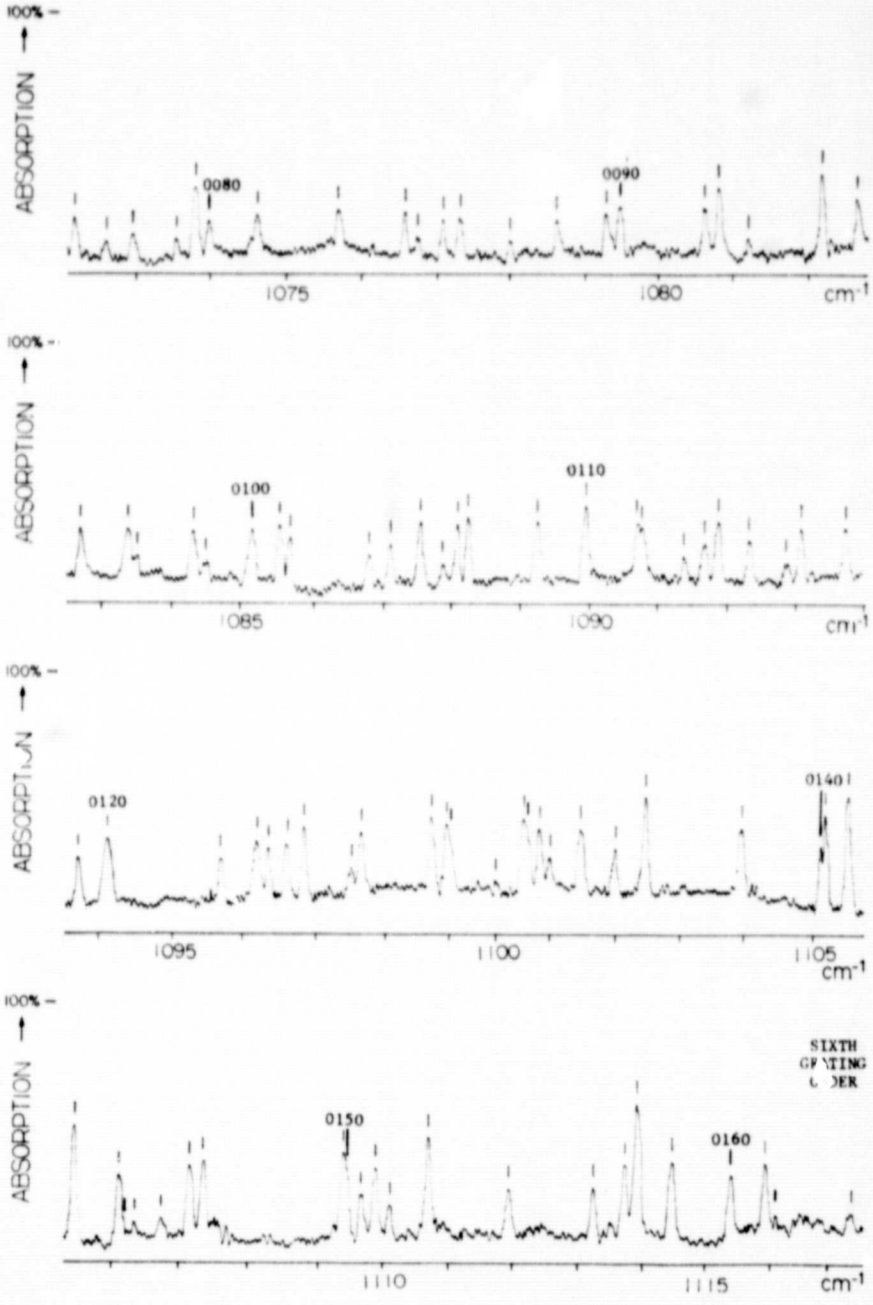

FIG. 1—*Continued*

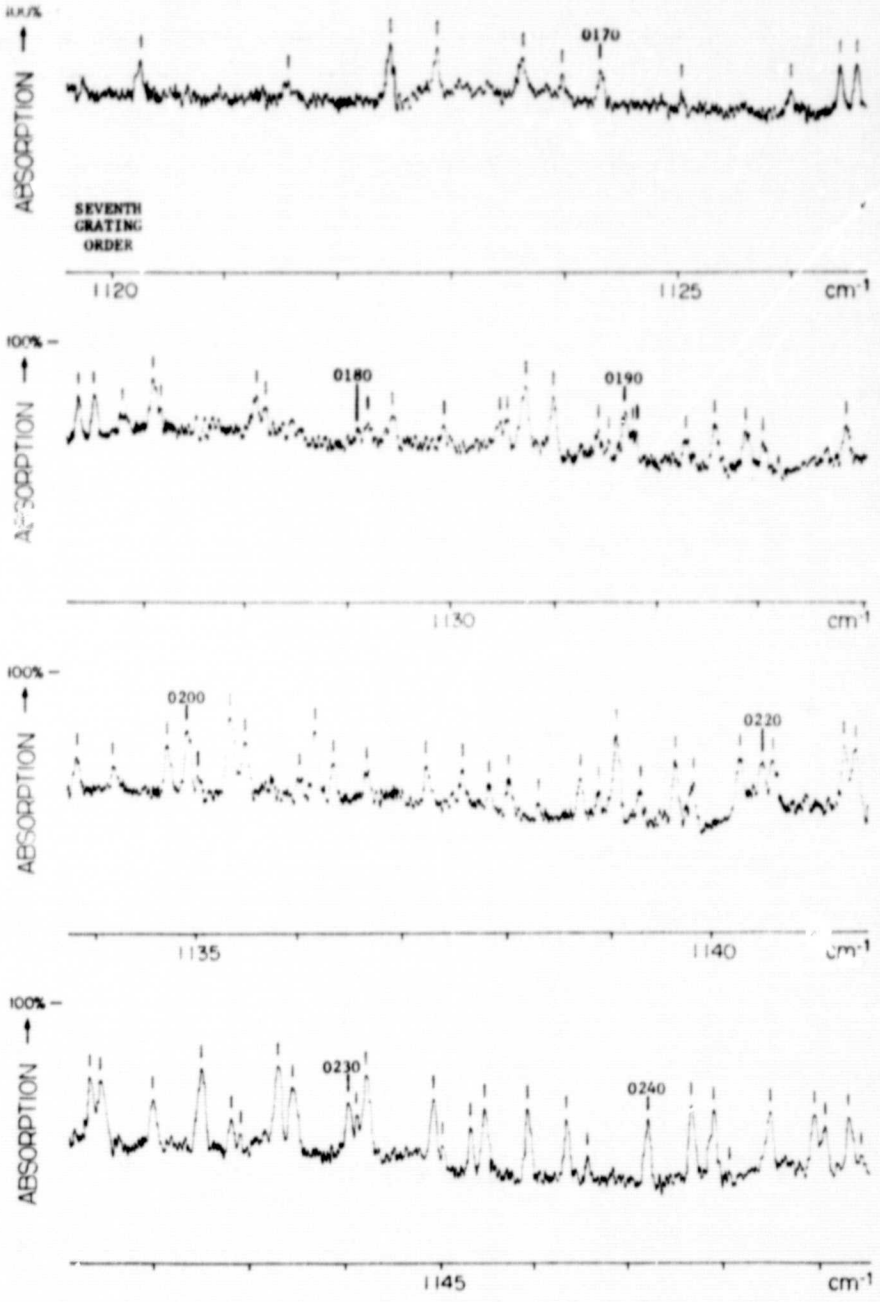

FIG. 1—*Continued*

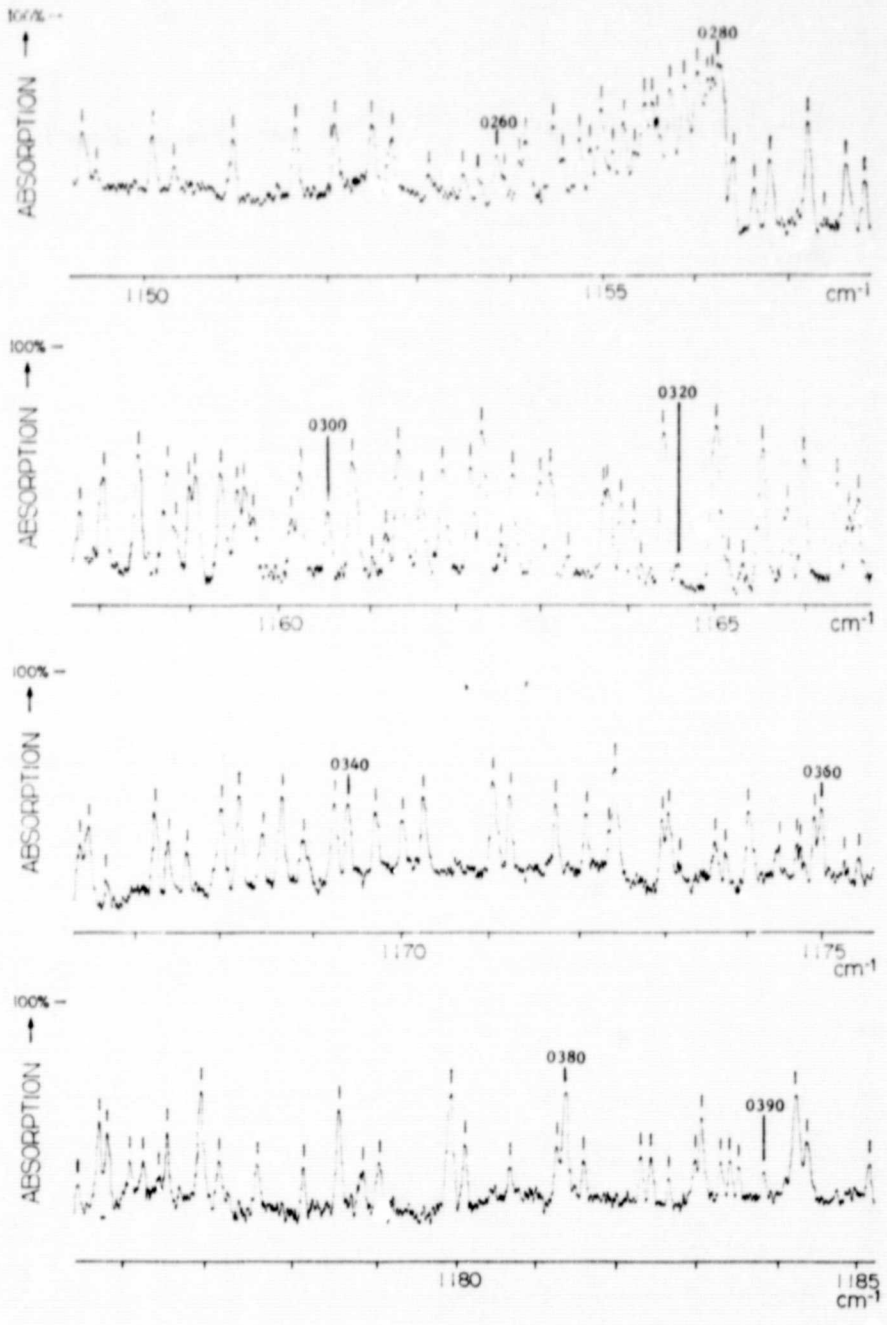

FIG. 1—*Continued*

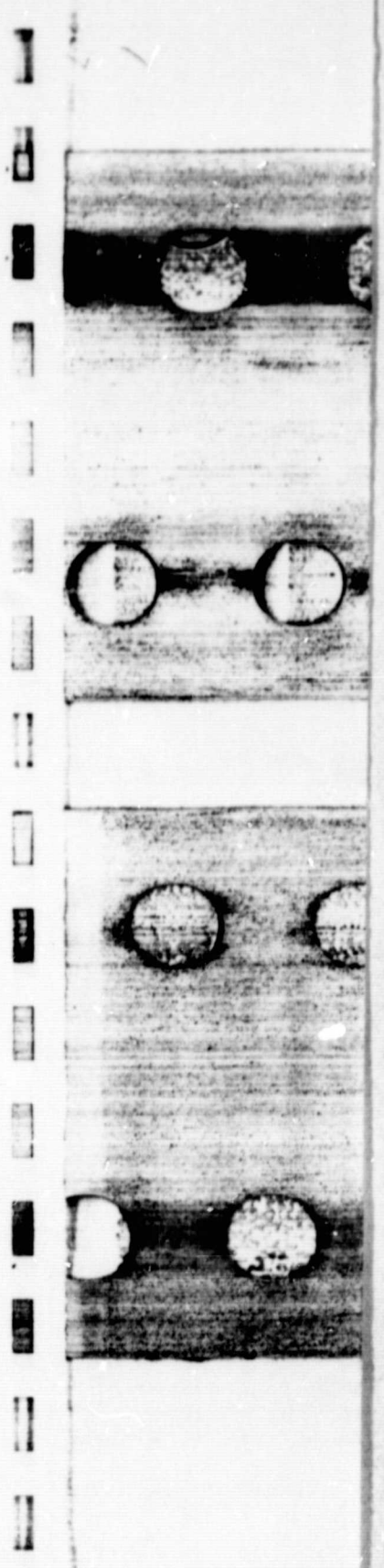

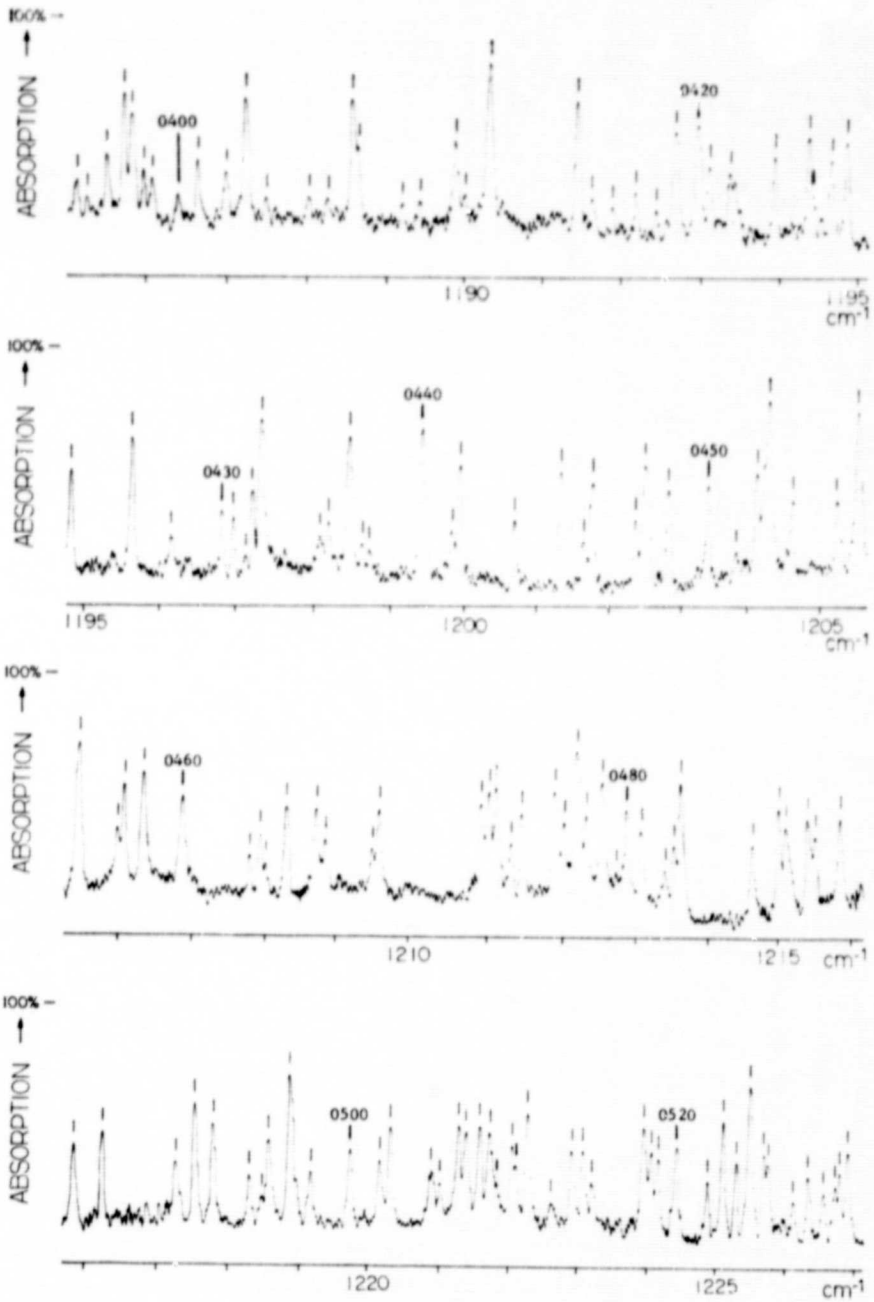

FIG. 1—*Continued*

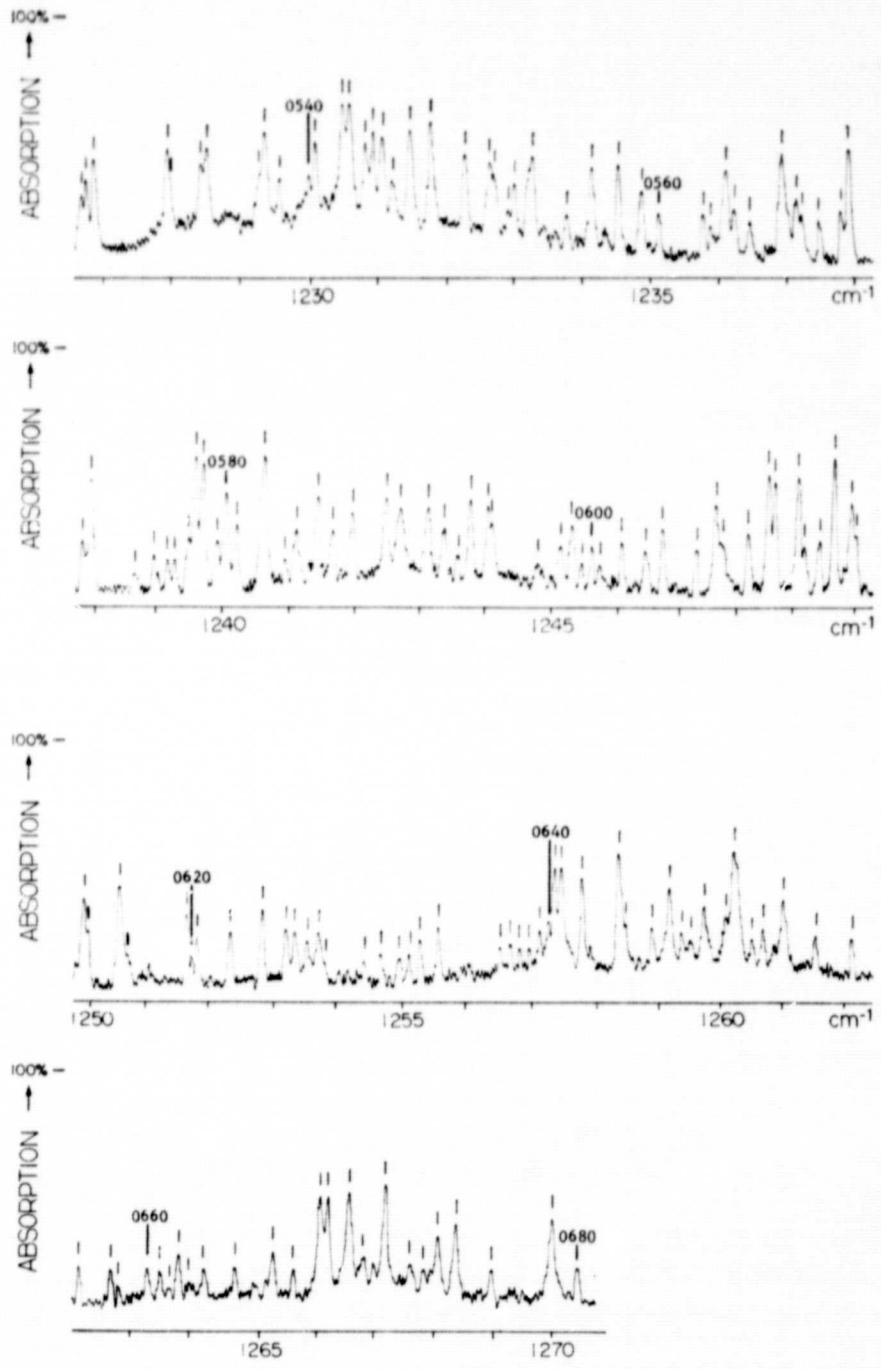

FIG. 1—*Continued*

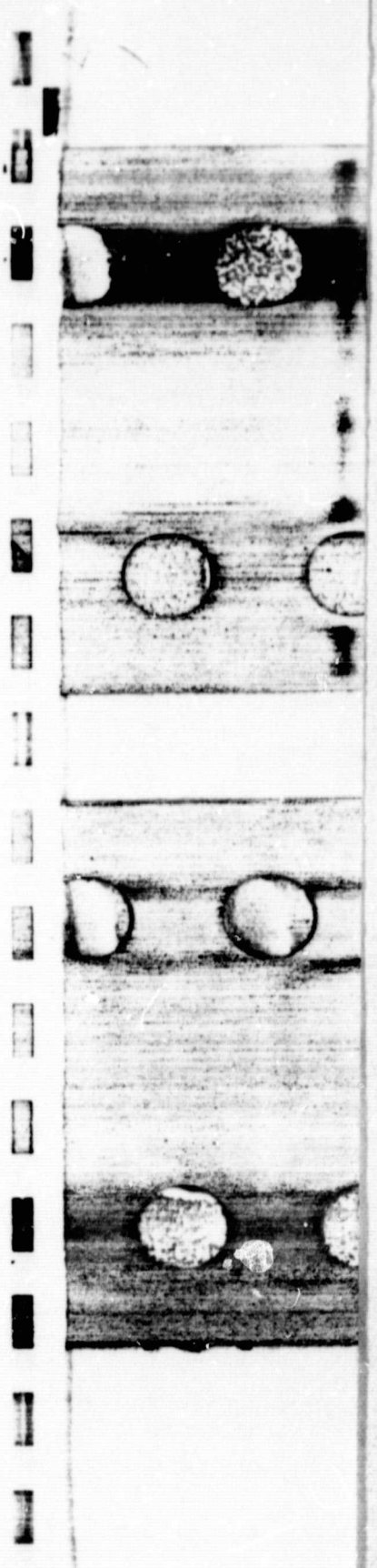

lines of ν_6 band, which is strongly overlapped on the high-frequency side by the parallel-type ν_2 band of $^{13}CH_3D$. The rotational structure in J and K is well resolved throughout the ν_6 band; even the very closely spaced components of the $^RQ_0$ subbranch could be measured from $J = 1$.

III. COMPUTATIONAL PROCEDURE

Assignments of the transitions to observed lines and the determination of molecular structure constants were performed in an iterative, three-step computational procedure:

1. Experimental values of the energies of the upper-state levels, E'_i, with $v_6 = 1$ were calculated using the expression

$$E_i' = hc\sigma_i + E_i'', \tag{1}$$

where σ_i are observed (and assigned) wavenumbers of ν_6 and E''_i are energies of the ground-state levels:

$$E''_i = E_i''^{o} + H_0^K K''^6. \tag{2}$$

Values of $E_i''^{o}$, including all but one term through the fourth order, were determined using the accurate values now available (*7*, *8*) for the ground-state structure constants. The term involving the fourth-order distortion constant H_0^K remains an unknown to be determined. Thus, Eq. (1) can be expressed as

$$E_i'^{e} = E'_i - H_0^K K''^6 \tag{3}$$

where $E_i'^{e} = hc\sigma_i + E_i''^{o}$ are considered to be experimental data and H_0^K is a constant to be determined. Because of the accuracy of the $E_i''^{o}$, the uncertainties of the $E_i'^{e}$ and $hc\sigma_i$ are equivalent.

2. Eigenvalues, E_i', and eigenvectors were approximated for the energy matrix expanded to fourth order for the vibrational state with $v_6 = 1$ (see below). In this approximation it was assumed that $H_0^K = H^K$ ($v_6 = 1$); H^J, H^{JJK}, and H^{JKK} were constrained to the values determined for the corresponding ground-state constants (*8*).

The unknown upper-state structure constants $t_1 \cdots t_k \cdots t_n$, with $t_k = H^K = H_0^K$, were determined utilizing a trivial iterative process based on the least-squares method applied to the function

$$W(t_1 \cdots t_k \cdots t_n). = \sum_{i=1}^{N} g_i[E_i'^{e} - E'_i(t_1 \cdots t_k \cdots t_n) + t_k K''^6]^2, \tag{4}$$

where N is the number of assigned transitions and g_i are suitable statistical weights defined so that $\sum_{i=1}^{N} g_i = N$.

3. Wavenumbers and relative intensities calculated from adjustable values of the molecular structure constants were used to extend progressively the assignments of the transitions to larger values of J and K.

IV. VIBROTATIONAL ENERGIES IN THE UPPER STATE

The energies of the levels of the $v_6 = 1$ vibrational state were calculated using the formulation developed in Ref. (*9*). The twice-transformed Hamiltonian H^+, including all terms through h_4^+, was utilized. The use of symmetrized functions, as defined in

Ref. (*10*) allows the energy matrix to be factored into four submatrices, i.e., A_1, A_2, E_a, and E_b, according to the irreducible representations of the C_{3v} group.[3] The energy eigenvalues and eigenvectors were calculated by diagonalization of the A_1, A_2, and E_a submatrices.

The contributions to the energy which originate from the term r^2P^2, in the second-order Hamiltonian $h_2{}^+$, are enhanced by the Coriolis interaction between states with $v_6 = 1$ and $v_3 = 1$:

(i) The totally diagonal elements are responsible for large vibrational corrections $\alpha_6{}^A$ and $\alpha_6{}^B$ to the rotational constants A_e and B_e.

(ii) The two nondiagonal elements

$$\langle v_6 = 1, J, K, l_6 = \mp 1 | r^2P^2 | v_6 = 1, J, K \pm 2, l_6 = \pm 1\rangle = 2q_{22}{}^6[J(J+1) - K(K \pm 1)]^{\frac{1}{2}}[J(J+1) - (K \pm 1)(K \pm 2)]^{\frac{1}{2}} \quad (5)$$

and

$$\langle v_6 = 1, J, K, l_6 = \pm 1 | r^2P^2 | v_6 = 1, J, K \pm 1, l_6 = \mp 1\rangle = 2q_{12}{}^6(2K \pm 1)[J(J+1) - K(K \pm 1)]^{\frac{1}{2}} \quad (6)$$

are responsible for a significant mixing in K and l_6. Even two fourth-order rotational corrections[4] to the terms given by Eqs. (5) and (6), i.e.,

$$\langle v_6 = 1, J, K, l_6 = \mp 1 | r^2P^4 | v_6 = 1, J, K \pm 2, l_6 = \pm 1\rangle = 2f_{22}{}^{6,J}J(J+1)[J(J+1) - K(K \pm 1)]^{\frac{1}{2}} \times [J(J+1) - (K \pm 1)(K \pm 2)]^{\frac{1}{2}} \quad (7)$$

and

$$\langle v_6 = 1, J, K, l_6 = \pm 1 | r^2P^4 | v_6 = 1, J, K \pm 1, l_6 = \mp 1\rangle = 2f_{12}{}^{6,K}(2K \pm 1)^2[J(J+1) - K(K \pm 1)]^{\frac{1}{2}} \quad (8)$$

appear to contribute significantly to the energies for $J \geq 10$. Also, the fourth-order doubling element

$$\langle v_6 = 1, J, K = \mp 2, l_6 = \pm 1 | r^2P^4 | v_6 = 1, J, K = \pm 2, l_6 = \mp 1\rangle = 2f_{12}{}^6J(J+1)[J(J+1) - 2] \quad (9)$$

gives significant contributions when $J \geq 8$. All these effects are observable in the spectra of the ν_6 band as an extended J and K structure, as well as by a rapidly increasing A_1A_2 splitting of the transitions with $|K' - l'_6| = 0$ and 3, as the value of J increases. Nevertheless, no A_1A_2 splitting has been observed for transitions with $|K' - l'_6| = 6, 9, \ldots$.

Since the mixing in K and l_6 is not extremely large the energy levels of the upper state will be labeled using the quantum numbers and indices $v_6 = |l_6| = 1, J, |K|, |K - l_6|$, and C ($C = A_1, A_2, E$). The species A_1 and A_2 are defined according to Refs. (*10*, *11*).

[3] E_a and E_b are the two components of an E basis, respectively, symmetric and antisymmetric with respect to the operation σ_v of the C_{3v} group.

[4] Note that the contributions due to $f_{22}{}^{6,K}$ and $f_{12}{}^{6,J}$ appeared to be insignificant. The fourth-order vibrational corrections due to r^4P^2, in $h_4{}^+$, are included in the effective values of A_v, B_v, $(q_{22}{}^6)_v$, and $(q_{12}{}^6)_v$ appearing in Table II.

V. RELATIVE LINE INTENSITIES

The relative line intensities were calculated using the expression

$$I_{m\to n} \propto \sigma_{mn} S_{mn} \exp(-E_m/kT), \tag{10}$$

where σ_{mn} is the wavenumber of the transition from E_m to E_n and S_{mn} is the square of the transition moment,

$$S_{mn} = 3 \sum_{ij} |\langle mi | M_Z^+ | nj \rangle|^2. \tag{11}$$

$|mi\rangle$ and $|nj\rangle$ are the eigenfunctions of H^+ which correspond to E_m and E_n, respectively. The subscripts i and j denote secondary quantum numbers: the magnetic quantum number M, the nuclear spin quantum numbers, and the index[3] a or b for eigenfunctions with symmetry species E. M_Z^+ is the twice-transformed component of the dipole moment (*12*) on the space fixed axis Z.

In the computations of the relative line intensities, M_Z^+ has been approximated by retaining only the leading term

$$(M_Z^+)_0 = M_Z = \sum_\alpha \cos(Z, \alpha) M_\alpha. \tag{12}$$

As usual, the molecule fixed components M_α of the dipole moment have been expanded in terms of the dimensionless normal coordinates q_n, q_{ta}, q_{tb}; then, the part responsible for the ν_6 transitions can be written as

$$\begin{aligned}(M_x)_{\nu_6} &= d_6 q_{6a}[1 + F^{A_1}(q_n, q_{ta}, q_{tb})],\\ (M_y)_{\nu_6} &= d_6 q_{6b}[1 + F^{A_1}(q_n, q_{ta}, q_{tb})],\\ (M_z)_{\nu_6} &= 0,\end{aligned} \tag{13}$$

$F^{A_1}(q_n, q_{ta}, q_{tb})$ is a totally symmetric expansion of q_n, q_{ta}, q_{tb} without a constant term.

When using Eq. (12), all terms of M_Z^+ which depend on the angular momentum components are neglected. Nevertheless, the contributions of these terms to the intensities can be roughly estimated from theoretical values of the $\zeta_{aa'\alpha}^{\alpha}$ constants, to be generally less than a few percent of the contributions due to Eq. (12). Only the intensities of the weakest transitions, especially the forbidden transitions, with $\Delta|K - l_6| \neq 0$, may be seriously affected (up to 50%).

All transitions obey the strict selection rules (*10, 11*)

$$\Delta J = 0, \pm 1 \quad \text{and} \quad A_1 \leftrightarrow A_2 \quad \text{or} \quad E \leftrightarrow E. \tag{14}$$

It should be noticed that the approximate selection rule $\Delta|K - l_6| = 0$ which holds for the allowed transitions in the zero-order approximation is not affected by the (2, 2) coupling (see Eqs. (5) and (7)), which is diagonal in $K - l_6$. Thus, no additional transitions can appear when only such a coupling occurs. However, the (1, −2) coupling (see Eqs. (6) and (8)), which obeys $\Delta(K - l_6) = \pm 3$, can be responsible for forbidden transitions. Of course, A_1 – A_2 splittings of energy levels with $|K| = 3, 6, \ldots$ in the ground state might also provide a breakdown of the rule $\Delta|K - l_6| = 0$, but such splittings are insignificant for the values of J considered here (*8*).

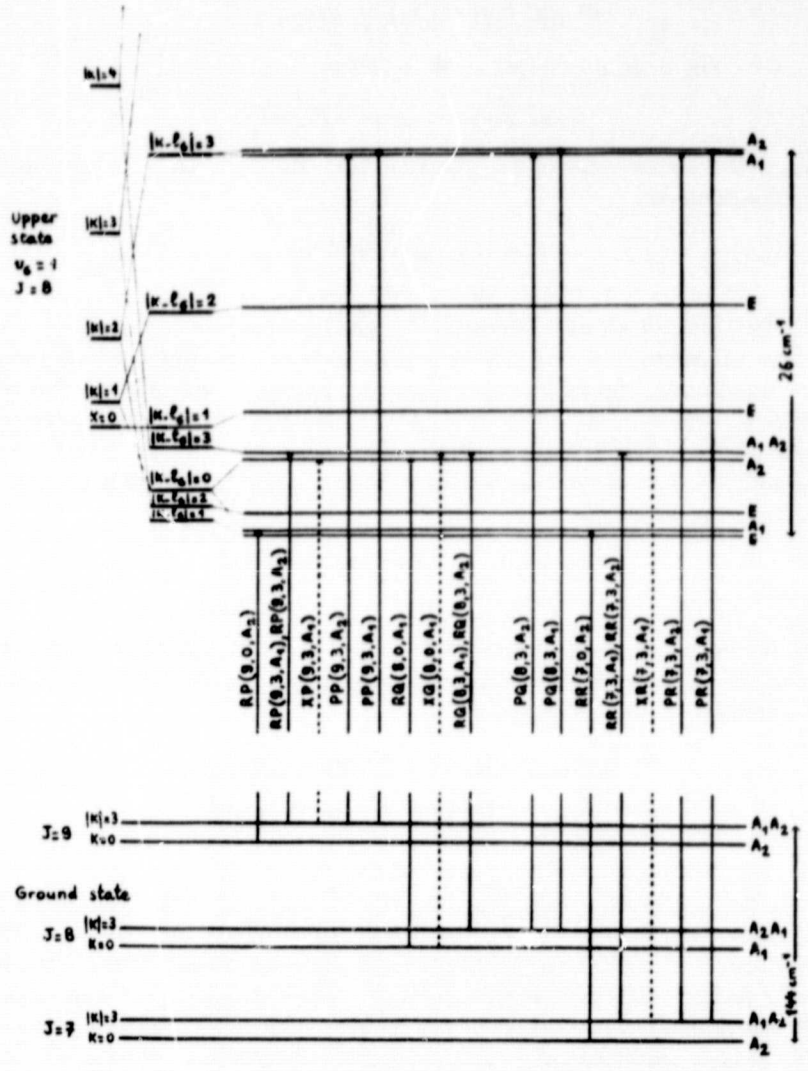

FIG. 2. The ν_6 band transitions of $^{12}CH_3D$ with $J' = 8$ and $|K' - l'_6| = 0$ and 3.

Actually, some forbidden transitions with $\Delta|K - l_6| = 3$, induced by the $(1, -2)$ coupling, are observed in our spectra: they involve upper-state levels with small values of $|K' - l'_6|$, i.e., those which are the most strongly affected by the mixing in K and l_6. In Fig. 2, as an example, the first few upper-state rotational levels with $J' = 8$ are represented along with the observed transitions having $|K' - l'_6| = 0$ or 3. The allowed transitions are represented by solid lines and are labeled $PP(J'', |K''|, C'')$, $PQ(J'', |K''|, C'')\ldots$, where the double prime indicates lower-state quantum numbers and PP, PQ, PR, ... have their usual meanings. The forbidden transitions are represented by broken lines and are labeled $XP(J'', |K''|, C'')$, $XQ(J'', |K''|, C'')$ ....

A more complete specification of the forbidden transitions is not necessary here, owing to the restricted number of observations.

VI. RESULTS AND DISCUSSION

Of the 689 lines measured in the range 1033–1270 cm^{-1}, 510 can be assigned to be totally or partially due to transitions of the ν_6 band of $^{12}CH_3D$, the other lines are due to transitions of the ν_3 band of $^{12}CH_3D$ or to transitions of $^{12}CH_4$ and H_2O impurities in the gas sample.

Assignments and observed wavenumbers of the transitions of the ν_6 band are listed in Table I, columns (II) and (IV); column (I) gives the correspondence with the lines of Fig. 1; column (III) gives the specification of the upper levels of the transitions. The transitions and upper-state energy levels are labeled as indicated in Part V of this paper, except that the pairs of transitions of the type

$$(J'', |K''|, A_1) \rightarrow (J', |K' - l'_6|, A_2)$$

and

$$(J'', |K''|, A_2) \rightarrow (J', |K' - l'_6|, A_1), \text{ with } |K' - l'_6| = 6, 9, \ldots, \qquad (15)$$

which coincide exactly (doublets unresolved in the present work), are tabulated according to the global notation

$$(J'', |K''|, A) \rightarrow (J' |K' - l'_6|, A) \qquad (16)$$

instead of as in representation (15) above.

Of the 680 transitions $E \leftrightarrow E$, $A_1 \leftrightarrow A_2$, or $A \leftrightarrow A$, which have been assigned to the 510 observed lines of the ν_6 band, 633 have been retained for calculation of molecular structure constants of the $v_6 = 1$ state. Statistical weights equal to 1.0 have been assigned to the 633 retained transitions; the weights for the transitions $A \rightarrow A$, have been distributed equally between the two components $A_1 \rightarrow A_2$ and $A_2 \rightarrow A_1$ and are indicated as *1.0 in Table I (see column VIII).

The 633 transitions were used to calculate values of molecular structure constants following the computational procedure outlined in Section III. The results of these calculations are listed in Table II. The standard deviations and 99.5% confidence intervals within the theoretical model adopted are also given. The values of the three constants H^J, H^{JJK}, and H^{JKKK} were constrained to the values listed at the bottom of Table II. The 633 values for the wavenumbers of the assigned transitions can be reproduced with an overall standard deviation of 0.013 cm^{-1} using the stated values for the molecular structure constants, which is within the experimental uncertainty of the experimental data.

The values of the molecular structure constants listed in Table II have been used to predict the spectral positions and relative intensities for all transitions of the ν_6 band of $^{12}CH_3D$ with $J' \leq 17$. The predicted transitions include 745 allowed transitions, with 659 observed, and 12 forbidden transitions, with 10 observed, which have a calculated intensity ratio $\geq 1/250$ with respect to the most intense lines of the ν_6 band (i.e., having intensities $\geq 0.20 \times 10^3$ in our arbitrary scale). The intensity ratio $\geq 1/250$ was selected to approximately correspond to the limit for observation of lines in the most favorably recorded portions of the spectrum. Predicted wavenumbers and relative intensities are

TABLE I

Observed and Calculated Wavenumbers of ν_6 of $^{13}CH_3D$

Note: The explanations for Columns I–VIII are given at the end of the table as a footnote.

(I)	(II)	(III)				(IV)	(V)	(VI)	(VII)	(VIII)
	RP(17, 3,A2)	16	4	3	A1		1001.4604		0.133E+03	
	RP(17, 3,A1)	16	4	3	A2		1001.4690		0.133E+03	
	RP(17, 0,A2)	16	1	0	A1		1004.8536		0.200E+03	
	RP(16, 3,A2)	15	4	3	A1		1010.9613		0.225E+03	
	RP(16, 3,A1)	15	4	3	A2		1010.9747		0.225E+03	
	RP(16, 2,E)	15	3	2	E		1012.8377		0.281E+03	
	RP(15, 6,A)	14	7	6	A		1013.6675		0.296E+03	
	RP(16, 0,A1)	15	1	0	A2		1014.7408		0.358E+03	
	RP(15, 5,E)	14	6	5	E		1015.9216		0.202E+03	
	RP(15, 4,E)	14	5	4	E		1018.0373		0.254E+03	
	RP(15, 3,A1)	14	4	3	A2		1020.3314		0.362E+03	
	RP(15, 3,A2)	14	4	3	A1		1020.3572		0.361E+03	
	RP(15, 2,E)	14	3	2	E		1022.3766		0.464E+03	
	RP(14, 6,A)	13	7	6	A		1022.6139		0.421E+03	
	RP(15, 1,E)	14	2	1	E		1023.9249		0.566E+03	
	RP(15, 0,A2)	14	1	0	A1		1024.5335		0.616E+03	
	RP(14, 5,E)	13	6	5	E		1024.9320		0.297E+03	
	RP(14, 4,E)	13	5	4	E		1027.4271		0.289E+03	
	RP(14, 3,A2)	13	4	3	A1		1029.5737		0.553E+03	
	RP(14, 3,A1)	13	4	3	A2		1029.6051		0.551E+03	
	RP(13, 6,A)	12	7	6	A		1031.4605		0.558E+03	
	RP(14, 2,E)	13	3	2	E		1031.7830		0.726E+03	
1	RP(14, 1,E)	13	2	1	E	1033.5165	1033.5162	0	0.915E+03	1.0
	RP(13, 5,E)	12	6	5	E		1033.8394		0.408E+03	
2	RP(14, 0,A1)	13	1	0	A2	1034.2243	1034.2249	-0	0.102E+04	1.0
	PP(17, 6,A)	16	5	6	A		1035.7746		0.241E+03	
3	RP(13, 4,E)	12	5	4	E	1036.3069	1036.3015	5	0.557E+03	1.0
4	RP(13, 3,A1)	12	4	3	A2	1038.6987	1038.6850	13	0.799E+03	1.0
4	RP(13, 3,A2)	12	4	3	A1	1038.6987	1038.7175	-18	0.795E+03	1.0
5	RP(12, 6,A)	11	7	6	A	1040.2039	1040.2089	-5	0.681E+03	*1.0
6	RP(13, 2,E)	12	3	2	E	1041.0484	1041.0501	-1	0.108E+04	1.0
7	PP(16, 5,E)	15	4	5	E	1041.2060	1041.1898	16	0.207E+03	1.0
8	RP(12, 5,E)	11	6	5	E	1042.6448	1042.6420	2	0.523E+03	1.0
10	RP(13, 1,E)	12	2	1	E	1042.9791	1042.9804	-1	0.141E+04	1.0
12	PP(15, 3,A2)	14	2	3	A1	1043.3060	1043.3067	-6	0.246E+03	1.0
13	RP(13, 0,A2)	12	1	0	A1	1043.8182	1043.8084	9	0.160E+04	1.0
13	PP(15, 3,A1)	14	2	3	A2	1043.8182	1043.8443	-26	0.250E+03	1.0
15	PP(16, 6,A)	15	5	6	A	1044.5584	1044.5584	-0	0.466E+03	*1.0
16	RP(12, 4,E)	11	5	4	E	1045.1634	1045.1591	4	0.757E+03	1.0
18	PP(17, 9,A)	16	8	9	A	1046.5907	1046.5633	27	0.271E+03	*1.0
18	PP(15, 4,E)	14	3	4	E	1046.5907	1046.5789	11	0.327E+03	1.0
19	RP(12, 3,A2)	11	4	3	A1	1047.6750	1047.6640	11	0.109E+04	1.0
19	RP(12, 3,A1)	11	4	3	A2	1047.6750	1047.6957	-20	0.108E+04	1.0
21	PP(16, 7,E)	15	6	7	E	1048.1149	1048.1094	5	0.250E+03	1.0
23	RP(11, 6,A)	10	7	6	A	1048.8578	1048.8616	-3	0.752E+03	*1.0
	PP(14, 2,E)	13	1	2	E		1049.2198		0.290E+03	
24	PP(15, 5,E)	14	4	5	E	1049.8626	1049.8554	7	0.388E+03	1.0
25	RP(12, 2,E)	11	3	2	E	1050.1790	1050.1732	5	0.151E+04	1.0
27	RP(11, 5,E)	10	6	5	E	1051.3430	1051.3414	1	0.618E+03	1.0
28	PP(14, 3,A1)	13	2	3	A2	1051.7913	1051.7771	14	0.459E+03	1.0
28	PP(16, 8,E)	15	7	8	E	1051.7913	1051.8230	-31	0.258E+03	1.0
29	PP(14, 3,A2)	13	2	3	A1	1052.1902	1052.1898	0	0.462E+03	1.0
30	RP(12, 1,E)	11	2	1	E	1052.3030	1052.3075	-4	0.205E+04	1.0
31	RP(12, 0,A1)	11	1	0	A2	1053.2869	1053.2781	8	0.243E+04	1.0
32	PP(15, 6,A)	14	5	6	A	1053.3559	1053.3391	16	0.864E+03	*1.0
33	RP(11, 4,E)	10	5	4	E	1053.9116	1053.9147	-3	0.942E+03	1.0
34	PP(14, 4,E)	13	3	4	E	1055.1563	1055.1263	29	0.594E+03	1.0
34	PP(13, 1,F)	12	0	1	E	1055.1563	1055.1770	-20	0.200E+03	1.0
	PP(16, 9,A)	15	8	9	A		1055.6909		0.518E+03	
36	RP(11, 3,A1)	10	4	3	A2	1056.5231	1056.5111	11	0.139E+04	1.0

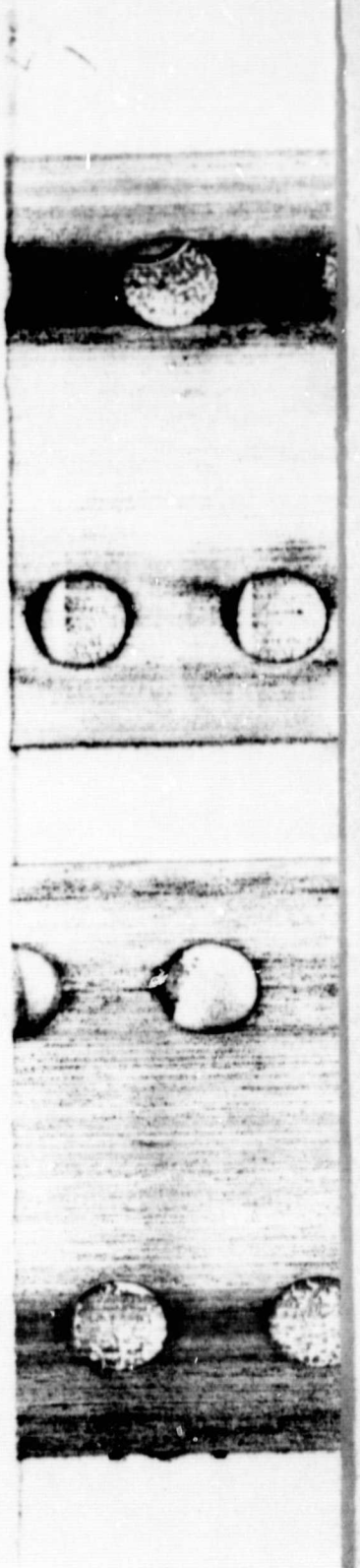

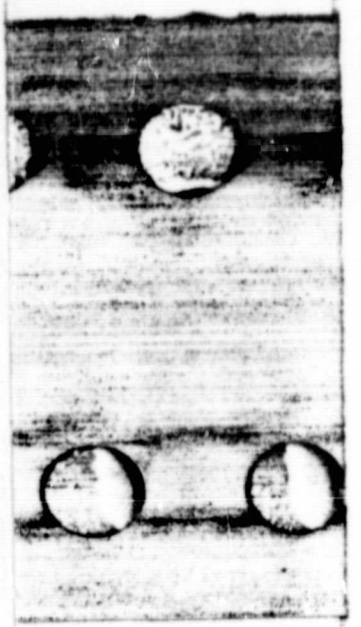

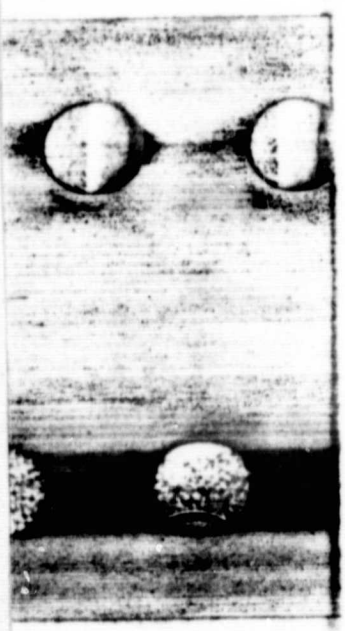

TABLE I—*Continued*

(I)	(II)	(III)				(IV)	(V)	(VI)	(VII)	(VIII)
36	RP(11, 3,A2)	10	4	3	A1	1056.5231	1056.5429	-19	0.138E+04	1.0
37	PP(15, 7,E)	14	6	7	F	1056.9972	1056.9974	-0	0.461E+03	1.0
38	RP(10, 6,A)	9	7	6	A	1057.4986	1057.4215	17	0.727E+03	*1.0
38	PP(13, 2,E)	12	1	2	E	1057.4986	1057.4781	-39	0.535E+03	1.0
40	PP(14, 5,E)	13	4	5	E	1058.5239	1058.5203	9	0.696E+03	1.0
	PP(17,12,A)	16	11	12	A		1058.7482		0.240E+03	
41	RP(11, 2,E)	10	3	2	E	1059.1521	1059.1505	1	0.198E+04	1.0
	PP(16,10,E)	15	9	10	E		1059.7114		0.254E+03	
42	RP(10, 5,E)	9	6	5	E	1059.9422	1059.9406	1	0.661E+03	1.0
43	PP(13, 3,A2)	12	2	3	A1	1060.2484	1060.2513	-2	0.813E+03	1.0
44	PP(13, 3,A1)	12	2	3	A2	1060.5647	1060.5603	4	0.816E+03	1.0
45	PP(15, 8,F)	14	7	8	F	1060.8156	1060.8149	0	0.475E+03	1.0
46	RP(11, 1,F)	10	2	1	E	1061.4843	1061.4885	-4	0.282E+04	1.0
49	PP(14, 6,A)	13	5	6	A	1062.1104	1062.1082	2	0.154E+04	*1.0
50	RP(10, 4,F)	9	5	4	F	1062.5305	1062.5629	-32	0.108E+04	1.0
51	RP(11, 0,A2)	10	1	0	A1	1062.6032	1062.6282	-24	0.350E+04	1.0
52	PP(12, 1,E)	11	0	1	E	1063.2591	1063.2590	0	0.380E+03	1.0
54	PP(13, 4,E)	12	3	4	E	1063.6776	1063.6767	0	0.103E+04	1.0
	PP(16,11,E)	15	10	11	E		1063.8875		0.243E+03	
56	PP(15, 9,A)	14	8	9	A	1064.7511	1064.7860	-34	0.952E+03	*1.0
57	RP(10, 3,A2)	9	4	3	A1	1065.2423	1065.2220	20	0.161E+04	1.0
57	RP(10, 3,A1)	9	4	3	A2	1065.2423	1065.2638	-21	0.165E+04	1.0
59	PP(12, 2,E)	11	1	2	E	1065.7571	1065.7549	2	0.938E+03	1.0
60	PP(14, 7,F)	13	6	7	E	1065.8785	1065.8636	14	0.816E+03	1.0
60	RP(9, 6,A)	8	7	6	A	1065.8785	1065.8917	-13	0.569E+03	*1.0
62	PP(13, 5,E)	12	4	5	E	1067.1796	1067.1761	3	0.119E+04	1.0
64	RP(10, 2,F)	9	3	2	E	1067.9806	1067.9832	-2	0.245E+04	1.0
	PP(16,12,A)	15	11	12	A		1068.2249		0.456E+03	
65	RP(9, 5,E)	8	6	5	E	1068.4343	1068.4432	-8	0.620E+03	1.0
66	PP(12, 3,A1)	11	2	3	A2	1068.7161	1068.7242	-8	0.137E+04	1.0
67	PP(15,10,E)	14	9	10	E		1068.9108		0.466E+03	
68	PP(12, 3,A2)	11	2	3	A1	1068.9595	1068.9487	10	0.138E+04	1.0
69	PP(14, 8,E)	13	7	8	E	1069.7769	1069.7752	1	0.839E+03	1.0
70	RP(10, 1,F)	9	2	1	E	1070.5131	1070.5151	-1	0.365E+04	1.0
71	PP(13, 6,A)	12	5	6	A	1070.8641	1070.8569	7	0.262E+04	*1.0
72	RP(9, 4,F)	8	5	4	F	1071.1028	1071.1060	-3	0.112E+04	1.0
73	PP(11, 1,F)	10	0	1	F	1071.3508	1071.3455	5	0.690E+03	1.0
74	RP(10, 0,A1)	9	1	0	A2	1071.8491	1071.8532	-4	0.481E+04	1.0
75	PP(12, 4,F)	11	3	4	E	1072.2221	1072.2214	0	0.171E+04	1.0
	PP(16,13,E)	15	12	13	E		1072.7311		0.210E+03	
77	PP(15,11,F)	14	10	11	F		1073.1935		0.445E+03	
78	XP(9, 3,A1)	8	1	0	A2	1073.5962	1073.5989	-3	0.340E+03	0.0
79	PP(14, 9,A)	13	8	9	A	1073.8604	1073.8399	20	0.168E+04	*1.0
79	RP(9, 3,A2)	8	4	3	A1	1073.8604	1073.8643	-3	0.182E+04	1.0
79	RP(9, 3,A1)	8	4	3	A2	1073.8604	1073.9033	-42	0.149E+04	0.0
80	PP(11, 2,E)	10	1	2	E	1074.0484	1074.0472	1	0.156E+04	1.0
	RP(8, 6,A)	7	7	6	A		1074.2750		0.290E+03	
81	PP(13, 7,F)	12	6	7	E	1074.7042	1074.6989	5	0.139E+04	1.0
82	PP(12, 5,F)	11	4	5	F	1075.8123	1075.8133	-0	0.196E+04	1.0
83	RP(9, 2,E)	8	3	2	E	1076.6780	1076.6755	2	0.283E+04	1.0
84	RP(8, 5,E)	7	6	5	E	1076.8480	1076.8530	-4	0.473E+03	1.0
85	PP(11, 3,A2)	10	2	3	A1	1077.1842	1077.1883	-4	0.221E+04	1.0
86	PP(11, 3,A1)	10	2	3	A2	1077.3242	1077.3459	-21	0.221E+04	1.0
	PP(15,12,A)	14	11	12	A		1077.6404		0.835E+03	
87	PP(14,10,E)	13	9	10	E	1078.0316	1078.0595	-27	0.821E+03	1.0
88	PP(13, 8,E)	12	7	8	E	1078.7127	1078.6948	17	0.142E+04	1.0
89	RP(9, 1,E)	8	2	1	E	1079.3877	1079.3818	5	0.440E+04	1.0
89	PP(10, 1,F)	9	0	1	F	1079.3877	1079.4486	-60	0.119E+04	0.0
90	RP(8, 4,F)	7	5	4	F	1079.5699	1079.5482	21	0.102E+04	1.0
90	PP(12, 6,A)	11	5	6	A	1079.5699	1079.5757	-5	0.429E+04	*1.0

TABLE I—*Continued*

(I)	(II)	(III)	(IV)	(V)	(VI)	(VII)	(VIII)
91	PP(11, 4,E)	10 3 4 E	1080.7472	1080.7537	-3	0.270E+04	1.0
92	PP(9, 0,A2)	8 1 0 A1	1080.9422	1080.9482	-6	0.630E+04	1.0
	PP(15,13,E)	14 12 13 E		1082.2595		0.389E+03	
	PP(16,15,A)	15 14 15 A		1082.2823		0.334E+03	
94	PP(10, 2,E)	9 1 2 E	1082.3541	1082.3486	5	0.246E+04	1.0
94	PP(8, 3,A1)	7 4 3 A2	1082.3541	1082.3511	3	0.183E+04	1.0
94	PP(8, 3,A2)	7 4 3 A1	1082.3541	1082.3557	-1	0.180E+04	1.0
	PP(14,11,E)	13 10 11 E		1082.4394		0.785E+03	
95	PP(13, 9,A)	12 8 9 A	1082.8401	1082.8437	4	0.285E+04	*1.0
96	PP(12, 7,E)	11 6 7 E	1083.5002	1083.4943	5	0.226E+04	1.0
98	PP(11, 5,E)	10 4 5 E	1084.4195	1084.4222	-2	0.308E+04	1.0
100	PP(7, 5,E)	6 6 5 E	1085.2323	1085.1734	58	0.235E+03	0.0
100	PP(8, 2,E)	7 3 2 E	1085.2323	1085.2330	-1	0.302E+04	1.0
101	PP(10, 3,A1)	9 2 3 A2	1085.6266	1085.6344	-7	0.337E+04	1.0
102	PP(10, 3,A2)	9 2 3 A1	1085.7398	1085.7406	-0	0.337E+04	1.0
	PP(14,12,A)	13 11 12 A		1086.9864		0.147E+04	
	PP(15,14,E)	14 13 14 E		1087.0589		0.345E+03	
104	PP(13,10,E)	12 9 10 E	1087.1506	1087.1491	1	0.139E+04	1.0
105	PP(12, 8,E)	11 7 8 E	1087.5746	1087.5649	9	0.232E+04	1.0
105	PP(9, 1,E)	8 0 1 E	1087.5746	1087.5702	4	0.195E+04	1.0
106	PP(7, 4,E)	6 5 4 E	1087.9027	1087.8941	8	0.758E+03	1.0
107	PP(9, 1,E)	7 2 1 E	1088.0855	1088.0872	-1	0.493E+04	1.0
108	PP(11, 6,A)	10 5 6 A	1088.2510	1088.2551	-4	0.672E+04	*1.0
109	PP(10, 4,E)	9 3 4 E	1089.2481	1089.2540	-5	0.408E+04	1.0
110	PP(8, 0,A1)	7 1 0 A2	1089.9051	1089.9086	-3	0.781E+04	1.0
111	PP(9, 2,E)	8 1 2 E	1090.6623	1090.6494	12	0.367E+04	1.0
112	PP(7, 3,A2)	6 4 3 A1	1090.7203	1090.7307	-10	0.162E+04	1.0
112	PP(7, 3,A1)	6 4 3 A2	1090.7203	1090.7316	-11	0.162E+04	1.0
114	PP(13,11,E)	12 10 11 E	1091.6134	1091.6170	-3	0.133E+04	1.0
115	PP(14,13,E)	13 12 13 E		1091.7088		0.676E+03	
115	PP(12, 9,A)	11 8 9 A	1091.7990	1091.7890	9	0.465E+04	*1.0
	PP(15,15,A)	14 14 15 A		1092.0463		0.610E+03	
116	PP(11, 7,E)	10 6 7 E	1092.2410	1092.2404	0	0.355E+04	1.0
118	PP(10, 5,E)	9 4 5 E	1092.9909	1092.9927	-1	0.464E+04	1.0
119	PP(7, 2,E)	6 3 2 E	1093.6652	1093.6671	-1	0.294E+04	1.0
120	PP(9, 3,A2)	8 2 3 A1	1094.0827	1094.0523	30	0.490E+04	1.0
120	PP(9, 3,A1)	8 2 3 A2	1094.0827	1094.1205	-37	0.490E+04	1.0
121	PP(8, 1,E)	7 0 1 E	1095.7018	1095.7074	-5	0.298E+04	1.0
122	PP(6, 4,E)	5 5 4 E	1096.2050	1096.1481	56	0.370E+03	0.0
122	PP(12,10,E)	11 9 10 E	1096.2050	1096.1712	33	0.228E+04	1.0
122	PP(13,12,A)	12 11 12 A	1096.2050	1096.2550	-49	0.250E+04	*1.0
123	PP(11, 8,E)	10 7 8 E	1096.3800	1096.3769	3	0.365E+04	1.0
	PP(14,14,E)	13 13 14 E		1096.6149		0.609E+03	
124	PP(7, 1,E)	6 2 1 E	1096.6334	1096.6349	-1	0.508E+04	1.0
125	PP(10, 6,A)	9 5 6 A	1096.8808	1096.8858	-5	0.101E+05	*1.0
127	PP(9, 4,E)	8 3 4 E	1097.7120	1097.7208	-8	0.588E+04	1.0
128	PP(7, 0,A2)	6 1 0 A1	1098.7248	1098.7301	-5	0.913E+04	1.0
129	PP(8, 2,E)	7 1 2 E	1098.9512	1098.9376	13	0.516E+04	1.0
130	PP(6, 3,A1)	5 4 3 A2	1099.0118	1099.0096	2	0.118E+04	1.0
130	PP(6, 3,A2)	5 4 3 A1	1099.0118	1099.0098	2	0.118E+04	1.0
132	PP(11, 9,A)	10 8 9 A	1100.6910	1100.6675	23	0.731E+04	*1.0
132	PP(12,11,E)	11 10 11 E	1100.6910	1100.7183	-27	0.218E+04	1.0
134	PP(10, 7,E)	9 6 7 E	1100.9246	1100.9287	-4	0.535E+04	1.0
135	PP(13,13,E)	12 12 13 E	1101.0577	1101.0714	-13	0.115E+04	1.0
136	PP(9, 5,E)	8 4 5 E	1101.5090	1101.5151	-12	0.669E+04	1.0
137	PP(6, 2,E)	5 3 2 E	1101.9768	1101.9840	-7	0.253E+04	1.0
138	PP(8, 3,A1)	7 2 3 A2	1102.4460	1102.4315	14	0.677E+04	1.0
138	PP(8, 3,A2)	7 2 3 A1	1102.4460	1102.4726	-26	0.677E+04	1.0
139	PP(7, 1,E)	6 0 1 E	1103.8537	1103.8514	2	0.422E+04	1.0
140	PP(6, 1,E)	5 2 1 E	1105.0392	1105.0339	5	0.476E+04	1.0

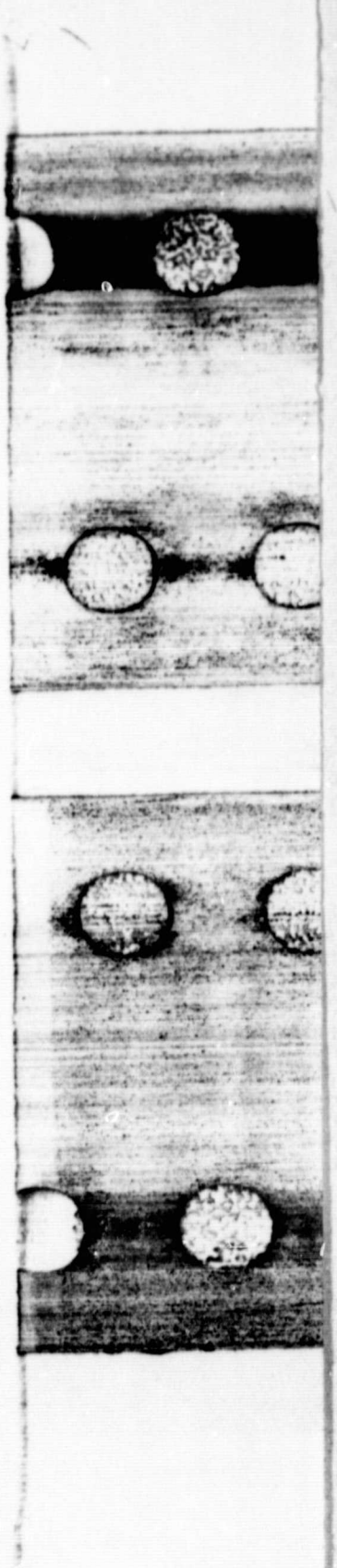

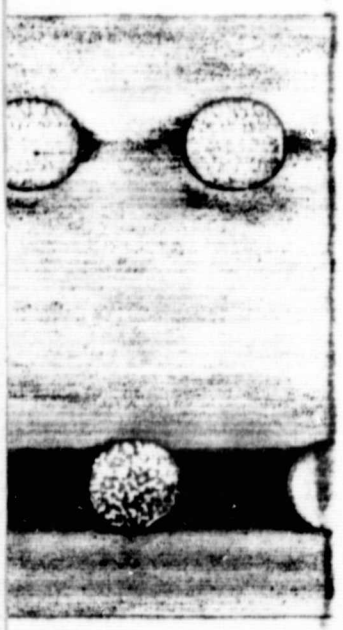

TABLE I—*Continued*

(I)	(II)	(III)				(IV)	(V)	(VI)	(VII)	(VIII)
141	PP(11,10,F)	10	9	10	E	1105.1167	1105.1179	-1	0.358E+04	1.0
141	PP(10, 8,F)	9	7	8	F	1105.1167	1105.1223	-5	0.551E+04	1.0
142	PP(12,12,A)	11	11	12	A	1105.4629	1105.4383	24	0.409E+04	*1.0
142	PP(9, 6,A)	8	5	6	A	1105.4629	1105.4587	4	0.146E+05	*1.0
143	PP(8, 4,E)	7	3	4	E	1106.1382	1106.1403	-2	0.812E+04	1.0
147	RP(5, 3,A1)	4	4	3	A2	1107.2004	1107.1995	6	0.568E+03	1.0
147	RP(5, 3,A2)	4	4	3	A1	1107.2004	1107.1995	6	0.569E+03	1.0
147	PP(7, 2,F)	6	1	2	E	1107.2004	1107.1997	0	0.685E+04	1.0
148	RP(6, 0,A1)	5	1	0	A2	1107.4093	1107.4087	0	0.100E+05	1.0
149	PP(10, 9,A)	9	8	9	A	1109.4964	1109.4711	25	0.111E+05	*1.0
150	PP(9, 7,F)	8	6	7	F	1109.5400	1109.5505	-10	0.776E+04	1.0
151	PP(11,11,F)	10	10	11	F	1109.7669	1109.7357	30	0.344E+04	1.0
152	PP(8, 5,F)	7	4	5	F	1109.9715	1109.9797	-8	0.926E+04	1.0
153	RP(5, 2,F)	4	3	2	E	1110.2018	1110.1936	8	0.181E+04	1.0
154	PP(7, 3,A2)	6	2	3	A1	1110.7636	1110.7611	2	0.891E+04	1.0
154	PP(7, 3,A1)	6	2	3	A2	1110.7636	1110.7840	-20	0.891E+04	1.0
155	PP(6, 1,E)	5	0	1	E	1111.9918	1111.9886	3	0.551E+04	1.0
156	RP(5, 1,F)	4	2	1	E	1113.3091	1113.2972	11	0.397E+04	1.0
157	PP(9, 8,E)	8	7	8	E	1113.7822	1113.7932	-11	0.802E+04	1.0
158	PP(8, 6,A)	7	5	6	A	1113.9596	1113.9651	-5	0.204E+05	*1.0
158	PP(10,10,E)	9	9	10	E	1113.9596	1113.9817	-22	0.544E+04	1.0
159	PP(7, 4,E)	6	3	4	E	1114.4979	1114.5025	-5	0.107E+05	1.0
160	PP(6, 2,E)	5	1	2	E	1115.4291	1115.4218	7	0.855E+04	1.0
161	RP(5, 0,A2)	4	1	0	A1	1115.9445	1115.9409	3	0.101E+05	1.0
	PP(8, 7,F)	7	6	7	E		1118.0979		0.108E+05	
	PP(9, 9,A)	8	8	9	A		1118.1925		0.162E+05	
	RP(4, 2,E)	3	3	2	E		1118.3039		0.866E+03	
	PP(7, 5,E)	6	4	5	E		1118.3776		0.123E+05	
	RQ(13,12,A)	13	13	12	A		1118.3971		0.204E+03	
	PP(6, 3,A1)	5	2	3	A2		1119.0309		0.112E+05	
	PP(6, 3,A2)	5	2	3	A1		1119.0424		0.112E+05	
164	PP(5, 1,E)	4	0	1	E	1120.1176	1120.1016	15	0.660E+04	1.0
164	RQ(16, 9,A)	16	10	9	A	1120.1176	1120.1337	-16	0.266E+03	*1.0
	RQ(14,10,E)	14	11	10	E		1120.8572		0.266E+03	
165	RP(4, 1,E)	3	2	1	E	1121.4449	1121.4392	5	0.278E+04	1.0
165	RQ(15, 9,A)	15	10	9	A	1121.4449	1121.5239	-78	0.445E+03	0.0
	RQ(13,10,E)	13	11	10	E		1122.0078		0.360E+03	
166	PP(8, 8,E)	7	7	8	E	1122.3709	1122.3823	-11	0.113E+05	1.0
166	PP(7, 6,A)	6	5	6	A	1122.3709	1122.3969	-26	0.273E+05	*1.0
167	PP(6, 4,E)	5	3	4	E	1122.7895	1122.7978	-8	0.136E+05	1.0
167	RQ(14, 9,A)	14	10	9	A	1122.7895	1122.8099	-20	0.697E+03	*1.0
	RQ(12,10,E)	12	11	10	E		1123.0632		0.417E+03	
	RQ(15, 8,E)	15	9	8	E		1123.5344		0.265E+03	
168	PP(5, 2,F)	4	1	2	E	1123.5945	1123.5904	4	0.101E+05	1.0
169	RQ(13, 9,A)	13	10	9	A	1124.0127	1123.9939	18	0.101E+04	*1.0
169	RQ(11,10,F)	11	11	10	E	1124.0127	1124.0257	-12	0.350E+03	1.0
170	RP(4, 0,A1)	3	1	0	A2	1124.3330	1124.3236	9	0.924E+04	1.0
	RQ(14, 8,E)	14	9	8	E		1124.8649		0.429E+03	
171	RQ(12, 9,A)	12	10	9	A	1125.0777	1125.0782	-0	0.132E+04	*1.0
	RQ(15, 7,F)	15	8	7	F		1125.6295		0.301E+03	
172	RQ(11, 9,A)	11	10	9	A	1126.0848	1126.0655	19	0.148E+04	*1.0
172	RQ(13, 8,F)	13	9	8	F	1126.0848	1126.0882	-3	0.649E+03	1.0
	RQ(16, 6,A)	16	7	6	A		1126.2350		0.362E+03	
173	PP(7, 7,F)	6	6	7	E	1126.5340	1126.5636	-29	0.146E+05	1.0
174	PP(6, 5,F)	5	4	5	E	1126.6916	1126.7007	-9	0.158E+05	1.0
175	RQ(10, 9,A)	10	10	9	A	1126.9928	1126.9587	34	0.120E+04	*1.0
175	RQ(14, 7,F)	14	8	7	F	1126.9928	1127.0122	-19	0.500E+03	1.0
176	RQ(12, 8,F)	12	9	8	F	1127.2279	1127.2068	21	0.909E+03	1.0
176	PP(5, 3,A2)	4	2	3	A1	1127.2279	1127.2317	-3	0.134E+05	1.0
176	PP(5, 3,A1)	4	2	3	A2	1127.2279	1127.2366	-8	0.134E+05	1.0

TABLE I—*Continued*

(I)	(II)	(III)				(IV)	(V)	(VI)	(VII)	(VIII)
	RQ(15, 6,A)	15	7	6	A		1127.7956		0.649E+03	
178	PP(4, 1,E)	3	0	1	E	1128.1901	1128.1717	18	0.718E+04	1.0
178	RQ(11, 8,E)	11	9	8	E	1128.1901	1128.2236	-33	0.115E+04	1.0
179	RQ(13, 7,E)	13	8	7	E	1128.2893	1128.2819	7	0.782E+03	1.0
180	RQ(10, 8,E)	10	9	8	E	1129.1506	1129.1417	8	0.125E+04	1.0
181	RQ(14, 6,A)	14	7	6	A	1129.2405	1129.2389	1	0.110E+04	*1.0
182	RQ(12, 7,E)	12	8	7	E	1129.4615	1129.4411	20	0.115E+04	1.0
182	PP(3, 1,F)	2	2	1	E	1129.4615	1129.4733	-11	0.134E+04	1.0
183	RQ(9, 8,E)	9	9	8	E	1129.9771	1129.9644	12	0.978E+03	1.0
183	RQ(15, 5,E)	15	6	5	E	1129.9771	1130.0377	-60	0.327E+03	0.0
184	RQ(11, 7,E)	11	8	7	E	1130.4862	1130.4929	-6	0.155E+04	1.0
185	RQ(13, 6,A)	13	7	6	A	1130.5539	1130.5638	-10	0.178E+04	*1.0
186	PP(6, 6,A)	5	5	6	A	1130.7255	1130.7469	-21	0.353E+05	*1.0
187	PP(5, 4,E)	4	3	4	E	1131.0118	1131.0179	-6	0.166E+05	1.0
188	RQ(10, 7,E)	10	8	7	E	1131.4417	1131.4406	1	0.190E+04	1.0
189	RQ(14, 5,E)	14	6	5	E	1131.5378	1131.5330	4	0.575E+03	1.0
190	PP(4, 2,F)	3	1	2	E	1131.6990	1131.6934	5	0.112E+05	1.0
191	RQ(12, 6,A)	12	7	6	A	1131.7613	1131.7718	-10	0.269E+04	*1.0
	RQ(15, 4,E)	15	5	4	E		1132.0865		0.284E+03	
193	RQ(9, 7,F)	9	8	7	E	1132.2873	1132.2881	-0	0.199E+04	1.0
	RQ(16, 3,A2)	16	4	3	A1		1132.3287		0.125E+03	
	RQ(16, 3,A1)	16	4	3	A2		1132.3372		0.126E+03	
194	PP(3, 0,A2)	2	1	0	A1	1132.5649	1132.5539	11	0.722E+04	1.0
195	RQ(11, 6,A)	11	7	6	A	1132.8757	1132.8657	10	0.382E+04	*1.0
195	RQ(13, 5,E)	13	6	5	E	1132.8757	1132.9194	-43	0.951E+03	0.0
196	RQ(8, 7,E)	8	8	7	E	1133.0449	1133.0388	6	0.151E+04	1.0
	RQ(14, 4,F)	14	5	4	E		1133.6814		0.460E+03	
197	RQ(10, 6,A)	10	7	6	A	1133.8485	1133.8492	-0	0.500E+04	*1.0
198	RQ(12, 5,E)	12	6	5	E	1134.1924	1134.1857	6	0.149E+04	1.0
198	RQ(15, 3,A2)	15	4	3	A1	1134.1924	1134.2399	-47	0.245E+03	0.0
198	RQ(15, 3,A1)	15	4	3	A2	1134.1924	1134.2533	-60	0.247E+03	0.0
199	RQ(9, 6,A)	9	7	6	A	1134.7229	1134.7263	-3	0.592E+04	*1.0
200	PP(5, 5,E)	4	4	5	E	1134.9235	1134.9416	-18	0.196E+05	1.0
202	RQ(11, 5,E)	11	6	5	E	1135.3516	1135.3313	20	0.219E+04	1.0
202	PP(4, 3,A1)	3	2	3	A2	1135.3516	1135.3550	-3	0.154E+05	1.0
202	PP(4, 3,A2)	3	2	3	A1	1135.3516	1135.3566	-5	0.154E+05	1.0
202	RQ(13, 4,F)	13	5	4	F		1135.4452		0.766E+03	
203	RQ(8, 6,A)	8	7	6	A	1135.4851	1135.5013	-16	0.602E+04	*1.0
204	RQ(14, 3,A1)	14	4	3	A2	1136.0154	1136.0009	14	0.457E+03	1.0
204	RQ(14, 3,A2)	14	4	3	A1	1136.0154	1136.0267	-11	0.464E+03	1.0
205	RQ(7, 6,A)	7	7	6	A	1136.1837	1136.1784	5	0.444E+04	*1.0
205	PP(3, 1,E)	2	0	1	F	1136.1837	1136.1814	2	0.704E+04	1.0
206	RQ(10, 5,E)	10	6	5	E	1136.3487	1136.3589	-10	0.300E+04	1.0
207	RQ(12, 4,E)	12	5	4	E	1136.6780	1136.6765	1	0.151E+04	1.0
208	RQ(9, 5,E)	9	6	5	E	1137.2706	1137.2727	-2	0.381E+04	1.0
209	RQ(13, 3,A2)	13	4	3	A1	1137.6315	1137.6157	15	0.809E+03	1.0
209	RQ(13, 3,A1)	13	4	3	A2	1137.6315	1137.6471	-15	0.828E+03	1.0
210	RQ(11, 4,E)	11	5	4	E	1137.8728	1137.8750	-2	0.232E+04	1.0
211	RQ(14, 2,E)	14	3	2	E	1138.0714	1138.0642	7	0.[illegible]1E+03	1.0
211	RQ(8, 5,E)	8	6	5	E	1138.0714	1138.0776	-6	0.437E+04	1.0
213	RQ(7, 5,E)	7	6	5	E	1138.7793	1138.7784	0	0.431E+04	1.0
214	RQ(10, 4,E)	10	5	4	E	1138.9575	1138.9567	0	0.332E+04	1.0
215	RQ(12, 3,A1)	12	4	3	A2	1139.1355	1139.0822	53	0.136E+04	0.0
215	RQ(12, 3,A2)	12	4	3	A1	1139.1355	1139.1148	20	0.140E+04	1.0
215	PP(4, 4,E)	3	3	4	E	1139.1355	1139.1552	-19	0.196E+05	1.0
216	RQ(6, 5,E)	6	6	5	E	1139.3687	1139.3800	-11	0.309E+04	1.0
217	PP(3, 2,F)	2	1	2	E	1139.7247	1139.7205	4	0.118E+05	1.0
	RQ(13, 2,E)	13	3	2	E		1139.8420		0.584E+03	
218	RQ(9, 4,F)	9	5	4	E	1139.9074	1139.9179	-9	0.443E+04	1.0
219	RQ(11, 3,A2)	11	4	3	A1	1140.4136	1140.4005	13	0.215E+04	1.0

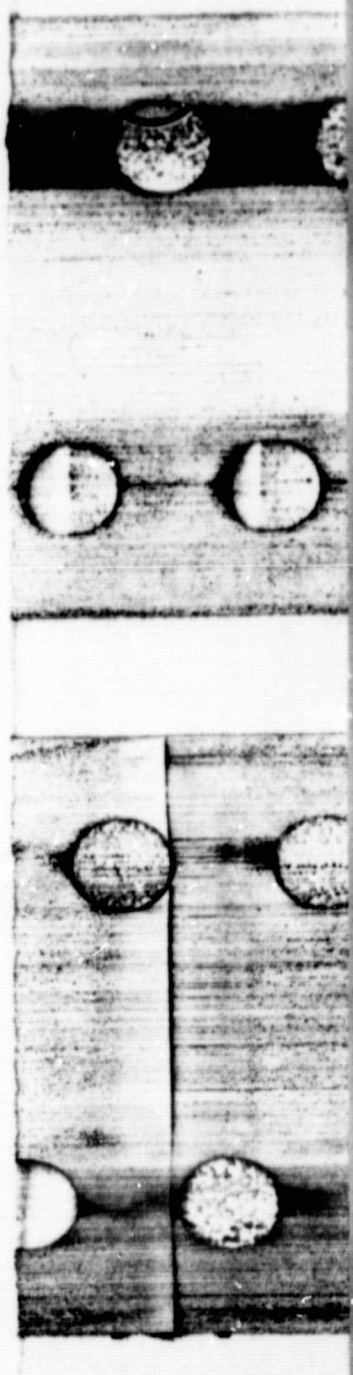

TABLE I—*Continued*

(I)	(II)	(III)	(IIII)	(IV)	(V)	(VI)	(VII)	(VIII)
219	R0(11, 3,A1)	11 4 3 A2		1140.4196	1140.4323	-13	0.222E+04	1.0
220	PP(2, 0,A1)	1 1 0 A2		1140.6345	1140.6293	5	0.407E+04	1.0
221	R0(8, 4,F)	8 5 4 F		1140.7552	1140.7605	-5	0.546E+04	1.0
222	R0(12, 2,E)	12 3 2 E		1141.4805	1141.4692	17	0.104E+04	1.0
222	R0(7, 4,F)	7 5 4 E		1141.4805	1141.4916	-11	0.608E+04	1.0
223	R0(10, 3,A1)	10 4 3 A2		1141.5830	1141.5721	10	0.317E+04	1.0
223	R0(13, 1,F)	13 2 1 E		1141.5830	1141.5854	-2	0.223E+03	1.0
223	R0(10, 3,A2)	10 4 3 A1		1141.5830	1141.6099	-20	0.332E+04	1.0
224	R0(6, 4,F)	6 5 4 E		1142.1154	1142.1165	-3	0.583E+04	1.0
225	R0(9, 3,A2)	9 4 3 A1		1142.6143	1142.5938	20	0.417E+04	1.0
225	R0(9, 3,A1)	9 4 3 A2		1142.6143	1142.6356	-21	0.466E+04	1.0
225	R0(5, 4,F)	5 5 4 E		1142.6143	1142.6407	-26	0.407E+04	1.0
226	R0(11, 2,E)	11 3 2 E		1142.9184	1142.9245	-6	0.176E+04	1.0
	X0(9, 3,A2)	9 1 0 A1			1143.1798		0.500E+03	
	X0(8, 3,A1)	8 1 0 A2			1143.2691		0.565E+03	
228	PP(3, 3,A2)	2 2 3 A1		1143.3959	1143.3939	1	0.172E+05	1.0
228	PP(3, 3,A1)	2 2 3 A2		1143.3959	1143.3949	1	0.172E+05	1.0
228	R0(12, 1,F)	12 2 1 E		1143.3959	1143.4030	-7	0.433E+03	1.0
229	R0(8, 3,A2)	8 4 3 A1		1143.5554	1143.5345	20	0.608E+04	1.0
229	R0(8, 3,A1)	8 4 3 A2		1143.5554	1143.5735	-18	0.553E+04	1.0
230	PP(2, 1,F)	1 0 1 F		1144.1264	1144.1166	9	0.609E+04	1.0
231	R0(10, 2,F)	10 3 2 F		1144.2186	1144.2251	-6	0.281E+04	1.0
232	R0(7, 3,A1)	7 4 3 A2		1144.3069	1144.3085	-1	0.731E+04	1.0
232	R0(7, 3,A2)	7 4 3 A1		1144.3069	1144.3132	-6	0.732E+04	1.0
233	R0(6, 3,A2)	6 4 3 A1		1144.9613	1144.9654	-4	0.793E+04	1.0
233	R0(6, 3,A1)	6 4 3 A2		1144.9613	1144.9663	-4	0.794E+04	1.0
234	R0(11, 1,F)	11 2 1 F		1145.0791	1145.0677	11	0.809E+03	1.0
235	R0(9, 2,F)	9 3 2 F		1145.3666	1145.3674	-0	0.420E+04	1.0
236	R0(5, 3,A1)	5 4 3 A2		1145.5140	1145.5127	1	0.741E+04	1.0
236	R0(5, 3,A2)	5 4 3 A1		1145.5140	1145.5129	1	0.741E+04	1.0
237	R0(4, 3,A2)	4 4 3 A1		1145.9561	1145.9576	-1	0.507E+04	1.0
237	R0(4, 3,A1)	4 4 3 A2		1145.9561	1145.9576	-1	0.507E+04	1.0
238	R0(8, 2,F)	8 3 2 F		1146.3544	1146.3569	-2	0.586E+04	1.0
239	R0(10, 1,F)	10 2 1 F		1146.5749	1146.5712	3	0.144E+04	1.0
240	R0(7, 2,F)	7 3 2 F		1147.1989	1147.2013	-2	0.756E+04	1.0
241	PP(2, 2,F)	1 1 2 F		1147.6644	1147.6634	1	0.120E+05	1.0
242	R0(9, 1,F)	9 2 1 F		1147.9051	1147.9067	-1	0.244E+04	1.0
242	R0(6, 2,F)	6 3 2 F		1147.9051	1147.9105	-5	0.896E+04	1.0
244	R0(5, 2,F)	5 3 2 F		1148.4903	1148.4946	-4	0.955E+04	1.0
245	R0(4, 2,F)	4 3 2 F		1148.9672	1148.9640	3	0.876E+04	1.0
246	R0(8, 1,F)	8 2 1 F		1149.0665	1149.0699	-3	0.386E+04	1.0
247	R0(3, 2,F)	3 3 2 F		1149.3300	1149.3277	2	0.592E+04	1.0
249	R0(7, 1,E)	7 2 1 F		1150.0611	1150.0606	0	0.569E+04	1.0
251	R0(6, 1,F)	6 2 1 F		1150.8815	1150.8835	-2	0.767E+04	1.0
252	R0(5, 1,F)	5 2 1 F		1151.5480	1151.5490	-1	0.935E+04	1.0
253	PP(1, 1,E)	0 0 1 E		1151.9797	1151.9670	12	0.441E+04	1.0
254	R0(4, 1,F)	4 2 1 E		1152.0797	1152.0713	2	0.101E+05	1.0
255	R0(3, 1,F)	3 2 1 E		1152.4711	1152.4660	5	0.933E+04	1.0
256	R0(2, 1,F)	2 2 1 F		1152.7598	1152.7479	5	0.639E+04	1.0
257	R0(17, 0,A2)	17 1 0 A1		1153.1300	1153.1152	14	0.496E+03	1.0
258	R0(16, 0,A1)	16 1 0 A2		1153.4663	1153.4827	-16	0.886E+03	1.0
259	P0(17, 1,F)	17 0 1 F		1153.6257	1153.6255	0	0.475E+03	1.0
260	X0(10, 0,A1)	10 4 3 A2		1153.8202	1153.7901	30	0.243E+03	0.0
260	R0(15, 0,A2)	15 1 0 A1		1153.8202	1153.8259	-5	0.152E+04	1.0
261	X0(14, 1,F)	14 5 4 F		1153.8687	1153.8721	-3	0.249E+03	0.0
262	P0(16, 1,F)	16 0 1 F		1154.0710	1154.0693	7	0.841E+03	1.0
263	R0(14, 0,A1)	14 1 0 A2		1154.1972	1154.1455	-8	0.251E+04	1.0
264	R0(13, 0,A2)	13 1 0 A1		1154.4428	1154.4420	0	0.395E+04	1.0
265	P0(15, 1,F)	15 0 1 F		1154.5140	1154.4943	19	0.141E+04	1.0
266	R0(12, 0,A1)	12 1 0 A2		1154.7168	1154.7159	0	0.597E+04	1.0

TABLE I—*Continued*

(I)	(II)	(III)				(IV)	(V)	(VI)	(VII)	(VIII)
267	XQ(9, 0,A2)	9	4	3	A1	1154.8341	1154.8341	0	0.106E+04	0.0
268	PQ(14, 1,F)	14	0	1	F	1154.9608	1154.9447	16	0.213E+04	1.0
268	RQ(11, 0,A2)	11	1	0	A1	1154.9608	1154.9681	-7	0.863E+04	1.0
269	PQ(13, 1,F)	13	0	1	F	1155.0730	1155.0774	-4	0.276E+04	1.0
270	RQ(10, 0,A1)	10	1	0	A2	1155.2043	1155.2002	4	0.118E+05	1.0
271	PQ(16, 2,F)	16	1	2	F	1155.3359	1155.3214	14	0.662E+03	1.0
271	PQ(17, 2,F)	17	1	2	F	1155.3359	1155.3299	6	0.295E+03	1.0
272	RQ(9, 0,A2)	9	1	0	A1	1155.4323	1155.4208	11	0.149E+05	1.0
273	RQ(8, 0,A1)	8	1	0	A2	1155.5236	1155.5286	-5	0.174E+05	1.0
274	PQ(12, 1,F)	12	0	1	E	1155.5896	1155.5996	-10	0.539E+04	1.0
275	XQ(13, 1,E)	13	5	4	E	1155.7269	1155.6814	45	0.942E+03	0.0
275	RQ(7, 0,A2)	7	1	0	A1	1155.7269	1155.7296	-2	0.239E+05	1.0
276	XQ(8, 0,A1)	8	4	3	A2	1155.8749	1155.8322	43	0.262E+04	0.0
276	RQ(6, 0,A1)	6	1	0	A2	1155.8749	1155.8783	-3	0.271E+05	1.0
277	RQ(5, 0,A2)	5	1	0	A1	1156.0149	1156.0025	12	0.288E+05	1.0
277	PQ(11, 1,E)	11	0	1	E	1156.0149	1156.0191	-4	0.776E+04	1.0
277	PQ(15, 2,E)	15	1	2	E	1156.0149	1156.0360	-21	0.127E+04	1.0
278	RQ(4, 0,A1)	4	1	0	A2	1156.1270	1156.1049	22	0.285E+05	1.0
279	RQ(3, 0,A2)	3	1	0	A1	1156.1915	1156.1864	5	0.258E+05	1.0
280	RQ(2, 0,A1)	2	1	0	A2	1156.2602	1156.2473	12	0.206E+05	1.0
280	RQ(1, 0,A2)	1	1	0	A1	1156.2602	1156.2879	-27	0.134E+05	1.0
	PQ(17, 3,A1)	17	2	3	A2		1156.3637		0.393E+03	
281	PQ(10, 1,E)	10	0	1	E	1156.4204	1156.4282	-7	0.104E+05	1.0
282	PQ(14, 2,E)	14	1	2	E	1156.6554	1156.6653	-9	0.208E+04	1.0
283	PQ(9, 1,E)	9	0	1	E	1156.8410	1156.8402	0	0.132E+05	1.0
284	PQ(16, 3,A2)	16	2	3	A1	1157.2618	1157.2532	8	0.688E+03	1.0
284	PQ(8, 1,E)	8	0	1	E	1157.2618	1157.2583	3	0.158E+05	1.0
284	PQ(13, 2,E)	13	1	2	E	1157.2618	1157.2788	-17	0.321E+04	1.0
285	PQ(17, 3,A2)	17	2	3	A1	1157.4050	1157.4072	-2	0.981E+03	1.0
286	PQ(7, 1,E)	7	0	1	E	1157.6870	1157.6807	6	0.177E+05	1.0
287	PQ(12, 2,E)	12	1	2	E	1157.8972	1157.8913	5	0.467E+04	1.0
288	PQ(6, 1,E)	6	0	1	E	1158.1056	1158.1001	5	0.186E+05	1.0
288	PQ(16, 3,A1)	16	2	3	A2	1158.1056	1158.1077	-2	0.674E+03	1.0
288	PQ(15, 3,A1)	15	2	3	A2	1158.1056	1158.1216	-15	0.115E+04	1.0
289	PQ(5, 1,E)	5	0	1	E	1158.5046	1158.5038	0	0.183E+05	1.0
289	PQ(11, 2,E)	11	1	2	E	1158.5041	1158.5061	-2	0.648E+04	1.0
290	PQ(15, 3,A2)	15	2	3	A1		1158.8063		0.113E+04	
290	PQ(4, 1,E)	4	0	1	E	1158.8825	1158.8758	6	0.168E+05	1.0
291	PQ(14, 3,A2)	14	2	3	A1	1158.9629	1158.9762	-13	0.182E+04	1.0
292	PQ(10, 2,E)	10	1	2	E	1159.1257	1159.1218	3	0.853E+04	1.0
293	PQ(3, 1,E)	3	0	1	E	1159.1994	1159.1985	0	0.142E+05	1.0
294	PQ(17, 4,E)	17	3	4	E	1159.4697	1159.4227	47	0.344E+03	0.0
294	PQ(2, 1,E)	2	0	1	E	1159.4697	1159.4560	13	0.107E+05	1.0
294	PQ(14, 3,A1)	14	2	3	A2	1159.4697	1159.5138	-44	0.180E+04	0.0
295	PQ(1, 1,E)	1	0	1	E	1159.6479	1159.6351	12	0.665E+04	1.0
296	PQ(9, 2,E)	9	1	2	E	1159.7306	1159.7328	-2	0.107E+05	1.0
297	PQ(13, 3,A1)	13	2	3	A2	1159.8150	1159.8190	-4	0.276E+04	1.0
298	PQ(13, 3,A2)	13	2	3	A1	1160.2949	1160.2318	3	0.273E+04	1.0
299	PQ(8, 2,E)	8	1	2	E	1160.3323	1160.3308	1	0.126E+05	1.0
299	PQ(16, 4,E)	16	3	4	E	1160.3323	1160.3593	-27	0.595E+03	0.0
300	PQ(12, 3,A2)	12	2	3	A1	1160.6409	1160.6486	-8	0.398E+04	1.0
301	PQ(7, 2,E)	7	1	2	E	1160.9291	1160.9050	24	0.141E+05	1.0
301	PQ(12, 3,A1)	12	2	3	A2	1160.9291	1160.9575	-28	0.395E+04	1.0
303	PQ(15, 4,E)	15	3	4	E	1161.2975	1161.2933	4	0.984E+03	1.0
304	PQ(6, 2,E)	6	1	2	E	1161.4481	1161.4431	4	0.149E+05	1.0
304	PQ(11, 3,A1)	11	2	3	A2	1161.4481	1161.4608	-12	0.547E+04	1.0
305	PQ(11, 3,A2)	11	2	3	A1	1161.6858	1161.6853	0	0.544E+04	1.0
306	PQ(5, 2,E)	5	1	2	E	1161.9375	1161.9324	5	0.148E+05	1.0
307	PQ(14, 4,E)	14	3	4	E	1162.2417	1162.2290	18	0.155E+04	1.0
307	PQ(10, 3,A2)	10	2	3	A1	1162.2417	1162.2493	-7	0.716E+04	1.0

TABLE I—*Continued*

(I)	(II)					(III)	(IV)	(V)	(VI)	(VII)	(VIII)
307	PQ(17, 5,E)	17	4	5	E	1162.2417	1162.2535	-11	0.298E+03	1.0	
308	PQ(4, 2,F)	4	1	2	E	1162.3789	1162.3608	18	0.135E+05	1.0	
308	PQ(10, 3,A1)	10	2	3	A2	1162.3789	1162.4069	-27	0.714E+04	1.0	
310	PQ(3, 2,E)	3	1	2	E	1162.7175	1162.7172	0	0.108E+05	1.0	
311	PQ(2, 2,E)	2	1	2	E	1163.0054	1162.9927	12	0.674E+04	1.0	
311	PQ(9, 3,A1)	9	2	3	A2	1163.0054	1163.0062	-0	0.891E+04	1.0	
312	PQ(9, 3,A2)	9	2	3	A1	1163.1220	1163.1124	9	0.889E+04	1.0	
312	PQ(13, 4,E)	13	3	4	E	1163.1220	1163.1445	-22	0.234E+04	1.0	
313	PQ(16, 5,E)	16	4	5	E	1163.3256	1163.3341	-8	0.312E+03	1.0	
314	PQ(8, 3,A2)	8	2	3	A1	1163.7303	1163.7226	7	0.105E+05	1.0	
315	PQ(8, 3,A1)	8	2	3	A2	1163.7768	1163.7907	-13	0.105E+05	1.0	
316	RR(0, 0,A1)	1	1	0	A2	1163.9259	1163.9084	17	0.931E+04	1.0	
317	PQ(12, 4,F)	12	3	4	F	1164.0524	1164.0517	0	0.336E+04	1.0	
319	PQ(7, 3,A1)	7	2	3	A2	1164.4066	1164.3889	17	0.117E+05	1.0	
319	PQ(15, 5,E)	15	4	5	E	1164.4066	1164.4068	-0	0.842E+03	1.0	
319	PQ(7, 3,A2)	7	2	3	A1	1164.4066	1164.4300	-23	0.117E+05	1.0	
321	PQ(11, 4,E)	11	3	4	F	1164.9964	1164.9373	59	0.461E+04	0.0	
321	PQ(6, 3,A2)	6	2	3	A1	1164.9964	1164.9957	0	0.122E+05	1.0	
321	PQ(6, 3,A1)	6	2	3	A2	1164.9964	1165.0187	-22	0.122E+05	1.0	
323	PQ(17, 6,A)	17	5	6	A	1165.3010	1165.3168	-15	0.510E+03	*1.0	
324	PQ(14, 5,E)	14	4	5	E		1165.4667		0.132E+[illegible]		
324	PQ(5, 3,A1)	5	2	3	A2	1165.5366	1165.5340	2	0.116E+[illegible]	1.0	
324	PQ(5, 3,A2)	5	2	3	A1	1165.5366	1165.5455	-8	0.116E+05	1.0	
325	PQ(10, 4,F)	10	3	4	F	1165.8049	1165.7927	12	0.600E+04	1.0	
326	PQ(4, 3,A2)	4	2	3	A1	1166.0012	1165.9957	5	0.973E+04	1.0	
326	PQ(4, 3,A1)	4	2	3	A2	1166.0012	1166.0007	0	0.973E+04	1.0	
327	PQ(3, 3,A1)	3	2	3	A2	1166.3741	1166.3738	0	0.612E+04	1.0	
327	PQ(3, 3,A2)	3	2	3	A1	1166.3741	1166.3754	-1	0.612E+04	1.0	
328	PQ(13, 5,E)	13	4	5	F	1166.5220	1166.5077	14	0.198E+04	1.0	
328	PQ(16, 6,A)	16	5	6	A	1166.5220	1166.5330	-11	0.870E+03	*1.0	
329	PQ(9, 4,E)	9	3	4	E	1166.6036	1166.6085	-4	0.741E+04	1.0	
331	PQ(8, 4,E)	8	3	4	F	1167.3704	1167.3753	-4	0.862E+04	1.0	
332	PQ(12, 5,F)	12	4	5	E	1167.5238	1167.5224	1	0.283E+04	1.0	
333	PQ(15, 6,A)	15	5	6	A	1167.7372	1167.7330	4	0.142E+04	*1.0	
334	PQ(7, 4,E)	7	3	4	E	1168.0755	1168.0838	-8	0.937E+04	1.0	
335	RR(1, 1,E)	2	2	1	F	1168.2734	1168.2663	7	0.137E+05	1.0	
336	PQ(11, 5,E)	11	4	5	E	1168.5098	1168.5026	7	0.384E+04	1.0	
	PQ(17, 7,E)	17	6	7	F		1168.5681		0.214E+03		
337	PQ(6, 4,E)	6	3	4	E	1168.7151	1168.7249	-9	0.931E+04	1.0	
338	PQ(14, 6,[illegible])	14	5	6	A	1168.9218	1168.9104	11	0.222E+04	*1.0	
339	PQ(5, 4,[illegible])	5	3	4	F	1169.2837	1169.2904	-6	0.806E+04	1.0	
340	PQ(10, 5,E)	10	4	5	E	1169.4468	1169.4397	5	0.494E+04	1.0	
341	PQ(4, 4,E)	4	3	4	E	1169.7676	1169.7732	-5	0.518E+04	1.0	
	PQ(16, 7,E)	16	6	7	F		1169.8136		0.364E+03		
342	PQ(13, 6,A)	13	5	6	A	1170.0698	1170.0580	11	0.329E+04	*1.0	
343	PQ(9, 5,E)	9	4	5	F	1170.3242	1170.3248	-0	0.599E+04	1.0	
344	PQ(8, 5,E)	8	4	5	E	1171.1640	1171.1494	14	0.677E+04	1.0	
344	PQ(12, 6,A)	12	5	6	A	1171.1640	1171.1681	-4	0.466E+04	*1.0	
	PQ(15, 7,E)	15	6	7	E		1171.2337		0.589E+03		
345	RR(1, 0,A2)	2	1	0	A1	1171.3567	1171.3481	8	0.135E+05	1.0	
346	PQ(7, 5,E)	7	4	5	E	1171.8919	1171.9051	-13	0.698E+04	1.0	
347	PQ(11, 6,A)	11	5	6	A	1172.2383	1172.2324	5	0.624E+04	*1.0	
348	PQ(14, 7,E)	14	6	7	E	1172.5219	1172.5213	0	0.911E+03	1.0	
349	PQ(6, 5,E)	6	4	5	F	1172.5909	1172.5842	6	0.625E+04	1.0	
349	RR(2, 2,E)	3	3	2	F	1172.5909	1172.6000	-9	0.206E+05	1.0	
350	PQ(5, 5,E)	5	4	5	E	1173.1764	1173.1787	-3	0.413E+04	1.0	
351	PQ(10, 6,A)	10	5	6	A	1173.2458	1173.2427	3	0.787E+04	*1.0	
	PQ(16, 8,E)	16	7	8	E		1173.4522		0.298E+03		
353	PQ(13, 7,E)	13	6	7	E	1173.7931	1173.7689	24	0.134E+04	1.0	
355	PQ(9, 6,A)	9	5	6	A	1174.1964	1174.1906	5	0.923E+04	*1.0	

TABLE I—*Continued*

(I)	(II)	(III)	(IV)	(V)	(VI)	(VII)	(VIII)
358	PQ(15, 8,E)	15 7 8 E	1174.8396	1174.8892	-59	0.479E+03	0.0
359	PQ(12, 7,E)	12 6 7 E	1174.9840	1174.9687	15	0.186E+04	1.0
359	PR(1, 1,E)	2 0 1 E	1174.9840	1174.9744	9	0.197E+04	1.0
360	PQ(8, 6,A)	8 5 6 A	1175.0548	1175.0684	-13	0.987E+04	*1.0
362	PQ(17, 9,A)	17 8 9 A	1175.5188	1175.5309	-21	0.286E+03	*1.0
363	PR(2, 1,E)	3 2 1 E	1175.7405	1175.7405	0	0.147E+05	1.0
364	PQ(7, 6,A)	7 5 6 A	1175.8670	1175.8685	-11	0.914E+04	*1.0
365	PQ(11, 7,E)	11 6 7 E	1176.1182	1176.1125	5	0.244E+04	1.0
366	PQ(14, 8,E)	14 7 8 E	1176.2725	1176.2840	-11	0.731E+03	1.0
368	PQ(6, 6,A)	6 5 6 A	1176.5856	1176.5842	-18	0.621E+04	*1.0
369	PR(3, 3,A2)	4 4 3 A1	1176.9803	1176.9764	3	0.249E+05	1.0
369	PR(3, 3,A1)	4 4 3 A2	1176.9803	1176.9764	3	0.249E+05	1.0
370	PQ(16, 9,A)	16 8 9 A	1177.1972	1177.1975	89	0.478E+03	0.0
370	PQ(10, 7,E)	10 6 7 E	1177.1972	1177.1935	4	0.298E+04	1.0
371	PQ(13, 8,E)	13 7 8 E	1177.6501	1177.6290	21	0.106E+04	1.0
372	PQ(9, 7,E)	9 6 7 E	1178.2003	1178.2010	-0	0.330E+04	1.0
373	PR(2, 0,A1)	3 1 0 A2	1178.6336	1178.6267	6	0.168E+05	1.0
373	PQ(15, 9,A)	15 8 9 A	1178.6336	1178.6910	-57	0.757E+03	0.0
374	PQ(12, 8,E)	12 7 8 E	1178.9228	1178.9165	6	0.144E+04	1.0
375	PQ(8, 7,E)	8 6 7 E	1179.1112	1179.1308	-19	0.316E+04	1.0
376	PQ(7, 7,E)	7 6 7 E	1179.9821	1179.9752	6	0.221E+04	1.0
376	PR(3, 2,E)	4 3 2 E	1179.9821	1179.9878	-5	0.198E+05	1.0
377	PQ(11, 8,E)	11 7 8 E	1180.1522	1180.1386	13	0.182E+04	1.0
377	PQ(14, 9,A)	14 8 9 A	1180.1522	1180.1928	-40	0.114E+04	*1.0
379	PQ(10, 8,E)	10 7 8 E	1181.3008	1181.2879	12	0.209E+04	1.0
380	PR(4, 4,E)	5 5 4 E	1181.3938	1181.3960	-2	0.263E+05	1.0
381	PQ(13, 9,A)	13 8 9 A	1181.6247	1181.6352	-10	0.160E+04	*1.0
382	PQ(9, 8,E)	9 7 8 E	1182.3589	1182.3572	1	0.207E+04	1.0
383	PR(2, 1,E)	3 0 1 E	1182.4813	1182.4731	8	0.336E+04	1.0
	PQ(15,10,E)	15 9 10 F		1182.6374		0.290E+03	
385	PQ(12, 9,A)	12 8 9 A	1183.0211	1183.0108	10	0.210E+04	*1.0
386	PR(3, 1,E)	4 2 1 E	1183.1014	1183.0981	3	0.157E+05	1.0
387	PQ(8, 8,E)	8 7 8 E	1183.3333	1183.3398	-6	0.149E+04	1.0
	PQ(14,10,E)	14 9 10 E		1184.2477		0.424E+03	
391	PR(4, 3,A1)	5 4 3 A2	1184.2873	1184.2768	10	0.224E+05	1.0
391	PR(4, 3,A2)	5 4 3 A1	1184.2873	1184.2770	10	0.224E+05	1.0
391	PQ(11, 9,A)	11 8 9 A	1184.2873	1184.3120	-24	0.250E+04	*1.0
395	PQ(10, 9,A)	10 8 9 A	1185.5379	1185.5318	6	0.257E+04	*1.0
396	PR(3, 0,A2)	4 1 0 A1	1185.7496	1185.7441	5	0.189E+05	1.0
396	PQ(13,10,E)	13 9 10 E	1185.7496	1185.7803	-30	0.576E+03	1.0
397	PR(5, 5,E)	6 6 5 E	1185.8514	1185.8500	-7	0.251E+05	1.0
398	PR(2, 2,E)	3 1 2 E	1185.9970	1185.9895	7	0.117E+04	1.0
401	PQ(9, 9,A)	9 8 9 A	1186.6619	1186.6635	-1	0.192E+04	*1.0
	PQ(15,11,E)	15 10 11 F		1186.7313		0.213E+03	
403	PQ(12,10,E)	12 9 10 E	1187.2654	1187.2540	10	0.711E+03	1.0
403	PR(4, 2,E)	5 3 2 E	1187.2654	1187.2650	0	0.188E+05	1.0
	PQ(14,11,E)	14 10 11 E		1188.4528		0.300E+03	
407	PR(5, 4,E)	6 5 4 E	1188.6120	1188.6091	2	0.225E+05	1.0
407	PQ(11,10,E)	11 9 10 E	1188.6120	1188.6374	-25	0.755E+03	1.0
	PQ(16,12,A)	16 11 12 A		1189.0621		0.203E+03	
411	PR(3, 1,E)	4 0 1 E	1189.9170	1189.9026	14	0.400E+04	1.0
411	PQ(10,10,E)	10 9 10 E	1189.9170	1189.9300	-13	0.583E+03	1.0
412	PQ(13,11,E)	13 10 11 E	1190.0966	1190.0964	-59	0.384E+03	0.0
413	PR(4, 1,E)	5 2 1 F	1190.3431	1190.3232	19	0.162E+05	1.0
413	PR(6, 6,A)	7 7 6 A	1190.3431	1190.3656	-22	0.441E+05	*1.0
	PQ(15,12,A)	15 11 12 A		1190.9784		0.297E+03	
414	PR(5, 3,A2)	6 4 3 A1	1191.4674	1191.4685	-1	0.198E+05	1.0
414	PR(5, 3,A1)	6 4 3 A2	1191.4674	1191.4694	-1	0.198E+05	1.0
415	PQ(12,11,E)	12 10 11 F	1191.6619	1191.6549	6	0.622E+03	1.0
419	PR(4, 0,A1)	5 1 0 A2	1192.7006	1192.7007	-0	0.196E+05	1.0

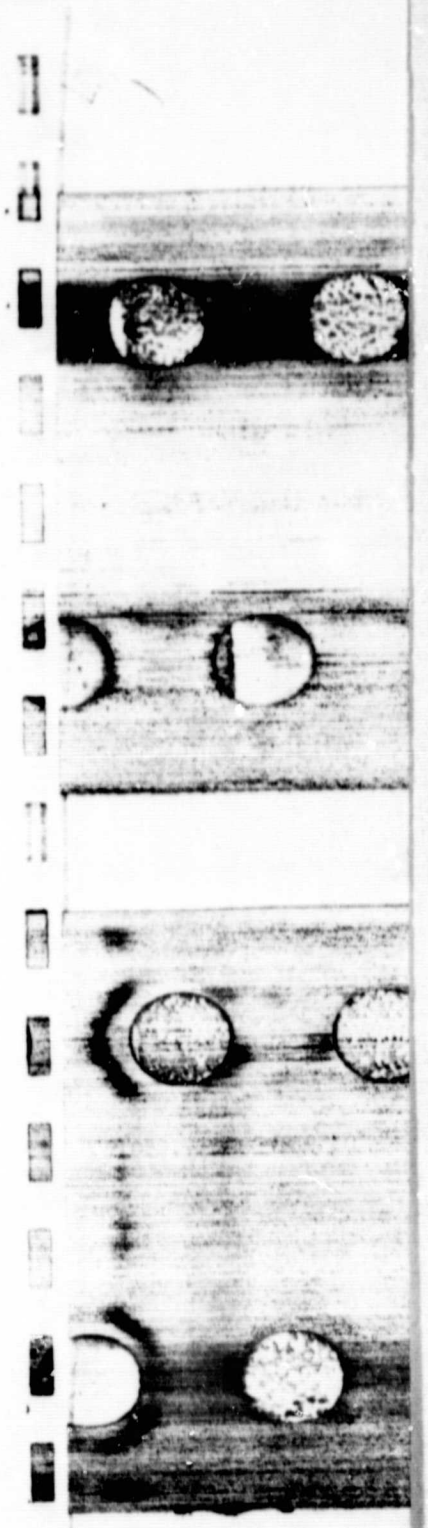

TABLE I—*Continued*

(I)	(II)	(III)				(IV)	(V)	(VI)	(VII)	(VIII)
	PQ(14,12,A)	14	11	12	A		1192.8146		0.393E+03	
420	RR(6, 5,E)	7	6	5	E	1192.9800	1192.9850	4	0.206E+05	1.0
421	PQ(11,11,E)	11	10	11	E	1193.1956	1193.1215	14	0.337E+03	1.0
422	RR(3, 2,E)	4	1	2	E	1193.4270	1193.3846	42	0.220E+04	0.0
424	RR(5, 2,E)	6	3	2	E	1194.4227	1194.4211	1	0.179E+05	1.0
425	PQ(13,12,A)	13	11	12	A	1194.5055	1194.5635	-57	0.447E+03	0.0
427	RR(7, 7,E)	8	8	7	E	1194.9130	1194.9161	-3	0.180E+05	1.0
428	RR(6, 4,E)	7	5	4	E	1195.7023	1195.7140	-11	0.188E+05	1.0
429	PQ(12,12,A)	12	11	12	A	1196.2099	1196.2183	-8	0.370E+03	*1.0
431	RR(3, 3,A2)	4	2	3	A1	1197.0194	1197.0145	4	0.732E+03	1.0
431	RR(3, 3,A1)	4	2	3	A2	1197.0194	1197.0195	-0	0.732E+03	1.0
433	RR(4, 1,E)	5	0	1	E	1197.2856	1197.2779	7	0.394E+04	1.0
434	RR(5, 1,E)	6	2	1	F	1197.3924	1197.3987	-6	0.160E+05	1.0
434	RR(7, 6,A)	8	7	6	A	1197.3924	1197.4047	-12	0.346E+05	*1.0
437	RR(6, 3,A1)	7	4	3	A2	1198.5393	1198.5431	-3	0.170E+05	1.0
437	RR(6, 3,A2)	7	4	3	A1	1198.5393	1198.5478	-8	0.169E+05	1.0
440	RR(5, 0,A2)	6	1	0	A1	1199.5006	1199.4971	3	0.190E+05	1.0
440	RR(8, 8,E)	9	9	8	F	1199.5006	1199.5109	-10	0.137E+05	1.0
442	RR(7, 5,E)	8	6	5	F	1199.9911	1200.0030	-11	0.164E+05	1.0
443	RR(4, 2,E)	5	1	2	E	1200.7096	1200.7038	6	0.280E+04	1.0
444	RR(6, 2,E)	7	3	2	F	1201.4401	1201.4447	-4	0.155E+05	1.0
446	RR(8, 7,E)	9	8	7	F	1201.8674	1201.8685	-1	0.135E+05	1.0
448	RR(7, 4,E)	8	5	4	F	1202.6779	1202.7030	-26	0.153E+05	1.0
452	RR(9, 9,A)	10	10	9	A	1204.1588	1204.1510	8	0.195E+05	*1.0
453	RR(4, 3,A1)	5	2	3	A2	1204.3074	1204.3981	9	0.143E+04	1.0
453	RR(6, 1,E)	7	2	1	F	1204.3074	1204.3082	-1	0.150E+05	1.0
453	RR(4, 3,A2)	5	2	3	A1	1204.3074	1204.3096	-2	0.143E+04	1.0
453	RR(8, 6,A)	9	7	6	A	1204.3074	1204.3360	-28	0.264E+05	*1.0
454	RR(5, 1,E)	6	0	1	E	1204.6149	1204.6152	-0	0.338E+04	1.0
455	XR(7, 3,A1)	8	1	0	A2	1205.2216	1205.2265	-5	0.201E+04	0.0
456	RR(7, 3,A2)	8	4	3	A1	1205.5088	1205.4910	17	0.142E+05	1.0
456	RR(7, 3,A1)	8	4	3	A2	1205.5088	1205.5309	-21	0.121E+05	1.0
458	RR(6, 0,A1)	7	1	0	A2	1206.1305	1206.1344	-3	0.174E+05	1.0
459	RR(9, 8,E)	10	9	8	F	1206.3928	1206.3765	16	0.990E+04	1.0
460	RR(8, 5,E)	9	6	5	F	1206.9015	1206.9071	-5	0.127E+05	1.0
462	RR(5, 2,E)	6	1	2	E	1207.9635	1207.9537	9	0.292E+04	1.0
463	RR(4, 4,E)	5	3	4	E	1208.0476	1208.0457	1	0.443E+03	1.0
464	RR(7, 2,E)	8	3	2	F	1208.3238	1208.3243	-0	0.133E+05	1.0
465	RR(9, 7,E)	10	8	7	F	1208.7193	1208.7130	6	0.989E+04	1.0
466	RR(10,10,E)	11	11	10	F	1208.8532	1208.8377	15	0.653E+04	1.0
468	RR(8, 4,E)	9	5	4	E	1209.5714	1209.5719	-0	0.120E+05	1.0
469	RR(10, 9,A)	11	10	9	A	1210.9378	1210.9299	7	0.136E+05	*1.0
470	RR(7, 1,E)	8	2	1	F	1211.0420	1211.0433	-1	0.134E+05	1.0
471	RR(9, 6,A)	10	7	6	A	1211.1481	1211.1539	-5	0.195E+05	*1.0
473	RR(5, 3,A2)	6	2	3	A1	1211.5145	1211.4988	15	0.184E+04	1.0
473	RR(5, 3,A1)	6	2	3	A2	1211.5145	1211.5218	-7	0.184E+04	1.0
474	RR(6, 1,E)	7	0	1	E	1211.9584	1211.9294	29	0.259E+04	1.0
476	RR(8, 3,A2)	9	4	3	A1	1212.2758	1212.2640	11	0.107E+05	1.0
476	RR(8, 3,A1)	9	4	3	A2	1212.2758	1212.3058	-29	0.114E+05	1.0
478	RR(7, 0,A2)	8	1	0	A1	1212.6107	1212.6140	-3	0.151E+05	1.0
479	XR(8, 3,A2)	9	1	0	A1	1212.8518	1212.8500	2	0.652E+03	0.0
481	RR(10, 8,E)	11	9	8	F	1213.1366	1213.1346	2	0.694E+04	1.0
483	RR(11,11,E)	12	12	11	F	1213.5843	1213.5732	11	0.412E+04	1.0
484	RR(9, 5,E)	10	6	5	E	1213.6911	1213.6910	0	0.948E+04	1.0
486	RR(8, 2,E)	9	3	2	E	1215.0458	1215.0488	-3	0.110E+05	1.0
487	RR(6, 2,E)	7	1	2	F	1215.1651	1215.1484	16	0.267E+04	1.0
487	RR(5, 4,E)	6	3	4	F	1215.1651	1215.2174	-52	0.908E+03	0.0
488	RR(10, 7,E)	11	8	7	F	1215.4534	1215.4449	8	0.700E+04	1.0
489	RR(11,10,E)	12	11	10	F	1215.5340	1215.5294	4	0.438E+04	1.0
491	RR(9, 4,E)	10	5	4	F	1216.3084	1216.3112	-2	0.914E+04	1.0

TABLE I—*Continued*

(I)	(II)	(III)	(IV)	(V)	(VI)	(VII)	(VIII)
493	RR(8, 1,E)	9 2 1 E	1217.5994	1217.5948	4	0.114E+05	1.0
493	RR(11, 9,A)	12 10 9 A	1217.5994	1217.6012	-1	0.915E+04	*1.0
494	RR(10, 6,A)	11 7 6 A	1217.8512	1217.8532	-2	0.139E+05	*1.0
495	RR(12,12,A)	13 13 12 A	1218.3644	1218.3604	4	0.491E+04	*1.0
497	RR(6, 3,A1)	7 2 3 A2	1218.6394	1218.6235	15	0.193E+04	1.0
497	RR(6, 3,A2)	7 2 3 A1	1218.6394	1218.6647	-25	0.193E+04	1.0
498	RR(8, 0,A1)	9 1 0 A2	1218.9610	1218.9377	23	0.125E+05	1.0
498	RR(9, 3,A1)	10 4 3 A2	1218.9610	1218.9440	17	0.873E+04	1.0
498	RR(9, 3,A2)	10 4 3 A1	1218.9610	1218.9757	-14	0.884E+04	1.0
	RR(5, 5,E)	6 4 5 E		1219.0632		0.290E+03	
499	RR(7, 1,E)	8 0 1 E	1219.2360	1219.2317	4	0.180E+04	1.0
500	RR(11, 8,E)	12 9 8 E	1219.7781	1219.7804	-2	0.471E+04	1.0
501	RR(12,11,E)	13 12 11 E	1220.1868	1220.1768	11	0.266E+04	1.0
502	RR(10, 5,E)	11 6 5 E	1220.3453	1220.3488	-3	0.686E+04	1.0
507	RR(9, 2,E)	10 3 2 E	1221.6104	1221.6093	1	0.874E+04	1.0
510	RR(11, 7,E)	12 8 7 E	1222.0477	1222.0593	8	0.479E+04	1.0
511	RR(12,10,E)	13 11 10 E	1222.1194	1222.1137	5	0.284E+04	1.0
512	RR(7, 2,E)	8 1 2 E	1222.2935	1222.2982	-4	0.219E+04	1.0
512	RR(6, 4,E)	7 3 4 E	1222.2935	1222.3061	-12	0.116E+04	1.0
514	RR(10, 4,E)	11 5 4 E	1222.9127	1222.9170	-4	0.668E+04	1.0
516	RR(13,13,E)	14 14 13 E	1223.1984	1223.2029	-4	0.138E+04	1.0
517	RR(9, 1,E)	10 2 1 E	1223.9604	1223.9628	-2	0.914E+04	1.0
519	RR(12, 9,A)	13 10 9 A	1224.1646	1224.1609	3	0.596E+04	*1.0
520	RR(11, 6,A)	12 7 6 A	1224.4254	1224.4286	-3	0.962E+04	*1.0
521	RR(13,12,A)	14 13 12 A	1224.8808	1224.8744	6	0.309E+04	*1.0
522	RR(9, 0,A2)	10 1 0 A1	1225.1003	1225.1077	-7	0.980E+04	1.0
524	RR(10, 3,A2)	11 4 3 A1	1225.4745	1225.4615	12	0.657E+04	1.0
524	RR(10, 3,A1)	11 4 3 A2	1225.4745	1225.4933	-18	0.660E+04	1.0
525	RR(7, 3,A2)	8 2 3 A1	1225.6837	1225.6800	3	0.177E+04	1.0
526	RR(7, 3,A1)	8 2 3 A2	1225.7488	1225.7481	0	0.178E+04	1.0
527	RR(6, 5,E)	7 4 5 E	1226.1009	1226.1117	-10	0.563E+03	1.0
528	RR(12, 8,E)	13 9 8 E	1226.3102	1226.3099	0	0.309E+04	1.0
529	RR(8, 1,E)	9 0 1 E	1226.5237	1226.5283	-4	0.115E+04	1.0
530	RR(13,11,E)	14 12 11 E	1226.6808	1226.6733	7	0.166E+04	1.0
532	RR(11, 5,E)	12 6 5 E	1226.8802	1226.8751	5	0.479E+04	1.0
533	RR(10, 2,E)	11 3 2 E	1228.0032	1227.9991	4	0.665E+04	1.0
534	RR(14,14,E)	15 15 14 E	1228.0688	1228.1058	-36	0.734E+03	1.0
536	RR(12, 7,E)	13 8 7 E	1228.5651	1228.5516	13	0.317E+04	1.0
536	RR(13,10,E)	14 11 10 E	1228.5651	1228.5870	-21	0.178E+04	1.0
537	RR(7, 4,E)	8 3 4 E	1229.3089	1229.3188	-9	0.121E+04	1.0
538	RR(11, 4,E)	12 5 4 E	1229.4056	1229.3924	13	0.464E+04	1.0
538	RR(8, 2,E)	9 1 2 E	1229.4056	1229.4142	-8	0.165E+04	1.0
539	RR(14,13,E)	15 14 13 E	1229.6141	1229.6249	-10	0.826E+03	1.0
540	RR(6, 6,A)	7 5 6 A	1230.0239	1230.0557	-31	0.354E+03	*1.0
541	RR(10, 1,E)	11 2 1 E	1230.1425	1230.1504	-7	0.698E+04	1.0
543	RR(13, 9,A)	14 10 9 A	1230.6298	1230.6053	24	0.376E+04	*1.0
544	RR(12, 6,A)	13 7 6 A	1230.8755	1230.8751	0	0.642E+04	*1.0
546	RR(10, 0,A1)	11 1 0 A2	1231.1227	1231.1266	-3	0.736E+04	1.0
547	RR(14,12,A)	15 13 12 A	1231.2448	1231.2816	-3	0.183E+04	*1.0
549	RR(11, 3,A1)	12 4 3 A2	1231.8922	1231.8188	13	0.473E+04	1.0
549	RR(11, 3,A2)	12 4 3 A1	1231.8922	1231.8513	-19	0.474E+04	1.0
551	RR(8, 3,A1)	9 2 3 A2	1232.7025	1232.6764	26	0.147E+04	1.0
551	RR(13, 8,E)	14 9 8 E	1232.7025	1232.7188	-16	0.196E+04	1.0
552	RR(8, 3,A2)	9 2 3 A1	1232.7653	1232.7827	-17	0.147E+04	1.0
554	RR(14,11,E)	15 12 11 E	1233.0654	1233.0595	5	0.999E+03	1.0
554	RR(7, 5,E)	8 4 5 E	1233.0654	1233.0748	-9	0.712E+03	1.0
554	RR(15,15,A)	16 16 15 A	1233.0654	1233.0750	-9	0.738E+03	*1.0
555	RR(12, 5,E)	13 6 5 E	1233.3071	1233.2658	41	0.322E+04	0.0
556	RR(9, 1,E)	10 0 1 E	1233.8187	1233.8199	-1	0.691E+03	1.0
557	RR(11, 2,E)	12 3 2 E	1234.2034	1234.2145	-11	0.483E+04	1.0

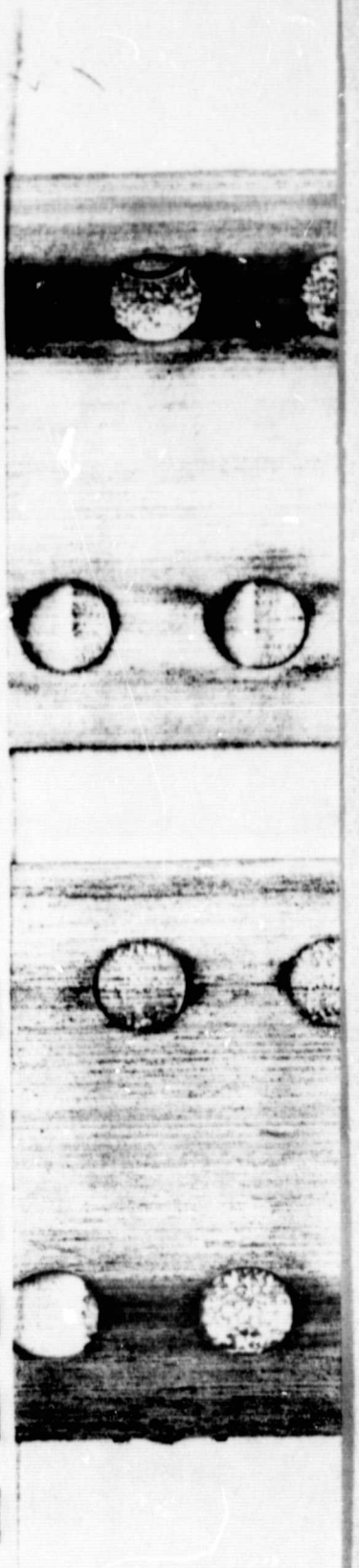

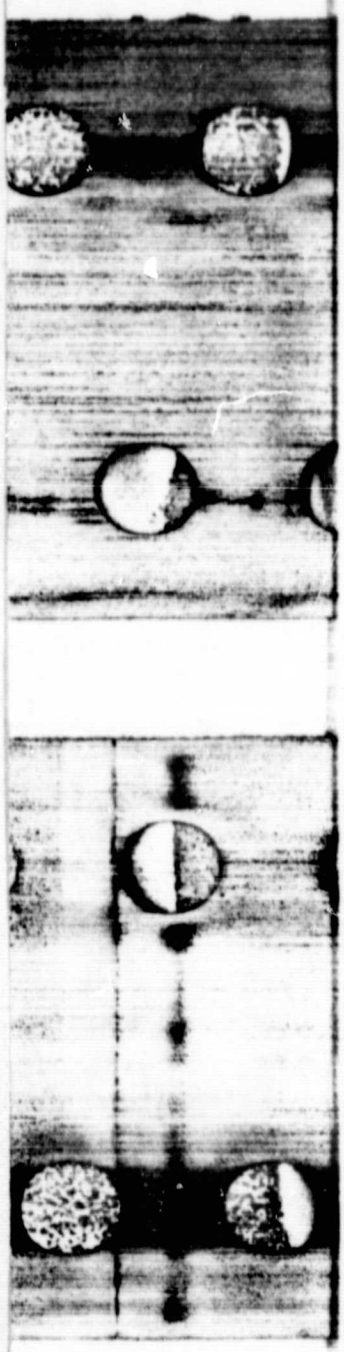

TABLE I—*Continued*

(I)	(II)	(III)				(IV)	(V)	(VI)	(VII)	(VIII)
	RR(15,14,E)	16	15	14	E		1234.4321		0.423E+03	
559	RR(13, 7,E)	14	8	7	E	1234.9356	1234.9175	18	0.202E+04	1.0
559	RR(14,10,F)	15	11	10	E	1234.9356	1234.9460	-10	0.108E+04	1.0
560	XR(12, 4,E)	13	0	1	E	1235.2015	1235.2160	-15	0.840E+03	0.0
561	RR(12, 4,E)	13	5	4	E	1235.8228	1235.8203	2	0.240E+04	1.0
562	RR(15,13,E)	16	14	13	E	1235.9429	1235.9405	2	0.477E+03	1.0
563	RR(11, 1,E)	12	2	1	E	1236.1423	1236.1632	-20	0.508E+04	1.0
564	PR(8, 4,E)	9	3	4	E	1236.2769	1236.2631	13	0.110E+04	1.0
565	PR(9, 2,F)	10	1	2	F	1236.5009	1236.5060	-5	0.115E+04	1.0
566	RR(14, 9,A)	15	10	9	A	1236.9774	1236.9306	46	0.229E+04	0.0
566	PR(7, 6,A)	8	5	6	A	1236.9774	1236.9718	5	0.676E+03	*1.0
566	RR(11, 0,A2)	12	1	0	A1	1236.9774	1236.9973	-19	0.529E+04	1.0
567	RR(13, 6,A)	14	7	6	A	1237.1911	1237.1887	2	0.413E+04	*1.0
569	RR(15,12,A)	16	13	12	A	1237.5848	1237.5792	5	0.106E+04	*1.0
571	RR(12, 3,A2)	13	4	3	A1	1238.0264	1238.0130	13	0.327E+04	1.0
571	RR(12, 3,A1)	13	4	3	A2	1238.0264	1238.0443	-17	0.327E+04	1.0
573	RR(14, 8,F)	15	9	8	E	1239.0064	1239.0035	2	0.120E+04	1.0
575	RR(16,15,A)	17	16	15	A	1239.3313	1239.3003	31	0.410E+03	*1.0
575	RR(15,11,F)	16	12	11	E	1239.3313	1239.3324	-1	0.582E+03	1.0
576	RR(13, 5,F)	14	6	5	E	1239.5282	1239.5204	7	0.208E+04	1.0
577	PR(9, 3,A2)	10	2	3	A1	1239.6404	1239.6211	19	0.111E+04	1.0
578	PR(9, 3,A1)	10	2	3	A2	1239.7643	1239.7787	-14	0.112E+04	1.0
579	PR(8, 5,F)	9	4	5	E	1239.9701	1239.9502	10	0.728E+03	1.0
581	RR(12, 2,F)	13	3	2	E	1240.2564	1240.2551	1	0.336E+04	1.0
582	RR(16,14,F)	17	15	14	E	1240.6633	1240.6523	11	0.235E+03	1.0
584	PR(10, 1,F)	11	0	1	E	1241.1576	1241.1018	55	0.392E+03	0.0
584	RR(14, 7,E)	15	8	7	E	1241.1576	1241.1534	4	0.125E+04	1.0
584	RR(15,10,F)	16	11	10	E	1241.1577	1241.1875	-29	0.630E+03	1.0
586	RR(13, 4,F)	14	5	4	F	1241.7019	1241.6995	2	0.191E+04	1.0
587	RR(12, 1,F)	13	2	1	E	1242.0036	1242.0081	-4	0.353E+04	1.0
	RR(16,13,F)	17	14	13	E		1242.1472		0.267E+03	
589	RR(12, 0,A1)	13	1	0	A2	1242.7279	1242.7233	4	0.363E+04	1.0
589	XR(13, 4,F)	14	0	1	E	1242.7279	1242.7716	-44	0.214E+03	0.0
590	RR(15, 9,A)	16	10	9	A	1243.1416	1243.1338	7	0.135E+04	*1.0
590	PR(9, 4,F)	10	3	4	E	1243.1416	1243.1471	-5	0.900E+03	1.0
591	RR(14, 6,A)	15	7	6	A	1243.3736	1243.3669	6	0.256E+04	*1.0
592	PR(10, 2,F)	11	1	2	E	1243.5776	1243.5807	-3	0.739E+03	1.0
593	RR(16,12,A)	17	13	12	A	1243.7865	1243.7646	23	0.595E+03	*1.0
593	PR(8, 6,A)	9	5	6	A	1243.7885	1243.8003	-11	0.836E+03	*1.0
594	RR(13, 3,A1)	14	4	3	A2	1244.0661	1244.0429	23	0.217E+04	1.0
594	RR(13, 3,A2)	14	4	3	A1	1244.0661	1244.0687	-2	0.217E+04	1.0
597	RR(15, 8,F)	16	9	8	E	1245.1989	1245.1609	37	0.710E+03	1.0
599	RR(16,11,F)	17	12	11	E	1245.4967	1245.4892	7	0.328E+03	1.0
600	RR(14, 5,F)	15	6	5	E	1245.6608	1245.6490	11	0.128E+04	1.0
602	RR(13, 2,F)	14	3	2	E	1246.1220	1246.1232	-1	0.224E+04	1.0
603	PR(10, 3,A1)	11	2	3	A2	1246.4959	1246.5218	-25	0.778E+03	1.0
604	PR(10, 3,A2)	11	2	3	A1	1246.7625	1246.7463	16	0.786E+03	1.0
604	PR(9, 5,F)	10	4	5	E	1246.7625	1246.7718	-9	0.648E+03	1.0
605	RR(15, 7,F)	16	8	7	E	1247.2835	1247.2570	26	0.741E+03	1.0
605	RR(16,10,F)	17	11	10	E	1247.2835	1247.3086	-25	0.356E+03	1.0
606	RR(13, 1,F)	14	2	1	E	1247.7008	1247.6925	17	0.234E+04	1.0
606	RR(14, 4,F)	15	5	4	E	1247.7008	1247.7306	-20	0.130E+04	1.0
608	RR(13, 0,A2)	14	1	0	A1	1248.3120	1248.3082	3	0.238E+04	1.0
608	PR(11, 1,E)	12	0	1	E	1248.3120	1248.3598	-47	0.212E+03	0.0
612	RR(16, 9,A)	17	10	9	A	1249.1854	1249.2121	-26	0.763E+03	*1.0
613	RR(15, 6,A)	16	7	6	A	1249.4187	1249.4096	9	0.153E+04	*1.0
615	RR(14, 3,A2)	15	4	3	A1	1249.9323	1249.9094	22	0.138E+04	1.0
615	RR(14, 3,A1)	15	4	3	A2	1249.9323	1249.9228	9	0.138E+04	1.0
616	PR(10, 4,F)	11	3	4	E	1249.9893	1249.9793	9	0.675E+03	1.0
	PR(9, 6,A)	10	5	6	A		1250.5474		0.836E+03	

TABLE I—*Continued*

(I)	(II)	(III)				(IV)	(V)	(VI)	(VII)	(VIII)
618	PP(11, 2,E)	12	1	2	E	1250.6366	1250.6426	-5	0.447E+03	1.0
	PP(16, 8,E)	17	9	8	E		1251.1888		0.405E+03	
620	PP(15, 5,E)	16	6	5	E	1251.7176	1251.7161	1	0.675E+03	1.0
621	PP(14, 2,E)	15	3	2	E	1251.8317	1251.8232	8	0.143E+04	1.0
624	PP(14, 1,E)	15	2	1	E	1253.2264	1253.2240	2	0.148E+04	1.0
624	PP(16, 7,E)	17	8	7	E	1253.2264	1253.2274	-0	0.424E+03	1.0
625	PP(11, 3,A2)	12	2	3	A1	1253.3701	1253.3852	-15	0.507E+03	1.0
626	PP(10, 5,E)	11	4	5	E	1253.5514	1253.5201	31	0.519E+03	1.0
626	PP(15, 4,E)	16	5	4	E	1253.5510	1253.5710	-20	0.803E+03	1.0
627	PP(11, 3,A1)	12	2	3	A2	1253.7125	1253.6941	18	0.516E+03	1.0
627	PP(14, 0,A1)	15	1	0	A2	1253.7925	1253.7961	-29	0.151E+04	1.0
629	PP(9, 7,E)	10	6	7	E	1254.4603	1254.4549	4	0.236E+03	1.0
633	PP(16, 6,A)	17	7	6	A	1255.3316	1255.3215	10	0.874E+03	*1.0
634	PP(15, 3,A2)	16	4	3	A1	1255.6181	1255.6073	10	0.840E+03	1.0
634	PP(15, 3,A1)	16	4	3	A2	1255.6181	1255.6158	2	0.841E+03	1.0
636	PP(11, 4,E)	12	3	4	E	1256.7610	1256.7676	-6	0.469E+03	1.0
637	PP(16, 5,E)	17	6	5	E	1256.9288	1256.9093	19	0.305E+03	1.0
639	PP(10, 6,A)	11	5	6	A	1257.2355	1257.2200	15	0.726E+03	*1.0
640	PP(15, 2,E)	16	3	2	E	1257.3636	1257.3612	2	0.872E+03	1.0
	PP(12, 2,E)	13	1	2	E		1257.6920		0.255E+03	
645	PP(15, 1,E)	16	2	1	E	1258.6376	1258.6098	27	0.903E+03	1.0
646	PP(15, 0,A2)	16	1	0	A1	1259.0692	1259.0716	-8	0.916E+03	1.0
	PP(16, 4,E)	17	5	4	E		1259.2430		0.471E+03	
651	PP(11, 5,E)	12	4	5	E	1260.2104	1260.2117	-7	0.391E+03	1.0
651	PP(12, 3,A1)	13	2	3	A2	1260.2104	1260.2143	-3	0.309E+03	1.0
653	PP(12, 3,A2)	13	2	3	A1	1260.6446	1260.6290	15	0.318E+03	1.0
	PP(10, 7,E)	11	6	7	E		1261.0645		0.229E+03	
655	PP(16, 3,A1)	17	4	3	A2	1261.1410	1261.1246	16	0.492E+03	1.0
655	PP(16, 3,A2)	17	4	3	A1	1261.1410	1261.1674	-26	0.492E+03	1.0
658	PP(16, 2,E)	17	3	2	E	1262.7432	1262.7446	-1	0.511E+03	1.0
661	PP(12, 4,E)	13	3	4	E	1263.5418	1263.5195	22	0.304E+03	1.0
663	PP(11, 6,A)	12	5	6	A	1263.8345	1263.8240	9	0.667E+03	*1.0
663	PP(16, 1,E)	17	2	1	E	1263.8345	1263.8574	-22	0.527E+03	1.0
665	PP(16, 0,A1)	17	1	0	A2	1264.2527	1264.2504	-6	0.533E+03	1.0
672	PP(12, 5,E)	13	4	5	E	1266.8409	1266.8541	-4	0.259E+03	1.0
680	PP(12, 6,A)	13	5	6	A	1270.3757	1270.3693	6	0.406E+03	*1.0
	PP(13, 6,A)	14	5	6	A		1270.8602		0.269E+03	

(I) SERIAL NUMBER

(II) TRANSITION

(III) VALUES OF $J'', |K''|, |K''-l_6''|, C''$ FOR UPPER LEVELS OF THE TRANSITIONS

(IV) OBSERVED WAVENUMBER IN CM^{-1}

(V) CALCULATED WAVENUMBER IN CM^{-1}

(VI) (EXPT-CALC) IN 10^{-3} CM^{-1}

(VII) CALCULATED RELATIVE INTENSITY

(VIII) STATISTICAL WEIGHT

given in the columns (V) and (VII) of Table I; column (VI) gives the deviations (expt − calc) corresponding to the observed transitions.

The 88 unassigned transitions either are blended by lines of much larger relative intensity or occur in portions of the spectra unfavorable for the observation (a small part near 1118 cm^{-1} could not be recorded). The transitions, assignments, upper-state

energy levels, calculated spectral positions, and calculated relative intensities of predicted transitions which were not assigned to observed lines are included in Table I.

In the first column of Table II, the indices of the magnitude of the constants, expected from the expansion in power series of the transformed Hamiltonian H^+ (see Ref. (9), Chapt. VII) are listed. The comparison between these indices and the corresponding values determined for the constants shows that the expansion of H^+ is satisfactorily convergent, with the ratio $\langle h_{m+1}{}^+\rangle/\langle h_m{}^+\rangle$ between consecutive terms, being about $\frac{1}{10}$. However, this ratio is not small enough for the successive orders of magnitude to be very well separated. Thus, some neglected terms of H^+, i.e., $h_5{}^+$ or $h_6{}^+$, may slightly contribute to the effective values of the smallest constants appearing in Table II. In addition, the matrix element of $h_2{}^+$ of the form $\langle v_6=1, J, K, l_6|P^4|v_6=1, J, K\pm3, l_6\rangle$, which could not be significantly determined, probably contributes in the same manner.

Finally, the validity of the formulation used in the present paper for analyzing ν_6

TABLE II

Structure Constants for the $v_6 = 1$ Vibrational State of $^{12}CH_3D$

Index of Magnitude	Constant[a]	Value in cm^{-1}	Standard Deviation in cm^{-1}	99.5% Confidence Interval in cm^{-1}
0	ν	1161.0975	0.0015	0.0085
2	$(A\zeta)_v$	3.1123	0.0002	0.0012
2	B_v	3.83430	0.00003	0.00015
2	A_v	5.26896	0.00007	0.00039
6	D_v^J	4.509×10^{-5}	0.009×10^{-5}	0.052×10^{-5}
6	D_v^{JK}	1.935×10^{-4}	0.004×10^{-4}	0.025×10^{-4}
6	D_v^K	-1.098×10^{-4}	0.005×10^{-4}	0.029×10^{-4}
6	H_v^J	1.608×10^{-3}	0.009×10^{-3}	0.049×10^{-3}
6	H_v^K	-8.20×10^{-4}	0.12×10^{-4}	0.66×10^{-4}
4	$(q_{22}^6)_v$	-1.7452×10^{-2}	0.0015×10^{-2}	0.0085×10^{-2}
8	$f_{22}^{6,J}$	4.31×10^{-6}	0.06×10^{-6}	0.35×10^{-6}
8	f_{42}^6	2.99×10^{-6}	0.04×10^{-6}	0.21×10^{-6}
10	$H^K - H_o^K$	1.89×10^{-7}	0.08×10^{-7}	0.45×10^{-7}
4	$\epsilon(q_{12}^6)_v$	1.93×10^{-2}	0.02×10^{-2}	0.11×10^{-2}
8	$\epsilon(f_{12}^{6,K})$	-1.40×10^{-5}	0.06×10^{-5}	0.36×10^{-5}
10	$H^J - H_o^J$	1.172×10^{-9}[b]		
10	$H^{JJK} - H_o^{JJK}$	1.200×10^{-8}[b]		
10	$H^{JKK} - H_o^{JKK}$	-1.042×10^{-8}[b]		

[a] All the constants are defined in Ref. (10); $\epsilon = \pm1$ cannot be determined by the fitting.

[b] Constants constrained to their ground state values (8).

can be discussed near the level crossings between the two rotational series of $v_6 = 1$ and of $v_3 = 1$. The elements of the untransformed energy matrix $[\mathcal{H}]$ responsible for the interactions between these two series are:

(a) a first-order term

$$\langle v_6 = 1, v_3 = 0, J, K, l_6 = \pm 1 | H | v_6 = 0, v_3 = 1, J, K \mp 1, l_6 = 0 \rangle$$

with a main part due to r^2P of H_1, and

(b) a second-order term

$$\langle v_6 = 1, v_3 = 0, J, K, l_6 = \pm 1 | H | v_6 = 0, v_3 = 1, J, K \pm 2, l_6 = 0 \rangle$$

with a main part due to r^2P^2 of H_2.

The crossing between the levels coupled by (a) occurs in the $v_6 = 1$ state for $Kl_6 \simeq -42$, i.e., very far from the observed values $|K|$. Such a situation explains that the first-order Coriolis interaction of $v_6 = 1$ with $v_3 = 1$ could not be clearly separated from all other vibration–rotation interactions. Therefore, the effective value of ζ_{36}^x determined in Ref. (*3*), i.e., $|\zeta_{36}^x| = 0.041$ is too small compared to the calculated value $(\zeta_{36}^x)_{cal} \simeq -0.23$.

The crossing between the levels coupled by (b) lies between $Kl_6 = -12$ and $Kl_6 = -13$; the interaction, expected to be very localized, must affect mainly the PP, PQ, and PR transitions belonging to the two subbands $|K| = 13$ and $|K| = 14$. But these transitions are too weak to be observed in our spectra and no discrepancy due to this second-order interaction could be effectively detected. Let us note that the effects of this interaction should be more easily detected in the parallel band ν_3, where the involved transitions correspond to the subbands with $|K| = 10$ and $|K| = 11$.

RECEIVED: February 1, 1977

REFERENCES

1. L. W. PINKLEY, Ph.D. Dissertation, The Ohio State University, 1974.
2. W. H. SHAFFER, H. H. NIELSEN, AND L. H. THOMAS, *Phys. Rev.* **56**, 895 (1939).
3. J. C. DEROCHE, G. GRANER, AND C. ALAMICHEL, *J. Mol. Spectrosc.* **43**, 175 (1972).
4. M. E. MICKELSON, Ph.D. Dissertation, The Ohio State University, 1969.
5. K. NARAHARI RAO, C. J. HUMPHREYS, AND D. H. RANK, "Wavelength Standards in the Infrared," Academic Press, New York, 1966.
6. R. M. ALEXANDER, M.S. Thesis, The Ohio State University, 1970.
7. W. BRUCE OLSON, *J. Mol. Spectrosc.* **43**, 190 (1972).
8. G. TARRAGO, G. POUSSIGUE, M. DANG-NHU, A. VALENTIN, AND P. CARDINET, *J. Mol. Spectrosc.* **60**, 429 (1976).
9. G. AMAT, H. H. NIELSEN, AND G. TARRAGO, "Rotation–Vibration of Polyatomic Molecules," Dekker, New York, 1971.
10. G. TARRAGO, *Cah. Phys.* **19**, 149 (1965).
11. J. T. HOUGEN, *J. Chem. Phys.* **37**, 1433 (1962); **38**, 1167 (1963).
12. F. LEGAY, *Cah. Phys.* **99**, 416 (1958).

JOURNAL OF MOLECULAR SPECTROSCOPY 84, 305–312 (1980)

Diode Laser Spectroscopy of the ν_6 Band of $^{12}CH_3I$

PALASH P. DAS,* V. MALATHY DEVI,† AND K. NARAHARI RAO

Department of Physics, The Ohio State University, Columbus, Ohio 43210

The vibration–rotation spectrum of the ν_6 fundamental of methyl iodide has been recorded in the 824 to 862 cm^{-1} region by using a tunable semiconductor diode laser spectrometer. The rotational analysis performed for six Q branches $^pQ(J,3)$, $^rQ(J,4)$, $^pQ(J,5)$, $^pQ(J,6)$, $^pQ(J,7)$, and $^pQ(J,8)$ led to accurate values for several molecular constants. The nuclear quadrupole splitting arising from the spin of iodine has been observed very clearly in the low J transitions and for various K values.

INTRODUCTION

For the methyl iodide molecule, as a result of extensive studies made in the past both in the microwave and the infrared regions, we now have available accurate values for the molecular constants of its ground state. However, not many microwave measurements have been made for the transitions in the ν_6-state (*1*) which is located at 883 cm^{-1}. Also, in the infrared studies made with a grating spectrometer by Matsuura and Overend (*2*) the resolution was not sufficient to resolve the Q branches completely. The present work relates to the study of portions of the vibration–rotation fundamental ν_6 of $^{12}CH_3I$ with a tunable diode laser spectrometer having a spectral resolution of 0.002 cm^{-1}. Figure 1 displays the structure observed for one of the Q branches to illustrate the type of spectral data available in this work. Since we have observed the structure in the Q branches to J values as high as 70, several molecular constants could be determined for the ν_6-state. The results are compared with the recent saturated absorption work of the ν_6 band by Arimondo and Glorieux (*3*) as well as the microwave and infrared results mentioned earlier.

EXPERIMENTAL DETAILS

The general experimental setup has been described elsewhere (*4*). In the present investigation a 2.54-cm-long germanium Fabry–Perot etalon was used to produce calibration fringes of about 0.049 cm^{-1} separations. To minimize variation in fringe spacing due to temperature changes to which germanium is very susceptible, the following steps were taken: (i) The germanium etalon was enclosed in a thermally isolated box. (ii) A mode was scanned in a few minutes and several repetitive scans were obtained for each mode. (iii) Temperature of the etalon enclosure was monitored continuously and only those scans in which temperature remained steady were used in obtaining the final data. (iv) In each mode which was typically about 0.5 cm^{-1} in extent, attempts were made to obtain at least two calibration lines so as to enable us to calculate the fringe spacings in addition to

Present Address: *Tachisto Inc., 13 Highland Circle, Needham, Mass. 02194 and †NOAA/NESS FB4, S/RE21 Washington, D. C. 20233.

0022-2852/80/110305-08$02.00/0

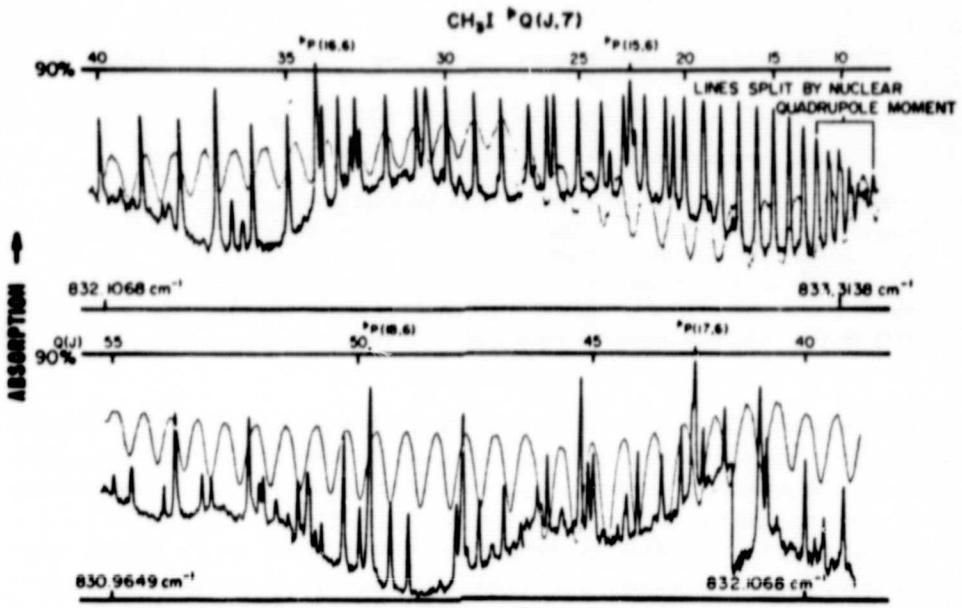

FIG. 1. $^rQ(J,7)$ structure in the ν_6 band of $^{12}CH_3I$ recorded with a diode laser spectrometer. Absorption path length = 12 m, pressure = 0.5 Torr approx.

providing absolute wavenumber standards. In this connection, the ν_1 band lines of OCS (*5*) were found useful.

Based on the quoted uncertainties of OCS lines, the absolute uncertainty of our measurements has been estimated to be about ± 0.002 cm^{-1}, whereas, the relative accuracy is about ± 0.0005 cm^{-1}.

A commercial sample of CH_3I was used without further purification. A multipass cell of base length 1 m was used to provide a total pathlength of 12 m. Pressures of the gas sample ranged from 0.2 to 1 Torr. A Ge:Cu detector cooled to about 4 K was used to detect the signal from the multiple path absorption cell and a HgCdTe detector operated at 77 K was used in the etalon arm.

RESULTS

Molecular Constants

A total of 219 rotational transitions were identified in the Q branches recorded in the present investigation and their measurements are presented in Table I. These data were fitted by least-squares techniques making use of the term value expressions given respectively in Eqs. (1) and (2) below for the ground state and the ν_6-state.

$$F''(J,K) = B_0[J(J+1) - K^2] + A_0K^2 - D_0^JJ^2(J+1)^2 - D_0^{JK}J(J+1)K^2 - D_0^KK^4 + H_0^{JKK}J(J+1)K^4, \quad (1)$$

$$F'(J,k,l) = \tilde{\nu}_6 + B_6[J(J+1) - K^2] + A_6K^2 - 2(A\zeta)_6kl + \eta_6^lJ(J+1)kl + \eta_6^Kk^3l - D_6^lJ^2(J+1)^2 - D_6^{lK}J(J+1)K^2 - D_6^KK^4 + H_6^{lK^2}J(J+1)K^4, \quad (2)$$

where $K = |k|$ except for $k = l = \pm 1$ and $\tilde{\nu}_6 = \nu_0 + (A\zeta^2)_3$. In the above evaluations the ground-state molecular constants were constrained to the values presented in Table II. The D_6^{lK} and η_6^K were constrained to the values of Matsuura and Overend (*2*) since the range of $K\Delta K$ values observed by them was much higher than in the present work. Finally, from preliminary calculations we found that it is adequate to set $D_6^K = D_6^K$ of Ref. (*6*). The present set of constants determined in this manner for the ν_6-state agree well with the microwave values given in Ref. (*1*). In view of the high J values obtained in the present data it was possible to determine an improved value for the constant η_6^l. However, there is one aspect which does not quite agree with the results of Arimondo and Glorieux (*3*). The value obtained by these authors for the effective band center, $\nu_0 + A_6(1 - \zeta^2) - B_6 + (3/4)\eta_6^K$ differs by about 0.01 cm^{-1} from the present result, which incidentally is within 0.002 cm^{-1} of the grating infrared work (*2*). Such a difference could be due to an absolute calibration error for the wavenumbers of the diode laser data. But, in view of the stated uncertainty of 0.002 cm^{-1} for the OCS lines used as calibration standards here (*5*), the difference of 0.01 cm^{-1} is outside the scope of the current measurements. It may also be mentioned that in our investigations related to the diode laser spectra of the ν_2 band of NO_2 (*7*), although some of the data were calibrated by the ν_1 band lines of OCS and others by the ν_2 band lines of CO_2, we found internal consistency between all the NO_2 data observed. As such, at this time we cannot completely account for the 0.01 cm^{-1} difference in the effective band center values.

Along with the Q branch data for $^{12}CH_3I$ we also observed other transitions belonging to $^pP(J,K)$ and $^pR(J,K)$ transitions. The molecular constants of Table II were used to calculate the positions for these P and R lines and Table III compares these calculated values with the actual measured data and there is good agreement as shown by the observed − calculated values.

Nuclear Quadrupole Hyperfine Structure

For many years now, it has been known from microwave studies (*8*) that CH_3I has a large quadrupole coupling constant. For $v = 0$, the (eqQ) value is -6.45×10^{-3} cm^{-1} (*1*) and for $v_6 = 1$ it is -6.47×10^{-3} cm^{-1} (*9*). The nuclear spin (I) of 5/2 of iodine combines with J and splits the rotational levels represented in Eqs. (1) and (2) into $2I + 1 = 6$ components for $J > 2$. The ^{12}C and H nuclei have spins 0 and 1/2, respectively, and hence give no quadrupole effects. The contribution due to the quadrupole effect to Eqs. (1) and (2) is

$$\left(\frac{E_Q}{hc}\right) = \frac{eqQ\left[\dfrac{3K^2}{J(J+1)} - 1\right][(3/4)C(C+1) - I(I+1)J(J+1)]}{2I(2I-1)(2J-1)(2J+3)}, \quad (3)$$

where $C = F(F+1) - I(I+1) - J(J+1)$ and $\mathbf{F} = \mathbf{I} + \mathbf{J}$ is the total angular

TABLE I

Measured Q Branch Wavenumbers (vac. cm^{-1}) of the ν_6 Band of $^{13}CH_3I$

J	$P_{Q(J,3)}$	(O-C)x10^4	$P_{Q(J,4)}$	(O-C)x10^4	$P_{Q(J,5)}$	(O-C)x10^4
6			855.3243	- 4		
7	862.7829	- 11	855.3147	9	847.9169	- 13
8	862.7737	21	855.3015	2	847.9051	- 5
9	862.7585	11	855.2870	- 1	847.8912	- 3
10	862.7417	0	855.2720	5	847.8760	1
11	862.7237	- 8	855.2543	1	847.8586	0
12	862.7079	21	855.2349	- 4	847.8397	0
13	862.6851	- 2	855.2143	- 6	847.8196	2
14	862.6636	1	855.1926	- 4	847.7973	0
15	862.6394	- 5	855.1690	- 5	847.7739	1
16	862.6148	0	855.1441	- 3	847.7481	- 5
17	862.5874	- 7	855.1180	3	847.7212	- 7
18	862.5610	10	855.0888	- 6		
19	862.5309	7	855.0590	- 6	847.6634	- 4
20	862.4986	- 1	855.0295	12	847.6320	- 4
21	862.4653	- 5			847.5996	1
22	862.4310	- 2			847.5650	1
23	862.3945	- 6	854.9249	3	847.5290	3
24	862.3574	- 1	854.8864	- 4	847.4908	- 1
25	862.3187	4			847.4518	1
26	862.2783	8	854.8056	- 11	847.4113	5
27	862.2356	5	854.7637	- 5	847.3673	- 9
28	862.1906	- 4	854.7203	0	847.3243	1
29	862.1453	0	854.6743	- 3	847.2787	1
30	862.0978	- 5	854.6269	- 5	847.2310	- 2
31	862.0496	0			847.1820	- 4
32	861.9991	- 1			847.1313	- 7
33	861.9470	- 3			847.0801	0
34	861.8943	4			847.0264	0
35					846.9711	- 1
36					846.9137	- 7
37					846.8558	- 3
38					846.7966	4
39					846.7342	- 3
40					846.6714	0
41					846.6070	3
42					846.5402	0

J	$P_{Q(J,6)}$	(O-C)x10^4	J	$P_{Q(J,6)}$	(O-C)x10^4
8	840.5862	1	36	839.5942	1
9	840.5721	1	37	839.5361	5
10	840.5556	- 6	38	839.4756	0
11	840.5394	4	39	839.4133	- 6
12	840.5205	4	40	839.3509	1
13	840.4997	0	41	839.2855	- 4
14	840.4778	1	42	839.2190	- 5
15	840.4538	- 2	43	839.1512	- 2
16	840.4289	0	44	839.0821	2
17	840.4024	1	45	839.0105	- 1
18	840.3743	3			
19	840.3442	1	55	838.2097	3
20	840.3125	0	56	838.1200	- 2
21	840.2799	3	57	838.0294	- 1
22	840.2453	3	58	837.9368	- 4
23	840.2091	3	59	837.8430	- 2
24	840.1716	6	60	837.7487	10
25	840.1322	5	61	837.6500	- 4
26	840.0913	6	62	837.5515	0
27	840.0487	5	63	837.4509	- 1
28	840.0039	- 1	64	837.3500	11
29	839.9588	4	65	837.2459	0
30	839.9116	5	66		
31	839.8624	1	67	837.0324	0
32	839.8119	1	68	836.9235	- 1
33	839.7598	0	69	836.8132	0
34	839.7065	4	70	836.7009	- 1
35	839.6509	0			

TABLE I--*Continued*

J	$^pQ(J,7)$	(O-C)x10^4	$^pQ(J,8)$	(O-C)x10^4
8	833.3427	- 9		
9	833.3292	- 3	826.1654	- 1
10	833.3138	0	826.1502	3
11	833.2960	- 5	826.1321	- 4
12	833.2765	-11	826.1135	- 1
13	833.2563	- 9	826.0938	6
14	833.2352	0	826.0717	0
15	833.2116	0	826.0484	8
16	833.1863	- 1	826.0224	0
17	833.1599	2	825.9958	2
18	833.1314	0	825.9680	8
19	833.1016	2	825.9377	4
20	833.0693	- 7	825.9057	0
21	833.0369	0	825.8726	0
22			825.8379	- 1
23			825.8011	- 6
24	832.9286	3	825.7631	- 8
25	832.8893	4	825.7248	3
26	832.8487	8	825.6820	-14
27	832.8063	10		
28	832.7605	- 6	825.5968	1
29	832.7159	4	825.5519	10
30	832.6684	3	825.5040	4
31	832.6194	2	825.4542	- 1
32	832.5690	3	825.4040	0
33	832.5172	6	825.3522	3
34	832.4637	8	825.2982	0
35	832.4077	0	825.2420	- 8
36	832.3510	2	825.1865	6
37	832.2926	3	825.1263	-10
38	832.2329	7	825.0662	10
39	832.1710	4	825.0055	0
40	832.1068	- 4	824.9419	- 2
41	832.0424	0	824.8762	-10
42	831.9763	4	824.8102	- 4
43	831.9085	7	824.7424	- 1
44	831.8374	- 7	824.6727	0
45	831.7675	7		
46	831.6946	7		
47	831.6191	- 2		
48	831.5428	- 4		
49	831.4654	0		
50	831.3857	- 3		
51	831.3052	1		
52	831.2229	4		
53	831.1383	1		
54	831.0514	- 8		
55	830.9649	1		

momentum of the molecule. The complete selection rules for the ^pQ branches are $\Delta v = 1$, $\Delta J = 0$, $\Delta K = -1$, and $\Delta F = 0, \pm 1$.

Figure 2 shows a comparison between the measured and calculated absorption spectra of the $^pQ(6,4)$ line located at 855.324 cm^{-1}. Using the selection rules given above, we find that this line splits into ten components corresponding to $\Delta F = \pm 1$ and six components corresponding to $\Delta F = 0$. The relative strengths of these lines (*10*) are indicated in Fig. 2a by the lengths of the vertical lines. The six $\Delta F = 0$ components account for about 85% of the line intensity. From these relative strengths and line positions determined from Eq. (3) the spectrum of the line was calculated assuming a Doppler absorption profile for each component convoluted by a Gaussian instrument function, which arises due to the finite linewidth of the laser. Under these conditions, the absorptance $A(\nu)$ can

TABLE II

Molecular Parameters (in cm^{-1}) for the ν_6 Band of $^{13}CH_3I$

B_o	0.2502156241 (Ref. 14)	D_o^J	2.103789×10^{-7} (Ref. 14)
A_o	5.1734 (Ref. 6)	D_o^{JK}	3.29436×10^{-6} (Ref. 14)
		D_o^K	8.97×10^{-5} (Ref. 6)
		H_o^{JKK}	1.424×10^{-10} (Ref. 13)
ν_6 State Constants:			
$\nu_o + (A\zeta^2)_6$	882.91083(31)	D_6^J	$2.11970(26) \times 10^{-7}$
B_6	0.24943054(28)	D_6^{JK}	3.29×10^{-6} (Ref. 2)
A_6	5.207589(16)	$D_6^K = D_o^K$	
$(A\zeta)_6$	1.097131(72)	$H_6^{JKK} = H_o^{JKK}$	
		η_6^J	$7.227(47) \times 10^{-6}$
		η_6^K	1.524×10^{-4} (Ref. 2)

Number of lines 219; standard deviation of residuals is 0.00055 cm^{-1}. Error limits given in parentheses are standard deviations in the last digits.

TABLE III

Wavenumbers (vac. cm^{-1}) of Some Selected $^pP(J,K)$ and $^pR(J,K)$ Transitions Observed in the Q Branch Regions of CH_3I

LINE	$\nu_{obs.}$	$(O-C)\times10^4$	LINE	$\nu_{obs.}$	$(O-C)\times10^4$
$^pP_{P(15,3)}$	855.1608	0	$^pP_{P(21,5)}$	837.1342	- 1
$^pP_{P(16,3)}$	854.6380	6	$^pP_{P(6,6)}$	837.6182	3
$^pP_{P(16,4)}$	847.1665	12	$^pP_{P(15,6)}$	832.9780	6
$^pP_{P(17,4)}$	846.6425	- 3	$^pP_{P(16,6)}$	832.4544	2
$^pP_{P(15,5)}$	840.2965	4	$^pP_{P(17,6)}$	831.9299	4
$^pP_{P(16,5)}$	839.7732	4	$^pP_{P(18,6)}$	831.4036	3
$^pP_{P(17,5)}$	839.2473	- 8	$^pP_{P(28,6)}$	826.0620	14
$^pP_{P(19,5)}$	838.1949	7	$^pP_{R(12,6)}$	846.9995	- 8
$^pP_{P(20,5)}$	837.6651	1	$^pP_{R(13,6)}$	847.4787	6

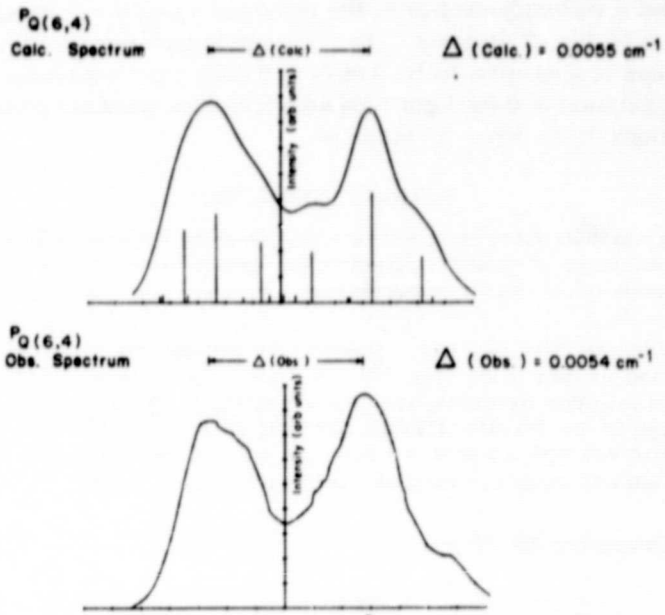

FIG. 2. Calculated and observed structure of $^{P}Q(6,4)$ line of ν_6 of $^{12}CH_3I$ illustrating the nuclear quadrupole splitting. Absorption path length = 12 m, pressure = 0.2 Torr.

be written in a series as given below (*11*):

$$A(\nu) = \sum_{n=1}^{\infty} (-1)^{n+1} \frac{(S')^n}{n!n^{1/2}} \left[\frac{1}{n} + \left(\frac{\delta}{\beta} \right)^2 \right]^{-1/2} \exp \frac{-(\nu^2)}{\beta^2[1/n + (\delta/\beta)^2]} ,$$

where

$$\beta = \frac{b_D}{(\ln 2)^{1/2}} , \qquad \delta = \frac{d}{(\ln 2)^{1/2}} , \tag{4}$$

b_D = Doppler half width at half height, d = instrument half-width at half-height, and S' is related to the strength of the line.

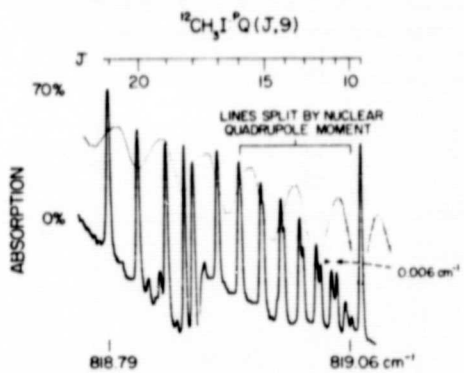

FIGURE 3

Both S' and δ were adjusted to fit the observed spectrum. The agreement, as demonstrated in Fig. 2 is good. The separation (Δ) between the two peaks of the split line is measured to be 0.0054 ± 0.0005 cm^{-1} which agrees with the calculated separation of 0.0055 cm^{-1}. Similar splittings were observed for several low J transitions in the other ^pQ branches.

ACKNOWLEDGMENTS

This research was done during the tenure of a grant from the National Aeronautics and Space Administration and one of us (KNR) is grateful for this support. We would also like to thank Drs. James K. G. Watson and T. Oka for reading the manuscript and making useful comments.

Note added after the above work was completed. The splittings due to nuclear spin molecular rotation interaction are more clearly seen in the spectrum of $^rQ(J,9)$ because of the large separation between the individual transitions. This is shown in Fig. 3. The observed values of $^rQ(J,9)$ for J = 9 through 21 are 819.0814, 819.0648, 819.0483, 819.0300, 819.0084, 818.9871, 818.9639, 818.9391, 818.9119, 818.8833, 818.8527, 818.8214, and 818.7878 cm^{-1}, respectively. These wavenumbers agree well with those calculated from the constants given in Table II.

RECEIVED: December 10, 1979

REFERENCES

1. Y. MORINO, J. W. SIMMONS, AND A. G. SMITH, *J. Mol. Spectrosc.* **22,** 99–104 (1967).
2. H. MATSURA AND J. OVEREND, *Spectrochim. Acta A* **27,** 2165–2170 (1971).
3. E. ARIMONDO AND P. GLORIEUX, *Phys. Rev. A* **19,** 1067–1083 (1979).
4. S. PADDI REDDY, W. IVANCIC, V. MALATHY DEVI, A. BALDACCI, K. NARAHARI RAO, A. W. MANTZ, AND R. S. ENG, *Appl. Opt.* **18,** 1350–1354 (1979).
5. A. G. MAKI, WM. BRUCE OLSON, AND R. L. SAMS, *J. Mol. Spectrosc.* **81,** 122–138 (1980).
6. P. D. MALLINSON, *J. Mol. Spectrosc.* **55,** 94–107 (1975).
7. J.-M. FLAUD, C. CAMY-PEYRET, V. MALATHY DEVI, PALASH P. DAS, AND K. NARAHARI RAO, *J. Mol. Spectrosc.* **84,** 234–242 (1980).
8. W. GORDY, A. G. SMITH, AND J. W. SIMMONS, *Phys. Rev.* **72,** 249L (1947).
9. E. ARIMONDO, P. GLORIEUX, AND T. OKA, *Phys. Rev. A* **17,** 1375–1392 (1978).
10. C. H. TOWNES AND A. L. SCHAWLOW, "Microwave Spectroscopy," McGraw–Hill, New York, 1955.
11. B. FRIDOVICH, V. MALATHY DEVI, AND P. P. DAS, *J. Mol. Spectrosc.* **81,** 269–272 (1980).
12. W. J. ORVILLE-THOMAS, J. T. COX, AND W. GORDY, *J. Chem. Phys.* **22,** 1718–1722 (1954).
13. T. E. SULLIVAN AND L. FRENKEL, *J. Mol. Spectrosc.* **39,** 185–201 (1971).
14. J. BURIE, D. BOUCHER, J. DEMAISON, AND A. DUBRULLE, *Mol. Phys.* **32,** 289–295 (1976); D. BOUCHER, J. BURIE, D. DANGOISSE, J. DEMAISON, AND A. DUBRULLE, *Chem. Phys.* **29,** 323–330 (1978).

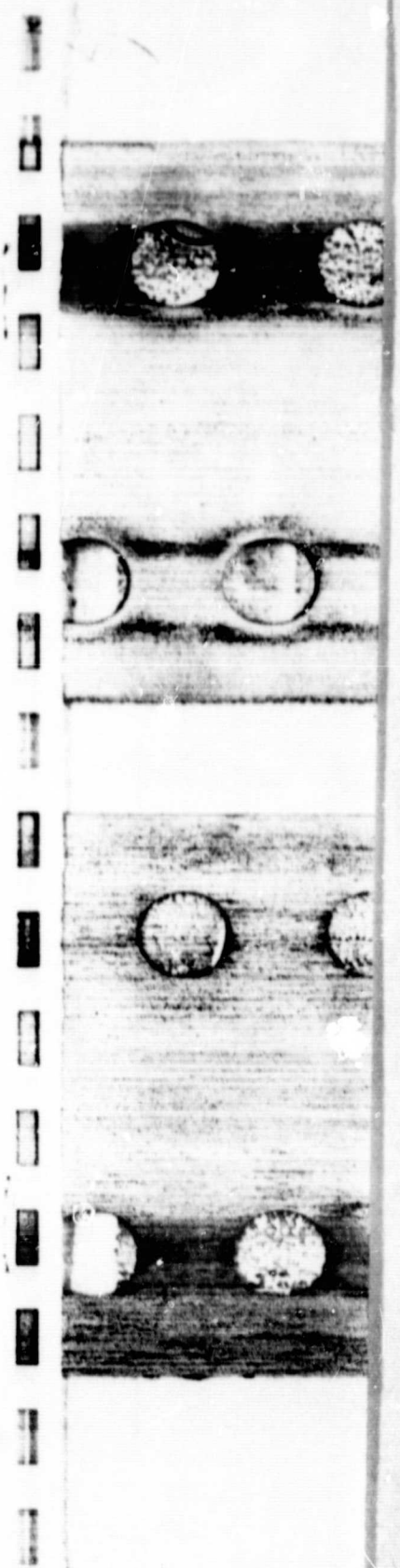

JOURNAL OF MOLECULAR SPECTROSCOPY 79, 455–495 (1980)

Coriolis and *l*-Type Interactions in the ν_2, $2\nu_2$, and ν_4 States of $^{14}NH_3$

Š. URBAN, V. ŠPIRKO, AND D. PAPOUŠEK

The J. Heyrovský Institute of Physical Chemistry and Electrochemistry, Czechoslovak Academy of Sciences, 160 00 Prague 6, Czechoslovakia

AND

ROBIN S. MCDOWELL AND NORRIS G. NERESON

University of California, Los Alamos Scientific Laboratory,[1] Los Alamos, New Mexico 87545

AND

S. P. BELOV, L. I. GERSHSTEIN, A. V. MASLOVSKIJ, AND A. F. KRUPNOV

Institute for Applied Physics, Academy of Sciences, USSR, Gorkii.

AND

JOHN CURTIS AND K. NARAHARI RAO[2]

Department of Physics, The Ohio State University, Columbus, Ohio 43210

High-resolution infrared spectra have been remeasured for the ν_2, $2\nu_2$, and ν_4 bands of $^{14}NH_3$ using a vacuum grating infrared spectrometer and a diode laser spectrometer. Far-infrared spectra of $^{14}NH_3$ have been measured with microwave accuracy in the 700–1100 GHz region by employing a submillimeter wave spectrometer (RAD) with acoustic detection. The pure inversion and inversion–rotation transition frequencies in the ν_2 excited state of $^{14}NH_3$ have been determined for the first time. The vibration–inversion–rotation Hamiltonian of ammonia [Špirko, Stone, and Papoušek, *J. Mol. Spectrosc.* **60**, 159–178 (1976)] has been used for a precise parameterization of the energy levels of ammonia. The ground state rotational and centrifugal constants of $^{14}NH_3$ have been determined using a modified method of combination differences. Coriolis and *l*-type interactions between ν_2, ν_4, $2\nu_2$, $\nu_2 + \nu_4$, and $3\nu_2$ states have been analyzed and the band parameters have been obtained which reproduce the transition frequencies within the accuracy of the experimental data.

I. INTRODUCTION

In previous papers (*1–5*) a new vibration–inversion–rotation Hamiltonian for ammonia has been developed and applied to the available experimental transition frequencies in the infrared, submillimeter, and microwave regions for $^{14}NH_3$, $^{15}NH_3$, $^{14}NH_2D$, $^{14}ND_2H$, $^{14}ND_3$, and $^{14}NT_3$. The main purpose of this work is to

[1] The Los Alamos portion of this work was supported by the United States Department of Energy.
[2] One of us (KNR) is grateful to the National Aeronautics and Space Administration for support of some of this research.

0022-2852/80/020455-41$02.00/0

obtain an accurate value of the inversion barrier in ammonia and to discuss certain anomalies in the spectra of this classic example of a nonrigid molecule (5).

In the present paper we have used this Hamiltonian for a precise parameterization of the energy levels of ammonia in the sense of obtaining the effective values of molecular parameters which reproduce the high-resolution infrared, submillimeter, and microwave data to within the accuracy of the experiments. Formulas which are obtained from this Hamiltonian to fit the experimental data are formally identical with those that would be obtained from the standard Darling–Dennison vibrational–rotational Hamiltonian. There are however two main advantages of our approach (Section II): (i) higher-order formulas can be obtained from the lower-order terms in the expansion of our Hamiltonian in terms of Q [cf. (6)]; and (ii) relations of the effective parameters to the basic molecular constants such as the molecular geometry and the potential energy function of ammonia are clearly defined in our treatment.

In the present paper we apply this treatment to the infrared data on $^{14}NH_3$ measured with the vacuum grating spectrometer at the Ohio State University in Columbus, Ohio, with the diode laser spectrometer at the Los Alamos Scientific Laboratory, and with the submillimeter wave spectrometer RAD at the Institute for Applied Physics at the Academy of Sciences USSR in Gorkii, (Section III). Although the infrared spectrum of ammonia has been studied in considerable detail (*7–23*), previous measurements (*7–13*) have been done with much lower resolution than achieved here. With the grating spectrometer, we have measured with resolution of about 0.03–0.06 cm^{-1} the ν_1, ν_2, ν_3, and ν_4 fundamental bands, the $2\nu_2$ and $2\nu_4$ overtone bands, and the "hot" bands for transitions from the ν_2 level to the $\nu_1 + \nu_2$, $\nu_2 + \nu_3$, ν_4, and $2\nu_2$ levels of $^{14}NH_3$. The 10^{-4}-cm^{-1} resolution of the diode laser spectrometer has made it possible to resolve certain features in the ν_2 band that remained unresolved in the grating measurements. We report here also for the first time the measured frequencies of the pure inversion and rotation–inversion transitions in the ν_2 state of $^{14}NH_3$ at 700–1100 GHz.

Combining these data with some other high- and ultra-high-resolution submillimeter and infrared data on the ν_2 (or $2\nu_2$) band of ammonia (*14*, *16–20*, *22–24*), we have determined the ground-state rotational and centrifugal distortion constants of $^{14}NH_3$ using a modified method of combination differences (Section IV). We have also analyzed in detail the Coriolis and l-type interactions between the ν_2, ν_4, $2\nu_2$, $\nu_2 + \nu_4$, and $3\nu_2$ states of ammonia (Section V). The results of analysis of the ν_1, ν_3, and $2\nu_4$ states including the perturbation-allowed transitions to the $2\nu_4$ level will be presented in a subsequent paper.

II. PARAMETERIZATION OF THE ENERGY LEVELS OF AMMONIA

If we expand the vibration–inversion–rotation Hamiltonian for NH_3 (*1*, *4*) in the vibrational coordinates Q, and retain only terms of order of magnitude $\kappa^2 T_v$, we obtain

$$H = T_i^0 + T_r^0 + T_{\text{Cent}} + T_{\text{Cor}} + T_{\text{Vib}} + V, \tag{1}$$

where

$$T_i^0 = (1/2)\mu_{\rho\rho}^0 J_\rho^2 + (1/2)(J_\rho \mu_{\rho\rho}^0) J_\rho + (1/2)(\mu^0)^{1/4}\{J_\rho \mu_{\rho\rho}^0 (\mu^0)^{-1/2}[J_\rho (\mu^0)^{1/4}]\} + U_0(\rho), \tag{2}$$

$$T_r^0 = (1/2)\mu_{xx}^0(J_x^2 + J_y^2) + (1/2)\mu_{zz}^0 J_z^2, \tag{3}$$

$$T_{\text{Cent}} = (1/2) \sum_{\alpha,\beta=x,y,z,\rho} [\sum_k X_k^{\alpha\beta} Q_k + \sum_{k,l} Y_{kl}^{\alpha\beta} Q_k Q_l] J_\alpha J_\beta + (1/2) \sum_{\alpha=x,y,z,\rho} [\sum_k (J_\rho X_k^{\rho\alpha}) Q_k + \sum_{k,l} (J_\rho Y_{kl}^{\rho\alpha}) Q_k Q_l] J_\alpha, \tag{4}$$

$$T_{\text{Cor}} = -(1/2) \sum_{\alpha=x,y,z,\rho} \mu_{\alpha\alpha}^0 (J_\alpha p_\alpha + p_\alpha J_\alpha) - (1/2)(J_\rho \mu_{\rho\rho}^0) p_\rho, \tag{5}$$

$$T_{\text{Vib}} = (1/2) \sum_k P_k^2 + (1/2) \sum_{\alpha=x,y,z,\rho} \mu_{\alpha\alpha}^0 p_\alpha^2, \tag{6}$$

$$V = V_0(\rho) + \sum_k \kappa_k(\rho) Q_k + (1/2) \sum_k \lambda_k(\rho) Q_k^2 + \sum_{klm} k_{klm}(\rho) Q_k Q_l Q_m + \cdots. \tag{7}$$

All the symbols have the same meaning as in Refs. (*1*, *4*, *5*); k, l, m take on the values 1, $3a$, $3b$, $4a$, $4b$. It should be emphasized that all parameters occurring in Eqs. (2)–(7) are functions of the coordinate measuring the large-amplitude inversion motion.

In the theory of centrifugal distortion described in Ref. (*4*) we used second-order perturbation theory and evaluated the matrix elements of the vibrational and rotational operators occurring in T_r^0, T_{Cent}, T_{Vib}, and V. Together with T_t^0, this gives an effective vibration–inversion–rotation Hamiltonian for NH_3 that contains only functions of ρ and the operator $J_\rho = -i\hbar\partial/\partial\rho$ [Eqs. (14)–(16) in (*4*)]. If the resulting Schrödinger equation is solved numerically as an "inverse" eigenvalue problem, we can obtain physically reliable information on the molecular potential function of ammonia including the "true" double-minimum potential function for the inversion motion (*5*). This is, however, a treatment which is not suitable for fitting experimental data with an accuracy comparable to that of the high-resolution infrared and microwave data.

We have now modified the treatment so that the parameterization of the energy levels can be achieved relatively easily. We do not obtain direct information on the whole potential function of ammonia, but effective molecular parameters such as rotational constants, band origins, and interaction parameters are obtained by a least-squares fit.

The basic idea of our treatment consists in the expansion of the ρ-dependent parameters in Eqs. (3)–(7) as a power series in the large-amplitude coordinate ρ in the point of the planar reference configuration of the atomic nuclei ($\rho = \pi/2$). The choice of the planar reference configuration in this expansion is the most natural from the point of view of the symmetry of the problem. All the ρ-dependent terms are either even or odd functions of $\tilde{\theta} = \rho - \pi/2$ [A_1' or A_2'' species in the D_{3h} permutation-inversion group of NH_3 (*1*, *5*)]. Let us denote these parameters in general as $M_p^{(A_1')}$ and $M_p^{(A_2'')}$. We can write

$$M_p^{(A_1')} = {}^{(0)}M_p^{(A_1')} + {}^{(1)}M_p^{(A_1')}\tilde{\theta}^2 + {}^{(2)}M_p^{(A_1')}\tilde{\theta}^4 + \cdots, \tag{8a}$$

$$M_p^{(A_2'')} = {}^{(1)}M_p^{(A_2'')}\tilde{\theta} + {}^{(2)}M_p^{(A_2'')}\tilde{\theta}^3 + \cdots, \tag{8b}$$

where ${}^{(s)}M_p$ are ρ-independent coefficients depending only on the molecular geometry and atomic masses.

If we substitute Eq. (8) into Eqs. (3)–(7), Eq. (1) can be written in the following form:

$$H = [T_i^0 + V_0(\tilde{\theta})] + [(1/2)\sum_k P_k^2 + (1/2)\sum_k {}^{(0)}\lambda_k Q_k^2] + [(1/2)^{(0)}\mu_{xx}^0(J_x^2 + J_y^2) + (1/2)^{(0)}\mu_{zz}^0 J_z^2] + H'$$
$$= H_0 + H', \tag{9}$$

where

$$H' = (1/2)\sum_{s=1}[{}^{(s)}\mu_{xx}^0\tilde{\theta}^{2s}(J_x^2 + J_y^2) + {}^{(s)}\mu_{zz}^0\tilde{\theta}^{2s}J_z^2] + T_{\text{Cent}} + T_{\text{Cor}} + (1/2)\sum\mu_{\alpha\alpha}^0 p_\alpha^2 + \sum_k\sum_s{}^{(s)}\lambda_k\tilde{\theta}^{2s}Q_k^2 + \sum_{klm}k_{klm}Q_kQ_lQ_m. \tag{10}$$

Wavefunctions ψ_0 that are solutions of the Schrödinger equation

$$H_0\psi_0 = E_0\psi_0 \tag{11}$$

can be written as the product functions

$$\psi_0(\tilde{\theta};\theta,\Phi,\chi;Q) = [\psi_i(\tilde{\theta})][S_{Jkm}(\theta,\Phi)\exp(ik\chi)][\prod_v\psi_v^0(Q)], \tag{12}$$

where v is summed over 1, $3a$, $3b$, $4a$, $4b$; here $\psi_i(\tilde{\theta})$ are the inversion wavefunctions, $S_{Jkm}(\theta,\Phi)\exp(ik\chi)$ the symmetric rotor wavefunctions, and $\psi_v^0(Q)$ the harmonic oscillator wavefunctions. The inversion wavefunctions $\psi_i(\tilde{\theta})$ are not obtained in the present treatment by a numerical integration of the Schrödinger equation with the operator $T_i^0 + V_0(\tilde{\theta})$; they are assumed to be known.

The product functions (12) are basis functions in which the Schrödinger problem with the Hamiltonian H is solved either by standard perturbation methods or by a variational approach (if there is a close coincidence of the interacting levels). In this Section, only a simple example will be discussed to demonstrate the usefulness of this approach.

Let us consider the so-called rigid bender approximation which has been treated numerically in Refs. (*1*, *2*) to obtain information on the inversion potential function in ammonia. The rigid bender Hamiltonian H_{rb}^0 can be written in the form (*1*)

$$H_{\text{rb}}^0 = [T_i^0 + V_0(\tilde{\theta})] + (1/2)\mu_{xx}^0(J^2 - J_z^2) + (1/2)\mu_{zz}^0 J_z^2. \tag{13}$$

If we expand μ_{xx}^0 and μ_{zz}^0 in a power series according to Eq. (8a), H_{rb}^0 has diagonal and off-diagonal matrix elements in $\psi_i(\tilde{\theta})(\equiv|i\rangle)$:

$$(hc)^{-1}\langle v;J,k,m;i|H_{rb}^0|v;J,k,m;i\rangle = E_i^0/hc + (h/4\pi^2c)[{}^{(0)}\mu_{xx}^0 + \sum_{s=1}{}^{(s)}\mu_{xx}^0\langle i|\tilde{\theta}^{2s}|i\rangle][J(J+1) - k^2] + (h/4\pi^2c)[{}^{(0)}\mu_{zz}^0 + \sum_{s=1}{}^{(s)}\mu_{zz}^0\langle i|\tilde{\theta}^{2s}|i\rangle]k^2$$
$$= E_i^0/hc + B_iJ(J+1) + (C_i - B_i)k^2, \tag{14}$$

$$(hc)^{-1}\langle v;J,k,m;i|H_{rb}^0|v;J,k,m;i+2\rangle = (h/4\pi^2c)[\sum_{s=1}{}^{(s)}\mu_{xx}^0\langle i|\tilde{\theta}^{2s}|i+2\rangle][J(J+1) - k^2] + (h/4\pi^2c)[\sum_{s=1}{}^{(s)}\mu_{zz}^0\langle i|\tilde{\theta}^{2s}|i+2\rangle]k^2. \tag{15}$$

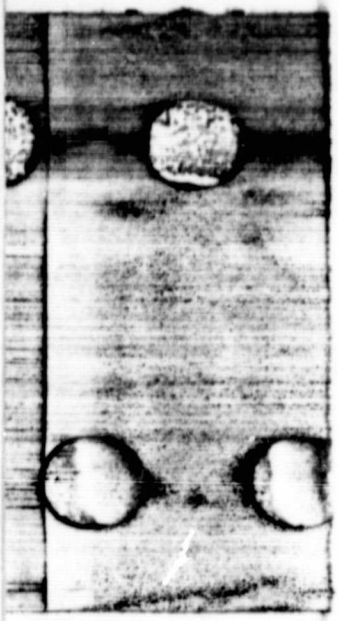

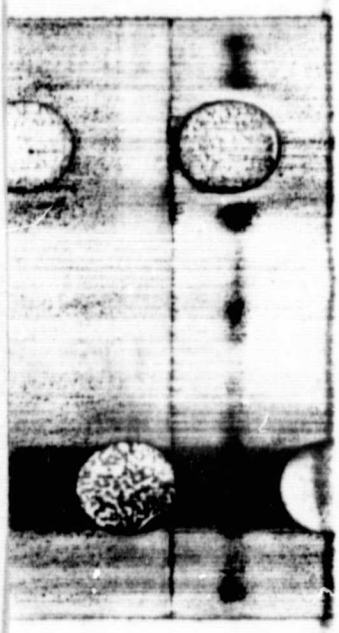

If we treat this problem by the standard perturbation theory up to third order, we obtain the well-known formula for the energy levels of a nondegenerate vibrational state and the ith inversion state including sextic centrifugal distortion coefficients:

$$\left(\frac{E_i}{hc}\right) = \left(\frac{E_i^0}{hc}\right) + B_i J(J+1) + (C_i - B_i)k^2 - D_J^{(i)} J^2(J+1)^2 - D_{JK}^{(i)} J(J+1)k^2$$
$$- D_K^{(i)} k^4 + H_{JJJ}^{(i)} J^3(J+1)^3 + H_{JJK}^{(i)} J^2(J+1)^2 k^2 + H_{JKK}^{(i)} J(J+1)k^4 + H_{KKK}^{(i)} k^6. \quad (16)$$

It should be mentioned that from the mathematical point of view such a treatment is correct if the series expansions (8) are convergent. We have verified a rapid convergence of the series expansions of all parameters occurring in the Hamiltonian H in Eq. (1), which justifies our procedure.

Rotational and centrifugal distortion coefficients in Eq. (16), and in other relations which could be obtained from higher-order terms in the Hamiltonian by perturbation treatment, are effective parameters for the ith inversion state. Their relation to the coefficients of the expansion (8a) could be found in explicit form. The algebra involved in such a treatment is straightforward but rather lengthy and will not be carried out in this paper. Instead we concentrate on the determination of the effective molecular parameters by a least-squares fit to the experimental data (Sections IV–VI).

It should be noted that in our approach to the parameterization of the energy levels, NH_3 is treated as a planar molecule of D_{3h} symmetry with a large-amplitude motion. Because we use the model Hamiltonian described in Refs. (*1*, *4*, *5*), such an approach is physically correct and its advantage is that higher-order effects can be described in a lower-order treatment (see the above discussion of the rigid bender approximation). Previous approaches (e.g., (*7*, *25*)) considered ammonia as a molecule of C_{3v} symmetry and the vibration–rotation Hamiltonian was expanded in terms of Q in the point group of the equilibrium configuration. Strictly speaking this is not physically correct, and the relation between the effective molecular parameters and the true physical parameters is not clear in such a treatment, especially for the excited vibrational–rotational states.

III. HIGH-RESOLUTION INFRARED MEASUREMENTS

The ν_2 and ν_4 bands of ammonia in the infrared were recorded with a 3.5-m focal length vacuum grating infrared spectrometer at the Ohio State University equipped with a 9 in. × 6 in. (22½ cm × 15 cm) Bausch and Lomb grating with 40 grooves per millimeter and used echelle fashion. The gas sample used was supplied by Matheson and Company and was quoted to have a purity of 99.4% of $^{14}NH_3$. The source of continuous radiation was a carbon rod furnace. The measurements were made relative to the 1–0 band lines of CO and the accuracy is believed to be about 0.005 cm^{-1}. Other experimental details have been given in detail by Curtis (*26*). Figures 1a, 1b, and 1c display the spectra recorded, along with pressures and path lengths used for the ammonia gas.

Portions of the ν_2 band were examined under Doppler-limited resolution using the diode laser spectrometer at Los Alamos Scientific Laboratory (*27*). This was

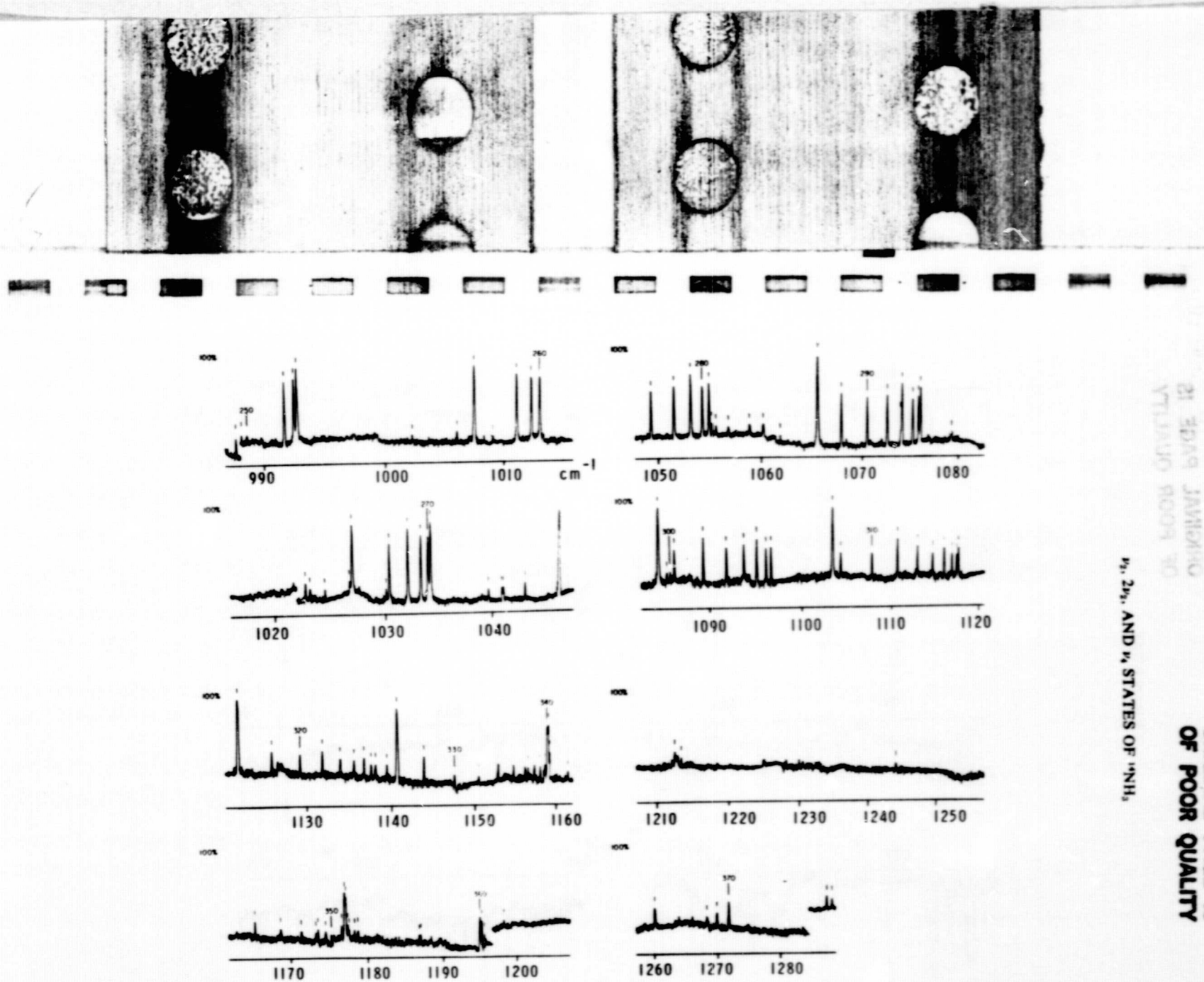

FIG. 1a. Low-pressure grating spectra in the ν_2 region of ammonia. Gas pressure used was 2 mm Hg in a 1-m-long absorption cell. At the upper and lower ends of the spectrum some data were observed with a sample pressure of 5.5 mm Hg.

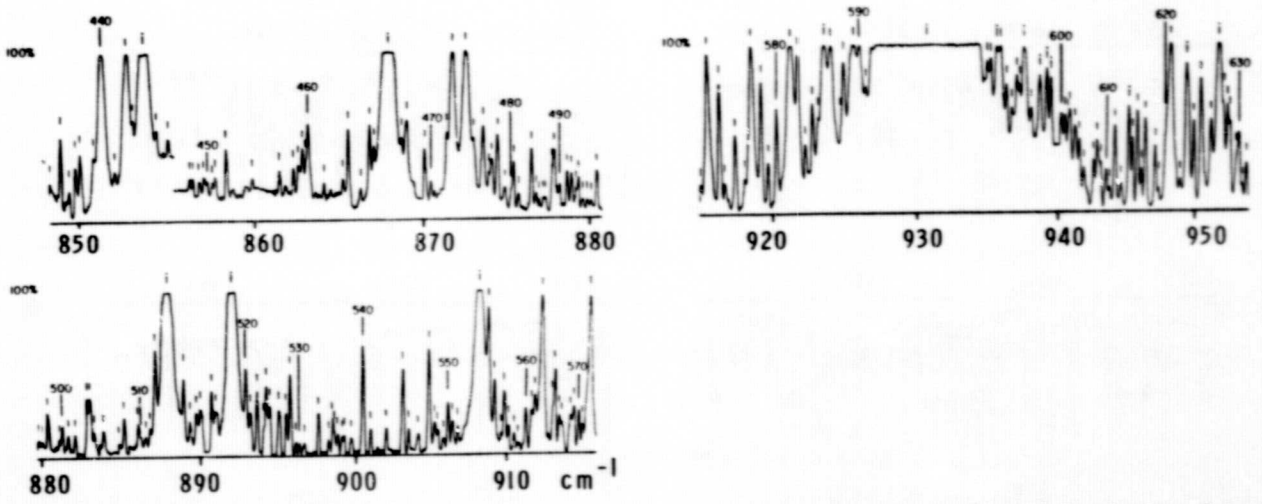

FIG. 1b. High-pressure grating spectra in the ν_2 region of ammonia. Gas pressure used was 1 cm Hg in an 11-m path. A line that has a dot over it is a blend of lines that are resolved in the low-pressure data.

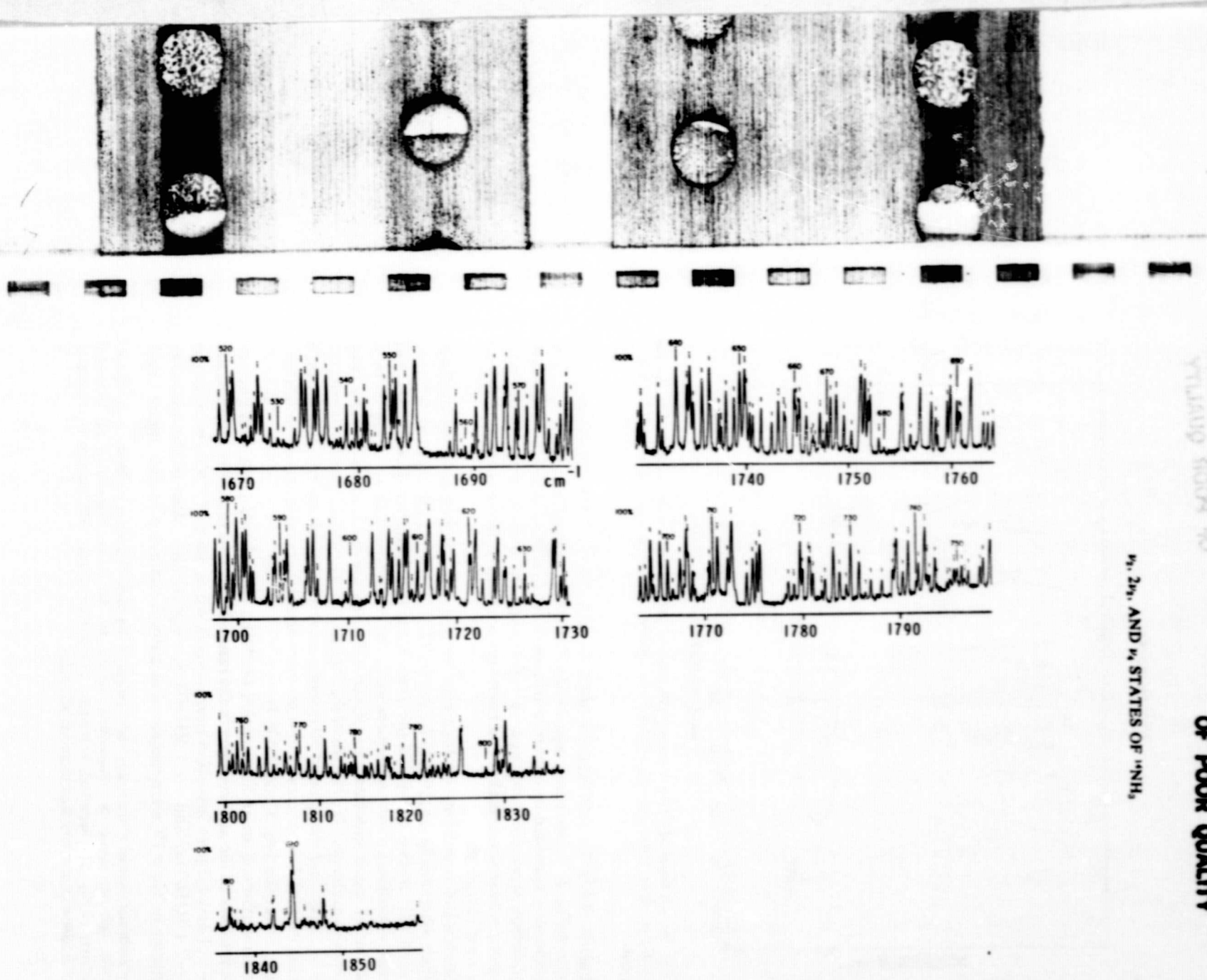

FIG. 1c. Grating spectra of the ν_4 region of ammonia. Gas pressure used was 1 cm Hg in a 1-m-long absorption cell. Line with a dot over it is an H_2O line or a blend with an H_2O line.

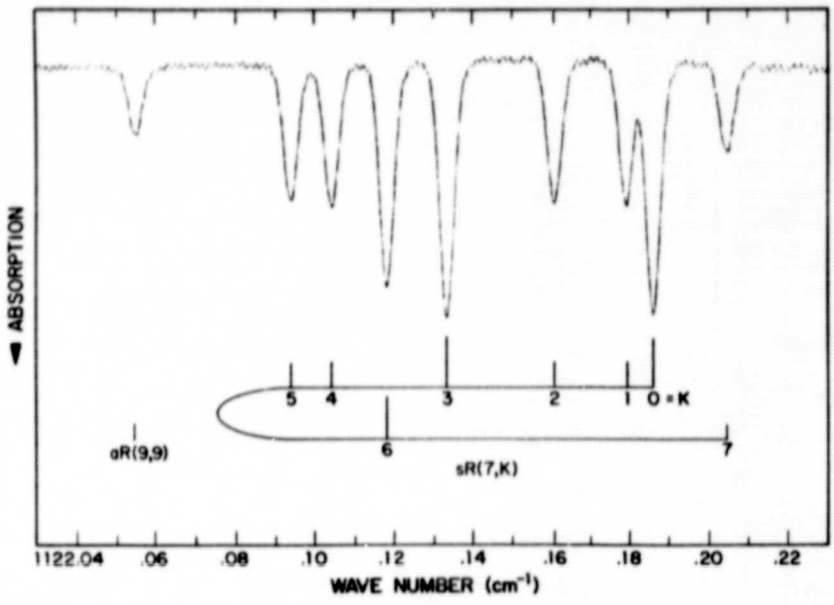

FIG. 2. The spectrum of $^{14}NH_3$ between 1122.03 and 1122.23 cm^{-1} as recorded with a tunable semiconductor diode laser, showing $sR(7,K)$ and $aR(9,9)$. Sample pressure was ~0.1 Torr in a 40-cm cell.

particularly useful for resolving the $sR(J,K)$ groupings; $sR(7,K)$ is shown as an example in Fig. 2. Relative line separations in these spectra were measured against simultaneously recorded interference fringes from a germanium etalon. Absolute wavenumbers were then obtained by referencing the lines to one transition in each group whose wavenumber had been very accurately determined as described in the next paragraph.

Experimental transition wavenumbers for the ν_2, $2\nu_2$, and ν_4 bands together with their assignments are given in Tables I to III. In the case of the ν_2 band, we have also used the precise values of the pure inversion transition frequencies and inversion–rotation transition frequencies in the ν_2 excited state as measured by a submillimeter wave spectrometer, RAD[3] (*28–30*), the infrared-microwave two-photon measurements (*16*, *17*, *31*) of the vibration–inversion–rotation transitions to the ν_2 state, and the ground-state pure inversion transition frequencies (*32*) to obtain precise frequencies of certain vibration–inversion–rotation transitions to the ν_2 state (see Fig. 3 and Table I).

The submillimeter-wave line centers of $^{14}NH_3$ were found to depend linearly on the pressure of the ammonia gas in the range 0.2–2 Torr (e.g., the slopes of the J,K = 1,1 and 2,2 pure inversion transitions in the ν_2 state of $^{14}NH_3$ were found to be −2.4 MHz/Torr and +1.5 MHz/Torr, respectively). Most of the transition frequencies in Table IV were measured at a single value of pressure (in the range

[3] The particular system of frequency stabilization of the backward wave oscillator used (Belov, Gershstein, and Maslovskii, *in* "Proceedings of the IV All Union Symposium on Molecular Spectroscopy of High and Superhigh Resolution, Tomsk-Novosibirsk, 1978") makes it possible to measure frequencies to a very high degree of accuracy.

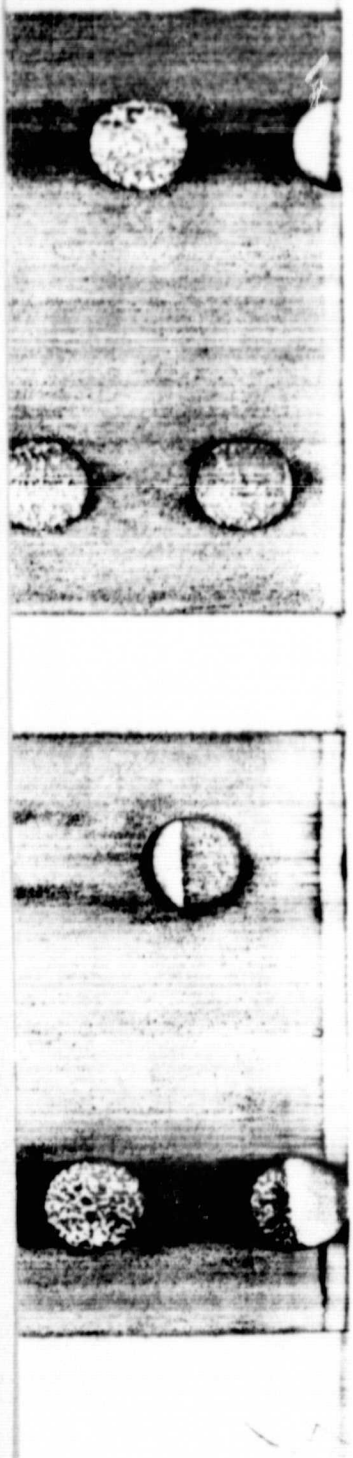

TABLE I

Observed and Calculated Transition Wavenumbers in the ν_2 Band of $^{14}NH_3$ (cm^{-1})[a]

J	K	ν_{obs}	ν_{calc}	$\nu_{cal}-\nu_{ob}$	ν_{obs}	ν_{calc}	$\nu_{cal}-\nu_{ob}$
		sP			aP		
1	0	948.2328[i] 948.232	948.2323	-0.0005	...	...	...
2	0	...	...	...	892.158	892.1570	-0.001
2	1	928.230	928.2322	0.002	891.884	891.8825	-0.001
3	0	908.190	908.1988	0.009	...	...	...
3	1	908.1795[h]	908.1767	-0.0018	872.565	872.5667	0.002
3	2	908.115	908.1124	-0.002	871.737	871.7371	0.000
4	0	...	...	...	*853.817	853.8186	0.002
4	1	888.0779[f] 888.035[b]	888.0788	0.0009	853.5467[h] 853.549	853.5472	0.0005
4	2	887.9998[f]	887.9995	0.0007	852.7237[h] 852.727	852.7239	0.0002
4	3	*887.87683[g] 887.8773[f] 887.878	887.8746	-0.0022	*851.32692[h] 851.330	851.3271	0.0002
5	0	*867.980[b]	868.0003	0.020	...	...	...
5	1	*867.980[b]	867.9682	-0.012	834.826	834.8230	-0.003
5	2	*867.882[b]	867.8723	-0.010	834.013	834.0112	-0.002
5	3	*867.717	867.7193	0.002	*832.635	832.6338	-0.001
5	4	867.517	867.5204	0.003	830.654	830.6533	-0.001
6	0	...	...	...	*816.649	816.6459	-0.003
6	1	847.876	847.8756	-0.000	816.388	816.3864	-0.002
6	2	847.765	847.7622	-0.003	815.585	815.5911	0.006
6	3	*847.578	847.5795	0.002	*814.239	814.2418	0.002
6	4	847.336	847.3375	0.001	812.297	812.3002	0.003
6	5	847.053	847.0517	-0.001	809.714	809.7151	0.001
7	0	*827.857[b]	827.8748	0.018	...	...	...
7	1	*827.857[b]	827.8329	-0.024	798.228	798.2239	-0.004
7	2	827.703	827.7014	-0.002	797.451	797.4491	-0.002
7	3	*827.491	827.4878	-0.003	*796.131	796.1347	0.004
7	4	827.202	827.2012	-0.001	794.240	794.2444	0.004
7	5	826.854	826.8553	0.001	791.723	791.7261	0.003
7	6	826.470	826.4705	0.000	788.506	788.5112	0.005
8	0	...	...	...	*780.565[b]	780.5523	-0.013
8	1	807.873	807.8714	-0.002	780.309	780.3161	0.007
8	2	807.716	807.7216	0.006	779.564	779.5657	0.002
8	3	*807.468	807.4768	0.009	*778.290	778.2932	0.003
8	4	807.148	807.1449	-0.003	776.458	776.4637	0.006
8	5	806.744	806.7382	-0.006	774.020	774.0264	0.006
8	6	806.281	806.2744	-0.007	770.913	770.9130	-0.000
8	7	805.775	805.7788	0.004	767.037	767.0387	0.002
9	0	*788.079[b]	788.0707	-0.008	...	...	...
9	1	*788.034[b]	788.0213	-0.013	762.639	762.6409	0.002
9	2	787.853	787.8533	0.000	761.921	761.9176	-0.003
9	3	*787.572	787.5776	0.006	*760.695	760.6919	-0.003
9	4	787.197	787.2009	0.004	758.927[b]	758.9313	0.004
9	5	786.728	786.7334	0.006	756.586	756.5871	0.001
9	6	786.184[b]	786.1914	0.007	753.590	753.5922	0.002
9	7	785.594	785.5964	0.002	749.862	749.8612	-0.001
9	8	784.976	784.9790	0.003	745.295	745.2938	-0.001

[a] Our infrared grating measurements unless stated otherwise; asterisk denotes that this value has not been used in the fit.

[b] Blended line.

[c] Ref. (*16*).

[d] Ref. (*14*).

[e] Ref. (*31*).

[f] Ref. (*17*).

[g] Ref. (*19*).

TABLE I—*Continued*

J	K	ν_{obs}	ν_{calc}	$\nu_{cal}-\nu_{ob}$	ν_{obs}	ν_{calc}	$\nu_{cal}-\nu_{ob}$
		sP			aP		
10	0	...	...	...	*745.409[b]	745.3761	-0.033
10	1	*768.309[b]	768.311.	0.002	*745.194[b]	745.1760	-0.018
10	2	*768.107[b]	768.1258	0.019	744.490[b]	744.4809	-0.009
10	3	*767.812	767.8199	0.008	*743.312	743.3047	-0.007
10	4	767.408	767.3994	-0.009	741.622	741.6179	-0.004
10	5	766.877	766.8733	-0.004	739.384	739.3754	-0.009
10	6	766.241[b]	766.2545	0.013	736.513	736.5129	-0.000
10	7	765.565	765.5621	-0.003	732.949	732.9456	-0.003
10	8	764.824	764.8227	-0.001	728.580[b]	728.5700	-0.010
10	9	764.074	764.0734	-0.001	723.275	723.2714	-0.004
11	0	*748.810[b]	748.8207	0.011	...	...	...
11	1	*748.810[b]	748.7689	-0.041	727.910	727.9026	-0.007
11	2	748.574[b]	748.5663	-0.008	727.251	727.2350	-0.016
11	3	*748.228[b]	748.2313	0.003	*726.109[b]	726.1077	-0.001
11	4	747.765	747.7687	0.004	724.517	724.4956	-0.021
11	5	747.179	747.1858	0.007	722.368	722.3585	-0.009
11	6	746.492	746.4935	0.001	719.647	719.6368	-0.010
11	7	745.703	745.7076	0.005	716.248	716.2486	0.001
11	8	744.869	744.8512	0.002	712.095	712.0894	-0.006
11	9	743.961	743.9555	-0.006	707.051	707.0372	-0.014
11	10	743.078	743.0644	-0.014	700.965	700.9650	0.000
12	0	...	...	...	*711.029	710.9625	-0.066
12	1	729.419	729.4196	0.001	*710.796[b]	710.8116	0.016
12	2	729.209	729.2006	-0.008	710.175	710.1682	-0.007
12	3	*728.822	728.8378	0.016	*709.098[b]	709.0851	-0.013
12	4	728.331	728.3350	0.004	*707.585[b]	707.5430	-0.042
12	5	727.699	727.6980	-0.001	*705.550[b]	705.5084	-0.042
12	6	726.943	726.9357	-0.007	702.943	702.9287	-0.014
12	7	*726.109[b]	726.0615	-0.047	699.727	699.7273	0.000
12	8	725.101	725.0940	-0.007	695.790	695.8018	0.012
12	9	724.052[b]	724.0600	0.008	691.030	691.0257	-0.004
12	10	723.007	722.9965	-0.011	685.281	685.2589	-0.022
12	11	721.978	721.9546	-0.023	678.376	678.3670	-0.009
13	0	*710.329[b]	710.3367	0.008	...	...	...
13	1	*710.329[b]	710.2892	-0.040	*698.811[b]	693.9096	0.099
13	2	*710.069[b]	710.0545	-0.015	*693.233[b]	693.2841	0.051
13	3	*709.669[b]	709.6649	-0.003	*692.298[b]	692.2358	-0.062
13	4	*709.098[b]	709.1235	0.026	690.767	690.7523	-0.017
13	5	708.420	708.4349	0.015	*688.849[b]	688.8087	-0.040
13	6	*707.585[b]	707.6063	0.021	*686.391[b]	686.3621	-0.029
13	7	706.645	706.6485	0.003	*683.356[b]	683.3448	-0.011
13	8	*705.550[b]	705.5769	0.027	679.653	679.6597	0.007
13	9	704.411	704.4136	0.003	*675.156[b]	675.1800	0.024
13	10	703.197	703.1896	-0.006		669.7556	
13	11	701.962	701.9477	-0.01[illegible]		663.2297	
13	12	700.774[b]	700.7468	-0.027		655.4683	
		sQ			aQ		
1	1	967.99774[c] 967.995	967.9980	0.0003	931.62776[h] 931.6280[f] 931.632	931.6286	0.0008

[h] Value calculated from the microwave ground state inversion frequencies, the submillimeter ν_2 inversion frequencies, and the high-resolution infrared vibration–inversion-rotation transition frequencies (see text).

[i] Ref. (*20*).

[j] Value calculated from the frequency difference (resolved K structure) in Ref. (*18*).

[k] Value calculated from the microwave ground-state inversion frequencies, the submillimeter ν_2 inversion–rotation frequencies, and the high-resolution infrared vibration–inversion-rotation transition frequencies (see text).

[l] Our diode laser measurements.

TABLE I—*Continued*

J	K	ν_{obs}	ν_{calc}	$\nu_{cal}-\nu_{ob}$	ν_{obs}	ν_{calc}	$\nu_{cal}-\nu_{ob}$
		sQ			aQ		
2	1	967.77467[h] 967.777[d]	967.7748	0.0001	932.13610[c] 932.107[b]	932.1361	0.0000
2	2	967.73860[h] 967.73859[c] 967.73841[g] 967.749	967.7386	0.0000	931.33342[g] 931.33348[f] 931.3336[c] 931.332	931.3338	0.0004
3	1		967.4490		932.886	932.8806	-0.005
3	2	967.40680[h] 967.4073[c]	967.4067	-0.0001	932.09402[c] 932.107[b]	932.0936	-0.0005
3	3	*967.34632[c] 967.367	967.3441	-0.0022	*930.75697[h] 930.7557[c] 930.760	930.7574	0.0004
4	1	967.0302[h] 966.965[b]	967.0307	0.0005	933.8419[f] 933.833[b]	933.8422	0.0003
4	2	966.9814[h] 966.965[b]	966.9808	-0.0006	933.0762[c] 933.063	933.0753	-0.0009
4	3	*966.908[d] 966.898	966.9049	-0.003	*931.773	931.7729	-0.000
4	4	966.8150[h] 966.816[d] 966.814	966.8148	-0.0002	929.8982[f] 929.8984[c] 929.894	929.8984	0.0002
5	1	968.530	966.5324	0.002	934.999	934.9948	-0.004
5	2	966.4739[h] 966.475[d] 966.476	966.4735	-0.0004	934.2524[f] 934.244[b]	934.2526	0.0002
5	3	*966.37987[h] 966.3804[c] 966.379	966.3821	0.0022	*932.99243[c] 932.99226[g] 932.994	932.9919	-0.0005
5	4	966.26931[c] 966.26935[g] 966.268	966.2691	-0.0002	931.17745[h] 931.17735[c] 931.1776[f] 931.165	931.1766	-0.0009
5	5	966.15100[c] 966.151	966.152	0.0002	928.7543[f] 928.7547[c] 928.755	928.7549	0.0006
6	1	965.982[b]	965.9678	-0.014	936.311	936.3068	-0.004
6	2	965.904	965.8989	-0.005	935.592	935.5933	0.001
6	3	*965.792[d] 965.787	965.7904	-0.002	*934.377	934.3814	0.004
6	4	965.65222[h] 965.6520[c] 965.649	965.6521	-0.0001	932.63589[f] 932.63582[g] 932.634	932.6359	0.0000
6	5	965.49939[h] 965.501[d] 965.496	965.4993	-0.0001	930.30653[c] 930.309	930.3058	-0.0007
6	6	965.355[d] 965.352	965.3540	-0.001	927.32328[f] 927.32323[g] 927.3234[c] 927.326	927.3240	0.0008
7	1	*965.360[b]	965.3515	-0.008	937.736	937.7424	0.006
7	2		965.2720		937.063	937.0609	-0.002
7	3	*965.1373[c]	965.1452	0.0079	*935.9034[h]	935.9038	0.0004

TABLE I—*Continued*

J	K	ν_{obs}	ν_{calc}	$\nu_{cal}-\nu_{ob}$	ν_{obs}	ν_{calc}	$\nu_{cal}-\nu_{ob}$
			sQ			aQ	
		965.140			935.914[b]		
7	4	964.9797[h]	964.9800	0.0003	934.2358[f]	934.2372	0.0014
		964.982[d]			934.244[b]		
		964.982					
7	5	964.79006[c]	964.7903	0.0002	932.01111[h]	932.0117	0.0006
		964.790			932.014		
7	6	964.5954[c]	964.5957	0.0003	929.1616[f]	929.1607	-0.0009
		964.596[b]			929.161		
7	7	964.42410[c]	964.4241	0.0000	*925.5977[f]	925.6016	0.0039
		964.428[b]			925.598		
8	1		964.6981		939.256[b]	939.2637	0.008
8	2	*964.596[b]	964.6077	0.012	*938.625[b]	938.6164	-0.009
8	3	*964.428[b]	964.4621	0.034	*937.516	937.5182	0.002
8	4	964.271	964.2692	-0.002	*935.914[b]	935.9376	0.024
8	5	964.04115[h]	964.0413	0.0002	933.82600[c]	933.8275	0.0015
		964.044			933.8265[f]		
					933.833[b]		
8	6	963.79607[h]	963.7962	0.0001	931.12190[c]	931.1227	0.0008
		963.651[d]			931.1227[f]		
		963.787			931.124[b]		
8	7	963.55939[h]	963.5587	-0.0007	927.74196[c]	927.7403	-0.0017
		963.5582[c]			927.739		
		963.555					
8	8	963.36262[c]	963.3627	0.0001	923.582	923.5827	0.001
		963.362					
9	1		964.0219		*940.850[b]	940.8335	-0.016
9	2		963.9206		*940.235[b]	940.2212	-0.014
9	3		963.7560		*939.197	939.1837	-0.013
9	4	963.5343[h]	963.5352	0.0009	937.6989[f]	937.6929	-0.0060
					937.701		
9	5	963.276[b]	963.2691	-0.007	935.710	935.7053	-0.005
9	6	962.97368[c]	962.9733	-0.0003	933.15745[h]	933.1588	0.0013
		962.975			933.1571[c]		
					933.152		
9	7	962.6705[h]	962.6698	-0.0007	929.9711[f]	929.9712	0.0001
		962.6736[c]			929.969[d]		
		962.673			929.954		
9	8	962.38850[h]	962.3888	0.0003	926.04584[c]	926.0424	-0.0034
		962.3878[c]			926.047		
		962.389					
9	9	962.167	962.1715	0.004	921.255	921.2611	0.006
10	1		963.3374		942.4206[i]	942.4201	-0.0005
10	2		963.2250		*941.872[b]	941.8415	-0.030
10	3		963.0415		*940.850[b]	940.8632	0.013
10	4		962.7931		*939.488[b]	939.4618	-0.026
10	5	962.4895[h]	962.4892	-0.0003	937.6119[f]	937.5988	-0.0132
					937.605		
10	6	962.1448[h]	962.1435	-0.0013	935.2216[f]	935.2169	-0.0047
					935.223		
10	7	*961.760[b]	961.7752		932.233[d]	932.2373	0.004
					932.233		
10	8	961.4113[h]	961.4110	-0.0003	928.5581[f]	928.5590	0.0009
		961.409			928.559		

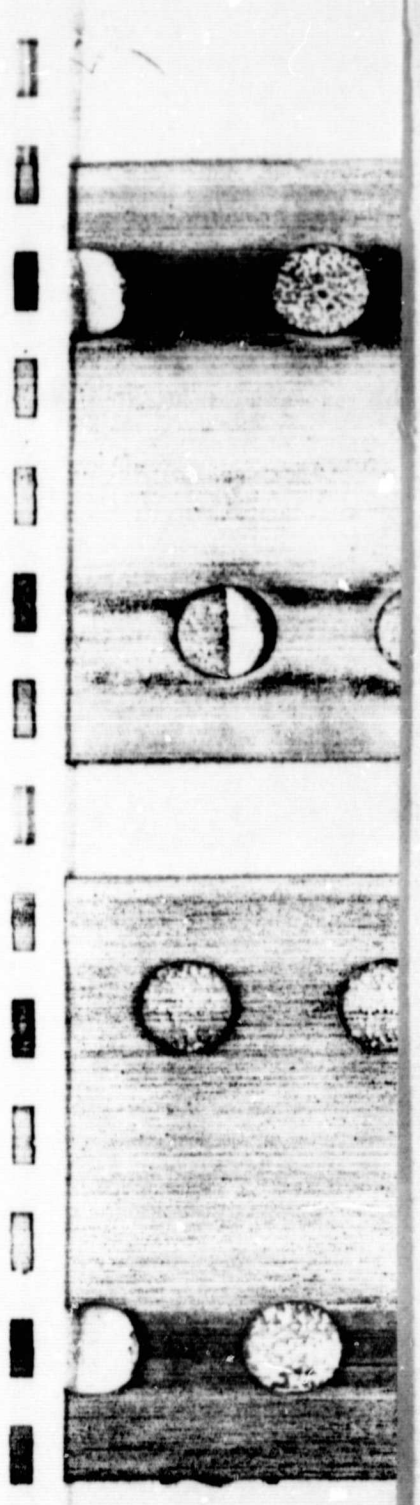

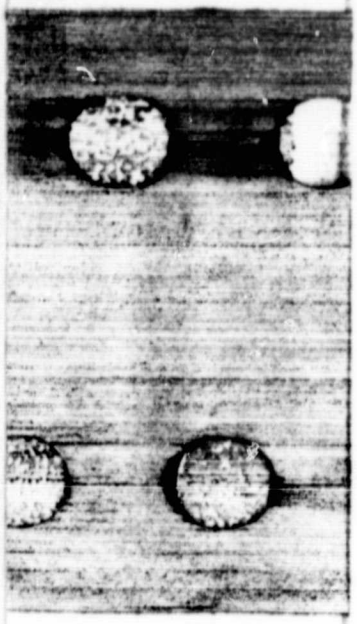

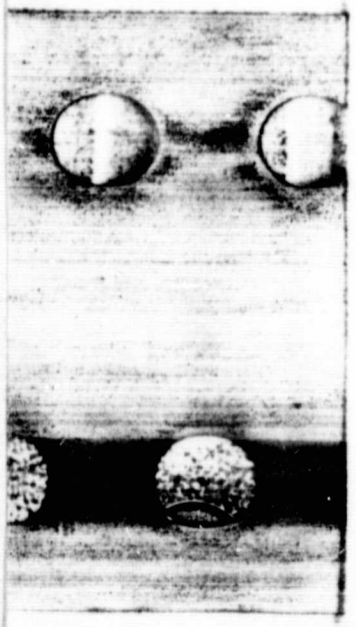

TABLE I—*Continued*

J	K	ν_{obs}	ν_{calc}	$\nu_{cal}-\nu_{ob}$	ν_{obs}	ν_{calc}	$\nu_{cal}-\nu_{ob}$
		sQ			aQ		
10	9	961.086	961.0870	0.001	924.068	924.0639	-0.004
10	10	960.85232[c]	960.8522	-0.0001	918.6209[f]	918.6296	0.0087
		960.857			918.620		
11	1		962.6590			944.0025	
11	2		962.5357		943.4481[i]	943.4536	0.0054
					943.486[b]		
11	3		963.3334		*942.5667[i]	942.5290	-0.0377
					942.569		
11	4		962.0576		*941.255[b]	941.2108	-0.044
11	5		961.7165		*939.488[b]	939.4676	-0.020
11	6	*961.325[b]	961.3219	-0.003	937.273[b]	937.2494	-0.024
11	7	*960.857[b]	960.8908	0.034	934.471[b]	934.4829	0.011
11	8	960.446	960.4463	0.000	*931.124[b]	931.0693	-0.055
11	9	960.01990[c]	960.0199	0.0000	926.88456[h]	926.8868	0.0022
		960.019			926.8844[c]		
					926.887		
11	10	959.656	959.6544	-0.002	921.8120[f]	921.7999	-0.0121
					921.810		
11	11	959.408	959.4071	-0.001	915.665	915.6800	0.015
12	1		962.0032			945.5772	
12	2		961.8687		*945.0918[ib]	945.0511	-0.0407
12	3		961.6475		*944.1835[i]	944.1696	-0.0141
12	4		961.3442		*942.9368[ib]	942.9217	-0.0151
12	5		960.9662			941.2849	
12	6		960.5237			939.2191	
12	7		960.0315			936.6600	
12	8		959.5098		*933.501[b]	933.5147	0.014
12	9	958.975	958.9858	0.011		929.6612	
12	10	958.499	958.4968	-0.002	924.9499[e]	924.9547	0.0048
					924.942		
12	11	958.089	958.0924	0.003	919.264	919.2443	-0.020
12	12	957.835	957.8390	0.004	912.385	912.4029	0.018
		sR			aR		
0	0	...	...	...	951.7794[i]	951.7769	-0.0025
					951.775		
1	0	1007.5474[j]	1007.5471	-0.0003	...	...	...
		1007.544[b]					
1	1	1007.54068[h]	1007.5406	-0.0001	971.882249	971.8821	-0.0001
		1007.544[b]			971.88204[c]		
					971.882		
2	0	...	...	...	*992.694	992.7003	0.006
2	1	1027.0467[f]	1027.0471	0.0004	992.45019[k]	992.4500	-0.0002
		1027.040[b]			992.452		
2	2	1027.0331[h]	1027.0329	-0.0002	991.69069[k]	991.6903	-0.0004
		1027.0335[f]			991.6914[c]		
		1027.040[b]			991.690		
3	0	*1046.4056[l]	1046.4053	-0.0003	...	...	...
		1046.392[b]					
3	1	1046.4008[l]	1046.4009	0.0001	1013.1758[h]	1013.1757	-0.0001
		1046.392[b]			1013.174		

TABLE I—*Continued*

J	K	ν_{obs}	ν_{calc}	$\nu_{cal}-\nu_{ob}$	ν_{obs}	ν_{calc}	$\nu_{cal}-\nu_{ob}$
		sR			aR		
3	2	1046.3881[l] 1046.392[b]	1046.3881	0.0000	1012.4452[h] 1012.442	1012.4449	-0.0003
3	3	*1046.37450[h] 1046.375[d] 1046.392[b]	1046.3745	0.0000	*1011.20350[e] 1011.2035[c] 1011.202	1011.2032	-0.0003
4	0	...	...	...	*1034.245	1034.2409	-0.004
4	1	1065.5944[f] 1065.576[b]	1065.5950	0.0006	1034.0128[h] 1034.011	1034.0141	0.0013
4	2	1065.5824[f] 1065.576[b]	1065.5820	-0.0004	1033.3165[h] 1033.316	1033.3166	0.0001
4	3	*1065.5655[f] 1065.576[b]	1065.5677	0.0022	*1032.1311[h] 1032.129	1032.1311	0.0000
4	4	1065.5636[f] 1065.576[b]	1065.5636	0.0000	1030.4222[h] 1030.421	1030.4217	-0.0005
5	0	*1084.6296[l]	1084.6276	-0.0020	...	...	...
5	1	1084.6244[l] 1084.608[b]	1084.6246	0.0002	1054.916	1054.9152	-0.001
5	2	1084.6082[c] 1084.608[b]	1084.6102	0.0020	1054.2511[h] 1054.254	1054.2548	0.0037
5	3	*1084.59306[c] 1084.608[b]	1084.5930	-0.0001	*1053.13044[h] 1053.135	1053.1320	0.0016
5	4	1084.58371[c] 1084.608[b]	1084.5837	0.0000	1051.51207[h] 1051.517	1051.5123	0.0002
5	5	1084.59924[c] 1084.608[b]	1084.5988	-0.0004	1049.34632[h] 1049.349	1049.3456	-0.0007
6	0	...	...	...	*1076.033	1076.0184	-0.015
6	1	1103.4846[l] 1103.452[b]	1103.4864	0.0018	1075.8218[h] 1075.824	1075.8254	0.0036
6	2	1103.4686[l] 1103.452[b]	1103.4696	0.0010	1075.2024[f] 1075.207	1075.2051	0.0027
6	3	*1103.4397[l] 1103.452[b]	1103.4478	0.0081	*1074.1477[h] 1074.152	1074.1505	0.0026
6	4	1103.4293[l] 1103.452[b]	1103.4310	0.0017	1072.6262[h] 1072.631	1072.6288	0.0026
6	5	1103.4324[l] 1103.452[b]	1103.4342	0.0018	1070.5909[f] 1070.594	1070.5914	0.0005
6	6	1103.4784[l] 1103.452[b]	1103.4792	0.0008	1067.9733[h] 1067.976	1067.9735	0.0002
7	0	*1122.1861[l] 1122.132[b]	1122.1784	-0.0077	...	...	...
7	1	1122.1792[l] 1122.132[b]	1122.1783	-0.0009	1096.6906[h] 1096.682	1096.6900	-0.0006
7	2	1122.1606[l] 1122.132[b]	1122.1582	-0.0024	1096.1132[f] 1096.112	1096.1117	-0.0015
7	3	*1122.1332[l] 1122.132[b]	1122.1305	-0.0027	*1095.1296[h] 1095.124	1095.1288	-0.0008
7	4	1122.1042[l] 1122.132[b]	1122.1043	0.0001	1093.7119[f] 1095.715	1093.7111	-0.0008
7	5	1122.0937[l] 1122.132[b]	1122.0934	-0.0003	1091.8120[h] 1091.816	1091.8128	0.0008
7	6	1122.1181[l] 1122.132[b]	1122.1175	-0.0006	1089.3704[h] 1089.370	1089.3704	0.0000

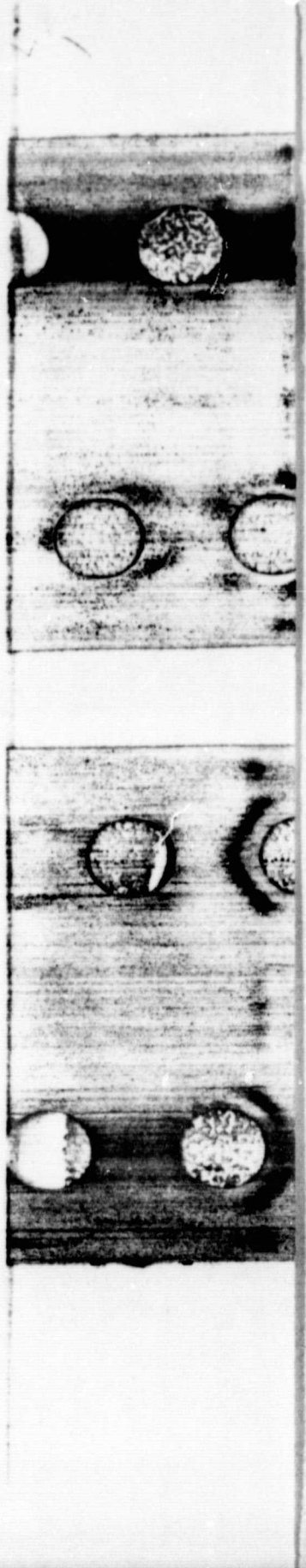

TABLE I—*Continued*

J	K	ν_{obs}	ν_{calc}	$\nu_{cal}-\nu_{ob}$	ν_{obs}	ν_{calc}	$\nu_{cal}-\nu_{ob}$
		sR			aR		
7	7	1122.2046[f] 1122.132[b]	1122.2039	-0.0007	1086.3044[h] 1086.295	1086.3032	-0.0012
8	0	...	...	...	*1117.642	1117.6036	-0.038
8	1	1140.697[f] 1140.628[b]	1140.6988	0.002	*1117.453[b]	1117.4563	0.003
8	2	1140.677[f] 1140.628[b]	1140.6749	-0.002	1116.922	1116.9200	-0.002
8	3	*1140.624[f] 1140.628[b]	1140.6404	0.016	*1116.015	1116.0100	-0.005
8	4	1140.601[f] 1140.628[b]	1140.6036	0.003	1114.703	1114.6992	-0.004
8	5	1140.575[b,f] 1140.628[b]	1140.5768	0.002	1112.941[b]	1112.9457	0.005
8	6	1140.575[b,f] 1140.628[b]	1140.5781	0.003	1110.687	1110.6893	0.002
8	7	1140.630[f] 1140.628[b]	1140.6322	0.002	1107.843	1107.8503	0.007
8	8	1140.768[f] 1140.628[b]	1140.7725	0.004	1104.329	1104.3313	0.002
9	0		1159.0418		...	...	...
9	1		1159.0479		1138.081	1138.0777	-0.003
9	2		1159.0198		1137.597	1137.5818	-0.015
9	3		1158.9776		*1136.759[b]	1136.7423	-0.017
9	4	*1159.165[b]	1158.9289		1135.559	1135.5368	-0.022
9	5	*1158.910[b]	1158.8851		1133.944	1133.9287	-0.015
9	6		1158.8624		1131.868	1131.8628	-0.005
9	7		1158.8830		1129.259	1129.2630	0.004
9	8		1158.9771		1126.025	1126.0314	0.006
9	9		1159.1851		*1122.132[b]	1122.0536	-0.078
10	0	...	...	...	*1158.663[b]	1158.6099	-0.053
10	1		1177.2275		*1158.493[b]	1158.5200	0.027
10	2		1177.1944		*1158.049[b]	1158.0600	0.011
10	3		1177.1436		*1157.301	1157.2846	-0.016
10	4		1177.0820		1156.209[b]	1156.1770	-0.032
10	5	*1176.999[b]	1177.0199		1154.734[b]	1154.7079	-0.026
10	6	*1177.131[b]	1176.9719		1152.851[b]	1152.8295	-0.022
10	7		1176.9583		1150.485	1150.4716	-0.013
10	8		1177.0061		1147.535	1147.5389	0.004
10	9		1177.1515		1143.908	1143.9135	0.005
10	10		1177.4422		1139.471	1139.4646	-0.006
11	0		1195.2250		...	...	...
11	1		1195.2426		*1178.703[b]	1178.7681	0.065
11	2		1195.2038		1178.319	1178.3365	0.018
11	3		1195.1431		*1177.591[b]	1177.6135	0.023
11	4	*1195.176[b]	1195.0669		*1176.618[b]	1176.5895	-0.028
11	5	*1195.531[b]	1194.9847		*1175.293[b]	1175.2441	-0.049
11	6	*1194.923[b]	1194.9099		*1173.583[b]	1173.5398	-0.043
11	7		1194.8609		1171.435	1171.4156	-0.019
11	8		1194.8620		1168.781	1168.7823	0.001
11	9		1194.9458		*1165.497[b]	1165.5222	0.025
11	10		1195.1547		*1161.483[b]	1161.4957	0.013
11	11		1195.5449		1156.555	1156.5574	0.002

Note added in proof: ν_{obs} for aR(9,9) is 1122.0555 cm^{-1} from our diode laser measurements (see Fig. 2).

TABLE II

Observed and Calculated Transition Wavenumbers in the $2\nu_2$ Band of $^{14}NH_3$ (cm^{-1})[a]

J	K	ν_{obs}	ν_{calc}	$\nu_{cal}-\nu_{ob}$	ν_{obs}	ν_{calc}	$\nu_{cal}-\nu_{ob}$
		sP			aP		
1	0	1862.285[c]	1862.2852	0.000	...	...	...
2	0	...	...	...		1557.4402	
2	1	1842.099[c]	1842.0978	-0.001	1556.904	1556.8966	-0.007
3	0		1821.0697		...	...	...
3	1	1821.255[c]	1821.2542	-0.001	*1538.012[b]	1538.0872	0.075
3	2	1821.814[c]	1821.8138	0.000	1536.458	1536.4411	-0.017
4	0	...	...	...	1520.442[b]	1520.4775	0.036
4	1	1799.9991[d]	1799.9994	0.0003		1519.8926	
4	2	1800.5218[d]	1800.5246	0.0028	1518.205	1518.1647	-0.040
4	3	1801.4303[d]	1801.4327	0.0024	*1515.337[b]	1515.4286	0.092
5	0	*1778.244[c]	1778.2226	-0.021	...	...	...
5	1	1778.399[c]	1778.3929	-0.006		1502.3794	
5	2	1778.876[c]	1778.8763	0.000	1500.522[b]	1500.5565	0.034
5	3	1779.714[c]	1779.7129	-0.001	*1497.672[b]	1497.6352	-0.037
5	4	1780.958[c]	1780.9556	-0.002	1493.875	1493.8663	-0.009
6	0	...	...	...	1486.245[b]	1486.2533	0.008
6	1	1756.508[c]	1756.5051	-0.003		1485.6175	
6	2	1756.935[c]	1756.9399	0.004		1483.6886	
6	3	1757.689[c]	1757.6934	0.004		1480.5728	
6	4	1758.812[c]	1758.8155	0.003	1476.431[b]	1476.4561	0.025
6	5	1760.390[c]	1760.3883	-0.002		1471.7713	
7	0	*1734.303[c]	1734.2412	-0.062	...	...	...
7	1		1734.4161			1469.6770	
7	2	1734.804[c]	1734.7962	-0.008	1467.645	1467.6287	-0.016
7	3	1735.460[c]	1735.4564	-0.004		1464.3072	
7	4		1736.4429			1459.8671	
7	5		1737.8324		1454.585[b]	1454.5813	-0.003
7	6	1739.739[c]	1739.7455	0.007	1449.227	1449.1740	-0.052
8	0	...	...	...		1455.3213	
8	1	1712.225[c]	1712.2137	-0.012		1454.6262	
8	2	1712.531[c]	1712.5341	0.003		1452.4369	
8	3	1713.084[c]	1713.0923	0.008		1448.8888	
8	4	1713.928[c]	1713.9301	0.003		1444.1324	
8	5		1715.1188			1438.3818	
8	6	1716.780[c]	1716.7706	-0.009		1431.9797	
8	7	1719.039[c]	1719.0563	0.017		1426.1235	
9	0		1689.7693		...	...	...
9	1	*1690.006[b]	1689.9922	-0.014		1440.5309	
9	2	1690.215[b]	1690.2488	0.034		1438.1608	
9	3	1690.664[b]	1690.6977	0.034	1434.318	1434.3468	0.029
9	4	1691.357[b]	1691.3764	0.019		1429.2631	
9	5	1692.354	1692.3494	-0.005		1423.1118	
9	6	1693.736	1693.7206	-0.015		1416.1252	
9	7	1695.6462[d]	1695.6492	0.0030		1408.6683	
9	8		1698.3710			1402.6953	
10	0	...	...	...		1428.2666	
10	1		1667.8509			1427.4485	
10	2		1668.0405			1424.8197	
10	3		1668.3745			1420.6748	
10	4		1668.8856			1415.2408	

[a] Our infrared grating measurements unless stated otherwise; asterisk denotes that this value has not been used in the fit.

[b] Blended line.

[c] Calculated from the frequency of the hot band $2\nu_2 \leftarrow \nu_2$ transition (our measurements), ν_2 frequency, and the ground-state pure inversion transition.

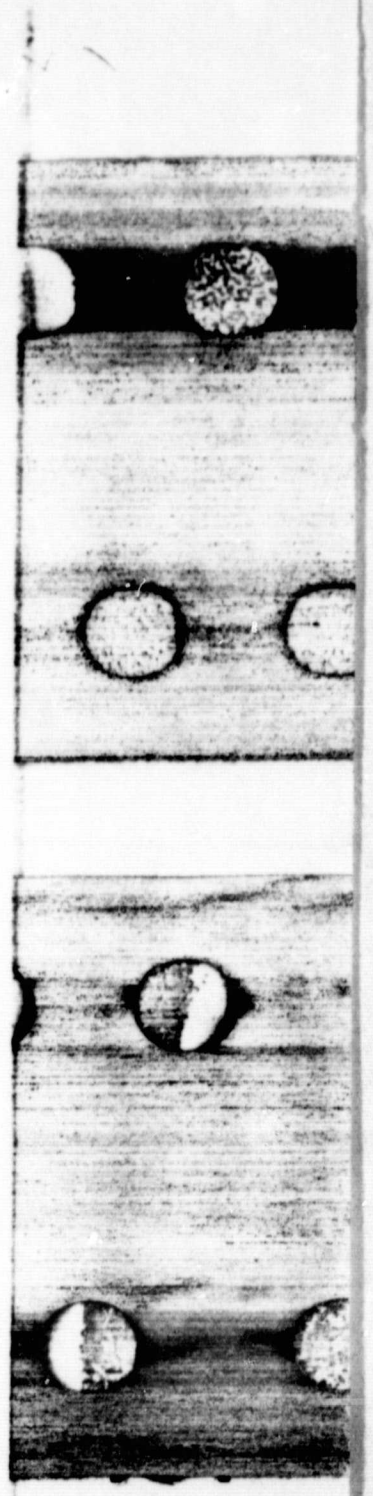

TABLE II—*Continued*

J	K	ν_{obs}	ν_{calc}	$\nu_{cal}-\nu_{ob}$	ν_{obs}	ν_{calc}	$\nu_{cal}-\nu_{ob}$
			sP			aP	
10	5		1669.6316			1408.7246	
10	6		1670.7066			1401.3108	
10	7		1672.2579			1393.1949	
10	8		1674.5058			1384.7213	
10	9		1677.7695			1378.9995	
11	0		1645.5558		...	...	...
11	1		1645.8935			1415.3953	
11	2		1646.0135			1412.3535	
11	3		1646.2283			1407.8008	
11	4		1646.5658			1415.2370	
11	5		1647.0759			1409.8936	
11	6		1647.8432			1402.8204	
11	7		1649.0019			1393.9842	
11	8		1650.7560			1383.3645	
11	9		1653.4042			1370.7866	
11	10		1657.3703			1355.1920	
12	0	...	...	...		1405.7387	
12	1		1624.2283			1404.1348	
12	2		1624.2769			1407.5765[f]	
12	3		1624.3694			1405.7684	
12	4		1624.5284			1402.4624	
12	5		1624.7966			1397.5366	
12	6		1625.2479			1390.8810	
12	7		1626.0030			1382.4472	
12	8		1627.2489			1372.2658	
12	9		1629.2630			1360.3733	
12	10		1632.4426			1346.6781	
12	11		1637.3413			1331.4857	
			sQ			aQ	
1	1	1881.8646[d]	1881.8637	-0.0009	1596.634	1596.6426	0.008
2	1	1880.8542[d]	1880.8523	-0.0019	*1597.594[b]	1597.6566	0.063
2	2	1881.4389[d]	1881.4400	0.0011	1596.046[b]	1596.0378	-0.008
3	1	1879.368[c]	1879.3695	0.001		1599.2261	
3	2	1879.9299[d]	1879.9319	0.0020	*1597.594[b]	1597.5343	-0.060
3	3	1880.8999[d]	1880.9022	0.0023	*1594.810[b]	1594.8588	0.049
4	1	1877.4586[d]	1877.4555	-0.0031		1601.3986	
4	2	1877.9836[d]	1877.9848	0.0012		1599.6205	
4	3	1878.8987[d]	1878.8985	-0.0002	1596.790[c]	1596.7743	-0.016
4	4	1880.2514[d]	1880.2501	-0.0013	1593.157[b]	1593.1115	-0.046
5	1	1875.168[c]	1875.1619	-0.006	1604.181[b]	1604.2259	0.045
5	2	1875.648[c]	1875.6511	0.003	1602.347[c]	1602.3501	0.003
5	3	1876.4937[d]	1876.4960	0.0023		1599.3234	
5	4	1877.74712[e]	1877.7471	0.0000	1595.341[c]	1595.3325	-0.008
5	5	1879.4923[d]	1879.4879	-0.0044	1590.859[b]	1590.8111	-0.048
6	1	*1872.561[c]	1872.5510	-0.010	1607.775	1607.7600	-0.015
6	2	1872.994[c]	1872.9937	0.000	1605.778[c]	1605.7729	-0.005
6	3	1873.7638[d]	1873.7590	-0.005	1602.543[c]	1602.5540	0.011
6	4	1874.887[c]	1874.8938	0.007	1598.248[c]	1598.2586	0.011
6	5	1876.4821[d]	1876.4764	-0.0057	1593.167[c]	1593.1610	-0.006
6	6	1878.6270[d]	1878.6290	0.0020	1588.016	1587.9868	-0.029

[d] Calculated as indicated in footnote c but the diode laser measurements of the $2\nu_2 \leftarrow \nu_2$ frequency (*20*) have been used.

[e] Ref. (*22*).

[f] Assigned as the $2\nu_2$ frequency although the corresponding upper state has the largest contribution from the $\nu_4(-l)$ state (see Section VI and Table XIII).

TABLE II—*Continued*

J	K	ν_{obs}	ν_{calc}	$\nu_{cal}-\nu_{ob}$	ν_{obs}	ν_{calc}	$\nu_{cal}-\nu_{ob}$
		sQ			aQ		
7	1		1869.6938		1612.064[c]	1612.0526	-0.011
7	2	1870.081[c]	1870.0846	0.003	1609.950[c]	1609.9321	-0.018
7	3	1870.735[c]	1870.7607	0.026	1606.501[c]	1606.4994	-0.002
7	4	1871.763[c]	1871.7653	0.002	1601.909[c]	1601.9059	-0.003
7	5		1873.1709		1596.373[b]	1596.3671	-0.006
7	6	1875.102[c]	1875.0919	-0.010	1590.225[c]	1590.2274	0.002
7	7	1877.681[c]	1877.7015	0.020	1584.615	1584.6865	0.072
8	1	1866.660[c]	1866.6690	0.009		1617.1537	
8	2	1866.979[c]	1867.0032	0.024		1614.8596	
8	3	1867.559[c]	1867.5822	0.024	1611.161	1611.1731	0.012
8	4	1868.410[c]	1868.4447	0.035	*1606.297[b]	1606.2694	-0.028
8	5	1869.661[c]	1869.6571	-0.004	*1600.278[b]	1600.3522	0.074
8	6	1871.343[c]	1871.3254	-0.018	1593.652	1593.6557	0.004
8	7	1873.6087[d]	1873.6116	0.0029	1586.534	1586.5474	0.013
8	8		1876.7547		1581.014[b]	1580.9841	0.029
9	1	1863.530	1863.5615	0.031		1623.1060	
9	2	1863.846	1863.8353	-0.011	*1620.601[b]	1620.5600	-0.041
9	3	1864.390[b]	1864.3105	-0.079		1616.5538	
9	4		1865.0214			1611.3158	
9	5		1866.0275		1605.018	1605.0545	0.037
9	6		1867.4255		1597.985	1597.9567	-0.028
9	7		1869.3657			1590.2206	
9	8		1872.0720		1582.219	1582.1937	-0.025
9	9		1875.8676			1576.9893	
10	1		1860.4619			1629.9128	
10	2		1860.6723			1626.9599	
10	3		1861.0386			1622.5564	
10	4		1861.5902		*1630.288[b]	1630.2032	-0.085
10	5		1862.3794			1625.1338	
10	6		1863.4932			1618.4005	
10	7		1865.0694			1609.9729	
10	8		1867.3158		1599.837	1599.8341	-0.003
10	9		1870.5357		1587.831	1587.8133	-0.017
10	10		1875.1581		1572.886	1572.8566	-0.029
11	1		1857.4677			1637.3257	
11	2		1857.6119		*1640.823[b]	1640.8619[f]	0.039
11	3		1857.8650			1639.2122	
11	4		1858.2510			1636.1302	
11	5		1858.8151			1631.4958	
11	6		1859.6341			1625.2017	
11	7		1860.8324			1617.2028	
11	8		1862.6012		*1607.502[b]	1607.5333	0.031
11	9		1865.2229			1596.2344	
11	10	1869.1010[d]	1869.1005	-0.0005	1583.192	1583.2191	0.027
11	11		1874.7939				
		sR			aR		
0	0	...	...	...	1616.980[b]	1617.0601	0.080
1	0		1920.4180		...	...	...
1	1	1920.6200[d]	1920.6181	-0.0019		1637.4027	

TABLE II—*Continued*

J	K	ν_{obs}	ν_{calc}	$\nu_{cal}-\nu_{ob}$	ν_{obs}	ν_{calc}	$\nu_{cal}-\nu_{ob}$
			sR			aR	
2	0	...	...	...	1659.336	1659.3593	0.024
2	1	1938.9681[d]	1938.9676	-0.0005	1658.777	1658.7954	0.018
2	2	1939.5562[d]	1939.5580	0.0018	1657.128[b]	1657.1310	0.003
3	0		1956.6277		...	...	...
3	1	1956.8292[d]	1956.8256	-0.0036	1680.700	1680.7321	0.032
3	2	1957.3904[d]	1957.3920	0.0016	1678.964	1678.9902	0.026
3	3	1958.3681[d]	1958.3680	-0.0001	1676.219	1676.2046	-0.014
4	0	...	...	...	1703.863	1703.8483	-0.014
4	1		1974.2245		1703.236	1703.2451	0.009
4	2		1974.7596		1701.399[b]	1701.4142	0.015
4	3	1975.6790[d]	1975.6816	0.0026	1698.441[b]	1698.4626	0.022
4	4	1977.0421[d]	1977.0416	-0.0005	1694.590	1694.5776	-0.012
5	0		1990.9939		...	...	...
5	1		1991.2078		1726.390[b]	1726.3683	-0.022
5	2		1991.7050		1724.444	1724.4344	-0.010
5	3		1992.5616		1721.289	1721.3046	0.016
5	4		1993.8254		1717.132	1717.1350	0.003
5	5	1995.5818[d]	1995.5760	-0.0058	1712.196[b]	1712.2008	0.005
6	0	...	...	...		1750.7875	
6	1		2007.8287		1750.154	1750.1356	-0.019
6	2		2008.2821		1748.088[b]	1748.0763	-0.012
6	3		2009.0633		1744.733	1744.7461	0.013
6	4		2010.2162		1740.312	1740.2974	-0.015
6	5		2011.8149		1734.952	1734.9469	-0.005
6	6	2013.9848[d]	2013.9755	-0.0093	1729.028	1729.0403	0.012
7	0		2023.8772		...	...	...
7	1		2024.1492			1774.5801	
7	2		2024.5537		*1772.334[b]	1772.3548	0.021
7	3		2025.2506		1768.769	1768.7837	0.015
7	4		2026.2798		1764.034	1764.0429	0.009
7	5		2027.7092		1758.376	1758.3375	-0.039
7	6		2029.6467		1751.931	1751.9034	-0.028
7	7		2032.2568		1745.084	1745.1103	0.026
8	0	...	...	...	1800.503	1800.4941	-0.009
8	1		2040.2383			1799.7288	
8	2		2040.5896		*1797.338[b]	1797.2588	-0.079
8	3		2041.1950			1793.3801	
8	4		2042.0897			1788.3221	
8	5		2043.3352		1782.291	1782.2949	0.004
8	6		2045.0303		*1775.598[b]	1775.4872	-0.111
8	7		2047.3281		*1768.133[b]	1768.0996	0.033
8	8		2050.4556		1760.428	1760.4826	0.055
9	0		2055.7768		...	...	...
9	1		2056.1725			1825.5703	
9	2		2056.4670			1822.7002	
9	3		2056.9746			1818.4355	
9	4		2057.7260			1826.2782	
9	5		2058.7753			1821.4637	
9	6		2060.2121		1815.080	1815.0464	-0.034
9	7		2062.1772		1806.919	1806.9986	0.080

TABLE II—*Continued*

J	K	ν_{obs}	ν_{calc}	$\nu_{cal}-\nu_{ob}$	ν_{obs}	ν_{calc}	$\nu_{cal}-\nu_{ob}$
			sR			aR	
9	8		2064.8819		1797.338	1797.3065	-0.031
9	9		2068.6338		1785.824	1785.8030	-0.020
10	0	...	...	...		1853.3861	
10	1		2072.0362			1851.8432	
10	2		2072.2707			1855.4684[f]	
10	3		2072.6752			1853.9678	
10	4		2073.2754			1851.0964	
10	5		2074.1185			1846.7360	
10	6		2075.2841			1840.7818	
10	7		2076.8999			1833.1915	
10	8		2079.1610			1824.0029	
10	9		2082.3544		*1813.351	1813.2611	-0.090
10	10		2086.8883		1800.850	1800.8838	0.034

0.3–0.6 Torr); the accuracy of those frequencies is about ±1 MHz. The frequencies obtained by extrapolating to zero pressure from at least three measurements at different pressures are determined with the accuracy of ±0.2 MHz (Table IV).

IV. GROUND-STATE ROTATIONAL AND CENTRIFUGAL DISTORTION CONSTANTS

Combination relations have been used in evaluating the molecular constants of the ground state of $^{14}NH_3$. In the standard application of this method to NH_3, rotational and centrifugal distortion constants are obtained separately for the symmetric and antisymmetric components of the inversion doublet. We have modified this treatment so that all the infrared data are processed simultaneously with the microwave pure inversion transition frequencies, using the following equation in addition to the standard combination relations:

$$\begin{aligned}\Delta_i(J,K) &= 0.7934115 + [{}^{(a)}B_0 - {}^{(s)}B_0]J(J+1) \\ &- [{}^{(a)}D_J^0 - {}^{(s)}D_J^0]J^2(J+1)^2 - [{}^{(a)}D_{JK}^0 - {}^{(s)}D_{JK}^0]J(J+1)K^2 \\ &+ [{}^{(a)}H_{JJJ}^0 - {}^{(s)}H_{JJJ}^0]J^3(J+1)^3 + [{}^{(a)}H_{JJK}^0 - {}^{(s)}H_{JJK}^0]J^2(J+1)^2K^2 \\ &+ [{}^{(a)}H_{JKK}^0 - {}^{(s)}H_{JKK}^0]J(J+1)K^4 + \{[{}^{(a)}C_0 - {}^{(a)}B_0] - [{}^{(s)}C_0 - {}^{(s)}B_0]\}K^2 \\ &- [{}^{(a)}D_K^0 - {}^{(s)}D_K^0]K^4 + [{}^{(a)}H_{KKK}^0 - {}^{(s)}H_{KKK}^0]K^6. \quad (17)\end{aligned}$$

The values of the molecular parameters obtained in this way are then consistent also with the experimental inversion frequencies; they are listed in Table V. In this and all other fits the weights of the experimental data have been chosen to be inversely proportional to the squares of their estimated dispersions.

V. CORIOLIS AND *l*-TYPE INTERACTIONS IN THE EXCITED VIBRATION-INVERSION STATES OF $^{14}NH_3$

The lowest-lying vibration–inversion energy levels of $^{14}NH_3$ (Fig. 4) form a complicated system of interacting levels. In order to keep the problem in a

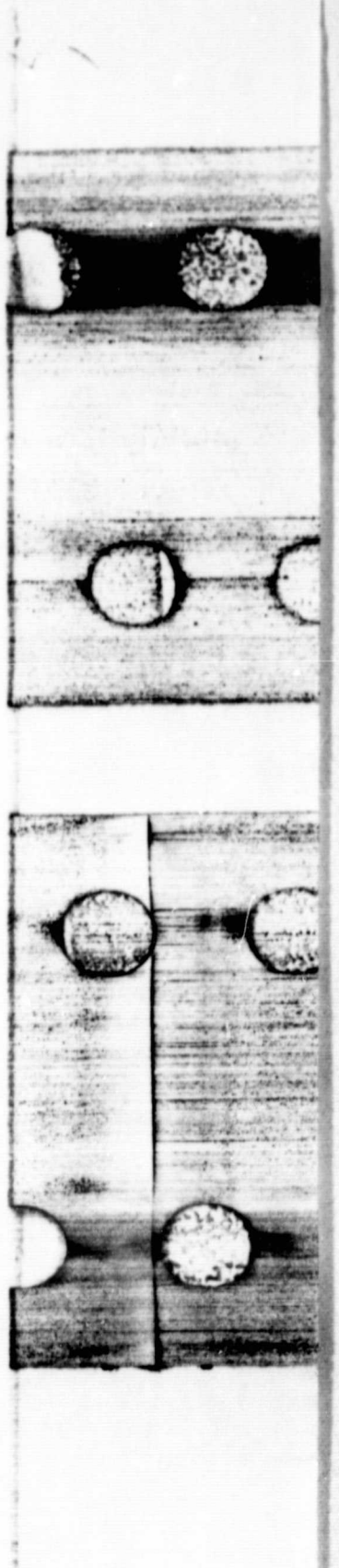

TABLE III

Observed and Calculated Transition Wavenumbers in the ν_4 Band of $^{14}NH_3$ (cm^{-1})[a]

J	K	ν_{obs}	ν_{calc}	$\nu_{cal}-\nu_{ob}$	ν_{obs}	ν_{calc}	$\nu_{cal}-\nu_{ob}$
		s^PP			a^PP		
1	1	1610.089	1610.0987	0.010	*1610.361[b]	1610.4571	0.096
2	1	1590.684	1590.6940	0.010	1591.085	1591.1419	0.057
2	2	1594.810[b]	1594.7855	-0.024	1595.072[b]	1595.1275	0.056
3	1	1571.823[b]	1571.8419	0.019	1572.483	1572.5064	0.024
3	2	1575.852	1575.8580	0.006		1576.3409	
3	3	1579.364	1579.3528	-0.011	1579.621[b]	1579.6732	0.052
4	1	1553.622[b]	1553.6469	0.025	1554.725	1554.7387	0.014
4	2	*1557.532[b]	1557.4948	-0.035	*1558.270[b]	1558.2431	-0.027
4	3	1560.893	1560.8956	0.003	1561.373	1561.3889	0.016
4	4	1563.829	1563.8094	-0.020	1564.075	1564.1027	0.028
5	1	1536.207	1536.2316	0.025	1538.012[b]	1538.0321	0.020
5	2	1539.756	1539.7715	0.016	1541.002	1540.9782	-0.024
5	3	1542.973	1543.0126	0.040	1543.844	1543.8055	-0.038
5	4	1545.796	1545.8165	0.020	1546.324	1546.3065	-0.018
5	5	1548.188	1548.1644	-0.024	1548.421	1548.4278	0.007
6	1	1519.659[b]	1519.6938	0.035	1522.388	1522.4910	0.103
6	2	*1522.712[b]	1522.7758	0.064	1524.736	1524.7068	-0.029
6	3	1525.761	1525.7670	0.006	1527.055	1527.0520	-0.003
6	4	1528.375	1528.4040	0.029	1529.287	1529.2215	-0.065
6	5	1530.613	1530.6304	0.017	1531.153	1531.1241	-0.029
6	6	1532.445	1532.4265	-0.018	1532.666	1532.6630	-0.003
7	1	1504.025	1504.0737	0.049		1508.1241	
7	2	*1506.604[b]	1506.5935	-0.010		1509.5679	
7	3	*1509.138[b]	1509.2316	0.094	1511.314	1511.2770	-0.037
7	4	1511.599	1511.6277	0.028	1513.054[b]	1512.9703	-0.084
7	5	1513.654	1513.6786	0.025	1514.599	1514.5373	-0.062
7	6	1515.337	1515.3466	0.010	1515.871	1515.8837	0.012
7	7	*1516.663[b]	1516.6045	-0.058	1516.840	1516.8229	-0.017
8	1	*1489.304[b]	1489.3635	0.059		1494.9140	
8	2	1491.320	1491.2920	-0.028	1495.726[b]	1495.6511	-0.075
8	3	1493.531	1493.4829	-0.048		1496.6293	
8	4	1495.527	1495.5537	0.027	1497.672[b]	1497.7002	0.028
8	5	1497.332	1497.3607	0.029	*1498.822[b]	1498.7882	-0.036
8	6	*1498.822[b]	1498.8457	0.024	1499.806	1499.8198	0.014
8	7	1499.940	1499.9734	0.033	1500.522[b]	1500.6392	0.117
8	8	1500.746	1500.7068	-0.039	1500.933	1500.9200	-0.013
9	1		1475.5394			1482.8682	
9	2	1476.879	1476.9114	0.032		1483.0076	
9	3		1478.5927		*1483.249[b]	1483.2377	-0.011
9	4	1480.191	1480.2554	-0.064		1483.5720	
9	5	1481.718	1481.7408	0.023		1484.0286	
9	6	1482.955	1482.9743	0.019		1484.5927	
9	7	1483.911	1483.9131	0.002		1485.1588	
9	8	1484.496	1484.5187	0.023		1485.4564	
9	9	1484.779	1484.7417	-0.037	1484.950	1484.9608	0.011
10	1		1462.5856			1472.0371	
10	2		1463.4693		1471.623[b]	1471.6845	0.062
10	3	1464.643	1464.6209	-0.022	*1471.147[b]	1471.2078	0.061
10	4		1465.8093		*1470.754[b]	1470.7456	-0.008
10	5	1466.939[b]	1466.8940	-0.045		1470.4355	

[a] Our infrared grating measurements unless stated otherwise; asterisk denotes that this value has not been used in the fit.

[b] Blended line.

[c] Assigned as the $\nu_4\ ^RX$ ($X = P, Q, R$) frequency although the corresponding upper state has the largest contribution from the $\nu_4(-l)$ state (see Section VI and Table XIII).

TABLE III—*Continued*

J	K	ν_{obs}	ν_{calc}	$\nu_{cal}-\nu_{ob}$	ν_{obs}	ν_{calc}	$\nu_{cal}-\nu_{ob}$
			s^PP			a^PP	
10	6	1467.783	1467.7981	0.015		1470.3631	
10	7	1468.466	1468.4752	0.009		1470.5058	
10	8	•1468.920[b]	1468.8873	-0.033		1470.6699	
10	9	•1468.920[b]	1468.9890	0.069		1470.4116	
10	10	1468.753[b]	1468.7170	-0.036	1468.920	1468.9406	0.021
11	1		1450.5043			1462.5162	
11	2		1450.9757			1461.7552	
11	3		1451.6141			1460.6378	
11	4		1452.2890			1459.3724	
11	5	•1452.828[b]	1452.9040	0.076		1458.1999	
11	6	•1453.335[b]	1453.3978	0.063		1457.3275	
11	7	1453.743[b]	1453.7303	-0.013		1456.8519	
11	8	1453.907[b]	1453.8682	-0.039		1456.6879	
11	9	1453.743[b]	1453.7729	0.030		1456.4945	
11	10	•1453.335[b]	1453.3899	0.055		1455.5894	
11	11	1452.662	1452.6405	-0.022	1452.828	1452.8387	0.011
12	1		1439.3178			1408.5551	
12	2		1439.4463			1453.3373	
12	3	•1439.621[b]	1439.6113	-0.010		1451.6431	
12	4		1439.7628			1449.6013	
12	5		1439.8582			1447.5176	
12	6		1439.8673			1445.7100	
12	7		1439.7681			1444.4163	
12	8	•1439.621[b]	1439.5399	-0.081		1443.6952	
12	9	•1439.208[b]	1439.1554	-0.053		1443.3408	
12	10	1438.563	1438.5725	0.010		1442.8008	
12	11	1437.684	1437.7260	0.042		1441.0792	
12	12	•1436.483[b]	1436.5199	0.037		1436.6113	
			s^PQ			a^PQ	
1	1	1630.444[b]	1630.4598	0.016	1630.878	1630.8879	0.010
2	1	1631.427	1631.4400	0.013	1632.028[b]	1632.0758	0.048
2	2	1635.520[b]	1635.4842	-0.036	1635.896[b]	1635.9376	0.042
3	1	1632.998	1633.0170	0.019	1634.076	1634.0721	0.004
3	2	1636.905	1636.9020	-0.003	•1637.544[b]	1637.6128	0.069
3	3	1640.358	1640.3651	0.007	1640.823	1640.8191	-0.004
4	1	1635.268	1635.2942	0.027	1637.023[b]	1637.0513	0.028
4	2	1638.881	1638.8801	-0.001	1640.075	1640.0422	-0.033
4	3	1642.176[b]	1642.1982	0.022	1643.003	1642.9447	-0.058
4	4	1645.117	1645.1109	-0.006	1645.588	1645.5516	-0.036
5	1	1638.325	1638.3506	0.025		1641.0993	
5	2	1641.515	1641.4870	-0.028	1643.382	1643.3683	-0.014
5	3	1644.588	1644.5696	-0.018		1645.8026	
5	4	•1647.406[b]	1647.3356	-0.070	1648.183	1648.0979	-0.085
5	5	1649.731	1649.7299	-0.001	1650.213	1650.1639	-0.049
6	1	•1642.176[b]	1642.2086	0.033		1646.2071	
6	2	1644.827	1644.7910	-0.036		1647.7121	
6	3	•1647.592[b]	1647.5341	-0.058	1649.582	1649.5238	-0.058
6	4	1650.062	1650.0786	0.017	1651.455	1651.3618	-0.093

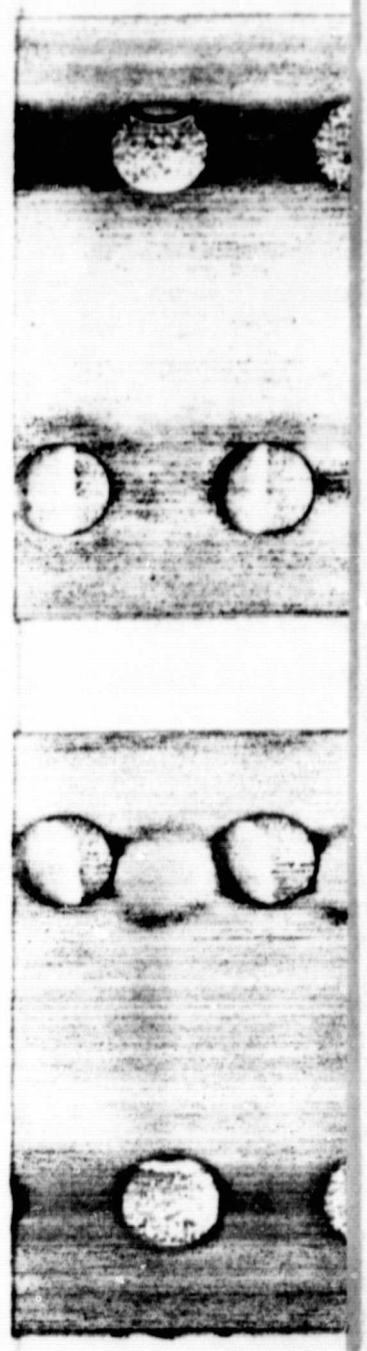

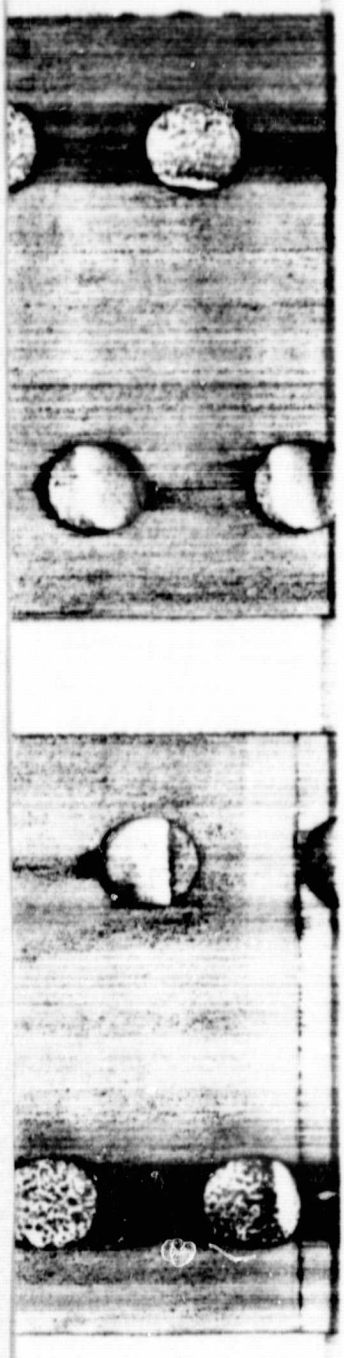

TABLE III—*Continued*

J	K	ν_{obs}	ν_{calc}	$\nu_{cal}-\nu_{ob}$	ν_{obs}	ν_{calc}	$\nu_{cal}-\nu_{ob}$
		s^PQ			a^PQ		
6	5	*1652.418[b]	1652.3226	-0.095		1653.1170	
6	6	1654.217[b]	1654.2301	0.013	1654.703	1654.6965	-0.007
7	1		1646.8437			1652.3403	
7	2	1648.857	1648.8425	-0.015		1653.1463	
7	3	1651.201	1651.1513	-0.050	*1654.217[b]	1654.2399	0.023
7	4	*1653.311[b]	1653.3888	0.078	*1655.431[b]	1655.4737	0.043
7	5	*1655.431[b]	1655.4128	-0.018	1656.839	1656.7735	-0.065
7	6	1657.128[b]	1657.1670	0.039	1658.071	1658.0675	-0.003
7	7	1658.601	1658.6187	0.018		1659.2021	
8	1		1652.2163		*1659.528[b]	1659.4910	-0.037
8	2		1653.6658			1659.7064	
8	3	*1655.431[b]	1655.4772	0.046		1660.0640	
8	4		1657.3237			1660.5783	
8	5	1659.056[b]	1659.0485	-0.007		1661.2690	
8	6	1660.560	1660.5791	0.019		1662.1232	
8	7	1661.833	1661.8755	0.043		1663.0379	
8	8	*1662.813[b]	1662.9024	0.089		1663.7453	
9	1		1658.2962			1667.6946	
9	2		1659.2641			1667.4248	
9	3	1660.560	1660.5569	-0.003		1667.0869	
9	4	1662.038	1661.9451	-0.094		1666.8207	
9	5	1663.270	1663.2899	0.020		1666.7655	
9	6	1664.510	1664.5170	0.007		1667.0090	
9	7	1665.565[b]	1665.5830	0.018		1667.5315	
9	8	1666.379[b]	1666.4534	0.075		1668.1423	
9	9	1667.066	1667.0871	0.021		1668.4014	
10	1		1665.0728			1677.0337	
10	2	*1665.565[b]	1665.6345	0.070		1676.3616	
10	3	*1666.379[b]	1666.4244	0.045		1675.3933	
10	4	*1667.349[b]	1667.3134	-0.036		1674.3386	
10	5		1668.2075			1673.4402	
10	6	1668.975[b]	1669.0478	0.074		1672.9076	
10	7		1669.7978			1672.8407	
10	8	1670.423	1670.4280	0.005		1673.1575	
10	9	1670.873	1670.9044	0.031		1673.5212	
10	10	*1671.197[b]	1671.1777	-0.019		1673.2540	
11	1		1672.5572			1641.2047	
11	2		1672.7814			1686.6227	
11	3		1673.1069			1685.0870	
11	4		1673.4854			1683.2691	
11	5		1673.8767			1681.4768	
11	6		1674.2535			1680.0308	
11	7		1674.5974			1679.1719	
11	8		1674.8921			1678.9627	
11	9		1675.1153			1679.2018	
11	10		1675.2304			1679.3418	
11	11		1675.1785			1678.3922	
			s^PR			a^PR	
1	1	1671.197[b]	1671.2058	0.009	1671.793	1671.8218	0.029

TABLE II.—*Continued*

J	K	ν_{obs}	ν_{calc}	$\nu_{cal}-\nu_{ob}$	ν_{obs}	ν_{calc}	$\nu_{cal}-\nu_{ob}$
		s^PR			a^PR		
2	1	1692.615	1692.6151	0.000	1693.643	1693.6415	-0.001
2	2	1696.516	1696.5282	0.012	1697.224	1697.2095	-0.015
3	1	1714.639	1714.6643	0.025	1716.357	1716.3848	0.028
3	2	1718.281	1718.2873	0.006	1719.430	1719.4119	-0.018
3	3	*1721.728[b]	1721.6678	-0.060	1722.425	1722.3749	-0.050
4	1	1737.388	1737.4132	0.025	*1739.982[b]	1740.1186	0.137
4	2	1740.601	1740.5956	-0.006	1742.433	1742.4324	-0.001
4	3	1743.727	1743.7552	0.028	1744.978	1744.9418	-0.037
4	4	1746.605[b]	1746.6301	0.025	1747.416	1747.3430	-0.073
5	1	*1760.802[b]	1760.8654	0.063	1764.804[b]	1764.8155	0.011
5	2	1763.527	1763.5022	-0.024	*1766.253[b]	1766.3736	0.121
5	3	*1766.252[b]	1766.3367	0.085	1768.294	1768.2744	-0.019
5	4	1768.980	1769.0103	0.030	*1770.340[b]	1770.2382	-0.102
5	5	*1771.287[b]	1771.4221	0.135	*1772.287[b]	1772.1568	-0.130
6	1	*1784.943[b]	1784.9786	0.036		1790.4233	
6	2	1787.051[b]	1787.0400	-0.011		1791.2904	
6	3	1789.512[b]	1789.4539	-0.058		1792.4866	
6	4	1791.843	1791.8397	-0.003	*1793.775[b]	1793.8652	-0.090
6	5	1794.030	1794.0568	0.027	1795.443	1795.3532	-0.090
6	6	*1796.093[b]	1796.0505	-0.042	1796.921[b]	1796.8803	-0.041
7	1		1809.6964			1816.9173	
7	2	1811.191[b]	1811.2162	0.025		1817.2016	
7	3	1813.121	1813.1456	0.024		1817.6746	
7	4	1815.080[b]	1815.1589	0.079		1818.3518	
7	5		1817.1006			1819.2543	
7	6	1818.914[b]	1818.9004	-0.014		1820.3709	
7	7		1820.5207			1821.6008	
8	1		1834.9730			1844.3174	
8	2		1836.0185			1844.1236	
8	3	1837.457	1837.4414	-0.015		1843.9132	
8	4		1839.0134			1843.8270	
8	5	1840.601	1840.5976	-0.003		1844.0058	
8	6	*1842.147[b]	1842.1217	-0.025		1844.5395	
8	7		1844.5454			1845.4106	
8	8		1847.8371			1846.4318	
9	1		1860.7833			1872.6912	
9	2		1861.4293			1872.1019	
9	3		1862.3604			1871.2724	
9	4		1863.4492			1870.4136	
9	5		1864.6034			1869.7701	
9	6		1865.7667			1869.5535	
9	7		1866.9055			1869.8663	
9	8		1867.9941			1870.6298	
9	9		1869.0027			1871.5110	
10	1		1887.1257			1855.7222	
10	2		1887.4401			1901.2291	
10	3		1887.9171			1899.8425	
10	4		1888.5098			1898.2353	
10	5		1889.1802			1896.7171	
10	6		1889.9035			1895.6109	

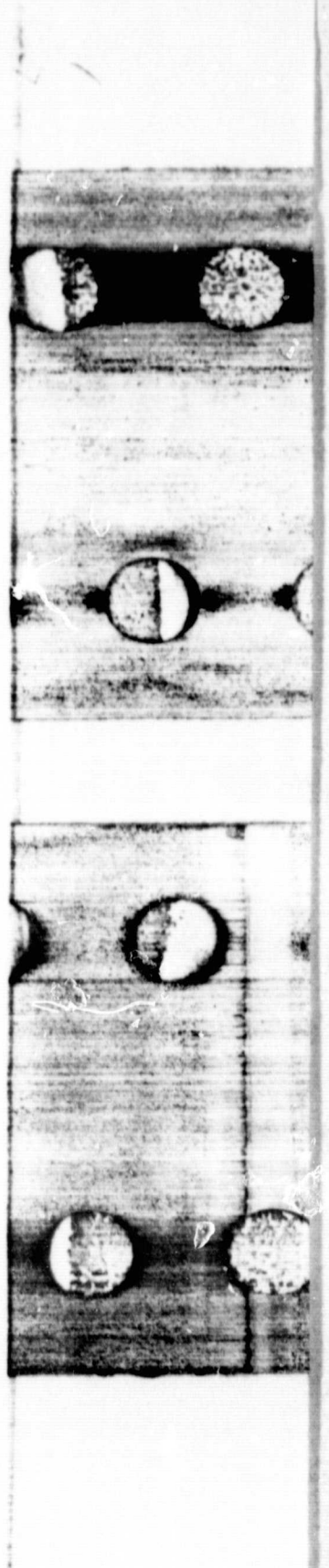

TABLE III—*Continued*

J	K	ν_{obs}	ν_{calc}	$\nu_{cal}-\nu_{ob}$	ν_{obs}	ν_{calc}	$\nu_{cal}-\nu_{ob}$
			s^PR			a^PR	
10	7		1890.6649			1895.1606	
10	8		1891.4519			1895.4323	
10	9		1892.2469			1896.2285	
10	10		1893.0182			1897.0065	
			s^RP			a^RP	
2	0	...	...	...	1586.859	1586.8905	0.031
3	0	1567.990	1567.9820	-0.008	...	...	...
3	1	1561.756	1561.7647	0.009	1562.369	1562.3783	0.009
4	0	...	...	...	1552.147	1552.0983	-0.049
4	1	1543.213	1543.2388	0.026	*1543.976[b]	1544.0147	0.039
4	2	1537.464	1537.4717	0.008	*1538.288[b]	1538.3108	0.023
5	0	*1533.361[b]	1533.7662	-0.095	...	...	...
5	1	1524.948	1524.9773	0.029	*1525.761[b]	1525.8208	0.060
5	2	1519.527	1519.5267	0.000	1520.747	1520.7207	-0.026
5	3	*1513.054[b]	1513.0786	0.025	1514.236	1514.2343	-0.001
6	0	...	...	...	1521.264	1521.2243	-0.040
6	1		1506.8824		*1507.809[b]	1507.7154	-0.094
6	2	*1501.859[b]	1501.9012	0.042	1503.431	1503.3869	-0.044
6	3	1495.726	1495.7247	-0.001	1497.518	1497.4829	-0.035
6	4	1488.596[b]	1488.5850	-0.011	1490.191	1490.1889	-0.002
7	0	1502.754	1502.7137	-0.040	...	...	...
7	1	1488.962[b]	1488.9154	-0.047		1489.7439	
7	2	1484.496	1484.5084	0.012	1486.245[b]	1486.2209	-0.024
7	3	1478.715	1478.7080	-0.007	1481.083	1481.0309	-0.052
7	4	*1471.889[b]	1471.8475	-0.041	1474.397	1474.3912	-0.006
7	5	1463.997	1463.9890	-0.008	1466.212	1466.2159	0.004
8	0	...	...	...	1494.241	1494.3012	0.060
8	1	1471.147	1471.0952	-0.052		1472.0249	
8	2	1467.344	1467.2891	-0.054	1469.180	1469.2347	0.055
8	3	1461.969	1461.9553	-0.013		1464.8287	
8	4	1455.495[b]	1455.4543	-0.041	1458.961	1458.9233	-0.038
8	5		1447.8958		1451.530	1451.4957	-0.034
8	6	1439.310[b]	1439.2895	-0.020		1442.3400	
9	0	1474.737	1474.7816	0.045	...	...	...
9	1		1453.4751			1454.7163	
9	2	1450.180	1450.2295	0.049		1452.5523	
9	3	1445.414	1445.4154	0.001		1448.9270	
9	4	*1439.310[b]	1439.3445	-0.035		1443.8018	
9	5	1432.170	1432.1498	-0.020		1437.1169	
9	6	1423.901	1423.8678	-0.033	1428.824	1428.7759	-0.048
9	7		1414.4866			1418.5357	
10	0	...	...	...		1471.6725	
10	1		1436.1282			1438.0228	
10	2		1433.3655			1436.4106	
10	3		1429.0762			1433.5140	
10	4		1423.4811			1429.1507	
10	5		1416.7038			1423.1851	
10	6		1408.7949			1415.5329	

TABLE III—*Continued*

J	K	ν_{obs}	ν_{calc}	$\nu_{cal}-\nu_{ob}$	ν_{obs}	ν_{calc}	$\nu_{cal}-\nu_{ob}$
			$^{s}R_{P}$			$^{a}R_{P}$	
10	7		1399.7610			1406.1186	
10	8		1389.5813			1394.7183	
11	0		1420.2757		...	...	...
11	1		1419.1469			1422.2458[c]	
11	2		1416.7782			1421.1994[c]	
11	3		1412.9757			1418.9497	
11	4		1407.8661			1402.0092	
11	5		1401.5382			1395.1671	
11	6		1394.0395			1387.4224	
11	7		1385.3862			1378.8971	
11	8		1375.5727			1369.7325	
11	9		1364.5766			1360.2282	
12	0	...	...	...		1454.1513	
12	1		1402.6499			1454.4490[c]	
12	2		1400.5891			1400.5114	
12	3		1397.2061			1395.5822	
12	4		1392.5536			1389.4992	
12	5		1386.6760			1382.3974	
12	6		1379.6030			1374.3996	
12	7		1371.3495			1365.5969	
12	8		1361.9180			1356.0518	
12	9		1351.3002			1345.8586	
12	10		1339.4772			1335.2400	
			$^{s}R_{Q}$			$^{a}R_{Q}$	
1	0	1625.487[b]	1625.4747	-0.013	...	...	...
2	0	...	...	...	1626.133[b]	1626.1827	0.050
2	1	1621.351	1621.3628	0.012	1621.934	1621.9477	0.014
3	0	1626.340[b]	1626.4059	0.066	...	...	...
3	1	*1622.623[b]	1622.6089	-0.014	1623.350	1623.3482	-0.002
3	2	*1616.833[b]	1616.8789	0.046	1617.668	1617.6804	0.012
4	0	...	...	...	1627.314	1627.4063	0.092
4	1	1624.005	1624.0399	0.035	1624.879[b]	1624.8401	-0.039
4	2	1618.613	1618.6352	0.022	1619.790	1619.7848	-0.005
4	3	1612.250	1612.2642	0.014	1613.336[b]	1613.3735	0.038
5	0		1627.9994		...	...	...
5	1	1625.599[b]	1625.5392	-0.059	1626.341[b]	1626.3237	-0.017
5	2	1620.601	1620.6125	0.011	1622.062	1622.0484	-0.013
5	3	1614.511	1614.5273	0.016	1616.273[b]	1616.2335	-0.039
5	4	1607.502	1607.5166	0.015	1609.045	1609.0653	0.021
6	0	...	...	...	1629.279[b]	1629.4055	0.127
6	1	1627.009[b]	1627.0503	0.041	*1627.875[b]	1627.8269	-0.046
6	2	*1622.623[b]	1622.7060	0.082	1624.387	1624.3651	-0.022
6	3	1616.980[b]	1617.0106	0.031	1619.320	1619.2776	-0.043
6	4	*1610.326[b]	1610.2984	-0.028	1612.801	1612.7827	-0.019
6	5	1604.627	1602.6330	0.006	1604.763	1604.7956	0.033
7	0	*1630.288[b]	1630.1886	-0.099	...	...	...
7	1	1628.608	1628.5753	-0.032		1629.4513	
7	2	*1624.879[b]	1624.8396	-0.039	1626.664	1626.7299	0.066
7	3	*1619.603[b]	1619.6238	0.021	*1622.383[b]	1622.4393	0.056

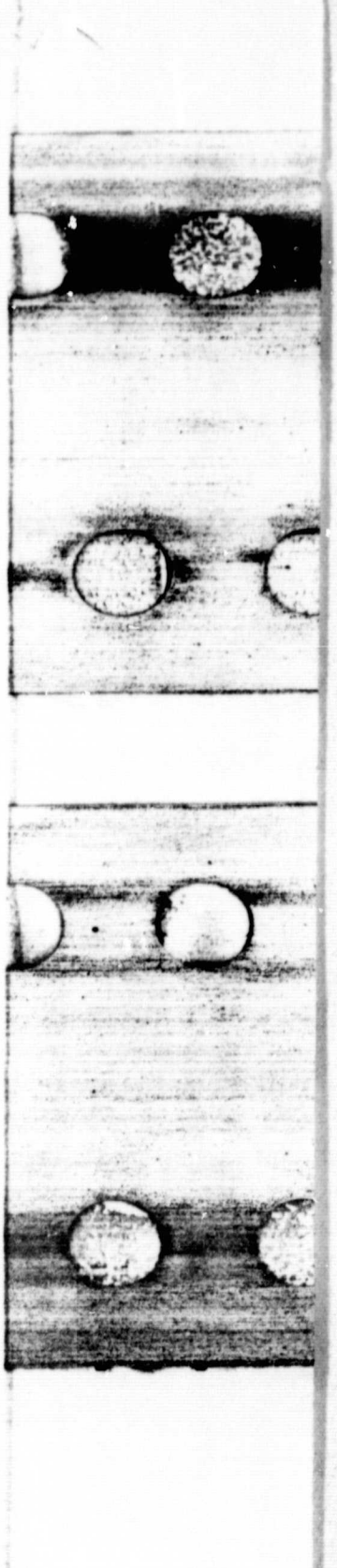

TABLE III—*Continued*

J	K	ν_{obs}	ν_{calc}	$\nu_{cal}-\nu_{ob}$	ν_{obs}	ν_{calc}	$\nu_{cal}-\nu_{ob}$
			s^RQ			a^RQ	
7	4	1613.336[b]	1613.2894	-0.047	*1616.716[b]	1616.6968	-0.019
7	5	1605.950	1605.9479	-0.002	*1609.458[b]	1609.4810	0.023
7	6	*1597.594[b]	1597.6108	0.017	1600.567	1600.5877	0.021
8	0	...	...	...		1632.5383	
8	1		1630.1519		*1631.284[b]	1631.3391	0.055
8	2	1627.009[b]	1626.9839	-0.025	1629.279	1629.2511	-0.028
8	3	*1622.383[b]	1622.2999	-0.083	*1625.599[b]	1625.7533	0.154
8	4	*1616.378[b]	1616.4128	-0.035	*1620.709[b]	1620.8081	0.099
8	5	*1609.458[b]	1609.4575	0.000	1614.367	1614.3572	-0.010
8	6	1601.469[b]	1601.4726	0.004	1606.297	1606.3064	0.010
8	7	1592.432	1592.4490	0.017	1596.373[b]	1596.4147	0.042
9	0	1632.998[b]	1633.0390	0.040	...	...	...
9	1	*1631.936[b]	1631.8388	-0.097		1633.6804	
9	2	1629.171[b]	1629.1603	-0.011		1632.1509	
9	3		1625.0123			1629.3931	
9	4	1619.603[b]	1619.6169	0.013		1625.2257	
9	5	1613.059	1613.0997	0.041		1619.5150	
9	6	1605.527[b]	1605.5138	-0.013	*1612.136[b]	1612.1788	0.043
9	7	1596.840	1596.8688	0.029	1603.130	1603.1443	0.014
9	8	1587.115[b]	1587.1474	0.032	1592.178[b]	1592.1907	0.012
10	0	...	...	...		1637.7580	
10	1		1633.7154			1636.7632[c]	
10	2	*1631.427[b]	1631.4369	0.010		1635.8058[c]	
10	3		1627.7859			1633.7053	
10	4		1622.8905		*1616.980[b]	1616.9754	-0.005
10	5	*1616.833[b]	1616.8416	0.008	*1610.326[b]	1610.4074	0.081
10	6		1609.6895		*1602.926[b]	1603.0025	0.078
10	7	1601.469[b]	1601.4537	-0.015	*1594.810[b]	1594.8858	0.076
10	8	1592.178	1592.1325	-0.046		1586.2020	
10	9	*1581.615[b]	1581.7082	0.093	*1577.276[b]	1577.2549	-0.021
11	0		1636.9352		...	...	...
11	1		1635.8893			1687.6396[c]	
11	2		1633.9242			1633.7968	
11	3		1630.7017			1629.0261	
11	4		1626.2762			1623.1670	
11	5		1620.6945			1616.3566	
11	6		1613.9892			1608.7203	
11	7		1606.1789			1600.3525	
11	8		1597.2703			1591.3194	
11	9	1587.269	1587.2601	-0.009		1581.7197	
11	10	*1576.198[b]	1576.1351	-0.063		1571.7810	
			s^RR			a^RR	
1	0	1667.349	1667.3303	-0.019	...	...	...
1	1	1661.140	1661.1286	-0.012	1661.685	1661.6937	0.009
2	0	...	...	...	1691.037	1690.9800	-0.057
2	1	1682.167	1682.2070	0.020	1682.925	1682.9176	-0.007
2	2	1676.509	1676.5051	-0.004	1677.263	1677.2771	0.014
3	0	1712.196[b]	1712.1712	-0.025	...	...	...
3	1	1703.382	1703.4100	0.028	1704.202	1704.1735	-0.028

TABLE III—*Continued*

J	K	ν_{obs}	ν_{calc}	$\nu_{cal}-\nu_{ob}$	ν_{obs}	ν_{calc}	$\nu_{cal}-\nu_{ob}$
		s^RR			a^RR		
3	2	1698.026	1698.0425	0.016	1699.181	1699.1544	-0.026
3	3	1691.746	1691.7338	-0.012	1692.792	1692.8037	0.012
4	0	...	...	...	1738.843	1738.8193	-0.024
4	1	1724.581	1724.6017	-0.021	1725.378	1725.3430	-0.035
4	2	1719.704	1719.7210	0.017	1721.151[b]	1721.1125	-0.038
4	3	1713.711	1713.7129	0.002	1715.405	1715.3727	-0.032
4	4	1706.818	1706.8110	-0.007	1708.306	1708.3104	0.004
5	0	1759.503	1759.4664	-0.037	...	...	...
5	1	*1745.743[b]	1745.7070	-0.036	1746.427	1746.4352	0.008
5	2	1741.417	1741.4172	0.000	1743.050[b]	1743.0266	-0.023
5	3	1735.817	1735.8132	-0.004	1738.075[b]	1738.0282	-0.046
5	4	1729.226	1729.2300	0.004	1731.694	1731.6591	-0.035
5	5	1721.728[b]	1721.7325	0.005	1723.821	1723.8354	0.014
6	0	...	...	...	1789.684	1789.7673	0.083
6	1	1766.751	1766.7102	-0.041	1767.504	1767.5343	0.030
6	2	1763.105	1763.0371	-0.068	1764.804	1764.8741	0.070
6	3	1757.932	1757.9263	-0.006	1760.693	1760.6861	-0.007
6	4	1751.749	1751.7403	-0.009	1755.100	1755.0883	-0.011
6	5	1744.604	1744.5919	-0.012	1748.088	1748.0607	-0.027
6	6	1736.504	1736.4944	-0.010	1739.386	1739.4010	0.015
7	0	1808.848	1808.8894	0.042	...	...	...
7	1		1787.6321			1788.7654	
7	2	1784.507	1784.5343	0.027		1786.7464	
7	3	1779.960	1779.9683	0.008		1783.3639	
7	4	1774.245	1774.2479	0.003	1778.512[b]	1778.5816	0.070
7	5	1767.504	1767.5096	0.005	1772.334[b]	1772.3425	0.009
7	6	1759.812	1759.7939	-0.018	1764.538	1764.5541	0.016
7	7	*1751.027[b]	1751.0942	0.067	1754.986	1754.9777	-0.009
8	0	...	...	...		1843.9000	
8	1		1808.5156			1810.3031	
8	2		1805.9146			1808.8497	
8	3	1801.872	1801.8967	0.025		1806.2194	
8	4	*1796.635[b]	1796.6852	-0.050		1802.2320	
8	5	1790.398	1790.4074	0.009		1796.7554	
8	6	1783.150[b]	1783.1186	-0.031	1789.684[b]	1789.7093	0.025
8	7	1774.848	1774.8316	-0.017	1781.028	1781.0233	-0.004
8	8	1765.504	1765.5311	0.027	1770.498	1770.4796	-0.018
9	0		1860.2487		...	...	...
9	1	*1829.411[b]	1829.4260	0.015		1832.4208[c]	
9	2		1827.2317			1831.5461[c]	
9	3		1823.7219			1829.5844	
9	4		1819.0263			1813.0504	
9	5		1813.2375			1806.7373	
9	6	*1806.393[b]	1806.4084	0.015	*1799.625[b]	1799.6484	0.023
9	7	1798.585	1798.5615	-0.024		1791.9115	
9	8	*1789.684[b]	1789.6986	0.014		1783.6744	
9	9	*1779.727[b]	1779.8062	0.079	1775.270	1775.2446	-0.026
10	0	...	...	...		1901.7987	
10	1		1850.4577			1902.1571[c]	
10	2		1848.5829			1848.4033	
10	3		1845.5119			1843.7816	
10	4		1841.3006			1838.1332	
10	5		1835.9979			1831.5969	
10	6		1829.6392			1824.3004	
10	7	*1822.154	1822.2464	0.092		1816.3412	
10	8	1813.852	1813.8301	-0.022		1807.7890	
10	9	1804.413	1804.3917	-0.022		1798.7464	
10	10	1793.775	1793.9120	0.137	*1789.512[b]	1789.4456	-0.066

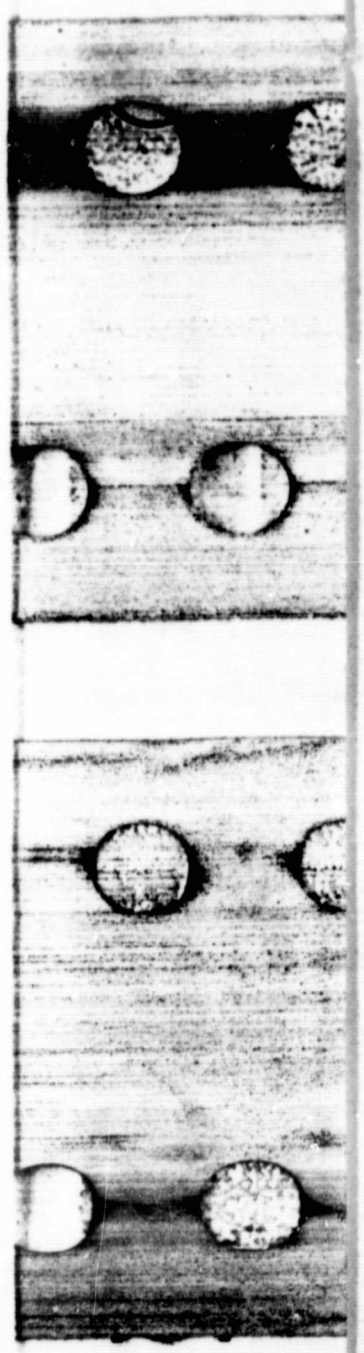

numerically manageable dimension, we have considered the interaction between the ν_2, $2\nu_2$, $3\nu_2$, ν_4, and $\nu_2 + \nu_4$ energy levels separately from the interaction between the ν_1, ν_3, and $2\nu_4$ levels. The Coriolis ζ coefficients for the interaction between the $\nu_1(A)$ and $\nu_4(E)$ as well as between the $\nu_2(A)$ and $\nu_3(E)$ states are very small and furthermore there is a large difference in energies between these states. This separation of the problem is therefore a very good approximation for the lowest-lying states ν_2, $2\nu_2$, and ν_4; parameters obtained for these states should be considered as the main result of our work.

In our scheme, Coriolis interactions between the ν_2, $2\nu_2$, $3\nu_2$, ν_4, and $\nu_2 + \nu_4$ energy levels are described by the operator (*4*, *5*)

$$H_{2,4} = (-i/2)[X^{\nu\rho}_{4a} J_\rho + (1/2)(J_\rho X^{\nu\rho}_{4a})](Q_4^- J_+ - Q_4^+ J_-), \tag{18}$$

where $Q_4^\pm = Q_{4a} \pm iQ_{4b}$, $J_\pm = J_x \pm iJ_y$. Besides this, there is a centrifugal distortion operator

$$H_{\text{Cent}} = (1/8)(Y^{xx}_{4a4a} - Y^{yy}_{4a4a})[(Q_4^+)^2 J_-^2 + (Q_4^-)^2 J_+^2] \tag{19}$$

which connects the $\pm l$ levels in the ν_4 and $\nu_2 + \nu_4$ states. The energy matrix of these interactions is thus the 7×7 matrix given in Table VI. For the nondegenerate vibrational states, the diagonal matrix elements of this matrix are given by Eq. (15). For the inversion–rotational energy levels in the degenerate vibrational states the following expression has been used:

$$\begin{aligned}\left(\frac{E_i}{hc}\right) = \left(\frac{E_i^0}{hc}\right) &+ B_i J(J+1) + (C_i - B_i)k^2 - 2C_i\zeta_4^{(i)} k l_4 - D_J^{(i)} J^2(J+1)^2 \\ &- D_{JK}^{(i)} J(J+1)k^2 - D_k^{(i)} k^4 + \eta_{4J}^{(i)} J(J+1) k l_4 + \eta_{4k}^{(i)} k^3 l_4 \\ &+ H_{JJJ}^{(i)} J^3(J+1)^3 + H_{JJK}^{(i)} J^2(J+1)^2 k^2 + H_{JKK}^{(i)} J(J+1)k^4 + H_{KKK}^{(i)} k^6 \\ &+ \tau_{4JJK}^{(i)} J^2(J+1)^2 k l_4 + \tau_{4JKK}^{(i)} J(J+1)k^3 l_4 + \tau_{4KKK}^{(i)} k^5 l_4 + \tau_{4KK}^{*(i)} k^3 l_4^3. \end{aligned} \tag{20}$$

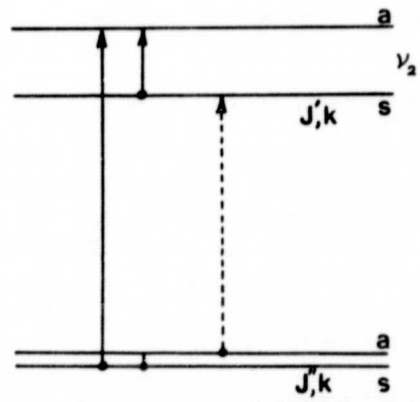

FIG. 3. Energy-level diagram illustrating the calculation of the ν_2 transition frequency (dashed line) from the known ν_2 frequency for a transition starting from a level with opposite parity and from the known pure inversion transitions in the ground and excited ν_2 states (see Table I).

TABLE IV

Submillimeter Wave Inversion and Rotation–Inversion Transitions of $^{14}NH_3$ in the ν_2 State (MHz)

Pure Inversion Transition Frequencies

J	K	$\nu_{inv.}$	J	K	$\nu_{inv.}$	J	K	$\nu_{inv.}$
1	1	1066 650.8[a]	7	1	810 918.7	10	6	790 818.2
			7	2	828 521.9	10	7	867 343.5
2	1	1045 318.7	7	3	858 394.2	10	8	964 060.3
2	2	1067 676.8[a]	7	4	902 459.2			
			7	5	961 885.4	11	6	706 899.0
3	1	1014 084.0	7	6	1039 360.8	11	7	775 717.6
3	2	1035 816.2				11	8	862 810.7
3	3	1073 050.7	8	1	747 286.8	11	9	972 301.6
			8	2	763 583.3			
4	1	973 826.5	8	3	791 531.4	12	8	763 996.2
4	2	994 747.8	8	4	831 969.3	12	9	861 672.9
4	3	1030 531.2	8	5	887 018.8			
			8	6	958 627.9	13	9	755 447.6
5	1	925 657.4	8	7	1050 521.5	13	11	1000 151.6
5	2	945 604.8						
5	3	979 650.0	9	3	721 263.7	14	12	1019 895.5
5	4	1029 374.5	9	4	759 001.2			
			9	5	809 481.9			
6	2	889 710.9	9	6	875 368.8			
6	3	921 940.3	9	7	959 569.0			
6	4	968 810.0	9	8	1065 868.2			
6	5	1032 323.0						

Rotation-Inversion Transition Frequencies

(J',K') - (J,K)	$\nu_{inv.-rot.}$
a(0,0) - s(1,0)[a,b]	466 245.1
s(2,1) - a(1,1)[c]	140 143.5
s(3,2) - a(2,2)[a]	741 788.1
s(3,1) - a(2,1)[a]	762 852.3
s(3,0) - a(2,0)[a]	769 710.2
a(3,3) - a(2,0)[d]	772 594.9
s(3,0) - s(3,3)[d]	1070 166.6

[a] Value obtained by extrapolating to zero pressure.
[b] Ref. (*29*).
[c] Ref. (*30*).
[d] Forbidden (or perturbation-allowed) transition.

The precision of our ν_2 data would require the additional introduction of operators that connect levels with $\Delta k = \pm 3$ in the ground and ν_2 excited state. A detailed study of this interaction using submillimeter wave data on the inversion and inversion–rotation transitions in the ν_2 excited state will be published in a separate paper. Therefore in the present paper we have not included in our fit transitions from the ground-state levels with $k'' = 3$ or 0 to those ν_2 excited states that are perturbed by this interaction (cf. Table I).

VI. SPECTROSCOPIC PARAMETERS OF $^{14}NH_3$

In Tables VII to XII, spectroscopic parameters of $^{14}NH_3$ are presented that have been obtained by a damped least-squares fit (*33*) to the experimental data

TABLE V

Ground-State Molecular Parameters of $^{14}NH_3$ (in cm^{-1})

	s	a
B_o	9.9466529 ± 0.0000004	9.9416356 ± 0.0000004
D_J^o	(8.4721 ± 0.0002) × 10^{-4}	(8.3184 ± 0.0002) × 10^{-4}
D_{JK}^o	(−15.6907 ± 0.0007) × 10^{-4}	(−15.2647 ± 0.0007) × 10^{-4}
H_{JJJ}^o	(2.298 ± 0.001) × 10^{-7}	(2.071 ± 0.001) × 10^{-7}
H_{JJK}^o	(−8.554 ± 0.006) × 10^{-7}	(−7.604 ± 0.006) × 10^{-7}
H_{JKK}^o	(11.49 ± 0.02) × 10^{-7}	(10.15 ± 0.02) × 10^{-7}
$[{}^{(a)}C_o - {}^{(a)}B_o] - [{}^{(s)}C_o - {}^{(s)}B_o]$		(6.9989 ± 0.0001) × 10^{-3}
$[{}^{(a)}D_K^o - {}^{(s)}D_K^o]$		(2.9512 ± 0.0002) × 10^{-5}
$[{}^{(a)}H_{KKK}^o - {}^{(s)}H_{KKK}^o]$		(6.3031 ± 0.0008) × 10^{-8}

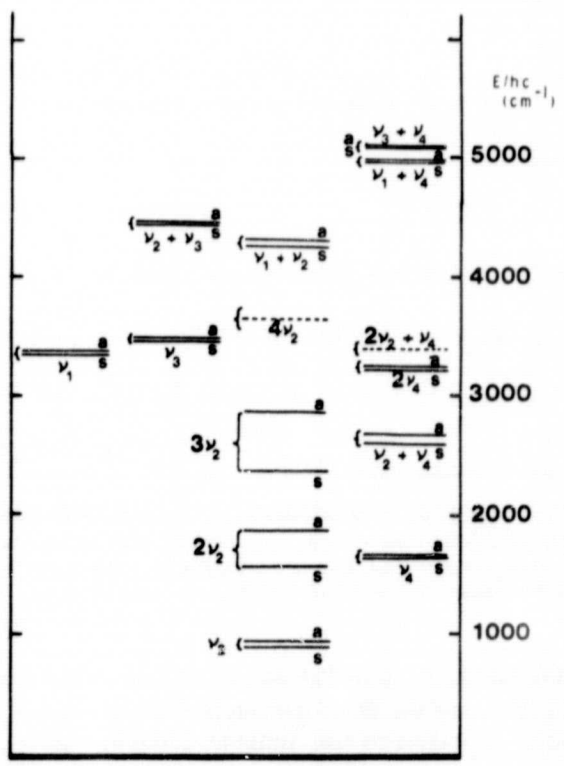

FIG. 4. The lowest vibration and inversion energy levels in NH_3.

TABLE VI

Energy Matrix of the Coriolis and l-Type Interaction Between the ν_2, $2\nu_2$, ν_4, $\nu_2 + \nu_4$, and $3\nu_2$ States of NH_3[a]

$\lvert v_2^{\pm}, v_4^{\ell_4}; J, k\rangle$	$3v_2^{\pm}$	$+\ell$ $(v_2 + v_4)^{\mp}$	$-\ell$ $(v_2 + v_4)^{\mp}$
$\lvert 3^{\pm}, 0^{o}; J, k\rangle$	$E_{3v_2}(J,k,\ell_4=0)^{\pm}$	$\langle 3^{\pm}\lvert\alpha\rvert 1^{\mp}\rangle f(J,k+1)$	$-\langle 3^{\pm}\lvert\alpha\rvert 1^{\mp}\rangle f(J,k-1)$
$\lvert 1^{\mp}, 1^{+1}; J, k+1\rangle$		$E_{v_2+v_4}(J,k+1,\ell_4=1)^{\mp}$	$\langle 1^{\mp}\lvert\beta\rvert 1^{\mp}\rangle q(J,k)$
$\lvert 1^{\mp}, 1^{-1}; J, k-1\rangle$			$E_{v_2+v_4}(J,k-1,\ell_4=-1)^{\mp}$
$\lvert 2^{\pm}, 0^{o}; J, k\rangle$			
$\lvert 0^{\mp}, 1^{+1}; J, k+1\rangle$	Hermitian		
$\lvert 0^{\mp}, 1^{-1}; J, k-1\rangle$			
$\lvert 1^{\pm}, 0^{o}; J, k\rangle$			

$2v_2^{\pm}$	$+\ell$ $v_4^{\mp}$	$-\ell$ $v_4^{\mp}$	$v_2^{\pm}$
0	$\langle 3^{\pm}\lvert\alpha\rvert 0^{\mp}\rangle f(J,k+1)$	$-\langle 3^{\pm}\lvert\alpha\rvert 0^{\mp}\rangle f(J,k-1)$	0
$\langle 1^{\mp}\lvert\alpha\rvert 2^{\pm}\rangle f(J,k+1)$	0	0	0
$-\langle 1^{\mp}\lvert\alpha\rvert 2^{\pm}\rangle f(J,k-1)$	0	0	0
$E_{2v_2}(J,k,\ell_4=0)^{\pm}$	$\langle 2^{\pm}\lvert\alpha\rvert 0^{\mp}\rangle f(J,k+1)$	$-\langle 2^{\pm}\lvert\alpha\rvert 0^{\mp}\rangle f(J,k-1)$	0
	$E_{v_4}(J,k+1,\ell_4=+1)^{\mp}$	$\langle 0^{\mp}\lvert\beta\rvert 0^{\mp}\rangle q(J,k)$	$\langle 0^{\mp}\lvert\alpha\rvert 1^{\pm}\rangle f(J,k+1)$
		$E_{v_4}(J,k-1,\ell_4=-1)^{\mp}$	$-\langle 0^{\mp}\lvert\alpha\rvert 1^{\pm}\rangle f(J,k-1)$
			$E_{v_2}(J,k,\ell_4=0)^{\pm}$

[a] $\alpha(\mathrm{cm}^{-1}) = h^{3/2}[2(2\pi)^{5/2}c]^{-1}[X^{\nu\rho}_{4\alpha}\partial/\partial\rho + \tfrac{1}{2}(\partial X^{\nu\rho}_{4\alpha}/\partial\rho)]\lambda_4(\rho)^{-1/4}$, where the first operator $\partial/\partial\rho$ operates outside the square brackets while the second one operates only within the brackets; $\beta(\mathrm{cm}^{-1}) = h^2[8(2\pi)^3c]^{-1}(Y^{xx}_{4\alpha 4\alpha} - Y^{yy}_{4\alpha 4\alpha})\lambda_4(\rho)^{-1/2}$; $f(J, k \pm 1) = +[J(J+1) - k(k \pm 1)]^{1/2}$; $g(J,k) = f(J, k+1) \times f(J, k-1)$; $\langle 3^{\pm}\lvert\alpha\rvert 1^{\mp}\rangle$ means $\langle v_2 = 3^{\pm}\lvert\alpha\rvert v_2 = 1^{\mp}\rangle$, etc.; and $E_n(J,k,l_4)^{\pm} = E_i/hc$, where E_i is defined in Eq. (20).

on the ν_2, $2\nu_2$, and ν_4 bands given in Tables I to III and on the data on the $\nu_2 + \nu_4$ and $3\nu_2$ bands (*11*). Because the fitted parameters are in general correlated, considerable care had to be taken to use suitable damping factors during the first cycles of iteration in order to reach the convergence region where the damping

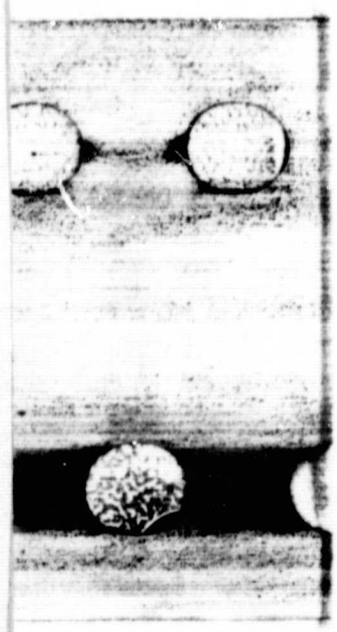

TABLE VII

Independent Linear Combinations of the Parameters of the ν_2 Band of $^{14}NH_3$ (in cm^{-1})

ν_0 (s → a)*	968.12224 ± 0.00006	ν_0 (a → s)*	931.64155 ± 0.00007
^aB	10.21521 ± 0.00007	^sB	10.50682 ± 0.00003
$(^aC - {}^aB) - (^sC^o - {}^sB^o)$	-0.33864 ± 0.00007	$(^sC - {}^sB) - (^aC^o - {}^aB^o)$	-0.65066 ± 0.00003
$^sD_J^o - {}^aD_J$	(0.655 ± 0.001)10^{-4}	$^aD_J^o - {}^sD_J$	(-2.325 ± 0.002)10^{-4}
$^sD_{JK}^o - {}^aD_{JK}$	(-1.875 ± 0.002)10^{-4}	$^aD_{JK}^o - {}^sD_{JK}$	(7.396 ± 0.004)10^{-4}
$^sD_K^o - {}^aD_K$	(1.095 ± 0.001)10^{-4}	$^aD_K^o - {}^sD_K$	(-5.500 ± 0.002)10^{-4}
$^aH_{JJJ} - {}^sH_{JJJ}^o$	(-1.950 ± 0.004)10^{-7}	$^sH_{JJJ} - {}^aH_{JJJ}^o$	(-0.58 ± 0.02)10^{-7}
$^aH_{JJK} - {}^sH_{JJK}^o$	(6.50 ± 0.02)10^{-7}	$^sH_{JJK} - {}^aH_{JJK}^o$	(0.54 ± 0.04)10^{-7}
$^aH_{JKK} - {}^sH_{JKK}^o$	(-7.59 ± 0.02)10^{-7}	$^sH_{JKK} - {}^aH_{JKK}^o$	(-1.41 ± 0.06)10^{-7}
$^aH_{KKK} - {}^sH_{KKK}^o$	(3.14 ± 0.01)10^{-7}	$^sH_{KKK} - {}^aH_{KKK}^o$	(1.46 ± 0.03)10^{-7}

Inversion splitting in the $J = k = 0$ ν_2 state: 35.68726 ± 0.00020

* The band origin ν_0 is defined as $\nu_0 = (E_i^0 - E_p^0)/hc$ [Eq. (16)].

factor could be put equal to zero. Calculations have been done with the CDC Cyber 172 computer using double-precision arithmetic (120 bits).

Because in the investigated system of interacting levels not k but $k - l_4$ is a good quantum number, the standard assignment of the transition frequencies to the ν_2, $2\nu_2$, ν_4, etc., bands is only approximate. This is especially true for the $s2\nu_2$, $a\nu_4$ levels because of the level crossing in this system. The only objective criterion on which such assignments can be based is to consider the coefficients of mixing of the wavefunctions in the system of interacting levels,

$$\psi_i = \sum_k c_{ik}\psi_{ik}^0, \tag{21}$$

TABLE VIII

Independent Linear Combinations of the Parameters of the $2\nu_2$ Band of $^{14}NH_3$ (in cm^{-1})

ν_0 (s → a)*	1882.1751 ± 0.0001	ν_0 (a → s)*	1596.6753 ± 0.0020
^aB	9.73747 ± 0.00009	^sB	10.5676 ± 0.0002
$(^aC - {}^aB) - (^sC - {}^sB)$	0.15203 ± 0.00008	$(^sC - {}^sB) - (^aC - {}^aB)$	-0.9084 ± 0.0002
$^sD_J^o - {}^aD_J$	(3.860 ± 0.006)10^{-4}	$^aD_J^o - {}^sD_J$	(3.23 ± 0.04)10^{-4}
$^sD_{JK}^o - {}^aD_{JK}$	(-10.225 ± 0.010)10^{-4}	$^aD_{JK}^o - {}^sD_{JK}$	(-6.56 ± 0.007)10^{-4}
$^sD_K^o - {}^aD_K$	(6.057 ± 0.007)10^{-4}	$^aD_K^o - {}^sD_K$	(4.94 ± 0.06)10^{-4}
$^aH_{JJJ} - {}^sH_{JJJ}^o$	(-0.478 ± 0.005)10^{-6}	$^sH_{JJJ} - {}^aH_{JJJ}^o$	(-0.227 ± 0.030)10^{-6}
$^aH_{JJK} - {}^sH_{JJK}^o$	(1.868 ± 0.020)10^{-6}	$^sH_{JJK} - {}^aH_{JJK}^o$	(3.22 ± 0.08)10^{-6}
$^aH_{JKK} - {}^sH_{JKK}^o$	(-4.179 ± 0.040)10^{-6}	$^sH_{JKK} - {}^aH_{JKK}^o$	(-14.67 ± 0.20)10^{-6}
$^aH_{KKK} - {}^sH_{KKK}^o$	(4.596 ± 0.030)10^{-6}	$^sH_{KKK} - {}^aH_{KKK}^o$	(13.87 ± 0.10)10^{-6}

Inversion splitting in the $J = k = 0$ $2\nu_2$ state: 284.7064 ± 0.0020

* The band origin ν_0 is defined as $\nu_0 = (E_i^0 - E_p^0)/hc$ [Eq. (16)].

TABLE IX

Independent Linear Combinations of the Parameters of the ν_4 Band of $^{14}NH_3$ (in cm^{-1})[a]

	s ↔ a, n = s	a ↔ a, n = a
$\nu_0 - (n_{C^0} - n_{B^0}) + \frac{1}{4}(n_{\eta_K} + n_{\tau^*_{KK}}) - \frac{2n}{3}\tau_{KKK}$	1629.99072 ± 0.00021	1630.3391 ± 0.0008
$n_C - n_B - n_C n_{\zeta_4} + n_{\eta_K} + n_{\tau^*_{KK}} - \frac{4}{3}\tau_{KKK}$	-2.43295 ± 0.00005	-2.41663 ± 0.00017
$n_C - n_B - (n_{C^0} - n_{B^0}) - \frac{5n}{2}\tau_{KKK} + \frac{3}{2}(n_{\eta_K} + n_{\tau^*_{KK}})$	-0.160203 ± 0.000035	-0.15235 ± 0.00008
n_B	10.040597 ± 0.000027	10.02747 ± 0.00006
$n_{D_J^0} - n_{D_J}$	$(-2.235 \pm 0.006)10^{-4}$	$(-0.871 \pm 0.019)10^{-4}$
$n_{D_{JK}^0} - n_{D_{JK}}$	$(5.503 \pm 0.014)10^{-4}$	$(1.393 \pm 0.044)10^{-4}$
$n_{D_K^0} - n_{D_K} + \frac{5n}{2}\tau_{KKK}$	$(-2.706 \pm 0.011)10^{-4}$	$(2.580 \pm 0.041)10^{-4}$
$n_{H_{JJJ}} - n_{H^0_{JJJ}}$	$(1.2014 \pm 0.0040)10^{-6}$	$(0.2486 \pm 0.0018)10^{-5}$
$n_{H_{JJK}} - n_{H^0_{JJK}}$	$(-3.685 \pm 0.015)10^{-6}$	$(-1.167 \pm 0.007)10^{-5}$
$n_{H_{JKK}} - n_{H^0_{JKK}}$	$(3.096 \pm 0.025)10^{-6}$	$(2.545 \pm 0.012)10^{-5}$
$n_{H_{KKK}} - n_{H^0_{KKK}}$	$(-0.557 \pm 0.013)10^{-6}$	$(-1.753 \pm 0.006)10^{-5}$
n_{η_J}	$(-0.967 \pm 0.038)10^{-4}$	$(5.08 \pm 0.17)10^{-4}$
$n_{\tau_{JJK}}$	$(1.1278 \pm 0.0042)10^{-5}$	$(0.2702 \pm 0.0025)10^{-4}$
$n_{\tau_{JKK}}$	$(-2.708 \pm 0.006)10^{-5}$	$(-1.3090 \pm 0.0028)10^{-4}$
$n_{D_K^0} + \frac{5n}{6}\tau_{KKK} - \frac{1}{4}(n_{\eta_K} + n_{\tau^*_{KK}})$	$(1.0438 \pm 0.0011)10^{-3}$	$(1.0501 \pm 0.0038)10^{-3}$
$n_{H^0_{KKK}} + \frac{1n}{6}\tau_{KKK}$	$(2.3124 \pm 0.0030)10^{-6}$	$(1.6732 \pm 0.0015)10^{-5}$
$n_{\eta_K} - n_{\eta_K^{(\nu_2+\nu_4)}} + n_{\tau^*_{KK}} - n_{\tau^{*(\nu_2+\nu_4)}_{KK}}$	$(-4.7168 \pm 0.0046)10^{-3}$	$(1.905 \pm 0.016)10^{-3}$
$n_{\tau_{KKK}} - n_{\tau_{KKK}^{(\nu_2+\nu_4)}}$	0[b]	0[b]
Inversion splitting in the J = k = 0 ν_4 state:	1.1488 ± 0.0010	

[a] The band origin ν_0 is defined as $\nu_0 = (E_1^0 - E_0^0)/hc$ [Eq. (20)].
[b] Constrained value.

where ψ_{ik}^0 are the unperturbed wavefunctions. Our assignments in Tables I to III are essentially based on the principle of the maximum contribution of the unperturbed wavefunction ψ_{ik}^0 to the perturbed state. This is illustrated by Table XIII which, however, also shows that in some cases this principle may not work.

TABLE X

Off-Diagonal Matrix Elements of the Coriolis and *l*-Type Interaction[a]

$\langle 3^-\|\alpha\|1^+\rangle$	6.6934 ± 0.0018	$\langle 3^+\|\alpha\|1^-\rangle$	-1.484 ± 0.021
$\langle 3^-\|\alpha\|0^+\rangle$	0.504 ± 0.011	$\langle 3^+\|\alpha\|0^-\rangle$	-5.9031 ± 0.0010
$\langle 2^-\|\alpha\|1^+\rangle$	5.2619 ± 0.0032	$\langle 2^+\|\alpha\|1^-\rangle$	11.3684 ± 0.0040
$\langle 2^-\|\alpha\|0^+\rangle$	-2.194 ± 0.006	$\langle 2^+\|\alpha\|0^-\rangle$	-1.2827 ± 0.0025
$\langle 1^-\|\alpha\|0^+\rangle$	10.338 ± 0.031	$\langle 1^+\|\alpha\|0^-\rangle$	11.461 ± 0.009
$\langle 1^+\|\beta\|1^+\rangle$	-0.244 ± 0.029	$\langle 1^-\|\beta\|1^-\rangle$	0.00466 ± 0.00041
$\langle 0^+\|\beta\|0^+\rangle$	-0.00291 ± 0.00011	$\langle 0^-\|\beta\|0^-\rangle$	-0.00701 ± 0.00021

[a] Matrix elements are defined in Table VI.

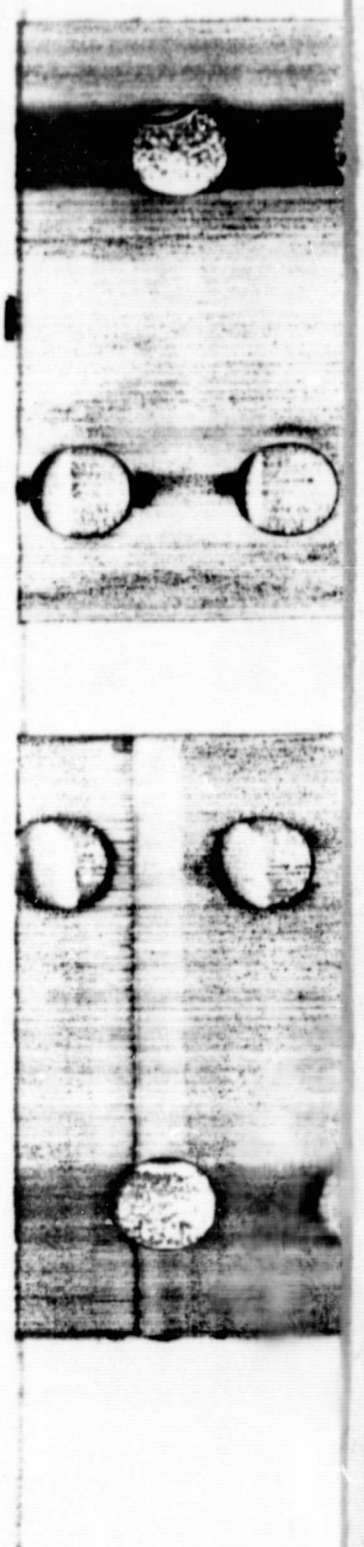

TABLE XI

Independent Linear Combinations of the Parameters of the $3\nu_2$ Band of $^{14}NH_3$ (in cm^{-1})

ν_0 (s + a)*	2895.6063 ± 0.0012	ν_0 (a + s)*	2383.3804 ± 0.0026
^aB	8.91779 ± 0.00026	^sB	9.42827 ± 0.00031
$(^aC - {}^aB) - (^sC^o - {}^sB^o)$	1.10027 ± 0.00018	$(^sC - {}^sB) - (^aC^o - {}^aB^o)$	0.47510 ± 0.00028
$^sD_J^o - {}^aD_J$	(1.179 ± 0.042)10^{-3}	$^aD_J^o - {}^sD_J$	(0.963 ± 0.019)10^{-3}
$^sD_{JK}^o - {}^aD_{JK}$	(-3.165 ± 0.058)10^{-3}	$^aD_{JK}^o - {}^sD_{JK}$	(-2.528 ± 0.043)10^{-3}
$^sD_K^o - {}^aD_K$	(1.994 ± 0.038)10^{-3}	$^aD_K^o - {}^sD_K$	(1.661 ± 0.038)10^{-3}
$^aH_{JJJ} - {}^sH_{JJJ}^o$	(-1.573 ± 0.049)10^{-5}	$^sH_{JJJ} - {}^aH_{JJJ}^o$	(-0.769 ± 0.026)10^{-6}
$^aH_{JJK} - {}^sH_{JJK}^o$	(4.618 ± 0.059)10^{-5}	$^sH_{JJK} - {}^aH_{JJK}^o$	(2.269 ± 0.061)10^{-6}
$^aH_{JKK} - {}^sH_{JKK}^o$	(-4.096 ± 0.058)10^{-5}	$^sH_{JKK} - {}^aH_{JKK}^o$	(-2.222 ± 0.038)10^{-6}
$^aH_{KKK} - {}^sH_{KKK}^o$	(1.039 ± 0.029)10^{-5}	$^sH_{KKK} - {}^aH_{KKK}^o$	(0.737 ± 0.032)10^{-6}

Inversion splitting in the J = k = 0 $3\nu_2$ state: 511.4325 ± 0.0040

* The band origin ν_0 is defined as $\nu_0 = (E_i^o - E_f^o)/hc$ [Eq. (16)].

For example, the 1855.468 cm^{-1} and 1901.229 cm^{-1} transitions should both be assigned as $a^PR(10,2)$, $\nu_4(-l)$. To avoid this, we assign the 1901.229 cm^{-1} transition as $a^PR(10,2)$, $\nu_4(-l)$ because it has a larger contribution from the $|0^-,1^{-1};\ 11,1\rangle$ state than the 1855.468 cm^{-1} transition. The latter is then assigned as $aR(10,2)$, $2\nu_2$ because its second-largest contribution is from the $|2^+,0^0;\ 11,2\rangle$ state. The few such cases that occurred in our data are indicated in Tables II and III by special labels.

TABLE XII

Independent Linear Combinations of the Parameters of the $\nu_2 + \nu_4$ Band of $^{14}NH_3$ (in cm^{-1})*

	s ↔ s, n = s	a ↔ a, n = a
$\nu_0 - (^nC^o - {}^nB^o) + \frac{1}{4}{}^n\eta_K$	2544.2587 ± 0.0012	2588.9592 ± 0.0017
$^nC - {}^nB - {}^n\zeta_4 + {}^n\eta_K$	-3.0029 ± 0.0006	-2.4137 ± 0.0008
$^nC - {}^nB - (^nC^o - {}^nB^o) + \frac{3}{2}{}^n\eta_K$	-0.6471 ± 0.0006	-0.1187 ± 0.0006
^nB	10.38786 ± 0.00021	9.97176 ± 0.00046
$^nD_J^o - {}^nD_J$	(5.302 ± 0.011)10^{-4}	(-1.759 ± 0.009)10^{-4}
$^nD_{JK}^o - {}^nD_{JK}$	(-4.539 ± 0.007)10^{-4}	(11.711 ± 0.047)10^{-4}
$^nD_K^o - {}^nD_K$	(-3.314 ± 0.021)10^{-4}	(-15.081 ± 0.051)10^{-4}
$^n\eta_J$	(2.369 ± 0.005)10^{-3}	(-6.503 ± 0.009)10^{-3}

Inversion splitting in J = k = 0 $\nu_2+\nu_4$ state: 45.4993 ± 0.0030

* The band origin is defined as $\nu_0 = (E_i^o - E_f^o)/hc$ [Eq. (20)]; sextic parameters have been neglected.

TABLE XIII

Example of the Assignments Based on the Values of $(c_{ik}^2/\sum_k c_{ik}^2) \times 100$ for $J = 11, k - l_4 = 2$

Calc. freq. (cm^{-1})	Assignment	$\|v_2^{\ell_2}, v_4^{\ell_4}; J, k\rangle$						
		$\|3^+,0^o;11,2\rangle$	$\|1^-,1^{+1};11,3\rangle$	$\|1^-,1^{-1};11,1\rangle$	$\|2^+,0^o;11,2\rangle$	$\|0^-,1^{+1};11,3\rangle$	$\|0^-,1^{-1};11,1\rangle$	$\|1^+,0^o;11,2\rangle$
1158.060	$aR(10,2),v_2$	0.0	0.0	0.0	0.0	3.3	3.3	93.4
1848.403	$a^RR(10,2),v_4(+\ell)$	0.2	0.8	0.8	42.5	51.9	2.6	1.3
1855.468	$aR(10,2),2v_2$	0.0	0.7	0.7	38.1	19.7	40.6	0.2
1901.229	$a^PR(10,2),v_4(-\ell)$	1.7	0.4	0.4	15.8	24.1	52.6	5.2
2557.356	$aR(10,2),3v_2$	97.4	0.3	0.3	0.1	0.9	1.0	0.0
2797.258	$a^RR(10,2),v_2+v_4(+\ell)$	0.1	73.9	25.8	0.2	0.0	0.0	0.0
2838.523	$a^PR(10,2),v_2+v_4(-\ell)$	0.6	23.9	72.1	3.3	0.0	0.0	0.0

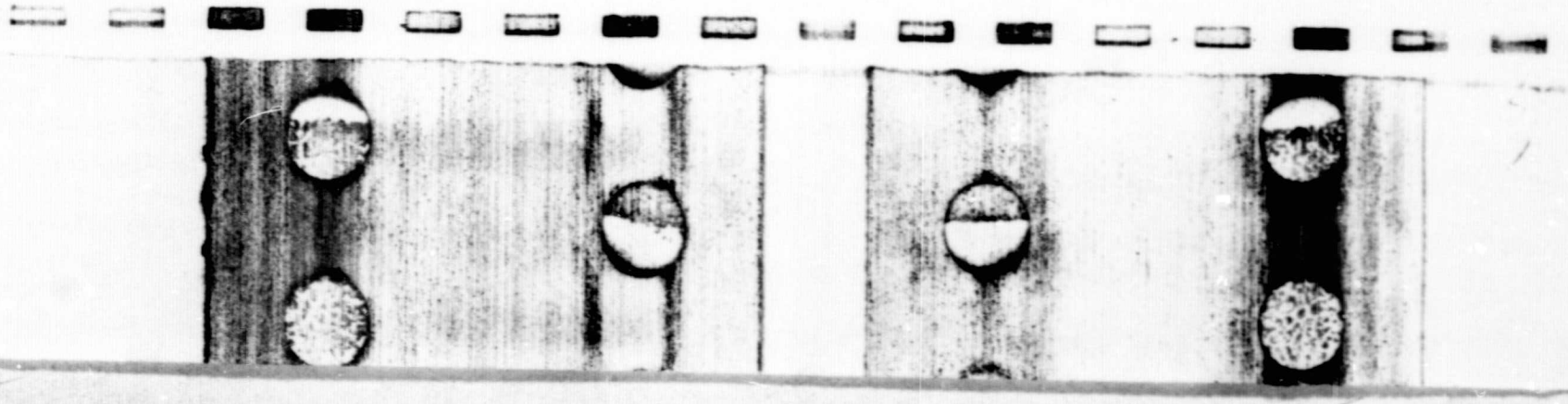

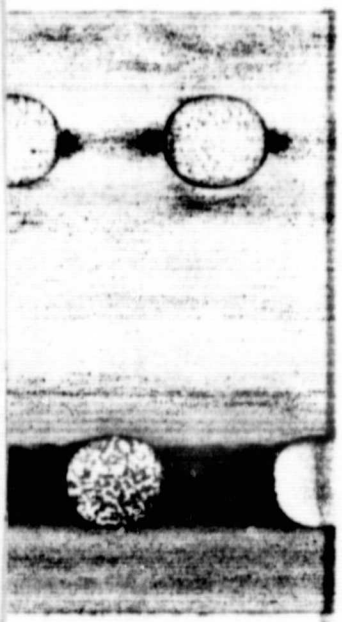

It should be emphasized that such assignments are only formal if there is strong mixing of the upper-state wavefunctions. Strictly speaking, we should give the same label to a series of lines originating from the same ground inversion-rotational level J'', k'' and terminating on upper-state levels with the same J', $k' - l_4$ quantum numbers.

REFERENCES

1. D. Papoušek, J. M. R. Stone, and V. Špirko, *J. Mol. Spectrosc.* **48,** 17–37 (1973).
2. V. Špirko, J. M. R. Stone, and D. Papoušek, *J. Mol. Spectrosc.* **48,** 38–46 (1973).
3. V. Danielis, D. Papoušek, V. Špirko, and M. Horák, *J. Mol. Spectrosc.*, **54,** 339–349 (1975).
4. V. Špirko, J. M. R. Stone, and D. Papoušek, *J. Mol. Spectrosc.* **60,** 159–178 (1976).
5. D. Papoušek and V. Špirko, *Top. Curr. Chem.* **68,** 59–102 (1976).
6. A. R. Hoy and P. R. Bunker, *J. Mol. Spectrosc.* **52,** 439–456 (1974).
7. J. S. Garing, H. H. Nielsen, and K. Narahari Rao, *J. Mol. Spectrosc.* **3,** 496–527 (1959).
8. H. M. Mould, W. C. Price, and G. R. Wilkinson, *Spectrochim. Acta* **15,** 313–330 (1959).
9. W. S. Benedict, E. K. Plyler, and E. D. Tidwell, *J. Res. Nat. Bur. Stand.* **61,** 123–147 (1958).
10. W. S. Benedict and E. K. Plyler, *Canad. J. Phys.* **35,** 1235–1241 (1957).
11. W. S. Benedict, E. K. Plyler, and E. D. Tidwell, *J. Chem. Phys.* **29,** 829–845 (1958).
12. W. S. Benedict, E. K. Plyler, and E. D. Tidwell, *J. Chem. Phys.* **32,** 32–44 (1960).
13. J. M. Dowling, *J. Mol. Spectrosc.* **27,** 527–538 (1968).
14. F. Shimizu, *J. Chem. Phys.* **52,** 3572–3576 (1970).
15. C. Chassagne, M. L. Grenier-Besson, and D. Bargues, *J. Phys. (Paris)* **37,** 71–80 (1976).
16. S. M. Freund and T. Oka, *Phys. Rev. A* **13,** 2178–2190 (1976).
17. H. Jones, *Appl. Phys.* **15,** 261–264 (1978).
18. J. P. Sattler and K. J. Ritter, *J. Mol. Spectrosc.* **69,** 486–488 (1978).
19. T. Kostiuk, M. J. Mumma, J. J. Hillman, D. Buhl, L. W. Brown, J. L. Faris, and D. L. Spears, *Infrared Phys.* **17,** 431–439 (1977).
20. N. Nereson, *J. Mol. Spectrosc.* **69,** 489–493 (1978).
21. D. Laughton, S. M. Freund and T. Oka, *J. Mol. Spectrosc.* **62,** 263–270 (1976).
22. W. K. Bischel, P. J. Kelly, and C. K. Rhodes, *Phys. Rev. A* **13,** 1829–1841 (1976).
23. P. Helminger, F. C. DeLucia, and W. Gordy, *J. Mol. Spectrosc.* **39,** 94–97 (1971).
24. A. F. Krupnov, L. I. Gershstein, V. G. Shustrov, and V. V. Polyakov, *Izv. Vyssh. Uchebn. Zaved. Radiofiz.* **12,** 1584–1586 (1969).
25. Y. Y. Kwan and E. A. Cohen, *J. Mol. Spectrosc.* **58,** 54–75 (1975).
26. J. B. Curtis, Ph.D. dissertation, The Ohio State University, 1974.
27. R. S. McDowell, H. W. Galbraith, C. D. Cantrell, N. G. Nereson, and E. D. Hinkley, *J. Mol. Spectrosc.* **68,** 288–298 (1977).
28. A. F. Krupnov and A. V. Burenin, *in* "Molecular Spectroscopy: Modern Research," Vol. 2, (K. Narahari Rao, Ed.) Academic Press, New York, 1976.
29. E. N. Karyakin, A. F. Krupnov, D. Papoušek, Ju. M. Schurin, and Š. Urban, *J. Mol. Spectrosc.* **66,** 171–173 (1977).
30. F. Y. Chu and S. M. Freund, *J. Mol. Spectrosc.* **48,** 183–184 (1973).
31. H. Jones, *in* "Proc. Vth Internat. Seminar on High Resolution Infrared Spectroscopy, Liblice near Prague, 18–22, Sept. 1978."
32. E. Schnabel, T. Törring, and W. Wilke, *Z. Phys.* **188,** 167–171 (1965).
33. D. Papoušek, S. Toman, and J. Plíva, *J. Mol. Spectrosc.* **15,** 502–505 (1965).

JOURNAL OF MOLECULAR SPECTROSCOPY **91**, 273 (1982)

ERRATUM

Volume **79**, No. 2, February (1980), in the article "Coriolis and *l*-Type Interactions in the ν_2, $2\nu_2$, and ν_4 States of $^{14}NH_3$," by Š. Urban *et al.*, pp. 455–495:

The value of $[^{(4)}D_k^k - {}^{(1)}D_k^k]$ in Table V should be considered with the negative sign. The value of ^1B in Table VII should be 10.44847 ± 0.00003.

JOURNAL OF MOLECULAR SPECTROSCOPY 88, 293–299 (1981)

The Diode Laser Spectrum of the ν_2 Band of $^{14}ND_3$ and $^{15}ND_3$

V. MALATHY DEVI,[1] P. P. DAS,[2] AND K. NARAHARI RAO

Department of Physics, The Ohio State University, Columbus, Ohio 43210

AND

Š. URBAN, D. PAPOUŠEK, AND V. ŠPIRKO

The J. Heyrovský Institute of Physical Chemistry and Electrochemistry, Czechoslovak Academy of Sciences, 160 00 Prague 6, Czechoslovakia

The spectra of the ν_2 bands of $^{14}ND_3$ and $^{15}ND_3$ were measured under Doppler-limited resolution with a diode laser spectrometer in order to resolve the K structure of the $sR(J, K)$ and $aR(J, K)$ multiplets. By a simultaneous least-squares analysis of these data, the Fourier spectra of the ν_2 band measured by Jones [*J. Mol. Spectrosc.* **74**, 409 (1979)], and the ground-state microwave transitions, sets of improved ν_2-band parameters were obtained, including the sextic centrifugal distortion coefficients.

INTRODUCTION

In our previous papers (*1–3*) we have measured and analyzed the high-resolution spectra of $^{14}NH_3$ in the submillimeter wave, far-infrared, and medium-infrared spectral regions. The ultimate goal of these studies is the determination of a complete anharmonic potential function of ammonia by a least-squares fit to the experimental data of various isotopically substituted ammonia molecules [cf. Ref. (*4*)].

There are, however, very few high-resolution infrared data on the deuterated ammonia. We have therefore undertaken a study of the spectra of the ν_2 bands of $^{14}ND_3$ and $^{15}ND_3$ (cf. Fig. 1) under Doppler-limited resolution with a diode laser spectrometer.

The Fourier spectra of the ν_2 fundamentals of $^{14}ND_3$ and $^{15}ND_3$ were recently measured by Jones (*5*) with 0.055-cm^{-1} resolution with apodization or slightly less than 0.04 cm^{-1} without apodization. This has made it possible to resolve many of the P, Q, and R lines and to determine the ν_2 band parameters including the quartic centrifugal distortion coefficients. Among the transitions which remained unresolved in the Fourier spectra were especially the $sR(J, K)$ and $aR(J, K)$ transitions which appear as multiplets within the 0.2–0.3 cm^{-1} interval.

In the present paper, we have resolved the K structure of these multiplets using a diode laser spectrometer operating between 818 and 852 cm^{-1}. In a simultaneous least-squares fit to the ν_2-band transition wavenumbers of Jones (*5*), the ground-

[1] Present address: NOAA-NESS, FB4, S/RE21, Washington, D. C. 20233.
[2] Present address: Tachisto Inc., 13 Highland Circle, Needham, Mass. 02194.

0022-2852/81/080293-07$02.00/0

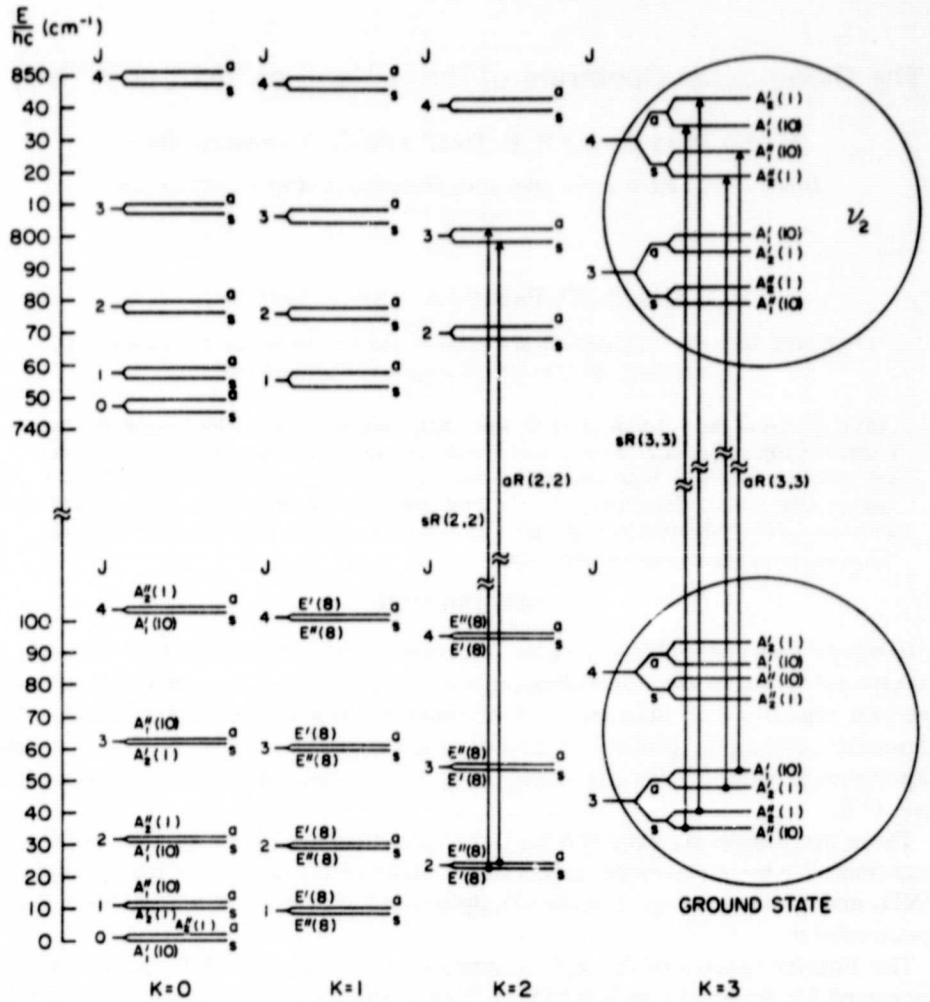

FIG. 1. Energy level diagram of the inversion–rotation levels in the ground and ν_2 state of ND_3 with examples of the $sR(J, K)$ and $aR(J, K)$ transitions. The inversion splittings and the A_1, A_2 splittings are not drawn to scale. Values in parentheses behind the symbol of the symmetry species denote the spin statistical weights. The species of the energy levels in the ν_2 state are the same as in the ground state. The symmetry species of the $K = 4, 5, 6$ levels are the same as for the $K = 1, 2, 3$ levels, respectively, except that $'$ should be changed to $''$ and vice versa (the rotational quantum number K should be considered with modulo 6 for obtaining the species of energy levels with higher K values).

state microwave frequencies of the inversion–rotation and inversion transitions (*6–8*), and our diode laser measurements, we arrived at an improved set of spectroscopic parameters for $^{14}ND_3$ and $^{15}ND_3$ including the sextic centrifugal distortion coefficients.

EXPERIMENTAL DETAILS

The diode laser spectrometer has been described earlier (*9*, *10*). The ν_1 band lines

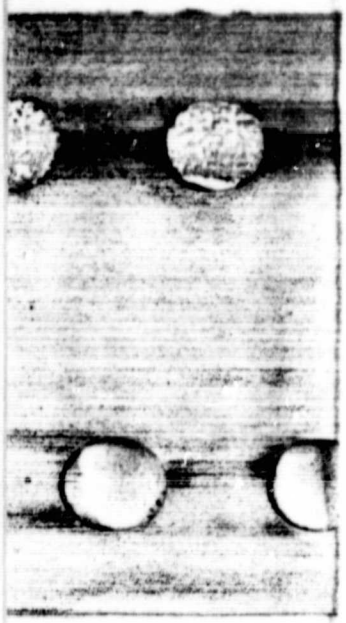

TABLE I

Calculated and Observed Wavenumbers (cm^{-1}) of the ν_2 Band of $^{14}ND_3$

J,K	ν_{calc}	ν_{obs}	ν_{calc}	ν_{obs}	J,K	ν_{calc}	ν_{obs}	ν_{calc}	ν_{obs}
	sR(6,K)		sR(6,K)			sR(9,K)		sR(9,K)	
6,0	819,2100	.2102	816,1535	-	9,0	848,0419	.0416	845,4256	.4245
6,1	819,2144	.2141	816,1444	-	9,1	848,0470	.0473	845,4193	.4189
6,2	819,2277	.2272	816,1188	-	9,2	848,0623	.0637	845,4003	.3973
6,3[a]	819,2504		816,0701	-	9,3[a]	848,0878		845,3682	
	817,2502	.2499	816,0703	-		848,0886	.0891	845,3674	.3660
6,4	819,2826	.2820	816,0029	-	9,4	848,1251	.1279	845,3206	.3218
6,5	819,3255	.3255	815,9130	-	9,5	848,1738	.1772	845,2572	.2572
6,6	819,3800	.3798	815,7979	-	9,6	848,2352	.2359	845,1760	.1737
	sR(7,K)		sR(7,K)		9,7	848,3106	.3120	845,0711	.0695
					9,8	848,4014	.3998	844,9416	.9417
7,0	828,9080	.9072	825,9883	.9884	9,9	848,5093	.5080	844,7815	.7822
7,1	828,9107	.9101	825,9802	.9802					
7,2	828,9248	.9246	825,9555	.9553		sR(10,K)		sR(10,K)	
7,3[a]	828,9485		825,9135	.9112	10,0	857,4787	-	855,0196	-
	828,9488	.9481	825,9133		10,1	857,484	-	855,0142	-
7,4	829,9828	.9821	825,8527	.8505	10,2	857,499	-	854,9981	-
7,5	829,0281	.0272	825,7715	.7701	10,3[a]	857,5270	-	854,9697	-
7,6	829,0854	.0839	825,6672	.6665		857,5258		854,9710	
7,7	829,1560	.1553	825,5365	.5357	10,4	857,5642	-	854,9301	-
	sR(8,K)		sR(8,K)		10,5	857,6141	-	854,8756	-
					10,6	857,6770	-	854,8047	-
8,0	838,5172	.5176	835,7471	.7478	10,7	857,7540	-	854,7144	.7168
8,1	838,5221	.5219	835,7399	.7412	10,8	857,8485	-	854,6012	.6008
8,2	838,5368	.5370	835,7180	.7186	10,9	857,9563	-	854,4802	.4593
8,3[a]	838,5620	.5618	835,6805	.6808	10,10	858,0852	-	854,2858	.2958
	838,5616		835,6809						
8,4	838,5975	.5972	835,6268	.6286					
8,5	838,6447	.6440	835,5544	.5537					
8,6	838,7043	.7035	835,4611	.4603					
8,7	838,7775	.7758	835,3437	.3433					
8,8	838,8660	.8664	835,1980	.1970					

[a] Upper value of ν_{calc} corresponds to the more intense line in the A_1, A_2 doublet

of OCS (*11*) were used for calibration purposes. Both $^{14}ND_3$ and $^{15}ND_3$ were obtained from Prochem Ltd. and were stated to be 98% pure. These gases were contained in 1-m-long Pyrex cells with KBr windows. The sample pressures ranged from 0.3 to 0.5 Torr. The relative uncertainty of the observed wavenumbers is about ± 0.0005 cm^{-1}, while the absolute uncertainty due mainly to OCS calibration is about ± 0.002 cm^{-1}.

The observed wavenumbers of the $R(J, K)$ multiplets obtained in this work are given in Tables I and II for $^{14}ND_3$ and $^{15}ND_3$, respectively. Figure 2 illustrates the resolution of the $sR(6, K)$ multiplet in the ν_2 band of $^{14}ND_3$. The corresponding FTS scan at 0.04-cm^{-1} resolution is also shown in this figure.

RESULTS

The experimental data which have been processed in a simultaneous least-squares fit for $^{14}ND_3$ were the transition wavenumbers in the ν_2 band measured

TABLE II

Calculated and Observed Wavenumbers (cm^{-1}) of the ν_2 Band of $^{15}ND_3$

J,K	ν_{calc}	ν_{obs}	ν_{calc}	ν_{obs}	J,K	ν_{calc}	ν_{obs}	ν_{calc}	ν_{obs}
	sR(7,K)		sR(7,K)			sR(9,K)		sR(9,K)	
7,0	822,4094	-	819,7656	.7651	9,0	841,5567		839,1983	.1989
7,1	822,4117	-	819,7559	.7557	9,1	841,5596	.5594	839,1905	.1906
7,2	822,4187	-	819,7267	.7267	9,2	841,5684	.5680	839,1669	.1675
7,3[a]	822,4315	-	819,6773	.6775	9,3[a]	841,5813	.5824	839,1273	.1267
	822,4306		819,6771			841,5836		839,1265	
7,4	822,4482	-	819,6061	.6062	9,4	841,6044	.6035	839,0694	.0692
7,5	822,4721	-	819,5114	.5107	9,5	841,6325	.6328	838,9927	.9941
7,6	822,5035	-	819,3906	.3897	9,6	841,6686	.6689	838,8944	.8950
7,7	822,5440	-	819,2403	.2393	9,7	841,7136	.7141	838,7717	.7700
	sR(8,K)		sR(8,K)		9,8	841,7695	.7697	838,6206	.6190
					9,9	841,8384	.8372	838,4361	.4360
8,0	832,0249	.0247	829,5200	.5196		sR(10,K)		sR(10,K)	
8,1	832,0275		829,5113	.5109					
8,2	832,0354	.0345	829,4850	.4844	10,0	851,0019	.0080	848,7970	.7907
8,3[a]	832,0490	.0487	829,4400	.4396	10,1	851,0051		848,7901	
	832,0485		829,4405		10,2	851,0146	.0168	848,7693	.7689
8,4	832,0681	.0680	829,3754	.3754	10,3[a]	851,0318	.0320	848,7332	.7326
8,5	832,0941	.0948	829,2903	.2894		851,0305		848,7345	
8,6	832,1277	.1290	829,1808	.1782	10,4	851,0545	.0543	848,6829	.6823
8,7	832,1705	.1709	829,0443	.0464	10,5	851,0851	.0845	848,6148	.6140
8,8	832,2243	.2227	828,8767	.8767	10,6	851,1237	.1230	848,5276	.5262
					10,7	851,1713	.1707	848,4184	.4191
					10,8	851,2294	.2287	848,2837	.2823
					10,9	851,3000	.2998	848,1186	.1179
					10,10	851,3856	.3856	847,9175	.9166

[a] Upper value of ν_{calc} corresponds to the more intense line in the A_1, A_2 doublet

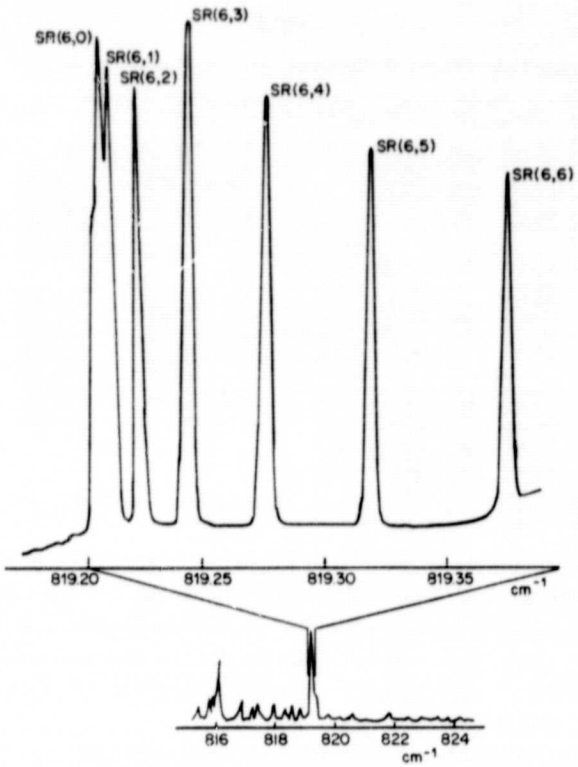

FIG. 2. Resolution of the $sR(6, K)$ multiplet in the ν_2 band of $^{14}ND_3$ along with the FTS scan by Jones (*5*).

by us with the diode laser spectrometer and by Jones with a Fourier spectrometer (*5*), the ground-state inversion frequencies (*6*), and the ground-state $J = 1 \leftarrow 0$ and $2 \leftarrow 1$ inversion–rotation transition frequencies (*7, 8*). For $^{15}ND_3$ only the inversion–rotation transition frequencies $J = 1 \leftarrow 0$ and $2 \leftarrow 1$ are available (*7, 8*) and these have been combined with the infrared data. A more detailed discussion of the simultaneous analysis of the infrared and microwave data of ammonia is given in Ref. (*3*).

The statistical weights assigned to the experimental data were $w_j = \delta_j^{-2}$, where δ_j is the estimated uncertainty of the measurement. We have used $\delta = 2 \times 10^{-3}$ cm^{-1} for our diode laser measurements, $\delta = 5 \times 10^{-3}$ cm^{-1} for the data of Jones (*5*) (except for few blended lines which have not been considered in the fit), and $\delta = 0.05$ MHz for the microwave inversion frequencies (*6*).

We have used a standard polynomial expression for the inversion–rotation energy levels in the ground and ν_2 excited states including the sextic centrifugal distortion constants. The A_1, A_2 splitting of the $K = 3$ levels was described by the parameter η_3 in the matrix element of the corresponding interaction (cf. Ref. (*3*)),

TABLE III

Ground-State and ν_2-State Molecular Parameters of $^{14}ND_3$ (cm^{-1})[a]

	Ground-state	ν_2-state
$(a)_{E(J=K=0)}$	0	745.5997(7)[b]
$(a)_B$	5.142763(2)	5.12251(5)
$(a)_{D_J} \times 10^4$	1.983(3)	1.964(9)
$(a)_{D_{JK}} \times 10^4$	-3.501(9)	-3.685(20)
$(a)_{H_{JJJ}} \times 10^8$	2.39(15)	2.11(48)
$(a)_{H_{JJK}} \times 10^8$	-5.69(63)	-8.7(17)
$(a)_{H_{JKK}} \times 10^8$	4.9(11)	12.1(20)
Inversion splitting Δ_{inv}	0.0530882(3)	3.5484(3)
$(a)_{B^-} - (a)_B$	$-1.7337(12) \times 10^{-4}$	$-1.047(5) \times 10^{-2}$
$[(a)_{C^-} - (a)_B] - [(a)_{C^-} - (a)_B]$	$2.6138(14) \times 10^{-4}$	$1.567(10) \times 10^{-2}$
$(a)_{D_J^-} - (a)_{D_J}$	$-2.14(17) \times 10^{-7}$	$-1.62(10) \times 10^{-5}$
$(a)_{D_{JK}^-} - (a)_{D_{JK}}$	$6.54(43) \times 10^{-7}$	$4.64(26) \times 10^{-5}$
$(a)_{D_K^-} - (a)_{D_K}$	$-4.66(28) \times 10^{-7}$	$-3.41(15) \times 10^{-5}$
$(a)_{H_{JJJ}^-} - (a)_{H_{JJJ}}$	$0.36(7) \times 10^{-10}$	$-1.26(52) \times 10^{-8}$
$(a)_{H_{JJK}^-} - (a)_{H_{JJK}}$	$-1.54(30) \times 10^{-10}$	$5.6(19) \times 10^{-8}$
$(a)_{H_{JKK}^-} - (a)_{H_{JKK}}$	$2.25(40) \times 10^{-10}$	$-8.8(24) \times 10^{-8}$
$(a)_{H_{KKK}^-} - (a)_{H_{KKK}}$	$-1.11(20) \times 10^{-10}$	$4.5(11) \times 10^{-8}$
$\eta_3 \times 10^{10}$	7.14(6)	(7.14)[c]
$[(a)_{C_{(\nu_2)}^-} - (a)_{B_{(\nu_2)}}] - [(a)_{C_0^-} - (a)_{B_0}]$		-0.01461(7)
$(a)_{D_K^{(\nu_2)}} - (a)_{D_K^0}$		$2.49(12) \times 10^{-5}$
$(a)_{H_{KKK}^{(\nu_2)}} - (a)_{H_{KKK}^0}$		$-4.13(78) \times 10^{-8}$

[a] Values in parentheses are standard deviations of the parameters, given in units of the last digit quoted; s and a denote respectively the lower and upper component of the inversion doublet.
[b] Band origin for the $a \rightarrow a$ transition is 749.1481(8), for the $s \rightarrow s$ transition 745.5466(7)cm^{-1}. [c] Constrained value.

$$\frac{1}{2}\left\langle\left(\frac{s}{a}\right)\right| [\langle J, +3| \pm \langle J, -3|](H'/hc) \left|\left(\frac{s}{a}\right)\right\rangle [|J+3\rangle \pm |J-3\rangle] = \pm\eta_3 (J+3)!/(J-3)!, \quad (1)$$

where s and a denote the parity of the corresponding inversion wavefunctions.

The calculated wavenumbers are compared with the measured wavenumbers for the $R(J, K)$ multiplets in Tables I and II; in Tables III and IV the values of the corresponding molecular parameters obtained for $^{14}ND_3$ and $^{15}ND_3$ by the least-squares fit are presented. The microwave data (*6–8*) and the Fourier data (*5*) have been described within their experimental accuracy.

The ground-state parameter η_3 [Eq. (1)] was determined for $^{14}ND_3$ from the ground-state inversion frequencies (*6*). This parameter (Table III) was assumed to have the same value in the ν_2 state of $^{14}ND_3$ and in the upper and lower states of $^{15}ND_3$. The magnitude of the splitting of the $R(J, 3)$ lines is given by the difference between the value of the splitting of the upper and lower state $K = 3$ energy

TABLE IV

Ground-State and ν_2-State Molecular Parameters of $^{15}ND_3$ (cm^{-1})[a]

	Ground-state	ν_2-state
$(s)_{E(J=K=0)}$	0	739.5343(9)[b]
$(s)_B$	5.129658(4)	5.10554(4)
$(s)_{D_J}\times10^4$	1.977(5)	1.986(6)
$(s)_{D_{JK}}\times10^4$	-3.500(18)	-3.733(18)
$(s)_{H_{JJJ}}\times10^8$	2.1(3)	2.75(25)
$(s)_{H_{JJK}}\times10^7$	-5.9(9)	-10.2(10)
$(s)_{H_{JKK}}\times10^8$	6.9(14)	13.3(15)
Inversion splitting Δ_{inv}	0.047791(5)	3.2454(18)
$(s)_{B_-}-(s)_B$	$-1.60(6)\times10^{-4}$	$-1.008(7)\times10^{-2}$
$[(s)_{C_-}-(s)_B] - [(s)_{C_-}-(s)_B]$	$2.23(11)\times10^{-4}$	$1.499(8)\times10^{-2}$
$(s)_{D_J}-(s)_{D_J}$	$0.95(70)\times10^{-7}$	$-1.82(12)\times10^{-5}$
$(s)_{D_{JK}}-(s)_{D_{JK}}$	$-25.2(32)\times10^{-7}$	$5.18(25)\times10^{-5}$
$(s)_{D_K}-(s)_{D_K}$	0[c]	$-3.32(12)\times10^{-5}$
$(s)_{H_{JJJ}}-(s)_{H_{JJJ}}$	$0.37(16)\times10^{-10}$	$-2.52(42)\times10^{-8}$
$(s)_{H_{JJK}}-(s)_{H_{JJK}}$	$-3.0(8)\times10^{-10}$	$8.0(14)\times10^{-8}$
$(s)_{H_{JKK}}-(s)_{H_{JKK}}$	$4.1(9)\times10^{-10}$	$-6.6(21)\times10^{-8}$
$(s)_{H_{KKK}}-(s)_{H_{KKK}}$	0[c]	0[c]
$\eta_3 \times 10^{10}$	(7.14)[c]	(7.14)[c]
$[(s)_{C_{(\nu_2)}}-(s)_{B_{(\nu_2)}}] - [(s)_{C_0}-(s)_{B_0}]$		-0.01632(5)
$(s)_{D_K(\nu_2)}-(s)_{D_K^0}$		$2.44(7)\times10^{-5}$
$(s)_{H_{KKK}(\nu_2)}-(s)_{H_{KKK}^0}$		$-1.5(5)\times10^{-8}$

[a] See footnote in Table III. [b] Band origin for the $s\rightarrow s$ transition is 742.7797(18), for the $s\rightarrow a$ transition is 739.4865(9) cm^{-1}. [c] Constrained value.

levels; due to the spin statistical weights, the ratio of the intensities of the split lines should be 1:10 (see also Fig. 1).

It can be seen from the calculated values of the $R(J, 3)$ transition wavenumbers (Tables I and II) that for $J \geq 10$ the splittings might be observable with the 0.002-cm^{-1} resolution of the diode laser spectrometer. We have observed shoulders

TABLE V

Comparison of Ground-State Constants (in cm^{-1}) Obtained from Vibration–Rotation Data and Pure Rotation Data

	$^{14}ND_3$			$^{15}ND_3$		
	Ref. 7	Ref. 5	This work	Ref. 7	Ref. 5	This work
B_0	5.14266(1)	5.14246(8)	5.142677(2)	5.12357(1)	5.12330(11)	5.123578(8)
$D_J^0\times10^4$	1.97(4)	1.930(3)	1.982(3)	1.98(4)	1.933(5)	1.978(5)
$D_{JK}^0\times10^4$	-3.50(2)	-3.407(6)	-3.498(10)	-3.52(1)	-3.434(5)	-3.513(18)

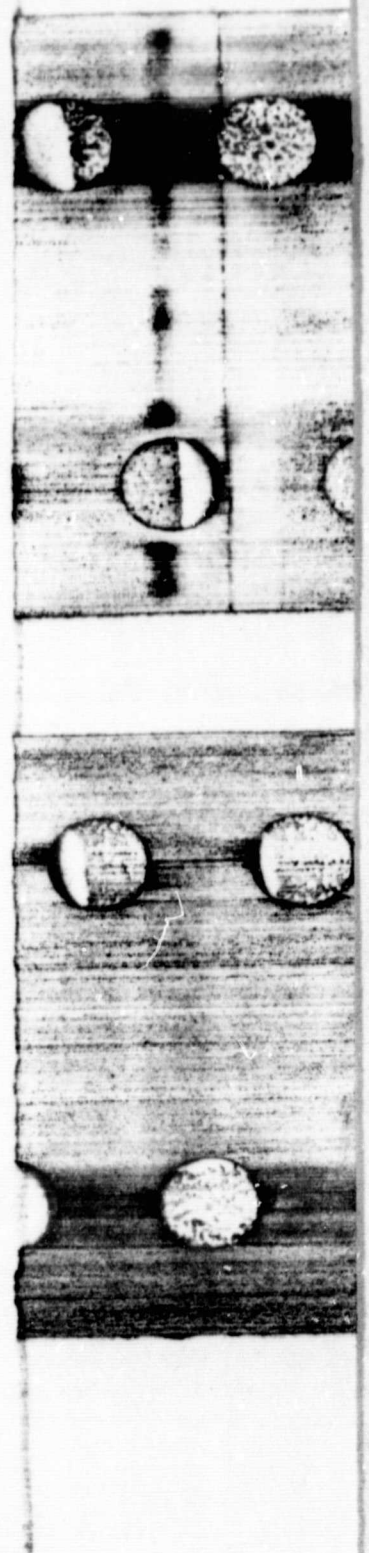

in the $R(10, 3)$ lines which probably correspond to this effect but this could be confirmed only by measuring transitions with $J \geq 10$.

In Table V, the ground-state constants of $^{14}ND_3$ and $^{15}ND_3$ obtained in our work are compared with those obtained previously by Helminger and Gordy (*7*) and Jones (*5*). Our values are much closer to the values obtained from pure rotation data (*7*) than those of Jones (*5*). The reason of the inconsistency in Ref. (*5*) is obvious: Jones (*5*) assumed that $^{(s)}B_0 = {}^{(a)}B_0$ in his simultaneous treatment of the observed rotational and vibrational–rotational transition frequencies which is not adequate to the accuracy of the experimental data.

ACKNOWLEDGMENT

This work was done during the tenure of a grant from the National Aeronautics and Space Administration. One of us (K.N.R.) acknowledges this support gratefully.

RECEIVED: August 29, 1980

REFERENCES

1. Š. URBAN, V. ŠPIRKO, D. PAPOUŠEK, R. S. MCDOWELL, N. G. NERESON, S. P. BELOV, L. I. GERSHTEIN, A. V. MASLOVSKIJ, A. F. KRUPNOV, J. CURTIS, AND K. NARAHARI RAO, *J. Mol. Spectrosc.* **79,** 455–495 (1980).
2. S. P. BELOV, L. I. GERSHTEIN, A. F. KRUPNOV, A. V. MASLOVSKIJ, Š. URBAN, V. ŠPIRKO, AND D. PAPOUŠEK, *J. Mol. Spectrosc.* **84,** 288–304 (1980).
3. Š. URBAN, V. ŠPIRKO, D. PAPOUŠEK, J. KAUPPINEN, S. P. BELOV, L. I. GERSHTEIN, AND A. F. KRUPNOV, *J. Mol. Spectrosc.*, **88,** 274–292 (1981).
4. D. PAPOUŠEK AND V. ŠPIRKO, *Top. Curr. Chem.* **68,** 59–102 (1976).
5. L. JONES, *J. Mol. Spectrosc.* **74,** 409–422 (1979).
6. G. HERRMAN, *J. Chem. Phys.* **29,** 875–879 (1958).
7. P. HELMINGER, F. C. DELUCIA, AND W. GORDY, *J. Mol. Spectrosc.* **39,** 94–97 (1971).
8. P. HELMINGER AND W. GORDY, *Phys. Rev.* **188,** 100–108 (1969).
9. S. P. REDDY, W. IVANCIC, V. MALATHY DEVI, A. BALDACCI, K. NARAHARI RAO, A. W. MANTZ, AND R. S. ENG, *Appl. Opt.* **18,** 1350–1354 (1979).
10. P. P. DAS, V. MALATHY DEVI, AND K. NARAHARI RAO, *J. Mol. Spectrosc.* **84,** 305–312 (1980).
11. A. G. MAKI, W. B. OLSON, AND R. L. SAMS, *J. Mol. Spectrosc.* **81,** 122–138 (1980).

JOURNAL OF MOLECULAR SPECTROSCOPY 92, 282 (1982)

ERRATUM

Volume **88,** No. 2 (1981), in the article "The Diode Laser Spectrum of the ν_2 Band of $^{14}ND_3$ and $^{15}ND_3$" by V. Malathy Devi, P. P. Das, K. Narahari Rao, Š. Urban, D. Papoušek, and V. Špirko, pp. 293–299:

In Tables III and IV, the ground state values of the differences $^{(a)}H - {}^{(s)}H$ should be with the factor 10^{-8} instead of 10^{-10}.

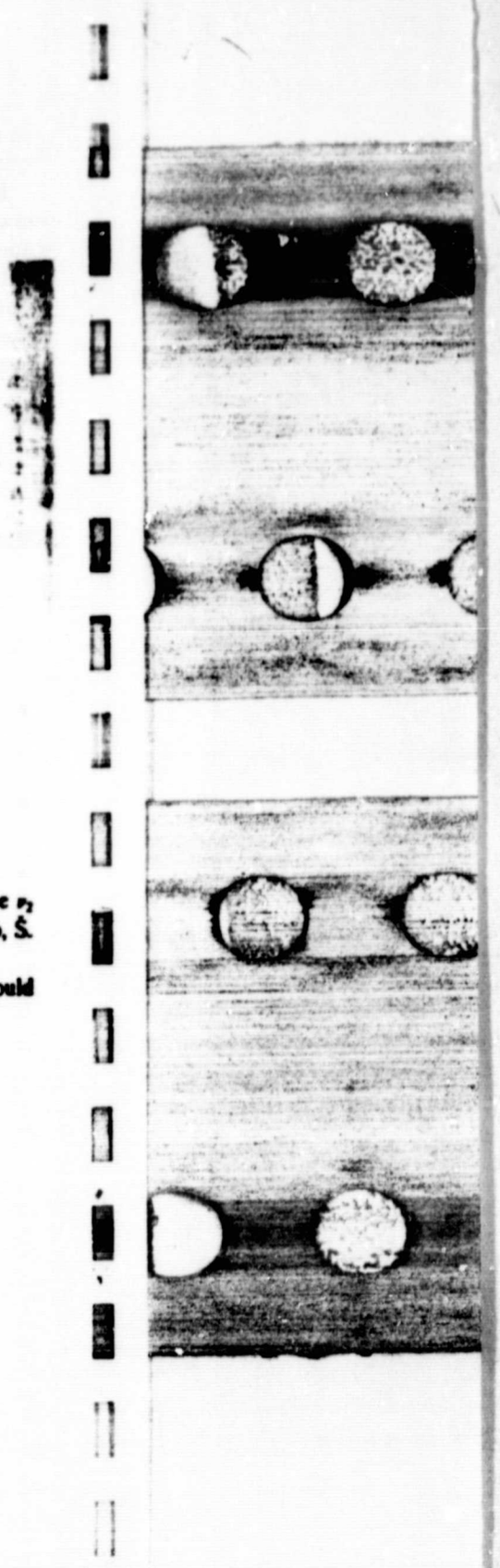

JOURNAL OF MOLECULAR SPECTROSCOPY 72, 135–142 (1978)

Interpretation of the $^{13}C^{16}O_2$ Spectrum at 4.4 μm

AGOSTINO BALDACCI, LOUISE LINDEN, V. MALATHY DEVI, AND K. NARAHARI RAO

Department of Physics, The Ohio State University, Columbus, Ohio 43210

AND

B. FRIDOVICH

National Oceanic and Atmospheric Administration, National Environmental Satellite Service Washington, D. C. 20233

The overlapping structure observed in the region of the ν_3 fundamental of $^{13}C^{16}O_2$ at 4.4 μm has been assigned to several transitions belonging to not only the 13-C variety of carbon dioxide ($^{13}C^{16}O_2$) but also to $^{13}C^{16}O^{17}O$ and $^{13}C^{16}O^{18}O$ species occurring in the sample. Molecular constants have been evaluated for the assigned transitions.

In a recent note (*1*) we reported the measurements and analysis of the ν_3 band of $^{13}C^{16}O_2$ recorded with a high resolution vacuum infrared spectrograph by using an enriched sample of this isotopic species. We now present the interpretation of most of the structure observed in the region where this ν_3 band occurs. The data were obtained in the spectral interval 2173 to 2334 cm^{-1} and the experimental conditions have already been described before (*1*). In all, 12 bands have been observed in the region, 10 belonging to $^{13}C^{16}O_2$ and the remaining two are the ν_3 fundamentals of $^{13}C^{16}O^{17}O$ and $^{13}C^{16}O^{18}O$. A few specific details are given below for some of the data pertaining to the current investigation.

$\Sigma^+{}_{u(g)} \leftarrow \Sigma^+{}_{g(u)}$ *Bands of* $^{13}C^{16}O_2$

Three bands belonging to this category were observed and the observational data are presented in Table I. For these three Σ–Σ bands, the lower states of the transitions observed are the levels 10^00, 02^00, and 00^01. Since the rotational constants for these lower levels are known with high accuracy from the laser studies (*2*), it was considered more appropriate to make use of these values and then determine the upper state constants of the three Σ–Σ bands studied here. Table V gives the rotational constants so obtained along with the band centers ($\nu_0 - B'l'^2 + B''l''^2$).

0022-2852/78/0721-0135$02.00/0

TABLE I

Measured Line Positions (cm^{-1}-vac.) of $^1\Sigma^+_{u(g)} \leftarrow {}^1\Sigma^+_{g(u)}$ Bands of $^{13}C^{18}O_2$

	$10^0 1 - 10^0 0$		$02^0 1 - 02^0 0$		$00^0 2 - 00^0 1$		
J	P OBS	R OBS	P OBS	R OBS	P OBS	R OBS	J
0				2262.6882			0
1							1
2		2265.1504	2260.3443	2264.2208			2
3							3
4	2259.6930	2266.6552	2258.7448	2265.7330			4
5						2264.5830	5
6	2258.0827	2268.1388	2257.1324	2267.2214			6
7					2254.5210	2266.0499	7
8	2256.4458	2269.5931	2255.4958	2268.6834			8
9					2252.6826	2267.4850	9
10	2254.7857	2271.0245	2253.8325	2270.1329			10
11					2251.2154	2268.8955	11
12	2253.1023	2272.4382	2252.1482	2271.5525			12
13							13
14	2251.3904		2250.4424	2272.9466			14
15					2247.8226		15
16		2275.1802	2248.7130	2274.3175			16
17						2272.9895	17
18	2247.9041	2276.5167	2246.9584	2275.6707			18
19							19
20	2246.1257	2277.8282	2245.1822	2276.9938			20
21					2242.5589		21
22	2244.3243	2279.1168	2243.3856	2278.2936			22
23					2240.7573	2276.8691	23
24	2242.4974	2280.3788	2241.5642	2279.5751			24
25					2238.9319	2278.1153	25
26	2240.6449	2281.6196	2239.7209				26
27					2237.0818	2279.3335	27
28	2238.7695	2282.8335	2237.8578				28
29					2235.2059	2280.5324	29
30		2284.0256	2235.9696	2283.2710			30
31					2233.3126	2281.7041	31
32		2285.1955		2284.4578			32
33							33
34	2233.0044	2286.3360		2285.6199			34
35					2229.4501	2283.9801	35
36	2231.0376			2286.7587			36
37						2285.0793	37
38	2229.0474	2288.5493		2287.8742			38
39							39
40	2227.0277	2289.6188	2226.1895	2288.9634			40
41					2223.4827	2287.2051	41
42	2224.9929		2224.1623	2290.0343			42
43					2221.4506		43
44	2222.9303		2222.1175	2291.0779			44
45							45
46	2220.8413	2292.6798	2220.0484	2292.0995			46
47					2217.3136		47
48	2218.7323						48
49						2291.1751	49
50	2216.6049	2294.5994	2215.8490	2294.0721			50
51							51
52	2214.4485	2295.5236	2213.7133	2295.0220			52
53					2210.9303		53
54	2212.2648	2296.4249	2211.5552				54
55							55
56	2210.0636	2297.2958	2209.3756	2296.8490			56
57					2206.5606		57
58	2207.8385		2207.1719	2297.7255			58
59					2204.3376		59
60	2205.5902	2298.9724	2204.9464	2298.5757			60
61							61
62	2203.3198		2202.7012	2299.4049			62
63					2199.8360		63
64	2201.0233		2200.4375				64
65							65
66	2198.7071						66
67							67
68	2196.3642	2302.0218	2195.8352				68
69							69
70	2193.9991			2302.4887			70
71							71
72	2191.6079		2191.1432	2303.2035			72
73							73
74	2189.2023	2304.0539	2188.7725				74
75							75
76	2186.7630		2186.3729				76
77							77
78			2183.9498				78

TABLE II

Measured Line Positions (cm^{-1}-vac.) of II_a — II_a Bands of $^{13}C^{18}O_2$

	$01^11 - 01^10$				
	e-e		f-f		
J	P OBS	R OBS	P OBS	R OBS	J
1		2273.3056			1
2	2269.3995	2274.6283	2270.1900	2274.0727	2
3	2267.7961	2276.3264	2268.5915	2275.5850	3
4	2266.1685	2277.7995	2266.9755		4
5	2264.5159	2279.2501	2265.3371	2278.5364	5
6	2262.8455	2280.6754	2263.6685	2279.9755	6
7	2261.1503		2261.9819	2281.3931	7
8		2283.4580	2260.2705	2282.7858	8
9	2257.6832	2284.8136	2258.5342	2284.1544	9
10	2255.9161	2286.1478	2256.7772	2285.5000	10
11	2254.1288	2287.4555	2254.9939	2286.8227	11
12	2252.3153	2288.7442	2253.1903	2288.1212	12
13	2250.4806	2290.0067	2251.3585	2289.3928	13
14	2248.6219	2291.2413	2249.5051	2290.6457	14
15	2246.7402	2292.4562	2247.6315	2291.8712	15
16	2244.8315	2293.6489	2245.7317		16
17	2242.9030	2294.8121	2243.8121	2294.2489	17
18	2240.9525	2295.9525	2241.8655	2295.4048	18
19	2238.9768	2297.0744	2239.8976	2296.5354	19
20	2236.9813	2298.1682	2237.9074	2297.6401	20
21	2234.9639	2299.2380	2235.8934	2298.7231	21
22	2232.9196	2300.2845	2233.8562		22
23	2230.8527	2301.3073	2231.7938	2300.8127	23
24	2228.7649		2229.7117	2301.8230	24
25	2226.6535	2303.2831	2227.6053	2302.8092	25
26	2224.5175	2304.2343	2225.4744	2303.7699	26
27	2222.3657	2305.1601	2223.3224		27
28	2220.1844	2306.0635	2221.1504	2305.6208	28
29		2306.9399	2218.9525	2306.5061	29
30	2215.7574	2307.7993	2216.7325	2307.3728	30
31	2213.5111	2308.6237	2214.4864		31
32	2211.2398	2309.4334	2212.2211		32
33	2208.9439	2310.2152		2309.8177	33
34	2206.6229	2310.9698	2207.6176	2310.5921	34
35	2204.2904	2311.7032	2205.2678		35
36	2201.9337		2202.9265	2312.0429	36
37	2199.5508	2313.1003	2200.5463	2312.7346	37
38		2313.7579	2198.1434		38
39	2194.7175		2195.7187	2314.0478	39
40	2192.2710	2315.0105	2193.2728	2314.6700	40
41	2189.8011	2315.5992	2190.8021		41
42			2188.3136	2315.8365	42
43			2185.8106		43
44	2184.7884		2183.2628		44
45			2180.7034		45
46	2179.6999				46

(continued)

TABLE II—*Continued*

	$11^11 - 11^10$				$03^11 - 03^10$				
	e-e		f-f		e-e		f-f		
J	P OBS	R OBS	P OBS	R OBS	P OBS	R OBS	P OBS	R OBS	J
			2249.0355	2252.9145		2252.2535		2253.0083	
			2247.4446				2247.5224		
	2246.6479		2245.8268					2256.0172	
		2256.6367		2257.3790			2244.2548		
			2242.5172	2258.8181	2243.4680		2242.5941	2258.9425	
	2241.6991	2259.5128	2240.8352	2260.2342	2241.8013	2259.6660		2260.3636	
	2240.0065	2260.9141	2239.1167	2261.6152	2240.1128	2261.0969	2239.1982	2261.7599	
	2238.2927	2262.2923			2238.4105	2262.4884	2237.4594		
	2236.5499	2263.6449			2236.6918		2235.7009	2264.4927	
	2234.7883		2235.6227	2264.3263		2265.2542	2233.9207	2265.8266	
		2266.2854		2265.6484	2233.2090			2267.1314	
				2266.9453	2231.4590	2268.0202		2268.4191	
	2229.3585	2268.8360	2230.2077	2268.2157			2228.4502		
		2271.0747			2227.9979	2270.8281	2226.5807	2270.9147	
	2225.6240		2226.6794	2270.6870		2272.2478	2224.6855	2272.1264	
	2223.7206		2224.6728	2271.8842			2222.7718		
	2221.7971	2273.6383	2222.6734	2273.0520	2222.8907				
	2219.6486	2274.7956	2220.7079	2274.1038	2221.7026				
	2217.8816	2275.8998		2275.3341			2218.8767	2275.6248	
	2215.8856			2276.4353			2216.8886	2276.7488	
		2278.0639		2277.5123					
			2212.6868				2212.8546		
	2209.7725		2210.6192				2210.8069		
	2207.6634	2281.1358	2208.5340	2280.5966			2208.7364	2280.9934	
			2206.4222	2281.5755					
				2282.5357				2282.9696	
	2203.4459	2283.0666	2202.1331				2202.3842	2283.9301	
	2201.2994			2284.3794			2200.2268		
	2198.1209		2197.7570				2198.0387		
	2196.9235		2195.5266						
							2193.6062		
	2192.4017		2191.0062						
			2188.7180				2189.0911		
	2187.9184						2184.8020		
	2185.4016								

$\Pi_u \leftarrow \Pi_u$ *Bands*

Table II gives the observational data for the three II–II bands measured in the present investigation. Two of the bands, namely the ones from the 11^10 and 03^10 have been identified for the first time, whereas in the case of the third band, 01^11–01^10, the rotational structure has been observed to J numbers about 30 higher than what was recorded in the emission work of Steiner, *et al.* (*3*). The band constants have been evaluated by using standard least squares programs and are included in Table V.

$\Delta_u \leftarrow \Delta_g$, $\Phi_u \leftarrow \Phi_u$ *and* $\Gamma_u \leftarrow \Gamma_u$ *Bands*

Again, in the case of the $\pi_u + 2\pi_g^2$ $2\pi_g^2$ band we have observed the rotational structure to very high J values. In fact, it has been possible to observe the rotational structure in

TABLE III

Measured Line Positions (cm^{-1}-vac.) of Some Other Bands of $^{13}C^{18}O_2$

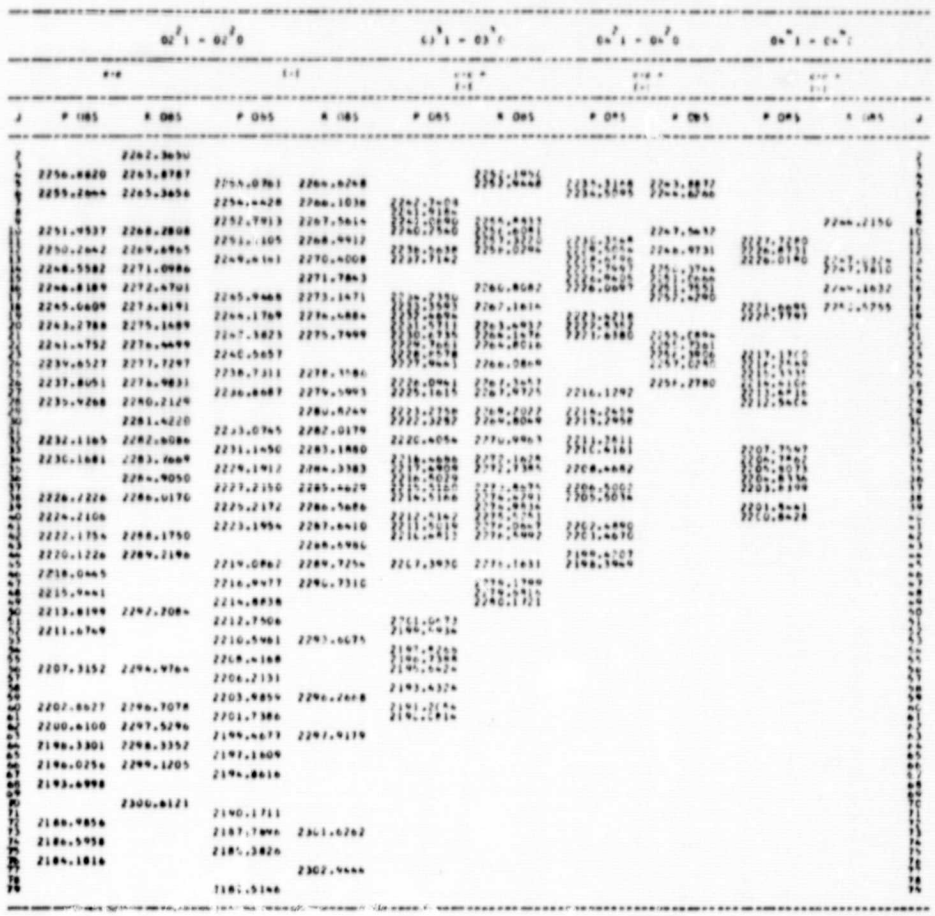

both the P and R branches to $P(79)$ and $R(77)$ as compared to $P(39)$ and $R(39)$ of the emission data (*3*). The data for this band as well as for the Φ–Φ and Γ–Γ bands identified in this region are included in Table III. The Q branches belonging to the $\nu_3 + 2\nu_2^2$–$2\nu_2^2$ and $\nu_3 + 3\nu_2^3$–$3\nu_2^3$ transitions could be distinguished without any ambiguity. However, in the case of the $\nu_3 + 4\nu_2^2$–$4\nu_2^2$ and $\nu_3 + 4\nu_2^4$–$4\nu_2^4$ bands, it was somewhat difficult to locate the band centers; therefore, the assignments had to be based upon calculated values for the band centers employing the molecular constants available in the literature (*4*, *5*). Thus, the J assignments for these bands should be regarded as tentative.

The oxygen-17 and oxygen-18 varieties of the carbon-13 carbon dioxide were detected in the sample used in this work. The ν_3 fundamental vibration rotation bands of these two isotopic species were identified and the observational data for them are given in

TABLE IV

Measured Line Positions (cm^{-1}-vac.) of the ν_3 Bands of $^{13}C^{16}O^{17}O$ and $^{13}C^{16}O^{18}O$

	$^{13}C^{16}O^{17}O$		$^{13}C^{16}O^{18}O$		
	$00^0 1 - 00^0 0$		$00^0 1 - 00^0 0$		
J	P OBS	R OBS	P OBS	R OBS	J
1				2267.4254	1
2	2272.5668				2
3			2263.7434	2268.8655	3
4			2262.9911	2269.5718	4
5			2262.2349		5
6	2269.4590		2261.4709		6
7	2268.6649	2279.9374	2260.7008	2271.6585	7
8	2267.8651	2280.6479	2259.9253	2272.3680	8
9	2267.0654		2259.1461	2273.0293	9
10	2266.2556		2258.3605		10
11	2265.4424	2282.7260	2257.5619	2274.3741	11
12		2283.4076		2275.0402	12
13	2263.7940	2284.0854	2255.9624	2275.6940	13
14	2262.9641	2284.7582	2255.1559		14
15	2262.1287	2285.4196	2254.3405		15
16		2286.0775	2253.5249	2277.6359	16
17	2260.4350	2286.7300	2252.6959	2278.2705	17
18	2259.5798	2287.3781	2251.8642	2278.9022	18
19	2258.7156	2288.0229	2251.0252	2279.5239	19
20	2257.8528	2288.6583	2250.1867	2280.1408	20
21	2256.9822	2289.2876	2249.3405	2280.7529	21
22	2256.1023	2289.9161	2248.4883	2281.3607	22
23	2255.2240	2290.5331		2281.9608	23
24		2291.1485	2246.7631	2282.5589	24
25	2253.4415	2291.7533	2245.8967	2283.1501	25
26	2252.5374	2292.3575	2245.0212	2283.7354	26
27		2292.9537	2244.1407	2284.3136	27
28	2250.7191	2293.5451	2243.2544		28
29	2249.8040	2294.1299			29
30	2248.8858	2294.7039			30
31	2247.9545	2295.2750			31
32	2247.0212				32
33		2296.4038		2287.6687	33
34	2245.1386	2296.9568	2237.8213	2288.2084	34
35		2297.5054	2236.8962		35
36					36
37	2242.2679		2235.0336	2289.7966	37
38	2241.3023		2234.0914	2290.3069	38
39	2240.3272		2233.1451	2290.8208	39
40			2232.1935	2291.3263	40
41	2238.3646		2231.2365	2291.8308	41
42			2230.2785	2292.3254	42
43			2229.3061	2292.8117	43
44	2235.3755			2293.2965	44
45	2234.3685		2227.3557	2293.7725	45
46			2226.3736		46
47	2232.3369		2225.3797		47
48	2231.3117		2224.3851	2295.1693	48
49			2223.3844	2295.6210	49
50	2229.2475				50
51			2221.3682		51
52			2220.3517	2296.9496	52
53			2219.3267	2297.3807	53
54			2218.3031	2297.8037	54
55			2217.2718		55
56			2216.2327	2298.6411	56
57					57
58			2214.1360		58
59			2213.0770		59
60			2212.0205		60
61					61
62			2209.8829		62

Table IV and the molecular constants of the levels involved are included in Table VI. These constants compare well with the ones calculated by Chedin (*6*).

The molecular constants obtained in this work for the levels 10^01 and 11^10 of $^{12}C^{16}O_2$ are consistent with the earlier results for the $(\nu_1 + \nu_2)$ and $(\nu_1 + \nu_3)$ bands (*7*, *8*).

C3

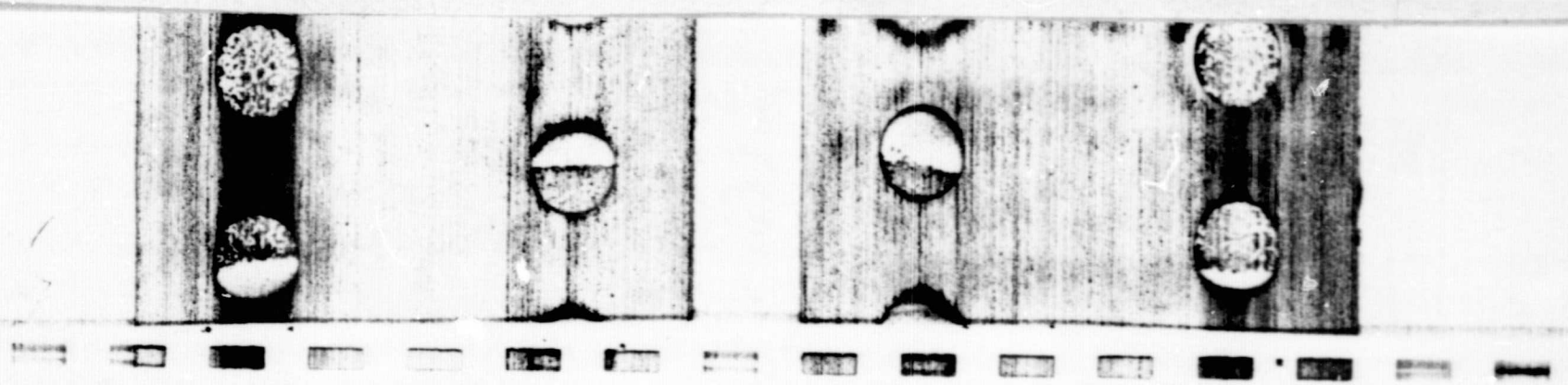

TABLE V

Molecular Constants[a] (cm^{-1}) of $^{13}C^{18}O_2$ Bands

BAND		SYMMETRY	ν_0	B'	B''	$D' \times 10^8$	$D'' \times 10^8$	$J_{max.}$ P,R
$10^01 - 10^00$		$\Sigma_u^+ - \Sigma_g^+$	2 262.8[illegible]0 ± 4	0.386 727 5 ± 23	0.389 721 4[e] ± 18	12.14 ± 2	12.149[e] ± 11	76, 74
$02^01 - 02^00$		$\Sigma_u^+ - \Sigma_g^+$	2 261.910 3 ± 5	0.388 041 3 ± 24	0.390 920 3[e] ± 19	15.95 ± 3	15.992[e] ± 12	78, 72
$00^02 - 00^01$		$\Sigma_g^+ - \Sigma_u^+$	2 260.064 3 ± 7	0.384 314 1 ± 30	0.387 277 7[e] ± 17	13.39 ± 5	13.465[e] ± 7	63, 49
$01^11 - 01^10$	e-e	$\Pi_g - \Pi_u$	2 271.759 9 ± 3	0.387 670 ± 5	0.390 601 ± 5	13.43 ± 5	13.48 ± 5	89, 81
	f-f			0.388 285 ± 5	0.391 236 ± 5	13.60 ± 5	13.64 ± 5	88, 82
$11^11 - 11^10$	e-e	$\Pi_g - \Pi_u$	2 250.606 2 ± 9	0.387 178 ± 16	0.390 097 ± 16	13.05 ± 42	13.15 ± 42	67, 51
	f-f			0.387 985 ± 17	0.390 960 ± 17	12.44 ± 40	12.52 ± 40	64, 54
$03^11 - 03^10$	e-e	$\Pi_g - \Pi_u$	2 250.693 4[c] ± 8					35, 29
	f-f			0.389 164 ± 18	0.392 041 ± 18	15.75 ± 43	15.84 ± 43	66, 52
$02^21 - 02^20$	e-e	$\Delta_u - \Delta_g$	2 260.049 1 ± 4	0.388 696 ± 8	0.391 611 ± 8	12.62 ± 12	12.77 ± 12	76, 70
	f-f					13.84 ± 8	13.90 ± 8	79, 77
$04^21 - 04^20$	e-e + f-f	$\Delta_u - \Delta_g$	2 239.300 0 ± 12	0.389 25 ± 4	0.392 13 ± 4	[d]	[d]	45, 26
$03^31 - 03^30$	e-e + f-f	$\Phi_g - \Phi_u$	2 248.357 1 ± 4	0.389 390 ± 12	0.392 275 ± 12	12.81 ± 33	12.96 ± 33	60, 49
$04^41 - 04^40$	e-e + f-f	$\Gamma_u - \Gamma_g$	2 236.674 2 ± 12	0.389 99 ± 4	0.392 82 ± 4	[d]	[d]	40, 18

The following ℓ-type doubling constants q and μ are given as defined by Baldacci, Malathy Devi, Chen, Rao & Fridovich, J. Mol. Spectros. (in press)

$q_{01}{}^1{}_0 = (0.635 \pm \text{[illegible]}) \times 10^{-3}$; $q_{11}{}^1{}_0 = (0.863 \pm 23) \times 10^{-3}$; $q_{01}{}^1{}_1 = (0.615 \pm 7) \times 10^{-3}$; $q_{11}{}^1{}_1 = (0.807 \pm 23) \times 10^{-3}$

$\mu_{01}{}^1{}_0 = (0.16 \pm 7) \times 10^{-8}$; $\mu_{11}{}^1{}_0 = (-0.63 \pm 58) \times 10^{-8}$; $\mu_{01}{}^1{}_1 = (0.17 \pm 7) \times 10^{-8}$; $\mu_{11}{}^1{}_1 = (-0.61 \pm 58) \times 10^{-8}$

$\mu_{02}{}^2{}_0 = (1.13 \pm 14) \times 10^{-8}$; $\mu_{02}{}^2{}_1 = (1.22 \pm 14) \times 10^{-8}$

[a] uncertainties quoted are standard deviations in units of the last digit.

a) see ref. (2).

b) constants for the e-e sub-band obtained by the least squares fitting are $(B'-B'') = (-3.030 \pm 34) \times 10^{-3}$; $(D'-D'') = (-102 \pm 3) \times 10^{-8}$

c) value obtained from the f-f sub-band.

d) not determinable.

Note: The complete reference by Baldacci *et al.* cited in the footnote to this table is *J. Mol. Spectrosc.* **70**, 143–159 (1978).

TABLE VI

Molecular Constants* (cm^{-1}) of the ν_2 Band of $^{13}C^{16}O^{17}O$ and $^{13}C^{16}O^{18}O$

MOLECULAR SPECIES	$\nu_0 - B'L'^2 + B''L''^2$	B'	B''	D' x 10^8	D'' x 10^8	J_{max} P,R
$^{13}C^{16}O^{17}O$	2274.0859 ± 4	0.375773 ± 11	0.378641 ± 11	10.8 ± 5	10.8 ± 5	50,35
$^{13}C^{16}O^{18}O$	2265.9717 ± 4	0.365403 ± 9	0.368193 ± 9	11.71 ± 20	11.78 ± 20	62,56

*Uncertainties quoted are standard deviations in units of the last digit.

ACKNOWLEDGMENTS

The support extended to the Ohio State University research programs by the National Environmental Satellite Service, National Oceanic and Atmospheric Administration (NESS-NOAA), the Atmospheric Research Section of the National Science Foundation, and the National Aeronautics and Space Administration is gratefully acknowledged.

RECEIVED: March 1, 1978

REFERENCES

1. V. MALATHY DEVI, A. BALDACCI, J. GRANGAARD, L. LINDEN, K. NARAHARI RAO, AND B. FRIDOVICH, *J. Mol. Spectrosc.* **70**, 160–162 (1978).
2. C. FREED, A. H. M. ROSS, AND R. G. O'DONNELL, *J. Mol. Spectrosc.* **49**, 439–453 (1974).
3. D. A. STEINER, T. R. TODD, C. M. CLAYTON, T. K. MCCUBBIN, JR., AND S. R. POLO, *J. Mol. Spectrosc.* **64**, 438–451 (1977).
4. C. P. COURTOY, *Ann. Soc. Sci. Bruxelles, Ser. I: Math. Astron. Phys.* **73**, 5 (1959).
5. K. NARAHARI RAO, "Exploration of the planetary system" (A. Woszczyk and C. Iwaniszewska, Ed.), D. Reidel Publishing Co. pp. 41–56 (1974), Dordrecht-Holland/Boston—U.S.A.
6. A. CHEDIN (private communication).
7. A. G. MAKI, E. K. PLYLER, AND R. J. THIBAULT, *J. Res. NBS* **67A**, 219–223 (1963).
8. H. R. GORDON AND T. K. MCCUBBIN, JR., *J. Mol. Spectrosc.* **19**, 137–154 (1966).

JOURNAL OF MOLECULAR SPECTROSCOPY 81, 179–206 (1980)

Spectrum of Phosphine at 4 to 5 μm: Analysis of ν_1 and ν_3 Bands

A. BALDACCI[1], V. MALATHY DEVI AND K. NARAHARI RAO

Department of Physics, The Ohio State University, Columbus, Ohio 43210

G. TARRAGO

Laboratoire d'Infrarouge, Laboratoire associé au CNRS, Université de Paris-Sud, Bâtiment 350, 91405 Orsay Cedex, France

The absorption spectrum of phosphine has been investigated in the region 2087–2482 cm^{-1}. About 1200 transitions belonging to the bands ν_1 and ν_3 were assigned. A strong Coriolis interaction between these bands gives rise to many "forbidden" transitions and large A_1A_2 splittings. The simultaneous analysis of the two bands enabled us to get a set of vibration–rotation constants for the vibrational states $v_1 = 1$ and $v_3 = 1$, and to obtain a value for the ratio S_1/S_3 between the band strengths of ν_1 and ν_3.

INTRODUCTION

Studies on the four fundamental bands of phosphine were reported in the past, under low resolution, by McConaghie and Nielsen (*1*), using a vacuum grating spectrometer. Subsequently, Hoffman *et al.* (*2*) and later Yin and Rao (*3*) measured and analyzed the two low-frequency fundamental vibration–rotation bands occurring at 8–12 μm with higher resolution. In attempting to obtain some information on the inversion barrier of PH_3, Maki *et al.* (*4*) studied the 3.4-μm region, where the $3\nu_2$ and $4\nu_2 - \nu_2$ bands were resolved. Molecular constants of the ground state are now well determined from the analysis of the "forbidden" rotational transitions (*5*, *6*) as well as from the above-mentioned infrared studies.

The present high-resolution study has been undertaken with a view to identifying the transitions involved in Jupiter's spectrum at 4–5 μm (*7*). The most prominent feature of the absorption by phosphine in this spectral range can be ascribed to the two strong overlapping fundamental bands ν_1 and ν_3 centered at 2321.131 and 2326.877 cm^{-1}, respectively. But weaker bands, $2\nu_2$, $\nu_2 + \nu_4$, and $2\nu_4$ also contribute to the absorption on the lower-frequency side.

This investigation relates to the two strongest bands ν_1 and ν_3. Their unusual and rather complicated rotational structures are well explained up to $J' = 10–11$ by a strong Coriolis-type interaction between them. Unfortunately, for higher J' values, Fermi-type interactions with the overtone $2\nu_4$ give rise to rapidly increasing dis-

[1] Present address: Istituto di Chimica Organica, Universita di Venezia, 2137 Calle Larga S. Marta, 30123 Venezia, Italy.

0022-2852/80/050179-28$02.00/0

crepancies between observed and calculated wavenumbers, so that the assignments became difficult beyond $J' = 13$. Nevertheless, more than 1200 transitions belonging to ν_1 and ν_3 could be assigned in the spectral interval 2184–2446 cm^{-1}.

EXPERIMENTAL METHOD

The entire spectrum was recorded at the Ohio State University by using a 10-m double-pass focal length Czerny–Turner-type vacuum infrared spectrograph equipped with a 31 groove/mm, 40 × 20 cm^2 (16 × 8 $in.^2$) echelle grating. The continuous source of radiation was provided by a carbon furnace heated to 2500 K. Argon gas was passed through the source tank in order to avoid the accumulation of CO during the scans. An InSb detector cooled to liquid nitrogen temperature was used and the data were obtained with a spectral resolution ranging between 0.025 and 0.035 cm^{-1}.

Interferometric fringes, which are recorded simultaneously with the observation of infrared spectra and absorption standards, were used in determining the spectral positions of the lines. A dispersion curve, for estimating the wavenumbers of the PH_3 lines, was then obtained from a least-squares fit of the internal calibration standards. 1–0 and 2–0 transitions of $^{12}C^{16}O$ were used as reference lines; wavenumbers (vac.-cm^{-1}) for the rotational structure of these two bands were taken from Rao (*8*).

In scanning the total spectral region, measurements were made with absorption path lengths of 10 and 100 cm at pressures ranging between 0.2 and 6.0 Torr. Under these conditions, data were recorded in the interval 2087–2482 cm^{-1} and about 3100 absorption lines were observed and measured.

The average of the stronger lines was taken over four or more measurements. The estimated accuracy is limited to ±0.005 cm^{-1}; however, for well-resolved lines the values are about ±0.003 cm^{-1}.

The spectrum showed lines due to atmospheric absorption of carbon dioxide, in the Q-branch region and among the lower first and R-branch lines of the ν_1 and ν_3 bands of PH_3. This overlapping CO_2 structure was easily identified (*9*).

ASSIGNMENTS—COMPUTATIONAL PROCEDURE

The two bands ν_1 and ν_3 are very close to each other. The strong Coriolis-type interaction between them is responsible for many "forbidden" (perturbation allowed) transitions as well as large A_1A_2 splittings. The first assignments were performed on the basis of the ground-state combination relations among transitions. The accurate values already available for the ground-state constants (*4*, *6*) were used to calculate the differences.

As a second step, we used an iterative computation as indicated in Ref. (*10*). This improved the assignments and allowed us to find the vibration–rotation constants related to the upper states $v_1 = 1$ and $v_3 = 1$. The energies in these states were obtained as eigenvalues of an effective twice-transformed Hamiltonian ${}^{(c)}_{(v_s,v_t)}H^+$, diagonal in v_s except for the two Coriolis terms T_1 and T_2, given by Eqs. (3) and (4) in Ref. (*11*). Besides these vibrational interactions (v_1, v_3, . . . $|v_1$

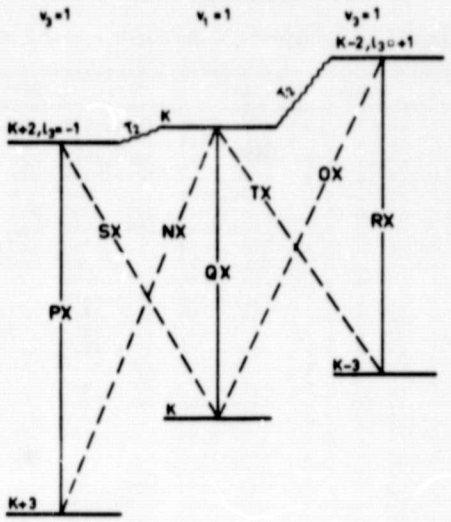

FIG. 1. "Forbidden" transitions induced by T_2 in ν_1 and ν_3. In the indicated notation, the first symbol refers to $K' - K''$, the second one, $X = P, Q, R$, to $J' - J''$.

$\pm 1, v_3 \mp 1, \ldots$) all essential resonances within $v_1 = 1$ and $v_3 = 1$ were also taken into account (*10*, *12*).

It may be noted that the first-order term T_1, which has only matrix elements in $\Delta(K - l_3) = 0$ cannot induce "forbidden" transitions, whereas, the second-order term T_2, with elements in $\Delta(K - l_3) = \pm 3$, breaks down the usual approximate selection rule $\Delta(K - l_3) = 0$, as sketched in Fig. 1. In the present analysis of ν_1 and ν_3, the great number of "forbidden" transitions observed in the spectrum is related to a large contribution of the term T_2.

LINE STRENGTHS

The line strengths were approximated from the leading operator responsible for the observed transitions, i.e.,

$$(M_\Gamma)_{1,3} = d_3[\cos(\Gamma,x)q_{3a} + \cos(\Gamma,y)q_{3b} + \rho_{1,3}\cos(\Gamma,z)q_1],$$

where q_1, q_{3a}, and q_{3b} are dimensionless normal coordinates related to ν_1 and ν_3

$$d_3 = \left(\frac{\partial M_x}{\partial q_{3a}}\right) = \left(\frac{\partial M_y}{\partial q_{3b}}\right); \qquad \rho_{1,3} = \left(\frac{d_1}{d_3}\right) \qquad \text{with} \qquad d_1 = \left(\frac{\partial M_z}{\partial q_1}\right).$$

M_Γ ($\Gamma = X, Y, Z$) and M_α ($\alpha = x, y, z$) are the usual dipole moment components on space- and molecule-fixed frames.

Therefore, the ratio $\rho_{1,3}$, as well as the eigenvectors arising from the diagonalization of the matrix ${}^{(c)}_{(v_1,v_3)}H^+$, are involved in the relative intensity calculations; absolute line strengths would also depend on the coefficient d_3 and experimental conditions (*13*).

The rigorous selection rules for the transitions are (*12*):

$$\Delta J = 0, \pm 1; \qquad A_1 \leftrightarrow A_2 \qquad \text{or} \qquad E \leftrightarrow E.$$

TABLE I

Wavenumbers and Intensities in the Bands ν_1 and ν_3 of PH_3

(I)	(II)	(III)				(IV)	(V)	(VI)	(VII)	(VIII)
1	RP(14,12,A)	13	13	1	A	2184.0785	3038.9929	-38	2.17-03	*1.0
2	RP(14,11,E)	13	12	1	E	2184.8219	3051.9604	-10	4.22-03	1.0
3	RP(14,10,E)	13	11	1	E	2185.5191	3063.7081	35	1.01-02	1.0
4	RP(14, 9,A)	13	10	1	A	2186.1347	3074.2357	47	3.83-02	*1.0
5	*RP(14, 1,E)	13	2	0	E	2186.3028	3115.1635	8	3.02-02	1.0
6	*SP(14, 4,E)	13	6	-1	E	2187.0589	3108.3930	317	1.19-01	.0
7	RP(14, 7,E)	13	8	1	E	2187.2029	3091.7888	-66	4.58-02	1.0
8	QP(14, 3,A)	13	3	0	A	2187.5198	3112.3730	145	3.87-01	* .0
9	QP(14, 2,E)	13	2	0	E	2187.8257	3115.1854	30	2.46-01	1.0
10	QP(14, 0,A1)	13	0	0	A2	2187.9485	3117.3090	38	1.95-01	1.0
11	QP(14, 1,E)	13	1	0	E	2188.0250	3116.8857	3	2.83-01	1.0
12	QP(14, 5,E)	13	5	0	E	2188.5799	3105.3721	73	6.28-02	1.0
13	*QP(14, 0,A1)	13	4	1	A2	2189.1974	3118.5579	13	1.45-01	1.0
14	QP(14, 4,E)	13	4	0	E	2189.4704	3110.8045	136	4.69-02	.0
15	*QP(14, 2,E)	13	1	0	E	2189.5152	3116.8748	-7	6.81-02	1.0
16	QP(14,13,E)	13	13	0	E	2190.5773	3032.0604	18	2.01-01	1.0
17	QP(14,12,A)	13	12	0	A	2190.6406	3045.5550	12	7.31-01	*1.0
18	QP(14,11,E)	13	11	0	E	2190.7520	3057.8905	-10	5.01-01	1.0
19	QP(14,10,E)	13	10	0	E	2190.9201	3069.1091	-26	6.11-01	1.0
20	QP(14, 9,A)	13	9	0	A	2191.1436	3079.2395	-26	1.40+00	*1.0
21	QP(14, 8,E)	13	8	0	E	2191.4279	3088.3146	0	7.70-01	1.0
22	QP(14, 7,E)	13	7	0	E	2191.7667	3096.3525	40	8.23-01	1.0
23	RP(14, 6,A)	13	7	1	A	2192.1366	3103.3514	66	1.72+00	*1.0
24	*NP(14, 3,A1)	13	0	0	A2	2192.4647	3117.3179	47	4.71-01	1.0
25	RP(14, 5,E)	13	6	1	E	2192.5476	3109.3398	74	8.85-01	1.0
26	*SP(13, 8,E)	12	10	-1	E	2192.8043	2966.1350	959	3.57-03	.0
27	RP(14, 4,E)	13	5	1	E	2193.0179	3114.3520	82	9.15-01	1.0
28	RP(14, 3,A2)	13	4	1	A1	2193.5781	3118.4313	21	8.88-01	1.0
29	RP(14, 3,A1)	13	4	1	A2	2193.7247	3118.5579	33	4.84-01	1.0
30	RP(14, 2,E)	13	3	1	E	2194.1772	3121.5368	21	8.10-01	1.0
31	RP(14, 1,E)	13	2	1	E	2194.8744	3123.7350	-30	7.62-01	1.0
32	*NP(14, 4,E)	13	1	0	E	2195.5490	3116.8831	0	7.06-02	1.0
33	RP(13, 9,A)	12	10	1	A	2195.9651	2960.4284	-17	3.[illegible]8-02	*1.0
34	*SP(14, 0,A1)	13	2	-1	A2	2196.4834	3125.8439	21	[illegible]	1.0
35	RP(13, 8,E)	12	9	1	E	2196.5351	2969.8659	-70	[illegible]	1.0
36	*SP(13, 4,E)	12	5	-1	E	2196.8369	2994.8244	[illegible]	[illegible]	.0
37	RP(13, 7,E)	12	8	1	E	2197.1873	2978.2836	[illegible]	6.[illegible]-02	1.0
38	PP(14, 1,E)	13	0	1	E	2197.3020	3126.1627	[illegible]	7.66-01	1.0
39	QP(13, 3,A)	12	3	0	A	2197.5054	2999.0416	[illegible]	6.75-01	*1.0
40	QP(13, 6,A)	12	6	0	A	2197.7538	2985.5359	-10	2.11-01	*1.0
41	QP(13, 2,E)	12	2	0	E	2197.9172	3001.9810	7	4.69-01	1.0
42	QP(13, 0,A2)	12	0	0	A1	2198.0067	3004.0881	39	2.46-01	1.0
43	QP(13, 1,E)	12	1	0	E	2198.1290	3003.7063	-4	5.47-01	1.0
44	QP(13, 5,E)	12	5	0	E	2198.3484	2991.7555	-4	1.42-01	1.0
45	*NP(14, 5,E)	13	2	0	E	2198.3846	3115.1768	21	2.22-01	1.0
46	PP(14, 2,E)	13	1	-1	E	2198.5850	3125.9446	34	7.02-01	1.0
47	PP(14, 3,A2)	13	2	-1	A1	2198.5850	3123.4382	-19	8.60-01	1.0
48	*QP(14, 2,E)	13	0	1	E	2198.7812	3126.1408	-2	1.32-04	1.0
49	QP(13, 4,E)	12	4	0	E	2199.0665	2997.0540	9	1.38-01	1.0
50	*QP(14, 3,A1)	13	1	1	A2	2199.5158	3124.3690	-64	6.43-01	1.0
51	*PP(13, 2,E)	12	1	0	E	2199.6475	3003.7112	0	1.00-01	1.0
52	*SP(13, 3,A)	12	5	-1	A	2200.0440	3001.5802	33	1.64-01	*1.0
53	QP(13,12,A)	12	12	0	A	2200.2948	2931.2813	16	6.84-01	*1.0
54	QP(13,11,E)	12	11	0	E	2200.3176	2943.6381	-6	6.26-01	1.0
55	QP(13,10,E)	12	10	0	E	2200.4164	2954.8855	-15	8.61-01	1.0
56	QP(13, 9,A)	12	9	0	A	2200.5511	2965.0144	-42	2.11+00	*1.0
57	PP(14, 4,E)	13	3	-1	E	2200.6984	3122.0325	22	7.71-01	1.0
58	QP(13, 8,E)	12	8	0	E	2200.7944	2974.1251	-11	1.21+00	1.0

(I) SERIAL NUMBER

(II) TRANSITION

(III) VALUES OF J', $|K'|$, ℓ_3', C', FOR UPPER LEVEL OF THE TRANSITION

(IV) OBSERVED WAVENUMBER IN CM^{-1}

(V) UPPER LEVEL ENERGY IN CM^{-1}

(VI) (OBS-CALC) WAVENUMBER IN 10^{-3} CM^{-1}

(VII) CALCULATED RELATIVE LINE STRENGTH

(VIII) STATISTICAL WEIGHT

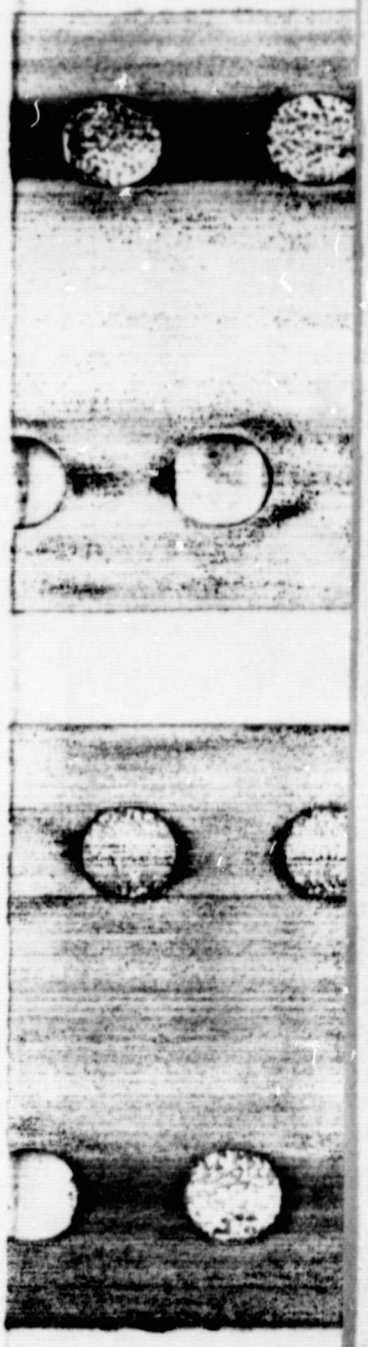

TABLE I—*Continued*

(I)	(II)	(III)				(IV)	(V)	(VI)	(VII)	(VIII)
59	*QP(14, 3,A2)	13	1	1	A1	2200.9580	3125.8112	36	8.01-02	1.0
60	PP(14, 3,A1)	13	2	-1	A2	2201.0078	3125.8610	38	2.17-01	1.0
61	QP(13, 7,E)	12	7	0	E	2201.0578	2982.1541	-15	1.32+00	1.0
62	*NP(14, 6,A)	13	3	0	A	2201.1636	3112.3784	150	9.38-01	* .0
63	*SP(13, 2,E)	12	4	-1	E	2201.2761	3005.3398	1	2.16-02	1.0
64	RP(13, 6,A)	12	7	1	A	2201.3885	2989.1706	-17	2.80+00	*1.0
65	RP(13, 5,E)	12	6	1	E	2201.7959	2995.2030	-22	1.44+00	1.0
66	RP(13, 4,E)	12	5	1	E	2202.3249	3000.3123	3	1.48+00	1.0
67	PP(14, 5,E)	13	4	-1	E	2202.3249	3119.1171	78	9.34-01	1.0
68	*QP(14, 4,E)	13	2	1	E	2202.3992	3123.7333	-31	5.07-03	1.0
69	*NP(13, 3,A2)	12	0	0	A1	2202.5585	3004.0947	46	1.18+00	1.0
70	*SP(13, 1,E)	12	3	-1	E	2202.7009	3008.2782	-28	6.28-03	1.0
71	RP(13, 3,A1)	12	4	1	A2	2202.9450	3004.4812	-12	1.46+00	1.0
72	RP(13, 3,A2)	12	4	1	A1	2203.1633	3004.6995	-9	4.20-01	1.0
73	RP(13, 2,E)	12	3	1	E	2203.6552	3007.7190	2	1.41+00	1.0
74	PP(14, 7,E)	13	6	-1	E	2203.8177	3108.4035	328	8.93-01	.0
75	PP(14, 6,A)	13	5	-1	A	2204.1887	3115.4035	164	1.69+00	* .0
76	RP(13, 1,E)	12	2	1	E	2204.4286	3010.0059	-13	1.39+00	1.0
77	RP(13, 0,A2)	12	1	1	A1	2204.6294	3010.7108	-29	6.91-01	1.0
78	*QP(14, 5,E)	13	3	1	E	2204.7373	3121.5295	14	8.31-04	1.0
79	*SP(13, 0,A2)	12	2	-1	A1	2205.7294	3011.8108	5	1.95+00	1.0
80	*QP(13, 2,E)	12	2	1	E	2205.9432	3010.0070	-12	1.50-01	1.0
81	PP(14, 8,E)	13	7	-1	E	2206.2400	3103.1267	503	1.38+00	.0
82	RP(12, 8,E)	11	9	1	E	2206.4450	2864.8685	-15	2.89-02	1.0
83	*SP(12, 4,E)	11	6	-1	E	2206.5692	2889.8480	38	2.18-01	1.0
84	PP(13, 1,E)	12	0	1	E	2206.7413	3012.3186	7	1.16+00	1.0
85	RP(12, 7,E)	11	8	1	E	2207.0699	2873.3221	-13	7.60-02	1.0
86	*QP(14, 6,A2)	13	4	1	A1	2207.2331	3118.4479	37	5.93-03	1.0
87	*QP(14, 6,A1)	13	4	1	A2	2207.3527	3118.5675	23	4.61-03	1.0
88	*SP(12, 3,A)	11	5	-1	A	2207.4581	2894.3138	15	1.08+00	*1.0
89	RP(12, 6,A)	11	7	1	A	2207.6513	2880.6432	-3	3.26-01	*1.0
90	QP(12, 2,E)	11	2	0	E	2207.9546	2897.3578	7	8.49-01	1.0
91	PP(13, 2,E)	12	1	-1	E	2207.9807	3012.0445	0	1.22+00	1.0
92	QP(12, 1,E)	11	1	0	E	2208.1741	2899.1029	7	1.01+00	1.0
93	QP(12, 5,E)	11	5	0	E	2208.1741	2886.8361	-18	2.80-01	1.0
94	QP(12, 0,A1)	11	0	0	A2	2208.2640	2899.7008	-59	1.08+00	1.0
95	PP(13, 3,A1)	12	2	-1	A2	2208.3490	3009.8852	-22	1.51+00	1.0
96	*NP(13, 5,E)	12	2	0	E	2208.5823	3001.9894	15	4.38-01	1.0
97	PP(14, 9,A)	13	8	-1	A	2208.6560	3096.7520	795	3.65+00	* .0
98	QP(12, 4,E)	11	4	0	E	2208.7621	2892.0409	-14	3.44-01	1.0
99	*QP(13, 3,A2)	12	1	1	A1	2209.1721	3010.7083	-32	1.08+00	1.0
100	QP(12, 3,A)	11	3	0	A	2209.5940	2896.4497	-6	4.84-01	*1.0
101	*PP(12, 2,E)	11	1	0	E	2209.6945	2899.0977	1	1.34-01	1.0
102	QP(12,11,E)	11	11	0	E	2209.9289	2838.0938	-10	5.59-01	1.0
103	QP(12,10,E)	11	10	0	E	2210.0045	2849.4111	34	1.03+00	1.0
104	QP(12, 9,A)	11	9	0	A	2210.0815	2859.5649	20	2.84+00	*1.0
105	QP(12, 8,E)	11	8	0	E	2210.2191	2868.6425	4	1.74+00	1.0
106	PP(13, 3,A2)	12	2	-1	A1	2210.2668	3011.0030	-2	3.63-01	1.0
107	PP(13, 4,E)	12	3	-1	E	2210.3092	3008.2967	-10	1.50+00	1.0
108	QP(12, 7,E)	11	7	0	E	2210.4254	2876.6776	-11	1.09+00	1.0
109	*QP(13, 3,A1)	12	1	1	A2	2210.4791	3012.0153	46	8.83-02	1.0
110	QP(12, 6,A)	11	6	0	A	2210.7246	2883.7165	-21	4.29+00	*1.0
111	*SP(12, 2,E)	11	4	-1	E	2210.7901	2900.1934	-32	8.04-02	1.0
112	RP(12, 5,E)	11	6	1	E	2211.1376	2889.7996	-22	2.22+00	1.0
113	PP(14,10,E)	13	9	-1	E	2211.1376	3089.3266	1173	2.22+00	.0
114	*NP(13, 6,A)	12	3	0	A	2211.2631	2999.0452	57	1.96+00	*1.0
115	RP(12, 4,E)	11	5	1	E	2211.6753	2894.9541	-17	2.24+00	1.0
116	PP(13, 5,E)	12	4	-1	E	2211.9387	3005.3458	7	1.60+00	1.0

TABLE I—*Continued*

(I)	(II)	(III)				(IV)	(V)	(VI)	(VII)	(VIII)
117	RP(12, 3,A1)	11	4	1	A2	2212.2858	2899.1415	26	2.47+00	1.0
118	RP(12, 3,A2)	11	4	1	A1	2212.3377	2899.1935	-21	2.22+00	1.0
119	RP(12, 2,E)	11	3	1	E	2213.1208	2902.5240	0	2.21+00	1.0
120	PP(14,11,E)	13	10	-1	E	2213.5413	3080.6798	1432	2.63+00	.0
121	PP(13, 7,E)	12	6	-1	E	2213.7465	2994.8428	165	1.88+00	.0
122	PP(13, 6,A)	12	5	-1	A	2213.7985	3001.5806	33	2.71+00	*1.0
123	RP(12, 1,E)	11	2	1	E	2213.9644	2904.8932	0	2.30+00	1.0
124	*SP(12, 0,A1)	11	2	-1	A2	2214.2186	2905.6554	-12	7.89-01	1.0
125	*QP(13, 5,E)	12	3	1	E	2214.3049	3007.7120	-4	2.94-03	1.0
126	*TP(11, 0,A2)	10	3	0	A1	2214.5322	2799.9953	-8	5.90-02	1.0
127	RP(12, 0,A1)	11	1	1	A2	2215.0276	2906.4644	-9	3.39+00	1.0
128	*NP(12, 4,E)	11	1	0	E	2215.8135	2899.0923	-3	2.99-01	1.0
129	*NP(13, 7,E)	12	4	0	E	2215.9712	2997.0675	23	8.07-01	1.0
130	PP(13, 8,E)	12	7	-1	E	2216.0574	2989.3881	359	2.74+00	.0
131	PP(12, 1,E)	11	0	1	E	2216.2291	2907.1579	14	1.76+00	1.0
132	*SP(11, 4,E)	10	6	-1	E	2216.2455	2793.4902	-17	2.29-01	1.0
133	RP(11, 8,E)	10	9	1	E	2216.2455	2768.4480	13	1.56-02	1.0
134	PP(14,12,A)	13	11	-1	A	2216.2891	3071.2035	1968	6.18+00	* .0
135	*RP(11, 1,E)	10	2	0	E	2216.3553	2801.3066	-9	6.13-02	1.0
136	PP(11, 7,E)	10	8	1	E	2216.9076	2776.9981	4	6.96-02	1.0
137	*SP(11, 3,A)	10	5	-1	A	2217.3269	2798.1751	-12	1.55+00	*1.0
138	PP(12, 2,E)	11	1	-1	E	2217.4393	2906.8426	0	2.03+00	1.0
139	RP(11, 6,A)	10	7	1	A	2217.4897	2784.3707	-7	4.33-01	*1.0
140	*QP(12, 2,E)	11	0	1	E	2217.7438	2907.1471	3	2.20-02	1.0
141	QP(11, 2,E)	10	2	0	E	2217.8985	2801.3130	-3	1.45+00	1.0
142	QP(11, 5,E)	10	5	0	E	2218.0128	2790.6063	5	4.86-01	1.0
143	PP(12, 3,A2)	11	2	-1	A1	2218.0745	2904.9302	-19	2.53+00	1.0
144	QP(11, 1,E)	10	1	0	E	2218.1116	2803.0629	-1	1.78+00	1.0
145	QP(11, 0,A2)	10	0	0	A1	2218.1853	2803.6486	-8	1.93+00	1.0
146	PP(13, 9,A)	12	8	-1	A	2218.1853	2982.6486	463	6.91+00	* .0
147	*NP(13, 8,E)	12	5	0	E	2218.4278	2991.7585	-1	3.40-01	1.0
148	QP(11, 4,E)	10	4	0	E	2218.4836	2795.7283	-3	7.47-01	1.0
149	PP(14,13,E)	13	12	-1	E	2218.5922	3060.0759	1980	3.62+00	.0
150	*NP(12, 5,E)	11	2	0	E	2218.6872	2897.3492	-1	7.93-01	1.0
151	PP(12, 3,A1)	11	2	-1	A2	2218.8003	2905.6560	-11	1.86+00	1.0
152	QP(11, 3,A)	10	3	0	A	2219.1502	2799.9984	-5	1.24+00	*1.0
153	QP(11,10,E)	10	10	0	E	2219.5386	2752.5784	-3	8.77-01	1.0
154	QP(11, 9,A)	10	9	0	A	2219.5795	2762.7736	15	3.24+00	*1.0
155	*QP(12, 3,A1)	11	1	1	A2	2219.6164	2906.4721	-1	4.92-01	1.0
156	QP(11, 8,E)	10	8	0	E	2219.6653	2771.8678	14	2.24+00	1.0
157	QP(11, 7,E)	10	7	0	E	2219.8200	2779.9106	3	2.74+00	1.0
158	PP(12, 4,E)	11	3	-1	E	2219.9182	2903.1970	-20	2.61+00	1.0
159	*QP(12, 3,A2)	11	1	1	A1	2219.9600	2906.8157	16	9.02-02	1.0
160	QP(11, 6,A)	10	6	0	A	2220.0784	2786.9594	-8	6.13+00	*1.0
161	*SP(11, 2,E)	10	4	-1	E	2220.2960	2803.7105	-22	2.17-01	1.0
162	RP(11, 5,E)	10	6	1	E	2220.4784	2793.0719	-16	3.19+00	1.0
163	PP(13,10,E)	12	9	-1	E	2220.4784	2974.9475	718	4.14+00	.0
164	PP(14,14,E)	13	13	-1	E	2220.8888	3047.6989	1903	4.25+00	.0
165	RP(11, 4,E)	10	5	1	E	2221.0392	2798.2839	-15	3.17+00	1.0
166	*NP(13, 9,A)	12	6	0	A	2221.0808	2985.5441	-2	2.89-01	*1.0
167	PP(12, 6,A)	11	5	-1	A	2221.3187	2894.3106	12	3.93+00	*1.0
168	PP(12, 5,E)	11	4	-1	E	2221.5445	2900.2065	-18	2.66+00	1.0
169	*QP(12, 4,E)	11	2	1	E	2221.6057	2904.8845	8	2.58-04	1.0
170	RP(11, 3,A)	10	4	1	A	2221.7465	2802.5947	13	6.68+00	*1.0
171	*QP(13, 8,E)	12	6	1	E	2221.8787	2995.2094	-18	1.80-02	1.0
172	RP(11, 2,E)	10	3	1	E	2222.5738	2805.9883	0	3.17+00	1.0
173	*NP(11, 3,A2)	10	0	0	A1	2222.7842	2803.6324	-24	1.74-01	1.0
174	PP(13,11,E)	12	10	-1	E	2222.8106	2966.1311	955	4.87+00	.0

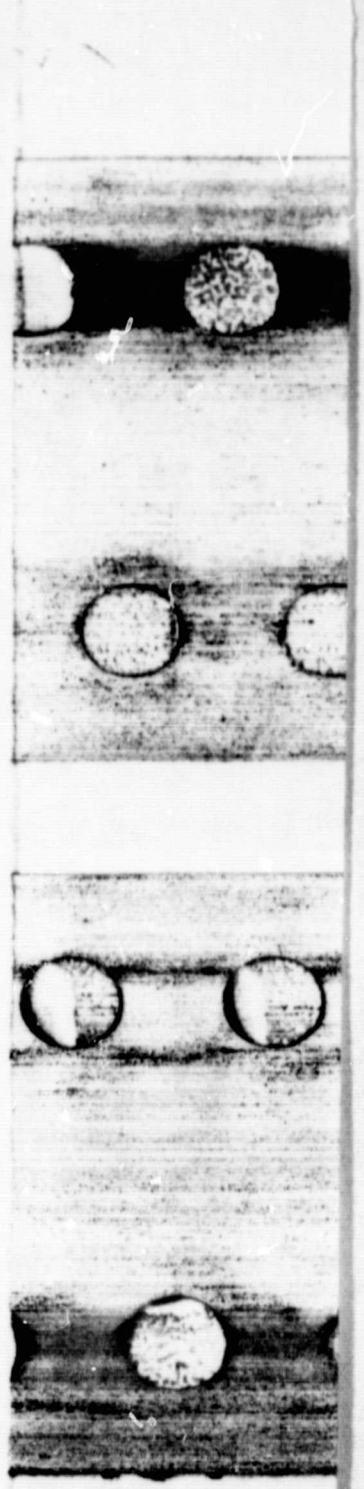

TABLE I—*Continued*

(I)	(II)	(III)				(IV)	(V)	(VI)	(VII)	(VIII)
175	RP(11, 1,E)	10	2	1	E	2223.4705	2808.4218	2	3.47+00	1.0
176	*NP(12, 8,A)	11	3	0	A	2223.4705	2896.4624	5	4.06+00	*1.0
177	PP(12, 7,E)	11	6	-1	E	2223.6040	2889.8562	46	3.69+00	1.0
178	*SP(11, 0,A2)	10	2	-1	A1	2223.7558	2809.2189	-1	5.49-01	1.0
179	*QP(12, 5,E)	11	3	1	E	2223.8607	2902.5227	0	5.10-03	1.0
180	RP(11, 0,A2)	10	1	1	A1	2224.4132	2809.8763	5	5.71+00	1.0
181	PP(13,12,A)	12	11	-1	A	2225.2408	2956.2273	1213	1.14+01	* .0
182	PP(12, 8,E)	11	7	-1	E	2225.6700	2884.0935	116	5.05+00	.0
183	PP(11, 1,E)	10	0	1	E	2225.7135	2810.6648	9	2.68+00	1.0
184	*NP(12, 7,E)	11	4	0	E	2225.7860	2892.0382	-16	9.38-01	1.0
185	*NP(11, 4,E)	10	1	0	E	2225.8165	2803.0612	-2	4.66-01	1.0
186	*SP(10, 4,E)	9	6	-1	E	2225.8558	2705.7755	-36	1.99-01	1.0
187	RP(10, 8,E)	9	9	1	E	2225.9374	2680.6405	24	3.62-03	1.0
188	*QP(12, 6,A)	11	4	1	A	2226.1417	2899.1336	18	2.20-02	*1.0
189	RP(10, 7,E)	9	8	1	E	2226.6620	2689.3085	17	4.33-02	1.0
190	PP(11, 2,E)	10	1	-1	E	2226.9199	2810.3344	4	3.26+00	1.0
191	*SP(10, 3,A)	9	5	-1	A	2227.1071	2710.6550	-28	1.91+00	*1.0
192	*QP(11, 2,E)	10	0	1	E	2227.2590	2810.6735	18	3.28-02	1.0
193	RP(10, 6,A)	9	7	1	A	2227.2784	2696.7628	-2	4.73-01	*1.0
194	PP(13,13,E)	12	12	-1	E	2227.3821	2944.8157	1100	6.72+00	.0
195	PP(12, 9,A)	11	8	-1	A	2227.7217	2877.2051	221	1.24+01	* .0
196	PP(11, 3,A1)	10	2	-1	A2	2227.7605	2808.6087	-7	4.06+00	1.0
197	QP(10, 2,E)	9	2	0	E	2227.7605	2713.8923	-10	2.34+00	1.0
198	QP(10, 5,E)	9	5	0	E	2227.7895	2703.0259	5	7.56-01	1.0
199	QP(10, 1,E)	9	1	0	E	2227.9657	2715.6448	1	2.92+00	1.0
200	QP(10, 0,A1)	9	0	0	A2	2228.0195	2716.2134	0	3.14+00	1.0
201	QP(10, 4,E)	9	4	0	E	2228.1613	2708.1010	3	1.41+00	1.0
202	PP(11, 3,A2)	10	2	-1	A1	2228.3722	2809.2204	0	3.29+00	1.0
203	QP(10, 3,A)	9	3	0	A	2228.6765	2712.2244	0	2.78+00	*1.0
204	*NP(11, 5,E)	10	2	0	E	2228.7166	2801.3102	-6	1.34+00	1.0
205	*QP(11, 3,A2)	10	1	1	A1	2229.0298	2809.8780	6	4.56-01	1.0
206	QP(10, 9,A)	9	9	0	A	2229.0729	2674.7039	-14	2.64+00	*1.0
207	QP(10, 8,E)	9	8	0	E	2229.1140	2683.8171	6	2.45+00	1.0
208	QP(10, 7,E)	9	7	0	E	2229.2209	2691.8674	13	3.38+00	1.0
209	QP(10, 6,A)	9	6	0	A	2229.4307	2698.9151	6	8.08+00	*1.0
210	PP(11, 4,E)	10	3	-1	E	2229.4953	2806.7400	-20	4.29+00	1.0
211	*SP(10, 2,E)	9	4	-1	E	2229.7443	2715.8761	-17	4.54-01	1.0
212	RP(10, 5,E)	9	6	1	E	2229.8113	2705.0478	-4	4.25+00	1.0
213	PP(12,10,E)	11	9	-1	E	2229.8619	2869.2685	374	7.34+00	.0
214	RP(10, 4,E)	9	5	1	E	2230.3960	2710.3157	-7	4.14+00	1.0
215	PP(11, 5,E)	10	4	-1	E	2231.1180	2803.7115	-21	4.28+00	1.0
216	RP(10, 3,A)	9	4	1	A	2231.1430	2714.6909	-1	8.38+00	*1.0
217	*QP(11, 4,E)	10	2	1	E	2231.1826	2808.4273	7	1.11-05	1.0
218	PP(11, 6,A)	10	5	-1	A	2231.2999	2798.1809	-6	7.56+00	*1.0
219	RP(10, 2,E)	9	3	1	E	2232.0163	2718.1481	2	4.20+00	1.0
220	PP(12,11,E)	11	10	-1	E	2232.0852	2860.2501	539	8.66+00	.0
221	*NP(10, 3,A1)	9	0	0	A2	2232.6660	2716.2139	0	3.74-01	1.0
222	RP(10, 1,E)	9	2	1	E	2232.9595	2720.6386	7	4.78+00	1.0
223	*NP(11, 6,A)	10	3	0	A	2233.1182	2799.9992	-4	5.57+00	*1.0
224	*SP(10, 0,A1)	9	2	-1	A2	2233.2269	2721.4213	10	1.48-01	1.0
225	PP(11, 7,E)	10	6	-1	E	2233.4030	2793.4936	-14	6.75+00	1.0
226	RP(10, 0,A1)	9	1	1	A2	2233.8554	2722.0498	17	8.68+00	1.0
227	PP(12,12,A)	11	11	-1	A	2234.2242	2849.9511	539	2.04+01	* .0
228	PP(10, 1,E)	9	0	1	E	2235.1932	2722.8723	7	3.97+00	1.0
229	PP(11, 8,E)	10	7	-1	E	2235.3260	2787.5285	14	8.74+00	1.0
230	*SP(9, 4,E)	8	6	-1	E	2235.3848	2626.7207	-41	1.39-01	1.0
231	*NP(11, 7,E)	10	4	0	E	2235.6423	2795.7328	1	9.38-01	1.0
232	*QP(11, 6,A)	10	4	1	A	2235.7177	2802.5987	17	3.28-02	*1.0

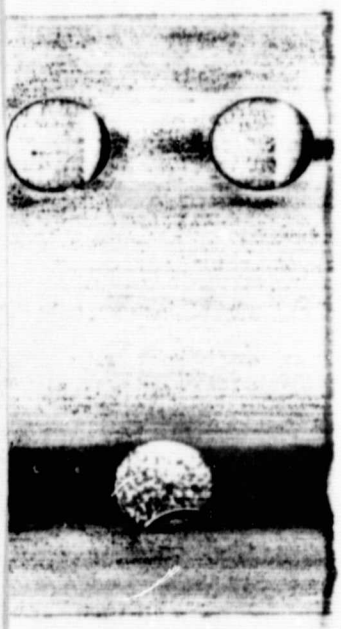

TABLE I—*Continued*

(I)	(II)	(III)	(IV)	(V)	(VI)	(VII)	(VIII)
233	*NP(10, 4,E)	9 1 0 E	2235.7177	2715.6374	-5	6.35-01	1.0
234	*RP(9, 1,E)	8 2 0 E	2235.9976	2635.1417	1	6.29-02	1.0
235	PP(10, 2,E)	9 1 -1 E	2236.3913	2722.5231	0	4.99+00	1.0
236	*OP(10, 2,E)	9 0 1 E	2236.7550	2721.8868	22	3.81-02	1.0
237	*SP(9, 3,A)	8 5 -1 A	2236.7896	2631.7766	-32	1.92+00	*1.0
238	RP(9, 6,A)	8 7 1 A	2236.9821	2617.8165	-13	3.99-01	*1.0
239	PP(11, 9,A)	10 8 -1 A	2237.2616	2780.4557	58	2.11+01	*1.0
240	PP(10, 3,A2)	9 2 -1 A1	2237.3752	2720.9231	-14	6.21+00	1.0
241	QP(9, 5,E)	8 5 0 E	2237.5078	2624.1308	-5	1.05+00	1.0
242	QP(9, 2,E)	8 2 0 E	2237.5450	2635.1321	-8	3.58+00	1.0
243	QP(9, 1,E)	8 1 0 E	2237.7170	2636.8611	-1	4.59+00	1.0
244	QP(9, 0,A2)	8 0 0 A1	2237.7542	2637.4168	0	4.81+00	1.0
245	QP(9, 4,E)	8 4 0 E	2237.8326	2629.1685	-2	2.38+00	1.0
246	PP(10, 3,A1)	9 2 -1 A2	2237.8732	2721.4211	10	5.52+00	1.0
247	QP(9, 3,A)	8 3 0 A	2238.1757	2633.1627	6	5.45+00	*1.0
248	*OP(11, 7,E)	10 5 1 E	2238.2039	2798.2944	-4	2.92-02	1.0
249	*OP(10, 3,A1)	9 1 1 A2	2238.5038	2722.0517	19	2.42-01	1.0
250	QP(9, 8,E)	8 8 0 E	2238.5557	2604.5140	-16	1.91+00	1.0
251	QP(9, 7,E)	8 7 0 E	2238.6103	2612.5631	6	3.54+00	1.0
252	*NP(10, 5,E)	9 2 0 E	2238.6625	2713.8990	-4	2.09+00	1.0
253	QP(9, 6,A)	8 6 0 A	2238.7661	2619.6005	13	9.57+00	*1.0
254	PP(10, 4,E)	9 3 -1 E	2239.0318	2718.9515	-12	6.75+00	1.0
255	RP(9, 5,E)	8 6 1 E	2239.1209	2625.7439	6	5.19+00	1.0
256	*SP(9, 2,E)	8 4 -1 E	2239.1493	2636.7364	-2	8.70-01	1.0
257	PP(11,10,E)	10 9 -1 E	2239.2771	2772.3167	123	1.25+01	.0
258	RP(9, 4,E)	8 5 1 E	2239.7312	2631.0671	-2	4.91+00	1.0
259	RP(9, 3,A)	8 4 1 A	2240.5275	2635.5146	-2	9.78+00	*1.0
260	PP(10, 5,E)	9 4 -1 E	2240.6435	2715.8799	-13	6.68+00	1.0
261	*OP(10, 4,E)	9 2 1 E	2240.7216	2720.6413	10	1.41-05	1.0
262	PP(10, 6,A)	9 5 -1 A	2241.1796	2710.6640	-19	1.40+01	*1.0
263	PP(11,11,E)	10 10 -1 E	2241.3695	2763.0800	187	1.48+01	.0
264	RP(9, 2,E)	8 3 1 E	2241.4359	2639.0230	0	5.12+00	1.0
265	RP(9, 1,E)	8 2 1 E	2242.4177	2641.5618	7	6.08+00	1.0
266	*SP(9, 0,A2)	8 2 -1 A1	2242.6247	2642.2873	8	2.74-04	1.0
267	*NP(10, 6,A)	9 3 0 A	2242.7459	2712.2303	5	6.75+00	*1.0
268	PP(10, 7,E)	9 6 -1 E	2243.1381	2705.7846	-26	1.15+01	1.0
269	RP(9, 0,A2)	8 1 1 A1	2243.3206	2642.9832	19	1.18+01	1.0
270	PP(9, 1,E)	8 0 1 E	2244.6571	2643.8012	10	5.66+00	1.0
271	*SP(8, 4,E)	7 6 -1 E	2244.8504	2556.3734	-27	7.09-02	1.0
272	PP(10, 8,E)	9 7 -1 E	2244.9642	2699.6673	-19	1.43+01	1.0
273	*OP(10, 6,A)	9 4 1 A	2245.2140	2714.6984	6	3.25-02	*1.0
274	*NP(10, 7,E)	9 4 0 E	2245.4616	2708.1082	10	8.02-01	1.0
275	*NP(9, 4,E)	8 1 0 E	2245.5323	2636.8682	5	7.55-01	1.0
276	PP(9, 2,E)	8 1 -1 E	2245.8622	2643.4493	9	7.27+00	1.0
277	*SP(8, 3,A)	7 5 -1 A	2246.3709	2561.5658	-24	1.48+00	*1.0
278	RP(8, 6,A)	7 7 1 A	2246.6387	2547.5997	5	2.05-01	*1.0
279	PP(10, 9,A)	9 8 -1 A	2246.8380	2692.4691	3	3.44+01	*1.0
280	PP(9, 3,A1)	8 2 -1 A2	2246.9493	2641.9363	-5	9.09+00	1.0
281	QP(8, 5,E)	7 5 0 E	2247.1803	2553.9633	-8	1.30+00	1.0
282	QP(8, 2,E)	7 2 0 E	2247.2434	2565.0533	-1	5.13+00	1.0
283	PP(9, 3,A2)	8 2 -1 A1	2247.2996	2642.2866	8	8.49+00	1.0
284	QP(8, 1,E)	7 1 0 E	2247.3790	2566.7547	7	6.60+00	1.0
285	QP(8, 0,A1)	7 0 0 A2	2247.3991	2567.2963	5	6.68+00	1.0
286	QP(8, 4,E)	7 4 0 E	2247.4466	2558.9696	0	3.61+00	1.0
287	QP(8, 3,A)	7 3 0 A	2247.6444	2562.8393	8	9.26+00	*1.0
288	*OP(10, 7,E)	9 5 1 E	2247.6746	2710.3211	-1	3.08-02	1.0
289	QP(8, 7,E)	7 7 0 E	2247.9855	2542.0251	-12	2.64+00	1.0
290	QP(8, 6,A)	7 6 0 A	2248.0725	2549.0335	5	9.67+00	*1.0

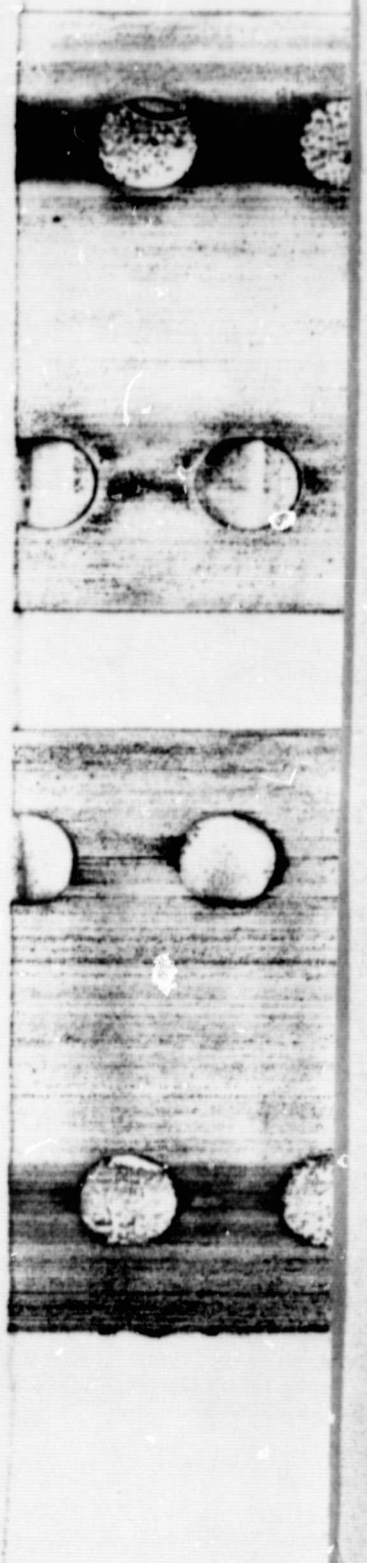

TABLE I—*Continued*

(I)	(II)	(III)	(IV)	(V)	(VI)	(VII)	(VIII)
291	RP(8, 5,E)	7 6 1 E	2248.3893	2555.1724	9	5.66+00	1.0
292	*SP(8, 2,E)	7 4 -1 E	2248.4926	2566.3025	0	1.21+00	1.0
293	*NP(9, 5,E)	8 2 0 E	2248.5148	2635.1378	-2	3.04+00	1.0
294	PP(9, 4,E)	8 3 -1 E	2248.5148	2639.8507	-8	1.02+01	1.0
295	PP(10,10,E)	9 9 -1 E	2248.7948	2684.1990	37	2.04+01	1.0
296	RP(8, 4,E)	7 5 1 E	2249.0397	2560.5627	0	5.10+00	1.0
297	*TP(7, 1,E)	6 4 0 E	2249.1083	2497.5092	1	8.13-03	1.0
298	RP(8, 3,A)	7 4 1 A	2249.8852	2565.0801	-3	1.03+01	*1.0
299	PP(9, 5,E)	8 4 -1 E	2250.1111	2636.7341	-4	1.01+01	1.0
300	*OP(9, 4,E)	8 2 1 E	2250.2293	2641.5652	11	1.22-04	1.0
301	RP(8, 2,E)	7 3 1 E	2250.8282	2568.6381	-2	5.76+00	1.0
302	PP(9, 6,A)	8 5 -1 A	2250.9539	2631.7883	-20	2.47+01	*1.0
303	RP(8, 1,E)	7 2 1 E	2251.8388	2571.2145	5	7.16+00	1.0
304	*SP(8, 0,A1)	7 2 -1 A2	2251.9957	2571.8929	21	4.76-02	1.0
305	*NP(8, 3,A1)	7 0 0 A2	2252.1040	2567.2989	8	5.19-01	1.0
306	*NP(9, 6,A)	8 3 0 A	2252.3355	2633.1699	13	6.83+00	*1.0
307	*OP(9, 5,E)	8 3 1 E	2252.4060	2639.0290	6	2.89-03	1.0
308	PP(9, 7,E)	8 6 -1 E	2252.7813	2626.7342	-28	1.83+01	1.0
309	RP(8, 0,A1)	7 1 1 A2	2252.7813	2572.6785	23	1.48+01	1.0
310	PP(8, 1,E)	7 0 1 E	2254.0866	2573.4623	10	7.71+00	1.0
311	PP(9, 8,E)	8 7 -1 E	2254.5532	2620.5115	-22	2.24+01	1.0
312	*OP(9, 6,A)	8 4 1 A	2254.6873	2635.5217	5	2.74-02	*1.0
313	*NP(9, 7,E)	8 4 0 E	2255.2118	2629.1646	-6	5.72-01	1.0
314	*NP(8, 4,E)	7 1 0 E	2255.2357	2566.7587	11	7.79-01	1.0
315	*RP(7, 1,E)	6 2 0 E	2255.2692	2503.6701	0	4.16-02	1.0
316	PP(8, 2,E)	7 1 -1 E	2255.2956	2573.1055	10	1.01+01	1.0
317	*SP(7, 3,A)	6 5 -1 A	2255.8457	2500.0445	-9	7.68-01	*1.0
318	PP(9, 9,A)	8 8 -1 A	2256.3915	2613.2190	-6	5.38+01	*1.0
319	PP(8, 3,A2)	7 2 -1 A1	2256.4619	2571.6568	2	1.27+01	1.0
320	PP(8, 3,A1)	7 2 -1 A2	2256.6889	2571.8838	12	1.22+01	1.0
321	RP(7, 5,E)	6 6 1 E	2256.8126	2492.5564	-4	1.33+00	1.0
322	QP(7, 2,E)	6 2 0 E	2256.8444	2503.6715	1	6.94+00	1.0
323	QP(7, 0,A2)	6 0 0 A1	2256.9375	2505.8625	4	9.14+00	1.0
324	QP(7, 1,E)	6 1 0 E	2256.9375	2505.3384	13	8.81+00	1.0
325	QP(7, 4,E)	6 4 0 E	2256.9969	2497.5049	-3	4.95+00	1.0
326	QP(7, 3,A)	6 3 0 A	2257.0816	2501.2804	7	1.35+01	*1.0
327	*OP(9, 7,E)	8 5 1 E	2257.1308	2631.0836	14	2.70-02	1.0
328	QP(7, 6,A)	6 6 0 A	2257.3498	2487.2415	-12	7.01+00	*1.0
329	*OP(8, 3,A1)	7 1 1 A2	2257.4809	2572.6758	20	1.20-02	1.0
330	QP(7, 5,E)	6 5 0 E	2257.6024	2493.3462	9	5.24+00	1.0
331	*SP(7, 2,E)	6 4 -1 E	2257.7905	2504.6176	6	1.42+00	1.0
332	PP(8, 4,E)	7 3 -1 E	2257.9584	2569.4814	3	1.48+01	1.0
333	*NP(8, 5,E)	7 2 0 E	2258.2775	2565.0605	5	4.05+00	1.0
334	RP(7, 4,E)	6 5 1 E	2258.3092	2498.8172	-1	4.35+00	1.0
335	RP(7, 3,A)	6 4 1 A	2259.2100	2503.4088	-6	9.47+00	*1.0
336	PP(8, 5,E)	7 4 -1 E	2259.5240	2566.3070	4	1.50+01	1.0
337	*OP(8, 4,E)	7 2 1 E	2259.6909	2571.2139	4	2.60-04	1.0
338	RP(7, 2,E)	6 3 1 E	2260.1836	2507.0197	-6	5.66+00	1.0
339	PP(8, 6,A)	7 5 -1 A	2260.6148	2561.5758	-14	4.07+01	*1.0
340	RP(7, 1,E)	6 2 1 E	2261.2129	2509.6138	-2	7.78+00	1.0
341	*NP(7, 3,A2)	6 0 0 A1	2261.6709	2505.8697	11	4.49-01	1.0
342	*TP(6, 0,A1)	5 3 0 A2	2261.7312	2448.5014	7	2.50-02	1.0
343	*OP(8, 5,E)	7 3 1 E	2261.8525	2568.6356	-5	1.66-03	1.0
344	*NP(8, 6,A)	7 3 0 A	2261.8852	2562.8462	15	5.51+00	*1.0
345	RP(7, 0,A2)	6 1 1 A1	2262.1923	2511.1173	12	1.74+01	1.0
346	PP(8, 7,E)	7 6 -1 E	2262.3432	2556.3828	-17	2.76+01	1.0
347	*QP(7, 1,E)	6 1 -1 E	2263.1228	2511.5237	19	7.19-02	1.0
348	PP(7, 1,E)	6 0 1 E	2263.4687	2511.8696	4	9.96+00	1.0

TABLE I—*Continued*

(I)	(II)	(III)	(IV)	(V)	(VI)	(VII)	(VIII)
349	PP(8, 8,E)	7 7 -1 E	2264.0794	2550.0779	-12	3.36+01	1.0
350	*DP(8, 6,A)	7 4 1 A	2264.1229	2505.0839	0	1.76-02	*1.0
351	PP(7, 2,E)	6 1 -1 E	2264.6984	2511.5135	9	1.33+01	1.0
352	*NP(7, 4,E)	6 1 0 E	2264.8325	2505.3405	15	6.76-01	1.0
353	*SP(6, 3,A)	5 5 -1 A	2265.2192	2447.2420	6	2.19-01	*1.0
354	PP(7, 3,A1)	6 2 -1 A2	2265.9874	2510.1062	6	1.70+01	1.0
355	PP(7, 3,A2)	6 2 -1 A1	2266.0417	2510.2404	14	1.66+01	1.0
356	QP(6, 2,E)	5 2 0 E	2266.3461	2451.0090	2	8.78+00	1.0
357	QP(6, 0,A1)	5 0 0 A2	2266.3849	2453.1551	8	1.12+01	1.0
358	QP(6, 1,E)	5 1 0 E	2266.3849	2452.6287	8	1.08+01	1.0
359	QP(6, 3,A)	5 3 0 A	2266.4775	2448.5003	6	1.66+01	*1.0
360	QP(6, 4,E)	5 4 0 E	2266.4775	2444.7930	-10	5.91+00	1.0
361	*DP(8, 7,E)	7 5 1 E	2266.5283	2563.5674	5	1.83-02	1.0
362	QP(6, 5,E)	5 5 0 E	2266.6559	2440.1856	-9	4.45+00	1.0
363	*DP(7, 3,A2)	6 1 1 A1	2266.9226	2511.1214	16	4.49-04	1.0
364	*SP(6, 2,E)	5 4 -1 E	2267.0433	2451.7062	12	1.28+00	1.0
365	*DP(7, 3,A1)	6 1 1 A2	2267.1587	2511.3575	-7	2.12-02	1.0
366	PP(7, 4,E)	6 3 -1 E	2267.3482	2507.8562	8	2.07+01	1.0
367	RP(6, 4,E)	5 5 1 E	2267.5363	2445.8517	-4	2.47+00	1.0
368	*NP(7, 5,E)	6 2 0 E	2267.9327	2503.6765	6	4.77+00	1.0
369	RP(6, 3,A)	5 4 1 A	2268.4933	2450.5161	-10	7.06+00	*1.0
370	PP(7, 5,E)	6 4 -1 E	2268.8791	2504.6229	11	2.17+01	1.0
371	*DP(7, 4,E)	6 2 1 E	2269.1087	2509.6167	0	3.79-04	1.0
372	RP(6, 2,E)	5 3 1 E	2269.4945	2454.1574	-9	5.23+00	1.0
373	PP(7, 6,A)	6 5 -1 A	2270.1618	2500.0535	0	6.19+01	*1.0
374	RP(6, 1,E)	5 2 1 E	2270.5415	2456.7853	-4	7.73+00	1.0
375	*NP(6, 3,A1)	5 0 0 A2	2271.1356	2453.1584	11	3.21+01	1.0
376	*DP(7, 5,E)	6 3 1 E	2271.2678	2507.0116	-5	8.82-04	1.0
377	*NP(7, 6,A)	6 3 0 A	2271.3988	2501.2905	17	3.17+00	*1.0
378	RP(6, 0,A1)	5 1 1 A2	2271.5619	2458.3321	10	1.92+01	1.0
379	PP(7, 7,E)	6 6 -1 E	2271.8281	2494.7625	2	3.97+01	1.0
380	*QP(6, 1,E)	5 1 -1 E	2272.4437	2458.6875	5	4.35-02	1.0
381	PP(6, 1,E)	5 0 1 E	2272.8079	2459.0517	4	1.21+01	1.0
382	*DP(7, 6,A)	6 4 1 A	2273.5240	2503.4157	0	9.37-03	*1.0
383	PP(6, 2,E)	5 1 -1 E	2274.0285	2458.6914	8	1.66+01	1.0
384	*NP(6, 4,E)	5 1 0 E	2274.3218	2452.6373	17	4.80-01	1.0
385	*DP(6, 2,E)	5 0 1 E	2274.3912	2459.0541	7	1.63-02	1.0
386	PP(6, 3,A2)	5 2 -1 A1	2275.2824	2457.3052	7	2.18+01	1.0
387	PP(6, 3,A1)	5 2 -1 A2	2275.3537	2457.3765	13	2.15+01	1.0
388	QP(5, 0,A2)	4 0 0 A1	2275.7352	2409.1895	10	1.26+01	1.0
389	QP(5, 1,E)	4 1 0 E	2275.7352	2408.6611	3	1.21+01	1.0
390	QP(5, 2,E)	4 2 0 E	2275.7352	2407.0741	-4	1.02+01	1.0
391	QP(5, 3,A)	4 3 0 A	2275.8076	2404.4961	-4	1.70+01	*1.0
392	QP(5, 4,E)	4 4 0 E	2275.8946	2400.8614	-11	5.41+00	1.0
393	*SP(5, 2,E)	4 4 -1 E	2276.2528	2407.5917	16	6.48-01	1.0
394	*DP(6, 3,A1)	5 1 1 A2	2276.3096	2458.3324	11	2.81-04	1.0
395	*DP(6, 3,A2)	5 1 1 A1	2276.4781	2458.5009	-9	1.01-02	1.0
396	PP(6, 4,E)	5 3 -1 E	2276.6869	2455.0023	11	2.75+01	1.0
397	*NP(6, 5,E)	5 2 0 E	2277.4814	2451.0111	4	4.64+00	1.0
398	RP(5, 3,A)	4 4 1 A	2277.7275	2406.4160	-15	3.46+00	*1.0
399	PP(6, 5,E)	5 4 -1 E	2278.1790	2451.7086	14	3.07+01	1.0
400	*DP(6, 4,E)	5 2 1 E	2278.4651	2456.7805	-9	2.00-04	1.0
401	RP(5, 2,E)	4 3 1 E	2278.7455	2410.0844	-19	3.87+00	1.0
402	PP(6, 6,A)	5 5 -1 A	2279.5986	2447.2476	12	8.75+01	*1.0
403	RP(5, 1,E)	4 2 1 E	2279.8058	2412.7317	-13	6.86+00	1.0
404	*NP(5, 3,A2)	4 0 0 A1	2280.4951	2409.1836	4	1.81-01	1.0
405	*DP(6, 5,E)	5 3 1 E	2280.6261	2454.1558	-11	5.49-04	1.0
406	RP(5, 0,A2)	4 1 1 A1	2280.8577	2414.3120	-2	1.97+01	1.0

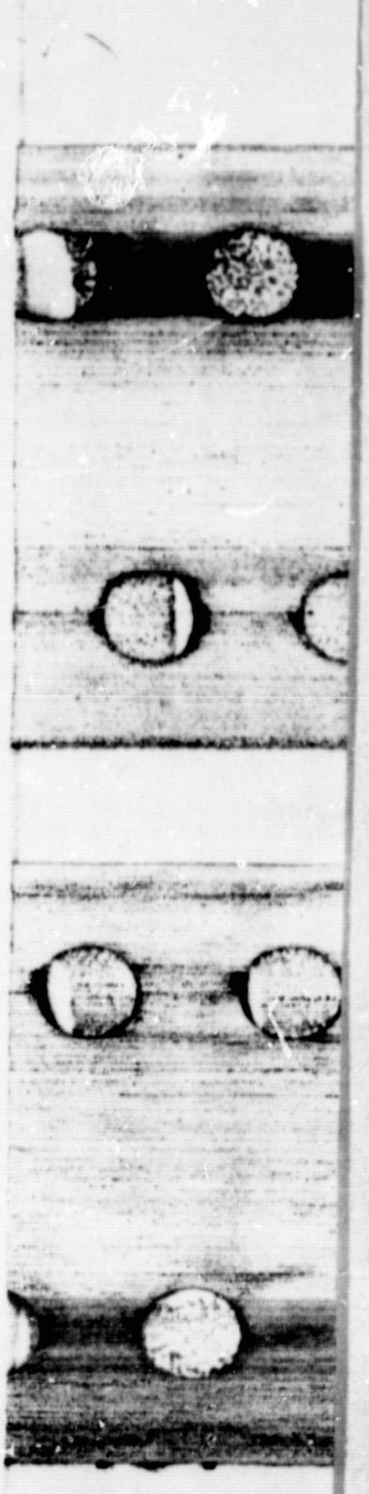

TABLE I—*Continued*

(I)	(II)	(III)				(IV)	(V)	(VI)	(VII)	(VIII)
407	*NP(6, 6,A)	5	3	0	A	2280.8577	2448.5087	14	1.08+00	*1.0
408	PP(5, 1,E)	4	0	1	E	2282.0837	2415.0096	0	1.38+01	1.0
409	*QP(6, 6,A)	5	4	1	A	2282.8682	2450.5192	-7	3.64-03	*1.0
410	PP(5, 2,E)	4	1	-1	E	2283.3129	2414.6518	8	1.97+01	1.0
411	*QP(5, 2,E)	4	0	1	E	2283.6832	2415.0221	12	1.42-02	1.0
412	PP(5, 3,A1)	4	2	-1	A2	2284.5927	2413.2812	13	2.68+01	1.0
413	PP(5, 3,A2)	4	2	-1	A1	2284.6167	2413.3052	9	2.66+01	1.0
414	QP(4, 0,A1)	3	0	0	A2	2284.9921	2373.9878	9	1.29+01	1.0
415	QP(4, 1,E)	3	1	0	E	2284.9921	2373.4577	0	1.22+01	1.0
416	QP(4, 2,E)	3	2	0	E	2285.0186	2371.8921	-6	1.00+01	1.0
417	QP(4, 3,A)	3	3	0	A	2285.0741	2369.2886	-8	1.25+01	*1.0
418	*QP(5, 3,A2)	4	1	1	A1	2285.6219	2414.3104	-4	4.52-04	1.0
419	*QP(5, 3,A1)	4	1	1	A2	2285.7343	2414.4229	-19	3.43-03	1.0
420	PP(5, 4,E)	4	3	-1	E	2285.9737	2410.9405	16	3.51+01	1.0
421	*NP(5, 5,E)	4	2	0	E	2286.9225	2407.0848	6	2.77+00	1.0
422	PP(5, 5,E)	4	4	-1	E	2287.4325	2407.5948	19	4.30+01	1.0
423	*QP(5, 4,E)	4	2	1	E	2287.7679	2412.7347	-10	1.09-05	1.0
424	RP(4, 2,E)	3	3	1	E	2287.9445	2374.8180	-20	1.90+00	1.0
425	RP(4, 1,E)	3	2	1	E	2289.0114	2377.4770	-17	5.10+00	1.0
426	*QP(5, 5,E)	4	3	1	E	2289.9293	2410.0916	-12	3.51-04	1.0
427	RP(4, 0,A1)	3	1	1	A2	2290.0946	2379.0903	-4	1.82+01	1.0
428	PP(4, 1,E)	3	0	1	E	2291.2983	2379.7639	-2	1.46+01	1.0
429	PP(4, 2,E)	3	1	-1	E	2292.5270	2379.4005	3	2.22+01	1.0
430	*QP(4, 2,E)	3	0	1	E	2292.8852	2379.7587	-7	4.02-03	1.0
431	PP(4, 3,A)	3	2	-1	A	2293.8236	2378.0381	4	6.31+01	*1.0
432	QP(3, 0,A2)	2	0	0	A1	2294.1527	2347.5627	0	1.17+01	1.0
433	QP(3, 1,E)	2	1	0	E	2294.1527	2347.0312	-10	1.05+01	1.0
434	QP(3, 2,E)	2	2	0	E	2294.1813	2345.4636	-14	6.86+00	1.0
435	*QP(4, 3,A1)	3	1	1	A2	2294.8746	2379.0891	-6	9.64-05	1.0
436	*QP(4, 3,A2)	3	1	1	A1	2294.9431	2379.1577	-14	8.46-04	1.0
437	PP(4, 4,E)	3	3	-1	E	2295.1969	2375.6776	18	4.33+01	1.0
439	RP(3, 1,E)	2	2	1	E	2298.1503	2351.0288	-18	2.60+00	1.0
440	RP(3, 0,A2)	2	1	1	A1	2299.2516	2352.6616	-10	1.44+01	1.0
441	PP(3, 1,E)	2	0	1	E	2300.4434	2353.3219	-3	1.41+01	1.0
442	PP(3, 2,E)	2	1	-1	E	2301.6764	2352.9586	3	2.37+01	1.0
443	*QP(3, 2,E)	2	0	1	E	2302.0531	2353.3354	10	5.32-04	1.0
444	PP(3, 3,A)	2	2	-1	A	2302.9763	2351.5927	9	7.26+01	*1.0
445	QP(2, 0,A1)	1	0	0	A2	2303.2303	2329.9400	-3	9.04+00	1.0
446	QP(2, 1,E)	1	1	0	E	2303.2303	2329.4075	-14	6.87+00	1.0
447	*TQ(9, 2,E)	9	5	0	E	2305.4363	2703.0234	2	4.33-02	1.0
448	*TQ(12, 0,A1)	12	3	0	A2	2307.6029	2949.0397	31	1.26-01	1.0
449	RQ(13,12,A)	13	13	1	A	2307.9975	3038.9840	-47	1.59-01	*1.0
450	*TQ(10, 1,E)	10	4	0	E	2308.0672	2795.7463	14	9.00-02	1.0
451	RP(2, 0,A1)	1	1	1	A2	2308.3256	2335.0353	-17	8.17+00	1.0
452	RQ(13,11,E)	13	12	1	E	2308.6283	3051.9488	-21	1.31-01	1.0
453	RQ(13,10,E)	13	11	1	E	2309.2396	3063.7087	36	1.63-01	1.0
454	PP(2, 1,E)	1	0	1	E	2309.5044	2335.6816	-11	1.22+01	1.0
455	*SQ(13, 5,E)	13	7	-1	E	2309.6907	3103.0978	474	2.49-03	.0
456	RQ(12,11,E)	12	12	1	E	2309.7568	2937.9217	11	1.55-01	1.0
457	RQ(13, 9,A)	13	10	1	A	2309.7748	3074.2381	50	3.63-01	*1.0
458	*VQ(12, 0,A1)	12	5	-1	A2	2310.1252	3001.5620	-6	1.40-01	1.0
459	RQ(13, 8,E)	13	9	1	E	2310.2280	3083.5587	-2	1.89-01	1.0
460	RQ(12,10,E)	12	11	1	E	2310.3629	2949.7695	-15	2.53-01	1.0
461	*SQ(13, 4,E)	13	6	-1	E	2310.4208	3108.4083	333	2.30-04	.0
462	RQ(13, 7,E)	13	8	1	E	2310.7054	3091.8018	-33	1.88-01	1.0
463	PP(2, 2,E)	1	1	-1	E	2310.7440	2335.3218	0	2.46+01	1.0
464	RQ(12, 9,A)	12	10	1	A	2310.9415	2960.4249	-21	6.09-01	*1.0
465	*TQ(11, 0,A2)	11	3	0	A1	2310.9937	2896.4568	-15	1.87-01	1.0

TABLE I—*Continued*

(I)	(II)	(III)				(IV)	(V)	(VI)	(VII)	(VIII)
466	*RQ(12, 1,E)	12	2	0	E	2311.0515	3001.9803	6	1.28-04	1.0
467	QQ(13, 2,E)	13	2	0	E	2311.1055	3115.1693	14	1.59-05	1.0
468	QQ(13, 6,A)	13	6	0	A	2311.2544	3099.0305	-20	3.58-01	*1.0
469	RQ(11,10,E)	11	11	1	E	2311.4535	2844.6931	35	2.78-01	1.0
470	RQ(12, 8,E)	12	9	1	E	2311.4535	2969.8770	-58	3.19-01	1.0
471	*SQ(12, 4,E)	12	6	-1	E	2311.5581	2994.8369	159	3.56-03	.0
472	*TQ(10, 0,A1)	10	3	0	A2	2311.7987	2799.9931	-21	2.22-01	1.0
473	*VQ(8, 0,A1)	8	5	-1	A2	2311.8985	2631.7957	-14	5.38-02	1.0
474	QQ(13, 5,E)	13	5	0	E	2311.9622	3105.3693	70	1.64-01	1.0
475	RQ(12, 7,E)	12	8	1	E	2312.0254	2978.2776	-12	3.03-01	1.0
476	RQ(11, 9,A)	11	10	1	A	2312.0754	2855.2695	1	8.78-01	*1.0
477	QQ(12, 3,A)	12	3	0	A	2312.1756	2999.0313	43	5.15-04	*1.0
478	QP(1, 0,A2)	0	0	0	A1	2312.2150	2321.1193	-12	4.98+00	1.0
479	QQ(12, 6,A)	12	6	0	A	2312.5343	2985.5262	-20	5.34-01	*1.0
480	QQ(12, 2,E)	12	2	0	E	2312.5781	3001.9814	7	6.15-05	1.0
481	RQ(11, 8,E)	11	9	1	E	2312.6670	2864.8695	-14	4.97-01	1.0
482	QQ(13, 4,E)	13	4	0	E	2312.8121	3110.7996	131	1.44-01	.0
483	RQ(10, 9,A)	10	10	1	A	2313.0957	2754.7267	38	9.07-01	*1.0
484	QQ(12, 5,E)	12	5	0	E	2313.0957	2991.7577	-2	2.23-01	1.0
485	RQ(11, 7,E)	11	8	1	E	2313.2383	2873.3289	-6	4.66-01	1.0
486	*TQ(8, 0,A1)	8	3	0	A2	2313.2816	2633.1787	18	2.44-01	1.0
487	*SQ(11, 3,A)	11	5	-1	A	2313.4568	2894.3050	6	1.04-02	*1.0
488	*RQ(10, 1,E)	10	2	0	E	2313.6337	2801.3128	-3	1.74-01	1.0
489	RQ(10, 8,E)	10	9	1	E	2313.7396	2768.4427	8	6.72-01	1.0
490	RQ(11, 6,A)	11	7	1	A	2313.7578	2880.6388	-7	7.44-01	*1.0
491	QQ(12, 4,E)	12	4	0	E	2313.7578	2997.0366	-7	1.83-01	1.0
492	*SQ(13, 3,A)	13	5	-1	A	2313.8630	3115.3992	160	2.38-01	* .0
493	QQ(11, 2,E)	11	2	0	E	2313.9193	2897.3338	-16	1.80-03	1.0
494	*TQ(7, 0,A2)	7	3	0	A1	2313.9193	2562.8443	11	2.05-01	1.0
495	QQ(11, 5,E)	11	5	0	E	2314.2493	2886.8428	-11	2.63-01	1.0
496	*RQ(12, 2,E)	12	1	0	E	2314.2991	3003.7024	-8	1.83-01	1.0
497	RQ(10, 7,E)	10	8	1	E	2314.3376	2776.9841	-9	6.65-01	1.0
498	*SQ(9, 4,E)	9	6	-1	E	2314.4351	2705.7710	-40	5.19-02	1.0
499	*TQ(6, 0,A1)	6	3	0	A2	2314.5273	2501.2975	23	1.45-01	1.0
500	QQ(13,12,A)	13	12	0	A	2314.5674	3045.5539	10	6.85+00	*1.0
501	QQ(13,11,E)	13	11	0	E	2314.5674	3057.8879	-13	3.08+00	1.0
502	QQ(13,10,E)	13	10	0	E	2314.6196	3069.0887	-46	2.81+00	1.0
503	QQ(13,13,E)	13	13	0	E	2314.6196	3032.0532	10	3.86+00	1.0
504	RQ(9, 8,E)	9	9	1	E	2314.6966	2680.6549	38	6.58-01	1.0
505	*SQ(12, 3,A)	12	5	-1	A	2314.7140	3001.5697	23	2.99-01	*1.0
506	QQ(13, 9,A)	13	9	0	A	2314.7768	3079.2401	-25	5.20+00	*1.0
507	QQ(11, 4,E)	11	4	0	E	2314.8049	2892.0496	-5	1.84-01	1.0
508	RQ(10, 6,A)	10	7	1	A	2314.8939	2784.3783	0	9.65-01	*1.0
509	QQ(13, 8,E)	13	8	0	E	2314.9851	3088.3158	0	2.43+00	1.0
510	*TQ(5, 0,A2)	5	3	0	A1	2315.0577	2448.5120	17	7.94-02	1.0
511	QQ(13, 7,E)	13	7	0	E	2315.2445	3096.3409	28	2.29+00	1.0
512	RQ(9, 7,E)	9	8	1	E	2315.3509	2689.3037	12	8.44-01	1.0
513	QQ(10, 5,E)	10	5	0	E	2315.3509	2790.5873	-13	2.57-01	1.0
514	QQ(12,10,E)	12	10	0	E	2315.4704	2954.8770	-24	4.66+00	1.0
515	QQ(12,11,E)	12	11	0	E	2315.4704	2943.6353	-9	5.17+00	1.0
516	QQ(12, 9,A)	12	9	0	A	2315.5299	2965.0133	-43	8.54+00	*1.0
517	RQ(13, 6,A)	13	7	1	A	2315.5555	3103.3376	52	4.34+00	*1.0
518	QQ(12,12,A)	12	12	0	A	2315.5555	2931.2824	18	1.17+01	*1.0
519	QQ(11, 3,A)	11	3	0	A	2315.5971	2896.4453	-11	2.89-01	*1.0
520	*SQ(9, 3,A)	9	5	-1	A	2315.6675	2710.6545	-28	1.42-01	*1.0
521	QQ(12, 8,E)	12	8	0	E	2315.6956	2974.1190	-17	3.98+00	1.0
522	QQ(10, 4,E)	10	4	0	E	2315.8061	2795.7258	-5	1.20-01	1.0
523	*TQ(3, 0,A2)	3	3	0	A1	2315.8651	2369.2751	-22	7.05-03	1.0

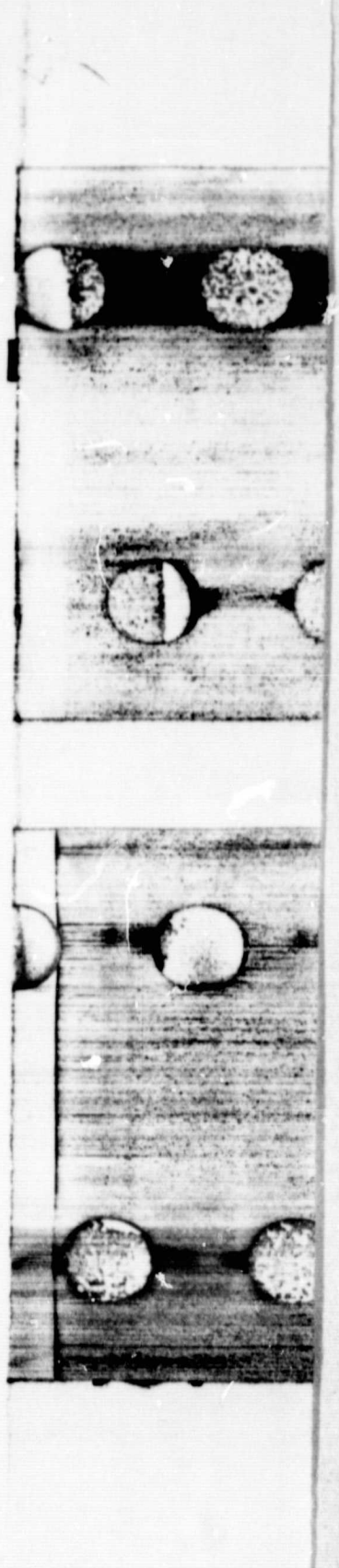

TABLE I—*Continued*

(I)	(II)	(III)				(IV)	(V)	(VI)	(VII)	(VIII)
524	QQ(12, 7,E)	12	7	0	E	2315.8927	2982.1449	-24	3.77+00	1.0
525	RQ(9, 6,A)	9	7	1	A	2315.9244	2696.7588	-6	1.16+00	*1.0
526	RQ(13, 5,E)	13	6	1	E	2315.9244	3109.3315	66	2.06+00	1.0
527	*TQ(10, 1,E)	10	4	-1	E	2316.0288	2803.7079	-25	9.47-02	1.0
528	RQ(12, 6,A)	12	7	1	A	2316.1681	2989.1600	-27	7.21+00	*1.0
529	RQ(8, 7,E)	8	8	1	E	2316.2347	2610.2744	22	7.81+01	1.0
530	QQ(11, 9,A)	11	9	0	A	2316.3686	2859.5627	18	1.35+01	*1.0
531	QQ(11,10,E)	11	10	0	E	2316.3686	2849.4082	31	7.45+00	1.0
532	QQ(11,11,E)	11	11	0	E	2316.3686	2838.0790	-25	8.42+00	1.0
533	RQ(13, 4,E)	13	5	1	E	2316.3686	3114.3560	86	1.85+00	1.0
534	QQ(10, 3,A)	10	3	0	A	2316.4374	2799.9853	-18	1.74+01	*1.0
535	QQ(11, 8,E)	11	8	0	E	2316.4374	2868.6399	2	6.22+00	1.0
536	*SQ(13, 1,E)	13	3	-1	E	2316.4374	3122.0147	4	8.16-02	1.0
537	RQ(12, 5,E)	12	6	1	E	2316.5456	2995.2076	-17	3.47+00	1.0
538	QQ(11, 7,E)	11	7	0	E	2316.5836	2876.6741	-15	5.90+00	1.0
539	*TQ(9, 1,E)	9	4	-1	E	2316.7382	2715.8823	-11	8.68-02	1.0
540	QQ(9, 4,E)	9	4	0	E	2316.7840	2708.1199	22	2.21-02	1.0
541	QQ(11, 6,A)	11	6	0	A	2316.8296	2883.7106	-27	1.14+01	*1.0
542	RQ(8, 6,A)	8	7	1	A	2316.8650	2617.8260	-3	1.22+00	*1.0
543	RQ(13, 3,A2)	13	4	1	A1	2316.9043	3118.4405	30	1.90+00	1.0
544	RQ(13, 3,A1)	13	4	1	A2	2317.0069	3118.5431	-1	2.66+00	1.0
545	RQ(12, 4,E)	12	5	1	E	2317.0069	3000.2857	-23	3.27+00	1.0
546	QQ(10, 9,A)	10	9	0	A	2317.1403	2762.7713	13	2.05+01	*1.0
547	QQ(10, 8,E)	10	8	0	E	2317.1625	2771.8656	12	9.33+00	1.0
548	QQ(10,10,E)	10	10	0	E	2317.1625	2752.5667	-15	1.16+01	1.0
549	RQ(11, 5,E)	11	6	1	E	2317.1923	2889.7858	-36	5.54+00	1.0
550	QQ(10, 7,E)	10	7	0	E	2317.2579	2779.9044	-2	8.78+00	1.0
551	QQ(9, 3,A)	9	3	0	A	2317.2579	2712.2449	20	1.85-02	*1.0
552	QQ(8, 2,E)	8	2	0	E	2317.3165	2635.1264	-14	1.56-01	1.0
553	QQ(8, 5,E)	8	5	0	E	2317.3650	2624.1480	11	5.86-02	1.0
554	QQ(10, 6,A)	10	6	0	A	2317.4724	2786.9568	-11	1.70+01	*1.0
555	RQ(13, 2,E)	13	3	1	E	2317.4724	3121.5362	20	1.29+00	1.0
556	*SQ(10, 2,E)	10	4	-1	E	2317.5775	2803.7094	-23	8.05-02	1.0
557	QQ(8, 4,E)	8	4	0	E	2317.6255	2629.1485	-22	4.42-02	1.0
558	RQ(12, 3,A1)	12	4	1	A2	2317.6255	3004.4812	-12	3.23+00	1.0
559	RQ(7, 6,A)	7	7	1	A	2317.7044	2547.5961	1	9.56-01	*1.0
560	RQ(11, 4,E)	11	5	1	E	2317.7044	2894.9491	-22	5.34+00	1.0
561	RQ(10, 5,E)	10	6	1	E	2317.8391	2793.0756	-12	8.38+00	1.0
562	QQ(9, 8,E)	9	8	0	E	2317.8654	2683.8237	13	1.35+01	1.0
563	QQ(9, 9,A)	9	9	0	A	2317.8654	2674.6928	-25	3.05+01	*1.0
564	RQ(12, 3,A2)	12	4	1	A1	2317.8654	3004.7211	11	4.18+00	1.0
565	QQ(9, 7,E)	9	7	0	E	2317.9104	2691.8633	9	1.25+01	1.0
566	QQ(8, 3,A)	8	3	0	A	2317.9595	2633.1544	-1	1.19+01	*1.0
567	*RQ(13, 2,E)	13	3	-1	E	2317.9595	3122.0233	13	8.69-01	1.0
568	QQ(9, 6,A)	9	6	0	A	2318.0794	2698.9138	4	2.42+01	*1.0
569	RQ(13, 1,E)	13	2	1	E	2318.1557	3123.7330	-32	1.46+00	1.0
570	QQ(7, 2,E)	7	2	0	E	2318.2327	2565.0598	5	4.09-01	1.0
571	QQ(7, 5,E)	7	5	0	E	2318.2327	2553.9765	4	1.09-02	1.0
572	RQ(11, 3,A1)	11	4	1	A2	2318.2793	2899.1275	12	3.09+00	1.0
573	RQ(12, 2,E)	12	3	1	E	2318.2950	3007.6983	-18	2.76+00	1.0
574	RQ(10, 4,E)	10	5	1	E	2318.3570	2798.2767	-22	8.17+00	1.0
575	RQ(11, 3,A2)	11	4	1	A1	2318.3570	2899.2052	-9	5.22+00	1.0
576	QQ(7, 1,E)	7	1	0	E	2318.3570	2566.7579	10	1.26-01	1.0
577	RQ(9, 5,E)	9	6	1	E	2318.4260	2705.0490	-2	1.20+01	1.0
578	QQ(7, 4,E)	7	4	0	E	2318.4542	2558.9622	-6	6.23-01	1.0
579	PP(1, 1,E)	0	0	1	E	2318.4978	2326.8688	-7	8.90+00	1.0
580	QQ(8, 7,E)	8	7	0	E	2318.5135	2612.5531	-3	1.70+01	1.0
581	QQ(8, 8,E)	8	8	0	E	2318.5135	2604.5120	-18	1.91+01	1.0

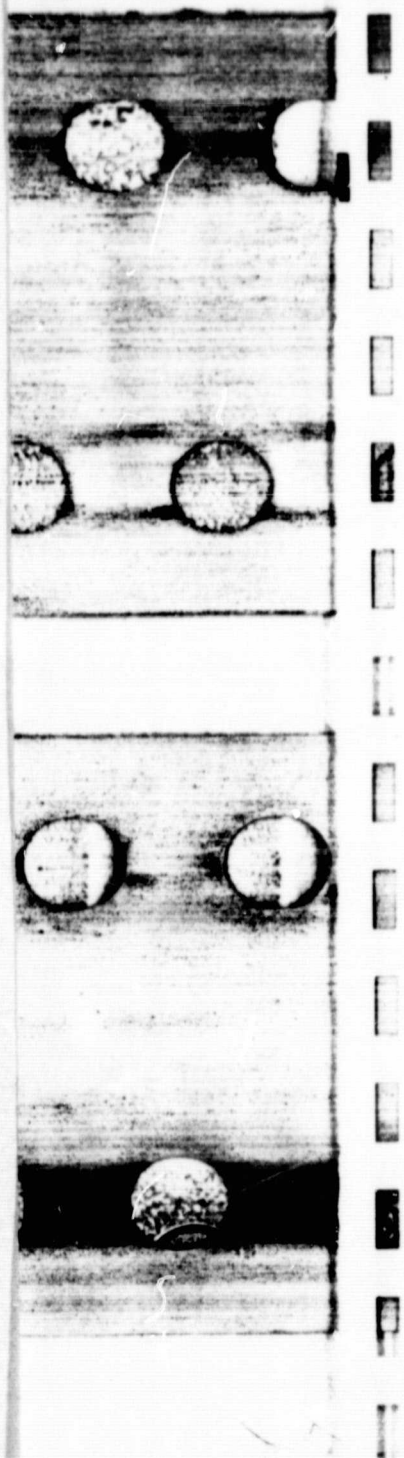

TABLE I—*Continued*

(I)	(II)	(III)	(IV)	(V)	(VI)	(VII)	(VIII)
582	QQ(8, 6,A)	8 6 0 A	2318.6395	2619.6005	13	3.25+01	*1.0
583	QQ(7, 3,A)	7 3 0 A	2318.6395	2562.8383	7	1.15+00	*1.0
584	*NQ(11, 3,A1)	11 0 0 A2	2318.8816	2899.7298	-30	3.44+00	1.0
585	*RQ(12, 2,E)	12 3 -1 E	2318.8816	3008.2849	-22	6.94-01	1.0
586	*SQ(8, 2,E)	8 4 -1 E	2318.9364	2636.7463	7	3.04-03	1.0
587	RQ(8, 5,E)	8 6 1 E	2318.9635	2625.7466	9	1.61+01	1.0
588	RQ(9, 4,E)	9 5 1 E	2318.9635	2710.2994	-23	1.17+01	1.0
589	QQ(6, 2,E)	6 2 0 E	2319.0148	2503.6777	7	9.71-01	1.0
590	RQ(6, 5,E)	6 6 1 E	2319.0328	2492.5625	1	4.96-01	1.0
591	RQ(10, 3,A)	10 4 1 A	2319.0328	2802.5807	0	1.41+01	*1.0
592	RQ(12, 1,E)	12 2 1 E	2319.0574	3009.9862	-33	2.49+00	1.0
593	QQ(7, 7,E)	7 7 0 E	2319.0880	2542.0224	-14	2.25+01	1.0
594	QQ(6, 1,E)	6 1 0 E	2319.0880	2505.3318	6	2.89-01	1.0
595	RQ(11, 2,E)	11 3 1 E	2319.0880	2902.5025	-21	4.80+00	1.0
596	QQ(7, 6,A)	7 6 0 A	2319.1425	2549.0342	5	4.14+01	*1.0
597	QQ(6, 4,E)	6 4 0 E	2319.1782	2497.4937	-14	2.79+00	1.0
598	QQ(6, 3,A)	6 3 0 A	2319.2571	2501.2799	7	4.14+00	*1.0
599	RQ(7, 5,E)	7 6 1 E	2319.4292	2555.1730	9	2.03+01	1.0
600	*SQ(11, 0,A2)	11 2 -1 A1	2319.4699	2904.9330	-17	3.54-04	1.0
601	RQ(8, 4,E)	8 5 1 E	2319.5483	2631.0713	1	1.56+01	1.0
602	QQ(6, 6,A)	6 6 0 A	2319.5859	2487.2369	-16	5.01+01	*1.0
603	QQ(5, 2,E)	5 2 0 E	2319.6663	2451.0052	0	2.12+00	1.0
604	RQ(9, 3,A)	9 4 1 A	2319.7018	2714.6888	-3	2.18+01	*1.0
605	QQ(5, 1,E)	5 1 0 E	2319.7018	2452.6277	7	5.94-01	1.0
606	RQ(13, 0,A2)	13 1 1 A1	2319.7402	3125.8216	46	4.56+00	1.0
607	QQ(5, 3,A)	5 3 0 A	2319.8180	2448.5065	12	1.05+01	*1.0
608	QQ(5, 4,E)	5 4 0 E	2319.8180	2444.7848	-19	8.90+00	1.0
609	QQ(6, 5,E)	6 5 0 E	2319.8180	2493.3477	10	2.33+01	1.0
610	RQ(10, 2,E)	10 3 1 E	2319.8540	2805.9858	-2	7.51+00	1.0
611	RQ(11, 1,E)	11 2 1 E	2319.9350	2904.8863	-6	4.08+00	1.0
612	QQ(5, 5,E)	5 5 0 E	2320.0201	2440.1826	-12	2.60+01	1.0
613	RQ(7, 4,E)	7 5 1 E	2320.0521	2560.5601	-1	1.90+01	1.0
614	*NQ(10, 3,A2)	10 0 0 A1	2320.0902	2803.6381	-18	2.39+00	1.0
615	QQ(4, 1,E)	4 1 0 E	2320.2010	2408.6666	9	1.11+00	1.0
616	QQ(4, 2,E)	4 2 0 E	2320.2010	2407.0745	-4	4.33+00	1.0
617	QQ(4, 3,A)	4 3 0 A	2320.2812	2404.4957	-5	2.21+01	*1.0
618	RQ(8, 3,A)	8 4 1 A	2320.3190	2635.5139	-2	2.98+01	*1.0
619	QQ(4, 4,E)	4 4 0 E	2320.3791	2400.8598	-12	2.49+01	1.0
620	*NQ(12, 4,E)	12 1 0 E	2320.4096	3003.6884	-22	9.05-01	1.0
621	*SQ(10, 0,A1)	10 2 -1 A2	2320.4396	2808.6040	-12	2.33-04	1.0
622	RQ(6, 4,E)	6 5 1 E	2320.4979	2498.8134	-5	2.02+01	1.0
623	RQ(9, 2,E)	9 3 1 E	2320.5652	2718.1523	6	1.09+01	1.0
624	QQ(3, 1,E)	3 1 0 E	2320.5652	2373.4437	-14	1.99+00	1.0
625	RQ(12, 0,A1)	12 1 1 A2	2320.5652	3012.0020	33	7.55+00	1.0
626	QQ(3, 2,E)	3 2 0 E	2320.6078	2371.8900	-8	8.38+00	1.0
627	QQ(3, 3,A)	3 3 0 A	2320.6680	2369.2844	-13	4.25+01	*1.0
628	RQ(10, 1,E)	10 2 1 E	2320.7475	2808.4266	6	6.39+00	1.0
629	QQ(2, 1,E)	2 1 0 E	2320.8637	2347.0409	0	3.59+00	1.0
630	QQ(2, 2,E)	2 2 0 E	2320.8817	2345.4595	-18	1.53+01	1.0
631	RQ(5, 4,E)	5 5 1 E	2320.8817	2445.8485	-7	1.62+01	1.0
632	RQ(7, 3,A)	7 4 1 A	2320.8817	2565.0805	-3	3.68+01	*1.0
633	QQ(1, 1,E)	1 1 0 E	2321.0414	2329.4124	-9	7.48+00	1.0
634	*SQ(7, 1,E)	7 3 -1 E	2321.0792	2569.4801	2	6.38-03	1.0
635	*QQ(12, 1,E)	12 1 -1 E	2321.1105	3012.0393	-5	8.67-01	1.0
636	*NQ(9, 3,A1)	9 0 0 A2	2321.2184	2716.2054	-7	1.94+00	1.0
637	RQ(8, 2,E)	8 3 1 E	2321.2184	2639.0283	5	1.47+01	1.0
638	*SQ(9, 0,A2)	9 2 -1 A1	2321.2720	2720.9346	-2	1.95-03	1.0
639	RQ(11, 0,A2)	11 1 1 A1	2321.3615	2906.8246	25	1.18+01	1.0

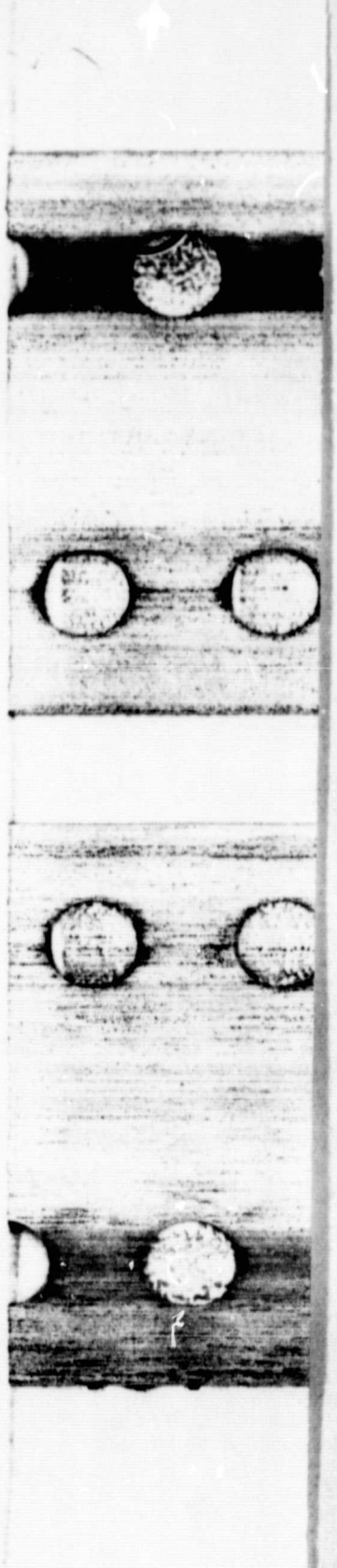

TABLE 1—*Continued*

(I)	(II)	(III)				(IV)	(V)	(VI)	(VII)	(VIII)
640	RQ(6, 3,A)	6	4	1	A	2321.3826	2503.4054	-9	4.07+01	*1.0
641	PQ(12, 1,E)	12	0	1	E	2321.3826	3012.3114	0	4.10+00	1.0
642	RQ(9, 1,E)	9	2	1	E	2321.4977	2720.6418	10	9.46+00	1.0
643	*SQ(6, 1,E)	6	3	-1	E	2321.6109	2507.8547	7	4.42-05	1.0
644	*NQ(13, 5,E)	13	2	0	E	2321.7751	3115.1822	27	8.57-01	1.0
645	RQ(5, 3,A)	5	4	1	A	2321.8221	2450.5107	-16	3.86+01	*1.0
646	RQ(7, 2,E)	7	3	1	E	2321.8221	2568.6492	8	1.84+01	1.0
647	*NQ(11, 4,E)	11	1	0	E	2321.8453	2899.0900	-5	1.11+00	1.0
648	*QQ(11, 1,E)	11	1	-1	E	2321.8882	2906.8395	-3	6.94-01	1.0
649	PQ(13, 3,A2)	13	2	-1	A1	2321.9194	3123.4556	-1	2.82+00	1.0
650	*SQ(8, 0,A1)	8	2	-1	A2	2322.0452	2641.9424	1	3.89-03	1.0
651	*QQ(13, 2,E)	13	0	1	E	2322.0830	3126.1468	3	5.83-01	1.0
652	*SQ(5, 1,E)	5	3	-1	E	2322.0830	2455.0089	18	1.83-03	1.0
653	RQ(10, 0,A1)	10	1	1	A2	2322.1109	2810.3053	12	1.76+01	1.0
654	RQ(4, 3,A)	4	4	1	A	2322.1951	2406.4096	-22	2.68+01	*1.0
655	PQ(11, 1,E)	11	0	1	E	2322.1951	2907.1464	2	6.94+00	1.0
656	RQ(8, 1,E)	8	2	1	E	2322.1951	2641.5708	16	1.32+01	1.0
657	*NQ(8, 3,A2)	8	0	0	A1	2322.2250	2637.4199	2	1.57+00	1.0
658	RQ(6, 2,E)	6	3	1	E	2322.3499	2507.0128	-4	2.12+01	1.0
659	*SQ(4, 1,E)	4	3	-1	E	2322.4721	2410.9377	13	4.27-03	1.0
660	PQ(12, 2,E)	12	1	-1	E	2322.6421	3012.0453	0	3.31+00	1.0
661	*SQ(7, 0,A2)	7	2	-1	A1	2322.7331	2571.6581	3	4.47-03	1.0
662	RQ(9, 0,A2)	9	1	1	A1	2322.8121	2722.4747	1	2.47+01	1.0
663	RQ(5, 2,E)	5	3	1	E	2322.8121	2454.1510	-16	2.21+01	1.0
664	RQ(7, 1,E)	7	2	1	E	2322.8121	2571.2130	3	1.72+01	1.0
665	*QQ(12, 2,E)	12	0	1	E	2322.9038	3012.3071	-4	4.89-01	1.0
666	PQ(10, 1,E)	10	0	1	E	2322.9860	2810.6651	9	1.05+01	1.0
667	PQ(12, 3,A1)	12	2	-1	A2	2323.0412	3009.8969	-10	4.46+00	1.0
668	*QQ(9, 2,E)	9	2	1	E	2323.0647	2720.6518	20	1.11-01	1.0
669	*NQ(7, 3,A1)	7	0	0	A2	2323.0990	2567.2978	7	1.16+00	1.0
670	*NQ(10, 4,E)	10	1	0	E	2323.1418	2803.0615	-2	1.29+00	1.0
671	RQ(4, 2,E)	4	3	1	E	2323.2125	2410.0860	-17	2.00+01	1.0
672	*NQ(12, 5,E)	12	2	0	E	2323.3170	3001.9790	5	1.28+00	1.0
673	*SQ(6, 0,A1)	6	2	-1	A2	2323.3348	2510.1050	5	3.40-03	1.0
674	RQ(6, 1,E)	6	2	1	E	2323.3746	2509.6184	2	2.08+01	1.0
675	PQ(11, 2,E)	11	1	-1	E	2323.4254	2906.8399	-3	5.79+00	1.0
676	RQ(8, 0,A1)	8	1	1	A2	2323.4676	2643.3647	0	3.28+01	1.0
677	RQ(3, 2,E)	3	3	1	E	2323.5303	2374.8126	-26	1.33+01	1.0
678	PQ(9, 1,E)	9	0	1	E	2323.7322	2722.8763	11	1.47+01	1.0
679	RQ(5, 1,E)	5	2	1	E	2323.8539	2456.7748	-10	2.32+01	1.0
680	*QQ(12, 3,A2)	12	1	1	A1	2323.8539	3010.7097	-31	1.37+00	1.0
681	PQ(13, 4,E)	13	3	-1	E	2324.0331	3122.0206	10	1.62+00	1.0
682	PQ(11, 3,A2)	11	2	-1	A1	2324.0662	2904.9144	-35	6.72+00	1.0
683	RQ(7, 0,A2)	7	1	1	A1	2324.0662	2572.9912	2	4.11+01	1.0
684	PQ(10, 2,E)	10	1	-1	E	2324.2012	2810.3330	3	9.04+00	1.0
685	RQ(4, 1,E)	4	2	1	E	2324.2755	2412.7411	-4	2.34+01	1.0
686	*NQ(9, 4,E)	9	1	0	E	2324.3074	2715.6433	0	1.36+00	1.0
687	PQ(8, 1,E)	8	0	1	E	2324.4252	2643.8009	10	1.92+01	1.0
688	*NQ(5, 3,A1)	5	0	0	A2	2324.4634	2453.1519	5	3.88-01	1.0
689	*QQ(10, 2,E)	10	0	1	E	2324.5331	2810.6649	9	3.23-01	1.0
690	RQ(3, 1,E)	3	2	1	E	2324.5895	2377.4680	-26	2.06+01	1.0
691	RQ(6, 0,A1)	6	1	1	A2	2324.5895	2511.3597	-4	4.84+01	1.0
692	*QQ(7, 1,E)	7	1	-1	E	2324.7011	2573.1020	7	1.39-01	1.0
693	*NQ(11, 5,E)	11	2	0	E	2324.7525	3097.3460	-4	1.82+00	1.0
694	PQ(11, 3,A1)	11	2	-1	A2	2324.7944	2905.6426	-25	2.82+00	1.0
695	RQ(2, 1,E)	2	2	1	E	2324.8488	2351.0260	-21	1.36+01	1.0
696	PQ(9, 2,E)	9	1	-1	E	2324.9394	2722.5265	3	1.29+01	1.0
697	PQ(12, 3,A2)	12	2	-1	A1	2324.9394	3011.7951	-10	2.04+00	1.0

TABLE I—*Continued*

(I)	(II)	(III)				(IV)	(V)	(VI)	(VII)	(VIII)
698	PQ(12, 4,E)	12	3	-1	E	2325.0139	2908.2927	-14	3.03+00	1.0
699	RQ(5, 0,A2)	5	1	1	A1	2325.0500	2458.5043	-6	5.33+01	1.0
700	PQ(10, 3,A1)	10	2	-1	A2	2325.0500	2808.5979	-18	9.62+00	1.0
701	PQ(7, 1,E)	7	0	1	E	2325.0500	2573.4509	0	2.35+01	1.0
702	*QQ(12, 3,A1)	12	1	1	A2	2325.1477	3012.0034	34	2.34-02	1.0
703	*QQ(6, 1,E)	6	1	-1	E	2325.2806	2511.5244	20	7.08-02	1.0
704	*QQ(9, 2,E)	9	0	1	E	2325.2806	2722.8677	3	2.47-01	1.0
705	*NQ(8, 4,E)	8	1	0	E	2325.3554	2636.8784	15	1.28+00	1.0
706	RQ(4, 0,A1)	4	1	1	A2	2325.4324	2414.4281	-14	5.42+01	1.0
707	PQ(8, 2,E)	8	1	-1	E	2325.6304	2643.4403	0	1.72+01	1.0
708	PQ(6, 1,E)	6	0	1	E	2325.6304	2511.8742	8	2.69+01	1.0
709	*QQ(11, 3,A1)	11	1	1	A2	2325.6304	2906.4786	4	2.62+00	1.0
710	PQ(10, 3,A2)	10	2	-1	A1	2325.6675	2809.2154	-4	5.65+00	1.0
711	RQ(3, 0,A2)	3	1	1	A1	2325.7450	2379.1550	-17	5.02+01	1.0
712	PQ(11, 4,E)	11	3	-1	E	2325.9528	2903.1975	-20	4.98+00	1.0
713	PQ(9, 3,A2)	9	2	-1	A1	2325.9528	2720.9398	2	1.30+01	1.0
714	RQ(2, 0,A1)	2	1	1	A2	2325.9852	2352.6949	-15	4.08+01	1.0
715	*NQ(12, 6,A)	12	3	0	A	2326.0598	2999.0517	63	3.97+00	*1.0
716	*NQ(10, 5,E)	10	2	0	E	2326.0805	2801.3170	0	2.44+00	1.0
717	RQ(1, 0,A2)	1	1	1	A1	2326.1322	2335.0365	-28	2.67+01	1.0
718	PQ(5, 1,E)	5	0	1	E	2326.1322	2459.0581	11	2.88+01	1.0
719	*QQ(4, 1,E)	4	1	-1	E	2326.1920	2414.6576	14	5.69-03	1.0
720	*NQ(7, 4,E)	7	1	0	E	2326.2487	2566.7567	9	1.03+00	1.0
721	PQ(7, 2,E)	7	1	-1	E	2326.2769	2573.1040	9	2.13+01	1.0
722	*QQ(10, 3,A2)	10	1	1	A1	2326.3236	2809.8715	0	2.55+00	1.0
723	PQ(9, 3,A1)	9	2	-1	A2	2326.4273	2721.4143	3	9.92+00	1.0
724	*QQ(3, 1,E)	3	1	-1	E	2326.5131	2379.3916	-5	2.45-03	1.0
725	PQ(4, 1,E)	4	0	1	E	2326.5428	2415.0084	-1	2.86+01	1.0
726	*QQ(7, 2,E)	7	0	1	E	2326.6299	2573.4570	5	1.14-01	1.0
727	PQ(12, 5,E)	12	4	-1	E	2326.6765	3005.3385	0	2.62+00	1.0
728	*QQ(12, 4,E)	12	2	1	E	2326.7198	3009.9986	-20	1.95-01	1.0
729	PQ(8, 3,A1)	8	2	-1	A2	2326.7485	2641.9434	2	1.67+01	1.0
730	PQ(10, 4,E)	10	3	-1	E	2326.8263	2806.7457	-14	7.55+00	1.0
731	PQ(6, 2,E)	6	1	-1	E	2326.8551	2511.5180	13	2.45+01	1.0
732	PQ(3, 1,E)	3	0	1	E	2326.8812	2379.7597	-6	2.59+01	1.0
733	*QQ(1, 1,E)	1	1	-1	E	2326.9398	2335.3108	-11	1.59-04	1.0
734	*NQ(6, 4,E)	6	1	0	E	2327.0239	2505.3383	13	6.67-01	1.0
735	*QQ(9, 3,A1)	9	1	1	A2	2327.0654	2722.0524	19	1.69+00	1.0
736	PQ(8, 3,A2)	8	2	-1	A1	2327.0925	2642.2874	9	1.46+01	1.0
737	PQ(2, 1,E)	2	0	1	E	2327.1436	2353.3208	-4	2.08+01	1.0
738	*QQ(6, 2,E)	6	0	1	E	2327.2108	2511.8737	8	6.68-02	1.0
739	*NQ(9, 5,E)	9	2	0	E	2327.2834	2713.9064	3	3.04+00	1.0
740	PQ(1, 1,E)	1	0	1	E	2327.3158	2335.6868	-6	1.34+01	1.0
741	PQ(5, 2,E)	5	1	-1	E	2327.3520	2458.6909	8	2.61+01	1.0
742	PQ(11, 6,A)	11	5	-1	A	2327.4336	2894.3146	16	6.37+00	*1.0
743	PQ(7, 3,A2)	7	2	-1	A1	2327.4576	2571.6564	2	2.01+01	1.0
744	*QQ(9, 3,A2)	9	1	1	A1	2327.4919	2722.4789	5	5.00-02	1.0
745	PQ(9, 4,E)	9	3	-1	E	2327.6186	2718.9545	-9	1.07+01	1.0
746	PQ(11, 5,E)	11	4	-1	E	2327.6186	2900.2121	-13	4.06+00	1.0
747	*QQ(11, 4,E)	11	2	1	E	2327.6414	2904.8861	-6	2.48-01	1.0
748	PQ(7, 3,A1)	7	2	-1	A2	2327.6897	2571.8885	16	1.87+01	1.0
749	PQ(4, 2,E)	4	1	-1	E	2327.7815	2414.6550	11	2.54+01	1.0
750	PQ(6, 3,A1)	6	2	-1	A2	2328.0873	2510.1101	10	2.24+01	1.0
751	PQ(3, 2,E)	3	1	-1	E	2328.1207	2379.4030	5	2.16+01	1.0
752	*QQ(8, 3,A1)	8	1	1	A2	2328.1757	2643.3706	6	5.14-02	1.0
753	PQ(6, 3,A2)	6	2	-1	A1	2328.2148	2510.2376	11	2.16+01	1.0
754	PQ(8, 4,E)	8	3	-1	E	2328.3380	2639.8610	2	1.40+01	1.0
755	*NQ(8, 5,E)	8	2	0	E	2328.3735	2635.1566	16	3.45+00	1.0

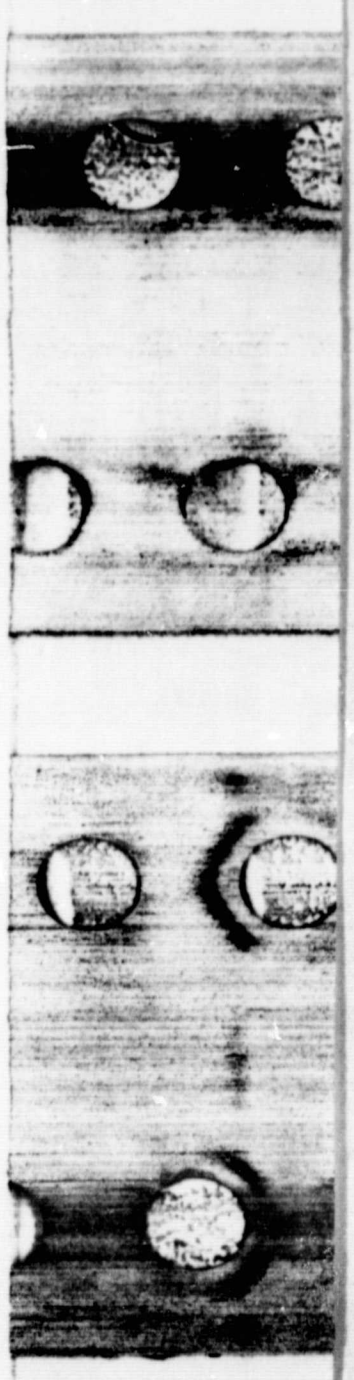

TABLE I—*Continued*

(I)	(II)	(III)				(IV)	(V)	(VI)	(VII)	(VIII)
756	PQ(2, 2,E)	2	1	-1	E	2328.3735	2352.9513	-3	1.39+01	1.0
757	PQ(10, 5,E)	10	4	-1	E	2328.4803	2803.7167	-16	5.91+00	1.0
758	*QQ(10, 4,E)	10	2	1	E	2328.5055	2808.4252	5	2.60-01	1.0
759	PQ(12, 7,E)	12	6	-1	E	2328.5899	2994.8421	164	2.79+00	.0
760	PQ(12, 6,A)	12	5	-1	A	2328.5899	3001.5818	35	3.48+00	*1.0
761	PQ(5, 3,A2)	5	2	-1	A1	2328.6165	2457.3050	7	2.28+01	1.0
762	PQ(5, 3,A1)	5	2	-1	A2	2328.6962	2457.3847	21	2.24+01	1.0
763	PQ(10, 6,A)	10	5	-1	A	2328.6962	2798.1806	-6	9.77+00	*1.0
764	*QQ(7, 3,A2)	7	1	1	A1	2328.7749	2572.9737	-14	4.60-02	1.0
765	PQ(7, 4,E)	7	3	-1	E	2328.9704	2569.4784	0	1.69+01	1.0
766	PQ(4, 3,A1)	4	2	-1	A2	2329.0656	2413.2802	12	2.01+01	1.0
767	PQ(4, 3,A2)	4	2	-1	A1	2329.0908	2413.3053	9	2.00+01	1.0
768	PQ(9, 5,E)	9	4	-1	E	2329.2599	2715.8829	-10	8.05+00	1.0
769	*NQ(7, 5,E)	7	2	0	E	2329.3171	2565.0609	6	3.42+00	1.0
770	PQ(3, 3,A)	3	2	-1	A	2329.4250	2378.0414	7	2.64+01	*1.0
771	PQ(6, 4,E)	6	3	-1	E	2329.5439	2507.8594	11	1.84+01	1.0
772	*NQ(11, 6,A)	11	3	0	A	2329.5690	2896.4500	-6	4.70+00	*1.0
773	*QQ(5, 3,A1)	5	1	1	A2	2329.6392	2458.3277	6	5.79-02	1.0
774	*NQ(13, 7,E)	13	[illegible]	0	E	2329.7124	3110.8087	140	6.23-01	.0
775	PQ(11, 7,E)	11	[illegible]	-1	E	2329.7669	2889.8575	47	4.39+00	1.0
776	PQ(9, 6,A)	9	5	-1	A	2329.8294	2710.6638	-19	1.41+01	*1.0
777	QK(0, 0,A1)	1	0	0	A2	2329.9466	2329.9466	3	5.32+00	1.0
778	PQ(8, 5,E)	8	4	-1	E	2329.9466	2636.7296	-9	1.02+01	1.0
779	PQ(5, 4,E)	5	3	-1	E	2330.0401	2455.0069	16	1.72+01	1.0
780	*QQ(4, 3,A2)	4	1	1	A1	2330.0954	2414.3099	-4	1.95-02	1.0
781	*NQ(6, 5,E)	6	2	0	E	2330.1457	2503.6754	5	2.71+00	1.0
782	*QQ(4, 3,A1)	4	1	1	A2	2330.2047	2414.4193	-23	1.11-02	1.0
783	PQ(4, 4,E)	4	3	-1	E	2330.4606	2410.9413	17	1.17+01	1.0
784	*NQ(10, 6,A)	10	3	0	A	2330.5224	2800.0068	3	5.61+00	*1.0
785	PQ(7, 5,E)	7	4	-1	E	2330.5546	2566.2984	-3	1.17+01	1.0
786	*QQ(13, 6,A2)	13	4	1	A1	2330.6468	3118.4289	18	1.65-01	1.0
787	*QQ(7, 4,E)	7	2	1	E	2330.7076	2571.2156	6	1.12-01	1.0
788	*QQ(10, 5,E)	10	3	1	E	2330.7583	2805.9948	6	2.53-01	1.0
789	*QQ(13, 6,A1)	13	4	1	A2	2330.7583	3118.5404	-3	1.41-01	1.0
790	PQ(10, 7,E)	10	6	-1	E	2330.8383	2793.4846	-22	6.26+00	1.0
791	*NQ(5, 5,E)	5	2	0	E	2330.8383	2451.0006	-5	1.35+00	1.0
792	PQ(8, 6,A)	8	5	-1	A	2330.8383	2631.7993	-9	1.84+01	*1.0
793	PQ(12, 8,E)	12	7	-1	E	2330.9676	2989.3911	362	3.07+00	.0
794	PQ(6, 5,E)	6	4	-1	E	2331.0921	2504.6218	10	1.18+01	1.0
795	*QQ(6, 4,E)	6	2	1	E	2331.3001	2509.6156	0	6.09-02	1.0
796	*NQ(9, 6,A)	9	3	0	A	2331.3963	2712.2307	5	5.66+00	*1.0
797	*QQ(12, 6,A1)	12	4	1	A2	2331.4953	3004.4872	-6	2.05-01	1.0
798	PQ(5, 5,E)	5	4	-1	E	2331.5394	2451.7018	7	8.74+00	1.0
799	PQ(7, 6,A)	7	5	-1	A	2331.6859	2561.5776	-12	2.03+01	*1.0
800	*QQ(12, 6,A2)	12	4	1	A1	2331.7239	3004.7158	6	1.36-01	1.0
801	PQ(9, 7,E)	9	6	-1	E	2331.8338	2705.7867	-24	7.90+00	1.0
802	PQ(11, 8,E)	11	7	-1	E	2331.8936	2884.0961	119	4.42+00	.0
803	*NQ(11, 7,E)	11	4	0	E	2331.9643	2892.0548	0	7.14-01	1.0
804	*NQ(8, 6,A)	8	3	0	A	2332.2105	2633.1715	15	4.45+00	*1.0
805	*QQ(11, 6,A1)	11	4	1	A2	2332.2437	2899.1247	9	1.85-01	1.0
806	*QQ(11, 6,A2)	11	4	1	A1	2332.3242	2899.2052	-9	2.25-01	1.0
807	PQ(6, 6,A)	6	5	-1	A	2332.3933	2500.0443	-9	1.57+01	*1.0
808	PQ(8, 7,E)	8	6	-1	E	2332.6982	2626.7379	-24	8.39+00	1.0
809	PQ(10, 8,E)	10	7	-1	E	2332.8318	2787.5349	20	5.66+00	1.0
810	*QQ(7, 5,E)	7	3	1	E	2332.8980	2568.6418	0	8.86-02	1.0
811	*NQ(7, 6,A)	7	3	0	A	2332.9584	2562.8501	19	2.48+00	*1.0
812	*QQ(10, 6,A)	10	4	1	A	2333.1123	2802.5967	15	4.12-01	*1.0
813	PQ(7, 7,E)	7	5	-1	E	2333.4523	2556.3867	-13	6.38+00	1.0

TABLE I—*Continued*

(I)	(II)	(III)	(IV)	(V)	(VI)	(VII)	(VIII)
814	*NG(6, 6,A)	6 3 0 A	2333.6361	2501.2871	14	7.38-01	*1.0
815	PQ(9, 8,E)	9 7 -1 E	2333.7109	2699.6692	-17	6.16+00	1.0
816	*OQ(9, 6,A)	9 4 1 A	2333.8654	2714.6998	7	3.41-01	*1.0
817	PQ(11, 9,A)	11 8 -1 A	2334.0063	2877.2003	216	7.62+00	* .0
818	*OQ(12, 7,E)	12 5 1 E	2334.0558	3000.3080	0	1.54-01	1.0
819	*NQ(9, 7,E)	9 4 0 E	2334.1533	2708.1061	8	3.70-01	1.0
820	PQ(8, 8,E)	8 7 -1 E	2334.5127	2620.5112	-22	4.82+00	1.0
821	*OQ(8, 6,A)	8 4 1 A	2334.5591	2635.5201	3	2.32-01	*1.0
822	PQ(10, 9,A)	10 8 -1 A	2334.8277	2780.4587	61	8.57+00	*1.0
823	*OQ(11, 7,E)	11 5 1 E	2334.8690	2894.9595	-12	1.68-01	1.0
824	RR(0, 0,A1)	1 1 1 A2	2335.0351	2335.0351	-17	1.86+01	1.0
825	*NQ(8, 7,E)	8 4 0 E	2335.1245	2629.1642	-6	1.77-01	1.0
826	*OQ(7, 6,A)	7 4 1 A	2335.1951	2565.0868	2	1.18-01	*1.0
827	PQ(9, 9,A)	9 8 -1 A	2335.6441	2692.4716	6	6.96+00	*1.0
828	*OQ(6, 6,A)	6 4 1 A	2335.7674	2503.4184	3	3.77-02	*1.0
829	PQ(11,10,E)	11 9 -1 E	2336.2282	2869.2679	373	2.86+00	.0
830	*OQ(9, 7,E)	9 5 1 E	2336.3711	2710.3239	1	1.20-01	1.0
831	PQ(10,10,E)	10 9 -1 E	2336.9104	2772.3146	121	2.41+00	.0
832	*OQ(8, 7,E)	8 5 1 E	2337.0411	2631.0807	11	7.07-02	1.0
833	*OQ(7, 7,E)	7 5 1 E	2337.6196	2560.5540	-8	2.54-02	1.0
834	*NQ(8, 8,E)	8 5 0 E	2338.1362	2624.1347	-1	5.65-03	1.0
835	PQ(11,11,E)	11 10 -1 E	2338.5388	2860.2492	538	1.60+00	.0
836	QR(1, 0,A2)	2 0 0 A1	2338.6585	2347.5628	0	1.03+01	1.0
837	QR(1, 1,E)	2 1 0 E	2338.6585	2347.0295	-11	7.96+00	1.0
838	*OQ(9, 8,E)	9 6 1 E	2339.1105	2705.0688	16	5.95-02	1.0
839	PQ(12,12,A)	12 11 -1 A	2340.4931	2956.2200	1206	2.05+00	* .0
840	RR(1, 1,E)	2 2 1 E	2342.6547	2351.0257	-21	2.67+01	1.0
841	RR(1, 0,A2)	2 1 1 A1	2343.7531	2352.6574	-14	2.67+01	1.0
842	PR(1, 1,E)	2 0 1 E	2344.9455	2353.3165	-8	4.38+00	1.0
843	QR(2, 0,A1)	3 0 0 A2	2347.2717	2373.9814	2	1.44+01	1.0
844	QR(2, 1,E)	3 1 0 E	2347.2717	2373.4489	-9	1.32+01	1.0
845	QR(2, 2,E)	3 2 0 E	2347.3119	2371.8857	-8	9.21+00	1.0
846	*SR(2, 1,E)	3 3 -1 E	2349.4976	2375.6748	15	2.37-02	1.0
847	RR(2, 2,E)	3 3 1 E	2350.2352	2374.8130	-25	4.03+01	1.0
848	*TR(3, 0,A2)	4 3 0 A1	2351.0758	2404.4858	-15	2.37-02	1.0
849	RR(2, 1,E)	3 2 1 E	2351.2984	2377.4756	-19	2.72+01	1.0
850	*SR(2, 0,A1)	3 2 -1 A2	2351.3235	2378.0332	0	4.27-02	1.0
851	RR(2, 0,A1)	3 1 1 A2	2352.3779	2379.0876	-7	3.25+01	1.0
852	*QR(2, 1,E)	3 1 -1 E	2353.2234	2379.4006	3	8.11-03	1.0
853	PR(2, 1,E)	3 0 1 E	2353.5843	2379.7615	-4	7.85+00	1.0
854	PR(2, 2,E)	3 1 -1 E	2354.8167	2379.3945	-2	2.74+00	1.0
855	QR(3, 0,A2)	4 0 0 A1	2355.7855	2409.1955	16	1.72+01	1.0
856	QR(3, 1,E)	4 1 0 E	2355.7855	2408.6640	6	1.67+01	1.0
857	QR(3, 2,E)	4 2 0 E	2355.7855	2407.0677	-10	1.42+01	1.0
858	QR(3, 3,A)	4 3 0 A	2355.8856	2404.5020	1	2.31+01	*1.0
859	*SR(3, 2,E)	4 4 -1 E	2356.3107	2407.5930	17	9.46-01	1.0
860	RR(3, 3,A)	4 4 1 A	2357.7998	2406.4162	-15	9.57+01	*1.0
861	*SR(3, 1,E)	4 3 -1 E	2358.0645	2410.9430	19	1.38-01	1.0
862	RR(3, 2,E)	4 3 1 E	2358.8061	2410.0886	-15	3.60+01	1.0
863	*TR(4, 0,A1)	5 3 0 A2	2359.4919	2448.4876	-6	6.38-02	1.0
864	RR(3, 1,E)	4 2 1 E	2359.8568	2412.7353	-10	2.68+01	1.0
865	*SR(3, 0,A2)	4 2 -1 A1	2359.9070	2413.3170	21	1.69-01	1.0
866	RR(3, 0,A2)	4 1 1 A1	2360.9062	2414.3162	1	3.53+01	1.0
867	*QR(3, 1,E)	4 1 -1 E	2361.7751	2414.6536	10	2.64-02	1.0
868	PR(3, 1,E)	4 0 1 E	2362.1346	2415.0131	3	1.00+01	1.0
869	PR(3, 2,E)	4 1 -1 E	2363.3699	2414.6522	9	5.33+00	1.0
870	*QR(3, 2,E)	4 0 1 E	2363.7363	2415.0186	8	1.31-02	1.0
871	QR(4, 2,E)	5 2 0 E	2364.1299	2451.0034	-2	1.59+01	1.0

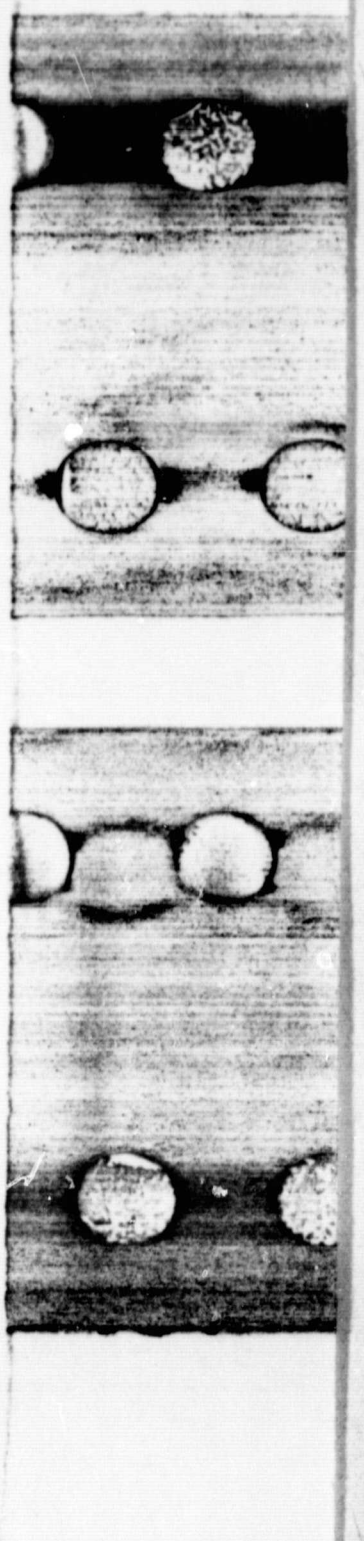

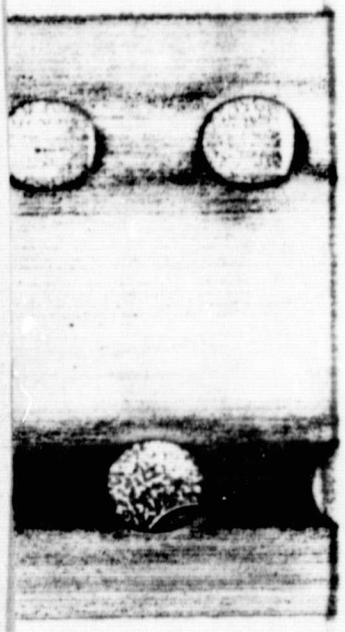

TABLE I—*Continued*

(I)	(II)	(III)				(IV)	(V)	(VI)	(VII)	(VIII)
872	QR(4, 0,A1)	5	0	0	A2	2364.1525	2453.1482	1	1.85+01	1.0
873	QR(4, 1,E)	5	1	0	E	2364.1525	2452.6181	-2	1.83+01	1.0
874	QR(4, 3,A)	5	3	0	A	2364.2855	2448.5000	5	3.67+01	*1.0
875	QR(4, 4,E)	5	4	0	E	2364.3119	2444.7926	-11	2.07+01	1.0
876	PR(3, 3,A1)	4	2	-1	A2	2364.6648	2413.2812	13	1.87+00	1.0
877	PR(3, 3,A2)	4	2	-1	A1	2364.6886	2413.3050	9	1.85+00	1.0
878	*SR(4, 2,E)	5	4	-1	E	2364.8336	2451.7071	13	2.59+00	1.0
879	RR(4, 4,E)	5	5	1	E	2365.3770	2445.8577	1	4.32+01	1.0
880	RR(4, 3,A)	5	4	1	A	2366.2998	2450.5143	-12	7.60+01	*1.0
881	*SR(4, 1,E)	5	3	-1	E	2366.5341	2454.9997	8	3.98-01	1.0
882	RR(4, 2,E)	5	3	1	E	2367.2759	2454.1494	-17	3.12+01	1.0
883	RR(4, 1,E)	5	2	1	E	2368.3145	2456.7801	-9	2.52+01	1.0
884	*SR(4, 0,A1)	5	2	-1	A2	2368.3731	2457.3686	5	4.74+01	1.0
885	RR(4, 0,A1)	5	1	1	A2	2369.3323	2458.3280	6	3.50+01	1.0
886	*QR(4, 1,E)	5	1	-1	E	2370.2280	2458.6936	11	8.16-02	1.0
887	PR(4, 1,E)	5	0	1	E	2370.5838	2459.0494	2	1.08+01	1.0
888	PR(4, 2,E)	5	1	-1	E	2371.8154	2458.6889	6	7.00+00	1.0
889	*QR(4, 2,E)	5	0	1	E	2372.1744	2459.0479	0	4.81-02	1.0
890	QR(5, 2,E)	6	2	0	E	2372.3329	2503.6718	1	1.59+01	1.0
891	QR(5, 0,A2)	6	0	0	A1	2372.3964	2505.8507	-7	1.83+01	1.0
892	QR(5, 1,E)	6	1	0	E	2372.3964	2505.3223	-2	1.82+01	1.0
893	RR(5, 5,E)	6	6	1	E	2372.3964	2492.5587	-1	5.21+01	1.0
894	QR(5, 4,E)	6	4	0	E	2372.5430	2497.5098	1	2.85+01	1.0
895	QR(5, 3,A)	6	3	0	A	2372.5905	2501.2791	6	4.22+01	*1.0
896	*TR(6, 1,E)	7	4	0	E	2372.7367	2558.9805	11	6.96-02	1.0
897	PR(4, 3,A2)	5	2	-1	A1	2373.0914	2457.3059	8	3.72+00	1.0
898	PR(4, 3,A1)	5	2	-1	A2	2373.1728	2457.3873	24	3.65+00	1.0
899	QR(5, 5,E)	6	5	0	E	2373.1728	2493.3351	-1	1.14+01	1.0
900	*SR(5, 2,E)	6	4	-1	E	2373.2784	2504.6173	6	3.99+00	1.0
901	*UR(7, 3,A)	8	7	1	A	2373.6311	2617.8299	0	2.93-02	*1.0
902	RR(5, 4,E)	6	5	1	E	2373.8512	2498.8180	0	2.84+01	1.0
903	*QR(4, 3,A2)	5	1	1	A1	2374.2784	2458.4930	-17	1.76-02	1.0
904	PR(4, 4,E)	5	3	-1	E	2374.5249	2455.6056	14	1.28+00	1.0
905	RR(5, 3,A)	6	4	1	A	2374.7250	2503.4135	-1	5.80+01	*1.0
906	*SR(5, 1,E)	6	3	-1	E	2374.9295	2507.8554	7	8.09-01	1.0
907	RR(5, 2,E)	6	3	1	E	2375.6735	2507.0124	-4	2.57+01	1.0
908	*TR(6, 0,A1)	7	3	0	A2	2376.0696	2562.8398	8	1.91+01	1.0
909	*SR(6, 5,E)	7	7	-1	E	2376.5348	2550.0645	-26	2.00-02	1.0
910	RR(5, 1,E)	6	2	1	E	2376.6882	2509.6141	-1	2.23+01	1.0
911	*SR(5, 0,A2)	6	2	-1	A1	2376.7866	2510.2409	14	1.07+00	1.0
912	RR(5, 0,A2)	6	1	1	A1	2377.6655	2511.1198	14	3.19+01	1.0
913	*SR(6, 4,E)	7	6	-1	E	2378.0599	2556.3754	-25	1.88-01	1.0
914	*QR(5, 1,E)	6	1	-1	E	2378.5848	2511.5107	6	1.55-01	1.0
915	PR(5, 1,E)	6	0	1	E	2378.9452	2511.8711	5	1.02+01	1.0
916	*SR(6, 3,A)	7	5	-1	A	2379.5449	2561.5677	-22	4.33+00	*1.0
917	RR(6, 6,A)	7	7	1	A	2379.9533	2547.6043	10	1.16+02	*1.0
918	PR(5, 2,E)	6	1	-1	E	2380.1759	2511.5148	10	7.56+00	1.0
919	QR(6, 2,E)	7	2	0	E	2380.3968	2565.0597	4	1.47+01	1.0
920	QR(6, 5,E)	7	5	0	E	2380.4369	2553.9666	-5	4.47+01	1.0
921	QR(6, 0,A1)	7	0	0	A2	2380.5223	2567.2925	2	1.68+01	1.0
922	QR(6, 1,E)	7	1	0	E	2380.5223	2566.7661	18	1.68+01	1.0
923	QR(6, 4,E)	7	4	0	E	2380.6568	2558.9723	3	2.94+01	1.0
924	QR(6, 3,A)	7	3	0	A	2380.8196	2562.8424	11	4.06+01	*1.0
925	QR(6, 6,A)	7	6	0	A	2381.3855	2549.0365	8	1.55+00	*1.0
926	PR(5, 3,A1)	6	2	-1	A2	2381.4097	2510.0982	0	4.90+00	1.0
927	PR(5, 3,A2)	6	2	-1	A1	2381.5526	2510.2411	15	4.70+00	1.0
928	RR(6, 5,E)	7	6	1	E	2381.6409	2555.1706	7	8.59+00	1.0
929	*SR(6, 2,E)	7	4	-1	E	2381.6409	2566.3038	1	4.83+00	1.0

TABLE I—*Continued*

(I)	(II)	(III)	(IV)	(V)	(VI)	(VII)	(VIII)
930	RH(6, 4,E)	7 5 1 E	2382.2476	2560.5630	0	1.87+01	1.0
931	*QR(5, 3,A2)	6 1 1 A1	2382.4297	2511.1186	13	8.94-02	1.0
932	*QR(5, 3,A1)	6 1 1 A2	2382.6778	2511.3663	1	4.16-02	1.0
933	PR(5, 4,E)	6 3 -1 E	2382.8900	2507.8568	9	2.49+00	1.0
934	RR(6, 3,A)	7 4 1 A	2383.0582	2565.0810	-3	4.24+01	*1.0
935	*SR(6, 1,E)	7 3 -1 E	2383.2342	2569.4780	0	1.31+00	1.0
936	*NR(5, 5,E)	6 2 0 E	2383.5111	2503.6735	3	1.74+01	1.0
937	RR(6, 2,E)	7 3 1 E	2383.9759	2568.6388	-2	2.01+01	1.0
938	*TR(7, 0,A2)	8 3 0 A1	2384.2346	2633.1596	3	2.43+01	1.0
939	PR(5, 5,E)	6 4 -1 E	2384.4534	2504.6158	4	7.39+01	1.0
940	*SR(7, 5,E)	8 7 -1 E	2384.7533	2620.4971	-36	7.69-02	1.0
941	RR(6, 1,E)	7 2 1 E	2384.9711	2571.2149	5	1.87+01	1.0
942	*SR(6, 0,A1)	7 2 -1 A2	2385.1190	2571.8892	17	2.10+00	1.0
943	*NR(6, 3,A1)	7 0 0 A2	2385.2691	2567.2919	1	2.39+01	1.0
944	RR(6, 0,A1)	7 1 1 A2	2385.9050	2572.6752	20	2.66+01	1.0
945	*QR(6, 1,E)	7 1 -1 E	2386.8615	2573.1053	10	2.42-01	1.0
946	*QR(5, 5,E)	6 3 1 E	2386.8615	2507.0239	6	7.01-03	1.0
947	PR(6, 1,E)	7 0 1 E	2387.2158	2573.4596	7	8.80+00	1.0
948	RR(7, 7,E)	8 8 1 E	2387.3411	2610.2755	23	5.16+01	1.0
949	*SR(7, 3,A)	8 5 -1 A	2387.5806	2631.7794	-29	7.19+00	*1.0
950	RR(7, 6,A)	8 7 1 A	2387.9400	2617.8317	1	9.12+01	*1.0
951	QR(7, 2,E)	8 2 0 E	2388.3143	2635.1414	0	1.27+01	1.0
952	QR(7, 5,E)	8 5 0 E	2388.3912	2624.1350	-1	3.63+01	1.0
953	PR(6, 2,E)	7 1 -1 E	2388.4440	2573.1069	12	7.15+00	1.0
954	QR(7, 1,E)	8 1 0 E	2388.4627	2636.8636	0	1.44+01	1.0
955	QR(7, 0,A2)	8 0 0 A1	2388.4952	2637.4202	2	1.45+01	1.0
956	QR(7, 4,E)	8 4 0 E	2388.6691	2629.1771	6	2.63+01	1.0
957	*QR(6, 2,E)	7 0 1 E	2388.7973	2573.4602	8	1.79-01	1.0
958	QR(7, 3,A)	8 3 0 A	2388.9663	2633.1651	8	3.45+01	*1.0
959	PR(6, 3,A2)	7 2 -1 A1	2389.6307	2571.6535	0	5.26+00	1.0
960	QR(7, 7,E)	8 7 0 E	2389.6307	2612.5651	8	5.92-02	1.0
961	QR(7, 6,A)	8 6 0 A	2389.7069	2619.5986	11	2.63+00	*1.0
962	PR(6, 3,A1)	7 2 -1 A2	2389.8612	2571.8840	12	4.85+00	1.0
963	*SR(7, 2,E)	8 4 -1 E	2389.8975	2636.7246	-14	4.96+00	1.0
964	RR(7, 5,E)	8 6 1 E	2390.0003	2625.7441	6	6.27+00	1.0
965	*PR(7, 2,E)	8 1 0 E	2390.0407	2636.8678	5	3.80-01	1.0
966	RR(7, 4,E)	8 5 1 E	2390.5604	2631.0684	-1	1.21+01	1.0
967	*QR(6, 3,A1)	7 1 1 A2	2390.6513	2572.6741	19	2.23-01	1.0
968	*QR(6, 3,A2)	7 1 1 A1	2390.9577	2572.9805	-7	7.17-02	1.0
969	PR(6, 4,E)	7 3 -1 E	2391.1629	2569.4784	0	3.14+00	1.0
970	RR(7, 3,A)	8 4 1 A	2391.3165	2635.5153	-1	2.96+01	*1.0
971	*SR(7, 1,E)	8 3 -1 E	2391.4564	2639.8573	-1	1.76+00	1.0
972	*NR(6, 5,E)	7 2 0 E	2391.5284	2565.0581	3	4.11-01	1.0
973	RR(7, 2,E)	8 3 1 E	2392.1963	2639.0234	0	1.49+01	1.0
974	*TR(8, 0,A1)	9 3 0 A2	2392.3249	2712.2220	-2	2.68-01	1.0
975	PR(6, 5,E)	7 4 -1 E	2392.7745	2566.3042	2	1.37+00	1.0
976	*QR(6, 4,E)	7 2 1 E	2392.8979	2571.2133	3	6.27-02	1.0
977	*TR(9, 2,E)	10 5 0 E	2393.0148	2790.6019	0	7.88-02	1.0
978	RR(7, 1,E)	8 2 1 E	2393.1605	2641.5614	7	1.48+01	1.0
979	*NR(7, 3,A2)	8 0 0 A1	2393.2283	2637.4271	9	3.10-01	1.0
980	*SR(7, 0,A2)	8 2 -1 A1	2393.3632	2642.2882	9	3.74+00	1.0
981	PR(6, 6,A)	7 5 -1 A	2393.9236	2561.5746	-15	1.13+00	*1.0
982	RR(7, 0,A2)	8 1 1 A1	2394.0588	2642.9838	20	1.97+01	1.0
983	RR(8, 8,E)	9 9 1 E	2394.6553	2680.6538	37	4.28+01	1.0
984	*UR(8, 0,A1)	9 4 1 A2	2394.7975	2714.6946	2	2.34-01	1.0
985	*QR(7, 1,E)	8 1 -1 E	2395.0443	2643.4452	5	3.20-01	1.0
986	*QR(6, 5,E)	7 3 1 E	2395.1004	2568.6301	-10	2.72-02	1.0
987	RR(8, 7,E)	9 8 1 E	2395.2583	2689.2979	6	3.88+01	1.0

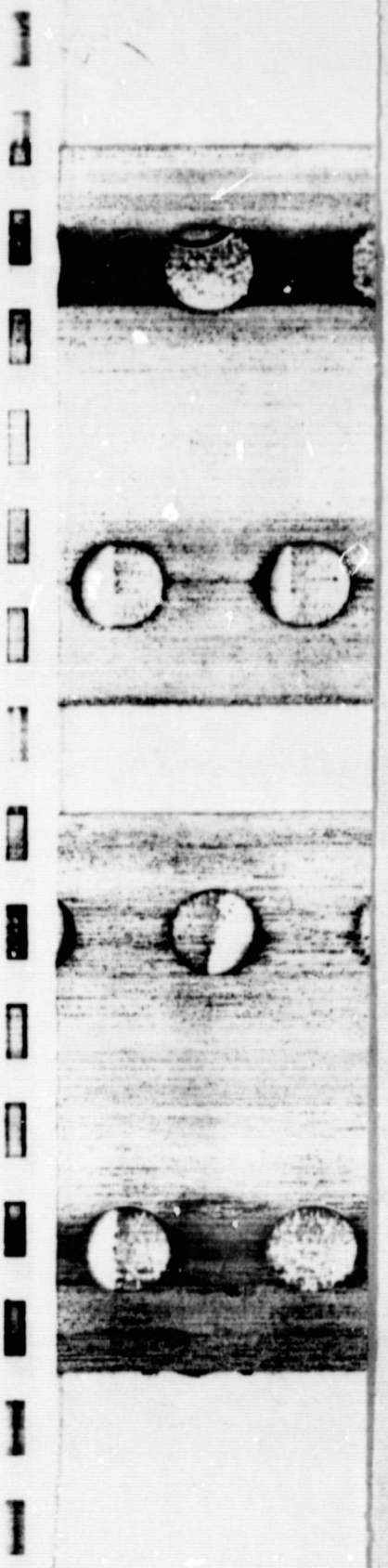

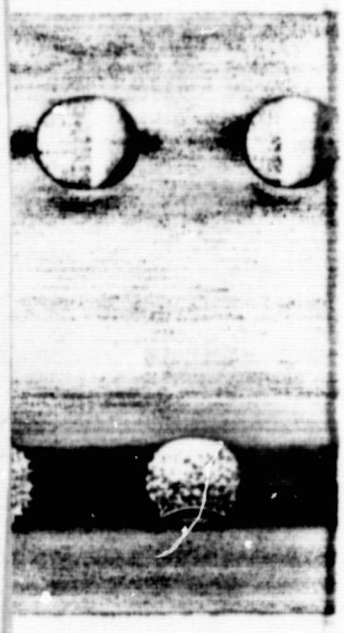

TABLE I—*Continued*

(I)	(II)	(III)	(IV)	(V)	(VI)	(VII)	(VIII)
988	PR(7, 1,E)	8 0 1 E	2395.4011	2643.8020	11	6.93+00	1.0
989	*SR(8, 3,A)	9 5 -1 A	2395.4639	2710.6588	-24	9.13+00	*1.0
990	RR(8, 6,A)	9 7 1 A	2395.8023	2696.7633	-1	6.81+01	*1.0
991	QR(8, 2,E)	9 2 0 E	2396.0910	2713.9009	-2	1.04+01	1.0
992	QR(8, 5,E)	9 5 0 E	2396.2443	2703.0273	6	2.79+01	1.0
993	QR(8, 1,E)	9 1 0 E	2396.2694	2715.6451	1	1.18+01	1.0
994	QR(8, 0,A1)	9 0 0 A2	2396.3168	2716.2140	1	1.17+01	1.0
995	*NR(7, 4,E)	8 1 0 E	2396.3595	2636.8675	4	2.95-01	1.0
996	QR(8, 4,E)	9 4 0 E	2396.5827	2708.1057	8	2.13+01	1.0
997	PR(7, 2,E)	8 1 -1 E	2396.6242	2643.4513	11	6.07+00	1.0
998	*QR(7, 2,E)	8 0 1 E	2396.9810	2643.8081	17	2.62-01	1.0
999	QR(8, 3,A)	9 3 0 A	2397.0323	2712.2272	2	2.64+01	*1.0
1000	*UR(10, 3,A)	11 7 1 A	2397.0917	2880.6396	-6	9.96-02	*1.0
1001	PR(7, 3,A1)	8 2 -1 A2	2397.7427	2641.9415	0	4.95+00	1.0
1002	QR(8, 8,E)	9 8 0 E	2397.8302	2683.8287	18	4.95-03	1.0
1003	QR(8, 7,E)	9 7 0 E	2397.8302	2691.8698	16	2.50-01	1.0
1004	*PR(8, 2,E)	9 1 0 E	2397.8302	2715.6401	-3	2.24-01	1.0
1005	QR(8, 6,A)	9 6 0 A	2397.9588	2698.9198	10	3.01+00	*1.0
1006	*SR(8, 2,E)	9 4 -1 E	2398.0792	2715.8891	-4	4.92+00	1.0
1007	PR(7, 3,A2)	8 2 -1 A1	2398.0792	2642.2780	0	4.19+00	1.0
1008	RR(8, 5,E)	9 6 1 E	2398.2693	2705.0523	0	4.43+00	1.0
1009	*VR(9, 0,A2)	10 5 -1 A1	2398.5200	2798.1826	-4	1.38-01	1.0
1010	RR(8, 4,E)	9 5 1 E	2398.7943	2710.3173	-5	7.72+00	1.0
1011	*UR(9, 1,E)	10 5 1 E	2399.1349	2798.2790	-19	9.41-02	1.0
1012	*QR(7, 3,A1)	8 1 1 A2	2399.1648	2643.3636	0	1.01+01	1.0
1013	PR(7, 4,E)	8 3 -1 E	2399.3499	2639.8579	0	3.18+00	1.0
1014	*NR(7, 5,E)	8 2 0 E	2399.4004	2635.1442	3	5.86-01	1.0
1015	RR(8, 3,A)	9 4 1 A	2399.5016	2714.6965	4	1.98+01	*1.0
1016	*SR(8, 1,E)	9 3 -1 E	2399.5805	2718.9562	-7	2.03+00	1.0
1017	RR(8, 2,E)	9 3 1 E	2400.3397	2718.1496	3	1.03+01	1.0
1018	*TR(10, 2,E)	11 5 0 E	2400.7120	2886.8438	-10	8.18-02	1.0
1019	PR(7, 5,E)	8 4 -1 E	2400.9947	2636.7385	0	1.65+00	1.0
1020	*NR(8, 3,A1)	9 0 0 A2	2401.0205	2716.2154	2	3.02-01	1.0
1021	*QR(7, 4,E)	8 2 1 E	2401.0587	2641.5667	12	1.14+01	1.0
1022	RR(8, 1,E)	9 2 1 E	2401.2668	2720.6425	11	1.09+01	1.0
1023	*SR(8, 0,A1)	9 2 -1 A2	2401.5209	2721.4181	7	5.92+00	1.0
1024	PR(7, 6,A)	8 5 -1 A	2401.9053	2631.7970	-12	1.95+00	*1.0
1025	RR(9, 9,A)	10 10 1 A	2401.9053	2758.7328	44	6.76+01	*1.0
1026	RR(8, 0,A1)	9 1 1 A2	2402.1554	2722.0526	19	1.22+01	1.0
1027	*SR(9, 4,E)	10 6 -1 E	2402.1554	2793.4913	-16	1.32+00	1.0
1028	RR(9, 8,E)	10 9 1 E	2402.4852	2768.4435	9	3.07+01	1.0
1029	*UR(9, 0,A2)	10 4 1 A1	2402.9229	2802.5855	4	5.56-01	1.0
1030	RR(9, 7,E)	10 8 1 E	2403.0387	2776.9915	-2	2.77+01	1.0
1031	*QR(8, 1,E)	9 1 -1 E	2403.1589	2722.5346	11	3.68-01	1.0
1032	*SR(9, 3,A)	10 5 -1 A	2403.1873	2798.1743	-13	9.33+00	*1.0
1033	*NR(7, 6,A)	8 3 0 A	2403.2812	2633.1729	16	4.36-01	*1.0
1034	*QR(7, 5,E)	8 3 1 E	2403.2812	2639.0250	2	6.15-02	1.0
1035	PR(8, 1,E)	9 0 1 E	2403.5050	2722.8807	16	5.03+00	1.0
1036	RR(9, 6,A)	10 7 1 A	2403.5425	2784.3769	-1	4.85+01	*1.0
1037	QR(9, 2,E)	10 2 0 E	2403.7255	2801.3126	-3	8.09+00	1.0
1038	PR(7, 7,E)	8 6 -1 E	2403.8028	2626.7372	-25	4.19-01	1.0
1039	QR(9, 1,E)	10 1 0 E	2403.9200	2803.0641	0	9.01+00	1.0
1040	QR(9, 0,A2)	10 0 0 A1	2403.9814	2803.6440	-12	8.61+00	1.0
1041	QR(9, 5,E)	10 5 0 E	2403.9814	2790.6044	3	2.03+01	1.0
1042	*NR(8, 4,E)	9 1 0 E	2404.1239	2715.6469	3	3.58-01	1.0
1043	QR(9, 4,E)	10 4 0 E	2404.3945	2795.7304	-1	1.58+01	1.0
1044	PR(8, 2,E)	9 1 -1 E	2404.7190	2722.5289	5	4.67+00	1.0
1045	QR(9, 3,A)	10 3 0 A	2405.0092	2799.9962	-7	1.89+01	*1.0

TABLE I—*Continued*

(I)	(II)	(III)	(IV)	(V)	(VI)	(VII)	(VIII)
1046	*QR(8. 2.E)	9 0 1 E	2405.0659	2722.8758	11	3.37-01	1.0
1047	*PR(9. 2.E)	10 1 0 E	2405.6724	2803.0595	-4	2.83-01	1.0
1048	*QR(7. 6.A)	8 4 1 A	2405.6334	2635.5251	8	5.39-02	*1.0
1049	PR(8. 3.A2)	9 2 -1 A1	2405.7364	2720.9313	-6	4.19+00	1.0
1050	QR(9. 8.E)	10 8 0 E	2405.9044	2771.8627	9	8.22-02	1.0
1051	QR(9. 9.A)	10 9 0 A	2405.9536	2762.7811	23	3.15-03	*1.0
1052	QR(9. 7.E)	10 7 0 E	2405.9536	2779.9065	0	4.56-01	1.0
1053	QR(9. 6.A)	10 6 0 A	2406.1242	2786.9586	-9	2.82+00	*1.0
1054	*SR(9. 2.E)	10 4 -1 E	2406.1242	2803.7113	-21	4.24+00	1.0
1055	PR(8. 3.A1)	9 2 -1 A2	2406.2224	2721.4173	6	2.96+00	1.0
1056	RR(9. 5.E)	10 6 1 E	2406.4502	2793.0732	-14	3.02+00	1.0
1057	*QR(8. 3.A1)	9 1 1 A2	2406.8569	2722.0518	19	9.11-01	1.0
1058	RR(9. 4.E)	10 5 1 E	2406.9500	2798.2859	-13	4.80+00	1.0
1059	*NR(8. 5.E)	9 2 0 E	2407.1204	2713.9034	0	6.49-01	1.0
1060	*QR(8. 3.A2)	9 1 1 A1	2407.2839	2722.4788	5	1.20-01	1.0
1061	PR(8. 4.E)	9 3 -1 E	2407.4304	2718.9534	-10	2.77+00	1.0
1062	*SR(9. 1.E)	10 3 -1 E	2407.6027	2806.7468	-13	2.03+00	1.0
1063	RR(9. 3.A)	10 4 1 A	2407.6027	2802.5897	8	1.30+01	*1.0
1064	*TR(10. 0.A1)	11 3 0 A2	2408.2520	2896.4484	-10	2.39-01	1.0
1065	RR(9. 2.E)	10 3 1 E	2408.4011	2805.9882	0	6.76+00	1.0
1066	*NR(9. 3.A2)	10 0 0 A1	2408.6623	2803.6493	-7	1.74-01	1.0
1067	PR(8. 5.E)	9 4 -1 E	2409.0924	2715.8755	-18	1.61+00	1.0
1068	RR(10.10.E)	11 11 1 E	2409.0924	2844.4966	39	2.54+01	1.0
1069	*QR(8. 4.E)	9 2 1 E	2409.1209	2720.6439	12	1.68-01	1.0
1070	RR(9. 1.E)	10 2 1 E	2409.2819	2808.4260	6	7.62+00	1.0
1071	*SR(9. 0.A2)	10 2 -1 A1	2409.5568	2809.2194	0	7.45+00	1.0
1072	RR(10. 9.A)	11 10 1 A	2409.6472	2855.2782	10	4.62+01	*1.0
1073	PR(8. 6.A)	9 5 -1 A	2409.7045	2710.6655	-17	2.14+00	*1.0
1074	*SR(10. 4.E)	11 6 -1 E	2409.9429	2889.8626	52	1.69+00	1.0
1075	RR(10. 8.E)	11 9 1 E	2410.1783	2864.3814	-2	2.07+01	1.0
1076	RR(9. 0.A2)	10 1 1 A1	2410.2135	2809.6761	4	5.76+00	1.0
1077	RR(10. 7.E)	11 8 1 E	2410.6843	2873.3308	-4	1.48+01	1.0
1078	*SR(10. 3.A)	11 5 -1 A	2410.7600	2894.3079	9	8.21+00	*1.0
1079	*UR(10. 0.A1)	11 4 1 A2	2410.9306	2899.1250	9	1.67+00	1.0
1080	RR(10. 6.A)	11 7 1 A	2411.1587	2880.6431	-3	3.30+01	*1.0
1081	QR(10. 2.E)	11 2 0 E	2411.2099	2897.3417	-8	5.96+00	1.0
1082	*QR(9. 1.E)	10 1 -1 E	2411.2099	2810.3540	24	3.84-01	1.0
1083	*NR(8. 6.A)	9 3 0 A	2411.2720	2712.2330	8	7.79-01	*1.0
1084	*QR(8. 5.E)	9 3 1 E	2411.3710	2718.1541	8	1.05-01	1.0
1085	QR(10. 1.E)	11 1 0 E	2411.4119	2899.0910	-4	6.52+00	1.0
1086	QR(10. 0.A1)	11 0 0 A2	2411.5102	2899.7046	-55	5.04+00	1.0
1087	PR(9. 1.E)	10 0 1 E	2411.5301	2810.6742	18	3.35+00	1.0
1088	QR(10. 5.E)	11 5 0 E	2411.6147	2886.8511	-3	1.40+01	1.0
1089	PR(8. 7.E)	9 6 -1 E	2411.7409	2705.7805	-31	7.57-01	1.0
1090	*NR(9. 4.E)	10 1 0 E	2411.7409	2803.0768	12	3.60-01	1.0
1091	QR(10. 4.E)	11 4 0 E	2412.1286	2892.0483	-6	1.07+01	1.0
1092	PR(9. 2.E)	10 1 -1 E	2412.7458	2810.3329	2	3.26+00	1.0
1093	QR(10. 3.A)	11 3 0 A	2412.9006	2896.4485	-7	1.28+01	*1.0
1094	*PR(10. 2.E)	11 1 0 E	2412.9570	2899.0888	-6	2.78-01	1.0
1095	*QR(9. 2.E)	10 0 1 E	2413.0785	2810.6656	10	3.90-01	1.0
1096	*TR(11. 0.A2)	12 3 0 A1	2413.5727	2999.0358	47	1.69-01	1.0
1097	PR(9. 3.A1)	10 2 -1 A2	2413.6175	2808.6045	-11	3.26+00	1.0
1098	PR(8. 8.E)	9 7 -1 E	2413.6772	2699.6757	-11	2.81-01	1.0
1099	*QR(8. 6.A)	9 4 1 A	2413.7405	2714.7015	9	1.10-01	*1.0
1100	QR(10. 8.E)	11 8 0 E	2413.9378	2868.6409	3	2.04-01	1.0
1101	QR(10. 9.A)	11 9 0 A	2413.9378	2859.5688	24	9.83-02	*1.0
1102	QR(10.10.E)	11 10 0 E	2414.0120	2849.4162	39	3.21-03	1.0
1103	QR(10. 7.E)	11 7 0 E	2414.0339	2876.6805	-8	5.48-01	1.0

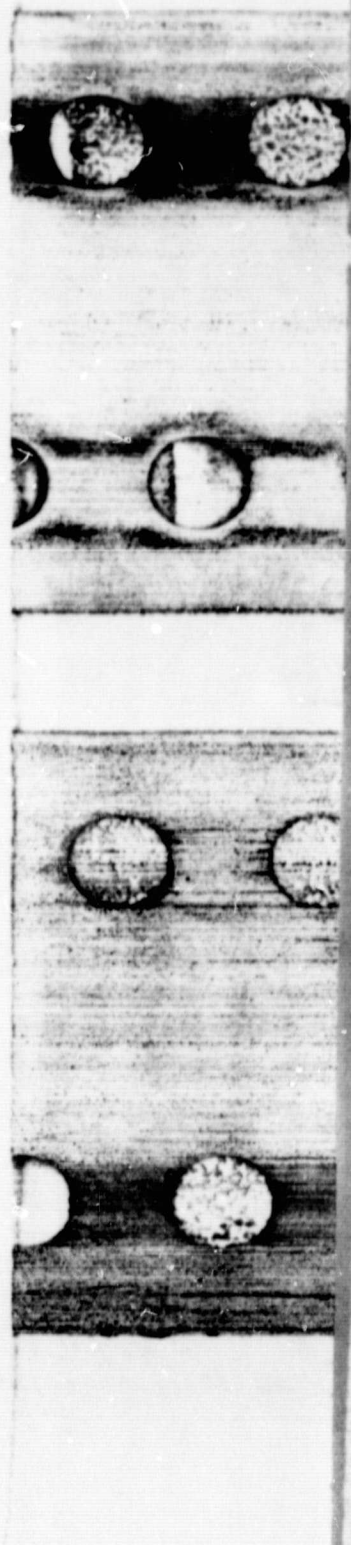

TABLE I—*Continued*

(I)	(II)	(III)				(IV)	(V)	(VI)	(VII)	(VIII)
1104	*SR(10, 2,E)	11	4	-1	E	2414.0739	2900.2057	-19	3.37+00	1.0
1105	QR(10, 6,A)	11	6	0	A	2414.2331	2883.7175	-20	2.30+00	*1.0
1106	PR(9, 3,A2)	10	2	-1	A1	2414.2331	2809.2201	0	1.63+00	1.0
1107	RR(10, 5,E)	11	6	1	E	2414.5615	2889.7979	-24	1.99+00	1.0
1108	*NR(9, 5,E)	10	2	0	E	2414.6919	2801.3149	-1	6.10-01	1.0
1109	*OR(9, 3,A2)	10	1	1	A1	2414.8899	2809.8769	5	1.31+00	1.0
1110	RR(10, 4,E)	11	5	1	E	2415.0324	2894.9521	-19	2.91+00	1.0
1111	*OR(9, 3,A1)	10	1	1	A2	2415.3185	2810.3055	12	1.22+01	1.0
1112	PR(9, 4,E)	10	3	-1	E	2415.4053	2806.7412	-19	2.15+00	1.0
1113	*SR(10, 1,E)	11	3	-1	E	2415.5130	2903.1921	-25	1.7[illegible]+00	1.0
1114	RR(10, 3,A1)	11	4	1	A2	2415.5796	2899.1275	12	4.20+00	1.0
1115	RR(10, 3,A2)	11	4	1	A1	2415.6491	2899.1970	-18	3.62+00	1.0
1116	*PR(11, 0,A2)	12	5	-1	A1	2416.1119	3001.5750	28	2.02+01	1.0
1117	*NR(10, 3,A1)	11	0	0	A2	2416.1721	2899.7200	-40	3.68-05	1.0
1118	RR,11,11,E)	12	12	1	E	2416.2076	2937.9181	7	1.83+01	1.0
1119	*OR(8, 7,E)	9	5	1	E	2416.2887	2710.3283	5	2.24-02	1.0
1120	RR(10, 2,E)	11	3	1	E	2416.3844	2902.5162	-7	4.20+00	1.0
1121	RR(11,10,E)	12	11	1	E	2416.7344	2949.7740	-10	1.66+01	1.0
1122	PR(9, 5,E)	10	4	-1	E	2417.0907	2803.7137	-19	1.36+00	1.0
1123	RR(10, 1,E)	11	2	1	E	2417.2084	2904.8875	-5	5.02+00	1.0
1124	RR(11, 9,A)	12	10	1	A	2417.2347	2960.4288	-17	3.00+01	*1.0
1125	PR(9, 6,A)	10	5	-1	A	2417.3468	2798.1812	-6	1.89+00	*1.0
1126	*SR(10, 0,A1)	11	2	-1	A2	2417.4529	2905.6473	-20	6.97+00	1.0
1127	*SR(11, 4,E)	12	6	-1	E	2417.5804	2994.8251	147	1.71+00	.0
1128	RR(11, 8,E)	12	9	1	E	2417.6713	2969.8738	-62	1.36+01	1.0
1129	RR(11, 7,E)	12	8	1	E	2418.1923	2978.2828	-7	1.22+01	1.0
1130	QR(11, 3,A)	12	3	0	A	2418.1923	2999.0405	52	6.45+00	*1.0
1131	RR(10, 0,A1)	11	1	1	A2	2418.2672	2906.4616	-12	2.15+00	1.0
1132	QR(11, 2,E)	12	2	0	E	2418.5598	3001.9743	0	4.17+00	1.0
1133	QR(11, 0,A2)	12	0	0	A1	2418.6175	3004.0806	32	3.75+00	1.0
1134	QR(11, 6,A)	12	6	0	A	2418.6498	2985.5308	-15	2.14+01	*1.0
1135	QR(11, 1,E)	12	1	0	E	2418.7471	3003.6984	-11	4.46+00	1.0
1136	QR(11, 5,E)	12	5	0	E	2419.1603	2991.7538	-6	9.00+00	1.0
1137	*QR(10, 1,E)	11	1	-1	E	2419.1603	2906.8394	-3	3.68+01	1.0
1138	*NR(10, 4,E)	11	1	0	E	2419.1947	2899.1144	18	3.11-01	1.0
1139	*QR(11, 0,A2)	12	4	1	A1	2419.2549	3004.7180	8	9.20-01	1.0
1140	*OR(9, 5,E)	10	3	1	E	2419.3687	2805.9917	3	1.43+01	1.0
1141	PR(10, 1,E)	11	0	1	E	2419.4680	2907.1471	3	2.06+00	1.0
1142	PR(9, 7,E)	10	6	-1	E	2419.5476	2793.5005	-7	8.65-01	1.0
1143	QR(11, 4,E)	12	4	0	E	2419.8090	2997.0537	9	6.75+00	1.0
1144	*PR(11, 2,E)	12	1	0	E	2420.2921	3003.7066	-3	2.39-01	1.0
1145	PR(10, 2,E)	11	1	-1	E	2420.7209	2906.8527	9	2.05+00	1.0
1146	*SR(11, 3,A)	12	5	-1	A	2420.7209	3001.5691	22	8.24+00	*1.0
1147	*OR(10, 2,E)	11	0	1	E	2421.0168	2907.1487	5	4.15-01	1.0
1148	PR(10, 3,A2)	11	2	-1	A1	2421.3847	2904.9326	-17	2.35+00	1.0
1149	PR(9, 8,E)	10	7	-1	E	2421.5772	2787.5355	21	5.00-01	1.0
1150	*QR(9, 6,A)	10	4	1	A	2421.7650	2802.5994	18	1.65-01	*1.0
1151	QR(11, 8,E)	12	8	0	E	2421.9264	2974.1289	-7	2.84-01	1.0
1152	*SR(11, 2,E)	12	4	-1	E	2421.9264	3005.3409	2	2.47+00	1.0
1153	QR(11, 7,E)	12	7	0	E	2422.0630	2982.1535	-15	5.20-01	1.0
1154	PR(10, 3,A1)	11	2	-1	A2	2422.1103	2905.6582	-9	7.35-01	1.0
1155	*NR(10, 5,E)	11	2	0	E	2422.1103	2897.3467	-3	5.06-01	1.0
1156	RR(11, 6,A)	12	7	1	A	2422.2858	2989.1668	-21	1.70+00	*1.0
1157	RR(11, 5,E)	12	6	1	E	2422.6154	2995.2089	-16	1.26+00	1.0
1158	*SR(11, 1,E)	12	3	1	E	2422.7553	3007.7066	-9	1.55-01	1.0
1159	*OR(10, 3,A1)	11	1	1	A2	2422.9158	2906.4637	-10	1.33+00	1.0
1160	RR(11, 4,E)	12	5	1	E	2423.0549	3000.2996	-9	1.75+00	1.0
1161	*NR(11, 3,A2)	12	5	0	A1	2423.2276	3004.0758	27	2.04+00	1.0

TABLE I—*Continued*

(I)	(II)	(III)				(IV)	(V)	(VI)	(VII)	(VIII)
1162	AR(12,12,A)	13	13	1	A	2423.2653	3038.9922	-39	2.51+01	*1.0
1163	PR(10, 4,E)	11	3	-1	E	2423.2653	2903.1850	-32	1.50+00	1.0
1164	*SR(11, 1,E)	12	3	-1	E	2423.3348	3008.2861	-20	1.27+00	1.0
1165	RR(11, 3,A1)	12	4	1	A2	2423.6342	3004.4824	-11	2.09+00	1.0
1166	PR(9, 4,A)	10	8	-1	A	2423.6342	2740.4616	64	3.64-01	*1.0
1167	AR(12,11,E)	13	12	1	E	2423.8023	3051.9672	-3	1.13+01	1.0
1168	RR(12,10,E)	13	11	1	E	2424.3036	3063.7102	37	1.03+01	1.0
1169	RR(11, 2,E)	12	3	1	E	2424.3036	3007.7181	1	2.50+00	1.0
1170	*OR(9, 7,E)	10	5	1	E	2424.3469	2798.2497	0	4.16-02	1.0
1171	RR(12, 9,A)	13	10	1	A	2424.7571	3074.2405	52	1.86+01	*1.0
1172	PR(10, 6,A)	11	5	-1	A	2424.8331	2894.3175	19	1.47+00	*1.0
1173	PR(10, 5,E)	11	4	-1	E	2424.9718	2900.2083	-17	1.03+00	1.0
1174	RR(11, 1,E)	12	2	1	E	2425.0469	3009.9982	-21	3.16+00	1.0
1175	RR(12, 8,E)	13	9	1	E	2425.1438	3083.5673	6	8.37+00	1.0
1176	RR(11, 0,A2)	12	1	1	A1	2425.2313	3010.6944	-46	5.23+00	1.0
1177	QR(12, 3,A)	13	3	0	A	2425.5094	3112.3651	137	4.62+00	* .0
1178	RR(12, 7,E)	13	8	1	E	2425.5421	3091.7943	-40	7.49+00	1.0
1179	QR(12, 2,E)	13	2	0	E	2425.7638	3115.1671	11	2.76+00	1.0
1180	QR(12, 0,A1)	13	0	0	A2	2425.8590	3117.2958	25	3.04+00	1.0
1181	QR(12, 1,E)	13	1	0	E	2425.9457	3116.8745	-8	2.85+00	1.0
1182	QR(12, 6,A)	13	6	0	A	2426.0372	3099.0291	-27	1.31+01	*1.0
1183	*SR(11, 0,A2)	12	2	-1	A1	2426.3293	3011.7924	-13	7.31-01	1.0
1184	*NR(11, 4,E)	12	1	0	E	2426.4575	3003.7022	-8	2.31-01	1.0
1185	QR(12, 5,E)	13	5	0	E	2426.7017	3105.3637	64	5.46+00	1.0
1186	*NR(10, 6,A)	11	3	0	A	2426.9721	2896.4565	0	9.37-01	*1.0
1187	*QR(11, 1,E)	12	1	-1	E	2427.0852	3012.0365	-7	3.43-01	1.0
1188	PR(10, 7,E)	11	6	-1	E	2427.2096	2889.8561	46	7.78-01	1.0
1189	*QR(10, 5,E)	11	3	1	E	2427.2792	2902.5157	-7	1.61-01	1.0
1190	PR(11, 1,E)	12	0	1	E	2427.3566	3012.3079	-3	1.13+00	1.0
1191	*PR(12, 2,E)	13	1	0	E	2427.4742	3116.87 5	-5	1.90-01	1.0
1192	QR(12, 4,E)	13	4	0	E	2427.5237	3110.8025	134	3.97+00	.0
1193	*SR(12, 3,A)	13	5	-1	A	2428.5328	3115.3885	149	5.00+00	* .0
1194	PR(11, 2,E)	12	1	-1	E	2428.6229	3012.0374	-7	1.13+00	1.0
1195	*QR(11, 2,E)	12	0	1	E	2428.8951	3012.3096	-1	4.20-01	1.0
1196	PR(11, 3,A1)	12	2	-1	A2	2429.0392	3009.8874	-26	1.58+00	1.0
1197	PR(10, 8,E)	11	7	-1	E	2429.3954	2884.0985	121	5.65-01	.0
1198	*NR(11, 5,E)	12	2	0	E	2429.3954	3001.9889	15	3.80-01	1.0
1199	*QR(10, 6,A1)	11	4	1	A2	2429.6458	2899.1302	14	8.72-02	1.0
1200	*SR(12, 2,E)	13	4	-1	E	2429.7176	3119.1208	82	1.66+00	1.0
1201	*QR(10, 6,A2)	11	4	1	A1	2429.7176	2899.2020	-13	1.05-01	1.0
1202	QR(12, 9,A)	13	9	0	A	2429.7576	3079.2410	-24	3.71-01	*1.0
1203	QR(12, 8,E)	13	8	0	E	2429.8890	3088.3125	-2	2.90-01	1.0
1204	*QR(11, 3,A2)	12	1	1	A1	2429.8890	3010.7372	-3	3.13-01	1.0
1205	QR(12, 7,E)	13	7	0	E	2430.0951	3096.3473	35	4.22-01	1.0
1206	RR(12, 6,A)	13	7	1	A	2430.3467	3103.3386	53	1.17+00	*1.0
1207	*NR(12, 3,A1)	13	0	0	A2	2430.4444	3117.3001	29	9.53-01	1.0
1208	RR(12, 5,E)	13	6	1	E	2430.6694	3109.3314	66	7.84-01	1.0
1209	PR(11, 3,A2)	12	2	-1	A1	2430.9386	301[illegible]7868	-18	1.05+00	1.0
1211	PR(11, 4,E)	12	3	-1	E	2431.0516	30[illegible]7963	-10	9.46-01	1.0
1212	RR(12, 4,E)	13	5	1	E	2431.0880	3114.3668	97	1.04+00	1.0
1213	*SR(12, 1,E)	13	3	-1	E	2431.0880	3122.0168	6	7.15-01	1.0
1214	*QR(11, 3,A1)	12	1	1	A2	2431.1434	3011.9916	22	9.01-02	1.0
1215	RR(12, 3,A2)	13	4	1	A1	2431.5721	3118.4279	17	1.17+00	1.0
1216	PR(10, 9,A)	11	8	-1	A	2431.5721	2877.2032	219	6.26-01	* .0
1217	RR(12, 3,A1)	13	4	1	A2	2431.6974	3118.5531	8	6.11-01	1.0
1218	RR(12, 2,E)	13	3	1	E	2432.1193	3121.5226	7	1.42+00	1.0
1219	*NR(11, 6,A)	12	3	0	A	2432.1614	2999.0424	54	1.04+00	*1.0
1220	*QR(10, 7,E)	11	5	1	E	2432.3157	2894.9622	-9	5.70-02	1.0

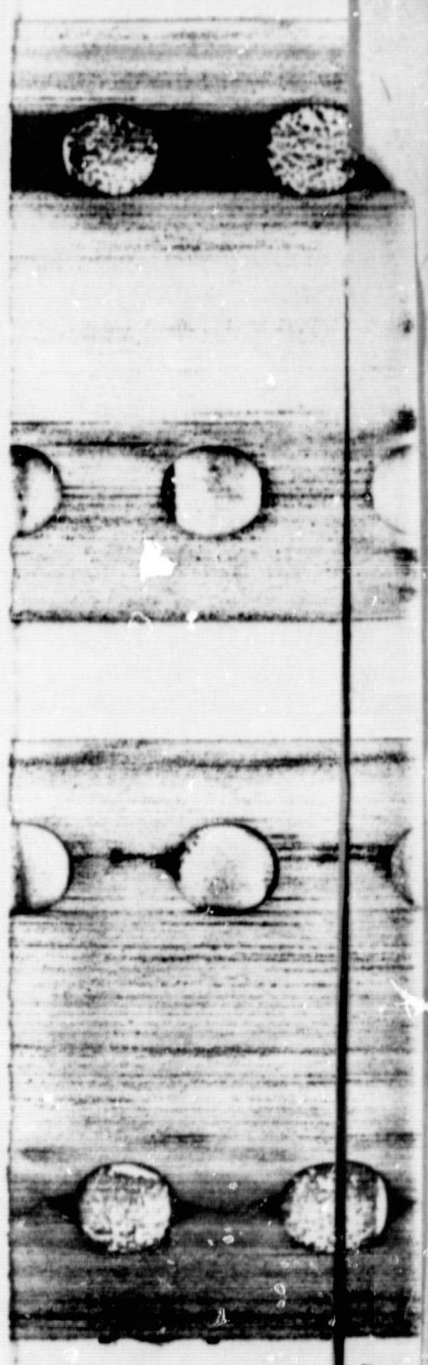

TABLE I—*Continued*

(I)	(II)	(III)	(IV)	(V)	(VI)	(VII)	(VIII)
1221	PR(11, 5,E)	12 4 -1 E	2432.7485	3005.3420	4	7.09-01	1.0
1222	PR(12, 1,E)	13 2 1 E	2432.8207	3123.7495	-15	1.91+00	1.0
1223	*NR(12, 4,E)	13 1 0 E	2433.5978	3116.8766	-5	1.42-01	1.0
1224	PR(10,10,E)	11 9 -1 E	2433.8428	2869.2470	352	1.13-01	.0
1225	PR(11, 6,A)	12 5 -1 A	2434.6956	3001.5766	29	7.74-01	*1.0
1226	PR(11, 7,E)	12 6 -1 E	2434.7465	2994.8370	159	5.96-01	.0
1227	*QR(11, 5,E)	12 3 1 E	2435.1147	3007.7086	-8	1.50-01	1.0
1228	PR(12, 1,E)	13 0 1 E	2435.2215	3126.1503	7	5.21-01	1.0
1229	*NP(12, 5,E)	13 2 0 E	2436.5142	3115.1762	21	2.59-01	1.0
1230	PR(12, 3,A2)	13 2 -1 A1	2436.5763	3123.4330	-25	9.98-01	1.0
1231	*QR(12, 2,E)	13 0 1 E	2436.7418	3126.1491	1	4.09-01	1.0
1232	PR(11, 8,E)	12 7 -1 E	2437.1897	2989.3922	363	5.06-01	.0
1233	*QR(12, 3,A1)	13 1 1 A2	2437.5279	3124.3836	-49	1.34-01	1.0
1234	PR(12, 4,E)	13 3 -1 E	2438.7388	3122.6176	7	5.15-01	1.0
1235	PR(12, 3,A1)	13 2 -1 A2	2438.9798	3125.8355	12	7.11-01	1.0
1236	*NR(12, 6,A)	13 3 0 A	2439.3779	3112.3696	142	6.88-01	* .0
1237	PR(11, 9,A)	12 8 -1 A	2439.4508	2982.6449	459	6.89-01	* .0
1238	PR(12, 5,E)	13 4 -1 E	2440.4513	3119.1133	74	4.53-01	1.0
1239	PR(12, 7,E)	13 6 -1 E	2442.1660	3108.4182	343	4.06-01	.0
1240	PR(12, 6,A)	13 5 -1 A	2442.3984	3115.3903	151	5.66-01	* .0
1241	*QR(12, 5,E)	13 3 1 E	2442.8681	3121.5301	14	1.12-01	1.0
1242	*QR(11, 8,E)	12 6 1 E	2442.9871	2995.1896	-35	3.24-02	1.0
1243	*QR(12, 6,A2)	13 4 1 A1	2445.4431	3118.4350	24	9.61-02	1.0
1244	*QR(12, 6,A1)	13 4 1 A2	2445.5578	3118.5497	5	8.36-02	1.0

RESULTS

The transitions assigned to ν_1 and ν_3 are listed in Table I with the asterisk denoting "forbidden" transitions. The weights given in column VIII are equal to either 1.0 for transitions unambiguously assigned to ν_1 or ν_3, or 0.0 for transitions which could be only tentatively assigned because of the Fermi interaction with $2\nu_4$. The weights noted with an asterisk correspond to doublets $A_1 \rightarrow A_2$, $A_2 \rightarrow A_1$ (with $|K| = 3, 6, \cdots$), unresolved experimentally and for which the expected splittings are small. The ground-state energy levels are labeled as $(J, |K|, C)$, where $C = A_1, A_2$ or E gives the symmetry species (*12*). In the upper states, the levels can be again specified unambiguously as $(J', |K'|, l_3' = 0, C')$ for $v_1 = 1$ and $(J', |K'|, l_3' = \pm 1, C')$ for $v_3 = 1$ although the mixing in v_1, v_3, K, and l_3' is large.

Twenty constants related to $v_1 = 1$ and $v_3 = 1$ were derived from the experimental data.[2] Six of them refer to $v_1 = 1$, ten to $v_3 = 1$, and four are interaction constants: $C_{11}^{(2)}$ and $C_{11}^{(3)}$ result from the first-order term T_1, $C_{21}^{(2)}$ and $C_{21}^{(3)}$ arise from the second-order term T_2; the first-order constant

$$C_{11}^{(1)} = \frac{B_e \zeta_{13}}{2} \times \frac{\lambda_1^{1/2} + \lambda_3^{1/2}}{\lambda_1^{1/4} \lambda_3^{1/4}}$$

is insignificant here, consistent with the very small value predicted for ζ_{13} in Ref. (*5*), viz., 0.004.

The derived constants are reported in Table II. They were obtained in two steps: first, the fitting was performed within the third order of approximation, the distortion constants D being fixed to their ground-state values. The fourth-order constants, introduced as a second step, were found to be insignificant except for the vibrational corrections to the constants D which improved the fitting significantly.

[2] These were the 1186 data points retained with weight equal to 1.0.

TABLE II

Vibration–Rotation Constants for $v_1 = 1$ and $v_3 = 1$ States of PH_3

$^{*}\nu_1$	2321.1314 (27)	$^{*}\nu_3$	2326.8766 (23)
$^{*}B_1$	4.406115(66)	$^{*}(C\zeta)_3$	$6.552\ (30)\times10^{-2}$
$^{*}C_1$	3.88468(13)	$^{*}B_3$	4.408738 (60)
$^{*}D_1^J$	$1.0876(42)\times10^{-4}$	$^{*}C_3$	3.90537 (12)
$^{*}D_1^{JK}$	$-9.97(14)\times10^{-5}$	$^{*}D_3^J$	$1.3130\ (35)\times10^{-4}$
$^{*}D_1^K$	$8.69\ (15)\times10^{-5}$	$^{*}D_3^{JK}$	$-2.500\ (15)\times10^{-4}$
$C_{11}^{(2)}$	$\epsilon\times6.084(34)\times10^{-3}$	$^{*}D_3^K$	$1.795\ (15)\times10^{-4}$
$C_{11}^{(3)}$	$-\epsilon\times2.898(29)\times10^{-4}$	$^{*}\eta_3^J$	$1.524\ (73)\times10^{-4}$
$C_{21}^{(2)}$	$\epsilon'\times9.595(23)\times10^{-3}$	$^{*}\eta_3^K$	$-8.49\ (11)\times10^{-4}$
$C_{21}^{(3)}$	$-\epsilon'\times2.781(38)\times10^{-4}$	$^{*}(q_{22}^3)_v$	$-1.628\ (14)\times10^{-3}$

constants constrained to their ground state values (4):

$$H_1^J = H_3^J = H_0^J = 1.83.10^{-8}$$
$$H_1^{JJK} = H_3^{JJK} = H_0^{JJK} = -6.2.10^{-8}$$
$$H_1^{JKK} = H_3^{JKK} = H_0^{JKK} = 8.0.10^{-8}$$

The errors quoted are one standard deviation

Also, the large deviations from their ground-state values, observed for these constants are, of course, related to strong vibrational interactions, especially with $2\nu_4$. The fourth-order distortion constants, H^J, H^{JJK}, and H^{JKK} were constrained for $v_1 = 1$ and $v_3 = 1$ to their ground-state values (*4*) recalled at the bottom of the table; no significant value of the constant, H^K, could be deduced from the present analysis. The 16 constants related to ν_1 and ν_3 are written in the usual notation (*12*), except that the asterisks point out that they do not involve exactly the same contributions as in the individual analyses of the bands. The set of constants of Table II reproduces the 1186 transitions assigned to ν_1 and ν_3 with an overall standard deviation of 0.017 cm^{-1}.

Concerning the intensities, the strengths of allowed and "forbidden" transitions could be deduced from measurement of equivalent widths (*14*), and compared together to adjust the ratio $\rho_{1,3}$ involved in the relative intensity calculations. In fact, the number of available data was very limited because of the intensity anomalies which appear early in the ν_1 and ν_3 bands as a result of the Fermi interaction with $2\nu_4$. Nevertheless, the comparison between experimental results and computed values of the relative intensities enabled us to approximate the coefficient $\rho_{1,3}$ to the value:

$$\rho_{1,3} = -0.75$$

with an uncertainty probably of less than 15%. This result leads to a ratio S_1/S_3 between the band strengths of ν_1 and ν_3 as equal to 0.28. Using the overall strength $S_1 + S_3$ measured in Ref. (*15*), one gets for S_1 and S_3, 114 and 406 cm^{-2} atm^{-1}, respectively. The present value of $\rho_{1,3}$ is smaller than the one predicted (1.04) in Ref. (*16*). The opposite signs are connected to opposite signs in the definition of the normal coordinates q_{3a} and q_{3b}.

Although no special effort has been made to record spectra from which absolute values for line strengths could be determined, the quantities reported in column VII of Table I can be considered as reasonable values for the dimensionless quantities $(S_i pl)/d_i$ at 300 K, where S_i are the absolute line strengths, d_i are the Doppler half-widths, $p \simeq 0.3$ T and $l = 100$ cm were defined by the experimental conditions.

CONCLUSIONS

The present analysis allowed us to explain the main features of the absorption by PH_3 in the extended range 2184–2445 cm^{-1}, and to evaluate the ratio between the band strengths of the two fundamental bands ν_1 and ν_3. Anomalies observed in frequencies and intensities pointed out that the Fermi interaction with $2\nu_4$ has to be taken into account for interpretation beyond $J' = 13$. This interaction is especially strong in the component $Kl_3 < 0$ of the ν_3 band, giving rise to serious anomalies in intensity distribution between *O*- and *S*-type "forbidden" transitions. See for example Fig. 2.

Many unassigned transitions, observed near 2200 cm^{-1} with intensities comparable to the ν_1 and ν_3 transitions, may be ascribed to the overtone band $2\nu_4$. The rotational structure of this band appears very complex at first sight; but a spectrum recorded at low temperature which would allow us to eliminate most of the ν_1 and ν_3

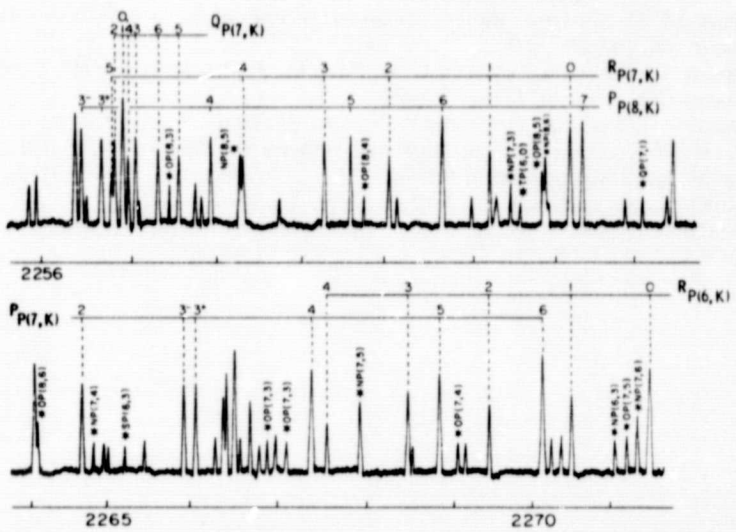

FIG. 2. Spectrum of PH_3 in the region 2256–2272 cm^{-1}. Pressure: 6 Torr; Pathlength: 1 m. The "forbidden" transitions are indicated by asterisks.

transitions, will probably be a good starting point for the analysis of this overtone band.

Finally, in the narrow region 2050–2120 cm^{-1} which was convenient for the detection of PH_3 in Jupiter's spectrum at 5 μm (7), the expected transitions for ν_1 and ν_3 correspond to high J values in the range 22–30, i.e., to ground-state energy levels very depopulated at low temperatures. So, the combination band $\nu_2 + \nu_4$—instead of ν_1 or ν_3—might be responsible for the PH_3 transitions observed in this region.

ACKNOWLEDGMENTS

One of us (K.N.R.) is grateful to the National Aeronautics and Space Administration for support of some of this research. A one-month stay of Baldacci at Orsay, France to do some of the computations was made possible by the joint scientific program CNR (Rome)—CNRS (Paris).

RECEIVED: October 1, 1979

REFERENCES

1. V. M. McConaghie and H. H. Nielsen, *J. Chem. Phys.* **21,** 1836–1838 (1953).
2. J. M. Hoffman, H. H. Nielsen, and K. Narahari Rao, *Z. Elektrochem.* **64,** 606–616 (1960).
3. P. K. L. Yin and K. Narahari Rao, *J. Mol. Spectrosc.* **51,** 199–207 (1974).
4. A. G. Maki, R. L. Sams, and W. B. Olson, *J. Chem. Phys.* **58,** 4502–4512 (1973).
5. F. Y. Chu and T. Oka, *J. Chem. Phys.* **60,** 4612–4618 (1974).
6. D. A. Helms and W. Gordy, *J. Mol. Spectrosc.* **66,** 206–218 (1977).
7. H. P. Larson, R. R. Treffers, and U. Fink, *Ap. J.* **211,** 972–979 (1977).
8. K. Narahari Rao, "High Resolution Infrared Spectroscopy: Aspects of Modern Research" (D. A. Ramsay, Ed.), Physical Chemistry Series Two, Vol. 3, pp. 352–358, Butterworths, London, 1976.
9. A. Baldacci, V. Malathy Devi, Da-Wun Chen, K. Narahari Rao, and B. Fridovich, *J. Mol. Spectrosc.* **70,** 143–159 (1978).
10. L. W. Pinkley, K. Narahari Rao, G. Tarrago, G. Poussigue, and M. Dang-Nhu, *J. Mol. Spectrosc.* **68,** 195–222 (1977).
11. G. Tarrago, K. Narahari Rao, and L. W. Pinkley, *J. Mol. Spectrosc.* **79,** 31–46 (1980).
12. G. Tarrago, *Cah. Phys.* **19,** 149–217 (1965).
13. G. Poussigue, G. Tarrago, P. Cardinet, and A. Valentin, *J. Mol. Spectrosc.*, in press.
14. L. A. Pugh and K. Narahari Rao, "Intensities from Infrared Spectra" (K. Narahari Rao, Ed.), Molecular Spectroscopy: Modern Research, Vol. 2, Academic Press, New York, 1976.
15. D. C. McKean and P. N. Schatz, *J. Chem. Phys.* **24,** 316–325 (1956).
16. A. J. van Straten and W. M. A. Smit, *J. Mol. Spectrosc.* **65,** 202–218 (1977).

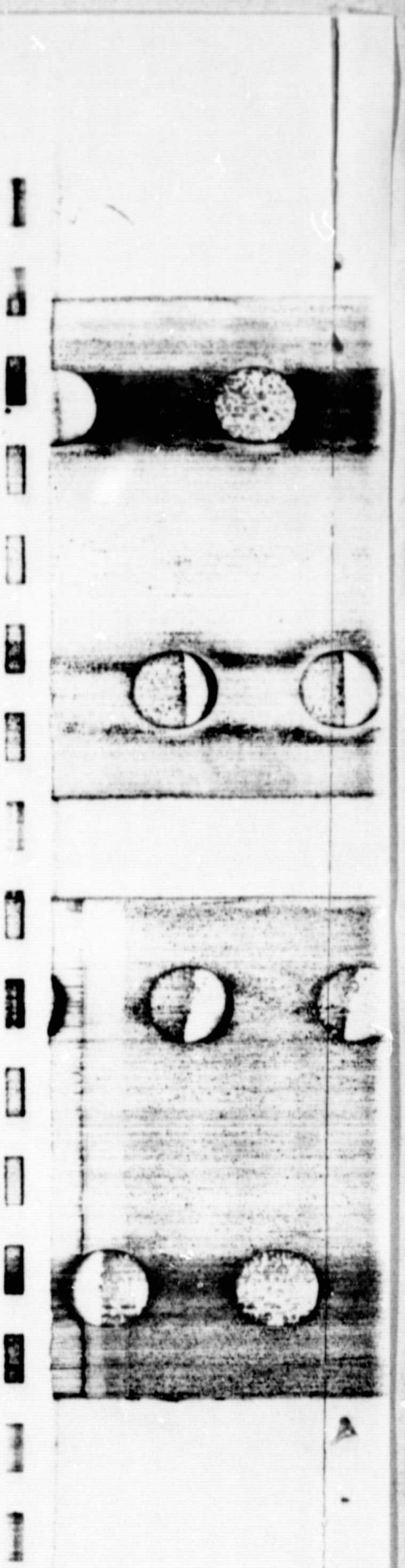

JOURNAL OF MOLECULAR SPECTROSCOPY 87, 578–581 (1981)

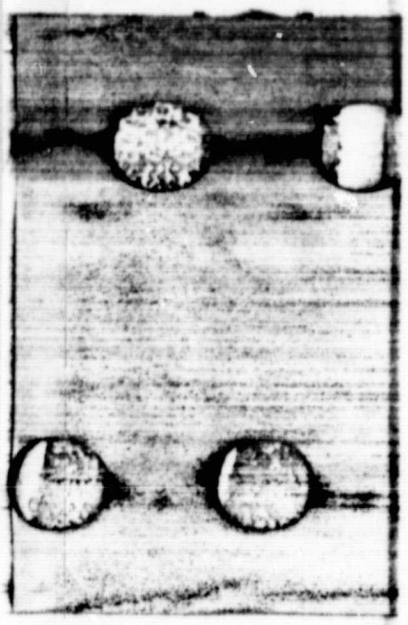

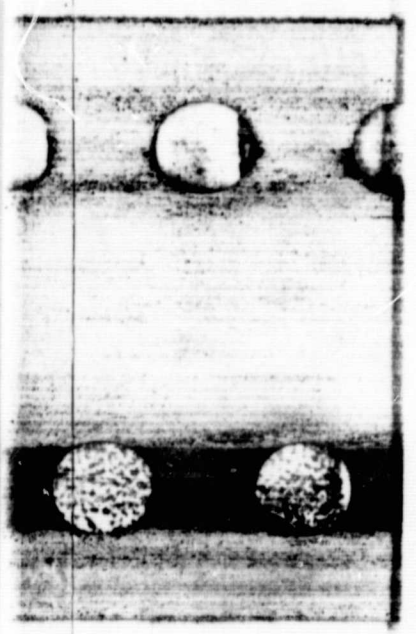

Diode Laser Measurements of Strengths of $^{16}O^{12}C^{32}S$ Lines at 12 μm[1]

Objective and experimental method. This note describes a study of individual line strengths of some lines of the ν_1 band of $^{16}O^{12}C^{32}S$ at 12 μm. Values for the total band intensity, pure vibration transition moment, and vibration–rotation interaction constants were deduced from the measured data. Also, strengths of a few lines of the "hot" band $(\nu_1 + \nu_2) - \nu_2$ were measured from which the total band intensity is estimated. Self-broadening coefficients of a few high J transitions of the ν_1 band were also determined.

The diode laser spectrometer has been described in detail elsewhere (*1*, *2*). A commercial sample of OCS with a minimum purity of 99.9% obtained from Matheson Gas Company was used without purification. A natural sample of OCS contains 93.72% of $^{16}O^{12}C^{32}S$. Pressures were measured with MKS Baratron gauges with 0–1 and 0–100 Torr pressure heads. The uncertainty of our measured pressures was estimated to be less than 1%. Pyrex cells of lengths 11.3, 21.7, 51.55, 101.6, and 201.6 cm fitted with KBr or KRS-5 windows were used. The cells were evacuated by a diffusion pump to less than 10^{-5} Torr. The pressures of OCS ranged from 0.040 to 0.280 Torr. All observations were taken within 1 h after filling the cells. Eight or more repetitive scans were made of each line at three or more pressure × pathlength values at room temperature (296–299 K). The cell temperatures were monitored during each scan by precision thermistor probes. The dispersion was calculated from the known fringe spacing of a one-inch germanium etalon. The analog records were digitized using a Bendix Datagrid Digitizer for processing.

Self-broadening parameters. The self-broadening parameter for OCS has been the subject of several experimental and theoretical investigations (*3*). However, they have all been done for $J < 30$. The theoretical self-broadening parameters calculated in Ref. (*3*) have been combined with the present high J measurements in order to determine this parameter for all values of J up to $J = 76$. For self-broadening measurements, a 11.3-cm cell was used and the pressures of OCS ranged from 33 to 55 Torr. At these pressures, the lines were essentially Lorentzian. From direct half-width measurements of $P(67)$, $P(72)$, and $P(76)$, a mean value of (0.108 ± 0.005) cm^{-1}/atm. at 300 K was determined. There was no clear J dependence for these lines. In Table I, the self-broadening parameters obtained from this combined work are listed for J up to 76.

Strengths of lines. At pressures of less than 0.280 Torr, self-broadening is negligible and thus the lines should be Doppler broadened. However, typical full widths at half height for the OCS lines were measured to be 0.0018 cm^{-1}, which is about 40% larger than the Doppler width. In previous publications from this laboratory (*2*, *4*) it has been shown that this broadening is due to an instrumental function with Gaussian characteristics related mostly to the diode laser linewidth. The method of equivalent width is therefore used to determine line strengths.

The equivalent width W is defined by

$$W = \int_{\text{line}} (1 - e^{-k(\nu)x}) d\nu, \tag{1}$$

where x is the measure of the number of absorbing molecules per unit area and $k(\nu)$ is the absorption coefficient which is related to the line strength S and the lineshape function $f(\nu - \nu_0)$ by the relation

$$k(\nu) = S \cdot f(\nu - \nu_0). \tag{2}$$

[1] Support extended this research by National Aeronautics and Space Administration is gratefully acknowledged.

0022-2852/81/060578-04$02.00/0

TABLE I

Strengths and Self-Broadening Parameters of Some ν_1 Band Lines of $^{16}O^{12}C^{32}S$ at 300 K

LINE	$S_{calc.}$ ($cm^{-2}atm^{-1}$)	$S_{obs.}$ ($cm^{-2}atm^{-1}$)	γ_L ($cm^{-1}atm^{-1}$)
P(76)	0.007	0.006	0.116
P(75)	0.008	0.007	0.117
P(72)	0.011	0.011	0.135
P(71)	0.013	0.014	0.137
P(67)	0.020	0.021	0.150
P(61)	0.037	0.037	0.163
P(55)	0.065	0.073	0.177
P(50)	0.096	0.103	0.190
P(45)	0.135	0.122	0.203
P(40)	0.180	0.170	0.215
P(35)	0.224	0.221	0.227
P(27)	0.277	0.312	0.258
P(20)	0.283	0.229	0.258
P(11)	0.206	0.210	0.235
R(7)	0.167	0.169	0.222
R(16)	0.297	0.303	0.252

A Voigt profile has been assumed for the OCS line, i.e.,

$$f(\nu - \nu_0) = (P'a/\pi) \int_{-\infty}^{\infty} (e^{-y^2})/(a^2 + (\xi - y)^2)dy, \tag{3}$$

where

$$P' = (1/b_D)\{(\ln 2)/\pi\}^{1/2},$$
$$a = (b_L/b_D)(\ln 2)^{1/2},$$
$$\xi = \{(\nu - \nu_0)/b_D\}(\ln 2)^{1/2}. \tag{4}$$

b_L and b_D denote the Lorentzian and Doppler half widths, respectively. The measured values of W ranged from 0.0004 to 0.001 cm^{-1} corresponding to Doppler lines on the linear part of the curve of growth.

The line strength S at a particular temperature was then calculated from W by iteration. From repeated measurements of line strengths at various pressure × pathlength values, the experimental uncertainty was estimated to be about ±5%. The line strength at a temperature T was converted to temperature $T = 300$ K by using the following expression,

$$S(T_0) = S(T)\frac{Q(T)}{Q(T_0)}\left(\frac{T}{T_0}\right)\exp\frac{hc\nu''}{k}\left(\frac{1}{T} - \frac{1}{T_0}\right), \tag{5}$$

where Q is the internal partition function (calculated in this work), and ν'', the energy of the lower level in cm^{-1}, evaluated from the molecular constants given in Ref. (6).

The line strength in a rovibrational band of OCS can be written as (5)

$$S(T) = \frac{8\pi^3 N_T}{3hcQ(T)}\,\nu_0 \exp\left(\frac{-hc\nu''}{kT}\right)\left(\frac{m^2 - l^2}{|m|}\right)|R_{vlJ}^{v'l'J'}|^2\left[1 - \exp\left(\frac{hc\nu_0}{kT}\right)\right], \tag{6}$$

where N_T is the total number of molecules per unit volume per unit partial pressure of the absorbing gas at temperature T, $R_{vlJ}^{v'l'J'}$ is the matrix element of the dipole moment of the vibrational transition; $m = J + 1$ for the R branch and $-J$ for the P branch, ν_0 is the wavenumber of the line. The square of the matrix element of the dipole moment of the vibrational transition $|R_{vlJ}^{v'l'J'}|^2$ can be expressed as

$$|R_{vlJ}^{v'l'J'}|^2 = |R_{vl}^{v'l'}|^2 F_{vR}(m), \tag{7}$$

where $F_{vR}(m)$ is the factor that accounts for the vibration–rotation interaction (nonrigidity correction)

TABLE II

Summary of Band Intensity Parameters for $^{16}O^{12}C^{32}S$

ν_1(859 cm^{-1}) Fundamental Band:

S_{Band} (300°K) = (26.93 ± 1.23) $cm^{-2}atm^{-1}$

$|R_{v\ell}^{v'\ell'}|^2$ = 0.00285 ± 0.00013 (Debye)^2

a = (1.7 ± 2.2) x 10^{-3}
b = (7.1 ± 3.1) x 10^{-5} Herman-Wallis coefficients

$(\nu_1 + \nu_2') - \nu_2'$ (852 cm^{-1}) Band

S_{Band} (300°K) = (4.05 ± 0.18) $cm^{-2}atm^{-1}$

$|R_{v\ell J}^{v'\ell'J'}|^2$ = 0.00246 ± 0.00011 (Debye)^2

and $|R_{ri}^{r'i'}|$ is the matrix element of the pure vibrational transition. For a linear molecule, $F_{vR}(m)$ may be expressed as a function of m by

$$F_{vR}(m) = 1 + am + bm^2 + \cdots. \tag{8}$$

By introducing the measured value of S and all known quantities into Eq. (6), $|R_{ri,J}^{r'i',J'}|^2$ was calculated for each line. These were then least-squares fitted to obtain a, b, and $|R_{ri}^{r'i'}|^2$. The line intensities were then calculated from $|R_{ri}^{r'i'}|^2$, a, and b. Table I presents these calculated values along with the mean line strengths of the measured lines.

Band strength of ν_1 of OCS. In Table II, the band strength for the ν_1 band obtained by direct summation of Eq. (6) is presented along with $|R_{ri}^{r'i'}|^2$, a, and b. As in the case of parallel bands of other linear molecules like CO_2, the constants a and b were not well determined.

Line strengths of four lines belonging to the $(\nu_1 + \nu_2) - \nu_2$ band were also measured. This band is much weaker than the ν_1 band. The measured intensities of $P_{ee}(35)$, $P_{ff}(35)$, $P_{ee}(40)$, and $P_{ff}(40)$ are 0.0149, 0.0157, 0.0121, and 0.0131 cm^{-2} atm^{-1} at 300 K. The calculated values of $|R_{ri,J}^{r'i',J'}|^2$ and the band strength are also presented in Table II.

The value of 26.93 ± 1.23 cm^{-2} atm^{-1} for the band strength of the ν_1 band of $^{16}O^{12}C^{32}S$ at 300 K obtained in this work translates to an integrated band intensity of 34.9 cm^{-2} atm^{-1} for all isotopes and hot bands of OCS at 12 μm.[2] This is in good agreement with the value of 33.4 cm^{-2} atm^{-1} obtained by Robinson (*8*) about 30 years ago. A value of (40.6 ± 4) cm^{-2} atm^{-1} has been recently reported by Foord and Whiffen (*9*) in 1973.

In conclusion, it may be mentioned that recently it was pointed out (*10*) that OCS could be a minor constituent in Io, the satellite of Jupiter. Estimates of its concentration were made from the strength of its ν_1 band.

[2] Dr. A. G. Maki of the National Bureau of Standards informed us that he and R. Kagann have measured the integrated intensity of the ν_1 band of OCS using a Fourier transform spectrometer and obtained 35.2 cm^{-2} atm^{-1} at 296 K (with an uncertainty of 15%) for the strength of this band. Oftentimes in the past, the band strengths determined at different times and in different laboratories differed by large amounts (see, for instance, Chapter IV on "Intensities in Infrared Spectra" in "Molecular Spectroscopy: Modern Research," Vol. II, (K. Narahari Rao, Ed.), Academic Press, New York, 1976). So, it is useful to note that the value of Maki and Kagann is close to the results obtained in the present investigation. We wish to thank Dr. Maki for bringing this to our attention and also for other useful comments.

REFERENCES

1. S. P. Reddy, W. Ivancic, V. Malathy Devi, A. Baldacci, K. Narahari Rao, A. W. Mantz, and R. S. Eng, *Appl. Opt.* **18**, 1350–1354 (1979).
2. P. P. Das, V. Malathy Devi, and K. Narahari Rao, *J. Mol. Spectrosc.* **84**, 305–312 (1980).
3. J. S. Murphy and J. E. Boggs, *J. Chem. Phys.* **49**, 3333–3343 (1968).
4. V. Malathy Devi, P. P. Das, A. Bano, K. Narahari Rao, J.-M. Flaud, C. Camy-Peyret, and J.-P. Chevillard, *J. Mol. Spectrosc.*, in press.
5. S. S. Penner, "Quantitative Molecular Spectroscopy and Gas Emissivities," Eq. (7-125), Chap. 7, Addison–Wesley, Reading, Mass., 1959.
6. A. G. Maki, W. B. Olson, and R. L. Sams, *J. Mol. Spectrosc.* **81**, 122–138 (1980).
7. E. K. Plyler, E. D. Tidwell, and W. S. Benedict, *J. Opt. Soc. Amer.* **52**, 1017–1022 (1962).
8. D. Z. Robinson, *J. Chem. Phys.* **19**, 881–886 (1951).
9. A. Foord and D. H. Whiffen, *Mol. Phys.* **26**, 959–968 (1973).
10. J. Pearl, R. Hanel, V. Kunde, W. Maguire, K. Fox, S. Gupta, C. Ponnamperuma, and F. Raulin, *Nature* **280**, 755–758 (1979).

V. Malathy Devi,[1]
P. P. Das,[2]
A. Bano,
K. Narahari Rao

Department of Physics
The Ohio State University
Columbus, Ohio 43210

Received August 29, 1980

[1] Present address: NOAA/NESS, FB4, S/RE21, Washington, D. C. 20233.
[2] Present address: Tachisto Inc., 13 Highland Circle, Needham, Massachusetts 02194.

JOURNAL OF MOLECULAR SPECTROSCOPY 91, 494–498 (1982)

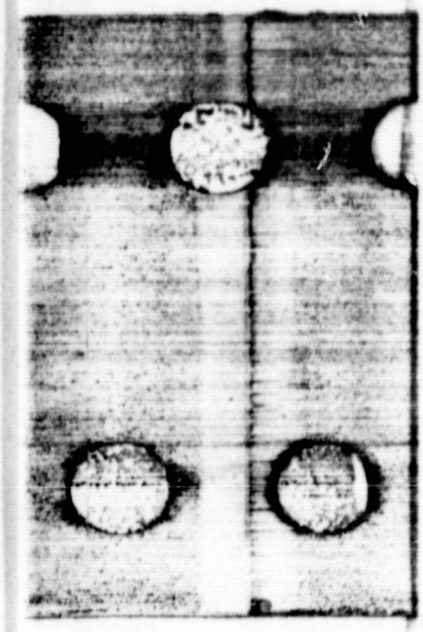

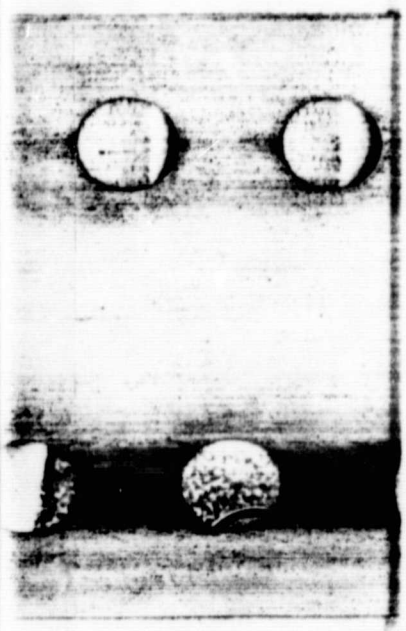

Tunable Diode Laser Study of the ν_4 Infrared Band of GeH_4

The ν_4 infrared band of GeH_4, centered close to 820 cm^{-1}, has been studied by several authors. The most recent rotational analysis is due to Kattenberg *et al.* (*1*), but the resolution in this work was comparatively modest so that almost none of the fine structure expected from tetrahedral splitting and from the different isotopic species of Ge was clearly resolved. Preliminary accounts have been given of spectra recorded at 0.06-cm^{-1} resolution, both using a natural sample of germane (*2*) and also with samples enriched in $^{70}GeH_4$, $^{72}GeH_4$, and $^{74}GeH_4$ (*3*). Improved values of the ground-state constants B_0, D_0, and H_0 have been derived from the latter spectra, but the full assignment of the ν_2 and ν_4 bands has not yet been completed (*4*).

Here we report measurements on the ν_4 band carried out with a tunable diode laser spectrometer (*5*, *6*). The diode laser provided wavenumber coverage from 818 to about 845 cm^{-1}. Assignments have been made to nearly 200 of the $R(0)$ through $R(10)$ transitions of the five naturally occurring species $^{70}GeH_4$, $^{72}GeH_4$, $^{73}GeH_4$, $^{74}GeH_4$, and $^{76}GeH_4$. In addition, the high-wavenumber Q-branch head of $^{70}GeH_4$ and a few high-J Q-branch lines of $^{72}GeH_4$ have also been assigned.

A commercial sample of germane (Matheson Gas Co., stated purity 99.9%) was used. Traces of H_2 were removed by freezing the sample at 77 K and pumping on the solid. Line positions were measured with ≤0.1 Torr of germane in a 1-m cell. ν_1 lines of OCS (*7*) were used for calibration. The absolute accuracy of measurement is believed to be about ±0.002 cm^{-1} (*8*). A typical scan, covering part of the overlapping $R(6)$ multiplets of four isotopic species, is shown in Fig. 1. It is clear that the high resolution achieved with the diode laser allows both the tetrahedral splitting and the isotope effects to be determined despite the high density of lines.

The results are summarized in Tables I–III. Table I gives the R-branch assignments and Table II the Q-branch assignments. In both cases the comparison between experimental line positions and those calculated from molecular constants given in Table III is also presented. The molecular constants were obtained from least-squares fits to the data of Tables I and II, using the Hamiltonian of Gray, Robiette, and co-workers (*9–11*) in which the Coriolis-coupled ν_2 and ν_4 bands are treated together. The ground-state constants (*3*) and ν_2 constants (*4*) were taken from analyses of the 0.06-cm^{-1} spectra and fixed during the fits of the diode laser data. Eventually, it should be possible to improve the constants by a combined analysis of the diode laser results and the 0.06 cm^{-1} results with appropriate weighting of the two types of data.

In the case of $^{70}GeH_4$, the observation of Q-branch transitions from $Q(3)$ through $Q(21)$ in addition to a complete set of transitions R(0) through R(9) allowed the refinement of nine parameters in the upper-state Hamiltonian of ν_4. The Q-branch assignment was not straightforward, but the GeH_4 line identifications given in Table II have been conclusively established by absolute intensity measurements on both Q-branch and R-branch lines. The analysis of the intensity measurements and their interpretation in terms of the ν_4 band strength will be reported subsequently.

For the other isotopic species, where fewer transitions were recorded, the number of parameters refined was always smaller and the poorly determined constants were fixed at their $^{70}GeH_4$ values. This procedure leads to a consistent set of molecular constants with a uniform quality of fit for the five isotopic species. A few lines, noted in Table I, were given zero weight in the final series of refinements. These lines are less accurate because of relatively poor diode laser performance where they appeared.

The constants of Table III are in satisfactory agreement with theoretical predictions of the isotope shifts. From an approximate harmonic force field adjusted to fit the ν_4 constants and the four fundamentals of $^{70}GeH_4$ (uncorrected for anharmonicity), we have calculated the isotope shifts in the band origin ν_4 and the Coriolis coefficient $2B\zeta_4$. These shifts are compared with experiment in the last four lines of Table III. The trends are well reproduced, especially when the uncertainties in the experimental shifts

0022-2852/82/020494-05$02.00/0

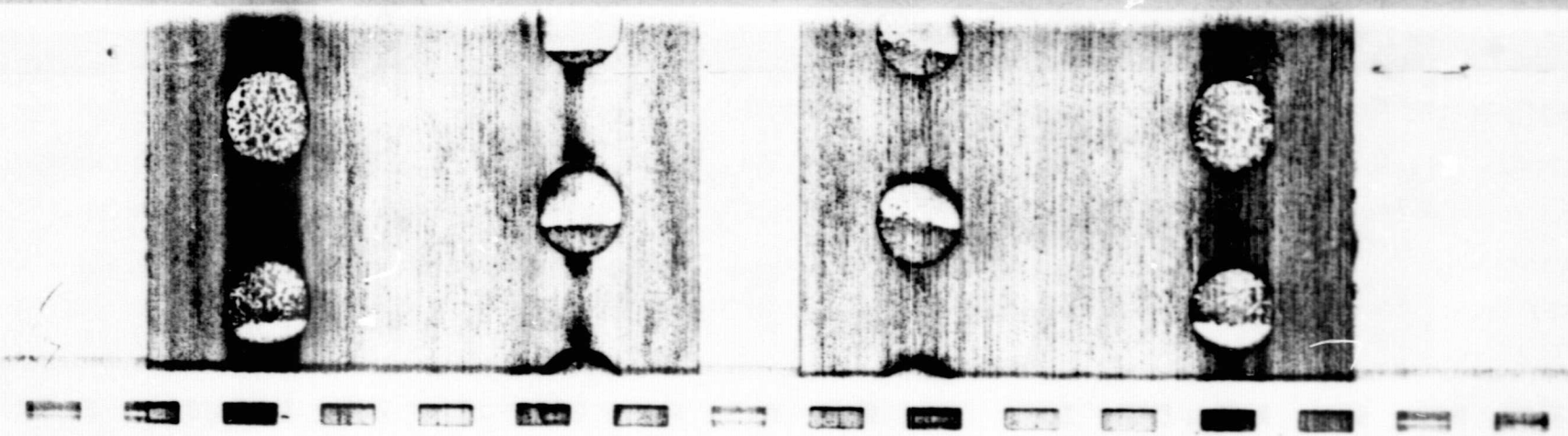

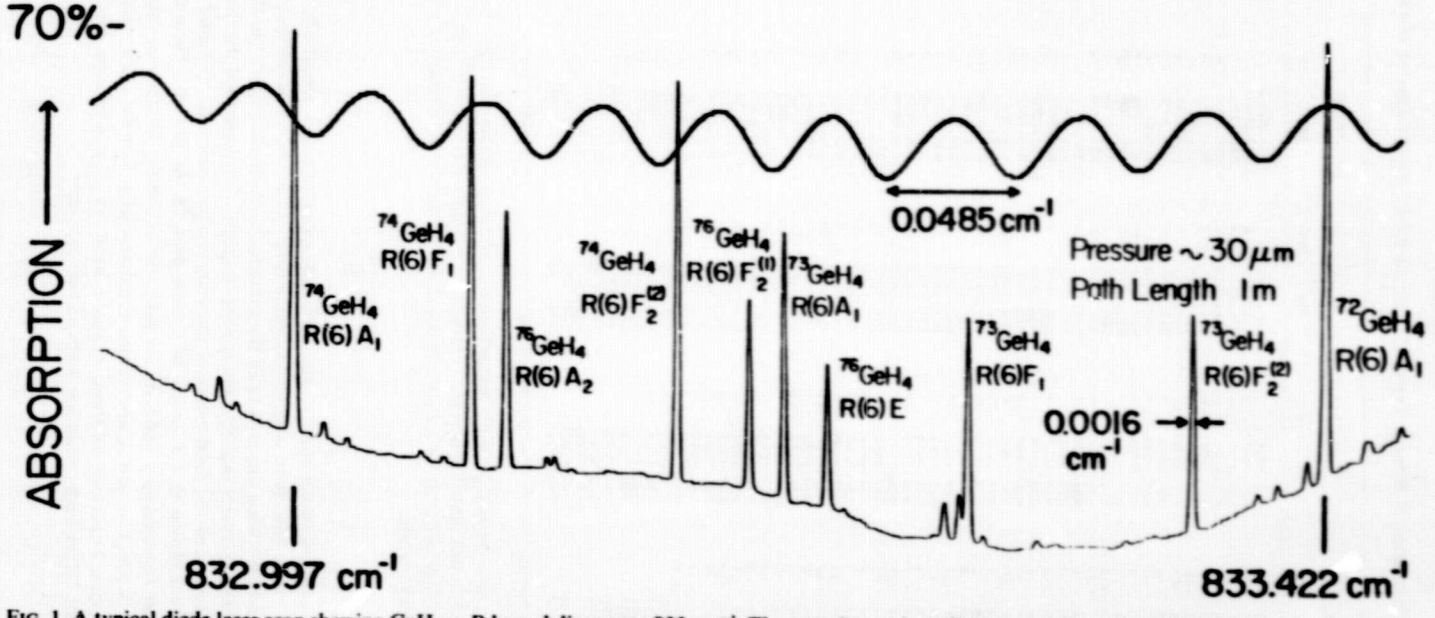

FIG. 1. A typical diode laser scan showing GeH_4 ν_4 R-branch lines near 833 cm^{-1}. The experimental conditions are indicated on the trace, and the assignments correspond to those in Table I.

TABLE I

Observed and Calculated *R*-Branch Transitions of the Five Isotopic Species of Germane

	$^{70}GeH_4$		$^{72}GeH_4$		$^{73}GeH_4$		$^{74}GeH_4$		$^{76}GeH_4$	
Transition	ν/cm^{-1}	o−c	ν/cm^{-1}	o−c	ν/cm^{-1}	o−c	ν/cm^{-1}	o−c	ν/cm^{-1}	o−c
R(0) A1	820.9128	-3	(820.4764)		(820.2672)		(820.0655)		(819.6722)	
R(1) F1	823.2212	-23	822.7849	9	822.5742	8	(822.3700)		(821.9743)	
R(2) F2	825.4816	38	825.0357	-2	824.8241	1	824.6194	4	(824.2211)	
R(2) E	825.5128	27	825.0680	0	824.8564	2	824.6515	4	(824.2531)	
R(3) A2	827.6124	-9	827.1689	-5	826.9571	8	826.7494	-6	826.3437	(-67)
R(3) F2	827.6991	-12	827.2565	5	827.0438	9	826.8363	-1	826.4341	-24
R(3) F1	827.7706	-19	827.3290	11	827.1153	5	826.9087	6	826.5069	-10
R(4) F2	829.7676	-6	829.3214	-7	829.1075	-2	828.8995	-7	(828.4987)	
R(4) E	829.9305	-4	829.4838	-4	829.2686	-13	829.0611	-7	(828.6598)	
R(4) F1	829.9895	9	829.5405	-12	829.3264	-9	829.1188	-3	(828.7169)	
R(4) A1	830.0728	21	829.6232	-3	829.4076	-15	829.1988	-18	(828.7981)	
R(5) F1(2)	831.8652	-18	831.4181	-9	831.2031	-5	830.9948	1	(830.5916)	
R(5) E	831.9129	-21	831.4660	-8	831.2509	-5	831.0422	-2	(830.6391)	
R(5) F2	832.1728	4	831.7228	-6	831.5063	-16	831.2975	-7	830.893[illegible]	-6
R(5) F1(1)	832.2809	-2	831.8305	-11	831.6148	-13	831.4045	-16	831.0013	-3
R(6) A1	833.8703	-15	833.4217	-4	833.2065	8	832.9971	13	832.5920	8
R(6) F1	833.9482	1	833.4975	-7	833.2822	5	833.0733	17	832.6676	8
R(6) F2(2)	834.0374	10	833.5852	-10	833.3698	1	833.1604	10	832.7539	-4
R(6) A2	834.3703	-10	833.9200	0	833.6984	(-50)	833.4919	-4	833.0874	12
R(6) F2(1)	834.4769	5	834.0262	15	833.8040	(-42)	833.5957	-10	833.1904	1
R(6) E	834.5115	5	834.0612	21	833.8394	-32	833.6292	-18	833.2244	-1
R(7) F1(2)	835.9094	9	835.4587	17	835.2398	3	835.0301	16	834.6258	34
R(7) E	836.0311	21	835.5782	10	835.3603	6	835.1490	6	(834.7419)	
R(7) F2(2)	836.1118	17	835.6582	2	835.4418	13	835.2290	0	(834.8223)	
R(7) A2	836.2665	5	835.8135	1	835.5957	-1	835.3843	4	834.9773	5
R(7) F2(1)	836.6798	-19	836.2291	14	836.0113	11	835.7977	6	835.3888	0
R(7) F1(1)	836.7389	-11	836.2867	9	836.0683	1	835.8555	5	835.4474	9
R(8) F2(2)	837.8950	-1	837.4422	4	837.2247	13	(837.0114)		836.6041	2
R(8) E(2)	837.9490	4	837.4956	4	837.2782	14	(837.0646)		836.6567	-3
R(8) F1(2)	838.1268	3	837.6736	10	837.4557	16	837.2439	23	(836.8334)	
R(8) F2(1)	838.3427	15	837.8855	-11	837.6679	-3	837.4557	7	(837.0463)	
R(8) E(1)	838.9253	-2	838.4679	-11	838.2528	23	838.0369	11	837.6263	9
R(8) F1(1)	838.9501	2	838.4925	-8	838.2726	-22	838.0608	8	837.6499	3
R(8) A1	838.9908	-6	838.5332	-16	838.3178	15	838.1019	6	837.6917	10
R(9) A2	839.8115	-2	(839.3567)		839.1388	13	838.9253	7	838.5153	-5
R(9) F2(2)	839.8757	-8	(839.4214)		839.2041	20	838.9908	17	(838.5801)	
R(9) F1(3)	839.9605	3	839.5053	4	(839.2856)		839.0725	1	(838.6632)	
R(9) A1	840.1626	1	839.7083	17	839.4887	13	(839.2737)		838.8642	2
R(9) F1(2)	840.3864	-17	839.9312	-4	839.7108	-15	839.4988	8	839.0878	0
R(9) E	840.4437	-5	839.9881	6	839.7675	-8	839.5545	7	839.1440	6
R(9) F2(1)	841.1709	7	840.7108	-5	840.4923	4	840.2753	-2	839.8633	2
R(9) F1(1)	841.2045	6	840.7458	10	840.5261	6	840.3078	-11	839.8955	-9
R(10) F2(3)	(841.7644)		841.3060	-15	841.0852	-23	(840.8737)		840.4631	-5
R(10) E(2)	(841.8528)		841.3948	-9	841.17[illegible]	-20	840.9581	-36	840.5529	15
R(10) F1(2)	(841.9329)		(841.4756)		841.2539	-17	841.0397	-17	840.6302	-7
R(10) A1	(842.1800)		(841.7220)		(841.5021)		841.2852	-21	(840.8762)	
R(10) F1(1)	(842.4478)		(841.9892)		(841.7692)		(841.5537)		841.1395	-24
R(10) F2(2)	(842.5483)		(842.0894)		(841.8694)		(841.6536)		841.2390	-26
R(10) A2	(843.4028)		(842.9414)		(842.7214)		(842.5033)		(842.0888)	
R(10) F2(1)	(843.4266)		(842.9631)		(842.7451)		(842.5269)		(842.1124)	
R(10) E(1)	(843.4376)		(842.9761)		(842.7560)		(842.5378)		(842.1233)	

Note. The transitions are labeled by their ground-state symmetry species. Columns headed o − c are the residuals (observed − calculated) from the least-squares fits, in units of 10^{-4} cm^{-1}. Bracketed line positions are calculated values for transitions which could not be measured. Bracketed residuals indicate transitions omitted from the fits.

are considered. The constants other than ν_4 and $2B\zeta_4$ are, as anticipated, essentially independent of isotopic species so far as we have been able to determine them. It should be noted that the upper-state constants of the ν_2 band have been assumed to be the same for all isotopic species, but that the strength of the ν_2/ν_4 Coriolis coupling varies slightly from species to species. We have used the theoretical isotope dependence of ζ_{24} to determine the fixed values of the coupling parameter R_{24} (*9*) used in the analysis.

In conclusion, we have shown that a wealth of precise data on the isotope effects in GeH_4 can be obtained by diode laser spectroscopy, and that the data can be readily interpreted using the Coriolis-coupled Hamiltonian in which ν_2 and ν_4 are treated simultaneously. The data discussed here establish for the first time the most important constants of the ν_4 band for all five isotopic species of germane, and provide a basis for future high-resolution work on this molecule.

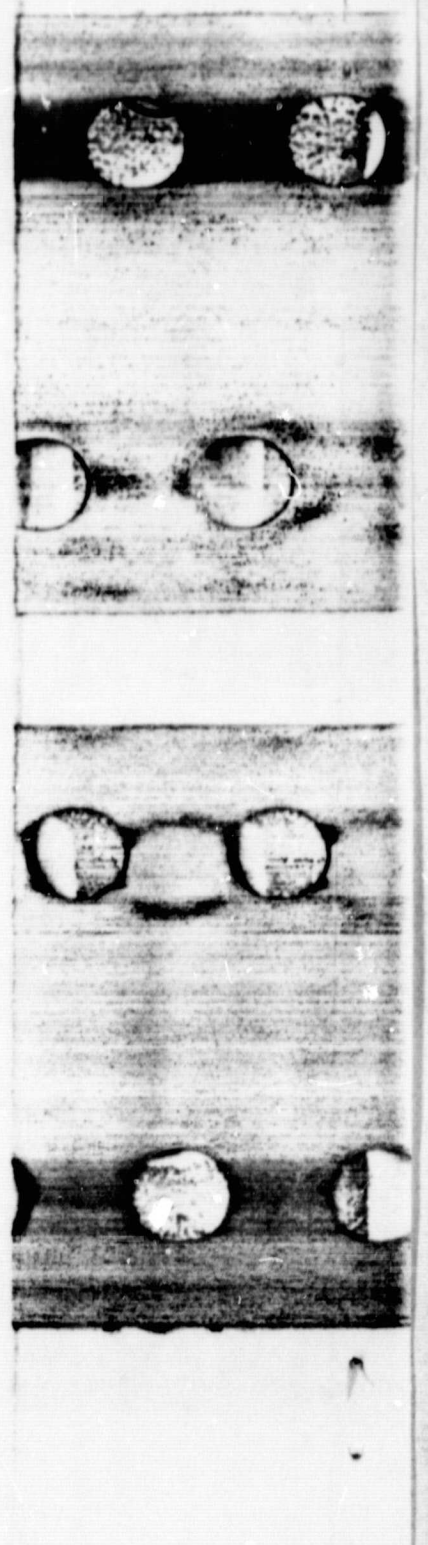

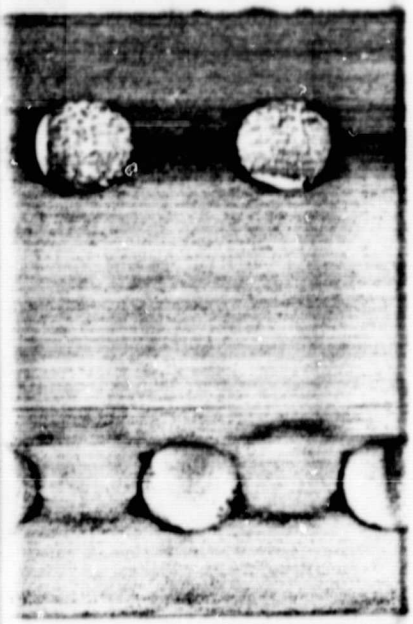

TABLE II

Observed and Calculated *Q*-Branch Transitions of $^{70}GeH_4$ and $^{72}GeH_4$, Listed in Order of Wavenumber

$^{70}GeH_4$ Transition	$^{72}GeH_4$ Transition	ν/cm^{-1}	^{70}Ge o−c	^{72}Ge o−c	$^{70}GeH_4$ Transition	$^{72}GeH_4$ Transition	ν/cm^{-1}	^{70}Ge o−c	^{72}Ge o−c
Q(8) F2(2)		818.6341	-11			Q(19) F1(5)	818.9028		-6
Q(7) F1(2)		818.6475	-6		Q(17) E(3)	Q(18) A1(2)	818.9202	0	-1
Q(3) A2		818.6590	-1		Q(14) F2(4)		818.9219	-4	
Q(12) F1(3)		818.6751	-2		Q(12) A1(2)		818.9332	-6	
	Q(15) A2(2)	818.6900		-1		Q(21) F2(5)	818.9567		3
Q(14) E(2)		818.6961	3			Q(20) F2(5)	818.9780		-6
Q(6) A1		818.7226	11		Q(19) E(3)		819.0476	-2	
Q(10) F2(3)		818.7401	7		Q(16) F2(4)		819.0801	-1	
Q(11) F1(3)		818.7537	10		Q(15) A2(2)		819.1132	-2	
Q(19) F2(5)	Q(20) E(4)	818.7682	1	18	Q(18) F1(4)		819.1132	17	
Q(16) E(3)		818.7703	3		Q(17) F1(5)		819.1432	-3	
Q(21) A1(2)		818.7866	4			Q(21) A2(2)	819.1665		-7
Q(9) A2		818.8067	0		Q(20) E(4)		819.1792	-6	
Q(18) F2(5)		818.8302	-3		Q(19) F1(5)		819.3197	-2	
Q(20) F1(5)		818.8511	-6		Q(19) A1(2)		819.3386	-5	
Q(15) F2(4)		818.8692	-1		Q(20) F2(5)		819.3937	5	
Q(13) F1(4)		818.8815	-1						

Note. The transitions are labeled by their ground-state symmetry species. Columns headed o − c are the residuals (observed − calculated) from the least-squares fits, in units of 10^{-4} cm^{-1}.

TABLE III

Molecular Constants (cm^{-1}) for the Five Isotopic Species of Germane, Derived from the Analysis of Diode Laser Measurements on the ν_4 Band

Constant[a]	$^{70}GeH_4$	$^{72}GeH_4$	$^{73}GeH_4$	$^{74}GeH_4$	$^{76}GeH_4$
ν_4	821.5392(12)	821.1084(23)	820.9025(11)	820.7046(10)	820.3166(12)
B	2.69569(8)	2.69570(5)	*b*	*b*	*b*
$2B\zeta_4$	3.0010(7)	3.0041(7)	3.0056(2)	3.0074(2)	3.0101(2)
q_{220}	9.45(12) × 10^{-3}	9.45(6) × 10^{-3}	*b*	*b*	*b*
q_{224}	-8.53(15) × 10^{-4}	-8.53(5) × 10^{-4}	-8.63(4) × 10^{-4}	-8.58(4) × 10^{-4}	-8.60(4) × 10^{-4}
D[c]	3.06(2) × 10^{-5}	3.07(2) × 10^{-5}	*b*	*b*	*b*
r_{110}	8.2(6) × 10^{-5}	*b*	*b*	*b*	*b*
F_{134}	6.0(9) × 10^{-5}	*b*	*b*	*b*	*b*
G_{224}	6.5(5) × 10^{-7}	6.4(5) × 10^{-7}	*b*	*b*	*b*
R_{24}[d]	2.5431	2.5413	2.5404	2.5395	2.5379
σ[e]	0.0012	0.0010	0.0013	0.0012	0.0012
$\Delta\nu_4$,obs	0.430_6	0.206_1	0.197_9	0.388_0	
$\Delta\nu_4$,calc[f]	0.438	0.211	0.205	0.394	
$\Delta(2B\zeta_4)$,obs	-0.0031	-0.0015	-0.0018	-0.0027	
$\Delta(2B\zeta_4)$,calc[f]	-0.0035	-0.0017	-0.0016	-0.0031	

a Nomenclature is that of Gray and Robiette (*9*). Ground state constants were fixed throughout at the values of Kreiner *et al.* (*3*) and Kagann *et al.* (*12*). ν_2 constants were preliminary values from Kreiner and Robiette (*4*), assumed the same for all isotopic species; the principal constants are: ν_2 929.921 cm^{-1}, B_2 2.6972 cm^{-1}, b_2 -0.00543 cm^{-1}, D_2 3.54 × 10^{-5} cm^{-1}, d_2 -6.77 × 10^{-6} cm^{-1}.

b Constant fixed at $^{70}GeH_4$ value.

c All upper state quartic and sextic centrifugal distortion constants other than D constrained to ground state values.

d ν_2/ν_4 Coriolis coupling parameter (*9*); fixed at values calculated from force field predictions of ζ_{24} for the five isotopic species.

e Standard deviation of the fit.

f Calculated value from approximate harmonic force field (see text).

Note. Errors in parentheses are one standard deviation in the last figure quoted.

REFERENCES

1. H. W. KATTENBERG, W. GABES, AND A. OSKAM, *J. Mol. Spectrosc.* **44,** 425–442 (1972).
2. W. A. KREINER, G. MAGERL, B. FURCH, AND E. BONEK, *J. Chem. Phys.* **70,** 5015–5020 (1979).
3. W. A. KREINER, R. OPFERKUCH, A. G. ROBIETTE, AND P. H. TURNER, *J. Mol. Spectrosc.* **85,** 442–448 (1981).
4. W. A. KREINER AND A. G. ROBIETTE, unpublished work.
5. S. P. REDDY, W. IVANCIC, V. MALATHY DEVI, A. BALDACCI, K. NARAHARI RAO, A. W. MANTZ, AND R. S. ENG, *Appl. Opt.* **18,** 1350–1354 (1979).
6. P. P. DAS, V. MALATHY DEVI, AND K. NARAHARI RAO, *J. Mol. Spectrosc.* **84,** 305–312 (1980).
7. A. G. MAKI, W. B. OLSON, AND R. L. SAMS, *J. Mol. Spectrosc.* **81,** 122–138 (1980).
8. V. MALATHY DEVI, P. P. DAS, AND K. NARAHARI RAO, *Appl. Opt.* **18,** 2918–2919 (1979).
9. D. L. GRAY AND A. G. ROBIETTE, *Mol. Phys.* **32,** 1609–1625 (1976).
10. D. L. GRAY, A. G. ROBIETTE, AND J. W. C. JOHNS, *Mol. Phys.* **34,** 1437–1453 (1977).
11. A. G. ROBIETTE, *J. Mol. Spectrosc.* **86,** 143–158 (1981).
12. R. H. KAGANN, I. OZIER, G. A. MCRAE, AND M. C. L. GERRY, *Canad. J. Phys.* **57,** 593–600 (1979).

P. P. DAS[1]
V. MALATHY DEVI[2]
K. NARAHARI RAO[3]

Department of Physics
The Ohio State University
Columbus, Ohio 43210

A. G. ROBIETTE

Department of Chemistry
University of Reading
Reading RG6 2AD, United Kingdom

Received March 16, 1981

[1] Present address: Tachisto Inc., 13 Highland Circle, Needham, Mass. 02194.
[2] Present address: NOAA-NESS, FB4, S/RE21, Washington D. C. 20233.
[3] K.N.R. expresses his gratitude to the National Aeronautics and Space Administration for support of this research.

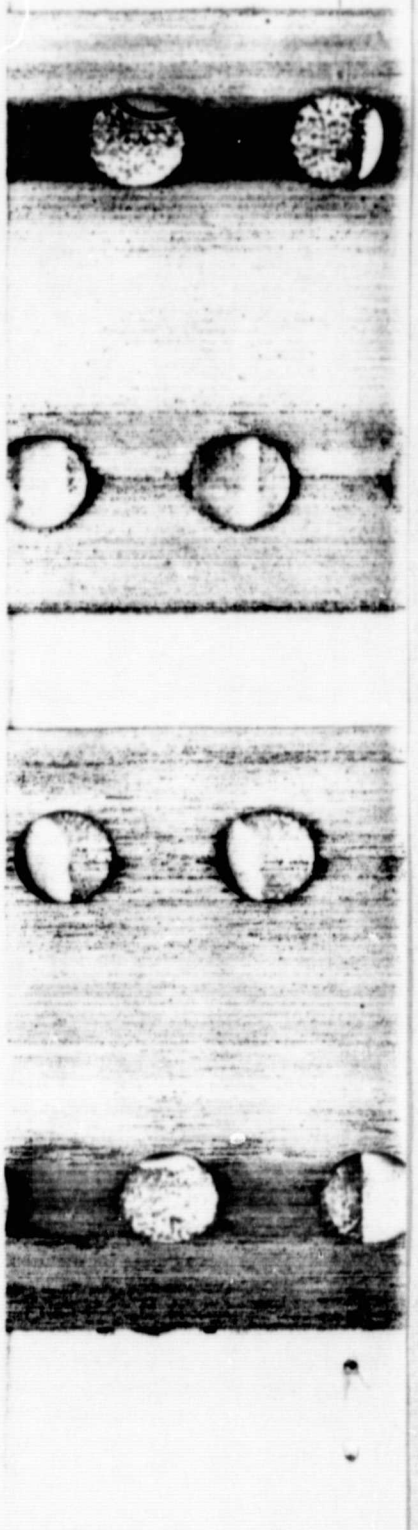

JOURNAL OF MOLECULAR SPECTROSCOPY 81, 269–272 (1980)

NOTE

Convolution of a Doppler Line by a Gaussian Instrument Function

In this note a simple method is derived for assessing the distortion of a Doppler line by a Gaussian instrument function. It has immediate applicability for diode laser measurements, and may be used whenever a Gaussian instrument function is a reasonable approximation to reality. The notation is similar to that of Penner (*1*). Define the absorptance

$$A(x) = 1 - \tau(x) = 1 - \exp[-P(x)], \tag{1}$$

where

$$P(x) = P' \exp[-(x/b_D)^2(\ln 2)], \tag{2}$$

$$P' = S/b_D \cdot (\ln 2/\pi)^{1/2} pl, \tag{3}$$

and

$$x = \nu - \nu_0.$$

Let the absorptance $A(x)$ be convoluted by a normalized Gaussian instrument function

$$f(x - x') = \frac{1}{\delta\pi^{1/2}} \exp[-(x - x')^2/\delta^2], \tag{4}$$

where $\delta = d/(\ln 2)^{1/2}$, and d is the half-width half-height (HWHH) of the convoluting function.

The convolution is

$$A'(x) = \int_{-\infty}^{\infty} A(x')f(x - x')dx'. \tag{5}$$

If we expand $A(x)$ in a series,

$$A(x) = \sum_{n=1}^{\infty} \frac{(-1)^{n+1}P'^n}{n!} \cdot \exp[-x^2/(\beta^2/n)], \tag{6}$$

where $\beta = b_D/(\ln 2)^{1/2}$, Eq. (5) becomes

$$A'(x) = \sum_{n=1}^{\infty} \frac{(-1)^{n+1}P'^n}{\delta\pi^{1/2}n!} \int_{-\infty}^{\infty} \exp[-x'^2/(\beta^2/n)] \cdot \exp[-(x - x')^2/\delta^2]dx'. \tag{7}$$

The form of Eq. (7) has been deliberately chosen to exhibit the fact that each term of the series for $A'(x)$ contains the convolution of the Gaussian instrument function with a Gaussian of $1/e$ half-width $\beta/n^{1/2}$.

For $n = 1$, the integration gives a Gaussian of $1/e$ half-width $(\beta^2 + \delta^2)^{1/2}$. This result was discussed by Van DeHulst and Reesinck (*2*). The other terms in the series can be written immediately, giving

$$A'(x) = \sum_{n=1}^{\infty} \frac{(-1)^{n+1}P'^n}{n!n^{1/2}} \exp\frac{[-x^2/\beta^2(1/n + r^2)]}{(1/n + r^2)^{1/2}}, \tag{8}$$

where $r = \delta/\beta = d/b_D$. If Eq. (6) or Eq. (8) is used to compute the equivalent width,

$$W = \int_{-\infty}^{\infty} A(x)dx = \int_{-\infty}^{\infty} A'(x)dx, \tag{9}$$

we get the result of Ladenburg (*3*),

$$W = Spl \sum_{n=0}^{\infty} \frac{(Spl/\beta\pi^{1/2})^n(-1)^n}{(n + 1)!(n + 1)^{1/2}}. \tag{10}$$

The form of Eq. (8) permits simple rapid calculation using a desktop programmable calculator.

0022-2852/80/050269-04$02.00/0

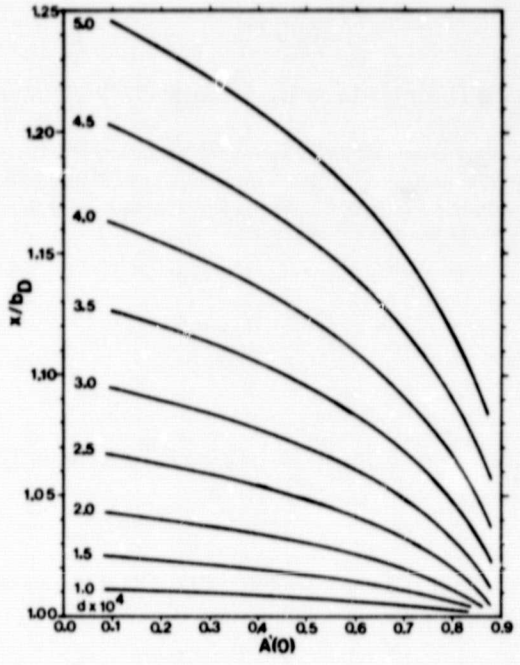

FIG. 1. Instrumental distortion, x/b_D, versus maximum observed absorptance, $A'(0)$, for various values of instrument HWHH, d.

The convergence of Eq. (8), as well as Eq. (10), is absolute. The rate of convergence depends mostly on the value of P'. For an accuracy of 10^{-5}, $P' = 0.2$ requires 5 terms, while $P' = 10$ requires 35 terms in the series. However, even the longer series is computed in a few seconds on a programmable calculator.

If there were no instrumental distortion we would measure the HWHH of a spectral line, b_D, at that point for which $\pi(x) = (\pi(0))^{1/2}$, or where $A(x) = 1 - [1 - A(0)]^{1/2}$. To find the error in this procedure for a convoluted line we iterated on Eq. (8) until we found an x such that

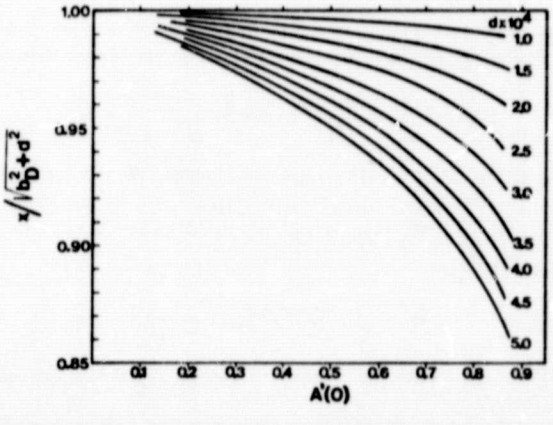

FIG. 2. The error in the first-order approximation to the instrumental distortion, $x/(b_D^2 + d^2)^{1/2}$, versus maximum observed absorptance for various values of instrument HWHH, d.

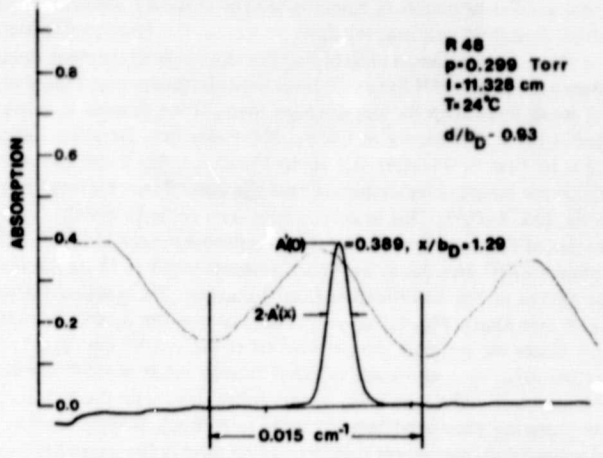

FIG. 3. Reproduction of laser diode spectrometer scan taken at OSU. Measurement of d/b_D is from Fig. 4.

$$A'(x) = 1 - [1 - A'(0)]^{1/2}. \tag{11}$$

This value, x (or x/b_D) is a measure of the broadening of the absorptance, or transmittance.

Figure 1 was prepared by choosing values for P', b_D, and d and computing $A'(0)$; then with this $A'(0)$ we compute $A'(x)$ to satisfy Eq. (11). Values of $d < b_D = 0.00066\ \text{cm}^{-1}$ were chosen to correspond to anticipated conditions for measurement in the 15 μm CO_2 bands. The results of these computations

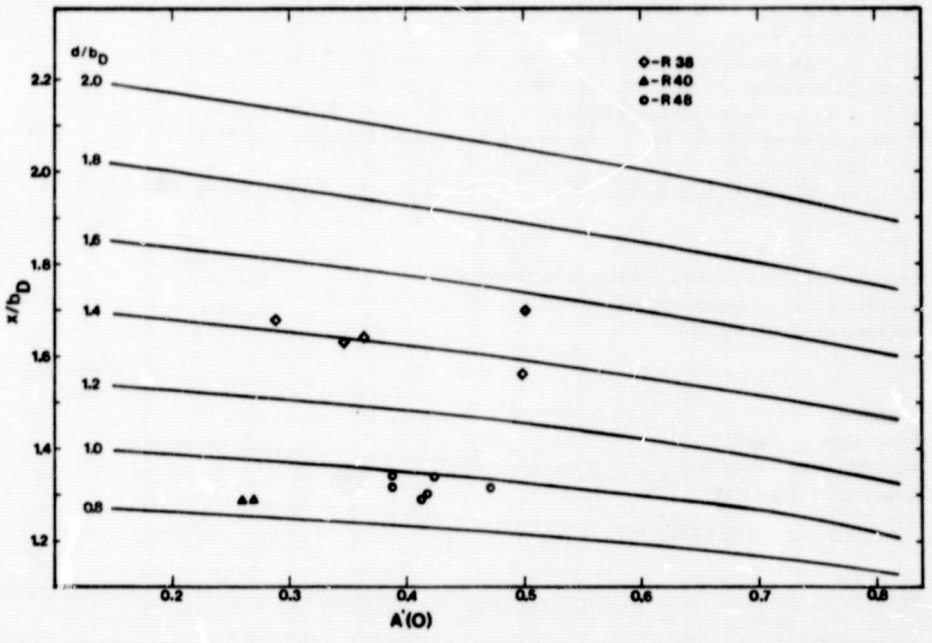

FIG. 4. Chart similar to Fig. 1 produced for larger values of instrument HWHH, shown as the ratio d/b_D.

agree perfectly with the published results of Kostkowski and Bass (*4*), who calculated the convolution, on a large computer by digital integration, for three values of the peak absorption.

The appearance of these curves shows clearly that for the same instrument function, and using the standard method of measuring HWHH for diode laser measurements (see Planet *et al.* (*5*, *6*)), the distortion is greater for weak lines than for the stronger ones. If we assume that the Doppler measurements of Ref. (*5*) had $A'(0) = 0.5$, then $x = 1.08b_D$, 8% wider than Doppler, indicates an instrument function of about 3.2×10^{-4} cm^{-1} (HWHH). If $A'(0)$ had been 0.3, Fig. 1 still shows $d \approx 2.9 \times 10^{-4}$ cm^{-1}.

Figure 2 shows the error incurred by assuming that the convoluted half-width is given by the first-order correction alone, $(b_D^2 + d^2)^{1/2}$. This assumption is seen to be better for weaker lines.

An example of the use of Fig. 1, or any similar chart, is demonstrated in Fig. 3. This is a reproduction of a measurement made at OSU on a diode laser spectrometer in the ν_2 15-μm band of $^{12}C^{16}O_2$. A simultaneous etalon trace serves as the wavenumber (cm^{-1}) marker. We measured $A'(0) = 0.389$, and the HWHH $x = 1.29b_D$. A new chart, Fig. 4, was prepared, because the instrument function was too large for Fig. 1. Using this figure we estimate $d/b_D \cong 0.93$ ($d \cong 6.1 \times 10^{-4}$ cm^{-1}).

The results of several other measurements in the *R* branch made at OSU are also shown in Fig. 4. The instrument function clearly changes with wavenumber, i.e., with diode laser mode.

The method of computation presented here is simple and direct. It suggests that a close approximation to the width of a Gaussian instrument function, or an almost Gaussian function may be found by measuring a line with a Doppler absorption coefficient. Charts for specific spectral regions and expected instrument widths can be easily prepared by the use of Eq. (8).

ACKNOWLEDGMENTS

Many fruitful discussions on various aspects of this problem were held with G. Tettemer of NOAA/NESS.

The support extended to the Ohio State University program by the National Aeronautics and Space Administration through grants made to Professor K. Narahari Rao is gratefully acknowledged.

REFERENCES

1. S. S. Penner, "Quantitative Molecular Spectroscopy and Gas Emissivities." Chap. 4, Addison–Wesley, Reading, Mass., 1959.
2. H. C. Van DeHulst and J. J. M. Reesinck, *Astrophys. J.* **106,** 121–127 (1947).
3. R. Ladenburg, *Z. Phys.* **65,** 200 (1930).
4. H. J. Kostkowski and A. M. Bass, *J. Opt. Soc. Amer.* **46,** 1060–1064 (1956).
5. W. G. Planet, G. L. Tettemer, and J. S. Knoll, *J. Quant. Spectrosc. Radiat. Transfer* **20,** 547–555 (1978).
6. W. G. Planet and G. L. Tettemer, *J. Quant. Spectrosc. Radiat. Transfer* **22,** 345–354 (1979).

B. Fridovich

National Oceanic and Atmospheric Administration
National Environmental Satellite Service
Washington, D. C. 20233

V. Malathy Devi
P. P. Das

Department of Physics
The Ohio State University
Columbus, Ohio 43210

Received August 3, 1979

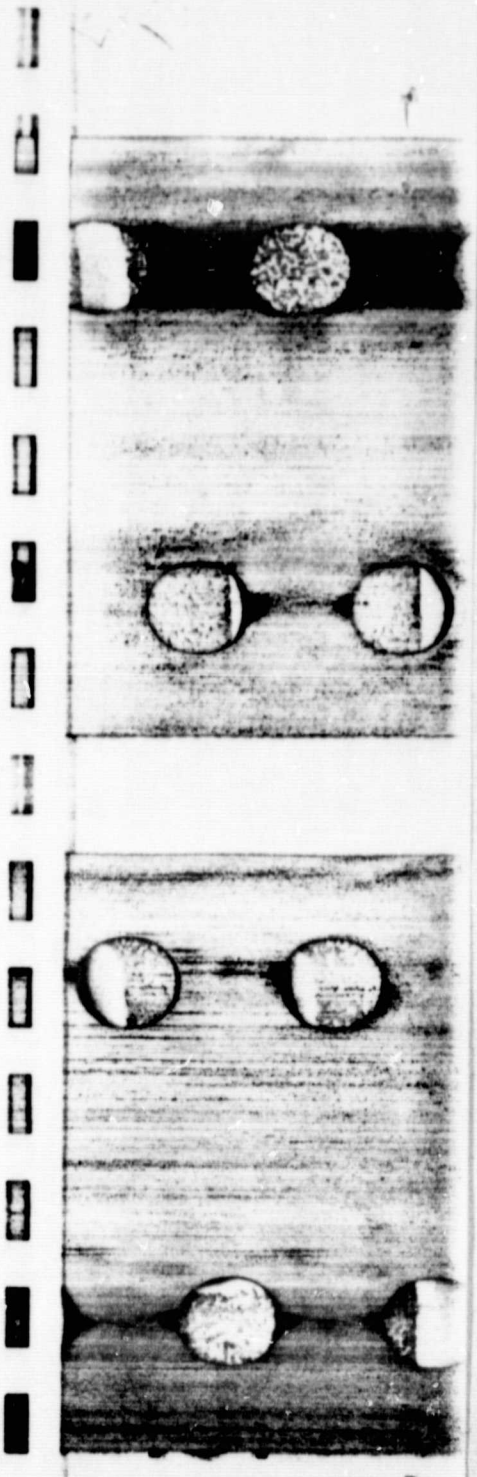

Reprinted from APPLIED OPTICS, Vol. 18, page 2918, September 1, 1979

Intercomparison of CO_2 and HCN wave numbers at 800–600 cm^{-1} with a diode laser spectrometer

V. Malathy Devi, Palash P. Das, and K. Narahari Rao

Ohio State University, Physics Department, Columbus, Ohio 43210.

Received 30 June 1979.
0003-6935/79/172918-02$00.50/0.

This investigation is based on two recent publications.[1,2] The high spectral resolution and sensitivity obtained with diode laser spectrometers are being increasingly used in procuring basic observational data for determination of molecular parameters. With diode lasers, typically we are able to scan spectral intervals of about 0.5–1 cm^{-1} at any one time, and quite frequently these spectral intervals do not have a continuity in them. Obviously, meaningful spectroscopic constants can be determined only when there is internal consistency in the wave-number data available for such disjointed spectral intervals. At the longer wavelengths of 12–17 μm where much useful information can be obtained by studying low-frequency fundamental vibration–rotation bands of polyatomic molecules, the band spectra of CO_2 and HCN seem to provide a set of convenient wave-number standards. The HCN data presented in Ref. 1 were generated from available rotational constants for its 01^10 and 00^00 levels combined with the ν_2 band center evaluated from grating measurements.[3] On the other hand, the CO_2 wave numbers of Ref. 2 were obtained with a high-resolution Fourier spectrometer, and their wave-number precision is quoted to be better than 0.001 cm^{-1} by relating the Fourier data for pure rotational water vapor lines to the values calculated from water vapor energy levels. We have intercompared these HCN and CO_2 data by making measurements at Doppler-limited spectral resolution with a diode laser spectrometer and find that there is internal consistency in the wave-number values of Refs. 1 and 2 within about ±0.0005 cm^{-1}.

The diode laser assembly described by Reddy *et al.*[1] has been used for the intercomparison of the measurements of

Table I. Comparison of the Present Measurements with the Fourier Data of Ref. 2

$R(76)$ of ν_2 of $^{12}C^{16}O_2$ relative to $R(5)$ of ν_2 of $H^{12}C^{14}N$ as standard		From Fourier	$R(56)$ of ν_2 of $^{12}C^{16}O_2$ relative to $Q(12)$ of ν_2 of $H^{12}C^{14}N$ as standard		From Fourier
729.6847			713.1348		
729.6844	Av. value		713.1350	Av. Value	
729.6847	729.6846	729.6847	713.1352	713.1350	713.1348

Table II. Wavenumbers (vac. cm^{-1}) of the Q Branches of the ν_1-ν_2 Bands of $^{12}C^{16}O_2$ and $^{13}C^{16}O_2$

	$^{12}C^{16}O_2$			$^{13}C^{16}O_2$		
Q(J)	Present obs. value[a]	High-resolution Fourier[b]	Diff. × 10^4	Present obs. value[c]	High-resolution Fourier[b]	Diff. × 10^4
$Q(2)$	720.7998	720.7994	4	721.5752	721.5749	3
$Q(4)$	720.7846	720.7845	1	721.5539	721.5536	3
$Q(6)$	720.7608	720.7610	−2	721.5206	721.5201	5
$Q(8)$	720.7292	720.7290	2	721.4745	721.4744	1
$Q(10)$	720.6890	720.6886	4	721.4165	721.4166	−1
$Q(12)$				721.3460	721.3466	−6
$Q(14)$				721.2644	721.2644	0
$Q(16)$				721.1692	721.1700	−8
$Q(18)$				721.0638	721.0635	3

[a] $^{12}C^{16}O_2$ lines were measured relative to $R(2)$ of ν_2 of $H^{12}C^{14}N$.
[b] Ref. 4; R. Antilla, U. Oulu, Finland; private communication.
[c] $^{13}C^{16}O_2$ lines were measured relative to $R(66)$ of the ν_2 of $^{12}C^{16}O_2$.

Table III. Wavenumbers (vac. cm^{-1}) of the Q Branch Lines of the ν_1-ν_2 Band of $^{12}C^{16}O^{17}$ and the ν_2 Band of $H^{13}C^{14}N$

$^{12}C^{16}O^{17}O$						$H^{13}C^{14}N$		
Q(J)	ν calc.[a]	(O-C) × 10^4	Q(J)	ν calc.[a]	(O-C) × 10^4	Q(J)	ν calc.[b]	(O-C) × 10^4
$Q(1)$	711.2981	2	$Q(16)$	711.0743	−11	$Q(4)$	706.0999	−3
$Q(4)$	711.2831	1	$Q(17)$	711.0462	−6	$Q(5)$	706.1672	−5
$Q(5)$	711.2748	0	$Q(18)$	711.0166	−1	$Q(6)$	706.2479	−5
$Q(6)$	711.2648	1	$Q(19)$	710.9854	2	$Q(7)$	706.3421	−1
$Q(7)$	711.2532	3	$Q(20)$	710.9526	4	$Q(8)$	706.4498	13
$Q(8)$	711.2399	3	$Q(21)$	710.9182	3	$Q(9)$	706.5709	16
$Q(9)$	711.2249	−1	$Q(22)$	710.8822	4	$Q(10)$	706.7055	−3
$Q(10)$	711.2083	3	$Q(23)$	710.8446	5	$Q(11)$	706.8535	−10
$Q(11)$	711.1900	3	$Q(24)$	710.8055	7	$Q(12)$	707.0150	−2
$Q(12)$	711.1701	−3	$Q(25)$	710.7649	0	$Q(13)$	707.1899	0
$Q(13)$	711.1486	−4	$Q(26)$	710.7227	−3			
$Q(14)$	711.1255	−5	$Q(27)$	710.6789	−4			
$Q(15)$	711.1007	−1	$Q(28)$	710.6337	−2			

[a] ν calc. = 711.29978 − 0.0008336 $J(J+1)$ + 1.64 × 10^{-8} J^2 $(J+1)^2$. The measurements were made relative to $P(13)$ of ν_1-ν_2 of $^{12}C^{16}O_2$.
[b] ν calc. = 705.96535 + 0.0067283 $J(J+1)$. The measurements were made relative to $R(48)$ of ν_2 of $^{12}C^{16}O_2$.

$^{12}C^{16}O_2$ lines relative to $H^{12}C^{14}N$ lines at 14 μm. It may be recalled that with a setup of this type, Fabry-Perot fringes of about 0.015 cm^{-1} apart produced with an air-spaced étalon are recorded simultaneously with the scanning of diode laser IR spectra. The absolute wave number on the fringe scale is obtained by recording an available absorption standard. By adopting this procedure, $R(76)$ and $R(56)$ lines of the ν_2 band of $^{12}C^{16}O_2$ have been measured, the first one by using an R branch line and the second one by using a Q branch line of the ν_2 band of $H^{12}C^{14}N$ as standards. The data presented in Table I show the extent of agreement between our measurements and the Fourier data[2] and also demonstrate that the reproducibility of diode laser measurements is excellent.

Another test for internal consistency between the R- and Q-branch wavenumbers of Ref. 1 was possible because we could measure the $R(1)$ of ν_2 of $H^{12}C^{14}N$ relative to the $Q(28)$ line of the same band. It has been found that such a measurement for $R(1)$ came out to be 717.8932 cm^{-1} as compared to the value 717.8927 cm^{-1} calculated in Ref. 1.

Table II compares the diode laser measurements for the ν_1-ν_2 bands of $^{12}C^{16}O_2$ and $^{13}C^{16}O_2$ with the Fourier spectroscopic data of Paso *et al.*[4] The agreement between the two sets of data is again within a few units in the fourth decimal place.

While performing the above described measurements, we have observed the ν_2 of $H^{13}C^{14}N$ and ν_1-ν_2 of $^{12}C^{16}O^{17}O$ in the natural sample. The wave numbers of the bands of these two molecules are given in Table III.

This paper was presented during the 34th Molecular Spectroscopy Symposium at the Ohio State University, 11–15 June 1979 (Paper TE10). This research was done during the period in which support was received from the National Aeronautics and Space Administration. One of us (KNR) is grateful for this support.

References

1. S. P. Reddy, W. Ivancic, V. Malathy Devi, A. Baldacci, K. Narahari Rao, A. W. Mantz, and R. S. Eng, Appl. Opt. 18, 1350 (1979).
2. J. Kauppinen, Appl. Opt. 18, 1788 (1979).
3. P. K. L. Yin and K. Narahari Rao, J. Mol. Spectrosc. 42, 385 (1972).
4. R. Paso, J. Kauppinen, and R. Antilla, J. Mol. Spectrosc. 78, Dec (1979).

1. Report No.	2. Government Accession No.	3. Recipient's Catalog No.
NASA CR-166494		

4. Title and Subtitle	5. Report Date
LABORATORY INFRARED STUDIES OF MOLECULES OF ATMOSPHERIC AND ASTROPHYSICAL INTEREST	October 1982
	6. Performing Organization Code
7. Author(s)	8. Performing Organization Report No.
K. Narahari Rao, Principal Investigator	
	10. Work Unit No.
	T 4183
9. Performing Organization Name and Address	11. Contract or Grant No.
The Ohio State University, Department of Physics 174 West 18th Avenue, Columbus, Ohio 43210	NSG-2175
	13. Type of Report and Period Covered
12. Sponsoring Agency Name and Address	Contractor Report
National Aeronautics and Space Administration Ames Research Center, Moffett Field, CA 94035	14. Sponsoring Agency Code 506-15-11-03

15. Supplementary Notes

Technical Monitor, Robert W. Boese, MS 245-6
Point of contact: Ames Research Center, Moffett Field, CA 94035
415-965-5501 or FTS 448-5501

16. Abstract

The report is a compilation of nineteen reprints on the molecular species:

NO_2 ν_2 & $2\nu_2$; H_2O (8050-9730 cm^{-1}); O_3 ν_2; C_2H_2 ν_5 & 6680-6460 cm^{-1};

CH_3D ν_3 & ν_6; CH_3I ν_6; NH_3 ν_2, $2\nu_2$, ν_4; ND_3 ν_2; $^{13}C^{16}O_2$ ν_3;

PH_3 ν_1 & ν_3; OCS ν_1; GeH_4 ν_4.

Much of the work was done by using the Doppler-limited resolution provided by diode lasers. The diode laser was used as a source to a grating spectrometer which has been used earlier for high resolution studies. This technique provided many advantages. Wherever possible, the studies have been directed to intensity determinations of infrared bands.

17. Key Words (Suggested by Author(s))	18. Distribution Statement
Molecular spectroscopy Absorption spectroscopy Gaseous absorption	UNCLASSIFIED - Unlimited STAR Category-72

19. Security Classif. (of this report)	20. Security Classif. (of this page)	21. No. of Pages	22. Price*
UNCLASSIFIED	UNCLASSIFIED	243	

*For sale by the National Technical Information Service, Springfield, Virginia 22161